

HULL, TIMOTHY STEPHEN
Ph.D. MARCH 1988

The University of Sydney

Copyright in relation to this thesis*

Under the Copyright Act 1968 (several provisions of which are referred to below), this thesis must be used only under the normal conditions of scholarly fair dealing for the purposes of research, criticism or review. In particular no results or conclusions should be extracted from it, nor should it be copied or closely paraphrased in whole or in part without the written consent of the author. Proper written acknowledgement should be made for any assistance obtained from this thesis.

Under Section 35(2) of the Copyright Act 1968 the 'author of a literary, dramatic, musical or artistic work is the owner of any copyright subsisting in the work'. By virtue of Section 32(1) copyright 'subsists in an original literary, dramatic, musical or artistic work that is unpublished' and of which the author was an Australian citizen, an Australian protected person or a person resident in Australia.

The Act, by Section 36(1) provides: 'Subject to this Act, the copyright in a literary, dramatic, musical or artistic work is infringed by a person who, not being the owner of the copyright and without the licence of the owner of the copyright, does in Australia, or authorises the doing in Australia of, any act comprised in the copyright'.

Section 31(1)(a)(i) provides that copyright includes the exclusive right to 'reproduce the work in a material form'. Thus, copyright is infringed by a person who, not being the owner of the copyright and without the licence of the owner of the copyright, reproduces or authorises the reproduction of a work, or of more than a reasonable part of the work, in a material form, unless the reproduction is a 'fair dealing' with the work 'for the purpose of research or study' as further defined in Sections 40 and 41 of the Act.

Keith Jennings
Registrar

*'Thesis' includes 'treatise', 'dissertation' and other similar productions.

THE STATIC BEHAVIOUR OF
LATERALLY LOADED PILES

Thesis submitted for the degree of
Doctor of Philosophy
The University of Sydney

June 1987

by

Timothy Stephen Hull, B.E.

CONTENTS

Synopsis

Preface

Acknowledgements

CHAPTER 1 - INTRODUCTION

1.1	General Introduction	1
1.2	Aim of Thesis	4
1.3	Thesis Outline	8
1.4	Notation	10

CHAPTER 2 - LITERATURE REVIEW

2.1	Introduction	13
2.2	Lateral Pile History and Analysis Classification	14
2.2.1	Winkler and p-y Methods	
2.2.2	Elastic Continuum Methods	
2.2.3	Finite Element Models	
2.3	Load Transfer Models	40
2.4	Field Tests	48
2.4.1	The Tests of Feagin (1935)	
2.4.2	The Test of McClelland and Focht (1956)	
2.4.3	Other Tests	
2.5	Model Parameters	61
2.5.1	p-y Approach	
2.5.2	Elastic Continuum Approach	
2.5.3	Other Approaches	
2.5.4	Gapping and Soil Parameters	
2.5.5	Summary	
2.6	Summary of Review	77

CHAPTER 3 - LATERAL PILE RESPONSE : LINEAR ANALYSIS

3.1	Introduction	92
3.2	Winkler Approach	95
3.2.1	Coefficient of Subgrade Reaction	
3.2.2	Uniform Soil Profile Winkler Analysis	
3.2.3	Linear Soil Profile Winkler Analysis	
3.3	Boundary Element Approach	117
3.3.1	Winkler Soil Element	
3.3.2	Mindlin Elastic Soil Element	
3.3.3	Boundary Element Analysis	
3.4	Finite Element Approach	134
3.4.1	Axisymmetric Finite Element Analysis	
3.4.2	Validation of Finite Element Analysis	
3.4.3	Mesh Boundary Investigation	
3.4.4	Profile Building Analysis	
3.5	Recommended Method for Linear Analysis	169
3.5.1	Mindlin-based Soil Layer of Finite Depth	
3.5.2	Modification for Non-Homogeneous Soil Profiles	
3.6	Conclusions	185

CHAPTER 4 - LATERAL PILE RESPONSE : EFFECTIVE LENGTH CONCEPT AND LINEAR RESULTS

4.1	Introduction and History	207
4.2	Effective Length Hypothesis	210
4.2.1	Critical Length Equation	
4.2.2	Effective Length and Presentation of Results	
4.3	Verification of Critical Length Concept and Results	225
4.3.1	Results of Winkler Analysis	
4.3.2	Results of MBEM Analysis	
4.3.3	Results of Finite Element Analysis	
4.3.4	Existence of Other Critical Lengths	
4.4	Critical Length Applied to Design of a Test Pit	252
4.5	Conclusions	258

CHAPTER 5 - LATERAL PILE RESPONSE : NON-LINEAR ANALYSIS

5.1	Introduction	300
5.2	Aspects of Non-linear Behaviour	303
5.2.1	Separation	
5.2.2	Soil Failure	
5.3	Winkler Model and Non-linear Behaviour	310
5.3.1	Winkler : Elastic Non-linear Gapping	
5.3.2	Winkler : Plastic Non-linear Soil Failure	
5.3.3	Winkler : Elastic Linear Soil and Pile Failure	
5.4	Boundary Element Method : Non-linear Behaviour	327
5.4.1	Soil-pile Deflection Mismatch Model	
5.4.2	Description of Non-linear MBEM Analysis	
5.4.3	Non-linear Soil Response : Parametric Study	
5.4.4	Comparison with Previous Non-linear Results	
5.5	Finite Element Method : Non-linear Behaviour	350
5.5.1	Soil Structure Interaction : Analysis	
5.5.2	Biface Analysis	
5.5.3	SSI Analysis Verification	
5.6	Non-linear Biface Model Response	383
5.7	Conclusions	400

CHAPTER 6 - LATERAL PILE RESPONSE : EXPERIMENTAL AND FIELD CASES

6.1	Introduction	434
6.1.1	Data Acquisition and Manipulation	
6.2	Closed-vessel Clay Tests	443
6.2.1	Apparatus and Procedure	
6.2.2	Dead Load Tests	
6.2.3	Load-deflection Response	
6.2.4	Summary of Closed-vessel Tests	
6.3	Open-vessel Clay Tests	457
6.3.1	Test with Different Pile Lengths	
6.3.2	Test Results and Theoretical Predictions	
6.3.3	Summary of Open-vessel Tests	

6.4	Field Case	466
6.5	Conclusions	471

CHAPTER 7 - SUMMARY OF CONCLUSIONS	496
------------------------------------	-----

REFERENCES	506
------------	-----

APPENDICES	
------------	--

SYNOPSIS

The elastic-continuum model of soil behaviour is used to predict the response of a single vertical pile to lateral loading. The range of methods developed to analyse this problem is reviewed and it is concluded that the continuum-based analysis represents the most likely one with which gains in understanding, and prediction of, pile response can be made. Other models represent mechanistic and isolated interpretations of soil behaviour.

A modified boundary element analysis is developed to produce linear continuum-based results comparable to more refined finite element analyses and is further extended to efficiently model non-linear soil response and incorporate gap formation within a non-linear interface element. The incremental plastic work in the non-linear interface element is defined in terms of a soil-pile deflection mismatch and restricted to have only a positive value, thus correctly modelling conditions where failed soil returns to an elastic state. The restricted nature of the interaction traction, modelled using closed-form solutions of an elastic continuum, means the case of unequal tractions on the back and front of the pile is not correctly modelled.

To correctly model unequal interaction tractions, a finite element-based soil-structure interaction analysis is developed, which employs a biface model of the pile-soil interface. With this analysis more accurate non-linear modelling is possible, also using the pile-soil mismatch and only positive plastic work.

The solution technique of both analyses are checked by employing a Winkler soil influence matrix, instead of an elastic-continuum one, and comparing the results with precise solutions of the Winkler-based pile problem with linear, elastic-gapping and

non-linear soil failure based responses.

All the analyses developed here present linear behaviour which is consistent with the existence of an effective pile length for lateral loading and the non-linear response is also shown to be explainable in terms of effective pile lengths. The concept of an effective ultimate load for the pile, at which pile deformations become excessive, is introduced.

A series of tests performed by the Author on model piles in normally consolidated and overconsolidated clay beds are described and shown to be amenable to elastic-continuum analysis and interpretation in terms of an effective length. The effective length is also found to simplify the back-analysis of results of a field test to allow accurate prediction of a pile with different dimensions tested in the same soil.

PREFACE

The candidate has carried out the work described in this thesis during the period 1982 to 1987. During most of that time the Author was employed as a research assistant. The work has been carried out under the supervision of Professor H.G. Poulos, Professor of Civil Engineering (Soil Mechanics), in the School of Civil and Mining Engineering. Six months were supervised by Dr. P.T. Brown during the absence of Professor Poulos.

In accordance with the By-Laws of The University of Sydney, a candidate for the degree of Doctor of Philosophy is required to indicate the sections of the thesis which are original. To this end the acknowledgement of ideas derived from other sources and references is made in the text and the Author claims originality for the following:

- (1) the Winkler analysis of piles in a linearly varying stiffness soil profile, presented in Chapter Three.
- (2) the average deflection-based soil interface element and the concept of a soil-pile mismatch developed in Chapter Three.
- (3) the profile building finite element analysis of Chapter Three.
- (4) the method of modifying the homogeneous soil response to obtain a non-homogeneous soil profile response, developed in Chapter Three.
- (5) the concept of an effective length based upon the actual or critical length and the equation for critical length, presented in Chapter Four.
- (6) the results of the Winkler, MBEM and finite element

analyses presented in Chapter Four.

- (7) the theoretical consideration of pile yield combined with a Winkler soil model, presented in Chapter Five.
- (8) the non-linear MBEM analysis and parametric results and the biface SSI analyses developed in Chapter Five, together with their treatment of plastic work based upon pile-soil deflection mismatches.
- (9) the conduct of the model pile tests, and their analysis, detailed in Chapter Six.
- (10) the interpretation and analysis of the field tests presented in Chapter Six.

During the period of the Author's candidature, two papers were prepared by the Author, Professor H.G. Poulos and E.W. Chua and are presented in support of his candidature:

Poulos, H.G., Hull, T.S. and Chua, E.W. (1984)
Foundation Behaviour in Calcareous Sands.
Ninth Australasian Conf. on the Mechanics of Structures and
Materials, The University of Sydney. pp 28 - 32.

Poulos, H.G., Chua, E.W. and Hull, T.S. (1984)
Settlement of Model Footings on Calcareous Sand
Geotechnical Engineering, Vol. 15, No. 1. pp 21 - 35.

ACKNOWLEDGEMENTS

The Civil and Mining Engineering Foundation made possible the commencement of study for this work and the Author expresses his gratitude for their generosity.

The academic staff and fellow research students in the School of Civil and Mining Engineering at The University of Sydney have been of assistance to me during many stages of my study, not least in their friendship which is much valued. In particular the moral support and hard work of Mr. K. Larrymore and Mr. R. Fraser in connection with the experimental work is greatly appreciated.

The assistance of Mrs J. MacLellan with the typing of this work, Mr. Frank Hull with the preparation of the figures and the help of Mr. M. Seidl in placing at my disposal the means to process and print the text is deeply appreciated.

Valuable discussions with Professor J.R. Booker, Dr. J.M. Rotter and the late Professor E.H. Davis are also gratefully acknowledged.

For his interest and helpful supervision during six months of my candidature I sincerely express my thanks to Dr. P.T. Brown.

For his constant support, enthusiasm for my work and guidance throughout a long and eventful course of study, I give many thanks to Professor H.G. Poulos.

In conclusion, I wish to thank my family, especially my wife Karen, for the encouragement, support and exceptional patience given to me during the long years of my candidature.

T.S.H.

CHAPTER ONE - INTRODUCTION

1.1 General Introduction

Any load, on a foundation supported by soil, can be defined in terms of six components related to a convenient reference system. The six components, consisting of three forces and three moments related to the Cartesian-coordinate reference system, are diagrammatically represented in Fig. 1.1. The resultant movement of the foundation will also be described by six concomitant components, three deflections and three rotations.

With the assumption of small strain and employing the principle of superposition, the general load-movement response of the foundation can be obtained by combining the results of three simplified types of analysis. These three classes of analysis, shown in Fig. 1.2, are

- a) lateral (antisymmetric response about a vertical plane),
- b) axial (axisymmetric radial and vertical response) and
- c) torsional (axisymmetric circumferential response).

If the resultant horizontal force and moment do not act in one vertical plane then two lateral load cases need to be analysed.

For a foundation with axially symmetric geometry, considering points along the axis to be representative of the foundation response, the three classes of loading do not interact with each other, e.g. no lateral deflection of the axis results from axial or torsional loads. Considering the symmetry in each class, prohibits across class induced average foundation response, although away from the axis the local deformation patterns for each class will interact. Thus, a pile foundation with an axisymmetric geometry, modelled by average deflections, has distinct analytical advantages over foundations without axial symmetry.

The simplification of the general load case, to the three cases of lateral, axial and torsional load, is thus directly applicable to pile foundations. Three separate models for pile response, each model simplified to a one-dimensional problem without introducing gross errors, will enable any load case to be analysed. The practical advantages of piles and this ease of analysis has ensured the popularity of piled foundations.

The wide range of piling applications and the variety of soil types encountered, have led to methods with considerable reliance upon empirical correlations of behaviour. While such correlations have been possible for land-based applications, it has proved difficult to obtain reliable data for off-shore piled foundation response. Therefore a need exists for a logical model of soil response to enable prediction of behaviour, as opposed to choosing a response from a series of empirical models, of possibly restricted applicability.

The elastic continuum model of soil provides one such theoretical framework, within which predictions of response are logically based upon measurable parameters that are basic (fundamental) soil properties. In contrast, the empirical approach employs parameters that are undetermined functions of the soil properties, the pile properties and the form of loading, while taking no account of interaction. The elastic-based theory provides a simple model that takes account of the interaction throughout the soil mass.

Elastic parameters are generally accepted to be functions of the state of effective stress in the soil and it has been suggested that use of elastic parameters based upon the mean

stress level, developed in an element of soil during load application, is appropriate. This must lead to a highly non-homogeneous distribution of elastic properties, even in an initially homogeneous soil, and is appropriate only for drained long-term response.

The inability of soil to sustain tension has previously been ignored, or the initial stress has been assumed sufficient to accommodate tensile stress increments without producing a tensile stress state. Very little work on the tensile breakaway of soil from the pile has been carried out, with most recommendations suggesting a reduction in stiffness for the parameters of the pile-soil model. The elastic continuum-based method represents a model that can logically be extended to encompass the problem of soil breakaway from the pile. An important aspect of tensile gapping, or breakaway, is a loss of antisymmetry of response and introduction of non-symmetric geometry, which requires a change of approach to modelling of pile-soil response.

This new approach requires some modifications to the standard model used by elastic-based theories. For example, the modified applicability of the concept of attaining an antisymmetric ultimate stress state in the soil at collapse, accompanied by antisymmetric flow of material around the pile. To assist the placing of the new model on a sound theoretical basis, the concept of eliminating negative plastic work in failed regions of soil is also essential. The non-linear response of piles is thus considered to consist of two phenomena, soil-pile breakaway, which is non-linear elastic, and local soil failure, which is non-linear and irrecoverable.

1.2 Aim of Thesis

The aim of this work is to improve the general understanding of the nature of laterally loaded pile behaviour but encompasses a wide range of foundations including,

- a) surface footings as a limiting case,
- b) short caissons,
- c) rigid piles,
- d) intermediate flexibility piles, and
- e) long flexible piles as the other limiting case.

In order to investigate the behaviour of the above cases, three broad methods have been employed. These are :

- a) The "Winkler" soil analysis, as typified by non-linear or linear spring models of soil behaviour.
- b) The linear elastic Finite Element method (FEM).
- c) The Modified Boundary Element method (MBEM) with modifications for non-linear behaviour.

It is demonstrated that the speed and versatility of the MBEM analysis, combined with the elastic-continuum soil model, can provide a useful method of solving the laterally loaded pile problem. The economics of using such a model for analysis, compared with the more commonly used "spring"-based formulations, are not as daunting as has been suggested. The FEM analysis, while more expensive in terms of computer time than MBEM analysis, gives results that are free of the simplifying assumptions inherent in the MBEM analysis. Objections to use of elastic based MBEM solutions can be removed by using the more respected FEM analysis to ensure the accuracy of the MBEM analysis is adequate.

The broader applicability and wider scope for development associated with elastic-continuum theory, compared with the empiricism and limited scope of the p-y methods, suggests that elastic-based analysis would be more useful. Inadequate computing facilities for standard use of elastic-based theories is no longer a problem, since most desk-top personal computers are now more than adequate for such analyses. Also the complex choice of parameters needed to give generality to the p-y models, would be replaced by elastic-based parameters that are available, in principle, from soil tests or, more directly, from pile tests.

One major source of reluctance to use elastic-continuum theory is the inability of the commonly employed homogeneous half-space Mindlin solution kernel to take account of non-uniform modulus distributions with depth. Ensuring the non-homogeneous modification of the Mindlin-based MBEM solution agrees with a sound FEM result can remove this criticism.

The transition from surface footing to pile foundation in terms of load-deflection behaviour is also presented, using a form of FEM analysis. The use of the method aims to give an indication of the wide range of problems that can be solved by an elastic continuum-based approach, and to illustrate the changing behaviour of circular foundations as the length to diameter ratio increases. The examination of such a range of different foundations places the extreme responses of rigid and flexible piles within the context of a wider class of foundation stiffnesses and geometries.

The use of a limiting interface reaction load, at which an element of the pile moves through the soil with no increase in interface stress, introduces a deflection-controlled aspect to the

analysis, similar to the ultimate reaction loads calculated by the p-y method. However, the interface element can also depict the form of behaviour that is governed by gapping around the pile. This aspect of pile behaviour is very poorly addressed by the current theories. Even the proposed MBEM analysis cannot provide a rigorous treatment of gapping, due to an assumption that is fundamental to both this method and the majority of p-y theories.

The versatile MBEM analysis developed in this work will thus overcome many of the drawbacks of earlier linear elastic-continuum models of soil response. Further, the analysis is capable of logical extension, to incorporate a reasonable form of non-linear behaviour, by use of an interface element based upon such concepts as are currently also employed in p-y analyses.

A fundamental change of approach is required in order to logically consider gapping, in relation to lateral pile response analysis using elastic-based theory. This is done for the Soil-Structure Interaction (SSI) method, which is perhaps more a research tool than a design tool, relying upon a finite element model of the soil. However, using the SSI method a number of new analyses may be attempted, covering the behaviour of piles with gapping and soil yielding incorporated in a more rigorous manner than has previously been attempted. The use of the SSI method, with assumptions consistent with real soil behaviour, provides a theoretical treatment of pile behaviour that previously relied upon empirical and mechanistic interpretations of soil response.

Thus the continuum nature of the soil can be fully modelled, and the model can be extended to include gapping and overcome many of the objections to the use of elastic-based theory.

Model pile tests are always subject to criticism because of the inability of most laboratory tests to give correct consideration to scale effects. While recognising that centrifuge tests are capable of overcoming most, if not all objections, it is usually not possible to gain enough access to such equipment in order to fully address the study of model pile behaviour. With this in mind, it remains to try and undertake model tests that provide some information that is capable of application to field situations. However, while it is possible to scale the overall geometry in model tests, this leaves the effects of uncontrollable parameters, such as stress distributions due to self-weight and the relative size of grains compared to the size of the pile, unaccounted for. Thus an important realisation is that stress levels and distributions in model tests usually do not compare to those in field tests.

It should be emphasised that the three factors of scale, stress distribution and geometry of the model test can be taken account of in an elastic continuum-based analysis. Despite difficulties associated with the direct application of model test data to prototype piles, it is considered that the quality of fit between elastic-based theoretical results and model test results is a good measure of predictive capability.

It is a logical treatment of interaction that makes elastic continuum theory most attractive as a model for comparison with field tests, and for general foundation analysis. It will automatically take account of factors that otherwise would need comprehensive empirical treatment in order to model their effect on foundation response. It is possible to maintain a constant set

of parameters, that are directly interpretable as material properties, when using an elastic-based model of soil response to fit or predict lateral pile behaviour.

With careful consideration of failure in the soil, the elastic-based model may be used with a limiting interface stress law in order to model highly non-linear responses that are so prevalent in the results of field and model tests. By recourse to more completely defined soil failure conditions, the aim is to show elastic-based predictions of non-linear pile behaviour may be formulated and placed upon a sound theoretical basis.

A brief outline of the thesis will now follow.

1.3 Thesis Outline

The thesis consists of seven chapters, with the main theoretical, experimental and field comparison work being presented in the five central chapters.

The second chapter is a review of previous work on the analysis of single piles subjected to lateral loading. In general, pile loadings may arise from loads from supported structures, inertial forces or movement of soil, and the subsequent pile response may be analysed by a variety of methods. The methods of soil modelling range from the assumption of simple spring supports replacing the soil response, to the use of complex non-linear elastic-viscoplastic soil models in three-dimensional finite element analyses, Winnicki and Zienkiewicz (1979).

A variety of field testing methods can be encountered in the literature and their application and suitability to particular methods of theoretical analysis is highlighted. The parameters required for certain analysis methods are also reviewed.

The linear analysis of lateral pile response is examined in Chapter three. An important parameter for any pile-soil system, the effective length, is defined and its effect upon present and previous thoughts on pile response is clarified in Chapter four. As an important part of the soil-pile interaction character, the critical length has long been recognised, but its ramifications for pile analysis have been explored by relatively few people.

Chapter five addresses the phenomenon of non-linearity of pile response, and a new form of lateral pile response analysis is introduced. The three phenomena of soil gapping behind piles, soil yield around piles, and briefly the prospect of yielding the pile itself are discussed. The continued importance of the pile effective length, even for non-linear response, is proposed.

Chapter six reports the results of experimental work carried out by the Author on model piles in prepared beds of clay. Comparisons are made between the experimental and theoretical results. The model tests are directed at improving the understanding of the response of piles of various diameters and lengths, in clay under essentially static load. Also, the various models of soil-pile behaviour that have been developed are used to analyse a field test of two piles reported in the literature.

The final chapter contains the conclusions and recommendations for future research.

1.4 Notation

A	area of pile cross-section
A^P	statics matrix, general matrix
B	general matrix
c_u	undrained shear strength of soil
c_v	coefficient of consolidation
C	coefficient, general matrix
C_I	one-dimensional Compression Index
C_R	one-dimensional Recompression Index
d	diameter or projected width of pile
e	eccentricity of applied shear force on pile
E	Young's modulus of soil
E	Young's modulus of pile (actual or equivalent)
E^P	Subgrade Modulus for soil (= k.d)
E^s	undrained Young's modulus of soil
E^u	fraction of failure load assumed to act in a gap
f	force
F	force
g	fraction of plastic deflection converted to a gap
G	Shear modulus of soil
h	depth of soil layer
H	horizontal shear force on pile head at ground level
H	ultimate horizontal shear force on pile head
H^u	influenced node number
i	influenced node number
I	Moment of Inertia of pile cross-section
I^P	dimensionless influence factors for head deflection
I_{uH}, I_{uM}	and rotation due to head shear and moment
$I_{\theta H}, I_{\theta M}$	influencing node number
j	influencing node number
k	Coefficient of Subgrade Reaction, Fourier term

K	relative stiffness factor for pile-soil system
R	
L	length of pile originally below the soil surface
L	critical length of pile-soil system
^c m	coefficient of increase of Young's modulus with depth
m	coefficient of increase of Subgrade Modulus with depth
^s M	bending moment in pile (normally at the head)
M	ultimate moment on pile head
^u n	number of terms used in a Fourier series
p	normal stress, traction, mean stress
p	active earth pressure
^a p	earth pressure at rest
^o p	passive earth pressure
^p P	axial load on a pile head
q	deviator stress, surcharge
r	radial coordinate
R	load vector length in M/L vs H space
t	shear stress, traction
u,v,w	deflections in direction of x, y and z axes
^k U	k.th Fourier Coefficient for deflection, $i = r, \theta, z$
ⁱ V	shear force in pile
W	uniformly distributed load per unit length of pile
x,y,z	Cartesian coordinate system
Y	wavelength parameter for Winkler solution
α	dimensionless measure of soil inhomogeneity
β	dimensionless head moment to shear ratio
θ	circumferential coordinate, pile head rotation
ν	Poisson's ratio
ϕ	angle of internal friction of soil
ω	ray angle of load R in M/L vs H space

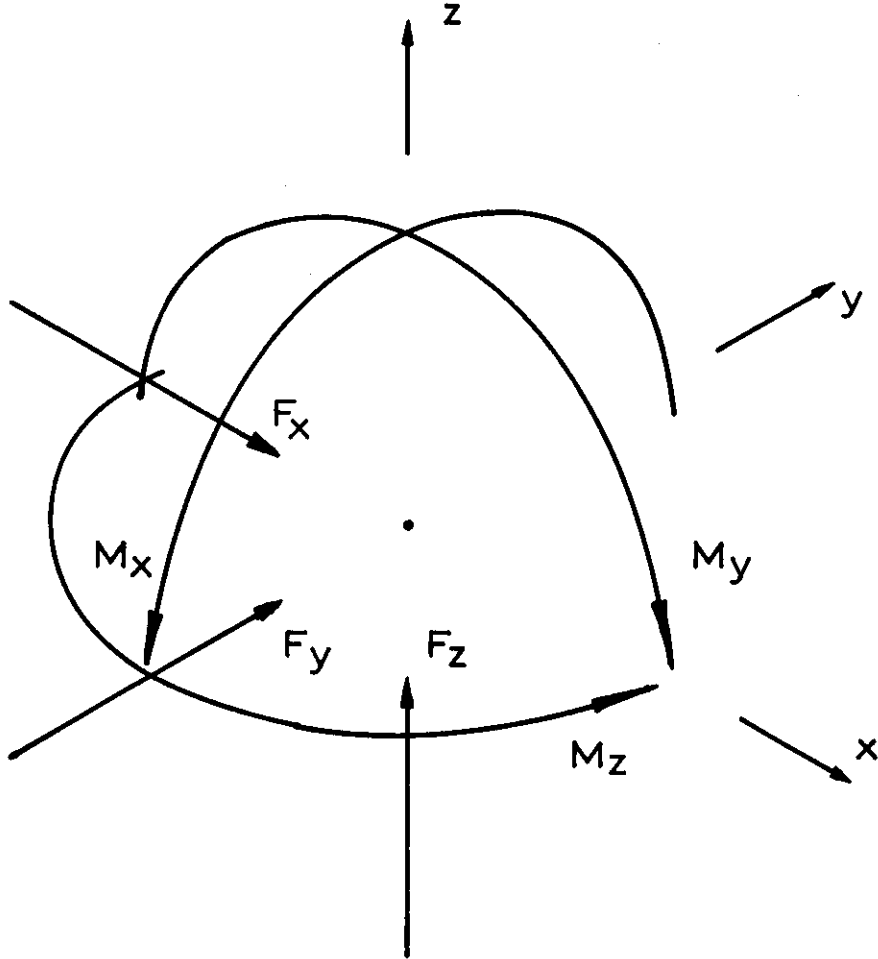


FIG. 1.1 THE SIX COMPONENTS OF LOAD IN CARTESIAN COORDINATES

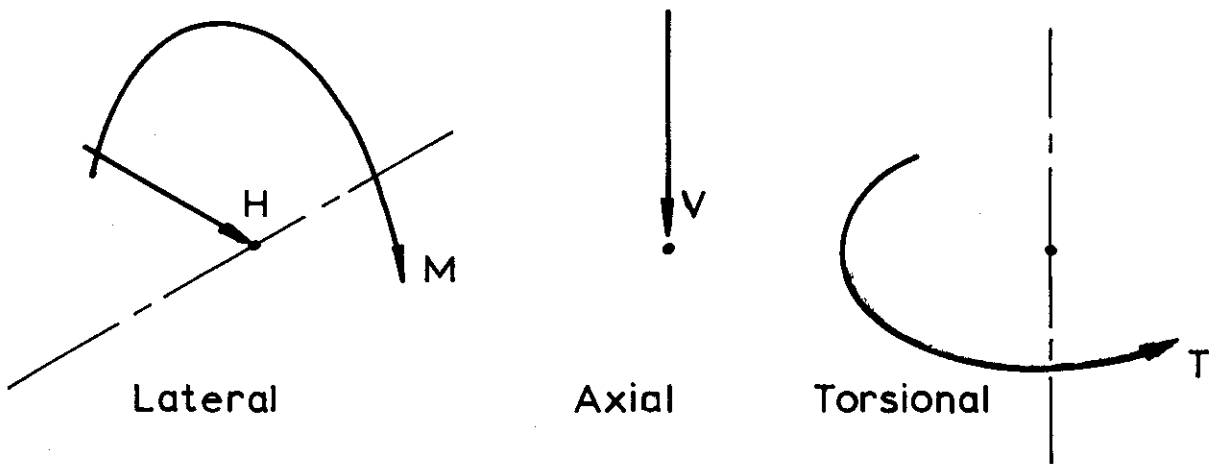


FIG. 1.2 THE THREE CLASSES OF LOAD COMMONLY CONSIDERED FOR LOADING ON ISOLATED PILES OF A FOUNDATION

CHAPTER TWO - LITERATURE REVIEW

2.1 Introduction

In this chapter a review is made of the methods that have been used, and are currently employed, for the analysis of the response of vertical piles to lateral loading.

Section 2.2 consists of a brief historical note, and the classification of the various methods into three categories, depending upon the soil model assumed and also the technique of solution employed. This approach has been adopted when reviewing laterally loaded pile analysis methods, although a subdivision on the basis of the model used for the behaviour of the pile might also have served as a means of classification.

The next section moves away from direct analysis of piles under head shear and moment loads, to consider methods that have been used in attempts to rationally analyse the underlying mechanisms of load transfer to the soil. Such methods include the plane strain pile segment in an elastic-continuum model of soil. In this section some of the methods used to introduce non-linear soil response are described.

Section 2.4 deals with field testing and includes examples of the types of test that have been reported in the literature. The in-situ measurement of material parameters and prediction of p - y response using pressuremeter results is also discussed briefly.

Following this is a section dealing with the evaluation of the parameters that are required for each major class of lateral pile analysis.

A summary of the major findings of the literature survey is then made with indications of the areas that will be investigated in this thesis.

2.2 Lateral Pile History and Analysis Classification

Lateral loading of piles is sometimes considered as a recently recognised solution to a foundation problem caused by man's quest for oil in the off-shore environment. However the laterally loaded pile has been a part of man's solution to the foundation problem for many hundreds of years.

One of the earliest documented uses of piles to withstand lateral forces is in the artificial islands (crannogs or terpens) that supported the lake villages of Meare and Glastonbury in Britain circa 50 B.C.. The island at Glastonbury consisted of a triangular platform in the shallows near the shore resting on a foundation of stones, faggots, brushwood, rushes and peat contained by horizontally laid logs restrained laterally by strong piles driven vertically into the swamp. The area was nearly 16000 square metres and contained about 90 huts relatively safe from raiding tribes. Nearby, connected to the shore was a 40 metre causeway of stone and clay, leading to a wooden jetty that was also kept in place by horizontal timber planks restrained by vertical piles which were topped by hurdles.

The outward lateral pressure of the island meant that throughout the life of the village, the boundary vertical piles had to be replaced and supported by offsets. This, together with the constant settlement of the peat, caused major engineering problems that even today would tax the ingenuity of engineers.

Today however, the remedial measures necessary when an off-shore oil rig installation settles or spreads unduly, would represent an economic constraint that may lead to severe financial loss for the rig operators. For this reason, as well as the

primary need for safety, the recent interest in behaviour of piles under lateral loading, such as occurs due to wind and wave action, has produced many solutions to the problem.

Prior to 1956, theoretical work was essentially an extension of the beam on a (Winkler) linear spring foundation study, so thoroughly addressed by Hetenyi (1946). The work of Matlock and Reese (1960) provides a general solution to the behaviour of laterally loaded piles in a medium obeying a linear law of the type commonly called "Winkler" (after Winkler, 1867), and represents the peak of the linear approach using Winkler theory.

Empirical treatment of off-shore problems using terrestrial-based experience was deemed to be unsatisfactory, in view of the vastly different environment and the larger dimensions of the piles required. Large scale field testing under conditions close to those existing off-shore provided the first means of examining the behaviour (McClelland and Focht, 1956). Their field test results showed a strong link between the pile distributed load and pile-displacement (p-y) curve and the triaxial stress-strain curve of samples taken from stations down the pile. This treatment of field test results led to the development of the widely used p-y method of predicting lateral pile behaviour.

In the p-y method, strain-gauged piles are used to provide distributions of bending moment down the pile when certain head loads are applied. The bending moments can then be integrated twice to find the bending deflections, which are combined with the measured head deflection and rotation to calculate the absolute value of deflection, "y" down the pile. Double differentiation of a curve fitted bending moment distribution provides the variation of distributed pile-reaction load, "p" with depth.

The studies of the 1970's have led to the unification of the p-y method and comprehensive representations of lateral pile behaviour in a wide variety of soils, e.g. Matlock (1970), Reese, Cox and Koop (1974 and 1975), Reese and Welch (1975), Lee and Gilbert (1979) and Sullivan, Reese and Fenske (1980). Using non-linear p-y curves at stations down the pile the lateral pile behaviour may be calculated, as long as the p-y curves are appropriate for the particular soil and pile.

Reliance upon empirical methods of modelling pile behaviour has prompted most of the research into lateral pile behaviour. Since much of the field-work was in conjunction with p-y research, it is not surprising that interpretations of field tests have been oriented towards ensuring that the p-y method works, rather than promoting or investigating the use of alternative methods. The policy of adapting the original approach to p-y curves, due to McClelland and Focht (1956), and catering for the most commonly experienced soil conditions, has proved acceptable for pile design, on the whole.

The Winkler or p-y approaches are of limited use since they only strictly apply to the case of a single pile of a given stiffness, and provide no information about the effect of pile loading on the soil anywhere other than at the interface. Even the information at the interface is only a value of pile-reaction load and deflection (p and y), and not actually a stress in the soil or the soil deflection. For these reasons, and others, various researchers have attempted to apply the elastic continuum model of soil behaviour.

The elastic-continuum model makes allowance for the continuous nature of the soil and has been widely used for a range

of foundation types, so a wide body of experience exists for choosing appropriate parameters. The parameters are few and can be obtained from triaxial testing at appropriate cell pressures, Davis and Poulos (1968). Further, the limiting cases of undrained and drained soil response are capable of inclusion.

The elastic continuum method thus offers three major improvements over the traditional p-y methods:

- a) Pile groups, and the effects of lateral loading of one pile upon nearby structures, can be logically treated.
- b) The parameters required by the model are few and can, in principle, be obtained from standard laboratory soil tests.
- c) Time-dependent behaviour may be incorporated.

In the light of the above it is not surprising that there have been many analyses based upon the soil modelled as an elastic continuum. A wide variety of approaches have been employed ranging from numerical, discrete methods such as the boundary element method to analytical procedures relying upon some form of numerical solution of the equations of an elastic continuum. In more recent years the finite element method has proved a popular method of obtaining results for lateral pile response using an elastic continuum model. It has been customary to isolate the finite element method as a separate class of analysis, mainly because soil nonhomogeneity can be included more rigorously than is possible with (say) boundary element based methods. Thus one of the often-referred-to limitations of elastic continuum theory, as embodied by the equations of Mindlin (1936), can be overcome.

From the above a convenient grouping of the methods of

analysis, based upon the complexity of the soil model, presents itself.

Thus, three classes of soil modelling can be proposed:

The first is the Winkler class that broadly includes any linear, and for the purposes of this classification also forms of non-linear, pile reaction load-deflection response. These responses have been measured in full scale tests and are generally assumed to apply to a limited range of piling situations, e.g. a specific p-y analysis for a particular soil type.

The second class consists of a wide variety of methods based upon elastic continuum theory, but limited to the case where Young's modulus of the soil is constant with depth. Although most methods are based upon a uniform modulus soil, some do make an attempt to model non-uniform soil modulus profiles in a systematic manner.

The third class consists of the finite element method in a variety of forms. Three dimensional approaches are few since the volume of soil to be discretised usually exceeds the practical limit for economical analysis. The more economical axisymmetric finite element method employing Fourier representation of circumferential behaviour dominates this class of analysis.

The three classes will now be reviewed, using several specific examples of the types of pile analysis methods mentioned above.

2.2.1 Winkler and p-y Methods

All the methods in the Winkler class of model rely upon the correlation of the distributed pile reaction load to lateral pile displacement at stations down the pile. The Winkler and, in particular, p-y approaches have proved to be very flexible when different soils have been encountered in practice.

However, this leaves the p-y method as a conceptual idealisation of pile response that has no link with the various soil constitutive models that have evolved. Other than the assumption that an empirically derived p-y curve will exist for the pile-soil interface, there is no modelling of the soil. Attention is limited to the behaviour, linear or non-linear, of the pile deflection and total reaction load at depths down the pile, with no consideration of the form of interface stress generated between pile and soil.

Reese and Cox (1969) have outlined a method whereby p-y curves may be derived from the results of a laterally loaded pile test in which only the response of the pile head has been measured. The non-linear form of the derived p-y curves depends upon the subgrade modulus distributions that best fit the value of head deflection and rotation at a number of loading levels.

Their aim was to present a method that would allow p-y curves to be correlated with a wide variety of sites, with different soil conditions. The basic assumption is that a secant model is appropriate for each pile deflected position, with a particular modulus distribution in a Winkler medium applying to the behaviour of the soil-pile system at any one instant of the loading sequence. The same Winkler medium parameters, however, are not

necessarily found to be applicable to any other combinations of head shear and moment or load level.

The cornerstone of their method is the assumption of superposition of the behaviour for shear and moment loading. This is proposed on the understanding that the deflection is small relative to the pile dimensions. Since the entire analysis is based upon small-strain differential equations and nowhere follows a strict load path approach to the problem, it is not made clear why this restriction of small strain is especially linked to the use of superposition.

The method culminates in relationships between a parameter defining the distribution of soil modulus with depth, and two relative measures of the pile head stiffness; one relationship for the deflection and one for the rotation. Figures 7 and 8 of Reese and Cox are reproduced here as Fig. 2.1 and illustrate the general procedure for obtaining p and y from test pile data. When their two relationships coincide, the pile-soil stiffness and the soil modulus distribution become uniquely defined. However if the two fail to cross, the procedure relies upon finding the point of closest matching of the two relationships. As pointed out by Reese and Cox, this case of no unique value will lead to poor correlation between the results of using the p - y curves in a numerical analysis and the pile results from which the curves were derived.

Points which the authors set outside the scope of their work include the correlation of soil properties to the p - y curves. Also no mention is made of the use of the p - y curves to model any combination of loads other than the one used to derive them, which limits their usefulness in predicting other test results. This is perhaps the major weakness of the p - y method as presented.

The paper however provides a very clear enunciation of the p-y hypothesis, and presents a method that seeks to maximise the information accumulated from a minimum number of data values collected. It seems that their method suffers from a major inadequacy when it is considered that the correlation does not ensure a coincidence of the two relationships used. This is due mainly to the reliance upon superposition of possibly non-linear behaviour and so it should not be surprising that such inadequacies exist. Also, only a limited number of simple linear distributions of soil modulus with depth are available to model a complex system of non-linear response. It follows that great care is needed when developing means of backfiguring soil parameters, and inadequacies in such methods should be well understood.

Examples of proposed p-y curve criteria are presented in Figs 2.2 and 2.3 for the two analysis methods derived for soft to medium clay soil sites, (Matlock, 1970), and stiff clay sites (Reese, Cox and Koop, 1975). Both methods are based upon values of ultimate pile reaction, p_u and the critical soil deflection, y_c which is related to the strain at half the maximum deviator stress in an undrained triaxial test. As shown in Fig. 2.4 the theoretically-derived values of ultimate soil reaction are not in agreement with the values deduced from the field test of Reese et al. (1975) and correction coefficients, A and B, are proposed to better model the behaviour. It is inherent in the method of back-analysis of the field test results that the value of pile reaction load is derived from measured bending moments. Thus the ultimate resistance of the soil is only assumed to be equivalent to this reaction load, with no information about the actual soil stress state which is commonly assumed to govern soil strength.

Because the same p-y curve may not be applicable to all the combinations of head shear and moment that might be applied to a pile, as pointed out by Lee and Gilbert (1979), the relative magnitudes of the desired pile head shear and moment should be duplicated in any testing designed to produce p-y curves. As an example the tests of Reese et al. (1975) may be considered where they compared the p-y curves from two tests on a six inch diameter pile in stiff clay, labelled 3 initially and 4 when re-driven. A free head and a restrained, "fixed" head condition were applied to piles 3 and 4 respectively and the p-y curves derived.

The curves for the free and restrained head cases are reproduced here in Fig. 2.5 and it is obvious that the two sets of p-y responses are not exactly equivalent, as is assumed in the p-y method. This is in part due to a lesser load having been applied to pile 3 than was applied to pile 4 and, as suggested by Reese et al., partly due to small variations in soil properties between the sites of each pile test. However, there is a consistent trend in the results for the two piles displayed in the curves.

The restrained-head pile exhibits a stiffer initial p-y response than the free head pile below a depth of one metre. At about one metre the stiffnesses are similar but the ultimate reaction loads for the restrained case are smaller. The fact that the ultimate reaction loads of the two piles at the same depths, of two and four diameters penetration, vary by a factor of as much as two is disturbing.

The correction coefficient, used by Reese et al. (1975), to ensure a match between experimental and theoretically-derived values of ultimate reactions, see Fig. 2.4, has typical values of 0.2 to 0.6. This coefficient varies with depth and thus it is not

surprising that similar variations exist between two ultimate reactions backfigured for any two piles at any depth. It would appear that the poor predictive capability of the p-y theory for, and the variation in the experimentally-derived values of, the ultimate reaction loads, indicates a response very sensitive to changes in material or geometrical properties.

The large change in ultimate reaction value corresponding to changes in material properties, or problem geometry, near the surface appears out of proportion to the magnitude of these small changes. When the range of ultimate reaction loads predicted by various theories is considered, as has been done by Stevens and Audibert (1979), it reveals a factor of two between most theoretical and observed values. These discrepancies will have a marked effect upon the pile load-carrying predictions and the load-deflection (p-y) curves which are based upon the ultimate reaction loads. Unfortunately, it is impractical to completely fail full scale test piles in order to verify the assumption that the failure stresses in the soil have been reached.

Thus, from consideration of the values found in many pile tests, ultimate reaction loads may even vary during continued loading. This is because no satisfactory definition of failure exists for the pile or soil response in most tests, and so there is no guarantee that failure loads have been achieved, or that the achieved loads can be maintained under an increment of head load. Indeed, the pile reaction from the stiff clay-based p-y curves suggest the soil failure load decreases with deflection, although the mechanics of this feature have not been explained.

From the two series of load tests that resulted in the p-y methods of analysis for laterally loaded piles in soft to medium clay and stiff clay, Sullivan, Reese and Fenske (1980) have synthesised what is referred to as a unified method for analysis of piles in clay. The essential differences between the two methods of Matlock (1970), for soft clay, and Reese et al. (1975), for stiff clay, and the unified method are the simplification of the p-y curve construction procedure and the depth to which "strain"-softening is allowed.

While representing a unification of the two separate p-y methods, two new parameters are introduced that have only limited empirical data to guide their choice. Since the variation of these two additional parameters represents the main difference between the unified and the two earlier p-y methods, reference to the recommendations of the soft and stiff clay methods will aid in the choice of values for the two parameters.

The p-y method, and generally any Winkler-type model, is thus seen to have a strongly empirical base and ultimately to rely upon limited data from field tests using a few head loading conditions. The variety of soils and pile dimensions encountered in the field, then requires a variety of models in order to cater for the practical needs of pile design.

2.2.2 Elastic Continuum Methods

Amongst the earliest uses of elastic continuum theory in a lateral pile application is the work of Spillers and Stoll (1964), who recognised the inability of Winkler or p-y methods of analysis to incorporate a constitutive equation for soil in a valid manner. The inability arises from the assumptions of the methods, especially the removal of interaction in the system of soil and pile, save that connected with bending of the pile. Spillers and Stoll preferred to use soil parameters arising from the basic constitutive equations of soil rather than define local "moduli" that are not independent of pile dimensions and stiffness.

They considered as their simplest model a homogeneous, isotropic, elastic continuum and emphasised the assumption of small strain. An elastic line inclusion in a linear elastic half-space represented a pile in the soil, and compatibility of pile and soil lateral deflections was employed at discrete nodal points. The interaction between pile and soil was approximated by concentrated forces at nodal points, and the soil response was provided by the equations of Mindlin (1936). As is usual with concentrated force methods, a special computational device was employed to avoid singularities associated with the deflections at the points of force application.

In recognition of the non-linear character of soil response, a limiting force was calculated for each node based upon a linearly varying yielding pressure law with depth. Although the method of implementing the non-linear behaviour was relatively crude, it marks an acceptance of the importance of the non-linear aspect of pile response.

Matters not considered by Spillers and Stoll, but which were thought to be worthy of future research, included the modelling of the non-homogeneous nature of soil.

If the restriction to an elastic homogeneous half-space is viewed, using the experience gained from studying the behaviour as if it were due to a Winkler response, it will appear patently inadequate. However, it is because the Winkler model has been used as a basis for comparison with field data that the assumption of an increasing modulus of soil reaction with depth becomes necessary, which says little about the variation of Young's modulus with depth. The elastic continuum model of soil is capable of displaying an increasing stiffness (modulus of soil reaction) with depth even for the homogeneous Young's modulus case without recourse to considering nonhomogeneous profiles. This will be shown in Chapter three.

The modulus of soil reaction and the soil Young's modulus, are two greatly different quantities that happen to have comparable numerical values in some circumstances. The modulus of soil reaction is a measurable quantity that is a result of the pile-soil interaction, whereas the form of the pile-soil interaction is largely a result of the Young's modulus of the soil in the elastic continuum model. Obviously it is better to consider a basic parameter of the soil rather than a measured response of very strictly limited applicability, i.e. the load-deflection response of a particular pile at one depth.

An obvious deficiency of the model of Spillers and Stoll is the assumption that the pile transmits load to the soil by concentrated forces at stations down the pile. The model proposed by Poulos (1971a) eliminated these point forces and modelled the interaction between pile and soil by elements of uniformly

distributed load. The rectangular elements of constant normal traction were again associated with the nodal points of a finite difference pile discretisation.

This improved the modelling of the interaction stresses, and also removed the need for special attention when the deflection of a point due to a concentrated force at that point was required. By using the integration of the Mindlin kernel (1936) that had been accomplished by Douglas and Davis (1964), the deflection of any point in the same plane as the thin strip pile could be obtained. By using a constant spacing of nodes for the pile, a model for the soil consisting of rectangular elements, of the same height as the spacing between pile nodes and the width of the pile, resulted. In this way the soil nodes along the pile centre-line, at which deflections were calculated, were situated at the centroid of elements internal to the pile and the centre of the top and bottom edges of half height elements at the pile extremities.

The resulting model gave improved analyses of laterally loaded piles and formed the basis of a presentation of behaviour that has gained wide acceptance both as a design aid and a benchmark against which other models are tested. The behaviour predicted by the elastic-continuum model showed some similarity with that from use of a Winkler soil model, but had marked differences. These differences are essentially due to the elastic model predicting results that have a complex dependency upon the slenderness ratio of the pile, while the Winkler model results simply normalise for any slenderness ratio to one curve.

Poulos relates the soil-pile interface uniform reaction load to the deflection of the centroid of internal elements, and the middle of the edges of elements at the upper and lower extremities

of the pile. This soil model has the drawback of over-estimating, by up to 30%, the deflection actually arising at the pile interface, as was pointed out by Randolph (1977). This is because the actual interface is essentially rigid across the width. By using the centroidal deflection the soil is given an opportunity to deform flexibly across the width that is not present in the real interface situation.

The results presented by Poulos suffer from inadequate pile discretisation for the case of very flexible pile-soil systems, because computational limitations precluded the use of a finer nodal spacing. This matter has subsequently been addressed by others, notably Evangelista and Viggiani (1976). Evangelista and Viggiani have drawn attention to the inadequacies of previous laterally loaded pile elastic continuum analyses. Although Poulos (1971a) is explicitly mentioned, their comments are applicable to perhaps the majority of results presented by others.

The major difference between the solutions of Evangelista and Viggiani and any previous elastic continuum solution, is the use of elements of varying length down the pile in an effort to model more accurately the region of greatest gradient for the displacement of the soil. The use of smaller elements at the pile head, grading to much larger elements at the tip, has two effects:

- a) Firstly, it allows a much finer modelling of pile bending near its head, and so would be expected to improve modelling of flexible piles, where large gradients of interaction stress occur near the pile head.
- b) Secondly, it detracts from modelling of the behaviour of the pile and soil near the base of a rigid pile, where the elements will have a much larger aspect ratio.

In Chapter four it will be shown that flexible piles of the same cross-section in the same soil, will exhibit equivalent responses to head loading, irrespective of their length. Flexible piles of solid circular cross-section are those having a pile to soil modulus ratio less than 524 for $L/d = 10$ and 5.24×10^6 for $L/d = 100$, from the use of the relationship of critical length and relative stiffness which is proposed in Chapter four.

When considering the results presented by Evangelista and Viggiani, their variable element length analysis gives improved results, with the deflections and rotations of piles longer than the critical length becoming constant, regardless of the actual pile length, and this response is tabulated in Table 2.1. This table also includes results from the MBEM analysis developed in this thesis, in which an equal number of elements for the modelling of the pile critical length was maintained for all but the longest pile. The solution of the longest pile is clearly seen to underestimate the response because of inadequate modelling of behaviour within the pile critical length. It has been assumed that the dimensionless influence coefficients in the table of Evangelista and Viggiani are in error and require the length terms to be replaced by the diameter.

The improved head response arises because the longer elements at the base have virtually no part to play in the analysis of flexible piles, and the head response is governed by the upper portion which has been discretised finely. However, for a long rigid pile ($L/d = 100$), because of the importance of the entire pile length in determining response, a finer discretisation over the lower pile portion is required. This may help to explain why there is nearly 15 % more deflection predicted by Evangelista and Viggiani for stiff piles of $L/d = 100$ than is predicted by the

Poulos analysis. It is also likely that the greatly increased possibility for flexibility across the pile face at the top of pile, is not consistent with the analysis of a rigid pile, even though such a slender rigid pile is not practically important.

Thus, the newer analysis using a fine discretisation near to the pile head obviously improves the accuracy of the answers for flexible piles. However it does so to the extent that it raises a question as to the applicability of the centroidal deflection based model. The use of a uniformly loaded area for the interface traction and the assignment of the centroid as the collocation of pile and soil, can be considered as being too conservative.

The work of Evangelista and Viggiani has highlighted two important aspects of pile analysis and response:

- a) All piles longer than their critical length have the same head response to head loads, regardless of actual pile lengths.
- b) The degree of pile discretisation may greatly affect the results of an analysis.

Although using variable lengths of elements improves the accuracy of the analysis of piles in an elastic continuum, there is the same deficiency in the formulation of the model, concerning the assumption of flexible behaviour across an element face, as in the method used by Poulos and discussed previously. By using an average deflection across the face, to approximate a rigid response, and employing a reasonable number of elements within the effective length, it will be shown in Chapters three and four that it is possible to achieve boundary element results that can be considered equivalent to results from more refined finite element analyses.

Examples of other uses of elastic continuum theory to analyse a problem related to the lateral loading of piles but suggested as including the behaviour of shear pins, are the papers of Apirathvorakij and Karasudhi (1980) and Selvadurai and Rajapaske (1985). Both methods employ the same fundamental solution technique involving Hankel transforms and Fourier expansions.

Apirathvorakij and Karasudhi employ a compatibility of both uniform horizontal shear and linearly varying vertical tractions, (shear forces and bending moments) acting over circular plane areas (where the pile is situated), between the elastic continuum and a pile whose modulus is reduced by the modulus of the elastic continuum. Selvadurai and Rajapaske use the same theory, but employ tractions acting upon a boundary of the pile. As such, neither method takes proper account of the displaced volume of soil due to the presence of the pile. Further, while Apirathvorakij and Karasudhi's method can be used to model solid circular pile foundations of any flexibility, the analysis of Selvadurai and Rajapaske is restricted to rigid piles but does allow the effect of varying the pile wall thickness to be found.

Apirathvorakij and Karasudhi's method is capable of calculating the entire consolidation response of an essentially permeable pile, although they only present the initial and final responses. Essentially, any elastic-continuum-based analysis is capable of giving these two results since the drained and undrained moduli of an elastic soil are simply related. The results are consistent with previous methods of analysis, e.g. Poulos (1971a), showing that the pile response depends upon the length to diameter ratio, the relative stiffness of the pile to the soil and, to a lesser extent, upon the value of Poisson's ratio of the soil.

However, piles that can be classed as flexible in the soil are shown to normalise to a common curve, while "rigid" piles produce curves of constant response for each particular length to diameter ratio when plotted against relative pile to soil modulus ratio. This is a result of using the pile diameter to normalise the head response and plotting against the ratio of pile to soil modulus, and will be further discussed in relation to the minimum lengths of flexible piles in Chapter four. Using the pile length to normalise head responses, and a relative stiffness based upon the pile length and section properties, would have produced results of a similar appearance to Poulos' results. However, Apirathvorakij and Karasudhi's results would in some respects be preferred, since some account has been taken of the need for changing the number of elements in the pile as the length changes to ensure there are sufficient elements in the effective length.

The results of Selvadurai and Rajapakse do not need consideration of critical pile lengths, since they analyse a rigid pile and thus the actual pile length is the effective length. A comparison with a Poulos-type analysis shows good agreement for the shear and moment distributions with depth for a pile with a length to diameter ratio of ten. For squatter, less slender piles the comparison is less satisfactory, but Poulos has not recommended his method for such a problem, suggesting the solutions of Douglas and Davis (1964) would be more appropriate for short rigid piles.

An interesting feature of Selvadurai and Rajapakse's analysis is the ability to consider a finite value of wall thickness to the circular pile. This leads to limiting cases of a thin rigid shell and a solid cross section pile, which they showed to have virtually no difference in response for lateral loading. This

suggests that it is the outside interface of pipe piles supporting the interface tractions that are of importance, not the enclosed region of soil or the pile base, even for relatively squat piles.

It can be seen that the isotropic homogeneous elastic continuum model has provided the basis for several analyses for lateral loading of piles. Several researchers, Poulos (1972), Banerjee and Davies (1978) and Pise (1982), have also considered means by which non-homogeneous and layered soil profiles can be treated. All the analyses contain assumptions about the behaviour of the pile-soil system whose validity is difficult to assess. However, it is evident in all the results that the pile-soil relative stiffness, the length to diameter ratio and Poisson's ratio of the soil all have some effect upon the response.

The different ways in which the results of the various elastic based models have been presented, tends to mask the similarities between them, and inconsistencies seem to be magnified. A natural caution in accepting results that rely upon theoretical assumptions which are difficult to justify and a preference for empirical approaches, has seen research emphasis on other types of models. However, recently there has been an increased effort to make elastic-continuum based results more acceptable. This has led to the application of elastic finite element methods to the problem of lateral loading of piles.

2.2.3 Finite Element Models

Since its introduction, the Finite Element Method has been applied to an increasingly wide range of problems in geotechnical engineering. The analysis of laterally loaded piles has been one such problem and has seen application of the method in two main forms. The first form is a fully three-dimensional formulation, using block elements of various degrees of sophistication. The second form is based upon a semi-analytic approach that analytically models variation of quantities in the circumferential direction by Fourier series, thus leaving only a two dimensional model to be discretised. Both forms are restricted to linear elastic response.

Of the two, the semi-analytic model is by far the most economical and consequently can provide results of a higher standard than the three-dimensional approach. This higher standard arises because of two factors. Firstly, the model uses an analytic treatment around the circumferential direction that is better than that available from standard finite element approximations. Secondly, the two-dimensional model can be used with a much finer discretisation than is possible three-dimensionally, thus leading to more accurate results.

Kuhlemeyer (1979a) has used a four-noded quadrilateral semi-analytic finite element model to analyse a laterally loaded pile in an elastic layer of soil, both statically and dynamically. A reduced integration procedure was found to be necessary to obtain economical and accurate modelling of the bending of a cantilever due to end loading. The standard element, without reduced integration, was shown to give a response that was too stiff, which is consistent with the restricted form of shape function.

Kuhlemeyer (1979b) has used the solution for a cantilever response given by Timoshenko and Gere (1972), as an analytic check on his finite element model. That solution provides a more accurate response than the predictions of simple bending theory by taking account of shear deformations. Using the predicted tip deflection for the tip loaded stocky cantilever, it is possible to show that the answer is at least five percent in error when using simple bending theory for beams with a length to diameter ratio of less than three.

This suggests that piles with an effective length in the soil of less than three diameters are likely to require consideration of deviations from the behaviour given by simple bending theory. This conclusion is based upon loading of the tip of a cantilever, but should provide an indication of the more complex behaviour arising from the distributed loading produced during interaction between the pile and soil. Thus a lower limit to the length of piles, of three diameters, can be suggested for any lateral pile analysis that uses simple bending theory for the pile response.

Kuhlemeyer (1979a) has indicated that the critical length of a pile can be estimated as the length that results in a relative pile-soil stiffness factor, $K_R = E_p I_p / E_L L^4$, of between 0.05 and 0.01 where the symbols are defined in section 1.4 and E_L is the soil Young's modulus at the pile tip. Kuhlemeyer's basis for these values is the results of Poulos (1972); choosing the K_R value where the tip fixity condition has no effect upon the head response to head loads. He proposes that for a given pile and soil combination, there is a critical length to diameter ratio, beyond which the head response to head loads is unchanged by increasing the pile length. This suggests that if a pile has an

effective length of less than three diameters, it may be necessary to use a more complex beam bending model than the simple beam theory which involves plane sections remaining plane. Even if the actual pile length is much greater than three diameters, then simple bending theory may still no longer be appropriate if the critical length is less than three diameters.

An expression that Kuhlemeyer fitted to the results of Poulos (1972), appears to be in error since Poulos' original results cannot be reproduced by its use. Instead of the influence coefficient for head deflection due to head shear increasing with increasing length to diameter ratio, it decreases. This is also contrary to the finite element based equations of Kuhlemeyer, which can be shown to include a term for the length to diameter ratio, when re-expressed in the form necessary for direct comparison with Poulos' results.

An important aspect of behaviour was identified by Kuhlemeyer with his recognition of the importance of the relative stiffness of the pile and soil and its relation to the critical length. He predicted that the non-dimensional deflection and rotation responses, normalised by the pile radius or diameter instead of length, will be proportional to a power of the ratio of the pile to soil Young's modulus. As long as the pile response is both:

- a) constant for increases of length, i.e. its length exceeds the critical length, and
- b) is also not a function of the actual value of critical length,

then Kuhlemeyer's predicted power coefficients are correct. However, his finite element results do not support his predicted coefficients derived from use of these two assumptions.

The existence of a critical length has been well documented and so the second assumption must be in error. Thus, the response of flexible piles (those of length greater than the critical length), will be seen to depend upon the critical length of the pile; more correctly the critical length to diameter ratio. A dependance upon length to diameter ratio is also seen in the response of stiffer piles with lengths less than critical.

This fact will explain why the correct powers in Kuhlemeyer's finite element result based equations differ from those of his theoretical predictions. Indeed it is necessary that the powers of the equations must be of lesser magnitude than those arising from Kuhlemeyer's argument. If the powers are larger, then the trend of solution with length to diameter ratio is reversed, just as it is in one of Kuhlemeyer's re-expressions of Poulos' results.

An important example in which the argument of Kuhlemeyer is correct, is the problem of a pile in a Winkler soil. In such a case the effective length to diameter ratio has no effect upon the deflection. This is consistent with the empirical basis of the Winkler model ignoring the effect of pile diameter, or width, upon the load deformation behaviour.

Randolph (1977) and (1981), also uses a semi-analytic finite element model to analyse the response of laterally loaded piles in an elastic soil mass. His resulting equations for the response of flexible piles can be expressed in a similar form to Kuhlemeyer's and are in broad agreement. Randolph (1977), has shown that the response of flexible piles in an elastic soil mass is a function of the relative stiffness of the soil and pile and the degree of inhomogeneity of the soil profile.

From dimensional analysis, Randolph has found the form of the

expressions for head load-deformation characteristics, and used the two extremes of a uniform Young's modulus and one that is proportional to depth, to ascertain the correct power relationships. Again expressions similar to Kuhlemeyer's are found for the uniform soil, but the expressions for the non-uniform profile are necessarily different. Randolph has then proposed expressions that include a non-homogeneity-related term and has checked their accuracy against the finite element results.

Randolph has also considered the problem of a pile in a Winkler soil, and for this simple model the actual powers used in the expressions can be shown to be determined by the restriction that the value of the critical length does not alter the non-dimensional response, as is implicit in Kuhlemeyer's argument. This will be discussed in more detail in the section of Chapter four in Section 4.2.2.

Randolph (1981) has presented the results of his finite element study in the form of simple equations that are convenient for design calculations using a small programmable calculator. His design charts allow bending moment, and deflected shape profiles to be calculated for any flexible pile in a wide range of soil Young's modulus profiles. The cornerstone of his presentation method is the pile "critical" length. By non-dimensionalising, using the critical length, the expressions obtained for head response to head loading of flexible piles are greatly simplified.

Randolph (1977), and Kuhlemeyer (1979a), both use the same concept of curve-fitted equations of response, based upon the results of finite element studies using the economical axisymmetric, semi-analytic model. This illustrates its power and versatility in solving problems in geotechnical engineering that

can be adequately approximated as being axially symmetric. The benefit of using the finite element method is the lack of difficult-to-verify simplifying assumptions, inherent in the modified Boundary Element method, leading to a confidence in the results that is governed only by the degree of discretisation in the finite element mesh used.

While the fully three-dimensional finite element method has been used in a few instances (e.g. Desai and Appel, 1976) it remains an unpopular choice of approach, because of the small size of problem that it can economically solve. A parametric study using three-dimensional finite elements is not feasible, and most applications have been for a particular pile and soil.

However, finite element modelling of lateral pile response has not been restricted to the axisymmetric geometry approach, nor to the analysis of the entire pile. Such exceptions include plane strain and plane stress finite element models, which have been used to model pile-soil load transfer behaviour, and also the use of other soil models than the elastic one, e.g. the hyperbolic stress-strain soil model. These approaches using the finite element method will be discussed in the next section.

2.3 Load Transfer Models

Several investigators have considered forms of the load transfer from the pile to the soil, that result from lateral loading of a pile, that are more involved than p-y curves. The work of Yegian and Wright (1973) and Baguelin, Frank and Said (1977), typify an approach to modelling lateral load transfer that considers the soil to behave like unconnected plane strain, or plane stress, discs. This greatly simplifies the modelling because a manageable, two dimensional analysis can replace the three dimensional reality. It also introduces conceptual problems that will be discussed during this section, and these raise some doubts about direct application of such a model to real pile analysis.

Baguelin, Frank and Said (1977), present a closed form two-dimensional plane strain solution for the stress distribution and displacement field, resulting from a rigid translation due to an applied force on a circular ring at the centre of an elastic body, confined by a circular rough rigid outer boundary. The expression for the displacement in the direction of the applied force predicts an infinite value of displacement, as the radial distance to the rough rigid boundary tends to infinity.

This infinite displacement typifies the results found from using infinite domain, full- or half-space, plane strain models. It occurs because the infinitely long pile involves an infinite total force acting upon the continuum, and further, the strains produced are integrated over an infinite domain. The combination of these two factors lead to theoretically infinite deflections, much in the same way as a point force results in an infinite stress and deflection at the point of application of the force.

This aspect of elastic continuum behaviour at first sight may seem alarming, but it must be realised that plane strain infinitely long footings or pile segments (and indeed point forces) do not exist in reality. Only finite areas ever need to be considered, and so the two limiting cases of infinite total load over an infinite area, and point forces, never actually arise.

Baguelin et al. proposed fixing of the outer boundary at the position which gives the same deformation in the x-coordinate direction for the plane strain solution as that for a solution based upon superposing a beam on a Winkler-support-theory-derived traction distribution on a point force Mindlin-based-elastic-continuum-model of deformation in the x-direction. This procedure seems cumbersome, and Baguelin et al. have outlined several difficulties associated with it. It does, however, lead to a value of fixed rough boundary radius for use in the plane strain pile segment model. Results from the elastic continuum based plane strain pile segment and three dimensional far-field model, are shown to give answers comparable to those of Poulos (1971a).

Another finding presented by Baguelin, Frank and Said in this paper, and in that of Baguelin, Trezos and Frank (1979), is the conclusion regarding the lack of influence of the pile segment cross-section shape upon load deformation behaviour. A circular pile and a square pile, with the same diameter and width are found to behave in essentially the same way. Thus, with the assumption of a rigid pile-soil interface, it seems the shape of the interface is not greatly important. This gives some support to the use of a thin strip pile idealisation, such as presented by Poulos and Davis (1980), which does not directly include the shape of the pile cross-section in the soil model.

Other aspects treated in the paper include the effect of a remoulded softened zone of elastic material near the pile and also the effect of soil yield using a Tresca criterion, both using the plane strain model. Neither the radial nor tangential shear traction distributions were greatly affected by the sizes of disturbed zone chosen or the degrees of modulus softening used.

Their solutions including soil yield show that the soil on the side face, where the shear traction is a maximum, fails in shear in a thin band first. The growth of plastic zones during loading is presented and does not show the mechanism that would need to form in the plastic region at collapse. From the shape of the load-deflection curve there is also no clear indication of collapse, even though the total load is near collapse according to the results presented by Randolph and Houlsby (1984). This will be considered again in Chapter five.

It would have been preferable if the loading could have been continued up to collapse, but the results do indicate that the component of total reaction arising out of shear along the side face becomes constant at relatively low load levels, namely about one fifth of collapse. This has importance as far as the rate of increase of the component of frontal reaction with deformation is concerned. The frontal reaction-deflection response actually appears to stiffen, to compensate for the loss of incremental side resistance and the initial portion of total reaction load-deflection response plots as if elastic behaviour applied right up to about two thirds of the collapse load.

This may well be a phenomenon associated with the plane strain confinement, or the rigid boundary assumed in the problem, but it still raises questions about commonly-held concepts of failure in soil masses. It challenges the concept of a softening

soil response as load levels increase. An isolated part of the soil may have a stiffening response according to these results.

The confinement raises a question as to the suitability of the analysis for application to the lateral loading of piles, especially when soil near the surface is considered. Breakout of the soil due to the proximity of the surface, will alter the plane strain state and lead to possibly a plane stress state. In the undrained state it can be shown theoretically that an increment of lateral load leads to an increase in the mean stress at the interface, equivalent to the increase of the radial normal stresses at any point around the circumference. Recourse to the Fourier representation leads to the radial normal stresses being a cosine function of the circumferential position multiplied by the stress increase occurring at the front of the pile, where the cosine takes a unit value, and the circumferentially directed shear stress is governed by a sine function and the shear value at the very edge of the pile, where the sine value is unity.

Thus zero mean stress increase is predicted at the sides of the pile-soil interface, while the circumferential shear is a maximum there. Since the three normal stresses are equal at any position around the pile-soil interface, it follows that soil yield is unlikely to occur close to the interface except at the two sides. The finite element analysis reproduces this behaviour with the sides failing first and then a zone of contained plastic flow appearing in front of and behind the pile, at some distance away from the interface.

All this presupposes that the soil is sufficiently contained to allow the generation of an increment of vertical stress, which will not be likely near the soil surface. Further, the plane

strain pile segment analysis predicts a wide variation of deflection response for different values of Poisson's ratio, as shown in Fig. 2.6. Not only is there a forty percent variation over the range of Poisson's ratio, but also there is a very steep rate of change of behaviour as a value of 0.5 is approached. Most researchers have concluded the value of Poisson's ratio has little effect upon pile behaviour and neglect it, or use parameters that effectively reduce its influence, (Randolph, 1977).

Yegian and Wright (1973) have described the application of a finite element analysis to model a thin horizontal slice of the strata through which a pile penetrates, using both plane strain and plane stress formulations. Their aim was to generate p-y curves by assuming both a non-linear soil stress-strain relationship and a non-linear interface joint element between the pile and soil. The analytic procedure for developing soil resistance to pile displacement relationships was presented and compared to the conventional method of predicting p-y curves, (Matlock, 1970). The soil model used is only applicable to saturated clays and has not been modified to allow for tensile breakaway of soil from the pile. The non-linear behaviour was implemented by an iterative, secant modulus procedure, converging upon the proper values. Unfortunately it was not made clear what was meant by "proper"; however it was pointed out that convergence was extremely rapid.

The soil behaviour was modelled by a hyperbolic stress-strain model, while the interface response was given by a bi-linear expression as a special case of a more general hyperbolic expression. The majority of results were found using a plane stress analysis, as this was anticipated to be applicable to the response at shallow depths where the pile action is concentrated.

An interesting point arises from the use of an interface element that could firstly, as a limiting case, withstand unlimited shear stress and secondly, model a case in which the interface shear strength and soil shear strength are equal. It would be expected that no gain in load could occur beyond that found for the second case. This is because any tendency to raise the interface shear stress above the soil shear strength would be expected to lead to failure of a thin band of soil close to the interface, regardless of the bonding strength. The fact that the fully bonded limiting case of infinite interface strength led to a higher load suggests there is a zone of overstress in the first solution.

Apparently the mesh was sufficiently fine to keep the overstressed zone small enough to produce only a load increase of less than 5 % above the theoretical maximum value, which corresponds to an interface shear strength equal to the undrained shear strength of the soil.

A comparison of the finite element and the standard method of predicting p-y curves was carried out for two cases:

- a) a "shallow" pile comparison.
- b) a "deep" pile comparison.

It was noted for the "shallow" case that Matlock's method predicts lower ultimate loads, in line with experience, than the finite element method. This was suggested as being a characteristic caused by breakaway of soil from the pile in reality which was not modelled in the method.

Further, a significant lack of agreement was found for the "deep" case, with lower ultimate loads being given by the finite element method. It was suggested that the deep case may have

significantly more vertical confinement and so a plane strain rather than plane stress analysis might be more appropriate.

No firm conclusions were drawn concerning ultimate loads other than to suggest that neither method, Matlock's nor the finite element analysis, can be put forward as the paragon since the accuracy of neither can be established unequivocally.

Group analyses were attempted by making efficient use of the periodicity induced by assuming smooth, reflective symmetry boundaries and restrained, antisymmetric boundaries. In this way an infinite row of pile segments between two fixed boundaries can be analysed for loading along and across the line of piles.

Not surprisingly the case of the pile loads along the line of the pile group gave much larger deflections. Indeed if an infinite extent were modelled instead of using a fixed boundary parallel to the line of piles then an infinite deflection would be expected, in much the same way as a strip footing on an infinite half-space would respond. The fact that any loading on the infinite number of pile segments causes an infinite total load to act upon the half-space, must result in infinite deflections.

The results from this approach should be viewed as an example of interaction between pile segments under highly artificial circumstances. Actual pile group behaviour is unlikely to consist solely of the responses depicted in this paper since:

- a) in general, individual pile reaction loads at any one depth are not necessarily equal as is assumed and
- b) as mentioned in the paper, plane strain and plane stress are likely to be only bounds to the true behaviour.

This paper highlights the lack of understanding of shallow

pile segment behaviour, especially with regard to pile-soil breakaway, and shows that the degree of confinement at greater depths may affect the non-linear response. Although in the paper importance is placed in the large variation of ultimate reaction load with interface shear strength, it is unlikely to be practically important. Since a fully smooth case is not realistic, and the maximum shear strength available near the pile-soil interface is only equal to the soil shear strength, there is less than a 20% change in ultimate reaction load when the expected range of interface strengths are considered.

It is clear that the load transfer mechanism for laterally loaded piles has only been successfully modelled for a restricted range of practical situations. Only coarse agreement has been achieved for these restricted cases, and obviously a more involved model than plane strain or plane stress is required. It does appear to be very important that the two situations of complete flow of soil around a pile, and breakaway of soil from the pile in regions of tensile stress, should be investigated using more refined models of behaviour. The deep flowing soil situation has received more attention and represents a fairly well-understood aspect of behaviour. Unfortunately it appears that the shallow breakaway behaviour will have a more important effect upon pile response, since the greater part of the effective length of a pile may be in the shallow behaviour zone.

2.4 Field Tests

The need for field tests was recognised very early in the study of lateral pile behaviour. The lack of models for predicting pile response led to an immediate need for field data concerning the suitability of piles to withstand lateral load. Normally the lateral loads were only a small component of the design loads and did not introduce areas of concern. However as piling became more widely used, especially for marine applications, the lateral load component became more significant.

The work of Feagin (1935) represents one of the earliest field tests reported in a comprehensive manner. His tests were aimed at proof testing the piles used in a lock, and so represent the class of field test designed to justify a foundation choice in a specific application.

When more advanced means of modelling lateral pile loading became available, the emphasis in pile tests shifted towards model evolution rather than proof testing. Such a test, in which the underlying mechanisms of laterally loaded pile behaviour are investigated, is that of McClelland and Focht (1956). They presented pile reaction load-deflection curves now known as p-y curves.

As confidence grew in the application of field test results to construct models of pile behaviour, the well known p-y curves became the standard approach to pile analysis. Once the p-y approach became accepted, then field tests were used as the means of correlating soil type and the form of p-y curve deemed to be appropriate, e.g. the curves of Reese et al. (1975) for sand and those of Lee and Gilbert (1979) for soft clay.

A general satisfaction with the use of p-y curves has resulted in less full scale field testing in recent years. However, recent activity in offshore areas that do not consist of terrestrial sands or soft marine clays has brought to the fore the problem of the behaviour of such soils as calcareous sands. While work upon the basic properties of calcareous sands is reasonably well advanced, much remains to be found out about the behaviour of piles under vertical and lateral load in such a soil. The need for improvement in understanding of such pile applications may well lead to a resurgence of interest in field testing.

The recent theoretical work, based upon elastic continuum principles, of Poulos (1971a), (1971b) and (1972), Randolph (1977), Banerjee (1978) and Banerjee and Davies (1978) could be used as a basis for comparison with the results of new tests. Such a thorough testing of elastic continuum models in predicting field tests that have been designed with that task in mind is long overdue. This would provide a better understanding of inadequacies of the model and may present means of overcoming them, much in the same way as field test results have modified p-y theories.

Two examples of field tests will now be given, one belonging to the class of proof testing of a foundation and the other to the class of tests investigating the underlying mechanism of load transfer down a pile in a marine environment.

2.4.1 The Tests of Feagin (1935)

Amongst the earliest works concerned with laterally loaded piles is the paper by Feagin (1935) in which the results were presented for tests on massive, concrete encased, monolithic pile groups in connection with the construction of a lock and dam on the Mississippi River, at Alton, Illinois. The soil consisted of river sand described as a medium sand with a water table 0.66 metres below the level of the base of the monoliths.

The procedures that were used have remained virtually unchanged until the present day and indeed the reporting of the results was of a standard that has seldom been achieved by more recent pile test reports. The loadings consisted of one-way cycles of horizontal load applied by a hydraulic jack acting between two monoliths or between two single piles.

The resulting load-deflection responses were decidedly non-linear with a reasonably well-defined failure load for the single piles, while the pile groups did not display such a marked deterioration in load carrying response with increasing deflection. This may in part be due to the fixed head condition that was enforced by the massive pile caps, as opposed to the free-head nature of the single piles.

The fixed head pile will provide a much higher failure load, since the fixing moment will cause more soil along the pile length to oppose the direction of pile movement. The free head pile will "waste" some of the soil response as a negative soil reaction in order to satisfy the restriction of moment equilibrium, whereas a restoring moment is provided by the pile cap in the fixed head case.

The pile groups were also shown to have a reduced efficiency for resisting deflection which was more noticeable at higher loads. This aspect of group behaviour is a well recognised phenomenon found in both sand and clay soils experimentally and also is evident in results from elastic-based analysis methods. The cycling of the load showed that the maximum deflections progressively increased upon returning to the same load level and that a permanent deflection remained upon load removal.

A further observation of interest was that of a gap behind the pile that extended to at least two metres depth when the maximum load was applied to the pile group. This gapping is somewhat at odds with the proposition made by Feagin that sand would have filled in behind the pile in order to produce a permanent deflection upon load removal. It would seem that a measure of both types of sand behaviour is required, both gapping and infilling, i.e. incomplete flow of sand into the gap.

The conclusions reached were of a specific nature and restricted to the soil conditions and piling arrangement tested. However, it is obvious from the discussions of this paper, that great interest was taken in the work and its value was recognised as shedding light on a subject that long had been "obscure". One particularly interesting discussion, by Y. L. Chang, (1937) proposed that a pile of sufficient length may be considered as infinitely long. This is an enunciation of the effective length concept, possibly the first of many forms taken by this concept. Chang uses what has now become known as the Winkler soil model to postulate a depth beyond which the pile is virtually vertical and undeformed. This depth is mathematically shown to be close to one wavelength of the pile deflection pattern.

Essentially the later results of Hetenyi (1946) for an infinitely long pile, are presented by Chang, (1937). Chang also uses the minimisation of internal energy to arrive at the same effective pile length as was proposed from finding the depth to zero deflection.

It is obvious from some of the statements made concerning the calibration bending tests on the piles when out of the soil that the concept of soil support and rigid body movements were not clearly linked. The terms such as "resistance to lateral movement supplied by passive pressure of the soil" and "the resistance of the pile itself" when used together suggest a lack of understanding of the nature of pile-soil interaction problems.

The fact that all of the support is achieved by the loading of the soil, and that the relative pile-soil stiffness modifies the form of the interaction traction distribution that is generated (and thus the relative importance of pile bending and rigid body components of deflection), is not apparent in the paper or its discussions.

A similar gap in understanding leads to a discussion of a point of rotation called the "zero point". Such a point was automatically assumed to correspond to a change in sign of reaction load as well as deflection. This is not necessarily true and is only an assumption made by the class of theories now referred to as Winkler soil models.

D. P. Krynine, (1937) introduces the zero point to the discussion, and also adds some interesting ideas, touching upon gapping behind piles, failure loads from a formula and pile structural failure, shakedown of pile-soil response, pre-loading

of piles and permanent deflections. Many of the problems mentioned are even today poorly understood and represent areas of research in which great gains in knowledge are possible.

Feagin's paper is a good example of the class of field test that seeks to justify the use of a type of foundation to carry the loads of a specific application. In this it was eminently successful and also led to great gains in the general understanding of lateral pile behaviour.

2.4.2 The Test of McClelland and Focht (1956)

Another paper in which progress was made in the understanding of laterally loaded pile behaviour was that of McClelland and Focht (1956). They investigated lateral behaviour of a strain gauged pile in a marine environment, concentrating upon the pile reaction loads induced by horizontal loading and the values of pile deflection accompanying the pile reaction loads. The test, see Fig. 2.7, was situated in the Gulf of Mexico about seven kilometres off the coast in water of about ten metres depth. The soil consisted of a deep clay layer which appeared to be slightly overconsolidated with a shear strength of finite value at the surface and a tendency to increase linearly with depth.

Their paper possibly represents the birth of the p-y method, although it has seen many changes from the form that was originally proposed. The contents of the paper present a correlation between consolidated undrained triaxial test results, in terms of stress and strain, with soil-pile reaction loads and pile deflections. The final result is an estimate of the "soil modulus of pile reaction". This reaction modulus at any point was found to vary with the depth of that point and also to vary with the deflection the point has undergone. This was evident in their

Fig. 4, a part of which is reproduced in Fig. 2.8, where a family of curves of soil reaction versus pile deflection for several depths is plotted.

In discussion of this paper Peck, Davisson and Hansen (1958), expressed some concern about the absolute magnitude of the deflections since no check upon actual deflections seemed to have been made. Their concern was that rigid body movements may have occurred and could well lead to a shift in the absolute value of deflections. Their objection was the failure of the point of zero soil reaction and point of zero pile deflection to coincide, as they state should happen if the subgrade modulus is not allowed a zero or negative value.

However the desire of the authors and discussers to ensure the depth to zero deflection and the depth to zero soil reaction coincide is perhaps an unfortunate limitation. The results from any investigation of a pile test should rely upon field measurement for their basis, not upon preconceived ideas of how soil reaction and pile movement should be related. Other models of soil behaviour, e.g. elastic continuum, do not require such limitations on the reaction and deflection and so this suggests that the results may not be inconsistent with the use of elastic theory. The reason why this aspect of behaviour was subsequently not considered as very important is that in the region where the soil reaction and pile deflection reach a zero value, the interaction loads between pile and soil have only a very small effect on the overall behaviour of the pile.

The doubts about the values of deflection derived are also strengthened when Fig. 2.7, taken from Figs 2 and 3 of the paper, is examined. The pile test setup appeared to consist of a rigid

pipe brace restraining the pile from translating, and presumably rotating, at a point just above the water level. The load was applied by a jack about 8.1 metres below the brace and 1.8 metres above the ground line. This setup however is not consistent with the zero moment depicted at the level of the pipe brace. If rotation was not restricted sufficiently to produce moments at that level, it is still inconsistent that the deflected shape should show pile translation at that level.

How badly the discrepancies affect the curves of Fig. 2.8 is not clear, since they occur at a large distance away from the main region of interest, which is just below the ground line. It is thus likely that the values of deflection used throughout the paper are more correctly interpreted as the bending deflections of the pile without any rigid body component.

In this regard the results presented should not be viewed as a reliable source of p - y curves as they are understood today. The current situation considers y as the absolute value of pile deflection and takes great care to assign a value of pile reaction p that will accommodate the effects of the loading history on the behaviour of any point on the pile-soil interface.

A further complication in understanding the significance of results presented in this paper lies in the method employed to obtain the data points. The method used by McClelland and Focht necessitated reloading the pile several times in order to obtain one full set of gauge readings at all levels. Although attempts were made to statistically cater for this in the test reduction procedure it is inevitable that some permanent soil deflections would have occurred, especially near the surface.

This is evident in the zero values of soil reaction measured

down to a depth of one metre when the maximum static loading was applied. Presumably this maximum load was applied several times to obtain a full set of gauge readings and a permanent gap may be assumed to exist after the first load. A permanent gap is defined as one that remains upon unloading with at least the front and possibly the back of the pile not touching the soil. This gap would not be expected to close at the front until the previous maximum load had been applied again, or exceeded. Unless the maximum loads were controlled precisely it is conceivable that a full gap around the upper section of the pile may have existed even when readings were made of the strain gauges at the intended maximum load.

Notwithstanding several shortcomings of the test, the paper represents a clear demystifying of laterally loaded pile response and introduces a direct and rational approach to correlations of pile behaviour with soil response in undrained triaxial tests. Judging from the twenty-three pages of lively discussion to the fourteen pages of the paper, there was a large degree of interest in the topic. The generation of this interest alone is sufficient to regard this paper as a significant contribution to the understanding of laterally loaded pile behaviour.

2.4.3 Other Tests

The paper of McClelland and Focht represents an example of a field test that helped a model of pile analysis to evolve rather than an attempt to answer a question as to the suitability of a particular pile to sustain a given load. The success of this paper has led to the large number of tests that have been undertaken in order to obtain details of the model that was first proposed in the pioneering paper of McClelland and Focht.

Such tests include those of Matlock (1970) for soft to medium stiffness clay sites, Reese, Cox and Koop (1975) for stiff clay, Lee and Gilbert (1979) for very soft clay and Reese, Cox and Koop (1974) for sand. Each of these tests involved the use of carefully instrumented piles loaded in a variety of head shear and applied head moment conditions in order to correlate the backfigured reaction load-pile deflection curves to these soil conditions. Thus the p-y approach to lateral pile analysis has been founded upon high quality field tests of the third type where neither pile suitability nor the underlying mechanism of load transfer are directly questioned.

Elastic-continuum-based analyses have not received the full benefit of pile tests specifically designed to investigate the applicability of an elastic model of soil-pile interaction. These analyses have only been applied in retrospect, after the aspects of pile-soil response felt to be important for p-y analyses have been reported. This generally means the region of loading that might realistically be expected to be elastic is not reported with the emphasis that later non-linear behaviour receives.

It seems that a deficiency exists in the range of field tests of laterally loaded piles in that the behaviour at low load

levels, so important for assessing the accuracy of elastic soil models, has been overshadowed by the intense study of later non-linear behaviour. The ability of the elastic models to provide excellent fits to a wide range of tests as reported by Poulos (1971a), Banerjee and Davies (1978), Randolph (1981) and others, suggests that study of a field test using low load levels would be most instructive.

Although not a field test of a pile the pressuremeter has been included in this section since it represents a test carried out in the field. Broadly three types of pressuremeter are found in use for soil investigation:

- a) The Menard pressuremeter that is used in pre-bored holes.
- b) The self-boring pressuremeter that cuts its way downwards with minimal disturbance to the soil that surrounds it.
- c) The full-displacement pressuremeter that remoulds the soil as it descends.

The Menard and self-boring type are generally assumed to best model the bored pile installation procedure, while the full-displacement version is felt to be more appropriate for driven piles. Much of the pioneering work in this field has been carried out by Wroth, Hughes, Gibson and Windle in Great Britain, and Menard, Baguelin and Jezequel in France. Work is currently underway to better understand the results that pressuremeters give in terms of basic soil properties, Yeung and Carter (1987). While such work is still in progress, many researchers have assumed that the results of pressuremeter tests can be used directly as a source of p-y curves for use in lateral pile analyses.

Many statements have been made, such as the opening one of

Briaud et al. (1984), that imply the pressuremeter test, and the theory used to backfigure soil parameters from the test results, have reached a stage of development sufficient to allow the prediction of the non-linear lateral response of piles, as described by p-y curves. Unfortunately such statements seem premature, and a more accurate assessment might be that the pressuremeter test has been found to produce a "load-deflection" curve that has the same general shape as a standard p-y curve.

It would be tempting to try and correlate the pressure and volume change response of the pressuremeter test with the pile reaction and lateral deflection response, as measured in lateral load tests. Obviously such an approach will meet with some level of success but several points may be raised:

- a) The pressuremeter test is ideally assumed to be an axisymmetric test.
- b) The p-y response is ideally assumed to be an anti-symmetric phenomenon.
- c) The pressuremeter test does not affect a region of soil of the same diameter as a pile and also has little in common with non-circular pile cross-sections.
- d) The pressuremeter test is isolated to a small region of depth in the soil profile, whereas a pile is a continuous member throughout its buried length.

Possibly the best way of expressing the viability of pressuremeter tests for modelling lateral pile behaviour, is to liken the connection to that existing between a triaxial compression test and a simple shear test. The non-linear form of the response from both tests are patently similar but two different sets of parameters are involved in each test; axial

strain and deviator stress for the triaxial test, and shear strain and shear stress for the simple shear test. The two responses of these soil laboratory tests can be individually interpreted to provide the same deformation and strength parameters, using a common model of soil behaviour. So the results of the pressuremeter and the p-y response should be viewed as two different soil responses but capable of being modelled by a common theory.

Such a theory of soil behaviour, allowing predictions of both the response of pressuremeter tests and lateral pile p-y responses, has not yet been fully developed. Robertson et al. (1984) have highlighted the fact that pressuremeter and p-y limit pressures are not equivalent from theory, and that initial stresses found in the pressuremeter are not considered by the standard p-y method. These facts alone place the problem of scaling of the pressuremeter curves, and the correlation of an axisymmetric normal pressure with the complex set of normal and shear tractions that combine to produce the pile reaction load, beyond current theoretical capability.

The pressuremeter is potentially one of the most important methods of in situ testing yet devised, and is destined to become a standard, reliable and indispensable tool of geotechnical engineering. It is hoped that such a desirable state can be achieved without recourse to the neglecting of a sound theoretical basis in order to hasten the use of the tool in an incomplete form. The rapid and indiscriminate creation of a body of analysis methods using pressuremeter results, that do not stand up to critical examination, may do more to harm the progress of the pressuremeter as a valuable tool than to promote it.

2.5 Model Parameters

Every laterally loaded pile analysis model will require the specification of a number of parameters in order to obtain response predictions. In general the more complex the model the greater the number of parameters that need to be found in order to use the model to analyse a particular pile and soil profile.

The pile properties are commonly believed to be known to a satisfactory extent and the use of simple engineering bending theory is taken to be adequate. The soil however represents a material that requires attention to the non-linear aspects of its response. For this reason the parameters chosen to model soil response have frequently been found by recourse to soil tests that include a large degree of non-linear behaviour.

2.5.1 p-y Approach

For clay soils, the family of laterally loaded pile analysis methods, known as the p-y approach, generally use a triaxial test to determine the axial strain at half the maximum deviator stress, (Matlock, 1970). This value of strain is then converted to units of displacement for use in the analysis by multiplying by the pile diameter and an empirical factor that depends upon the type of soil, e.g. Sullivan et al. (1980). This critical displacement is then used to construct the pile reaction load-displacement (p-y) curve for the depth from which the triaxial sample was obtained.

The initial stage of the p-y curve (except for Matlock, 1970 and Lee and Gilbert, 1979) is given by a straight line that corresponds directly to Winkler theory of soil response. This requires a coefficient of subgrade reaction, k (units of FL^{-3}), which is correlated directly, or indirectly, with the value of

soil shear strength. This coefficient may thus be constant with depth in a highly over-consolidated soil profile, where the undrained shear strength is found to be constant with depth. However, the defined p-y response is controlled by the "secant modulus" of the soil E_s (units of FL^{-2}), which is found by multiplying the coefficient k by the depth of the station considered. Thus, a linear increase of soil stiffness with depth will result even if k is constant with depth.

Matlock (1970) does not explicitly use a value of E_s but computer programs using his p-y curves presumably have a piecewise linear representation of the p-y curve and so a linear portion at the start of the curve is still evident. Lee and Gilbert essentially employ the same procedures as Matlock and only the p-y curve will change, not the method of solution. Thus both these soft clay p-y curves will still have an initial straight line portion. This means that the generally accepted increase of soil strength with depth associated with soft normally consolidated clay, will lead to a parabolic increase of Subgrade Modulus, E_s with depth.

In this way, the variation of initial stiffness of the clay with depth is approximated and also the soil shear strength is found, e.g. from the maximum deviator stress obtained from tri-axial tests. The choice of axial strain at half of the maximum deviator stress, as a means of obtaining the critical deflection y_c , means there will be a considerable degree of non-linear behaviour included in the specification of the soil stiffness. Thus, the instantaneous stiffness of the soil upon initial load application is not strictly modelled by the p-y approach.

In the approach of Sullivan et al. (1980) the strength,

obtained from the unconsolidated undrained triaxial tests at an isotropic confining stress equal to the overburden, is then used with an appropriate bearing capacity factor to predict the ultimate reaction load available from the soil. The testing of soil samples from various depths will then produce a knowledge of soil ultimate resistance variation with depth.

More complex analyses, including those for cyclic loading, employ a depth parameter defined by the transition from shallow, surface-influenced soil failure to the deeper, "constant" ultimate reaction load involving flow of soil around the pile. This transition depth is used in an expression used to describe the manner in which the residual, large-deflection ultimate reaction load varies from the surface down to the transition depth. In this way the model can reduce the "stiffness" of the pile-soil system in the upper layers and take some account of the results of gapping. The numerical value of this transition depth is calculated by equating the two expressions for the surface-influenced and the deep-pile failure loads per unit depth and thus depends heavily upon the accuracy of these two expressions.

The unified clay method of Sullivan et al. (1980) has a transition depth but it is maintained at a constant value of twelve pile widths. This is regardless of the point at which the two ultimate reaction load calculations give the same value, which is usually between four and six diameters depth. The unified clay criterion introduce a new parameter, F , for the prediction of the ultimate reaction load at large deflections in the upper soil layers where the surface has influence. The unified method also uses another parameter, A , that parallels an empirical correction for theoretically-derived ultimate reaction loads first used for p - y curves in stiff clay, Reese et al. (1975).

All the clay p-y models also include a term incorporating the value of effective unit weight of the soil although it is generally acknowledged to have little influence on the computed results for piles in clay. The effective unit weight actually appears as the source of the vertical overburden stress in the expression for ultimate reaction load near the surface, and thus can be seen to represent the effect of initial stress. How this initial stress has been theoretically incorporated is not clear, but it is still included, in the majority of recent p-y models.

The p-y methods for clay thus require a knowledge of :

- a) the material and geometrical properties of the pile,
- b) the axial strain at half the maximum deviator stress in triaxial compression tests of the soil from various depths,
- c) the value of soil strength from the triaxial tests or in situ vane tests at various depths,
- d) a soil effective unit weight at the pile stations and
- e) a variety of soil properties such as Liquidity index, Plasticity index, Liquid limit, over-consolidation ratio and sensitivity, and their variation with depth.

The above information is then combined with a construction procedure that relies heavily upon the estimation of the soil as being a stiff or soft clay. A knowledge of the type of clay aids in the choice of the value of the numerical constants in the unified model, that were proposed in their original form by Reese et al. (1975) for stiff clay. The original constants were corrections for the inadequacy of the theory used to predict the ultimate reaction loads in stiff clays, but the unified model has generalised the constants to allow for both stiff and soft clay.

The case of lateral loading of piles in sand has received somewhat less attention, and the model of Reese et al. (1975) is commonly used, see Fig. 2.8. Once again, the theoretical predictions for ultimate soil reactions were found to be unsatisfactory and a set of corrections based upon the Mustang Island pile tests is now in wide use. The sand type is broadly classed as being of a loose, medium or dense nature for the determination of the coefficient of subgrade reaction. The variation of friction angle and density with depth are also required in order to construct the non-linear portion of the p-y curves.

For sand, the effective unit weight becomes much more important than it was for the case of clay, since it directly controls the confining pressure and thus the strength in cohesionless soil. Essentially the two cases of surface-influenced and deep-flow failure loads are assumed to exist in sand, as they did in clay. The postulated sand failure mechanisms are similar in concept to those of clay, but are based upon assumptions that cannot be observed in the field. The ultimate reaction load theory depends upon an assumed geometry of a failed wedge of soil, and it is possible this assumed wedge is not always correct. This may help to explain why the empirical correction factor, multiplying the theoretical ultimate loads, reaches a value of nearly three at the sand surface for static loading conditions.

It is clear that the p-y approaches to predicting the behaviour of laterally loaded piles in both sand and clay are based upon theories that require considerable assistance from empirically-derived corrections. The choice of material parameters for the soil has been confined to the commonly-obtained material properties. These parameters are incorporated into theories and

pile reaction-deflection curve-fitting devices that have been shown to be applicable to a range of tests. The final result, the p-y curve, is then taken to be an envelope of behaviour which hopefully predicts the worst possible situation that can arise.

It is of the utmost importance that this last statement is fully understood. The p-y curve was not originally conceived as a description of a load-deflection path, but was a description of a secant type of behaviour that only depicts a final value of reaction-load and deflection without any information of how that was achieved. This is nowhere more clearly seen than in the method of catering for cyclic loading where a completely different p-y curve to the static one is proposed even though the same soil is being considered.

Because of this the material parameters that are used can be assessed as convenient measurements of the soil from which simple theories can predict a response, which subsequently requires empirical adjustment in order to agree with experience. As such the material properties are not used as the sole factors in the determination of the response of piles. Further the response predicted is not necessarily the response one should expect, except under a range of circumstances that would be deemed to be the worst situation possible.

2.5.2 Elastic Continuum Approach

In contrast to the envelope philosophy of the p-y method most other analyses require the best possible realistic model parameters in an attempt to follow a load path technique of analysis. This is because many of these methods are directly based upon continuum mechanics principles. Unfortunately, to date, it appears that no attempts to systematically reproduce the extensive

testing and calibration associated with the p-y method have been made for a continuum model.

This is largely due to the restrictions imposed upon the continuum models in the past to allow rigorous solutions. These restrictions such as uniform Young's modulus with depth have seemed highly unrepresentative of real soil. This is perhaps unfair, when it is noted that often the pre-conceived ideas of how real soil behaves have been formed in the light of experience obtained using a soil model that has none of the continuum properties such as interaction.

The Winkler model, in which the much used assumption of no interaction throughout the soil mass is made, has often served as a method of interpreting pile response. The conclusions reached about the soil response from using such a simplistic model should not have undue emphasis when considering the adequacy of other, more sophisticated continuum based models of soil.

The most valid criticism of continuum-based models is the argument that linear response is only rarely found in soil whereas, an elastic continuum model can only present linear responses. Thus, the convenient practice of selecting soil moduli that are representative of the stress range, expected in reality in the soil, evolved. Although this presents a response that might be appropriate to one load level, strictly, it invalidates the use of elastic continuum theory.

It amounts to the entire elastic soil mass having to change its Young's modulus with increasing applied load level, which will greatly affect the amount of interaction throughout the mass. This is unrealistic, and a better method of accounting for non-linear behaviour would be to maintain the same elastic properties

for the main mass of soil, but allow a softening or even a complete loss of incremental load transmission at highly stressed regions on the pile-soil interface. This is a non-rigorous application of theories of soil failure mechanisms, but at least the elastic continuum model has retained some integrity.

The continuum model in its simplest form, will require the Young's modulus and Poisson's ratio of the soil. The Young's modulus value should ideally be a representative one at the state of stress expected to be found in the soil, and the value of Poisson's ratio one that best fits the nature of the loading. A "rapid" load, that is rapidly applied and also quickly removed, will require only consideration of the undrained soil model parameters. However, even if it is rapidly applied, if a load is to be maintained then drained soil parameters are required in the analysis of the long term response. The word "rapid" covers a range of loading rates which rely upon the rate of redistribution of excess pore pressure in the soil, i.e. the soil permeability is the governing property.

This introduces an aspect not considered directly by the p-y method, that of the time-dependant nature of soil response. If the soil is assumed to be a two-phase (elastic-solid and fluid) material there will be an unique relationship between the values of undrained and drained model parameters. Any load that is applied and maintained will evoke an immediate undrained response followed by the slow progression to a drained response. Carter and Booker (1981) have explored such behaviour briefly using finite elements while Apirathvorakij and Karasudhi (1980) have also presented an analysis capable of such a prediction of lateral pile response as a function of time.

Very little work has been carried out in this area with most researchers content to consider the response as either essentially undrained or drained in nature, thus employing the appropriate value of either the undrained Young's modulus, E and Poisson's ratio, ν or drained values E' and ν' ; where ν^u is one half and $E = 3 E' / 2(1 + \nu')$ from the assumption of the shear modulus being always constant. The validity of such a procedure cannot be proved for every case in which it can be employed, but it does at least represent a systematic method of accounting for the increased deformation associated with drained soil response. Indeed, it appears that no other way of theoretically accounting for the time-dependant consolidation behaviour of pile-soil response is available, except the two-phase continuum model of soil.

In order to make some allowance for the non-linear nature of the soil there appear to be two choices. Firstly the soil modulus can be obtained from tests on soil samples at stress states similar to those existing in the ground and subjecting the samples to the same stress increments that would occur due to loading, as proposed by Lambe (1964). This modulus can then be adjusted during loading in the analysis in line with the reduction in stiffness evidenced in say a triaxial test on a soil sample, although as previously mentioned this is not a strictly valid use of the elastic model.

Alternatively, the appropriate initial modulus may be held constant and the device of limiting soil strength employed at the pile-soil interface which is more consistent with the use of an elastic model.

Poulos and Davis (1980) have outlined such approaches in the introductory chapter of their book on pile foundations, where they also emphasise the necessity of considering models of soil

behaviour that can cover the response over the entire range of load levels, using the best possible engineering approximation. This leads to the model requiring a value for p_u , the ultimate interface interaction stress that the soil can withstand, in much the same way as the p-y approach does. A generally accepted method for clays is to use a value of nine times the undrained shear strength of the soil for the deep value of ultimate average pressure. A linear variation from a reduced value at the surface to the deep value at between three and five diameters is a common way of modelling the effect of the free surface.

However, the elastic continuum method makes no assumptions about the pre-failure soil response based upon the ultimate interaction stress value that is chosen. This means that the fully elastic behaviour of the pile-soil system is not affected by the ultimate soil resistance profile chosen. This is not to say that the choice of ultimate interaction stress will not affect the response of the pile when using a continuum model. The load level at which soil yielding first occurs will vary when the ultimate interaction stress is changed in an elastic-limiting interface stress model. Indeed, failure of soil at one level will be seen to affect even the elastic response of nearby soil horizons because the system of interaction between horizons has been incrementally changed. This means that even elements of soil that have not reached a limiting stress, will exhibit a non-linear response simply because nearby elements have reached a failure interaction stress and will no longer contribute to the nature of the incremental pile response.

2.5.3 Other Approaches

Apart from the well known p-y and continuum analyses, there are other analyses that provide a link between the two approaches. The p-y curve is defined in terms of a load-deflection path and the parameters involved are based upon elastic theory in one such model proposed by Carter (1984). The initial slope of the p-y curve has been related to the Young's modulus of a soil using a form of the relationship proposed by Vesic (1961a) and (1961b).

The Young's modulus for a sand is found from the equations for shear modulus attributed to the work of Hardin and Richart (1963), but more probably due to Hardin and Black (1966). The modulus depends upon the effective confining pressure and the void ratio of the soil and also the nature of the particle e.g., round or angular grained. An estimate of Poisson's ratio of the sand is also required to estimate the initial stiffness of the p-y curve, since the shear modulus must be converted to a Young's modulus.

The Young's modulus for a clay was estimated from a correlation of shear modulus to undrained shear strength, Pender (1983) which, together with experience, suggested a ratio of between 100 and 200 which is similar to the values suggested by other authors, e.g. Poulos (1971a). The same form of the relationship between the coefficient of subgrade reaction and Young's modulus was then used.

This form of Vesic's original expression was proposed by Bowles (1982) and is interesting, since it marks an attempt to introduce the concept of a "back" and "front" to the soil-pile interface. The original expression of Vesic is multiplied by two in order to model the increase in stiffness due to both the front and back faces of the pile contacting the soil.

The load-deflection transition from the initial stiffness to the ultimate load, is modelled using a hyperbolic type expression involving the soil reaction to some power, the value of initial stiffness and the ultimate reaction load. The ultimate reaction load was assessed by a bearing capacity factor for clay that varied from five at the surface to twelve at a depth of 3.5 pile diameters, thereafter remaining constant. Cohesionless soils were treated using an ultimate reaction derived from a limiting pressure on the pile given by five times the Rankine passive pressure. These ultimate reaction loads are in broad agreement with both the p-y and continuum-based recommendations.

The power used in the hyperbolic expression was found by back analysis to be unity for the case of sand and to range from 0.2 to 0.3 for clay. Good agreement was generally found between the results of the model and several field cases that have been reported in the literature. The simple p-y load path employed by Carter (1984) showed that it is not necessary to maintain exactly the shape of the curve found in the field test in order to obtain adequate predictions of pile behaviour. This was also evident in the simplifications that Sullivan et al. (1980) made to the p-y curve definition in proposing the unified clay approach.

2.5.4 Gapping and Soil Parameters

Only a few examples of theoretical work considering the possibility of gapping around a pile can be found, e.g. Poulos and Davis (1980), Matlock, Foo and Bryant (1978) and Swane and Poulos (1982). The material parameters required are thus not as well known as those for analyses which neglect gap formation.

The Poulos and Davis analysis requires a knowledge of the in-

situ lateral stress via a value of coefficient of lateral earth pressure and the overburden stress given by the effective unit weight of the soil.

Matlock et al. (1978) employ the standard p-y approach, but with the non-linear spring replaced by an assemblage of elastic-plastic sub-elements at each node. Each sub-element acts in parallel such that their reactions can be summed to give the total reaction at one node. By varying the number of sub-elements at each node that are allowed to behave as if a gap were possible, from all sub-elements at the surface to none at the previously mentioned transition depth, a behaviour pattern commonly felt to be appropriate is produced.

Near the surface the pile passes through a "slack"-zone in which only a minimal side resistance to movement is evident. Deeper down the pile the confining stress is sufficient to result in confined flow of soil around the pile. At even greater depth the response is essentially linear. These three responses are depicted in Fig. 2.10.

Figure 2.10a depicts behaviour in terms of reaction load and deflection at a station on the surface, showing non-linear initial loading to a maximum, followed by a cycle of load. Since the loading is not symmetrical, the response also is not symmetric. Reloading and unloading are shown to have different stiffnesses, which have been magnified here for clarity. The movement of the pile through the softened (or gapped) zone is accompanied by a small resistance. Some degree of adhesion is assumed, leading to slightly larger negative loads at the point of breakaway than can be sustained in the "gap".

In Fig. 2.10b the initial non-linear portion remains, but is stiffer due to the larger depth. Unloading and reloading at this

depth do not lead to great changes in the position of the pile and a confined flow of soil around the pile is assumed.

In the deep zone of response (Fig. 2.10c), the non-linear behaviour is all but absent and an elastic response is evident. This would necessarily mean the initial stresses are much larger than the changes in stress brought about by soil-pile interaction.

Since the transition depth is governed by the ultimate reaction load, which incorporates a term for the soil unit weight, there is possibly some validity in Matlock, Foo and Bryant using the above approach with sub-elements. However, the effect of unit weight is disguised and no theoretical examination of its importance alone is possible since varying it would also vary every aspect of the p-y curve. There is little help available for choosing parameters above that already given in the various p-y methods, and since the analysis is intended to model the dynamic response of piles it is outside the main scope of this thesis.

Swane and Poulos (1985) have used two spring supports, one at the back and one at the front of each pile node, and have given the springs a variable stiffness dependent upon the soil model and loading condition. In this way the three major types of response, as in Fig. 2.10, can be broadly modelled. Their model was relatively simple since it was used to analytically investigate the cyclic lateral loading of single piles using a load path technique. The material parameters are based upon similar correlations with soil strength parameters to those of the Elastic method and p-y analyses. A significant difference in their method is the inclusion of initial stress resultants acting on the two sides of the pile before loading commences.

It is surprising that, with the exception of Poulos and Davis (1980), the methods that attempt to consider the effect of gapping on pile response have been for cyclic, and even dynamic, behaviour. A more logical approach would be to first consider the simpler case of static loading of piles. The repeated loading, and even dynamic, aspects of the other two methods requires careful choice of soil parameters with little guidance and, as used by Swane and Poulos, some consideration of material property degradation with the number of cycles and stress level.

2.5.5 Summary

The strong similarity between all the approaches is that linear, or elastic, parameters govern the initial response and continued loading leads to local failure of the soil at a constant ultimate interface load. The amount of empiricism and complexity of the soil model varies greatly between the methods as does the underlying philosophy of each approach. It seems that with the same soil parameters one could expect to adjust the empirical coefficients of any of the analyses and obtain agreement.

The parameters that are important for analysis of laterally loaded piles have been found to be,

- a) the initial soil stiffness, either as a load-deflection ratio or in terms of soil Young's modulus and Poisson's ratio which take account of soil permeability and loading rate,
- b) the ultimate reaction load, as a function of a bearing capacity factor times the undrained shear strength for clay, or the Rankine passive earth pressure coefficient, multiplied by an empirical correction for the three-dimensional effects, for sand and

c) the depth below which the confining stress limits soil failure to essentially plane strain flow; this has loosely been related to the overburden stress by the expressions for ultimate reaction load for shallow and deep cases.

Thus the parameters for the various models fall into three categories, namely those dealing with the initial stiffness of the pile-soil system, the ultimate strength of the soil when load is transmitted to it by a pile and the initial stress conditions in the soil prior to loading. Of these, the last is the most poorly understood but may well prove to be of great importance in understanding the finer points of pile-soil interaction response.

2.6 Summary of Review

Although this chapter has by no means given an exhaustive treatment of the wide range of literature concerned with the behaviour of laterally loaded piles, it does cover a number of significant aspects.

The progression from engineering approximation (e.g. the equivalent cantilever) methods (where the soil is all but ignored) up to the early attempts at assigning a response law to the soil, such as a Winkler model, has been omitted. It was felt that such early work, prior to the interest shown in applying say a Winkler type of soil model, provided very little insight into the basic nature of soil-pile behaviour.

A standard division into three classes of model has been used, in a manner that has previously been employed to consider the literature of lateral pile analysis. These three classes are shown to have some degree of overlap and also a degree of diversity, even within one class. As an example, both the modified boundary element elastic continuum and p-y methods employ the same basic soil properties when assigning model parameters concerned with soil limiting stresses and ultimate reaction loads. But the p-y method also maintains a distinct difference from almost all other methods in the Winkler class of model by following a philosophy of an envelope to behaviour.

The changing role of a field test from a proof-testing tool, to a soil-pile model developing tool, and finally a soil-pile model testing tool, has been traced. Many field tests have been reported in the literature but only two have been considered in

detail here. The undertaking of more field tests in the future to provide information about the lateral response of piles in unusual soils (e.g. calcareous sand), and to check the suitability of some of the newer methods of analysis, is seen to be most desirable.

Model pile tests have not been reviewed but they do play an important role. They have only limited credibility as means of predicting large prototype behaviour. Even the use of centrifuge modelling to obtain stress distributions similar to field conditions may suffer from the difficulties associated with the relative size of the soil fabric and the pile. Model tests are of most use in confirming the response predictions of analyses that allow for geometrical changes, such as the elastic model can. In such a case it is the ability of the analysis to theoretically predict model response, rather than the dubious extrapolation of the model response to full-scale response, that is the reason for the test. It then remains to assess the accuracy of the analysis with regard to full-scale tests before the analysis can be considered as appropriate.

The parameters required by the various models have been reviewed with attention being concentrated in three areas:

- a) The initial stiffness of pile response,
- b) the ultimate soil resistance to pile movement and
- c) the change from surface-affected to deep-pile response.

The commonly-used properties of the soil have been correlated with experience to allow prediction of behaviour as contained in the above three areas. The use of empirical calibration is widespread and is a cause for concern when comparisons are made between various models using the same parameters. Such inconsistencies between models is dangerous and suggests that the

whole topic of parameters for use in prediction of lateral pile behaviour would benefit from closer scrutiny.

A promising tool, with which a much better inspection of in-situ parameters is possible, is the pressuremeter. Despite the claims of some authors, it appears that correlation between pressuremeter results and lateral pile behaviour is not well catered for theoretically. Much work is possible in this area, paying more attention to the constitutive model used and its behaviour under both axisymmetric and antisymmetric imposed loadings. The expanding cavity solutions, so widely used to interpret pressuremeter results, are usually based upon a horizontally oriented plane strain approximation. This is thought to be appropriate at "great depth", but what amount constitutes a "great depth" is open to many interpretations. Improvements in understanding in this area may well lead to a clearer knowledge of the depth to reduced resistance used throughout the range of p-y methods.

Although not discussed in the main body of this chapter, plane strain cavity expansion theory has also been used to estimate the state of stress after driving of a pile in a clay soil, Carter, Randolph and Wroth (1980). The results suggest the long term final state of stress around a driven pile has a radial major principal stress, and the circumferential and vertical stresses are equal and represent the minor principal stress. This stress state is fortunately similar to that in a triaxial strength test rotated through a right angle, and may help to explain why p-y curves based upon triaxial test results have correlated well with measured p-y responses.

However, any anisotropy of the soil (or if the pile was pre-bored), would lead to a different predicted state of stress in the

soil. It means that the state of stress in a triaxial test would not necessarily be such a good representation of the stresses in the soil near a pile face. For this reason it would be necessary to alter the p-y criteria based upon triaxial results. In practice this may help to explain the large number of different p-y models proposed for different pile and soil conditions.

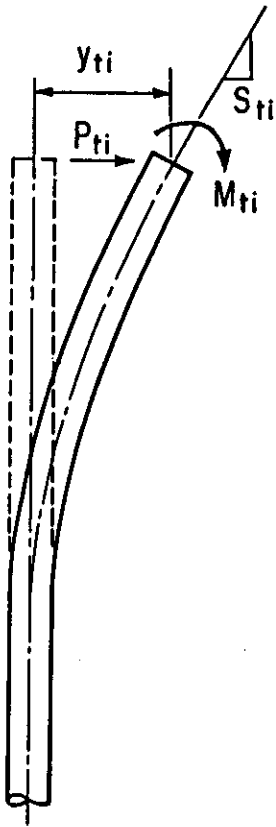
A major finding of this review is that the empirical correlations from one theory cannot always be employed successfully in other theories. Associated with this fact it is also apparent that the assumed soil response, based upon one theory, should not be used to gauge the performance of another theory, especially when one of the theories lacks the complexity of the other. Such a mixture of theories can only lead to misunderstandings or half-truths which obscure the important issues and give false conclusions.

Flowing of soil around piles is one area in which much research could be done. A soil's propensity to flow, or its ability to maintain a stress-free gap, is one of the most poorly understood aspects of soil response pertaining to laterally loaded piles. Very little work has been done in investigating the formation of gaps in the soil in regions of tensile stress. Although many analyses indirectly include some effects from gap formation, due to the use of empirically-based models, there is no way to isolate the importance of gapping on the overall response. The effect of gapping on the behaviour of laterally loaded piles is an area in which much work remains to be done, even before it is possible to be definite about the importance, or otherwise, of soil breaking away from the pile.

The main areas in which gains in understanding of laterally loaded pile behaviour are possible are those of non-homogeneous soil profile response, non-linear modelling of the soil-pile interface in combination with an elastic continuum model of the soil, and the study of the formation of breakaway between pile and soil. The most promising means of accomplishing these gains are by the very economical Modified Boundary Element Method (MBEM) and the more accurate but less economical Axisymmetric Geometry Finite Element Method (AGFEM).

Elements in a Pile Length	50	50	50	25	Variable
L/d	10	25	50	100	Evangelista and Viggiani any L/d
uEd/H	0.580	0.580	0.580	0.482	0.691
$\theta Ed^2/H$	0.233	0.233	0.233	0.153	0.313
uEd^2/M	0.238	0.238	0.238	0.157	0.313
$\theta Ed^3/M$	0.304	0.304	0.304	0.301	0.344

TABLE 2.1 *Results of Evangelista and Viggiani (1976) Compared with the Results of the Recommended MBEM Analysis of Chapter Three with up to Six Elements in the Critical Length, for $E/E_p = 10^{-2}$.*



Known

$$y_{ti} = \left[\frac{P_{ti} T_i^3}{EI} \right] A_{yt} + \left[\frac{M_{ti} T_i^3}{EI} \right] B_{yt} \quad (17)$$

$$S_{ti} = \left[\frac{P_{ti} T_i^2}{EI} \right] A_{st} + \left[\frac{M_{ti} T_i^3}{EI} \right] B_{st} \quad (18)$$

$$T_i^{n_i+4} = \frac{EI}{k_i} \quad (13)$$

Given

1. P_{ti} , M_{ti} , y_{ti} , S_{ti} , and EI .
2. A_{yt} , B_{yt} , A_{st} , and B_{st} as functions of n .

Solve for n_i and k_i from above 3 equations.

Use values of n_i and k_i to find E_{si}

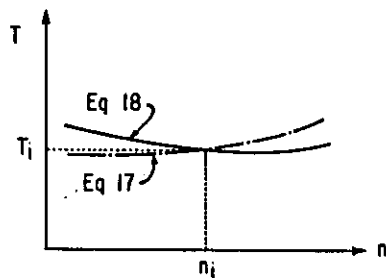
$$E_{si} = k_i \times^{n_i}$$

Solve for the deflected shape of the pile by substituting E_{si} for E_{sn} in Eq 3, and solving Eq 3 for y_i vs. n .

Find p_i vs. y_i at depth x .

$$p_i = -E_{si} y_i \quad (2)$$

General procedure for obtaining p-y relationships from test-pile data.



Values of n and T obtained from Eqs 17 and 18.

FIG. 2.1 GENERAL PROCEDURE USED BY REESE AND COX TO BACKFIGURE p-y CURVES, FROM REESE AND COX (1969)

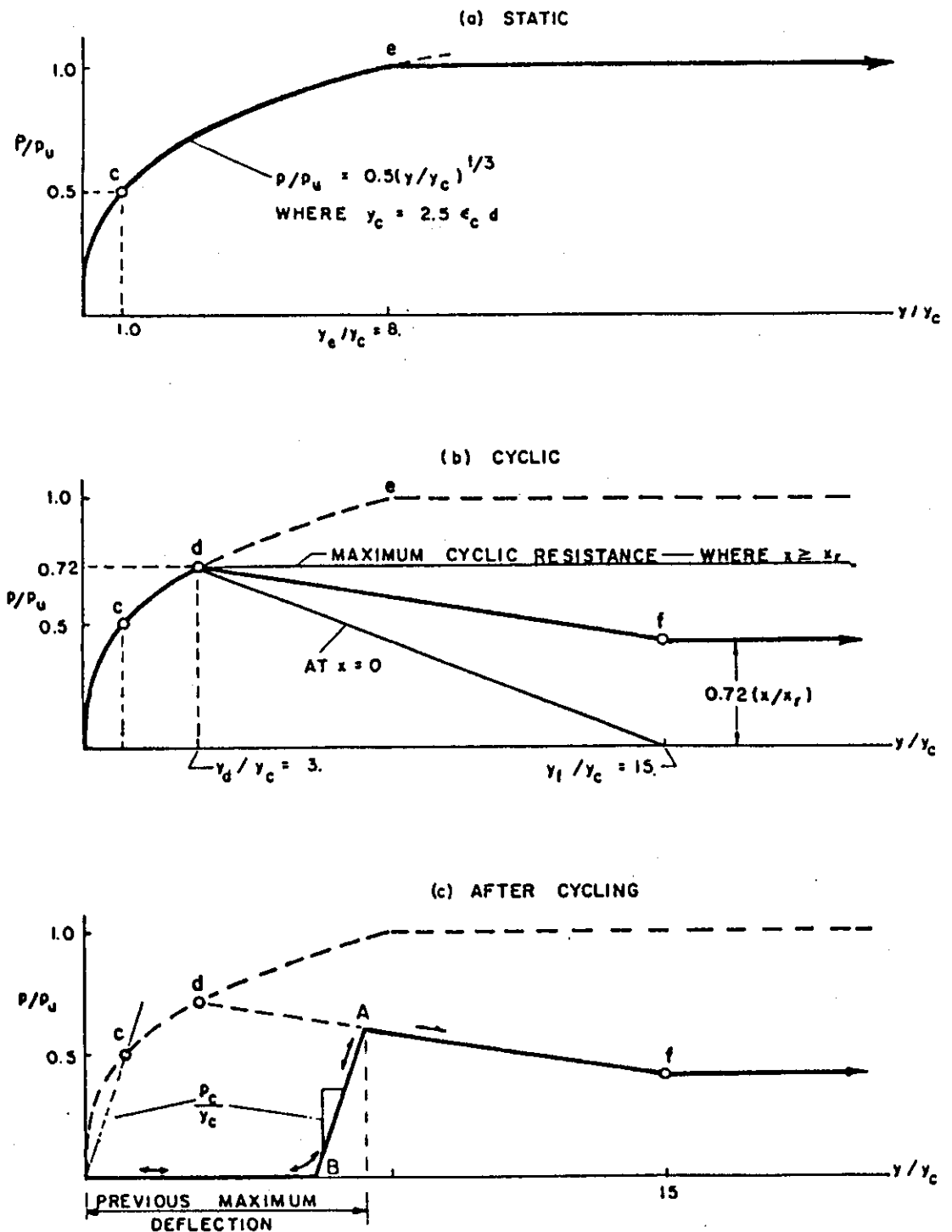


FIG. 2.2 CRITERIA FOR PREDICTING $p - y$ CURVES FOR (a) SHORT-TIME STATIC LOADING, (b) EQUILIBRIUM UNDER INITIAL CYCLIC LOADING AND (c) RELOADING AFTER CYCLING, MATLOCK (1970).

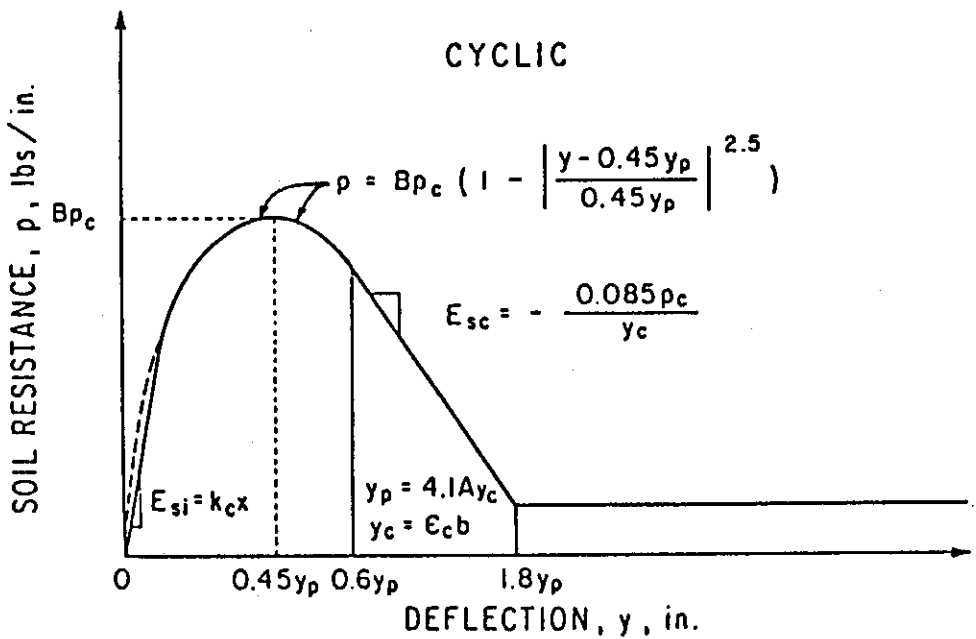
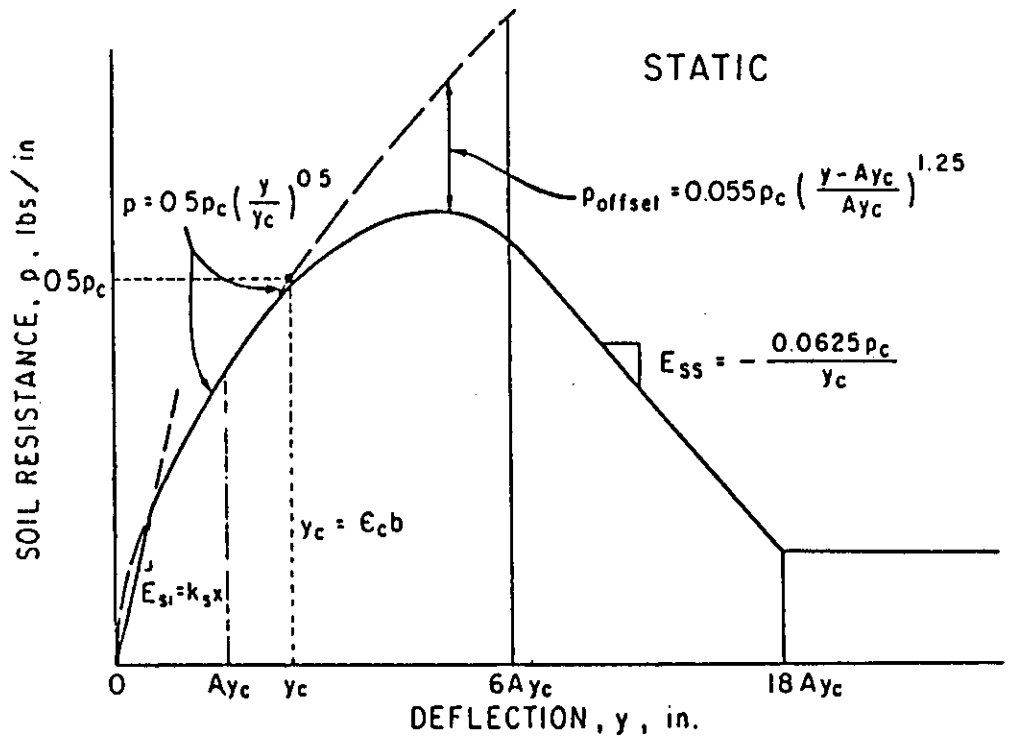


FIG.2.3 CHARACTERISTIC SHAPE OF PROPOSED p - y CRITERIA FOR LATERAL LOADING IN STIFF CLAY, REESE ET AL.,(1975)

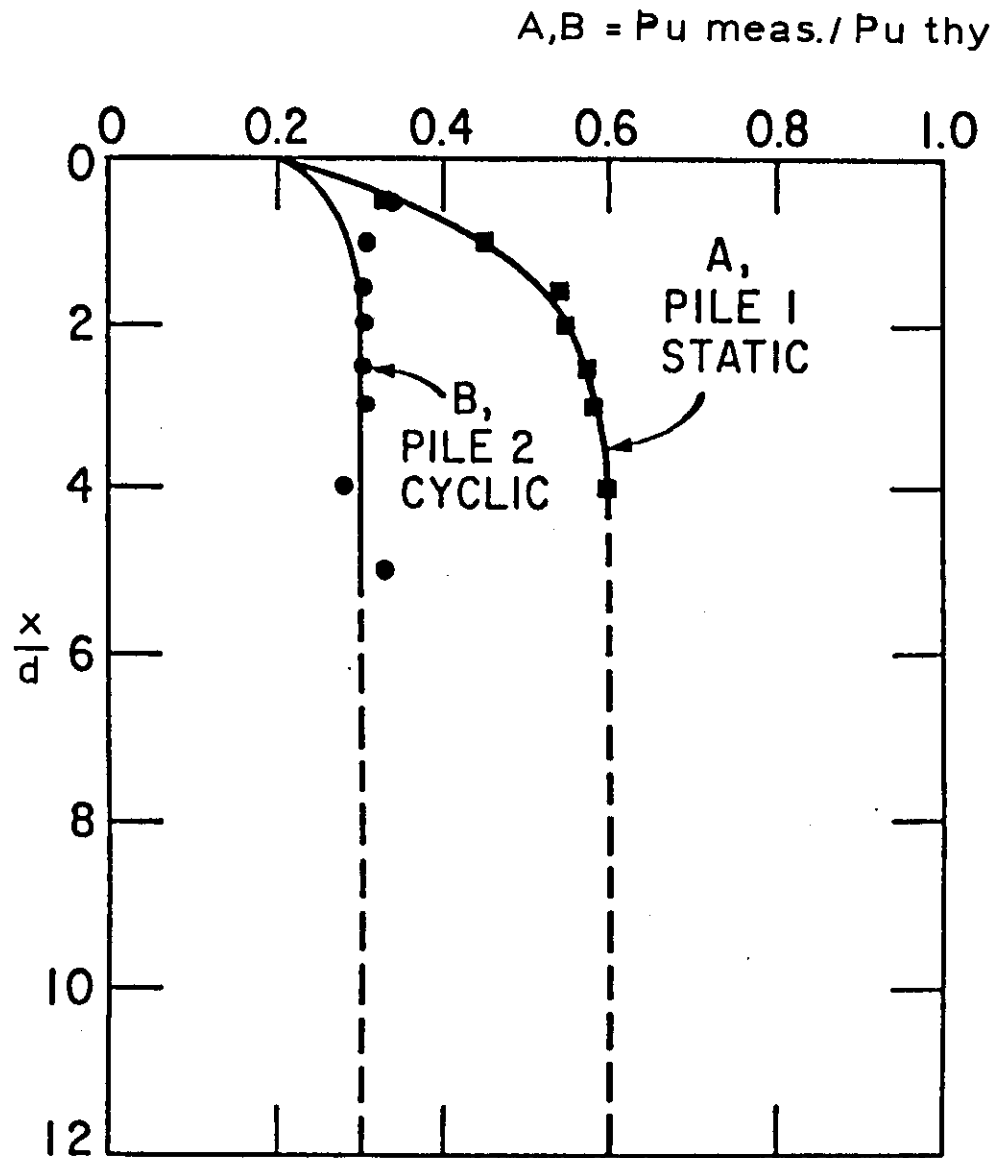


FIG.2.4 NON-DIMENSIONAL COEFFICIENTS A AND B OF
 ULTIMATE SOIL RESISTANCE VS NON-DIMENSIONAL DEPTH.
 REESE ET AL.,(1975)

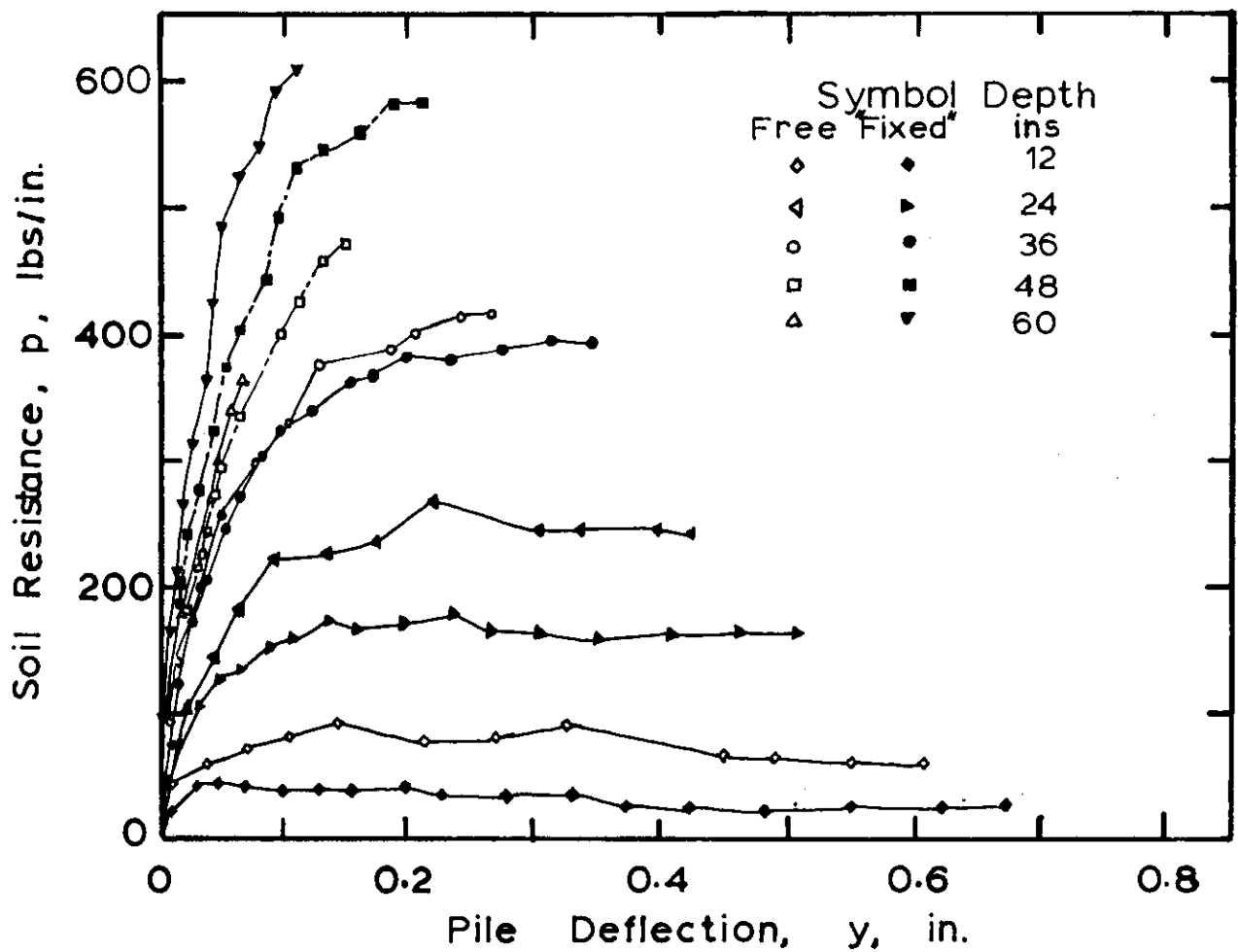


FIG. 2.5 FREE AND "FIXED" HEAD p - y CURVES Reese et al (1975).

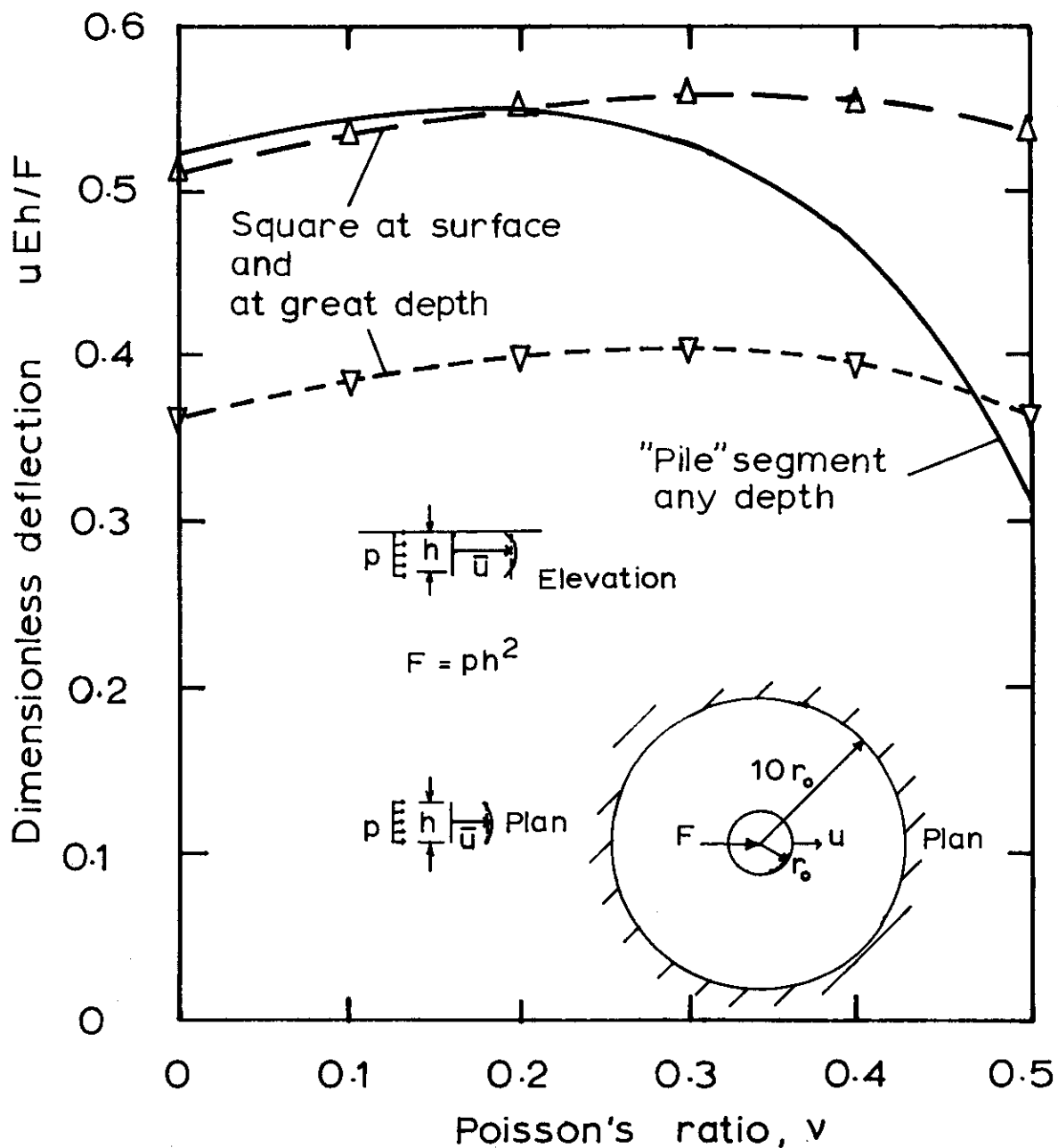


FIG. 2.6 DEFLECTION OF A RIGID PLANE STRAIN "PILE" SEGMENT & MEAN DEFLECTION OF A UNIFORMLY-LOADED VERTICAL SQUARE vs SOIL POISSON'S RATIO.

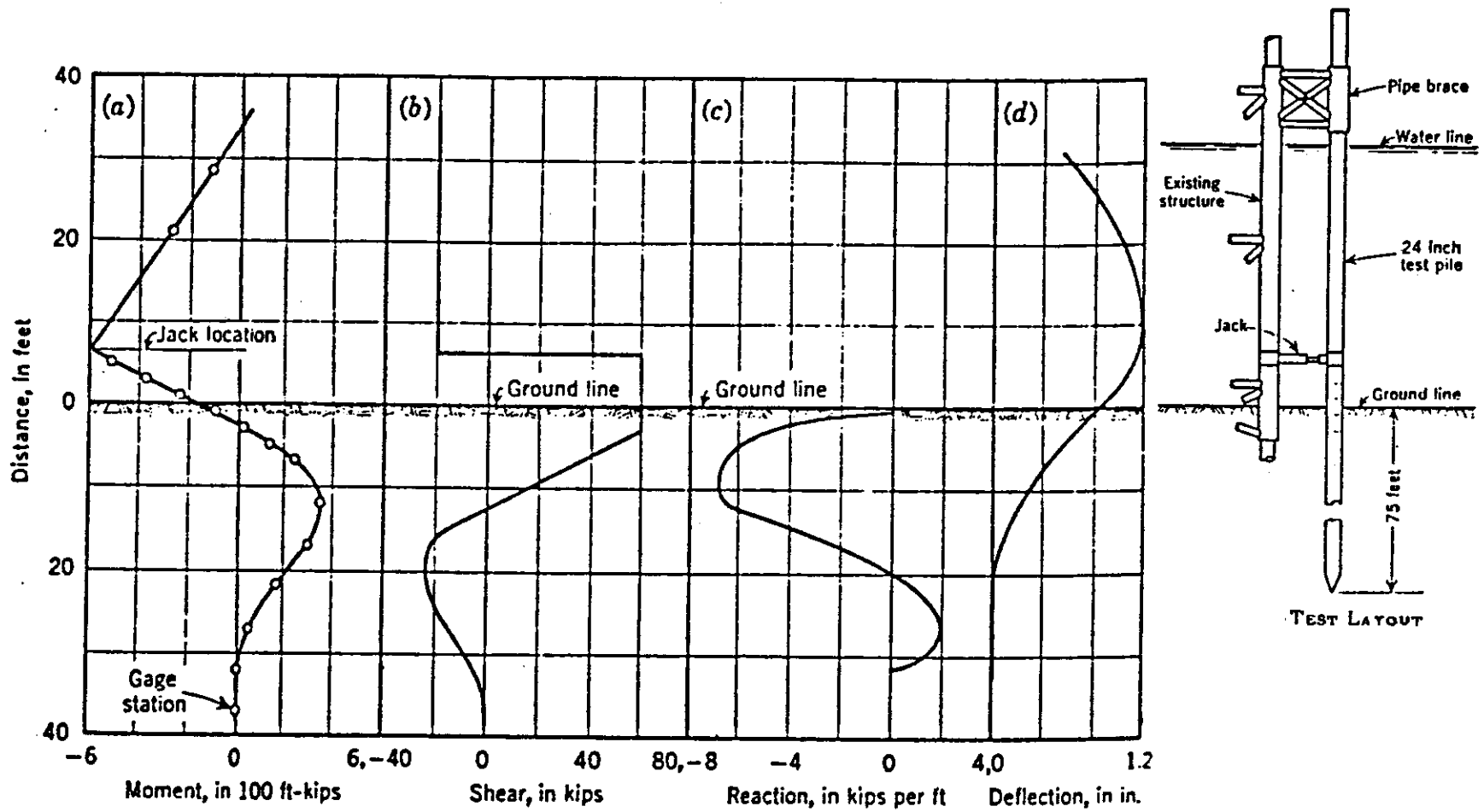


FIG. 2.7 RESULTS FOR 80 KIP LOAD TEST FROM McCLELLAND AND FOCHT, (1956)

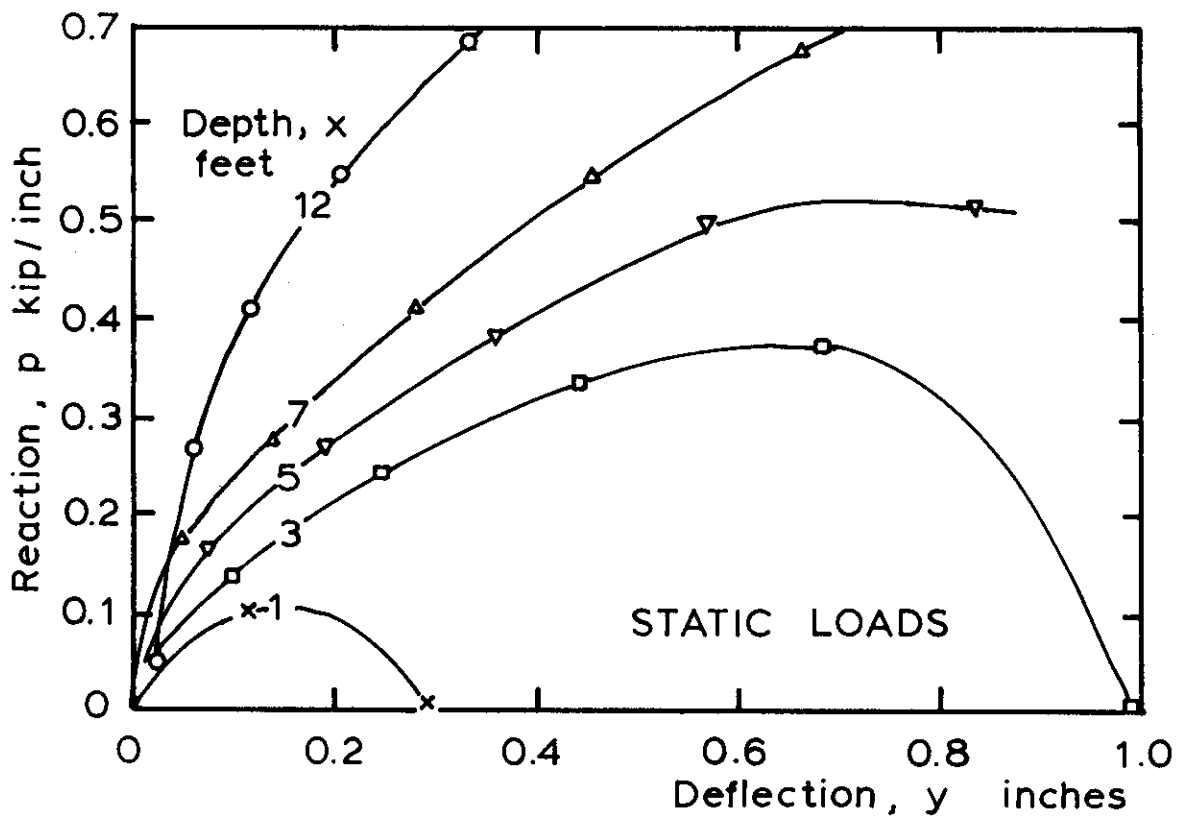


FIG. 2.8 PILE REACTION VERSUS PILE DEFLECTION FROM McCLELLAND AND FOCHT, (1956).

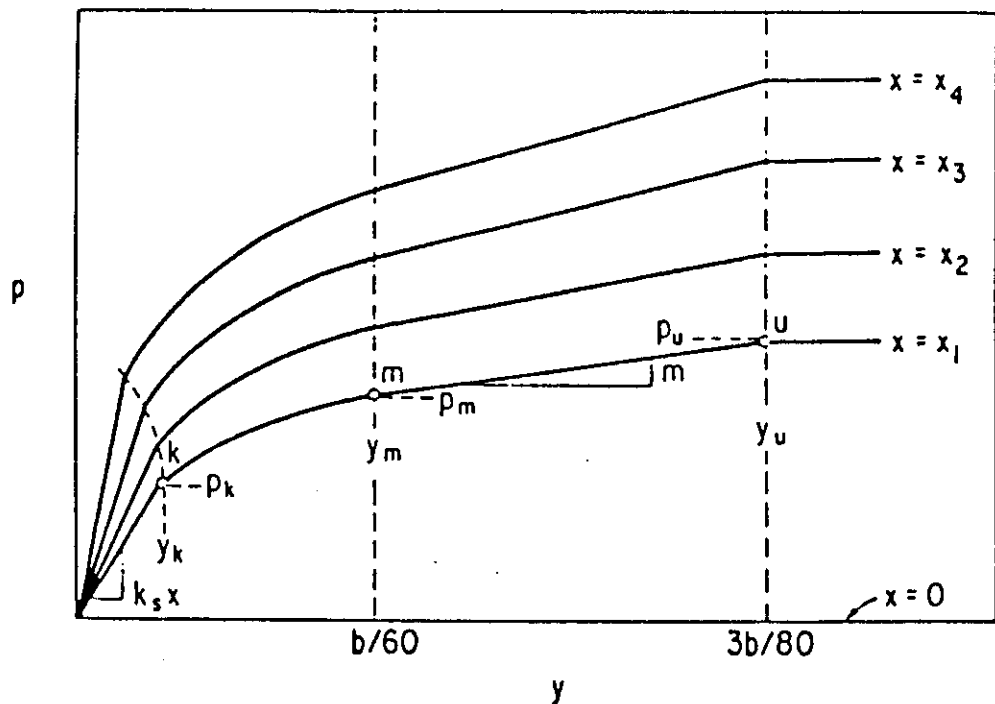
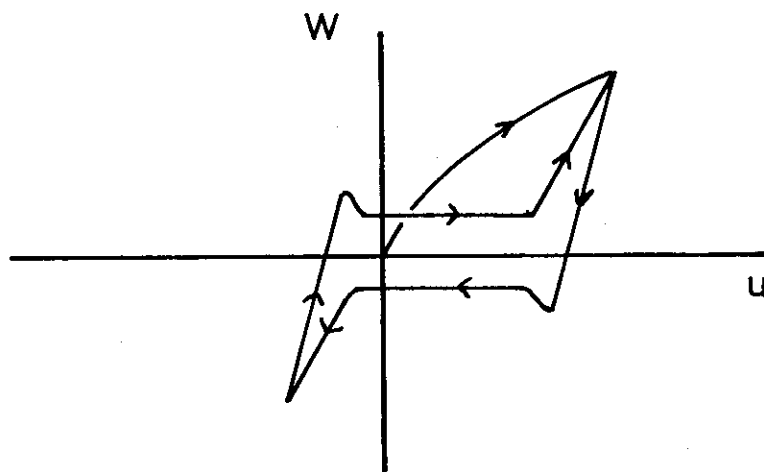
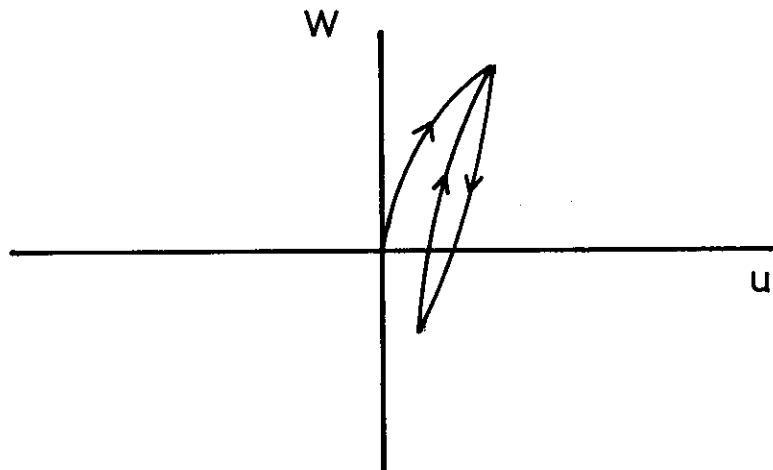


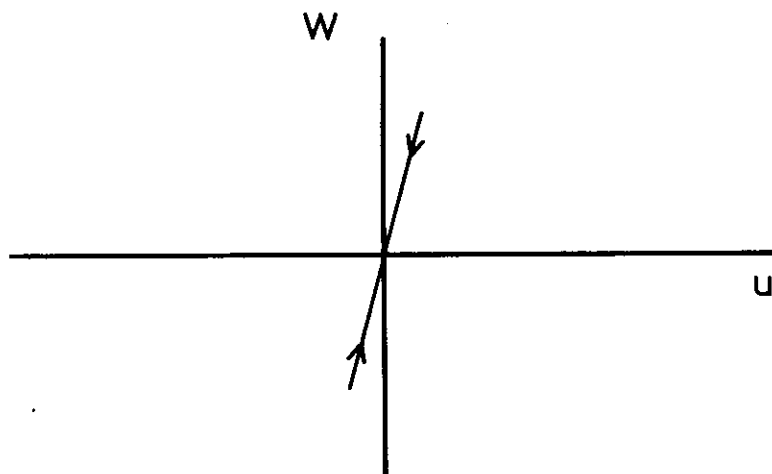
FIG. 2.9 TYPICAL FAMILY OF p - y CURVES FOR SAND FROM REESE ET AL., (1974).



a) Gapped Response in Upper Zone



b) Confined-Flow Response in Middle Zone



c) Linear Response in Deep Zone

FIG. 2.10 GRAPHICAL REPRESENTATIONS OF THE THREE COMMONLY ASSUMED PILE REACTION LOAD-DEFLECTION ($W-u$) RESPONSES

CHAPTER THREE - LATERAL PILE RESPONSE : LINEAR ANALYSIS

3.1 Introduction

In Chapter 2 a range of vertical pile lateral loading analyses were discussed within three categories, namely:

- a) Winkler methods using empirically-based models of soil behaviour with elastic simple beam theory to model the pile,
- b) numerical (Boundary Element) continuum methods of soil modelling, with elastic simple beam theory for the pile, and
- c) a direct application of the elastic Finite Element method to analyse both the soil and the pile.

The empirical, Winkler class of method includes the simplest possible model for the soil that originally appeared as the beam on elastic foundation solution of Hetenyi (1946), but also extends to the highly developed 'p-y' method of Matlock (1970), Reese, Cox and Koop (1974, 1975). The simpler methods in this class are amenable to analytic solution, but the more complex ones require an iterative numerical solution procedure.

It is expedient to initially consider the empirical class of solution to the laterally loaded pile problem, since an analytic result can be obtained that is free from discretisation error, i.e. a precise solution of the model but not necessarily an accurate solution to the real pile problem. It must be emphasised that this class of solution is only as good as the empirical correlations that have been derived from the years of application and research of the method. It is also a restricted area of research since it cannot be logically extended to incorporate interaction between piles in a group.

Notwithstanding this criticism, the accurate solution of this class of problem will provide answers that bear some relation to

those from the other two classes, one common characteristic of all the methods being the use of an elastic-based model of the pile.

The Winkler analysis relies upon the concept of a uniform traction over a small region on the pile-soil interface producing a uniform deflection of the region of soil which is proportional to the traction. This proportionality is governed by a constant that is termed the Coefficient of Subgrade Reaction and is usually connected with a traction and deflection which are normal to the foundation and in the direction of loading.

The shear traction analogy to this normal traction relationship is sometimes referred to as the 't-z' method and has been employed in axially loaded pile load transfer analyses, (Coyle and Reese, 1966; Murff, 1975). As a member of the class of solutions employing a Winkler hypothesis it is therefore useful to also, briefly, consider axial load behaviour and hence in the present study a solution has been found for a compressible axially loaded pile in a Winkler soil.

Using both the axially and laterally loaded pile solutions, the general characteristics of pile behaviour, including the dependence upon geometry and pile-to-subgrade stiffness ratio, can be analytically found for the Winkler soil model.

The Modified Boundary Element Method (MBEM) is not restricted to the (elastic) continuum soil model and can provide numerical solutions using a Winkler soil model. By this means the accuracy of the MBEM numerical solution technique can be assessed. Consequently, the technique can be used in conjunction with the elastic continuum soil model with a clearer understanding of the requirements for a numerically accurate solution. The MBEM technique, using elastic-continuum theory for the soil model,

while an advance on the Winkler class, also requires some approximations to be made that should be investigated.

To this end, it is fruitful to employ the third class of method, the Finite Element Method. Using the FEM has the benefit of a rigorous application of the Theory of Elasticity that is only restricted in its accuracy by an ability to refine the mesh used to discretise the continuum and maintain a numerically viable solution. By comparing the finite element answers for problems allied to pile loading with existing solutions, the ability of the method to model the effects of lateral or axial load on a pile can be assessed.

In this chapter the three methods are studied, and a reliable and computationally inexpensive pile analysis method for an elastic-continuum soil is recommended. This method (MBEM) uses well-accepted concepts and provides adequately accurate solutions for an elastic pile in a linearly elastic soil. Although it does not take proper account of the processes that cause non-linear behaviour, some modifications are possible and provide an insight into the effects of soil yield and soil-pile separation on overall response. However, the basic concept on which it is based is a linear elastic soil element in which all the interaction traction is shared equally between the "back" and "front" of the pile.

In order to extend the analysis of pile-soil interaction a new Soil-Structure Interaction (SSI) solution is required that will logically incorporate the possibility of gap formation along the pile length. This new method can be applied using either the Winkler or elastic-continuum soil models and is described in detail in Chapter five.

3.2 Winkler Approach

In the analysis of laterally loaded piles, frequent use has been made of the concept of a Winkler response from the soil in contact with the pile. The simple assumption of the deflection of a uniformly loaded area being proportional only to the applied traction has supported a wide range of analysis methods in geomechanics. Its simple form has attracted much attention since an analytic solution may be possible. Also, solutions can always be checked by referring to the restriction of proportionality between load and deflection.

Having attracted the engineer by its uncomplicated nature, the Winkler-based analysis must then be extensively correlated with field results in order to provide adequate estimates of real behaviour of laterally loaded piles. This area of research has been well addressed, especially in connection with p-y methods, as discussed in Chapter 2. The correlation of the Winkler solution with actual behaviour, or even with the results of more rigorous types of analysis, must provide excellent agreement for the fitted response over some range of the problems encountered. However a different response, or problem outside of the fitted range, may be poorly modelled by such an approach and lead to the miscalculation of some aspect of behaviour, (Stevens and Audibert, 1979).

The approach that p-y researchers have employed, has been to use a range of empirical correlations between soil type and the relevant parameters used in the p-y curve fitting devices, e.g. those for soft clay, stiff clay and sand that have been developed by Matlock (1970), Reese et al. (1974) and Reese et al. (1975). This complexity in the choice of model and reliance upon empirical correlations detracts from the initially uncomplicated relation-

ship that would seem to be a prime reason for the use of the method. It can be argued that the application of the simple Winkler concept does not warrant the complexity of extensively correlating it with other results since this will negate its most attractive feature, that of being a palatable, quick solution.

The most obvious benefit from use of the Winkler method seems to be the precision of its analytic solution and not necessarily the accuracy with which the solution models the real problem. Recently the Winkler concept has been used by Swane (1983) to consider the difficult problem of shakedown of a single pile subjected to cyclic lateral load. It is this consistent use of this concept, in order to provide an insight into more complex behaviour, that is the strength of the Winkler method.

With the understanding that use of the Winkler concept here is intended to provide an insight into the theoretical behaviour of laterally-loaded piles, including the efficacy of numerical models, and is not presented as a final design method, the linear response Winkler method will now be considered.

3.2.1 Coefficient of Subgrade Reaction

In order to study the problem posed by the pile in a Winkler medium model, it is necessary to consider the basic assumption in more detail than has been commonly used. The Winkler medium has often been thought of as a collection of discrete springs to which the foundation loads are transferred by horizontal displacement from the bending action of the pile. The discrete spring analogy obviously highlights one of the major deficiencies of the method. Each spring will act in isolation and have no influence upon any

other spring, save through the condition of compatibility with the pile. This lack of continuity within the medium precludes any systematic consideration of pile group interaction behaviour. While the spring analogy has its uses, it can only provide a very mechanical or structural quality to the response that belies the continuum nature of the soil.

In general, the traction developed by interaction between the soil and an element of the foundation can have a normal and a shear component. To more comfortably include both, it is proposed here to approach the Winkler concept from a viewpoint different to the spring analogy. Here the relationship between load and deflection will be seen as an expression of behaviour in the form of an isolated Influence Coefficient, i.e. the resulting soil deflection is isolated to the loaded region, and deflection other than at the load is zero.

From the wide range of expressions that might be considered for variation of the Winkler soil stiffness with depth, a useful and tractable form is chosen as a linear increase with depth, from an initial surface value which may be zero. Attention is now given to the form of the isolated Influence Coefficient.

Following the usual convention, the increase of traction existing at the interface between the pile and soil is taken to be directly proportional to the increase in displacement, in the same direction as the traction, i.e. for a normal traction increment p_n and a normal displacement increment u_n ,

$$p_n = k_n u_n \tag{3.1a}$$

and for a shear traction increment p_s and an in-plane displacement

increment u_s ,

$$p_s = k_s u_s \quad 3.1b$$

Therefore the proportionality constants k_n and k_s have units of FL^{-3} . Experience and intuition suggest that these constants will vary with depth and loading level, but this only applies to Winkler-related soil constants as defined here. To understand the dimensional units it is necessary to examine more closely the assumed interface conditions.

First it must be recognised that the Winkler concept, as proposed here, has no meaning if applied outside of the surfaces that are common to the pile and soil, i.e. the interface between pile and soil. This leads to a consideration of the likely traction distribution that will develop at the interface when head loading occurs. Across the pile width, or around the pile perimeter, the deflection at any depth in the direction of loading, u_x will be sensibly uniform, i.e. a rigid deflection pattern. However, down the length of the pile the deflection pattern will not necessarily be of a rigid nature.

Lateral behaviour of the Winkler medium can be represented in terms of a coincident deflection and traction over a small area, within which both are sensibly constant. Thus, we picture the interface having a constant x-directed traction around the pile, varying along the length and proportional to u_x . Similarly for the axial behaviour a variation will occur with depth, while now the vertical shear traction is constant around the pile perimeter and proportional to the vertical deflection, u_z .

Considering the normal traction at the interface and using an

elemental area of width b and depth h , as in Fig. 3.1, equ. 3.1a yields,

$$I_{nF} = \frac{u_n k_n bh}{F_n} = 1 \quad 3.2a$$

and for the same element with a shear traction resisting an applied vertical or horizontal load,

$$I_{sF} = \frac{u_s k_s bh}{F_s} = 1 \quad 3.2b$$

Equations 3.2 define the isolated Influence Coefficients I_{nF} and I_{sF} , for the deflections, u_n and u_s , of the pile-soil interface with respect to normal and shear total loads, F_n and F_s , generated at the interface over the elemental area, $b \times h$. By integrating the elemental forces, F_n and F_s , generated by rigid displacements, u_x and u_z , around the rough pile circumference we arrive at the total load per unit depth of

$$F_x/h = u_x \cdot (k_{sh} + k_n) \pi d/2 \quad 3.3a$$

$$F_z/h = u_z \cdot k_{sv} \pi d \quad 3.3b$$

This applies to a circular pile of diameter d . For a pile idealised as a thin strip of width d eqns 3.4 result.

$$F_x/h = u_x \cdot k_n \cdot 2d \quad 3.4a$$

$$F_z/h = u_z \cdot k_{sv} \cdot 2d \quad 3.4b$$

Equations 3.3 and 3.4 do not provide information about the distribution of traction (around the circumference, or across the width of the idealised pile), but show that the basic form of the

equations involving the Coefficient of Subgrade Reaction, k incorporates the pile diameter, or width, d .

Since k_n and k_s are purely theoretical parameters and not readily amenable to direct measurement or interpretation, the form of eqns 3.3 and 3.4 is usually shortened so that

$$p = k u \quad 3.5$$

where p is defined as $p = F / hd$.

The three equations 3.3, 3.4 and 3.5 essentially express the same relationship and demonstrate that k in equ. 3.5 is not an elementary property of the soil, since it will depend upon the geometry of a problem. Also p is not the pressure existing at the soil interface, i.e. for the thin strip model it is the force resultant of the pressures on the front and the back divided by the frontal area $h \times d$. Thus, the Coefficient of Subgrade Reaction k has the dimensional units of FL^{-3} and does not involve the stress in the soil in its definition. The Coefficient of Subgrade Reaction is related to the purely theoretical proportionality constants k_n and k_s but since these are not readily available, the value of k is usually defined by equ. 3.5 and deduced from insitu measurements.

As pointed out by Terzaghi (1955) and more recently Horvath (1983), the determination of a Coefficient of Subgrade Reaction from surface plate loading tests is fraught with difficulties, since it appears to vary with the size of plate used. Horvath presents various suggestions, including one that the variation is hyperbolic with respect to plate diameter, corresponding to the use of a Boussinesq-based Elastic theory to interpret the plate load test. This would suggest that $k \cdot d (= E_s)$ is a more fundamental

parameter and this has two results for pile analysis. The units of E are then comparable to those of Young's modulus and the "pressure" becomes more realistically defined as the load per unit depth ($W = F/h$) as is used by most p-y theories, giving

$$W = E u_s \quad 3.6$$

It might then appear that the necessary parameter can be found from plate loading tests performed at the site of the pile installation or from laboratory investigations. Unfortunately the situation is more complex. The non-homogeneous nature of the soil in the field, and the limited size of the soil mass in tests that are possible in laboratories, preclude direct applications of Boussinesq's Theory. Also, any analysis of experimental results that does not attempt to consider at least the limited soil depth for vertical plate loading, will not allow comparison with behaviour from elastic continuum theory.

A further complication is that the normal type of test for obtaining an estimate of the soil Elastic Young's modulus, or the Coefficient of Subgrade Reaction, is the vertically loaded plate test referred to by Horvath (1983). Even for a homogeneous isotropic medium, there is no reason to assume that the lateral value of Coefficient is the same as the vertical. In order to quantify the possible error involved, the results of an elastic-continuum analysis may be used to compare the response of plates at the surface and deeply buried plates.

Two types of plate geometry, square and circular, and the two situations, at the soil surface and at great depth, are considered. The deflection of a rigid circular plate at the

surface, Poulos and Davis (1974), and at depth, Selvadurai (1976), are given in Table 3.1. It should be noted that the orientation of a deep plate with respect to the surface will have no effect upon the response. Also in Table 3.1 are the mean deflections of a uniformly loaded square at the surface, due to Giroud from Poulos and Davis (1974) and an approximate solution for response of a square at great depth. The approximate solution for a square at great depth is based on the use of Elastic Theory and is described in section 3.3 of this chapter. As stated, the response of the deep square is unaffected by orientation but the surface response (of Giroud) is valid only for a uniformly vertically loaded square situated horizontally on the surface.

From the solutions, for surface and deep plates, approximations for the ratio of the horizontal to vertical Coefficients of Subgrade Reaction, for a circle and a square, may be found. The ratio of the influence coefficients of the vertically loaded surface area to any deep loaded area varies between 2.0 and 2.5 as Poisson's ratio varies from one-half to zero. A value of approximately two is expected, since at depth the load is transferred to the soil by both the front and back of the buried body. If two surface loading solutions were used in an attempt to model the effect of burying the area between two half-spaces, the result would give a surface (vertical) to deep (horizontal or vertical) influence coefficient ratio of two exactly. Since such an attempt makes no allowance for the continuity of the free surfaces of the two half-spaces, that are here facing each other, it would be expected that the correct deep solution would be more than twice as stiff as the surface solution.

The use of an elastic-continuum model will thus predict the buried horizontal and surface vertical Coefficients of Subgrade Reaction to be different. This is a reasonable result that could have been predicted from considering the form of equ. 3.4a for the thin strip pile element ($p = 2 k_n u$) and at the surface equ. 3.1a ($p = k_n u$).

A commonly accepted characteristic of the Coefficient of Subgrade Reaction is an increasing value with depth and this trend can also be seen if an elastic-continuum solution is used to backfigure the Coefficient for a particular problem. The problem chosen here is a vertically oriented rectangular area buried in an elastic half-space and loaded horizontally by a uniform pressure. Interaction within the elastic mass and the proximity of the surface give an average deflection of the rectangle that varies with embedment depth and width to height ratio of the rectangle. Analysis by the Winkler method does not include the effects of interaction within the mass, or the proximity of the free surface, and so would predict a constant deflection response for any depth, unless the Coefficient of Subgrade Reaction varied with depth.

Using equ. 3.5 as the definition of the Coefficient of Subgrade Reaction k and letting $E_s = kd = pd/\bar{u}$, the value of E_s that gives the same deflection as would occur for the same problem in an elastic mass can be found. Therefore the resulting value of E_s will vary in some manner and this can be compared to the variations commonly assumed for E_s . As a specific illustration, the dimensionless average deflection response, $I = \bar{u}E_s/pd$, of a square element of soil with length of sides d , is presented in Fig. 3.2 and is seen to be a function of depth below the surface. With the elastic soil Young's modulus, E constant with depth and noting $E_s = E/I$ represents the Subgrade Modulus, the plot in

Fig. 3.3 results, showing a value heading towards zero at the surface and reaching a limiting value with increasing depth.

It would be tempting to pursue this approach but it would result in a poor model because the use of elastic-derived quantities in a Winkler analysis, will ignore the effect of interaction in the soil and lead to an inconsistent modelling. As an example, consider uniform vertical loading of a square on the surface and horizontal loading of two vertical squares within the soil, one at great depth and one at the surface. Thus, a square loaded by a normal traction of unit total load is analysed to obtain the average deflection of the square, that being taken as an approximation for the behaviour of a rigid area.

Each of the three squares is composed of two component rectangles. At great depth the orientation of the square makes no difference to the deflection response providing the material is isotropic. So at depth, as for vertical loading on the surface, it is sufficient to consider the square symmetrically divided into two component rectangles without specifying their orientation. At the surface the orientation of the buried square is vertical and has one side parallel to and at the surface. The vertical surface case will thus allow two methods by which the square may be equally divided; parallel and at right angles to the surface.

By taking a mean of the two average deflections of the component rectangles, the deflection of the rigidly loaded square can be estimated, based on a Winkler-style of superposition excluding interaction. The elastic-continuum based mean deflections of the squares, the deflection from use of Winkler theory and from Winkler-style superposition of the elastic-continuum based deflections of the component rectangles are presented in Table 3.2.

It is obvious that the application of the Winkler-style of superposition, to the component rectangle deflections from elastic theory, underestimates the average deflection of the square soil element. However, direct use of the Winkler method, assuming E_s is constant with depth and equivalent to E , results in the predicted deflection being 0.5 for the buried cases and 1.0 for the case of surface loading, from use of equ. 3.4a and 3.1a.

Although the direct use of the Winkler method overpredicts the average deflection of both the surface horizontal and deep uniformly loaded squares and underpredicts the response of the vertical square at the surface, it does have an advantage over the mixed Winkler and Elastic-derived method. This advantage is that it is consistent, with the result of using Winkler style superposition on the two Winkler-based deflections of the component rectangles being the same as the prediction using the full square. The correct use of the elastic-continuum method, including interaction between rectangles, provides consistent behaviour but incorrect use of elastic-continuum based deflections with Winkler-style superposition leads to inconsistent results.

Because of the small dependence of pile head response on the soil response at depth, the value of isolated Influence Coefficient at depth (as was recognised by McClelland and Focht, 1956) would be difficult to measure accurately by field testing of piles. This may explain the wide range of soil stiffness variations with depth that have been proposed. It may be conjectured that the apparent increase of soil stiffness with depth obtained from field test data, is not solely a function of basic soil properties increasing with depth and that such a stiffness increase will not necessarily continue indefinitely.

Thus the Coefficient of Subgrade Reaction, or Subgrade Modulus, for normal loading in an isotropic homogeneous elastic mass is a function of orientation near the surface and varies with depth, becoming a constant at great depth, independent of orientation.

No matter how "unified" a method using Subgrade Reaction becomes, it still relies upon empirical correlations and strictly only applies to analysis of one type of pile loading with limited predictive capabilities. The Elastic method on the other hand is quite general and, used intelligently, will allow a far more unified approach to modelling of a variety of foundation problems.

In this thesis the Coefficient of Subgrade Reaction k will be combined with the width or diameter of the pile and therefore have the same units as Young's modulus. To avoid confusion the term "Subgrade Modulus" will be used and given the symbol E_s , as distinct from the soil Young's modulus, which will be denoted by the symbol E . Thus, $E_s = kd$ where the diameter d will be the projected width of the pile for lateral loading and will be the diameter of a circle with a perimeter equal to that of the pile for axial loading.

The argument as to which of the two methods of modelling the soil, Winkler or Elastic, is more accurate for pile analysis, is not answered in this section. The consideration of how the soil behaves compared with the two approaches is very much a personal judgement. While the Winkler parameters are only pertinent to the analysis of laterally loaded piles, and the model lacks any interaction between elements of the soil, the Winkler model represents a way to obtain analytic results free from discretisation errors for verification of the numerical technique of the MBEM analysis.

3.2.2 Uniform Soil Profile Winkler Analysis

Under this heading, the linear analysis of a single pile in a Winkler soil with a uniform Subgrade Modulus is outlined. Both the lateral and axial loading of single piles are considered, with the solutions being capable of closed form expression. It is useful to review the form of this solution for lateral loading and then consider the companion problem of an axially loaded pile in a soil modelled by a constant vertical Subgrade Modulus. The solutions will be valuable for comparison with other methods of analysis, checking of computer coding and indicating trends of response that might be expected in more complex analyses.

Lateral Case

The first complete solution of this problem was by Hetenyi (1946), in his work on beams on elastic foundations. He presented the deflection, rotation, bending moment and shear force due to end loading of an infinitely long beam, and a beam of finite length, supported by a Winkler soil. The behaviour of a pile in a Winkler soil, as well as that of a beam on an elastic foundation, is governed by the differential equation of simple beam bending which can be expressed as

$$E I \frac{d^4 u}{dz^4} = W \quad 3.7$$

where $E I$ is the constant beam bending stiffness and u is the deflection of the beam in the direction of W the distributed reaction load acting on the pile (pd).

Equation 3.7 will define the behaviour of the pile, and from

the compatibility of the soil with the pile, will also define the soil response. The distributed soil loading caused by the interaction of the pile and soil will, for the simple Winkler analysis, depend solely upon the distribution of soil deflection. This dependence is governed by equ. 3.6, namely $W = E_s u$.

The combination of eqs 3.6 and 3.7 together with the fact that the soil interaction load must act in opposite sense to the pile interaction load, leads to the differential equation

$$d^4 u/dz^4 + 4Y_s^4 u = 0 \quad 3.8$$

where $Y_s^4 = E_s / (4E_p I_p)$.

The definition and sign convention of variables used in the analysis are shown in Fig. 3.4a. The solution of equ. 3.8 is straightforward, resulting in the general solution

$$u = e^{Yz} (C_1 \cos Yz + C_2 \sin Yz) + e^{-Yz} (C_3 \cos Yz + C_4 \sin Yz). \quad 3.9$$

Any particular solution will specify the values of the constants $C_1, C_2, C_3,$ and C_4 , from the boundary conditions at the head and base of the pile. The boundary conditions involve the specification of the moment or rotation and shear or translation of the pile tip or head. Successive differentiation of equ. 3.9 will provide the analytic expressions for rotation, moment and shear, see Fig. 3.4a. Since four constants are involved there must be four equations, usually in terms of the boundary conditions at the head and tip but sometimes a restraint or fixity may be required at intermediate positions along the pile.

The four constants may be found numerically or by analytic inversion of the four equations in four unknowns. If the inversion is performed analytically, then closed form expressions such as those of Hetenyi result. It is very often more convenient to solve numerically for the constants and thereby allow a range of boundary conditions to be incorporated. For computer applications it is especially useful to allow the four equations to be produced for a generally defined set of head and tip boundary conditions. In this way a large variety of head and tip restraints may be easily incorporated in one program.

The solution can be expressed in non-dimensional terms which result in the unique specification of any pile in a uniform Winkler soil in terms of a relative pile to soil stiffness ratio

$$K_R = \frac{E I_p^4}{p_p / E L_s^4} \quad 3.10$$

where L is the pile length and $4(YL)^4 = K_R$.

The relative stiffness, K_R , has been used previously by Poulos (1971a) and Bannerjee and Davies (1978) with continuum analyses, and in other forms that are directly related (Barber, 1953). The results for head response from the analysis are then presented in a form that is non-dimensionalised with respect to head loads H and M , the soil modulus E_s and the pile length, L . These influence coefficients are

$$\begin{aligned} \frac{u E_s L}{H} &= I_{uH} \\ \frac{\theta E_s L^2}{H} &= I_{\theta H} : \frac{u E_s L^2}{M} = I_{uM} \\ \text{and } \frac{\theta E_s L^3}{M} &= I_{\theta M} \end{aligned} \quad 3.11$$

It is important to note that $I_{uM} = I_{\theta H}$ since the pile and soil obey the reciprocal theorem, attributed to Betti by Love (1928).

Therefore a method exists by which the problem of a laterally loaded pile in a uniform Winkler soil can be solved for deflections, rotations, moments and shears for a wide range of tip and head boundary conditions. The solution is valid for all pile to soil stiffness ratios, from rigid to flexible, as long as the pile and soil remain in intimate contact along the pile length. An important characteristic of the solution is that the results do not depend upon the pile length to diameter ratio and the diameter only appears in the definition of the Subgrade Modulus, E_s .

Axial Case

For the case of axial loading of a pile in a Winkler profile with a uniform vertical Subgrade Modulus, a similar solution may be found to provide the axial deflection, axial load and side shear acting on the pile at any depth. Considering the equilibrium of a small segment of pile as shown in Fig. 3.4b, it is found that

$$\frac{d\sigma}{dz} = \frac{t_s}{A} \quad 3.12$$

where σ is the axial compression stress acting over A the pile cross-section area and t_s is the shear traction acting around S the pile perimeter with $S = \pi d$.

The pile axial stiffness (assuming Poisson's ratio of the pile is zero) can be expressed as

$$E_p \frac{dw}{dz} = -\sigma \quad 3.13$$

where E_p is the pile Young's modulus and w is the deflection, positive downwards. Combining eqs 3.12 and 3.13 provides the

differential equation

$$\frac{d^2 w}{dz^2} = \frac{-t_s S}{E_p A_p} \quad 3.14$$

The soil response can be expressed by using a vertical Coefficient of Subgrade shear reaction, k_s with

$$t_s = k_s w \quad 3.15$$

where t_s is the soil shear traction.

Noting that the soil and pile interaction shear tractions will be of equal magnitude and opposite sign, the resulting differential equation is

$$\frac{d^2 w}{dz^2} - a^2 w = 0 \quad 3.16$$

with $a^2 = \frac{\pi E_s}{E_p A_p}$ and $E_s = k_s d$.

The general solution takes the form of

$$w = C_1 e^{az} + C_2 e^{-az} \quad 3.17$$

which will require two boundary conditions in order to produce a particular solution. The applied head load may be used with equ. 3.13 and the derivative of equ. 3.17 to provide one boundary condition. The pile tip will provide the other boundary condition with the base axial compressive stress, as from equ. 3.13, equated with the vertical normal traction generated at the soil-base interface as given by

$$\sigma_b = k_b w \quad 3.18$$

The appropriate choice of k will cover the range of base conditions from a zero base load to a fully fixed base. This is similar to a previous solution (Murff, 1975) but, like the laterally loaded pile model using a Winkler soil, is of limited use because of their restriction to a medium with a constant horizontal and vertical Subgrade Modulus with depth.

These two methods of analysis, for the lateral and axial response of single piles in a soil that obeys a Winkler response law, result in closed form analytic solutions that are unaffected by numerical methods of solution. Also, the effect of a variety of base and head boundary conditions may be investigated. However, the specification of the various Coefficients of Subgrade Reaction is not felt to be possible except via extensive empirical correlation, since they have no theoretical link between themselves or any measurable property of soil.

3.2.3 Linear Soil Profile Winkler Analysis

The problem of axial and lateral loading of an elastic pile in a Winkler medium with a Subgrade Modulus that varies linearly with depth may be expressed in two equations:

axially equ. 3.14, i.e.

$$\frac{d^2 w}{dz^2} = - \frac{t \pi d}{E A}$$

and laterally equ. 3.8, i.e.

$$\frac{d^4 u}{dz^4} = \frac{p d}{E I}$$

where z is the coordinate aligned with the pile length,

d is the diameter, (effective pile width for the laterally loaded case or effective pile diameter for the same circular pile perimeter for the axially loaded case),

u, w are the deflections in the lateral and axial cases respectively,

E is the pile modulus,

I, A are the Second Moment of Area and cross section area of the pile and

t, p are the axial pile-soil interface vertical shear traction and the lateral pile-soil interface normal traction respectively.

The basic Winkler assumption leads to eqs 3.5 and 3.15, i.e.

$$p = k_n u \quad \text{and} \quad t = k_s w.$$

Further, the normal traction at the base of the axially loaded pile requires equ. 3.18, namely

$$\sigma_b = k_b w.$$

Also, $E(z) = E_s + m \cdot z$ where k_s , k_n and k_b are the Coefficients of Subgrade side shear, side normal and base normal Reaction while E_{so} is the pertinent value of Subgrade Reaction Coefficient at the surface multiplied by the pile diameter, to obtain units of stress, and m is the increase of the value of Coefficient of Subgrade Reaction with unit depth, again multiplied by the pile diameter. Note that E_s is not the same value for side shear, side normal and base normal traction cases.

The substitution $Z = (E_s + m z)/E_{so}$ is made and the solution expressed as a power series,

$$u_m \text{ or } w_m = Z^m \sum_{n=0}^{\infty} a_n Z^n \quad 3.19$$

Substitution of equ. 3.19 into eqs 3.8 and 3.14 results in two polynomials in Z with coefficients that must vanish for a non-trivial solution. Equating each coefficient to zero provides the information that m will take values 0, 1, 2 and 3, for the lateral case and m becomes 0 and 1 for the axial case. Further consideration provides a recurrence relationship for the terms a_n . Choosing any convenient value for a_0 the remaining values of a_n can be found for any n . For each m the particular solution will require integration constants providing the general solutions,

$$u = C_{00} u_0 + C_{11} u_1 + C_{22} u_2 + C_{33} u_3 \quad 3.20a$$

and

$$w = C_{00} w_0 + C_{11} w_1 \quad 3.20b$$

Successive differentiation of Eqns 3.20 provides the means of incorporating the boundary conditions relevant to each problem. Laterally the boundary conditions arise from a knowledge of the

values of moment, (M) and shear, (H) occurring at both the top and base of the pile, and the relationships

$$\begin{aligned}
 M &= \frac{E I}{p p} \frac{d^2 u}{dz^2} = \frac{E I}{p p} \left(\frac{m}{s} / \frac{E}{s_o} \right)^2 \frac{d^2 u}{dZ^2} \\
 H &= \frac{E I}{p p} \frac{d^3 u}{dz^3} = \frac{E I}{p p} \left(\frac{m}{s} / \frac{E}{s_o} \right)^3 \frac{d^3 u}{dZ^3}
 \end{aligned}
 \tag{3.21}$$

The resulting four equations can then be solved for the four integration coefficients C_0 , C_1 , C_2 , and C_3 .

Axially the boundary conditions arise from the known axial compressive stress σ_o , at the top of the pile from the applied load, P, and the relationship between the base deflection w_b , and normal stress generated at the base of the pile σ_b .

$$\begin{aligned}
 \sigma_o &= P/A = -E \frac{dw}{dz} : z = 0 \\
 \sigma_b &= E \frac{w_b}{b} = -E \frac{dw}{dz} : z = L
 \end{aligned}
 \tag{3.22}$$

The resulting two equations can then be solved for the two coefficients C_0 and C_1 .

Equations 3.20 and 3.21 or 3.22 are then used to calculate the desired variable at any depth along the pile. The axial problem can be seen to have two types of Winkler relationships with side shear traction related to vertical displacement and base normal traction related to vertical base displacement. This means that in general E_{sb} at the base does not equal E_{sL} ($= E_{s_o} + \frac{m L}{s}$) on the pile circumference.

The strict application of Winkler theory to the laterally loaded pile case would lead to inclusion of a base (moment and shear) response as it rotated and translated, governed by extra

coefficients of a similar nature to the Coefficients of Subgrade Reaction already mentioned. This condition is usually ignored by most lateral pile analyses, since it is expected that the response of the long flexible piles usually encountered in practice, have a minimal effect from the base interface stresses.

It must be emphasised that the models used in this section to solve the pile problem contain no interaction within the soil mass and, especially for the axial case, this may lead to poor correlation with observed behaviour. However, it is expected that the general trends with variation of relative pile-soil stiffness, displayed by these models, will also occur in practical situations and in more complete elastic continuum analyses. The benefit of using such simple models is the exactness of the solutions obtained, with no ambiguity arising from the use of the numerical procedures that are usually required by more complex models.

Once the simple model behaviour is known, the knowledge can then be applied to the investigation of the behaviour of the more complex models that use solution techniques that have been checked for broad agreement with the Winkler results. This is especially true for the Modified Boundary Element Method approach that will now be described.

3.3 Boundary Element Approach

The general name for the method used in this section is Boundary Element Method and the specific model employed here is sometimes called the Modified Boundary Element Method (MBEM). It consists of determining a set of soil deflection influence coefficients in terms of distributed loads on a defined surface (interface) and the enforcing of compatibility between the soil and pile interface deflections. To analyse the pile, the method of Finite Differences proves most amenable to this type of problem and it is used here, although it is possible to use other methods such as a Finite Element Beam model for the pile (Poulos and Adler, 1979, and Swane, 1983).

With compatibility between pile and soil enforced, the boundary conditions at the head and tip of the pile are required to complete the solution. The four conditions are composed of a set of two alternative states, at each end of the pile,

- a) a defined translation or horizontal shear value and
- b) a defined rotation or moment value.

The chosen boundary conditions can be combined to provide a full range of socketed, pinned, fixed or floating ends to the piles analysed.

The soil influence coefficients may be found by a number of methods including

- a) a theory based upon the Winkler assumption or
- b) an elastic-continuum based theory.

By using the Winkler assumption the results can be directly compared with the analytic methods developed in section 3.2. This provides a check upon numerical accuracy of the Finite Difference

scheme employed to model the pile and will provide a guide to the degree of discretisation necessary to obtain accurate numerical solutions. The continuum based theory may then be employed with some degree of confidence and the spurious behaviour due to discretisation errors can be more easily assessed.

At this stage the use of elastic theory, based upon the results of Mindlin (1936), is limited to consideration of a homogeneous elastic half-space model for the soil. This model is thus restricted in its application to real problems and so requires a number of approximations in order to extend its usefulness. These extensions will be considered in section 3.5 following the section on use of finite elements to model the elastic soil and pile.

3.3.1 Winkler Soil Element

The MBEM analysis requires an influence matrix that connects soil deflections, at stations down the pile to the distributed loads that are generated by the interaction between soil and pile. In the terminology of the p-y method, the distributed load is given the symbol "p" and the lateral deflection the symbol "y". In this thesis "p" will be more correctly given the symbol "W" and "y" changed to "u" to avoid confusion with normal traction, p and Cartesian coordinate, y. Thus "p-y" becomes "W-u" and eqn 3.6 will replace the familiar "p = ky" expression, namely $W = E_s u$.

It should be noted that W is the total distributed load acting between the pile and soil, which does not directly give the stress state in the soil. The assumption of complete adherence between the pile and soil, together with the inherent assumption

that only the total reaction load is necessary to define both the pile and soil response, leads to the stress state in the soil being antisymmetric. Thus, the stress change in the soil close to the pile face due to pile-soil interaction, can be calculated on the basis that half the distributed load on the pile will act upon both the back and front face of the soil.

A more complex picture will evolve when non-linear soil response and soil-pile breakaway are considered. In this chapter attention is restricted to a soil element, either Winkler-based or Mindlin-based, that always transfers load at the pile-soil interface in an antisymmetric manner.

The value of E_s for loading of a pile modelled as a thin plate, will thus be seen to be twice that which would be associated with loading of a surface foundation assuming the Coefficient of Subgrade Reaction, k is a constant. This agrees with intuition, as long as the n adhesion and antisymmetric assumptions are valid. Assuming a linear distribution of E_s with depth leads to

$$E_s(z) = E_{so} + m_s \cdot z \quad 3.23$$

where the subscript "s" identifies the property as a Subgrade related (Winkler) property. The above two equations may be combined to provide a variety of expressions for the isolated Influence Coefficient as a function of soil modulus distribution defining parameters $n_{sd} = E_{so} / E_s(d)$ or $n_s = E_{so} / E_s(L)$:

$$u_s E(d)d / F = (d/h) / (n_{sd} + (1 - n_{sd})z/d) \quad 3.24a$$

$$u_s E(L)d / F = (d/h) / (n_{sL} + (1 - n_{sL})z/L). \quad 3.24b$$

Where F is the total force acting over the rectangle of width d and height h .

Thus, a set of influence coefficients consisting of a matrix with the on-diagonal terms given by either of the eqs 3.24, and the off-diagonal terms set to zero, can be used in the MBEM numerical analysis to model a pile in a Winkler-based soil profile. This is valid for a soil response described by a surface Subgrade Modulus value, E_s and an increase of Subgrade Modulus with depth, m_s . Any distribution of Subgrade modulus may be considered by using

$$u_s E(z)d / F = (d/h) \quad 3.24c$$

allowing any soil modelled by a Winkler-medium problem to be analysed by the numerical MBEM program developed in this thesis.

3.3.2 Mindlin Elastic Soil Element

The elastic method of analysing laterally loaded piles, that is used here, is based upon the equations of Mindlin (1936) for the displacements produced by point forces in an elastic homogeneous half space. The integration of the Mindlin equations, and expression of deflections due to uniform loading of a buried rectangle, was accomplished by Douglas and Davis (1964). They presented the expressions for both the top and bottom corner deflection of a rectangular, vertically oriented, plane area due to a uniform normal pressure acting over the area.

Using superposition with the results of Douglas and Davis it is possible to find the deflection anywhere within the plane containing the loaded rectangle, both inside and outside the loaded area.

The use of the integrated Mindlin result obviates the need for special attention, that other elastic methods require, when the deflection of the loaded area due to its own point load is considered. Several authors have reported various methods by which an infinite deflection at the point of application of a point force can be bypassed, e.g. Spillers and Stoll (1964) and Randolph (1977), but the chosen method avoids such approximation.

The use of a normal uniform pressure will also provide a more realistic model of the soil stress conditions than point loads and gives the width of the pile some influence. If the point-force method were employed directly, the result would not depend upon the width or diameter of the pile, unless a form of width integration were introduced.

Since the soil-pile interface is modelled as a flat plate it has been common to regard the pile as a thin strip, buried within the soil but not altering the response of the soil i.e., no account is taken of the existence of the hole within which the pile is situated. The origin of lateral forces must be either an inertial effect or from some movement of a buried object. The present case is the latter, with the pile being the buried structure moving through the soil. As mentioned the soil idealisation makes no allowance for the buried structure shape; however, for the distributed load to exist, the structure must be present.

The easiest concept to accept is the thin strip model (Poulos 1971a), which implies that, provided the pile is given the correct bending stiffness, the pile cross-section has no effect on the pile response to uniformly distributed loading. The results of Baguelin, Trezos and Frank (1979) suggest that the pile cross-section is of little importance to the overall soil response

either, supporting a similar argument for the soil. The actual shape of the soil interface element appears to have little effect providing the width of the projected area is the same as the buried structure width, measured at right angles to pile movement.

The model used here is a rectangular area (plate) that incorporates the loading due to the pile-soil interaction but does not include the changes in soil response caused by the physical presence of the pile. In this model the normal stresses that are generated within the soil near the front and back of the plate, are of equal magnitude and opposite in sign, from the condition of complete adherence that is implicit in the elastic solution. Alternatively, it can be said that the symmetric nature of the pile geometry and antisymmetric nature of the loading would require any solution, with a discontinuity at the plate, to have antisymmetric load in order to maintain the continuity of the soil with the plate back and front.

The uniformly distributed load is represented in the elastic mass in the form of a stress jump. Therefore the stress generated in the soil immediately in front of the pile and that immediately behind the pile, will sum to balance the uniformly distributed load applied by the pile.

It will be apparent that the restriction of adherence between pile and soil is not always a completely accurate model of the behaviour of laterally-loaded piles. The occurrence of gapping behind piles has been noted many times in the literature of laterally loaded piles. However, since most other investigators have assumed the pile and soil remain in contact, it is prudent to adopt this assumption in order to gain a result that is comparable with their solutions.

Isolated Response of Mindlin Soil Element

In order to introduce the elastic soil model, based upon the results of Douglas and Davis (1964), it is useful to present the results of a specific investigation using the elastic-based approach and compare it with the results of a Winkler approach. To this end the average deflection response of a uniformly loaded rectangular area for varying depths of embedment, in an elastic half-space will be investigated.

Any rectangular area may be divided into four component rectangles, and a deflection at the point of their common corners found by summing the individual deflections of the corners of the components. This follows from the property of superposition, that all elastic-linear materials will possess, and allows the calculation of the deflection at any point within, or outside the loaded rectangle.

If an average deflection of the loaded rectangle were required (say) as an estimate of the deflection likely if, as in this thesis, the response were rigid, then Gaussian quadrature may be employed. By sampling the deflection distribution at points, as defined by this integration rule, it is possible to calculate the mean deflection of the loaded area. Because of a vertical line of symmetry, it is only necessary to calculate half the number of deflections needed by the rule if an even number of Gauss points are used.

The mean deflection, \bar{u} of a uniformly loaded rectangular area in an isotropic elastic continuum can be shown to vary with the depth of embedment. Figure 3.2 shows the average deflection response of a vertical square due to uniformly distributed lateral load p , at various depths of embedment z . This is not a

deflection profile but may be considered as a plot of the on-diagonal values of an influence matrix connecting mean deflection and uniformly distributed load. When the embedment reaches twice the height of the square, h (or the width, d) the response has virtually reached a limiting value.

As well as variations with depth there will be variations in the average deflection response as the aspect ratio (h/d) of a rectangular area changes. Figure 3.5 shows the deflection response for a rectangle at the surface, and at great depth, as a function of aspect ratio and its inverse. The case of a square is in the centre of the diagram and either side the dimensionless form is different so as to avoid plotting infinite values of influence coefficient at both extremes of aspect ratio. The variation with Poisson's ratio is shown for the surface-response while the depicted deep-response is for one value of Poisson's ratio only, since a closed form expression for the influence of Poisson's ratio will allow all other values to be derived, see Table 3.1.

It can be noted that the deep-response gives a symmetrical plot about the aspect ratio of unity, whereas the surface-response curves are not quite symmetrical, as would be expected. The deflection response variation with Poisson's ratio is about ten percent over the range 0 to 0.5, and displays a maximum for a value of about one-third. This agrees well with the generally accepted fact that Poisson's ratio, for laterally loaded foundations, is not an important parameter.

A Winkler analysis of a square loaded area (assuming $E_s = E$) predicts a constant value of dimensionless response, \bar{u}_s / pd of unity, unaffected by embedment depth. In fact, the Winkler model would replace all the curves of the Elastic model with just one,

which is also shown in Fig. 3.5. The two straight lines, at different slopes, result from non-dimensionalising the response using the Subgrade Modulus, E_s , which is obtained by multiplying the Coefficient of Subgrade Reaction by the horizontal width of the loaded area, d .

This set of curves sheds light upon the reasons for the often favourable agreement found between Winkler and Elastic results. For small d/h ratios (narrow, vertical areas akin to a pile) the Winkler results are similar to those for a continuum, although Poisson's ratio now has no meaning in the comparison with Winkler results. This agreement is a consequence of the width or diameter having been used in the definition of Subgrade modulus. If the height were used instead, the agreement would be improved for small h/d ratios (akin to a buried horizontal pipe). This agreement is subject to the Subgrade Modulus being taken as numerically equal to the Young's modulus, which is only felt to be a rough approximation. The definition of the Subgrade Modulus merely provides it with similar dimensions to the Young's modulus and it is strictly not a material parameter but is more correctly a measured response from a particular test.

The agreement found in Fig. 3.5 must be qualified by noting that the effects of interaction between elements in the Elastic model, will modify the behaviour in any specific application but the dominant role is still taken by the self-influence response compared here.

The Mindlin soil element used above is an approximation to the deflection of a rigid loaded area. To test if this approximation gives reasonable results for rigid areas in an

elastic continuum, it is possible to compare the trends of the deep-response with the results of Brown (1978) for the settlement of a rigid loaded rectangle at the surface. Figure 3.6 presents the two sets of results normalised for variation of Poisson's ratio, as a dimensionless influence factor plotted against the aspect ratio of the rectangle. As mentioned before, there is a symmetry of the responses with respect to aspect ratio, and so the plot only covers aspect ratios between zero and one. Both curves have the same trend with aspect ratio and the ratio of the two influence factors is close to $3/7$ throughout the range, which indicates that the approximate method of predicting the response of rigid loaded rectangles is appropriate.

A further test is to use the numerical results of Douglas and Davis (1964) for a rigid vertical plate foundation with one edge at the surface of an elastic-continuum. By using a force at the head and a restoring moment equal to the force multiplied by half of the plate buried length, the equivalent of a uniformly distributed load on a rigid plate can be synthesised. Douglas and Davis present results for Poisson's ratio of 0.5 only for this case and the mean deflection of the rigid uniformly loaded plates from their results, for five values of buried length to breadth ratio, are presented in Table 3.3. Also in the table are results from the approximate mean deflection analysis of a Mindlin soil element and the results from using the recommended MBEM lateral pile analysis developed in this chapter.

For realistic plate aspect ratios the results of the approximate, mean deflection Mindlin plate analysis developed in this thesis are less than 10% in error, and the MBEM analysis results are generally in error by much less, when compared to the analysis of Douglas and Davis. The use of Mindlin's equations, in

the integrated form presented by Douglas and Davis (1964), has been shown to be capable of providing reliable results for the response of a rigid rectangular loaded area. Further, the results, when compared with those from Winkler theory, help to explain why and where Winkler and Elastic results might be expected to agree. The details of the elastic-based soil model based upon the integration of Mindlin's equations will now follow.

Soil Model Description

The situation of a representative Mindlin-based loaded soil element, j is depicted in Figs 3.7a and 3.7b and the assembled model of a pile and soil in Fig. 3.7c. By superposition of positive and negative uniformly distributed loads, the effect of any loaded rectangular "plate" element upon any point (say i) in the same plane as the plate element can be found. Thus, the value of the deflection at any point across the pile in any element can be found for the desired vertical element spacing.

The method of Poulos used the centre deflection of the flexible rectangular element for the overall plate deflection. As revealed by Poulos (1982), this approach overestimates the deflections of the pile, since it takes no account of the rigid behaviour across the width of the interface when it transfers load to the soil. Consequently in the present study it was decided to approximate this rigid behaviour by averaging the deflection due to a uniformly distributed load on the soil. This averaging could be accomplished in many ways, including,

- a) a factor applied to the central deflection,
- b) approximation of the deflection distribution across the width by a simple function and taking the average value and
- c) averaging the deflection over the entire element area.

The simple factoring of the central deflection would not take proper account of any effect from variation of the height to width ratio of the plate and so was deemed unsuitable.

The method of finding an average using a simple function approximation is very attractive. From the nature of the model it is possible to find the centre deflection and both edge deflections, which are the same from symmetry. Having three known values of deflection at one depth it is convenient to employ a parabolic approximation for the variation with width, such that Simpson's rule for integration is easily applied. The resulting average deflection, \bar{u} , using the centre deflection, u_c , and edge deflection, u_e , is thus given by

$$\bar{u} = (2u_c + u_e) / 3 \quad 3.25$$

The third way mentioned could be accomplished by using Gaussian integration over the entire rectangular area, as was done for the approximation of a centrally loaded rigid rectangle. This involves finding the value of deflection at the Gauss point coordinates inside the rectangle, given by the integration rule, and summing these deflection values. If use is again made of symmetry there is little extra effort involved in calculating the deflections at the Gauss points.

The resulting stiffening of the response, due to the averaging of variations of the deflection with height, was deemed to be a pre-empting of the deflection pattern that is meant to be governed by the pile bending. Further, the results from using Gaussian integration were generally very close to those from use of the simpler method and, because it gives a somewhat conservative stiffness, the second method was adopted.

Thus a set of Influence Coefficients $[I]_s$, relating the uniform distributed load W , to the average deflection across the plate u_s , for the nodes of the soil plate elements can be found for the thin strip pile model as shown in Fig. 3.7.

$$u_s = [I]_s W \quad 3.26$$

This solution is valid for an elastic homogeneous half-space with properties defined by a Young's modulus and a Poisson's ratio.

3.3.3 Boundary Element Analysis

A variety of approaches was tried using a finite difference representation of the pile and a Winkler or Mindlin-based soil model. In the chosen method the soil and pile stiffnesses are combined and the conditions that are required to produce known boundary conditions at nodal points are enforced. Using the finite difference approximation for a fourth order differential (with errors of order 2), the matrix for the pile bending stiffness may be found, giving a relationship between pile distributed loads and deflections.

Extension to non-uniform pile properties was not done, since evidence suggests that the stiffness of the upper portion of the pile will be appropriate in most cases. Poulos and Adler (1979) have derived correction factors for non-uniform piles, which are considered an adequate solution to most tapered pile problems.

The pile stiffness may be written as

$$[K]_p u_p = W_p - W_u \quad 3.27$$

and the corresponding soil stiffness as

$$[K]_s u_s = W_s + W_u \quad 3.28$$

for $[K]_s = [I]_s^{-1}$, where $[I]_s$ is the influence matrix for the soil as described in section 3.3.2. Subscripts p and s relate the quantity to pile and soil respectively and subscript u identifies the interface interaction distributed load, W_u , that must act in opposite senses on the pile and soil, see Fig. 3.7d. The matrix $[K]_s$ and all except four rows and columns of matrix $[K]_p$ relate the incremental loads per unit depth, W acting over internal buried (real) elements, to the incremental deflections, u at nodal points. The vectors W_s and W_p therefore contain externally induced uniformly distributed loads at real elements, and vector W_p contains four extra terms which are determined by the boundary conditions and equilibrium of the pile. Soil loads W_s in equ. 3.28, could arise from free-field soil movements u_{sm} , i.e. $W_s = [K]_s u_{sm}$, and the uniformly distributed pile loads W_p , in equ. 3.27, from inertial forces on the pile.

A further relationship is proposed to relate the pile and soil incremental deflections at real nodal points

$$u_p = u_s + \Delta u \quad 3.29$$

where Δu is the mismatch in deflection increment between the pile and soil, i.e. the extra deflection of the pile relative to the soil, when the contact between pile and soil is lost (from both front and back). It is necessary to emphasise the difference between this approach and the normal understanding encapsulated in the concept of gapping behind the pile. "Behind" in most instances, refers to the soil side the pile is moving away from,

but more correctly should refer to the pile face that experiences tension, which may not be consistent with pile movement.

The gapping of the pile and soil is a complete separation here, introducing the concept of a pile node passing freely through the elastic soil. This concept is also employed for the pair of imaginary nodes, Fig. 3.7, used at the tip of the pile to enforce boundary conditions.

Combining equations 3.27, 3.28 and 3.29 at soil nodes

$$[K_p + K_s] u_p = W_p + W_s + [K_s] \Delta u \quad 3.30$$

an expression may then be found for incremental deflections u_p , in terms of the externally applied head and tip loads, W_p and distributed traction increments of the pile W_s , the distributed load increments from such sources as soil movements, W_s , and distributed load increments associated with the stiffness loss of the pile at "gapped" elements, $[K_s] \Delta u$.

This may be expressed as

$$u_p = [C] (W_p + W_s + [K_s] \Delta u) \quad 3.31$$

where $[C] = [K_p + K_s]^{-1}$

Considering the pile as elastic and infinitely strong, the vector W_p consists purely of external loads applied to the pile and may be assumed constant for any one load increment. For this reason it is permissible to introduce the vector u_e ,

$$\text{where } u_e = [C] W_p \quad 3.32$$

is the elastic, or externally (head and pile inertial loading) induced, deflection vector for the pile-soil system with no free-field soil movement, gapping or soil yield. At this point it must be emphasised that $[K]_p$ has four more rows and columns than $[K]_s$, due to the use of the two imaginary pile nodes at each end, see Fig. 3.7d, which enable any combination of defined shear force, bending moment, rotation and deflection as the end boundary conditions of the pile to be specified.

The form of the complete W vector may vary between load increments, depending on the boundary conditions and the external loading, but the terms associated with distributed loading at real nodes can be taken as zero, for static behaviour. The same real pile nodes will always have uniformly distributed interaction load terms, W_u , compatible with the soil nodes. Understanding this provides a means of simplifying the pile stiffness eqs 3.27 and 3.31 to give at real nodes

$$\begin{aligned} \text{or} \quad - W_u &= [K]_p u_e + [K]_p [C] W_s + [K]_p [C] [K]_s \Delta u \\ - W_u &= W_e + [A] W_s + [B] \Delta u \end{aligned} \quad 3.33$$

$$\begin{aligned} \text{where} \quad W_e &= [K]_p u_e \\ \text{and} \quad [A] &= [K]_p [C] \\ [B] &= [A] [K]_s \end{aligned}$$

This establishes a relationship for the actual interface interaction loads W_u , in terms of the interface loads W_e (resulting from a purely elastic response to external head loading), the loads arising from the direct external loading of

the soil $[A]W$ and the free standing, gapped element load correction $[B]\Delta u$.

At this stage equ. 3.33 is capable of incorporating external soil movements and both soil yield and soil breakaway from the pile. For linear problems all that is required is for equ. 3.31 and equ. 3.33 to be applied in order to calculate pile displacements and soil-pile interaction distributed loads due to head loading.

Once the pile displacement pattern is known it is a simple matter of using the appropriate finite difference operators (with errors of order 2) and the equations in Fig. 3.4a to recover values of pile rotation, bending moment and shear force at nodal positions down the pile.

3.4 Finite Element Approach

The finite element method (FEM) has been used increasingly in the past two decades to solve a wide range of problems in geomechanics which previously had been solved by less rigorous engineering approximations. Such problems usually involve complex geometries and/or complex distributions of material properties that are found to make analytic, closed form solution impractical, if not impossible.

Examples include soil-structure interaction, seepage, non-linear elasto-plastic, dynamic and many other problems. Some uses of the method have possibly been of dubious merit considering the extent to which the analyses rely upon material properties that, if they can be found, may be of such an uncertain accuracy as to not warrant as precise an analysis as the FEM.

The behaviour of single piles in an elastic continuum is one problem that lends itself to a treatment by FEM, and which would otherwise leave the only rigorous treatment for their analysis to the boundary element method (BEM). It is true that the BEM is satisfactory for a pile in an isotropic uniform modulus elastic half space, (Poulos, 1971a, Bannerjee and Davies, 1978), but this leaves the cases of piles in soil of limited depth and non-uniform modulus without rigorous treatment.

The improvement in computer capabilities in recent years has led to the use of FEM in more adventurous applications, perhaps unfortunately, at the expense of more elegant methods of solution. It is felt however that the semi-analytic FEM using Fourier series, as used in this thesis, represents a valid use of a most powerful tool for analysis. Such a finite element method is very versatile and has been employed in the analysis of wall loads in

squat steel silos during earthquake loading, using a quasi-static approach, by Rotter and Hull (1985).

In this section the use of the Axisymmetric Geometry Finite Element Method (AGFEM), as applied to the analysis of piles, is outlined and then verified as giving an adequate solution to a wide range of problems, especially for problems allied to pile behaviour. Following the validation, Section 3.4.4 describes the extension of the AGFEM analysis to economically model an elastic soil profile built up of layers of finite elements that can include a pile. Later in the thesis, Chapter five describes a specialised use of the AGFEM analysis to take some account of gapping in a non-linear analysis of a pile in an elastic soil.

3.4.1 Axisymmetric Finite Element Analysis

The theory of finite elements, and in particular its use with Fourier Series for problems with axially symmetric geometry, has been presented elsewhere by Wilson (1965) and Zienkiewicz (1971). Here only the modifications pertinent to the use of the method to analyse piles under lateral loading, and the important restrictions that are imposed by the method, will be outlined.

The basis of any finite element model is the expression of the distribution of the variables of interest, throughout the domain of the problem, in an approximate form as a function of discrete values at nodal points. The displacement shape function used here is of second order and the nodal points are situated at the corners and midsides of a rectangular element. This is the well known isoparametric eight-noded quadrilateral finite element which, due to its second order shape function, can allow for a curved sided geometry if required.

With the displacements approximated by a shape function, it is possible to differentiate that function and produce a relationship for the strains at any point in terms of nodal values of displacement.

Employing an elastic constitutive relationship between stress and strain within the domain, the values of stress may similarly be expressed in terms of nodal deflections. The Principle of Virtual Work may then be employed to solve for the nodal displacement in terms of the nodal loading, which is required to involve the same total work as the imposed loading. The application of Virtual Work will involve integrations over the volume of the element domain to produce a stiffness matrix and over the loaded area to produce the equivalent nodal load vector.

The use of Fourier series to model antisymmetric loads acting on an axisymmetric body will require the cylindrical polar coordinate strain relationships to be modified to account for the analytic integration that is performed in the circumferential direction. This effectively removes from the formulation of the problem any further dependence upon the circumferential variation of deflections.

In cylindrical polar co-ordinates, see Fig. 3.8, the radial, circumferential and vertical deflections for the k.th harmonic will take the form

$$\begin{aligned}
 u_r &= U_r^k \cos(k\theta + \varepsilon) \\
 u_\theta &= U_\theta^k \sin(k\theta + \varepsilon) \\
 u_z &= U_z^k \cos(k\theta + \varepsilon).
 \end{aligned}
 \tag{3.34}$$

where ε (without a subscript) is a parameter to interchange the

sine and cosine functions and is defined to be zero or $\pi/2$. This form is the one that proves most convenient for computation and will allow the more general form of the Fourier series to be easily produced (with a_k associated with $\varepsilon = 0$ and b_k with $\varepsilon = \pi/2$), namely

$$u = a_0 + \sum_{k=1}^n a_k \cos k\theta + b_k \sin k\theta. \quad 3.35$$

Employing equ. 3.34 in the expressions for first order strains in cylindrical polar co-ordinates (Love, 1928), results in the expressions below (omitting the superscript k and using $\varepsilon = 0$, for clarity),

$$\begin{aligned} \varepsilon_{rr} &= \frac{dU}{dr} \cos k\theta \\ \varepsilon_{\theta\theta} &= \frac{1}{r}(kU + U_r) \cos k\theta \\ \varepsilon_{zz} &= \frac{dU}{dz} \cos k\theta \\ \gamma_{rz} &= \left(\frac{dU}{dz} \frac{1}{r} + \frac{dU}{dr} \frac{1}{z} \right) \cos k\theta \\ \gamma_{er} &= \left[\frac{dU}{dr} \frac{1}{e} - \frac{1}{r}(kU + U_r) \right] \sin k\theta \\ \gamma_{z\theta} &= \left(\frac{dU}{dz} \frac{1}{e} - \frac{kU}{r} \right) \sin k\theta \end{aligned} \quad 3.36$$

It is seen that the individual expressions for strain contain only one trigonometric term each, either a sine or cosine. This fact causes the integral over the domain volume to involve terms that are multiplied by either the square of the sine or the square of the cosine. The integration in the circumferential direction will thus depend upon the values of the following integrals:

$$\int_0^{2\pi} \sin^2(k\theta + \varepsilon) d\theta = \pi \left(1 - \frac{\sin 2\pi k \cdot \cos 2(\pi k + \varepsilon)}{2\pi k}\right)$$

$$\int_0^{2\pi} \cos^2(k\theta + \varepsilon) d\theta = \pi \left(1 - \frac{\sin 2\pi k \cdot \cos 2(\pi k + \varepsilon)}{2\pi k}\right).$$

3.37

For integral values of k and ε taking values of zero or $\pi/2$, there are three possible values for the above integrals namely, zero, π or 2π . If k is non-zero then both integrals are equal to π . For $k = 0$ the integrals are equal to 0 or 2π , depending upon the value used for ε . There is a physical interpretation to these results when k equals zero. If ε is equal to zero, then the case corresponds to one in which no y_{θ} or $y_{z\theta}$ strains are evident i.e., the well known axisymmetric case in which volume integrals involving 2π will appear. When ε is equal to $\pi/2$ every strain except y_{θ} and $y_{z\theta}$ will disappear and again 2π will appear in the integrals. This case corresponds to a torsional type of loading.

It is interesting to note that for the elastic constitutive law, the stiffness matrices that result for k equals zero when ε is zero and $\pi/2$, mirror the uncoupling of the two forms of loading, i.e. the axisymmetric and torsional cases may be analysed using one large stiffness matrix or by splitting the zero harmonic matrix into two smaller stiffness matrices.

For other harmonics, the stiffness matrix does not uncouple in this way and the use of $\varepsilon = 0$ or $\pi/2$ will involve an apparent change in co-ordinate direction only. This means that although the general form of the Fourier series, equ. 3.35, has two sets of

Fourier Coefficients, a_k and b_k , the same stiffness matrix relating nodal loads and deflections may be used to find the complete response, providing the circumferential load and deflection signs are changed appropriately.

This fact would save time when analysing a problem with a very general load form. In practice, however, the Fourier series that result from approximating most load forms will not need more than the Fourier Coefficients implied in equ. 3.34. This is because the loads usually possess a line or plane of symmetry that will eliminate the equivalent of one set of Fourier Coefficients, a_k or b_k , as defined by equ. 3.34.

When considering the particular case of a vertical pile in an Elastic medium the loading required to produce torsional, axial or lateral response may be represented as a Fourier series. If we assume a general load that would require a number of harmonics in order to model it satisfactorily, then the stiffness matrix that results would involve an unique set of deflections and loads associated with each Fourier term.

The situation would seem to require a large stiffness matrix relating all these loads and deflections involving all terms. Fortunately the volume integration for the stiffness associated with deflections and loads for dissimilar Fourier terms result in integrals of the form:

$$\int_0^{2\pi} \sin(k_1 \theta + \epsilon) \cdot \cos(k_2 \theta + \epsilon) d\theta = 0.$$

where $k_1 \neq k_2$ 3.38

In this manner the various Fourier terms uncouple and the

resulting stiffness matrix may be solved for, one term at a time, since the "off diagonal" stiffness matrices for individual Fourier terms are identically zero.

This is a fundamental aspect of the method as it has been used for many types of analysis. The three-dimensional problem is reduced to one containing two dimensions, with the third dimension analytically modelled by a Fourier series. Further, the number of Fourier terms used does not increase the size of a particular problem; it only increases the time needed to solve the problem, since the response of each term is solved for separately.

For axial loading, an inspection of the Fourier terms that produce axisymmetric vertical loading will result in the reduction of all terms to zero except for the zero harmonic, i.e. k equal zero and ε equal zero. Any other terms induce an antisymmetric lateral load or self equilibrating loads.

For torsional loading the axisymmetric solutions will again require the k equals zero term and no other non-zero terms. Now the value of ε is $\pi/2$ and, as previously mentioned, this case may be incorporated in the case with ε equal to zero since the torsional and axial responses are uncoupled.

For lateral loading the only term that contributes to the antisymmetric behaviour is k equal to unity. This one term will model an antisymmetric load distribution that produces a resultant load in the x -direction if ε is zero, or y -direction if ε is $\pi/2$, from the vectorial combination of radial and circumferential tractions. It will also model a linear variation of vertical load that will produce an applied moment load. This means that only

one harmonic is required to analyse the case of symmetric axial or torsional load, and only one harmonic is required for the case of antisymmetric lateral (horizontal and moment) load upon a body that possesses an axisymmetric geometry, see Fig. 3.9.

In the use of the two harmonics, zero and unity, to analyse a pile in an Elastic medium, the axis of the pile is the axis of symmetry and will require special attention. In order that the resulting deflection in the x, y or z direction on the centre line of the discretisation is single-valued, there is a restriction placed upon the radial, circumferential and vertical deflections.

Consideration of the transformation from cylindrical polar to Cartesian co-ordinates for the Fourier term k leads to

$$\begin{aligned} u_x &= A \cos(k-1)\theta + B \cos(k+1)\theta \\ u_y &= -A \sin(k-1)\theta + B \sin(k+1)\theta \\ u_z &= C \cos k.\theta \end{aligned} \quad 3.39$$

where

$$A = \frac{U - U}{2} e$$

$$B = \frac{U + U}{2} e \quad \text{and}$$

$$C = \frac{U}{z}$$

If u_x , u_y and u_z are to be single valued at any radius (but especially along the z axis), for any θ value then

$$\frac{d}{d\theta} u_x = \frac{d}{d\theta} u_y = \frac{d}{d\theta} u_z = 0 \quad 3.40a$$

or

$$\begin{aligned}
 -A(k-1)\sin(k-1)\theta - B(k+1)\sin(k+1)\theta &= 0 \\
 -A(k-1)\cos(k-1)\theta + B(k+1)\cos(k+1)\theta &= 0 \\
 -C k \sin k\theta &= 0 \quad 3.40b
 \end{aligned}$$

For equ. 3.40 to have a non-trivial solution it must have a determinant equal to zero, i.e.

$$-k (k-1) (k+1) \sin k\theta \sin 2k\theta = 0 \quad 3.41$$

From this, the three values of k of zero, -1 and $+1$ are seen to provide the necessary conditions for a non-trivial solution for A , B and C . When it is considered that this non-trivial solution restriction can be interpreted as a rigid body component of any deformation, it is clear that only these terms result in any rigid body movements.

When considering the case of $k = 0$, equ. 3.39 shows that the values of u_x and u_y depend upon the value of U_z and the value of u_z is identical to U_z . From this it can be deduced that U_r must be zero along the centre line or a multi-valued response is implied. The value of U_θ is not directly restricted by equ. 3.39 but for axisymmetric vertical or radial load it is necessarily zero everywhere. The case of torsional loading can be shown to lead to u_x and u_y being dependant upon U_θ and for these to be single valued U_θ must be equal to zero. This means the value of U_r is zero along the axis for the case of torsional loading and U_z and U_θ are not restricted but will necessarily be zero for purely torsional behaviour. This is consistent with the note made previously about the uncoupling of the torsional and the axially symmetric load cases. Thus when $k = 0$

$$U_r = U_\theta = 0. \quad 3.42$$

The case of $k = 1$ results in a form of equ. 3.39 that is similar to the Mohr circle representation of stress on a plane.

$$\begin{aligned} u &= A + B \cos 2\theta \\ u_x &= B \sin 2\theta \\ u_y &= C \cos \theta \\ u_z & \end{aligned} \quad 3.43$$

If u and u_x are to be single-valued on the centre line, the term B , connected with $\cos 2\theta$, will need to be equal to zero. Likewise, the value of U_z must be zero for the value of deflection u_z on the z axis to be single-valued.

This leads to:

$$\begin{aligned} U_r + U_\theta &= 0 \\ \text{and } U_z &= 0 \end{aligned} \quad 3.44$$

The case with $k = -1$ could be thought of as a mirror image of the last case discussed. The only difference in the result is a reversal of the circumferential coordinate direction and equ. 3.44 is then unchanged.

When the case of k greater than or equal to two is considered, it becomes necessary to use the trivial solution to enforce a single value to the Cartesian components of deflection.

$$U_r = U_\theta = U_z = 0 \quad 3.45$$

This special treatment of the axis of symmetry has not received great attention in the literature. The special cases above have been mentioned by Carter and Booker (1981); however most investigators have made no reference to the centre line

constraints and often have used a hollowed discretised form, thus eliminating the centre line nodes.

Consistent treatment of the continuity of material across the centre line of a circular beam is essential in order to reproduce simple Elastic beam theory results. For this reason it was found necessary to incorporate into the analysis a means of relating the values of nodal deflection on the centre-line. The constraint used may be written

$$u_i = m u_j + b \quad 3.46$$

This means m equal -1 and b equal zero, for u_i equal U_r and u_j equal U_e , provides the necessary restrictions for the $k = 1$ case along the centre of the mesh. As well as enforcing the uniqueness of deflections along the axis of the mesh, the constraint coding could also be used to rigidly or flexibly link degrees of freedom. In this way it becomes possible to introduce rigid body movements and sloping, smooth (shear free but fixed normal deflection) boundary conditions if required.

Before the AGFEM analysis computer program was used to analyse laterally loaded pile problems an extensive series of analytic checks were conducted, some of which are reported here.

3.4.2 Validation of Finite Element Analysis

The Finite Element program that was written to analyse the laterally loaded pile problem was tested against a large number of elastic solutions. The tests were chosen to check the accuracy of the solutions for various loading forms and different harmonic terms.

The most obvious test was to analyse a free-standing cantilever, using $k = 1$, for end shear and moment loading. This

establishes the suitability of the selected type of element for analysis of the response of the pile to head loads. A further check was on the pile response to uniformly distributed loads, which is a similar type of loading to that induced by the interaction of the buried pile in the soil.

To verify the program coding for the zero harmonic, and to investigate the ability of the finite element program and the arithmetic accuracy of the computer to model nearly incompressible problems, a sphere and a cylinder of elastic material under internal and external pressure was analysed.

To establish the suitability of the method for analysing the response of an Elastic half-space, the results of Gerrard and Harrison, as presented in Poulos and Davis (1974), for the loading of a circular area on the surface were compared with results of the finite element analysis. The loading was for uniformly distributed vertical load, uniformly distributed horizontal load, vertical traction proportional to distance along the $\theta = 0$ ray (moment) load and a circumferential (torsion) load proportional to radial distance, see Fig. 3.9.

Cantilever Response

One of the most pertinent tests for the validation of the analysis are those for the behaviour of a pile when built-in at one end. Indeed, this cantilever response has been used in some methods as a means of analysis of pile foundations, by choosing what is considered as an appropriately reduced cantilever length to cater for the reduction of head flexibility arising from the soil support (equivalent bent method).

Broadly, the behaviour of a pile may be characterised by two types of load :

- a) The load transferred through the supported structure to the pile head in the form of a bending moment and shear force.
- b) The tractions acting along the length of the pile caused by interaction of the pile with the soil.

The first aspect can be investigated by loading across the tip face of a circular cantilever beam, modelled by finite elements, with a uniformly distributed lateral shear and a linearly varying axial normal traction, which produces a shear force resultant and an applied moment, as in Fig. 3.9b and 3.9c. Simple bending theory provides a solution that can be compared with the results of the finite element analysis and this has been done for two pile geometries.

The pile geometries considered have length to diameter ratios of five and fifty with eleven elements lengthwise and one radially. The longer cantilever had an element aspect ratio of five compared with a ratio of unity for the shorter cantilever. Such slender elements for the long cantilever did not cause serious errors in the tip deflection due to shear and moment loadings, as the deflections were less than half a percent below the simple bending theory answers. The solution of the shorter cantilever gave an answer 0.8% higher than simple bending theory for shear load and 1.0% lower for moment loading. In this case good agreement was not necessarily expected, since a slenderness ratio of five for the pile is near to the lower limit of three for applicability of simple bending theory, as outlined in Chapter two.

Since most pile applications will involve length to diameter ratios greater than five but less than fifty, for the effective length of pile, and because the AGFEM analysis uses a more complete treatment of elasticity theory than simple bending theory, it is felt that the AGFEM analysis provides adequate modelling of the head loading condition.

An important requirement of the soil-structure interaction method is the ability of the model used to provide influence coefficients for deflection, to give reliable answers for loading of sections of the pile with uniformly distributed loads. For the pile in a soil these loads arise from its interaction with the soil when head loads are applied. The interaction loading referred to here is not exactly the traction on the pile from the soil but is a resultant, or an equivalent, of such tractions. This point is often overlooked in analysis of the pile response due to pile-soil interaction but, as will be shown in Chapter five, is of importance for the behaviour of the soil.

For verification purposes this loading is modelled as a uniform x-directed traction around the entire circumference and extending down the full face of an element of the pile. Using simple bending theory it is possible to calculate the deflection of any point on the beam when a uniformly distributed load is applied over one section of the beam. Here the loaded sections are taken to be the element lengths and the points at which deflections are calculated are the centres of the regions of load.

The analysis of two load cases were performed, using the previously generated cantilever meshes, with uniform x-directed tractions and deflection comparisons on the fifth (interior) and eleventh (tip) element from the base. The free end and built-in

base elements were both chosen to be half the length of the interior elements, in an attempt to refine the regions in which internal stresses might be expected to vary quickly with position.

For the long cantilever, the worst error in the comparison was for the deflection of the centroid of the interior element due to load on the tip element. This error was -0.9 % while the actual deflection of the fifth element was only 22% of the deflection of the tip element.

When loaded at the fifth element the long cantilever analysis gave answers for the deflections of both elements that were in error by less than -0.9%. The accuracy of the deflection of the tip, when load is applied near the centre of the beam, proves that rigid body movements are well catered for in the finite element model.

When results for the short cantilever are compared with simple bending theory predictions, it is found that agreement is not so favourable. The worst error is 9.6% for the deflection at the mid-element centroid due to load on the mid-element. This is expected since effectively it represents a tip loaded cantilever with a length to diameter ratio of only two. The behaviour of such a squat cantilever is influenced by extra deformation due to shear and so simple bending theory cannot apply.

The deflection of the tip element centroid due to the mid-element loading is only 1.8% in error compared to the simple theory. It can be argued that the AGFEM solution to this problem is preferable to the one from the simple theory of bending. Since it is not envisaged that results for such squat piles would be practically useful this remains of theoretical interest only.

The final check using the two cantilevers was for the response arising from a uniformly distributed loading over the entire length of the beam. This load was applied to the finite element problem as a self weight of the beam material. The errors in the mid and tip element deflections were -0.9% and -0.5% respectively for the long cantilever and 4.7% and 1.2% for the squat cantilever. The results confirm the accuracy of the modelling of pile bending and also give confidence that the self-weight capability of the analysis is correctly implemented.

It can be noted that generally the errors for the long pile were very small and negative while for the short pile they were positive. This may be interpreted as saying the simple theory of bending, in which plane sections remain plane, will underestimate the deflections of short squat beams while the simple theory results agree well with finite element results for beam slenderness ratios of up to fifty.

The load cases considered as important for modelling the pile, with regard to pile-soil interaction, have been analysed using the finite element approach and comparisons made with simple bending theory. Recognising the inapplicability of the simple theory for squat beams, and considering the likely slenderness ratio of piles in common use, it is shown that the finite element analysis using eleven elements is more than adequate to model the pile response. The validation also confirms the implementation of traction and self weight loading in the finite element analysis has been successful.

This represents a good check upon the method for the case of analyses using the first non-zero harmonic. The next two cases will examine the use of the method with the zero harmonic.

Elastic Sphere and Cylinder

The analytic solution for an elastic cylinder and an elastic sphere under both internal and external pressure has been presented by Lin (1968). The expressions for radial deflections, radial-, axial- and circumferential-stresses are given and the results of a finite element analysis of a sphere and a cylinder using the zero harmonic can be compared with them. The meshes used are shown in Fig. 3.10 and the results were obtained for a number of Poisson's ratios in order to gauge the viability of modelling nearly incompressible behaviour. The true radial deflection is a function involving both a linear and an inverse squared function of the radius for the sphere and a function of the radius and the inverse of radius for the cylinder problem.

The isoparametric element used in the finite element program allows for a quadratic variation of deflection which proves to be able to closely model the above distributions. The problem with the finite element formulation, however, is that the fully incompressible case cannot be modelled because the bulk modulus becomes infinite and cannot be handled by the normal mathematical framework. Poisson's ratio ranging from 0 to 0.495 was used and an internal to external pressure ratio of 0.5 for both the sphere and cylinder test cases.

Typically the answers from the finite element program for the spherical problems were well within 0.5% of the analytic solution for radial deflections and within 1% for the stresses over the range of Poisson's ratio used. For the cylindrical case, with Poisson's ratio zero, the finite element analysis gave the exact solution for deflection and stresses. However, as Poisson's ratio was increased the solution strayed slightly from perfect agreement

so that at 0.495 the response was nearly 4% in error for deflection of the outer radius and for some of the stresses.

The reason for this is that the near incompressibility of the material causes the numerical stiffness matrix terms to become very large. It was also noticed that there were small deflections occurring in the axial direction of the cylinder that violated the plane strain condition. These deflections were removed by fixing all the axial degrees of freedom to zero, but no appreciable change in accuracy was achieved.

It was felt that, considering the accuracy with which the spherical problem and the plane strain cylinder problem were solved, further development of the cylinder mesh was unnecessary. Further, using a Poisson's ratio between 0.48 and 0.49 would provide reasonable estimates of undrained behaviour with the value similar to that chosen by other investigators, Rowe (1977), Balaam (1978) and Redman (1980). It should be noted that the value of Poisson's ratio at which the near-incompressible analysis becomes unstable is largely a function of the word length of the computer used. The above authors all used the same computer as the present writer and employed double precision arithmetic.

Thus, problems modelled by the zero harmonic can be analysed successfully using the finite element program.

Half-space Response

In order to gauge the ability of the program to analyse the response of the soil, four load cases were modelled using a mesh of large enough dimensions to allow comparison with the elastic continuum half-space results of Gerrard and Harrison, as presented in Poulos and Davis (1974). The mesh is depicted in Fig. 3.11 and

contains 501 nodes and 150 rectangular elements.

The four load cases involve the analysis of two different Fourier terms, zero and one. The zero harmonic will model the vertical mode and also the rotational mode of deformation about the vertical axis. The first harmonic provides a solution for lateral deflection and lateral rotation. Superimposing the four cases encompasses any possible mode of deformation of the vertical axis in one particular vertical plane.

The deformation in the direction at right angles to the previous vertical plane follows as a simple new load case and a 90° rotation of axes about the z-axis. In this way the three deflections and three rotations that completely define a general response can be obtained. This work is limited to the response of, and load in, only one vertical plane but it is entirely possible to extend the methods used to a general method, such as would be required for pile group analysis.

Considering the zero term, the two cases of uniform vertical surface traction and radially linearly increasing circumferential shear traction, see Fig. 3.9a, on a material with Poisson's ratio of 0.3 are analysed. The deflections at the surface on the edge of the loaded circle are compared with the tabulated solution given by Gerrard and Harrison. The circumferential deflection was 0.7% below the tabulated value for the torsion load and the radial and vertical deflections for the uniform load were underestimated also, by 1.0% and 2.4% respectively, see Table 3.4.

The errors in deflections resulting from a uniform horizontal traction (shear load) and a linear variation, in the x-direction, of vertical normal traction (moment load) from the analysis by the

first harmonic are tabulated in Table 3.4. Once again the deflections compared are those at the surface on the edge of the loaded area. The radial and vertical deflection values occur along the $\theta = 0$ ray while the circumferential deflection value is for the $\theta = \pi/2$ ray. The values of error at other values of θ may be found by multiplying by cosine θ for the radial and vertical, and sine θ for the circumferential, deflections. This means the tabulated values of error are the maximum values that occur around the circumference of the loaded circle.

Table 3.4 shows that the worst error is for the vertical deflection of the shear load case. This result is not as bad as it appears when it is realised that the actual deflection is only 11% of the maximum deflection, occurring at the centre of the circle, and is also at right angles to the direction of load. Generally the response of the mesh gives results that are within three percent of the values predicted using the results of Gerrard & Harrison.

The deformed mesh geometry of three of the test cases is shown in Fig. 3.12. It is obvious that more mesh refinement is possible in the region of the load, but it can be said that even with this relatively coarse modelling the results are more than adequate for engineering purposes.

Cases of the above loading were also applied to other meshes with values of Poisson's ratio of 0 and 0.48. When Poisson's ratio is zero the results of the finite element program agree very closely with the published results. This might be expected since the effect of confinement from the rigid boundaries used on the mesh will be minimised for this case. When approximating an incompressible material the worst deflection error in the direction of loading is about 6%, and generally is of the order of 4%.

Thus the response of an elastic isotropic homogeneous half-space can be modelled with sufficient accuracy. The finite element method however is capable of analysing an elastic isotropic medium that has a non-homogeneous Young's modulus. This fact is crucial for the development of an approximate method for modifying the Mindlin, homogeneous medium, results to cater for non-homogeneous modulus distributions with depth.

To test the non-uniform modulus response of the method it is possible to use the results of Brown and Gibson (1972). In their paper the form of the vertical deflection profile at the surface and the magnitude of the central deflection are presented for uniform vertical loading of a circular area. Poisson's ratio and the degree of inhomogeneity are varied for the case of a deep stratum of elastic material. In a previous paper considering the case of zero surface modulus, Gibson et al. (1971), it was stated that when the incompressibility condition was relaxed (i.e. $0 < \nu < 0.5$) the settlement within the loaded area became unbounded and non-uniform. The response of uniform settlement within the loaded area, and zero outside it, is only associated with the loading of an incompressible half-space having zero surface modulus, with the result resembling the behaviour predicted by a Winkler foundation, i.e.

$$\frac{w m d^2}{P} = \frac{6}{\pi} \tag{3.47}$$

in the loaded area where $E = mz$.

Thus, using equ. 3.47, it is possible to approximately check the finite element program answers for the results of uniform loading of a circle on a nearly incompressible material, Poisson's ratio of 0.49. As mentioned previously Poisson's ratio of one

half is not accommodated by the FEM formulation. Also the non-homogeneous nature of the material is numerically modelled. The variation of modulus with position has been achieved by varying the value of modulus for each Gaussian integration point used in the integration scheme. Four integration points per element were used and so in that sense the modelling for modulus variation is approximate.

With the above approximations it was still expected that the finite element analysis would provide a reasonably comparable result to the published values. The results indicate that the settlement is overpredicted in the loaded region at the centre by 2.6%, in the middle of the (largest) first radial element by 13.8% and at the corner of the first element by 7.2%. Use of a finer mesh size for the remaining two elements under the uniform load kept the deflection errors to between 6.4% and 11.8%.

The node at the edge of the loaded area theoretically has a multi-valued response since outside the loaded circle there is no vertical deflection from the analytic solution. The finite element solution for deflection of this node can be compared to the analytic solution if the average of zero and the uniform internal deflection is compared. This gives an error of 4.1%. The area outside the loaded region showed insignificant deflections when compared to the maximum deflection.

Consideration of this "Gibson" soil problem provides an encouraging degree of agreement and suggests that the AGFEM program provides solutions that are probably of comparable accuracy to those from analysis of a homogeneous half-space. The use of near-incompressibility and the finite depth of layer for the AGFEM analysis means that comparison with an incompressible and semi-infinite mass of elastic material is only approximate.

Although no analytic solution has been found, the problem of lateral shear and moment loadings may also be considered for the "Gibson" soil profile and both provide Winkler type results. Lateral shear gives a uniform horizontal rigid body deflection of the loaded area, and the area outside the load has no appreciable lateral deflection when compared with the loaded area. The vertical deflections are also very small everywhere for shear loading. The linear vertical traction (moment) case also showed much smaller deflections outside than inside the loaded area. The vertical deflections are now virtually linear, just like the traction distribution, and the horizontal deflections in the x-direction change sign within the radius of the loaded area, leading to a very small average deflection.

Approximate expressions for the influence coefficients for mean deflection and rotation due to shear and moment loading were found to be

$$u_m d^2 / H = 16$$

$$\theta_m d^3 / H = u_m d^3 / M = 2.7$$

$$\text{and } \theta_m d^4 / M = 32 \qquad 3.48$$

The cross-terms are equal, due to the reciprocal theorem, but the responses given for deflection and rotation are an approximate average because the distribution of vertical or x-directed deflection varies with radial position.

Since Gerrard and Harrison's results for a uniform medium show the cross-term influence coefficients for average deflection or rotation tend quickly towards zero as Poisson's ratio increases to one half, the small magnitude of the cross-term coefficients

from the FEM result is entirely appropriate. It would be expected that a "Gibson" soil would behave in such manner, especially considering the analogy to Winkler behaviour for surface deflection response. It is worth noting that only the surface behaves like a Winkler material; the material away from the zone of zero modulus quickly shows the type of deflection response more commonly found from elastic homogeneous continuum analyses.

The finite element program has proved capable of reproducing the results of loading of an elastic half-space by horizontal, vertical, torsional and lateral moment tractions. The case of vertical deflection response is an aspect that is not modelled entirely satisfactorily since the finite depth of the elastic layer, as modelled using finite elements, affects the response.

Because the vertical response is usually of very little interest in cases of lateral loading, it is considered that the finite element method provides the most accurate and convenient available method for obtaining the response of the soil. This is especially true when it is realised that, to date, the behaviour of generally non-homogeneous soil profiles is only practically possible using the method of finite elements.

In order to check the program validity for terms greater than one, in the Fourier series representation of loading, a series of analyses was also carried out on a cylinder of Elastic material, which will not be reported here. The final comparison, which is not reported here, involved the effect of gravitational load upon a simple plane strain cylinder of Elastic material with a free internal and a rigid outer boundary. The gravitational loading acts across the axis of the cylinder, requiring the first non-zero Fourier term to model the antisymmetric load.

3.4.3 Mesh Boundary Investigation

The Finite Element Method has been applied to problems that involve an infinite extent to the body that is modelled. Accurate modelling of such a problem can proceed in two ways:

- a) The mesh may be terminated with an appropriate boundary condition at a distance from the load that is thought to give almost no effect upon the response of interest.
- b) The mesh may be extended only to a relatively close boundary, but one that is given a freedom of movement consistent with the response achieved if the material were to continue to infinity.

Method a) can be called the "equivalent half-space" method while b) is referred to as the "infinite super element" method (Rowe et al., 1978). The methods have both been used widely in numerical studies with the second method usually thought of as being the more theoretically sound. However, the type of problem will determine the most suitable method for any particular application. For instance, the boundaries in meshes used for dynamic analyses may introduce reflected energy that distorts the model's true response. In these cases it has been found necessary to use energy-absorbing boundary infinite super elements to give the far field response correct modelling (Velez, Gazettas and Krishnan, 1983). However, this is needed as a result of the dynamic nature of the problem.

An example of the equivalent half-space method is the use of smooth lateral boundaries with fixed normal deflections for both plane strain and axisymmetric finite element meshes. The extra freedom gives larger deflections that agree more closely with theoretical results based on infinite lateral or vertical extent.

This is probably a misleading improvement for plane strain problems. The reason is that, from consideration of symmetries, the shear-free laterally fixed boundary effectively converts the problem to a system of periodic strip loads. In such a case it is quite possible that reducing the distance from the centreline of the strip to the shear-free boundary may actually increase the vertical deflections, since this represents a system of more closely spaced strip footing loads and thus larger total load on the continuum. With axisymmetric analyses it is not clear how such a shear-free boundary affects the response. Balaam (1978) has successfully used such a boundary, see Fig. 3.13, to model a hexagonal region of influence for sand drains by analysing a circular pile-soil-unit region with a shear-free radial boundary in an axisymmetric finite element analysis.

Since axisymmetric finite element analysis is a subset of the more general finite element method used in this work it is obvious that careful attention must be paid to the position and type of boundary to be used in the analyses carried out. The analysis of major interest to this work is that for the first non-zero Fourier harmonic term, although other harmonic terms will be important for modelling asymmetric load cases. The first non-zero term is the one that governs the behaviour of axisymmetric geometry problems under antisymmetric load. Without this term there is no net load or displacement laterally and so this term is the one required in order to model laterally loaded piles.

A series of test cases were performed with meshes with different radial and vertical boundary dimensions and different boundary conditions. A range of pile-soil stiffnesses were modelled to cover pile responses from flexible through to rigid.

Uniform soil case

The meshes were automatically generated using an algorithm for the radial element widths, such that on a logarithmic scale the radii of the Gauss points fall on a more or less regular spacing. This gives the elements of the soil near the pile face an opportunity to model the complex and rapid rate of change of displacements and stresses that must occur in this region. Such a treatment can produce very thin elements near the pile face and very wide elements at the outer boundary to the mesh.

While not appearing to be a good method of discretisation it was found that very large aspect ratios for the element sides could be employed and still provide a reasonable solution. Although not proven, it seems likely that meshes retaining the rectangular geometry of the element, rather than making use of the capability of the finite element method to model non-rectangular geometries, will provide a better modelling of stresses at Gauss points. The improved stresses are then reflected in improved strains and thus deflected shapes.

The meshes consisted of 8 elements radially, and 12 elements vertically with the central uppermost 8 elements representing the pile. A pile with $L/d = 20$ was chosen and the values of the depth and radial width of the entire mesh were varied in order to gauge the effect of the proximity of the boundaries. After a preliminary study, a completely rough boundary condition was chosen, in order to model the far field behaviour of zero strain. As noted previously, smooth boundaries are sometimes used, but can cause unexpected results. This was particularly so for the smaller radial boundary meshes and the response connected with moment loading.

If a smooth boundary, only radially fixed, was used for the smaller radius meshes it was possible to obtain larger deflections and rotations than were achieved with larger radius meshes. The sliding, both vertically and circumferentially, at the radial boundary led to a larger than desired set of radial stresses directly in front of and behind the pile and consequently larger radial strains and hence deflections.

Such behaviour near the pile was deemed to be unrepresentative of both the theoretical half-space response and any practical single pile situation. Thus, nodes which were fixed in all three directions were used on the radial boundary. The boundary conditions on the base of the mesh had a less severe influence upon results and a realistic condition was assessed as being also the one of fully fixed nodes on the base.

The above discussion is based upon results using Poisson's ratios of 0.3 and 0.48 for the soil and of 0.2 for the pile. From the results of analyses in which Poisson's ratio was varied, it was found that it had only a minor effect, as long as results were presented normalised to the Young's modulus, rather than the Shear modulus. Thus the bulk of results presented in this thesis are for Poisson's ratio of 0.3 unless stated otherwise.

The analyses performed covered a range of radial boundaries from 3.75 to 60 pile diameters for a vertical height of mesh equal to twice the pile length and a range of vertical heights of mesh from 1.1 to 4 times the pile length for a radial boundary at 30 pile diameters.

The results of the two series of analyses are presented in Tables 3.5 to 3.10 as a tabulation of influence coefficient

against relative stiffness. The non-dimensional influence coefficient is based upon the pile length and the uniform Young's modulus of the soil, while the pile-soil system relative stiffness is measured by the factor $K = \frac{E I}{E L} \frac{P P}{R}$. For the case of a pile in a homogeneous elastic soil the value of K can be related to the ratio of critical length to real pile length by the equation $L_c / L = \pi \sqrt[1/4]{\frac{2 K}{R}}$.

The full height of the mesh is given the symbol h and the distance from the centre to the radial boundary the symbol s . Throughout the analyses the pile length and diameter were kept constant, as were the number of elements in the mesh. It would appear desirable to also change the number of elements in the mesh to maintain a similar element geometry near the pile. This was not done for two reasons:

1) part of the aim was to model the half-space response as economically as possible. Thus, performing the parametric study using more elements was prohibitive because of the computer time needed. Also, there would have been some analyses at smaller s/d ratios that would have meshes with very few elements radially and thus a poorer modelling ability. It must be remembered that it is the influence of the position of the boundary that is being studied, not the ability of the analysis to be accomplished by a minimum of elements. The chosen number of elements was considered optimal for the accuracy of modelling required.

2) the study would provide an indication of the limit of feasible solution by exhibiting a deterioration of response once the mesh became over-stretched.

Table 3.5 shows the half-space head response due to head shear is poorly modelled, i.e. lower influence coefficient values, for the smallest radial dimensioned mesh. This is true for the full range of pile/soil stiffness but is most severe for the rigid piles and less severe for the most flexible piles. As the radial dimension increases the response improves, i.e. the influence coefficient increases, until a mesh of 30 diameters lateral extent is reached. The mesh with the radial boundary at 60 diameters exhibits a reduced influence coefficient value for all pile-soil stiffnesses and suggests that a practical limit on the radial dimension, using 8 radial elements, is somewhere between 30 and 60 diameters.

The reduction in influence coefficient at the large radius, from the maximum that was obtained, is less severe than for the smaller radius mesh. This suggests the finite element model is still capable of reasonable economic solutions at least up to the radius of 60 pile diameters. Further, it may be said that adequate solutions are possible from meshes of a radius of 15 diameters.

These comments must be viewed in the light of the pile geometry employed and the value of critical length as characterised by the pile-soil relative stiffness factor K_R . Considering the head deflection due to head shear, it can be seen from Table 3.5 that, for the most flexible pile ($K_R = 10^{-6}$) the influence coefficient increases with increasing s/d ratio upto a ratio of 15. Thereafter it decreases slightly due mainly to the reduction in the number of effective elements near the pile. This is because the number of radial elements is fixed at 8, which means only one or two radial elements were expected to model the response in the soil over a distance of a pile critical length.

From the calculation of pile critical length, L_c , it can be shown that the most flexible pile and the smallest radial boundary mesh have a s/L_c ratio of 1.34 and the influence coefficient is only 91% of the maximum response. The maximum response occurs for an s/d of 15 and reduces by only 1% at s/d of 30 thus suggesting the optimum response will be at some intermediate distance. If s/d of 30 is used this represents a mesh with the radial boundary at about ten critical lengths from the pile.

Considering the same deflection response for the next most flexible pile ($K_R = 10^{-4}$) we find a similar picture but with an increased variation between the largest influence coefficient and the influence value obtained from the smallest radial mesh. The smallest radial boundary mesh gives an answer only 83% of the maximum value. This is because now the boundary is fixed at a radial distance of less than half the critical length.

For the almost rigid piles analysed in the test ($K_R > 1$), the effect of lateral boundary position played a major role in the maximising of the deflection and rotation response. With the radial boundary at the shortest distance, 3.75 pile diameters, a 40% reduction in head response was obtained. This is consistent with the important pile dimension, the actual length for rigid piles, being much greater than the distance to the radial boundary. As for the case of flexible pile response, it was found that the depth of layer had very little effect on the response of piles for layer depths down to just 1.1 times the pile length, as shown in Tables 3.8 and 3.9.

The results suggest an optimum is a radial boundary at between 5 and 10 times the pile critical length or the real length, whichever length is shorter, and a layer depth between 1.5 and 2 times the pile critical length or the real length.

3.4.4 Profile Building Analysis

This analysis uses layers of finite elements to build a series of soil profiles of increasing depths. The initial base layer of the profile is analysed to get an influence matrix relating nodal deflections and loads on its upper surface. The next layer to be added is analysed separately to provide a second influence matrix relating nodal deflections and loads on both its upper and lower surfaces. For each of the two layers, the following relationship is derived:

$$[I] F = u \quad 3.49$$

where $F = \begin{pmatrix} F_1^T \\ F_2^T \end{pmatrix}$ is a vector of nodal loads,

$u = \begin{pmatrix} u_1^T \\ u_2^T \end{pmatrix}$ is a vector of nodal deflections

$$[I] = \begin{bmatrix} I_{11} & I_{12} \\ I_{21} & I_{22} \end{bmatrix} \text{ is the influence matrix}$$

and subscripts 1 and 2 correspond to the upper and lower surfaces of one layer.

Figure 3.14 shows the original layer and illustrates the situation before the two layers are combined on their common interface, (lower surface of body (ii) and upper surface of body (i)). Compatibility conditions can be derived for the nodal loads and deflections at this interface, as follows:

$$\begin{aligned} u_{-1} - u_{=2} &= \Delta u \\ F_{-1} - F_{=2} &= \Delta F \end{aligned} \quad 3.50$$

where Δu and ΔF are the mismatch of nodal deflections and loads occurring at the interface and the number of underlines indicates the body number (i) or (ii).

Equations 3.49 and 3.50 can be used to derive the influence matrix for the deflections of the upper surface of body (ii) $u_{=1}$, in terms of the loads on that upper surface $F_{=1}$, for the combined body composed of bodies (i) and (ii), i.e.

$$u_{=1} = \begin{bmatrix} I_{=11} & -I_{=12} \\ I_{=12} & -I_{=11} \end{bmatrix}^T F_{=1} + I_{=11} [\Delta F_{=1} - \Delta u_{=1}] \quad 3.51a$$

$$\text{where } I_{=11} = \begin{bmatrix} I_{=12} & -I_{=11} \\ I_{=12} & -I_{=11} \end{bmatrix}^{-1}$$

and using the fact that ΔF and Δu are normally zero, leads to

$$u_{=1} = [I'_{=1}] F_{=1} \quad 3.51b$$

where $I'_{=1} = \begin{bmatrix} I_{=11} & -I_{=12} \\ I_{=12} & -I_{=11} \end{bmatrix}^T$ is the new influence matrix of the combined bodies (i) and (ii). By introducing a new body (ii) the procedure can be repeated using the previously calculated response of the already combined bodies as a new initial, base layer. Considerable computational economy can be achieved if the body (ii) is the same for each layer, thereby necessitating its stiffness formulation and solution once only during the entire building of a particular profile.

Because the end result is simply an influence matrix relating the loads and deflections on the surface of the soil profile, it is a simple task to store this matrix for later use in further analyses. For example, the solutions presented herein are produced by first analysing a finite layer composed of soil elements, increasing the profile depth until the average deflection of a circular loaded area on the soil surface does not

significantly change when the depth is further increased. This "converged" influence matrix can then be used to calculate the average deflection and rotation of the soil within the loaded area to provide an estimate of the response of a rigid surface footing on an elastic half-space.

The same influence matrix can then be used as the starting base layer for an analysis with layers containing both soil elements and the stiffer elements of the foundation. This saves analysis of the same "converged" block of soil layers for each pile to soil stiffness ratio that is considered. The depth of the "converged" base layer is sufficient to eliminate the effect of the finite depth of the soil profile for all but long stiff piles.

The present analysis uses fully fixed boundaries to the base and sides of the final solution in order to simplify the influence matrix formulation. This is not a restriction of the method as special substructuring techniques can be employed to account for any rigid body modes of movement that require arbitrary fixities to be incorporated, c.f. Rowe et al. (1978). The chosen boundary conditions were considered the only appropriate ones for the comparison of various Poisson's ratios of the soil and the different types of loading employed on the half-space model.

Ten radial elements in total, with two of these elements under the loaded area to represent the pier, or the soil under the surface footing, were used in order to retain a reasonable size for the deflection influence matrix. A banded solver was used for the small half-bandwidth system of equations of the finite element layer stiffness matrix, and a Gaussian solver with partial pivoting was used for the inversion of the combined influence matrix.

The use of two equation solution techniques actually results in a reduction of storage requirements when ten or more radial elements are used in the analysis. The fully populated nature of the combined influence matrix reduces any benefit from the use of the banded solver while the Gaussian solver provides an accurate matrix inversion. During the solution process, the symmetry of the influence matrices used, and also the range of the maximum and minimum pivot, were monitored to indicate numerical instability.

For the case of axial load the use of thin layers of finite elements to model the soil, means the in-plane stiffness far exceeds the normal stiffness of the layer. This has the effect of introducing large differences in the magnitude of terms in the influence matrices and results in numerical difficulties. For this reason, and the fixed vertical extent of the depth of soil beneath the pile base, the method is not suitable for analysis of long stiff piles.

All analyses presented in this thesis were carefully checked against standard finite element solutions of each problem, and where possible analytic solutions, to ensure the accuracy of the results. The results obtained using this method are considered to be accurate and are likely to be better than standard finite element solutions because of the finer overall discretisation of the problem.

3.5 Recommended Method for Linear Analysis

The three approaches described in the previous sections have dominated the analysis of laterally loaded piles. None of the approaches represent a definitive version of laterally loaded pile analysis:

- a) The Winkler type of method requires extensive calibration with experience to become practically useful and has limited predictive capabilities.
- b) The MBEM analysis requires assumptions about non-homogeneous elastic-continuum interaction with the pile that reduce its theoretical integrity.
- c) The FEM analyses are usually impracticable for most real problems, although Elastic Theory is given its most rigorous treatment by this method.

All these models are restricted to soil-pile interfaces that do not exhibit theoretically predicted non-linear response, nor do they allow for pile-soil breakaway.

In this section the MBEM analysis is modified in a logical manner to allow for consideration of limited soil depth and soil non-homogeneity with depth. Recourse is made to the AGFEM analysis to check the modification proposed for the homogeneous elastic-continuum model in order to give non-homogeneous soil behaviour.

The possibility of localised soil bearing capacity failure at stations down the pile and the concept of a non-linear interface element, between the pile and soil, will be introduced to model non-linear behaviour in Chapter five.

3.5.1 Mindlin-based Soil Layer of Finite Depth

The elastic Mindlin soil element is derived from the behaviour of a homogeneous elastic half-space. It follows that a finite depth layer of soil cannot be strictly modelled. The work of Poulos (1972) presented a variety of methods by which the Mindlin based analysis can be adjusted to provide adequate approximation to the behaviour of a pile with a socketed or pinned tip in a soil of limited depth. In general the choice of method of approximation made very little difference to the head response, with the largest effect for rigid piles with fixed tips. The various approximations attend to the problem of reducing the half-space influence coefficients in order to give zero displacement at the bottom of the layer, where the pile tip is pinned or socketed.

The horizontal equivalent of the Steinbrenner approximation was intuitively found unsatisfactory by Poulos. The correction of the influence matrix values by subtracting the deflections at the tip, for the loading of successive elements, will overcompensate for the lack of stiffness of the upper elements. The further the element is from the rigid base, the smaller becomes the expected effect of the rigid base upon the element deflections. This method also makes no allowance for the conservation of symmetry of the influence matrix that is required by the use of elastic theory.

When the influence matrix is expressed in terms of average element displacements and total forces at elements, the use of elastic theory should result in a symmetric matrix. This feature of elastic theory should also be displayed in the head response, with the deflection due to applied moment and the rotation due to applied shear being equal from the reciprocal theorem.

This conservation of symmetry is not observed in the preferred "mirror image" method of Poulos. However, it seems likely that the preferred form of the approximation, for the behaviour of elements distant from the rigid base, provides a gain in accuracy of modelling of behaviour, that gain being greater than the errors involved in using a slightly non-symmetric soil influence matrix.

Another possibility that was considered is to use the influence coefficients for an elastic half-space in the boundary element analysis without modification, but with the displacement of the tip element restrained to be zero. This method takes no account of the layer depth and arbitrarily assumes a displacement profile for the soil below the supposed rigid base.

A more satisfactory approximation is to use the fact that the displacements of any soil at and below the level of the pile tip should be zero in the rigid base. This will still be an approximation, since the displacements of points in the rigid base, other than on the extended pile length, will not necessarily be zero. One possible way of achieving this zero displacement regime is as follows.

The soil elements in the model may be extended below the actual pile tip, for some length deemed sufficient to model the rigid base. It can be seen that the previous fixing of just one node at the tip is one limit of such a method, while extending the zero deflection soil elements to infinity is the other limit. A convenient distance to maintain zero displacement elements might be seen as five pile diameters, since the influence of a loaded soil element upon another element is very small at that spacing when compared to the self influence.

The soil influence matrix for a homogeneous soil may be partitioned, so as to separate the quantities of load and displacement into one set for the soil layer and another set for those in the "rigid base layer".

$$\begin{bmatrix} I_{ss} & I_{sb} \\ I_{bs} & I_{bb} \end{bmatrix} \begin{bmatrix} W_s \\ W_b \end{bmatrix} = \begin{bmatrix} u_s \\ u_b \end{bmatrix} \quad 3.52$$

where subscripts s and b refer to the upper soil layer and lower rigid base layer. If the lower deflections, u_b , are equated to zero, then there is established a relationship between the upper soil loads, W_s , and the lower soil loads, W_b . Employing this relationship for the upper deflections u_s we find

$$u_s = \begin{bmatrix} I_{ss} & -I_{sb} I_{bb}^{-1} I_{bs} \end{bmatrix} W_s \quad 3.53.$$

Equation 3.53 shows the modification would retain any symmetry in the original influence matrix, unlike the "mirror image" modification preferred by Poulos (1972). The modified influence matrices from both the "mirror image" and the new method outlined here, have been found to be very similar from a limited number of calculations made for an $L/d = 10$ pile.

It is considered that the elastic analysis of a relatively stiff socketed or pinned tip pile is best accomplished by using the Finite Element Method, since there are none of the above approximations involved in this form of elastic analysis. The stiff piles encountered in practice are usually short enough to allow good modelling with an economical number of finite elements. Further, socketed rigid piles are less common than the more practical case of flexible piles. Very few piles would be designed

outside of the flexible range, and as such have a head behaviour that is virtually independent of the tip condition.

Various researchers, including Carter and Booker (1981), and Velez, Gazetas and Krishnan (1983), have used this aspect of pile behaviour to employ limited depth finite element mesh geometries, for essentially socketed piles, to provide results for the behaviour of flexible floating piles.

In respect of the above it was deemed unnecessary to deeply investigate this aspect of behaviour and felt sufficient to outline the possibility of adapting the Mindlin based solution. The results of Poulos (1972) and the trends evident in the results presented later for the Winkler soil model are suggested as adequate solutions, while the use of Finite Element Methods in particular cases may be worthwhile when a more accurate solution is desired.

3.5.2 Modification for Non-Homogeneous Soil Profiles

The often referred-to limitation of analyses based upon Mindlin's equations, is the restriction to soils that are homogeneous and isotropic. While the isotropic restriction remains, it is possible to postulate a non-homogeneous response, as has been done by Poulos (1972), Pise (1982) and also by Banerjee and Davies (1978). While such methods have provided useful results, there has been little checking of the analytical basis of the modified solutions, with the exception of Banerjee and Davies.

Any result of the modification of the homogeneous response should be expected to obey, at least approximately, the reciprocal law, as typified by the Maxwell-Betti theorem in structures, which leads to symmetric influence matrices. The modifications must then be shown to be symmetric in their effect upon the influence matrix. For this reason the early results of Poulos for non-homogeneous soil have been shown to be approximate in the sense that his method of modification was not symmetric. In a later paper (Poulos, 1979), it was recommended that the mean of the soil moduli at the influencing and influenced element be taken in order to modify a homogeneous solution. This does represent a symmetric effect upon the influence coefficients and has been generally adopted in analyses that use a modified form of the equations of an homogeneous elastic half-space response.

This mean-modulus modification pays some regard to the importance of the elastic properties of the soil between the influencing and influenced elements. It represents a form of the equivalent modulus concept, which assumes the essential response of some system composed of non-homogeneous material can be represented by taking an equivalent modulus in a homogeneous model. This approach is attractive for its economy but must be used with caution since there is no sound theoretical reason for its use and virtually resorts to a Winkler based approach.

The Poulos-type mean modulus method was tested in an axially-loaded pile application, where all the elements were of the same size. However, the modified boundary element model used here for laterally-loaded pile response involves half elements at the head and toe of the pile. This introduces a disturbance to the natural trend for symmetry in the influence coefficient matrix, that should naturally result from observance of the reciprocal law.

Using a definition for the influence matrix based upon unit uniform normal tractions acting over elements, leads to the head and toe elements sustaining only half the total force that arises at internal, full elements. Further, the use of displacements at discrete points, and at both the centre depth of internal elements and top or bottom edge of the first and last elements, will lead to inconsistent sampling of the changing patterns of response within elements. For these reasons the influence matrix relating traction and displacement for the soil model will not be symmetric, although it should show a strong tendency to symmetry for internal element response.

In order to properly assess the modification to the homogeneous solution, it is necessary first to ensure that there is no contradiction of the reciprocal nature of elastic behaviour. According to Love (1928), Maxwell in 1864, demonstrated the reciprocal theorem with particular reference to structural behaviour, and by formulating the problem in terms of work, the elastic continuum behaviour may also be demonstrated to obey the reciprocal theorem. To this end it is convenient to define the interface traction to be uniform and then it becomes necessary to define the deflection to be an average over the element.

These definitions of distributed load and average deflection over areas ensure the symmetry of the influence matrix, because the terms to be related can be used directly to calculate the work done by the total force at an influencing element over the displaced region of its own or any other element. Brown and Booker (1976) have pointed out the facility of using such definitions for a numerical model of a raft interfaced to a visco-elastic soil

model. The resultant symmetric, positive definite influence matrix, I_{ij} , can be expressed as

$$\left(\frac{u_{ij} E_{ref} d}{F_j} \right) = I_{ij} \quad 3.54$$

where u_{ij} is the average normal displacement at the i .th element due to load on the j .th element, E_{ref} is a convenient reference Young's modulus, d is a representative dimension (here the element width is used) and F_j is the total force resulting from a uniform normal traction over A_j , the j .th element area.

The form of u_{ij} will vary depending upon the form of the non-homogeneity and for the homogeneous case is given directly by the equations of Mindlin integrated over a rectangular vertically plane region. Any postulated form of modification must allow the recovery of the homogeneous answer and also maintain a symmetrical effect. To this end a form of modification similar in nature to the mean modulus proposal is defined as

$$u_{ij} = u_{ij}^* E_{ref} / E_{ij} \quad 3.55$$

where u_{ij}^* is the mean displacement at a node in a homogeneous soil whose modulus is E_{ref} and $E_{ij} = (E_i A_i + E_j A_j) / (A_i + A_j)$, a weighted modulus for interaction between elements i and j in a non-homogeneous case.

In this way the influence matrix, I_{ij} , can be prepared for a non-homogeneous material. The method gives extra weighting to whichever of the loaded or influenced areas is the largest. The modulus values that correspond to each element are taken to be the average value over the depth of the element, in keeping with the concept of an equivalent modulus. This average also avoids the possibility of assigning zero modulus to the element at the

surface for the case of soil modulus proportional to depth. It is convenient to take the reference modulus, E_{ref} , to be the value at the tip of the pile, noting that this is not necessarily the same value as for the modulus of the element at the pile tip.

This formulation results in a symmetric modification of the influence matrix and gives extra weight to the moduli of larger elements of the discretised soil. While this appears intuitively correct it is no more than an approximation, and it is necessary to investigate the worth of such an approach before applying it to lateral pile response analysis. It must be emphasised that the adequacy of this approach for lateral pile response analysis will not mean that a universal application of such an approach to other problems will always be adequate.

Indeed, the modification depends upon the region of major straining being close to at least one of the points at which the weighted average modulus would be found. A hypothetical example where this is not true is a cantilever with non-homogeneous modulus with length, where the largest bending moment, and therefore strain, being at the base means the major straining may well occur away from either of the influencing or influenced points on the beam. In such a case the required equivalent modulus has no similarity to the weighted average modulus employed in this modification.

Mindlin Non-Homogeneous Soil Verification

Apart from the work of Davies and Bannerjee (1978) there has been little advance in the analysis of point loads acting in elastic continua with non-homogeneous Young's modulus. The results of Mindlin (1936), say expressed in the form derived by Douglas and Davis (1964), remain the most commonly employed model upon which some modification is imposed to approximate the effect of non-homogeneity. The finite element method currently provides the best means with which to properly take account of non-homogeneous Young's modulus. Thus, the method of modifying the Mindlin solution, if it is to provide adequate modelling of lateral loading of non-homogeneous soil profiles, must be shown to work satisfactorily on the results from a finite element analysis of a similar problem.

The Mindlin-based model is a strip in an elastic half-space, i.e. a region in the continuum corresponding to the pile, but with zero thickness and width equal to the pile. The Mindlin-based problem is defined by applying an x-directed uniformly distributed loading on rectangular elements of the discretisation, which is not defined in terms of stress resultants on the soil but is directly related to the resultant distributed load acting.

The axisymmetric geometry finite element model consists of a large cylinder of elastic soil of finite radius and depth, with a central circular hole where the pile would be situated. In a similar manner to the Mindlin-based analysis, the finite element model uses an x-directed distributed traction, but now around the circular hole face. Both of the assumed interface tractions have no resultant load across the direction of loading, i.e. across the pile face. However, the finite element modelling does include

circumferential shear, but it is self-equilibrating in the y-direction.

The deflection of the Mindlin soil element, is at the mid-height of internal elements of constant height and the upper and lower edges of the top and bottom half-height elements, see Fig. 3.7. An average deflection across the element face at these nodal depths is found, as defined in Section 3.3.2. This means a similarly defined deflection should also be found from the finite element-based response. In this case, with load in the $\theta = 0$ direction, it can be shown that the average of the x-directed deflections at $\theta = \pi/2$ and $\theta = 0$ can be used. This means the deflections found in the finite element analysis, Fourier coefficients U_r and U_θ , can be directly used.

While the finite element model has been devised to be similar to the Mindlin model, this leads to two results:

The average deflection used to describe the soil behaviour is not a true average deflection over the entire height of the elements of either model, although the value is close to the true average. If an average deflection over the entire surface area of the applied load were used, in conjunction with unit resultant force applied by the uniform tractions, a symmetric set of influence matrices results. Thus the soil influence matrices from both analyses are somewhat non-symmetric. While this does not affect the quality of the eventual pile solution, it makes checking for errors in formulation more difficult.

Secondly, it is a characteristic of the finite element formulation that any coarseness of the mesh will result in locally poor deformation patterns for some elements; this is especially

true for the elements with lower modulus near the surface in highly non-homogeneous profiles. When the average deflection of an entire element is found, the locally-affected deflection pattern smooths to give a more satisfactory result. This complete averaging is not the method that was employed by the Mindlin-based soil analysis, and so the comparison here has been restricted to averaging the deflection at the same depth as the Mindlin-based soil nodes, see Fig. 3.7b.

Two finite element meshes were used, to analyse pile length to diameter ratios of ten and twenty. Both meshes had eleven elements for the pile length, a rough radial boundary at twenty pile radii and a rough base boundary at a depth of two pile lengths. The uniform uni-directional traction was applied to each element of the interface in turn and the deflections of the desired nodes recorded in a soil influence matrix. This procedure was followed for the soil non-homogeneity ratio, E_o/E_L equal to 1.0, 0.5, 0.3 and zero.

The eight interface geometries were also analysed using the Mindlin soil element, using the suggested modification procedure to predict the non-homogeneous response. The resulting soil influence matrices were then output for comparison with those from the finite element analyses. This comparison indicated that the soil response from the finite element method was 82% of that obtained from the Mindlin half-space approach for the deflections due to self influence of loaded elements.

This difference was expected and arises because the results from using the finite element mesh are affected by the proximity of the boundaries, mainly the radial boundary. The infinitely large volume of material in the Mindlin solution, that can strain

and add to the total deflection, can never be modelled using conventional finite elements. However, this extra deflection presents itself as a rigid body motion that is fairly constant over the entire length of the interface. As such, it will have little effect upon the interaction behaviour between loaded elements, which is of importance here.

Despite the differences between the two problems in form of loading and geometry of the discretised elastic soil, the two sets of results are very similar. This similarity of both responses, suggests that soil response is not sensitive to changes of pile cross-section geometry, as was suggested by Baguelin et al. (1977).

Because there is some difference between the deflections predicted by the two models of the interface, direct deflection comparison of the two does not represent a fair nor appropriate test of the prediction of non-homogeneous behaviour by the proposed method of modifying the homogeneous response. In order to accomplish this, the finite element results for a homogeneous soil will be modified using the chosen method to predict the non-homogeneous deflection response. This modified homogeneous finite element solution can in turn be compared with results using the non-homogeneous soil profiles directly in a finite element model.

Figure 3.15 shows the deflected soil profiles based upon the influence matrices found by the modified Mindlin analysis and the direct finite element approach, for $L/d = 10$. The load is applied at the depth of the third element from the surface. It should be noted that the actual soil profiles differ slightly from those in the figure, since only one horizontally averaged deflection point at the centre depth of each element is used to define the curve.

It is apparent that the two methods of analysis have their worst agreement in the upper portion of the curves, for the highly non-homogeneous case of a modulus proportional to depth. This arises because the average deflection across one depth (at the centre of the element) is used in the influence matrix. If the average deflections over the entire area of the elements were compared, the discrepancy would be less severe than this method of plotting the profiles suggests.

The two sets of curves also display the larger bulk movement of the soil in the results based upon an elastic half-space, compared to the finite element results. As mentioned, this is due to the finite boundary to the region modelled by the finite element analysis. But, significantly the two methods both give the same trends with depth and non-homogeneity factor. A similar picture to that depicted for $L/d = 10$ was found for the longer length to diameter ratio case of twenty.

The appropriate comparison, to check the modification procedure, is that between the results of the non-homogeneous finite element analyses and the predictions for non-homogeneous response from the modified homogeneous finite element response. This has been done in Figs 3.16 and 3.17. Figure 3.16 is a profile of the ratio of predicted to actual soil deflection for loading of the third element. Figure 3.17 is a plot of the same ratio of deflections, but for the self-influence of loaded elements and is not a soil response profile.

It is clear from the plots of the ratio of predicted soil deflection (using the modified homogeneous solution) to the deflection from the actual non-homogeneous solution, that the modification generally leads to an over-prediction of the

deflections down the profile. While this may reach a value of thirty percent near the base of the profile, the large apparent error should be viewed in the perspective that the total deflection involved is several orders of magnitude smaller than the maximum deflection due to self influence. Also, the largest influenced-deflections are typically only between one third and one half of the self-influence deflection. When these errors are scaled it becomes apparent that they are not significant.

For the response depicted in Fig. 3.16 near the surface above the third element, the highly non-homogeneous nature of the soil leads to localised perturbations in the deflected shape from the finite element analysis that make the comparison based on only one deflection magnify the apparent error. In the case of longer piles, the local deformation means the top element deflection has been over-predicted and second element deflection under-predicted by the finite element analysis of the non-homogeneous profile. The predicted response from the homogeneous analysis possesses errors that are in the opposite sense. Thus, the modification of the homogeneous solution actually seems to improve the accuracy of the non-homogeneous solution that results.

The adequacy of the modification method is better displayed in Fig. 3.17, where the accuracy ratio for the self-influenced behaviour is plotted against position in the profile. This figure shows the accuracy of the upper two elements are the worst. But again it could be argued that the non-homogeneous responses, predicted using the modified homogeneous response, are preferable to those from the actual finite element analysis of highly non-homogeneous profiles. The trend is consistent with the large strains and magnified errors of the smaller modulus material leading to an over-prediction for the top element and an under-

prediction for the second element responses.

It may be that finer meshes and the definition of the influence coefficient in terms of the average deflection over an entire element area, would lead to a better performance in the above tests. However, these improvements concern the behaviour of the finite element model, not the method of modification of the homogeneous elastic half-space used in the boundary element model.

It has been shown that the proposed method of modification of the homogeneous soil influence matrix gives adequate influence matrices for non-homogeneous elastic soil profiles, based upon the results of its application to a finite element model. Thus, the modification is expected to give satisfactory answers when applied to the Mindlin-based elastic model of the soil. This adequacy is strictly only limited to the behaviour of the types of soil profiles checked here, i.e. with a linear increase of Young's modulus with depth. Severe step changes in Young's modulus might not be expected to be as accurately modelled by the modification, but their consideration will be delayed until Chapter five, where they will be considered in association with the new analysis method developed there.

3.6 Conclusion

Section 3.2 describes an analytic solution of single laterally loaded piles using a Winkler soil model, which gives a discretisation-free result of a problem that can also be solved numerically using the MBEM approach of section 3.3. This provides a valuable check upon the accuracy of the MBEM solution procedure and indicates the degree of discretisation necessary to achieve this accuracy. Further, the simple Winkler-based answers agree favourably with elastic continuum-based ones for the problem of distributed loading of thin vertical regions of soil, akin to a pile projected shape, see section 3.3.2 and Fig. 3.5.

The elastic finite element method employing analytic modelling of the circumferential behaviour (section 3.4), has been used as a benchmark program against which to assess the accuracy of the modifications in the recommended soil model that was developed from an isotropic homogeneous elastic half-space model. Extensive checks of the accuracy of the finite element program have been made and some of them reported here in section 3.4.2.

The recommended method for analysis of single laterally loaded piles in an elastic continuum is presented in section 3.3 and 3.5. The necessary modifications for soil of limited depth and non-homogeneous Young's modulus with depth have been described. Checks with the finite element answers were made for the non-homogeneous modification and the limited depth modification method was compared with existing methods. In this chapter the MBEM analysis has been developed to give accurate linear elastic solutions to the problem of a single laterally loaded pile in both a Winkler and elastic continuum soil.

Load Type	Deflection of a Uniformly Loaded Rigid Circle	Mean Deflection of a Uniformly Loaded Square
Vertical at Surface	$\frac{wE}{pvd} = \frac{\pi}{4} (1 - \nu^2)$ (Poulos & Davis, 1974)	$\frac{\bar{w}E}{pd} = \frac{\pi}{3.32} (1 - \nu^2)$ (Giroud, 1972)
Normal at Depth	$\frac{uE}{pd} = \frac{\pi^2}{32} \frac{(1 + \nu)(3 - 4\nu)}{\pi(1 - \nu)}$ (Selvadurai, 1976)	$\frac{\bar{u}E}{pd} = \frac{\pi^2}{26} \frac{(1 + \nu)(3 - 4\nu)}{\pi(1 - \nu)}$ (Section 3.3)

TABLE 3.1 Equations for Deflection of Uniformly Loaded Rigid Circular Plates and Mean Deflection of Uniformly Loaded Squares in an Isotropic Homogeneous Elastic Medium.


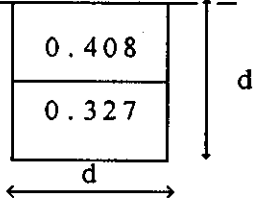
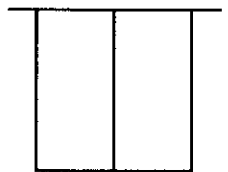
Load Case	Elastic E, ν	Winkler $E_s = E$ $pd = E_s u$	No Interaction: Superposition Winkler/ Solution Elastic
<i>Horizontal Surface Square</i> 	0.861	1.0	0.592
<i>Vertical Shallow Square</i> 	0.559	0.5	0.367
	0.559	0.5	0.364
<i>Any Orientation Deep Square</i>	0.404	0.5	0.278

TABLE 3.2 Average Deflection Resulting from Loading of a Unit Square by Unit Applied Traction for Surface and Buried cases ($E = 1$ $\nu = 0.3$, Elastic Theory Parameters).

$\frac{L}{d}$	$\frac{\bar{u}E}{pd} (\nu = 0.5)$		
	Rigid Plate Douglas and Davis (1964)	Approx. Mean of Flexible Area	MBEM Rigid Pile Analysis (21 elements)
0.25	0.230	0.267	0.247
0.5	0.394	0.390	0.367
1.0	0.500	0.535	0.508
2.0	0.665	0.694	0.662
5.0	0.900	0.910	0.879

TABLE 3.3 Various Estimates of the Mean Lateral Deflection of Vertical Rigid Plates and Piles of Different Buried Length to Breadth Ratios in an Elastic Isotropic Homogeneous Soil Due to Uniformly Distributed Lateral Load, p .

Load Case	Error in Deflection %		
	u	v	w
Axial	-1.0	-	-2.4
Torsional	-	-0.7	-
Horizontal	-2.0	-2.2	-7.6
Moment	-2.8	-0.8	-0.6

TABLE 3.4 Differences in Maximum Deflection at the Edge of a Circular Loaded Region on an Elastic Half-space, $\nu = 0.3$, between the AGFEM Analysis and the Results of Gerrard and Harrison (Poulos and Davis, 1974).

		$\frac{u E L}{H}$				
K_R	s/d	3.75	7.5	15	30	60
	10^{-6}	14.74	15.78	16.12	15.96	15.53
	10^{-4}	6.96	8.02	8.40	8.24	7.79
	10^{-2}	2.53	3.22	3.68	3.75	3.45
	10^{-1}	1.89	2.54	3.00	3.09	2.82
	10^0	1.80	2.45	2.91	3.01	2.73
	10^1	1.79	2.44	2.90	3.00	2.73
	10^2	1.79	2.44	2.90	2.99	2.72

TABLE 3.5 Influence Coefficient for Deflection due to Shear for a $L/d = 20$ pile and $h/L = 2$.

		$\frac{u E L^2}{M}$ and $\frac{\theta E L^2}{H}$				
K_R	s/d	3.75	7.5	15	30	60
	10^{-6}	193.4	195.7	195.2	193.9	192.9
	10^{-4}	55.5	58.5	58.4	57.1	55.7
	10^{-2}	6.72	7.78	8.30	8.14	7.52
	10^{-1}	3.14	4.02	4.54	4.46	3.96
	10^0	2.66	3.54	4.06	3.98	3.48
	10^1	2.61	3.49	4.01	3.93	3.44
	10^2	2.61	3.48	4.00	3.92	3.43

TABLE 3.6 Influence Coefficient for Deflection due to Moment and Rotation due to Shear for a $L/d = 20$ pile and $h/L = 2$.

		$\frac{\theta E L^3}{M}$				
K_R	s/d	3.75	7.5	15	30	60
	10^{-6}	23001	22996	22970	22940	22936
	10^{-4}	1038	1053	1049	1040	1034
	10^{-2}	36.6	39.1	40.1	39.5	38.0
	10^{-1}	8.78	10.4	11.3	11.1	10.0
	10^0	5.44	7.03	7.89	7.62	6.66
	10^1	5.09	6.69	7.54	7.28	6.31
	10^2	5.06	6.65	7.51	7.24	6.27

TABLE 3.7 Influence Coefficient for Rotation due to Moment
for a $L/d = 20$ pile and $h/L = 2$.

K_R	h/L	$\frac{u E L}{H}$				
		1.1	1.25	1.5	2	4
	10^{-6}	15.92	15.93	15.95	15.96	15.96
	10^{-4}	8.21	8.22	8.23	8.24	8.24
	10^{-2}	3.71	3.73	3.74	3.75	3.74
	10^{-1}	3.06	3.08	3.09	3.09	3.09
	10^0	2.97	2.99	3.00	3.01	3.00
	10^1	2.96	2.98	2.99	3.00	2.99
	10^2	2.96	2.98	2.99	2.99	2.99

TABLE 3.8 Influence Coefficient for Deflection due to Shear for a $L/d = 20$ pile and $s/d = 30$.

K_R	h/L	$\frac{u E L^2}{M}$ and $\frac{\theta E L^2}{H}$				
		1.1	1.25	1.5	2	4
	10^{-6}	193.8	193.8	193.8	193.8	193.8
	10^{-4}	57.0	57.0	57.0	57.0	57.0
	10^{-2}	8.11	8.12	8.13	8.14	8.13
	10^{-1}	4.41	4.44	4.46	4.46	4.45
	10^0	3.92	3.96	3.98	3.98	3.97
	10^1	3.87	3.92	3.93	3.93	3.92
	10^2	3.87	3.91	3.92	3.92	3.92

TABLE 3.9 Influence Coefficient for Deflection due to Moment and Rotation due to Shear for a $L/d = 20$ pile and $s/d = 30$.

		$\frac{\theta E L^3}{M}$				
K_R	h/L	1.1	1.25	1.5	2	4
	10^{-6}	22943	22942	22941	22940	22939
	10^{-4}	1040	1040	1040	1040	1040
	10^{-2}	39.3	39.4	39.5	39.5	39.5
	10^{-1}	10.7	10.9	11.0	11.0	11.0
	10^0	7.25	7.49	7.59	7.62	7.60
	10^1	6.90	7.14	7.25	7.28	7.26
	10^2	6.86	7.10	7.21	7.24	7.22

TABLE 3.10 Influence Coefficient for Rotation due to Moment
for a $L/d = 20$ pile and $s/d = 30$.

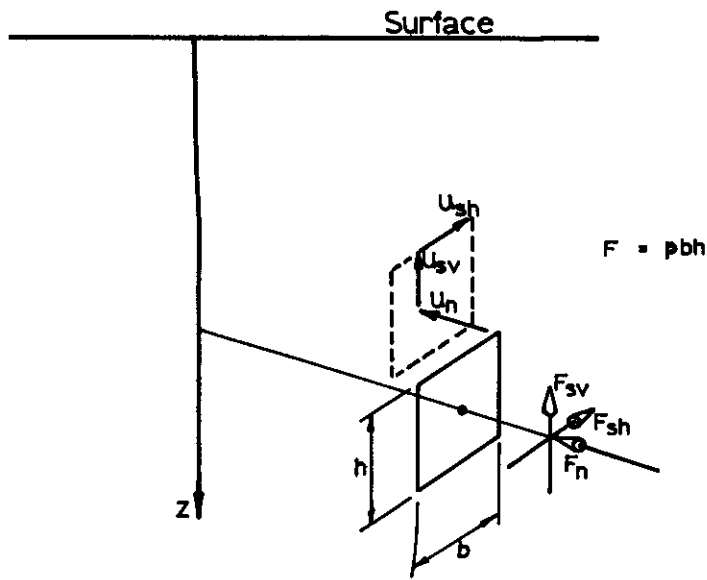


Fig 3.1 ELEMENT OF SOIL USED IN THE WINKLER
BASED ANALYSIS.

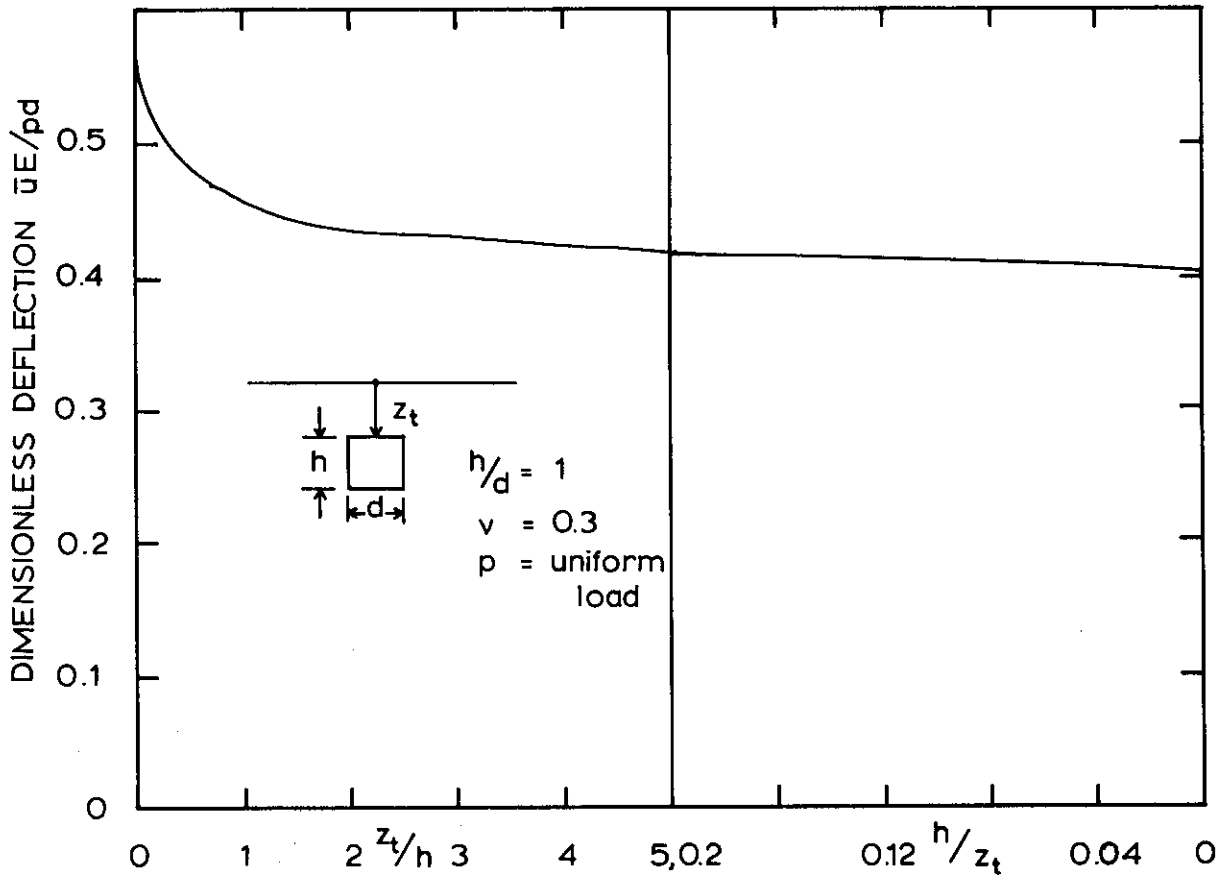


FIG. 3.2 VARIATION OF MEAN DEFLECTION INFLUENCE COEFFICIENT WITH DEPTH

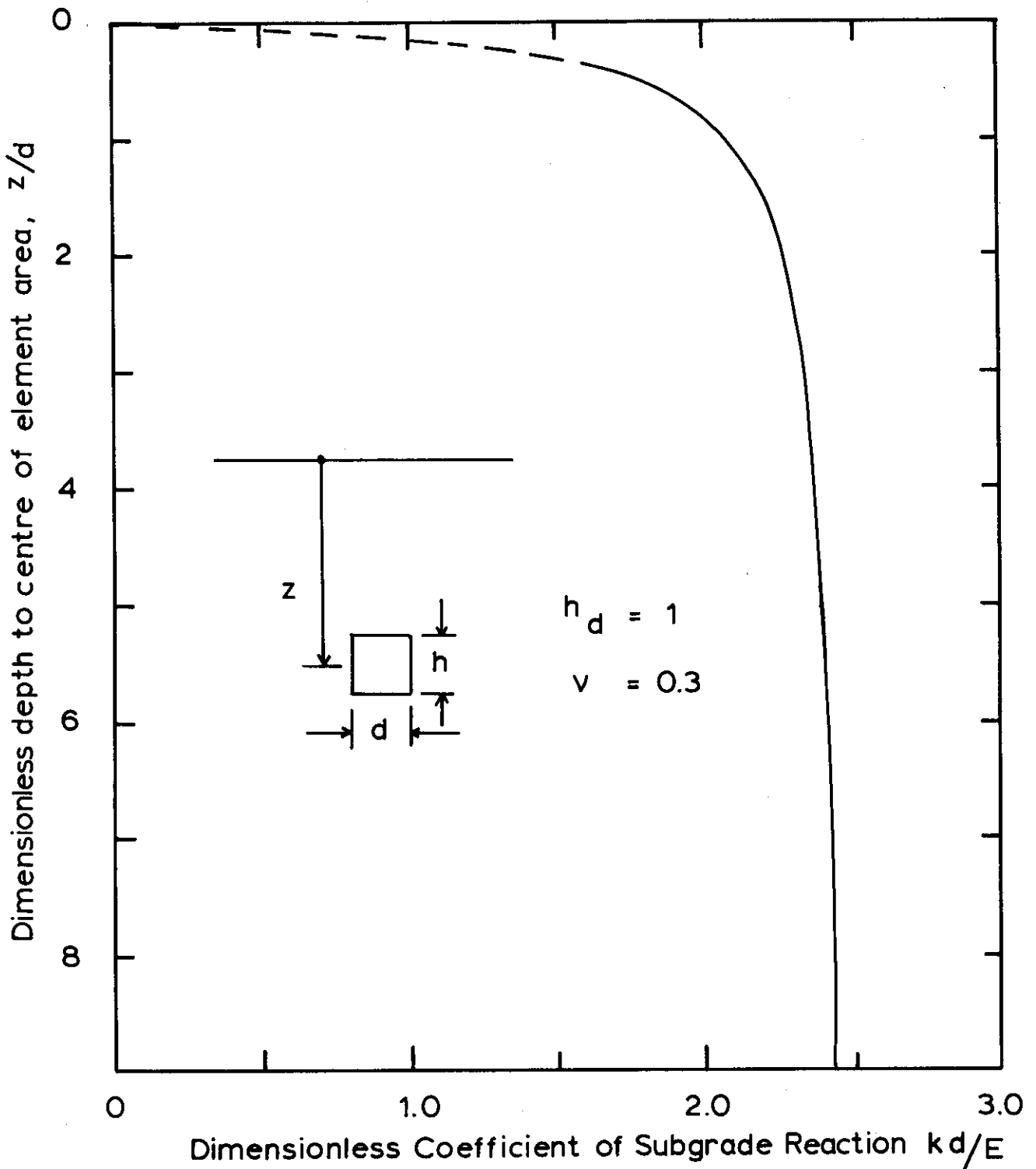
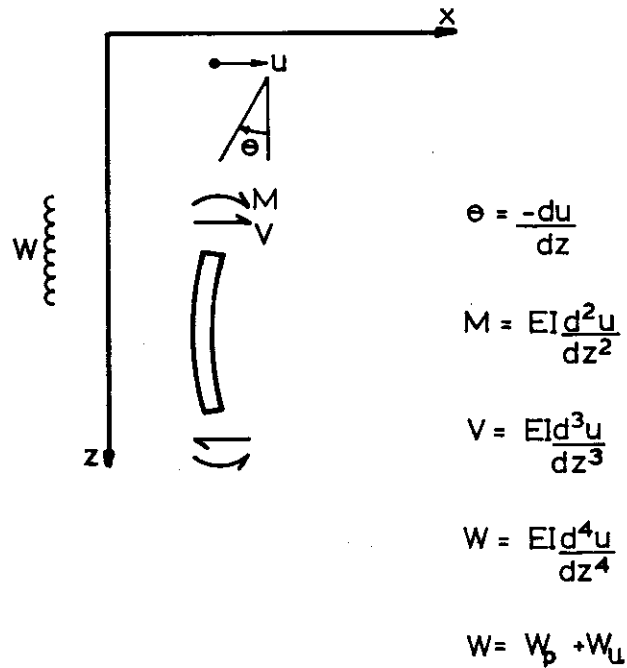


FIG. 3.3 VARIATION OF COEFFICIENT OF SUBGRADE REACTION NORMALISED BY ELEMENT WIDTH AND YOUNG'S MODULUS, E AS DEPTH INCREASES

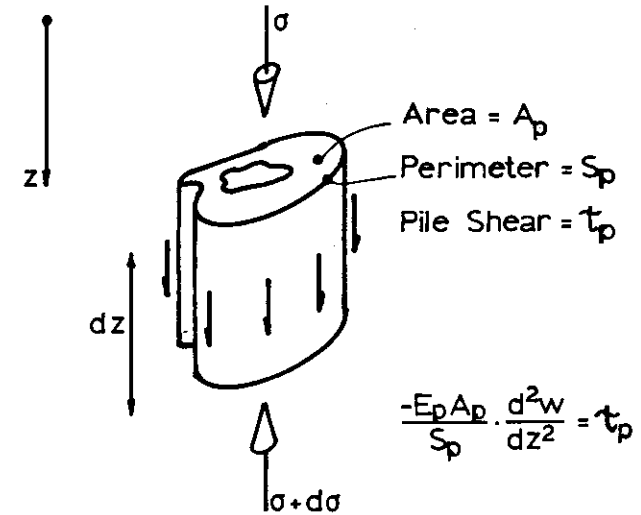


W_p = External pile loads
(usually zero)

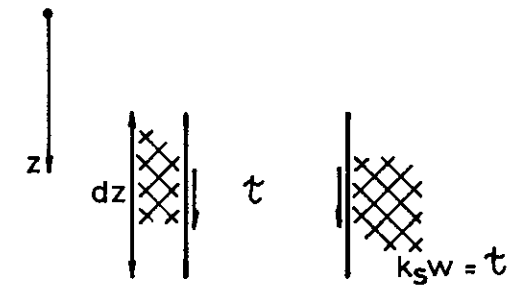
W_u = Subgrade reaction loads. (Interaction loads.)

and $W_u = -E_s u$

Fig3-4a DEFINITIONS OF PARAMETERS IN THE WINKLER PILE/SOIL ANALYSIS.



a) Pile Segment Equilibrium and Resulting Stiffness Relationship



b) Soil Segment and Stiffness Relationship

Fig3-4b AXIAL WINKLER ANALYSIS: PILE AND SOIL REPRESENTATION.

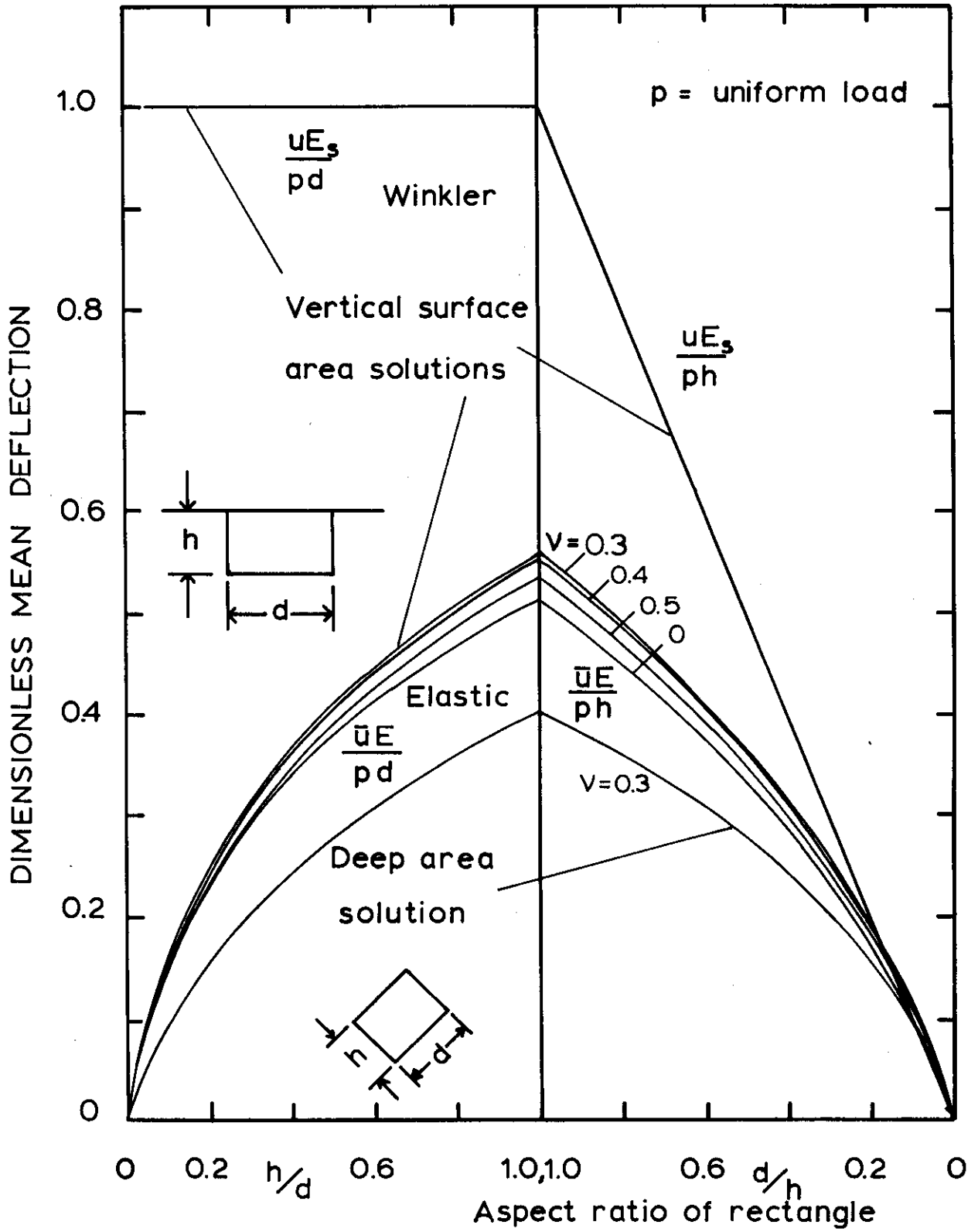


FIG. 3.5 MEAN DEFLECTION OF UNIFORMLY LOADED RECT-ANGLES : ELASTIC HALF-SPACE AND WINKLER MODELS

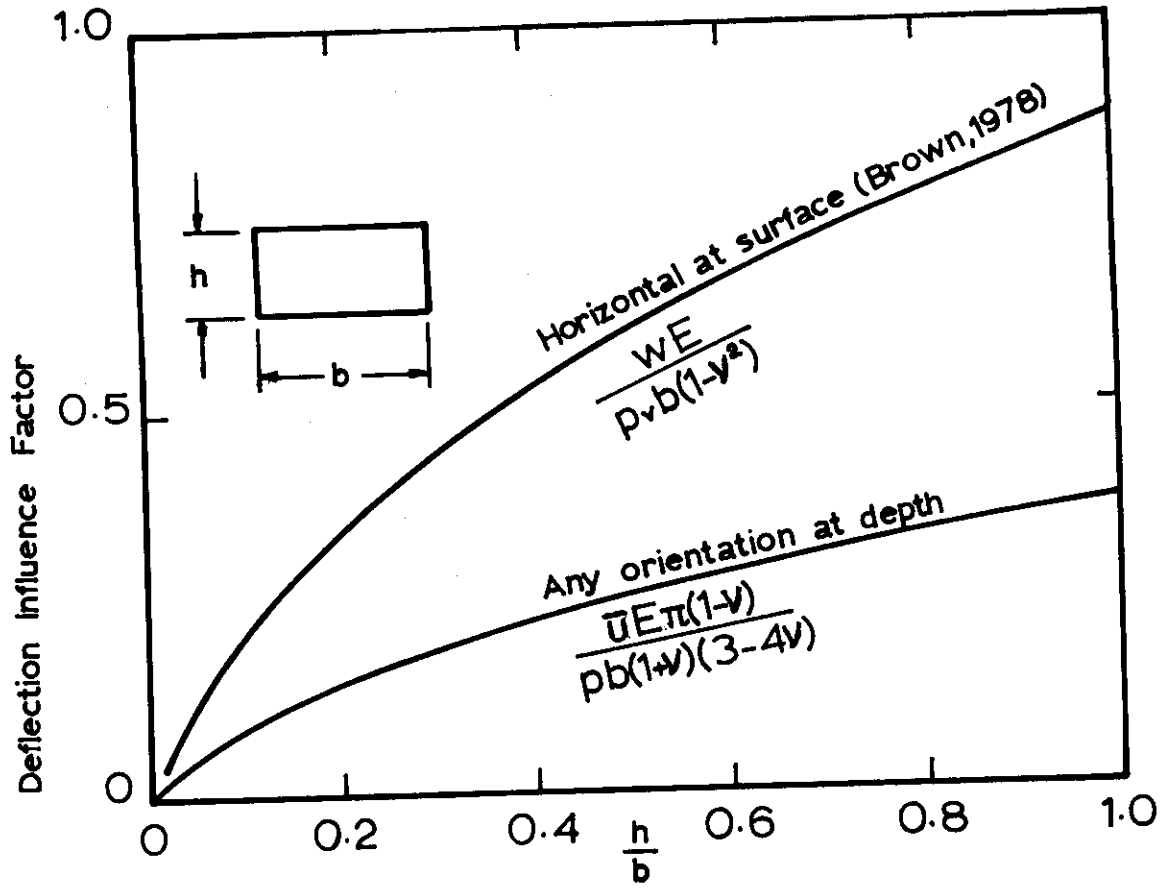


FIG. 3.6 SETTLEMENT OF SYMMETRICALLY LOADED RIGID RECTANGLE

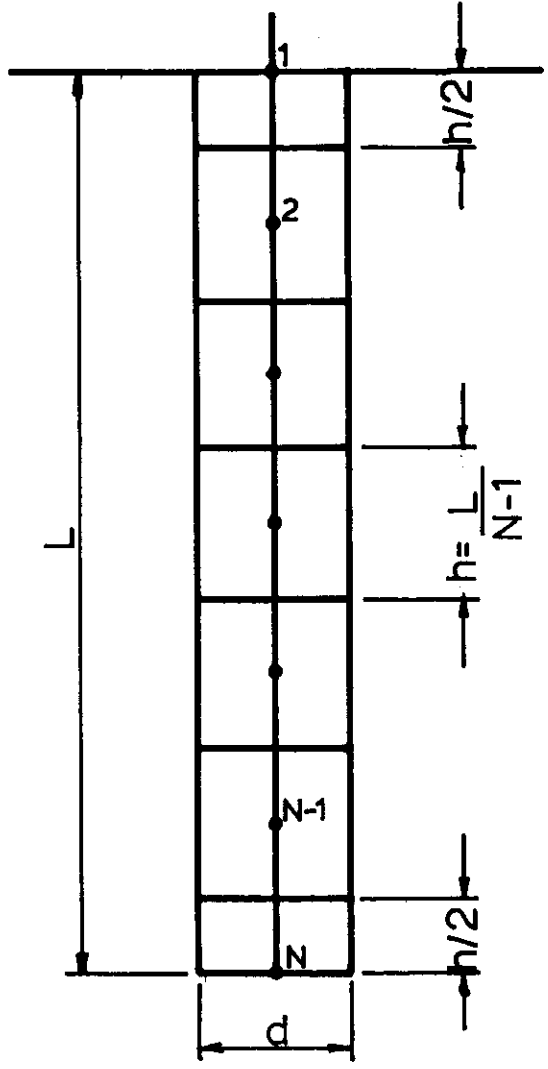
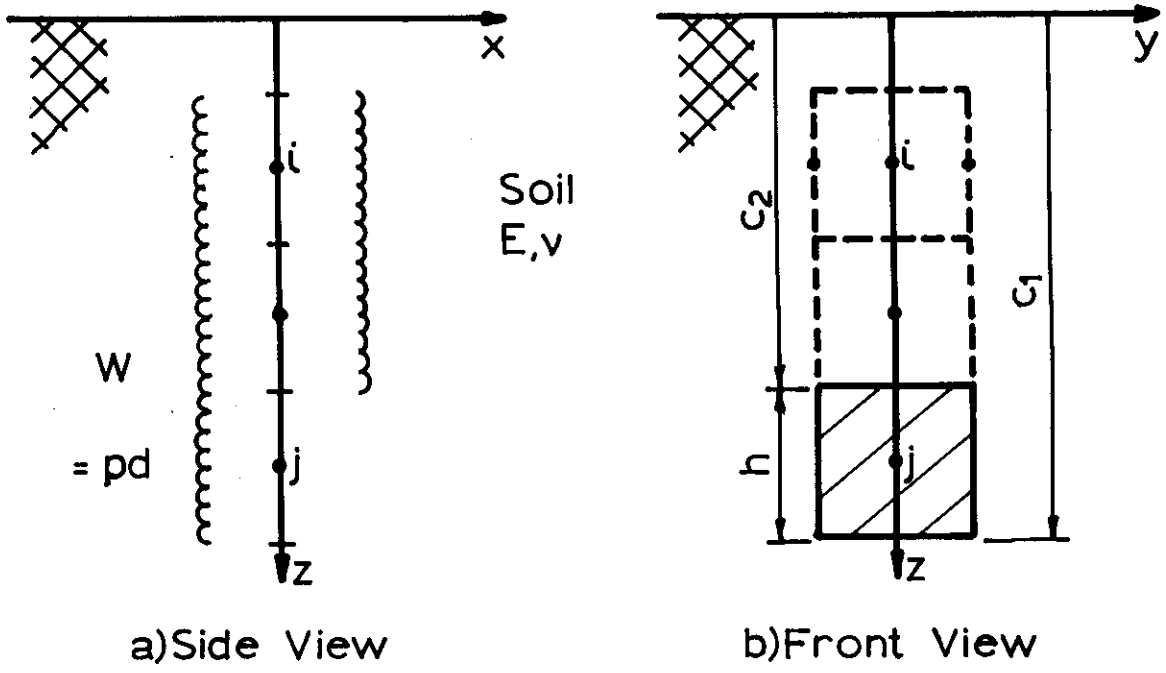


Fig 3.7 MINDLIN SOIL PLATE ELEMENT.

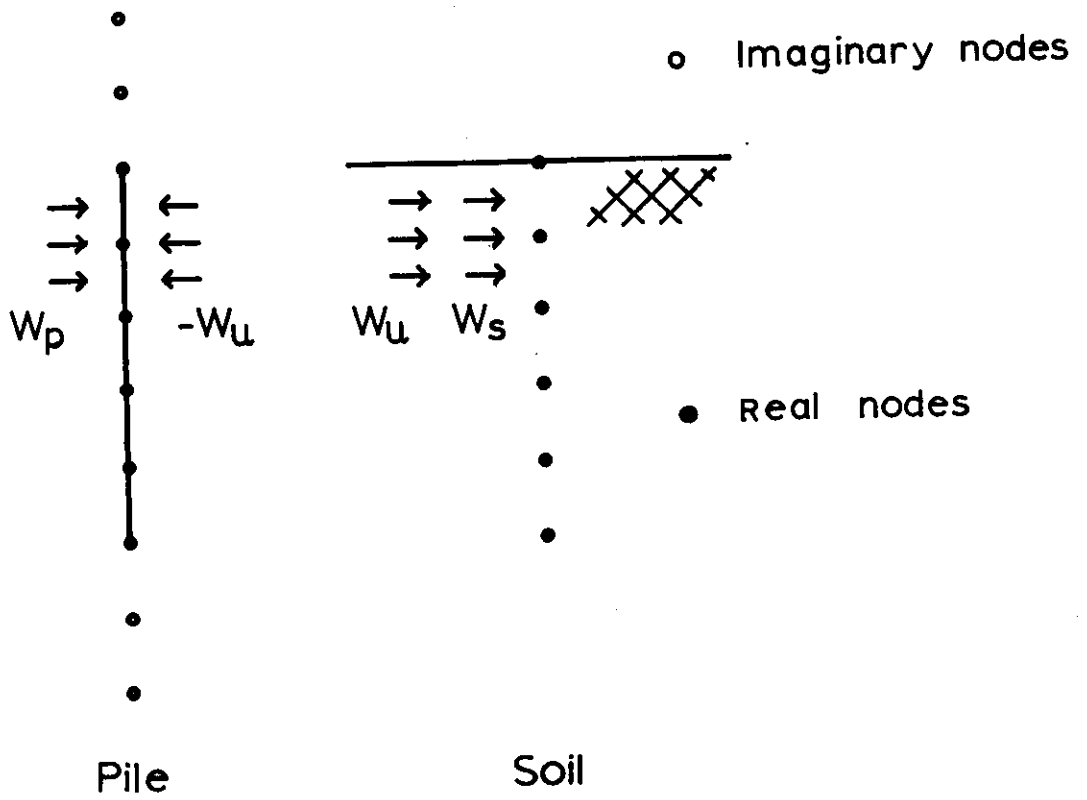


FIG 3.7 CONT'D d) DISTRIBUTED LOAD SIGN CONVENTION

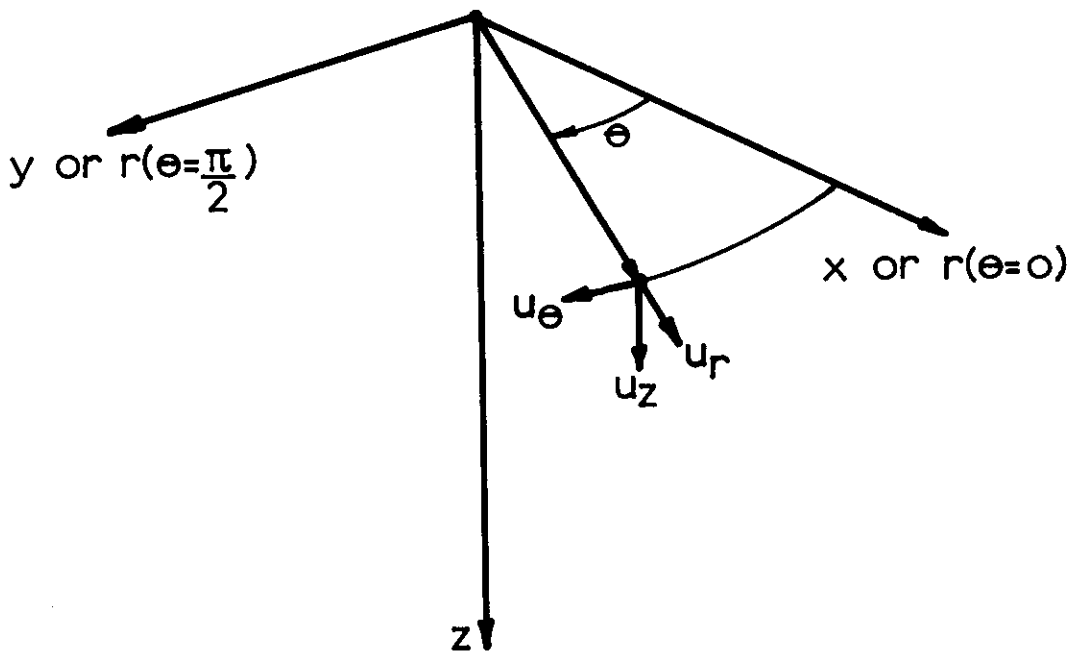
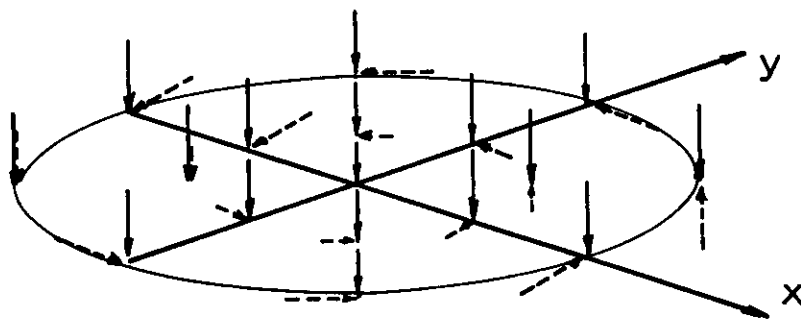
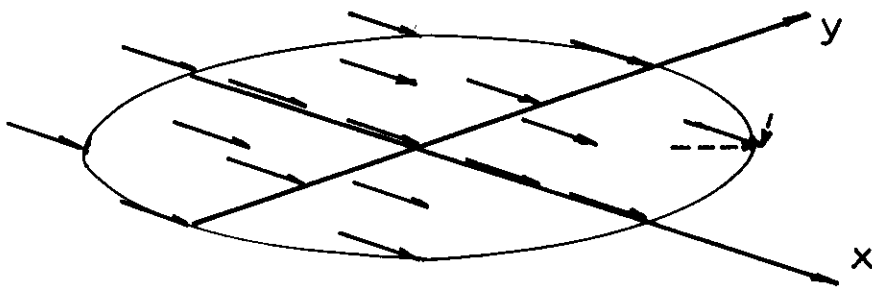


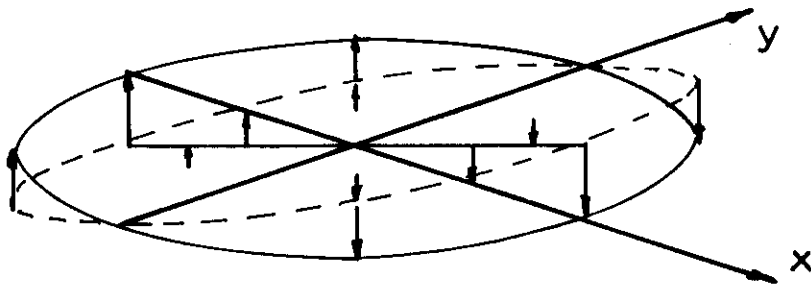
Fig 3.8 CYLINDRICAL-POLAR AND CARTESIAN COORDINATE SYSTEMS.



a) Uniform axial and linear torsional tractions $k = 0$

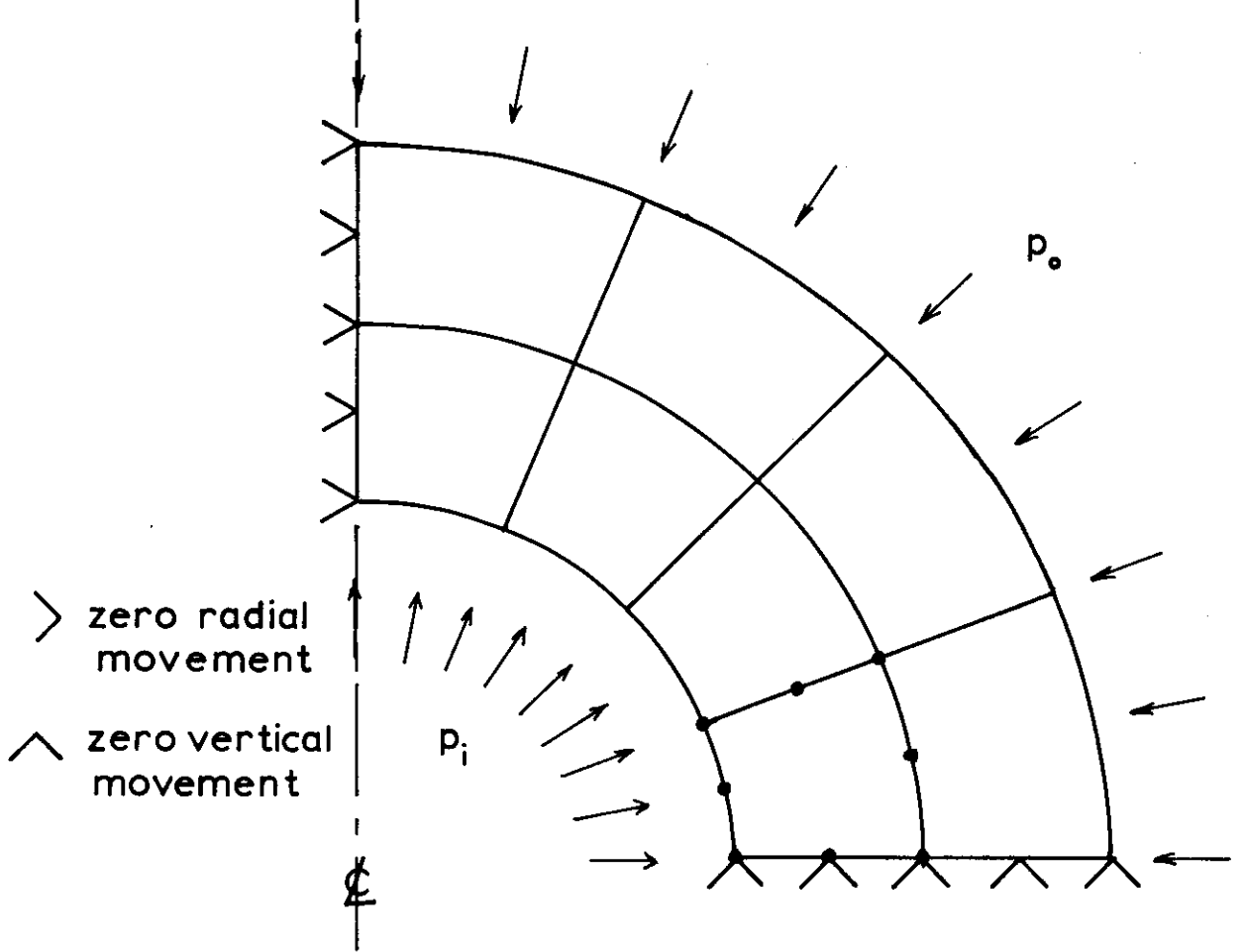


b) Uniform horizontal traction $k = 1$

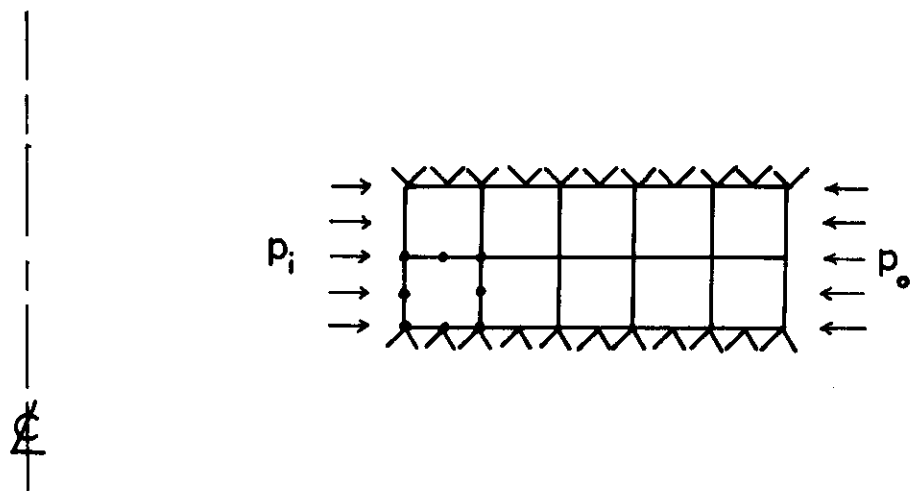


c) Moment inducing linear traction $k = 1$

FIG. 3.9 AXIAL, TORSIONAL, HORIZONTAL AND MOMENT OVER A CIRCULAR AREA : FOURIER TERMS ZERO AND 1



a) Spherical mesh



b) Cylindrical mesh

FIG. 3.10 FINITE ELEMENT MESHES FOR SPHERE AND
 CYLINDER ELASTIC TEST CASES: INTERNAL PRESSURE p_i
 EXTERNAL PRESSURE p_o

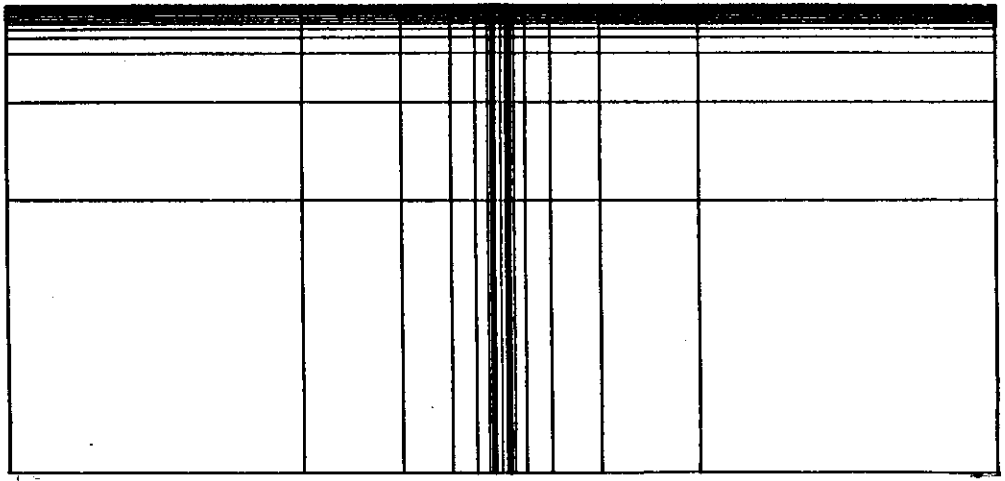
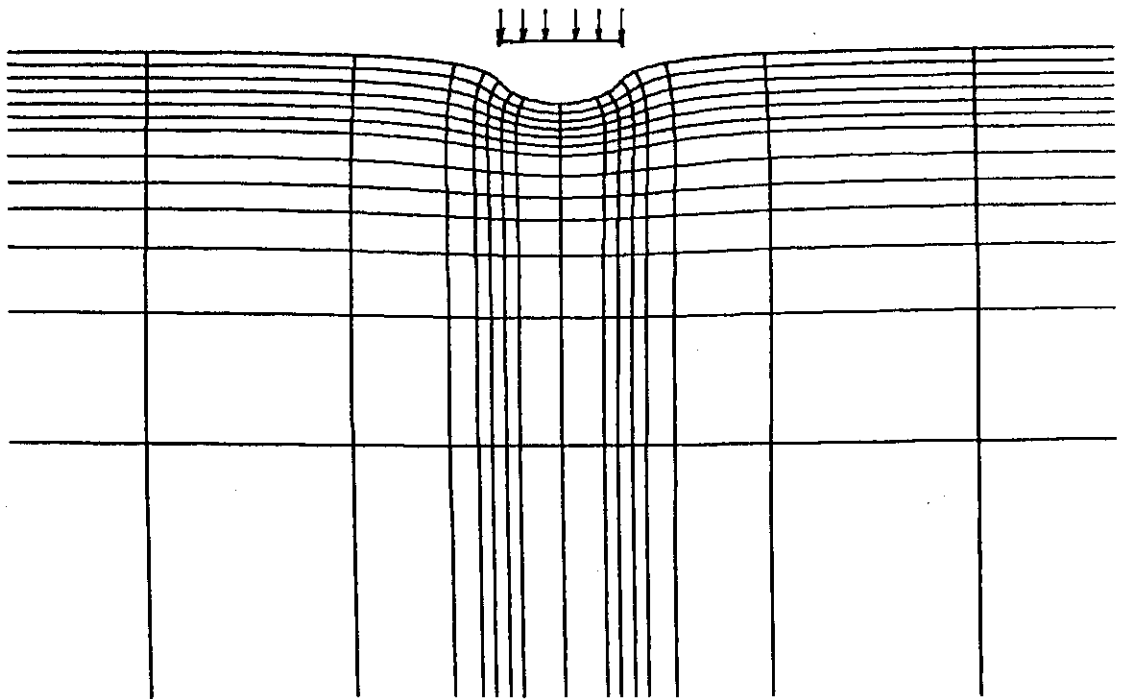
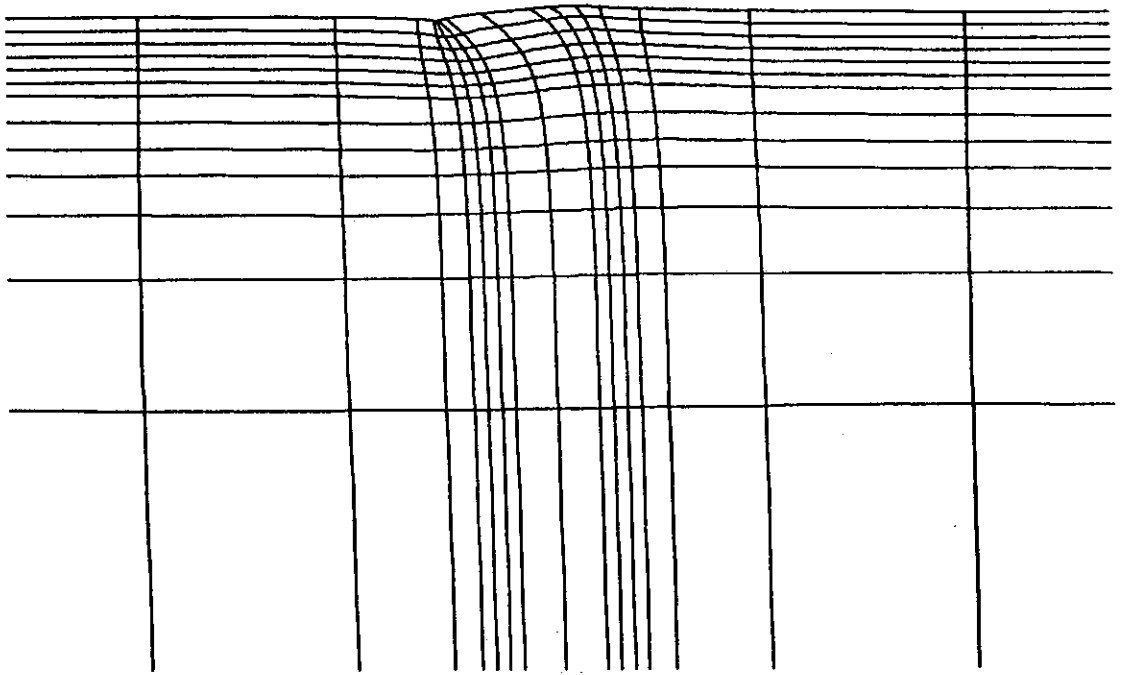


FIG 3.11 FINITE ELEMENT MESH FOR COMPARISON WITH GERRARD AND HARRISON ISOTROPIC ELASTIC HALF-SPACE RESPONSE TO CIRCULAR LOADINGS.

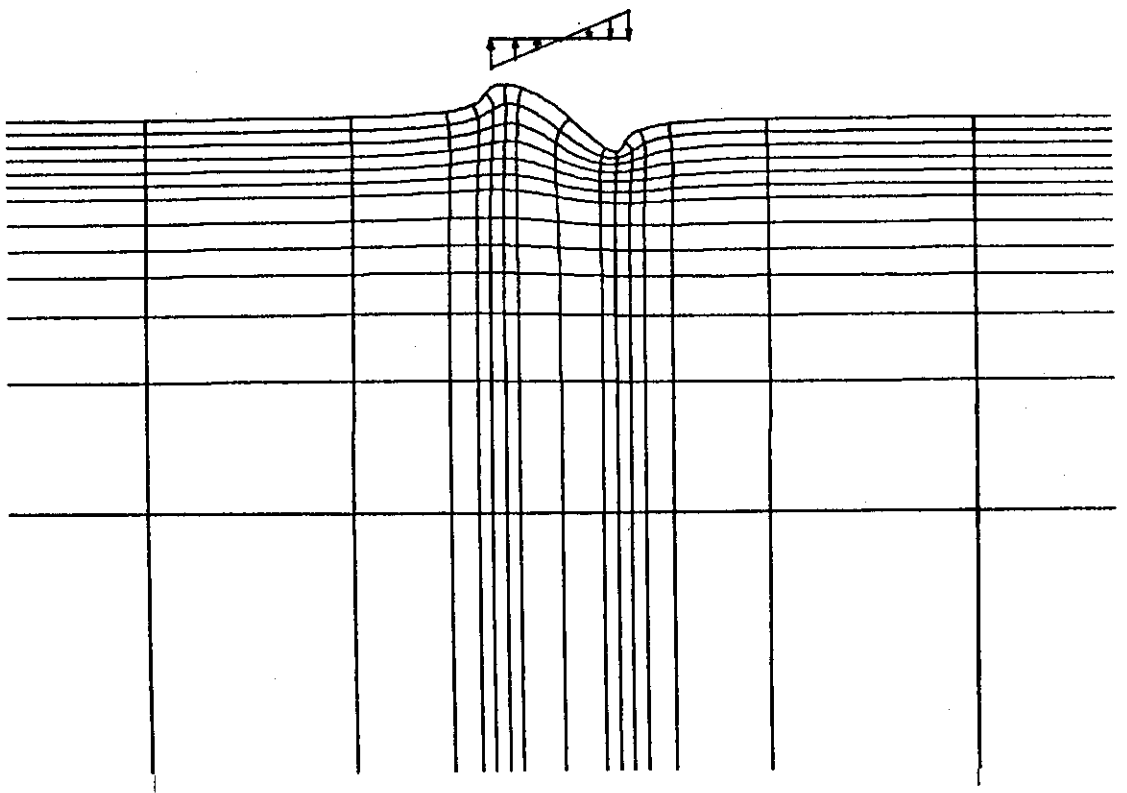


a) Uniform vertical load

FIG 3.12 DEFORMED MESH FOR RESPONSE OF ISOTROPIC HOMOGENEOUS ELASTIC HALF-SPACE DUE TO CIRCULAR LOADING.

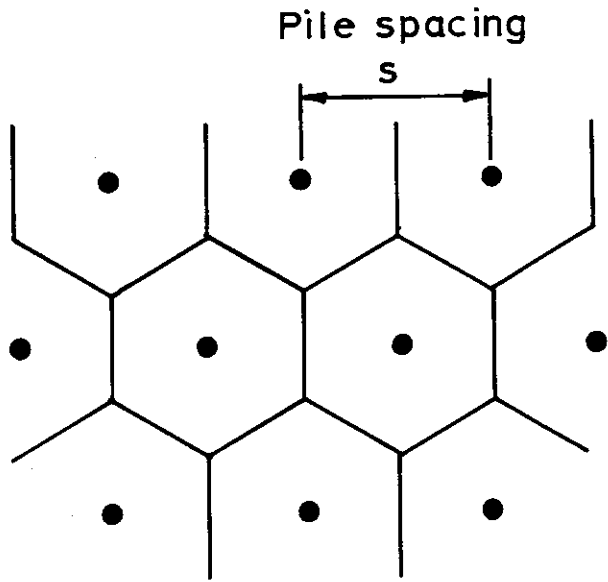


b) Uniform horizontal shear load

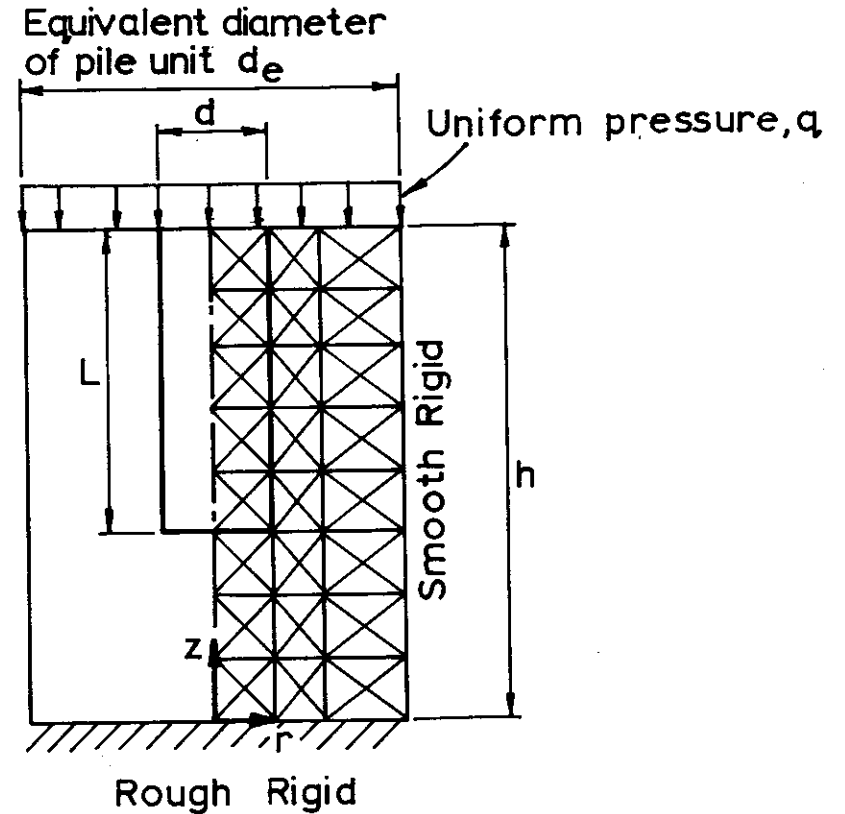


c) Linear vertical load (Moment)

FIG 3:12 CONT'D DEFORMED MESH FOR RESPONSE OF ISOTROPIC HOMOGENEOUS ELASTIC HALF-SPACE DUE TO CIRCULAR LOADING.



(a) Plan of regular triangular pattern of granular piles

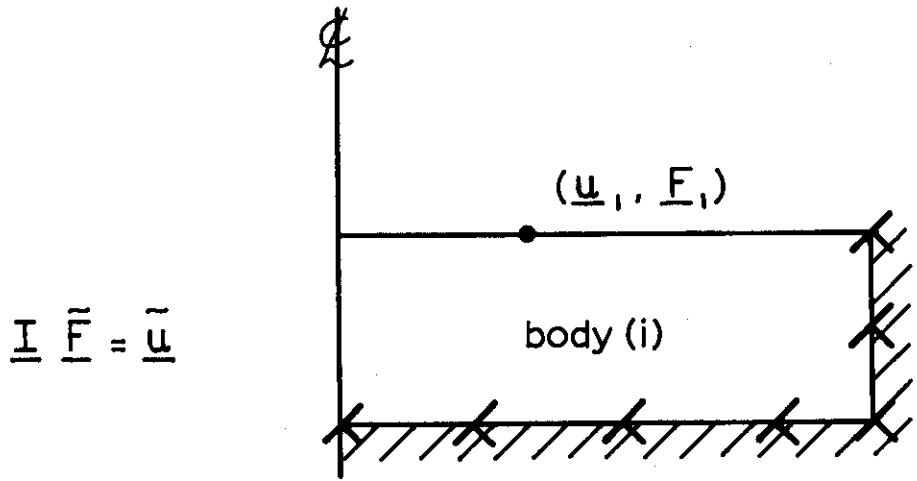


(b) Finite element model of a pile-soil unit

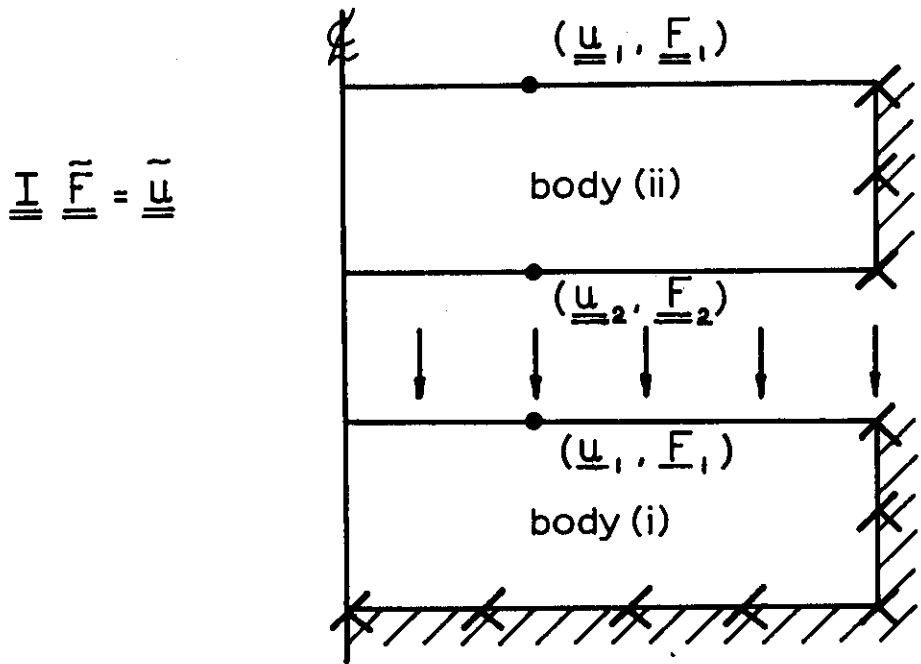
FIG. 3.13 FINITE ELEMENT MODEL USED FOR SETTLEMENT ANALYSIS OF LARGE GROUPS OF GRANULAR PILES from Balaam 1978

< zero radial movement

^ zero vertical movement



a) Original layer



b) Combination on common interface

FIG 3.14 TYPICAL ARRANGEMENT OF LAYERS PRIOR TO COMBINATION

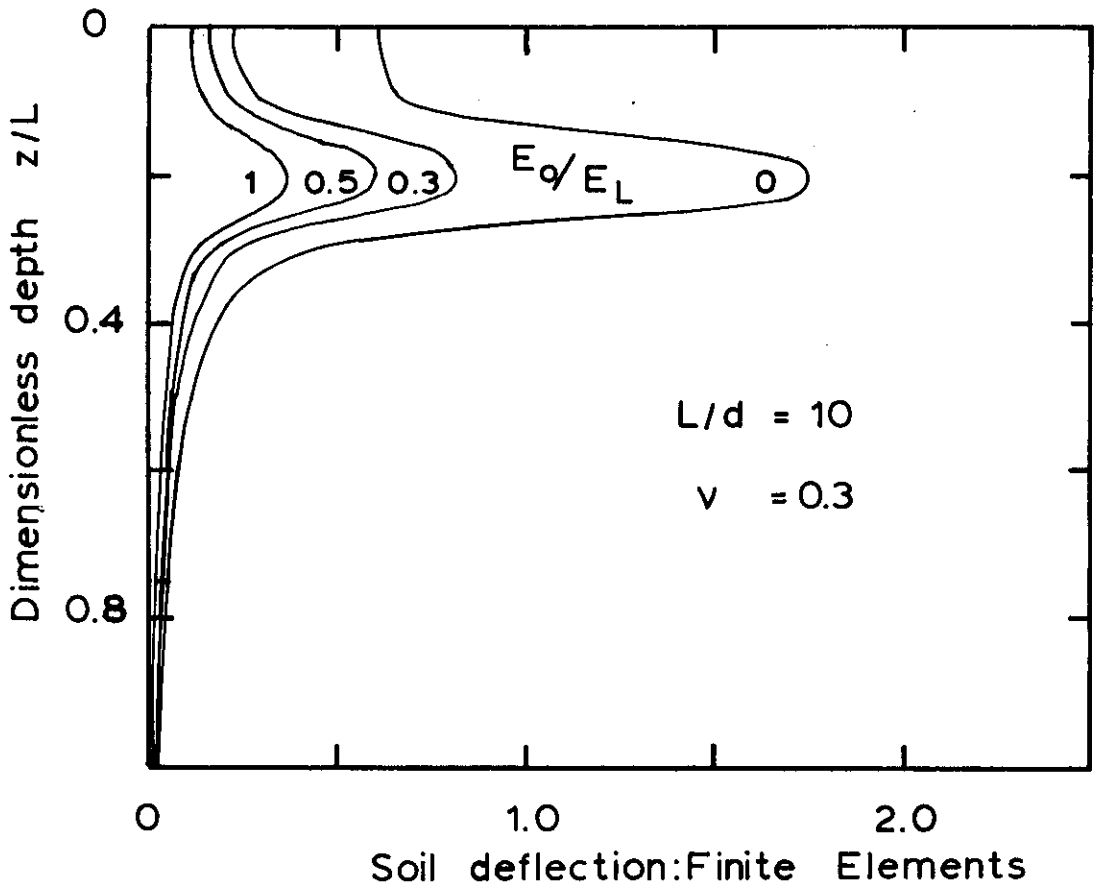
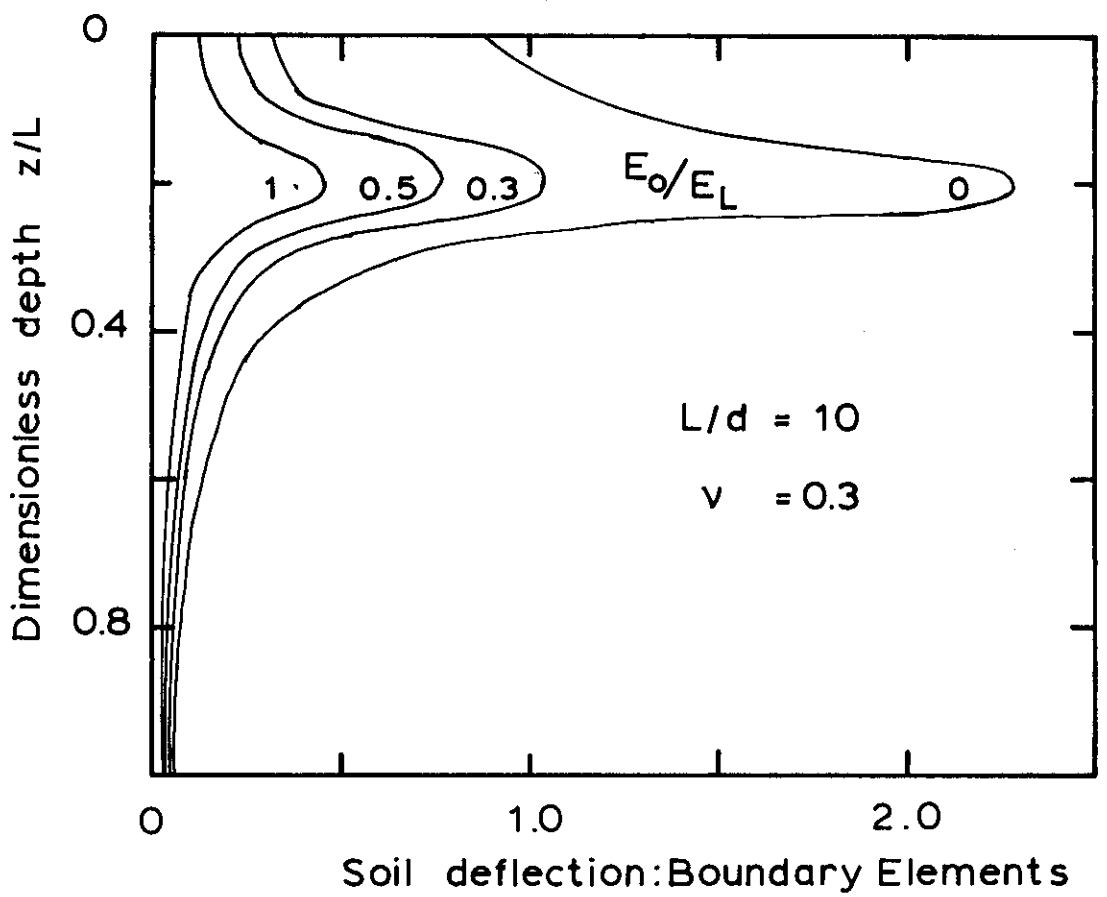


FIG. 315 PROFILES OF SOIL DEFLECTION DUE TO LOAD AT THE DEPTH OF THE THIRD ELEMENT

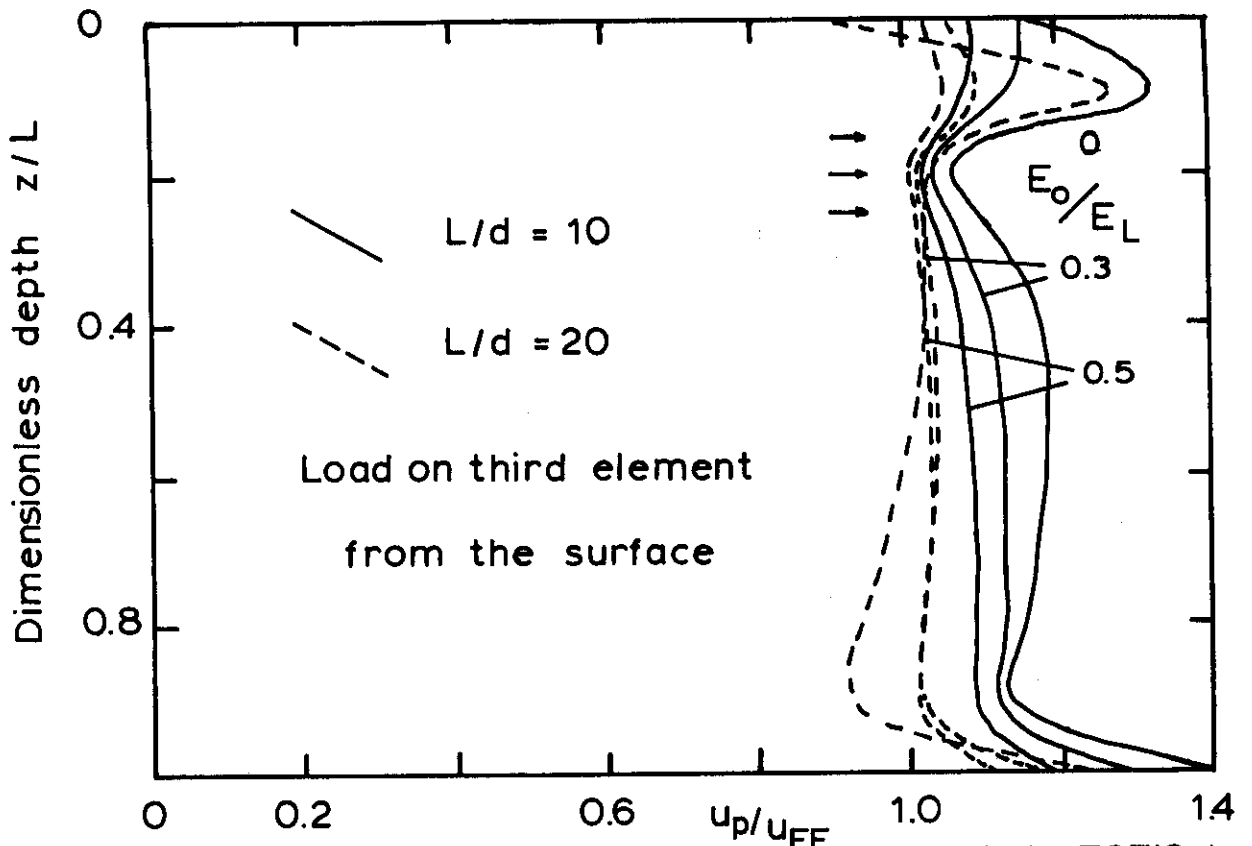


FIG. 3.16 PROFILE OF RATIO OF PREDICTED DEFLECTION, u_p TO DEFLECTION FROM FINITE ELEMENT ANALYSIS, u_{FE}

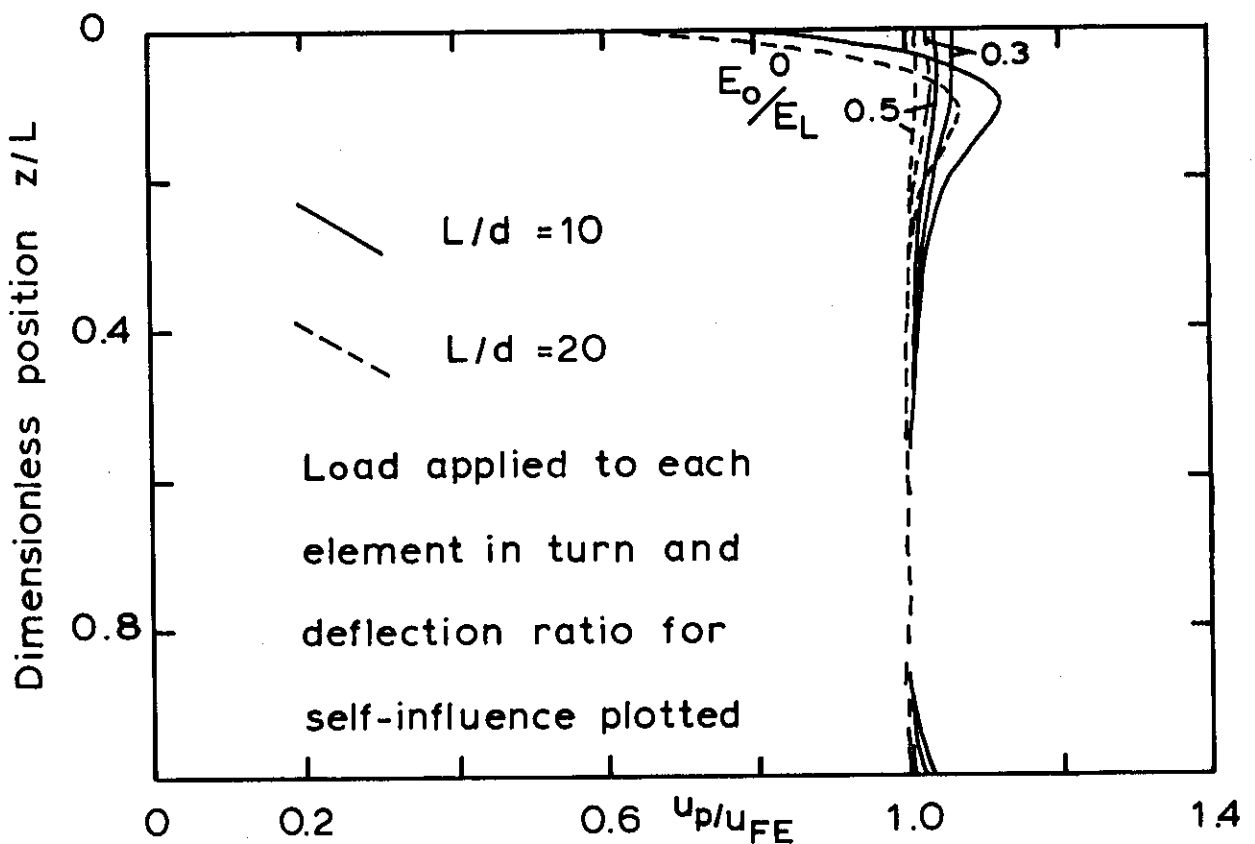


FIG. 3.17 VARIATION OF RATIO OF PREDICTED DEFLECTION, u_p TO DEFLECTION FROM FINITE ELEMENT ANALYSIS, u_{FE}

CHAPTER FOUR - LATERAL PILE RESPONSE : EFFECTIVE LENGTH CONCEPT
AND LINEAR RESULTS

4.1 Introduction and History

In order to provide a clear picture of the effect of relative pile-soil stiffness, recourse can be made to the proposition that an effective length of pile, equal to or shorter than the actual pile length, is associated with lateral pile behaviour. Such hypotheses have been proposed many times in the past. The name of the original proposer is difficult to determine from the literature. The American Society for Testing and Materials Special Technical Publications 154 and 154a (1953) include perhaps the earliest public discussions of the existence of an effective pile length which refer to work published in 1935.

The commonly held belief that only a limited number of diameters of a flexible pile length were active (or effective) in resisting load was also evident in the discussion of McClelland and Focht's paper of 1956. However, it was clear that the idea had not gained complete acceptance and that much of the quantitative work was based on the recommendations of Hetenyi (1946) or the work of Reese and Matlock (1956). While the lack of importance of the real pile length for flexible pile behaviour has been discussed widely, it has been assumed without comment that it is the actual pile length that is effective, if the pile is relatively stiff with respect to the soil.

During the 1950's, the emphasis of research was directed at correlating the Coefficient of Subgrade Reaction with soil type and even elastic parameters. The question of effective length remained relatively inconspicuous. One use of it was to explain why inconsistent field test and theoretical results beyond the effective (or critical) length were unimportant.

To a large extent, the critical length of a pile remained as a property of the Winkler soil model applied to lateral pile behaviour. The elastic continuum analyses, that were produced to model pile behaviour, were not expected to give results for which the Winkler critical length applied.

Poulos (1971a) showed that for a particular pile in a soil with a uniform Young's modulus, the effect of increasing the pile length was to reduce the head deflection due to shear loading until a limiting value was achieved. His analysis of a concrete pile for three values of soil Young's modulus showed that the length at which the pile head response achieved this limiting value changed with the soil parameters. The trend was for the pile in a softer soil to achieve a constant head response, with increasing pile length, at a longer pile length than in the stiffer soil profile. This trend was the one predicted from using the various estimates of critical length that had been proposed in the literature for piles modelled using subgrade-reaction theory.

Reese and Matlock (1956), Matlock and Reese (1960), Vesic (1961), Oteo (1972) and others have proposed equations that give the length within which the pile was deemed to be effective. None of the equations appear to have been tested against the results of elastic analyses although such a move was often recognised as potentially interesting and worthy of further consideration.

Apparently, it was not until the finite element work of Randolph (1977) that a serious attempt was made to predict the critical length of a flexible pile in an elastic continuum. Randolph's recommendations are based upon fitting a curve through points of estimated critical length, based upon the results of a finite element parametric treatment of piles of varying length,

and relative pile-soil stiffness. In other words, a matter of judgement was involved in the choice of the length beyond which extra pile length was deemed ineffective, although the application of dimensional analysis defined the general form of the variation of the critical length with relative pile-soil stiffness.

At present, the work of Randolph represents the most complete investigation of critical length for an elastic medium containing a laterally loaded pile. For the subgrade reaction method, Matlock and Reese have provided the most commonly-used expression. In the present work, the equation for the critical length will be defined for the Winkler soil model and shown to apply to the results from the elastic continuum method. As both methods support the same expression for critical length, it can be concluded that it is a theoretical property of lateral pile response, not just a result associated with one method of analysis.

In section 4.2 the effective length hypothesis and comparison of the equation for critical length, based upon the Winkler model, with other proposed expressions is made. Also the use of the pile critical length for presentation of results is discussed.

After this is a section verifying the hypothesis using three approaches to the analysis of laterally loaded piles. Included is a section about the general position which piles occupy in the wider class of problems that are amenable to elastic continuum analysis. Then the critical length of flexible laterally loaded piles will be shown to have parallel lengths for axially loaded compressible piles and flexible strip footings.

Section 4.4 considers the problem of dimensioning a test pit for the large scale model testing of off-shore piles with due regard to the existence of a pile critical length.

4.2 Effective Length Hypothesis

When the response of a pile head to lateral loading is considered, it is postulated that:

For a given soil, containing a pile of certain cross-sectional properties, there exists a length of pile that provides a critical head stiffness which is not increased by an increase of pile length.

Such a definition has been implicit in many previous statements on the behaviour of piles. The word "critical" is sometimes replaced by the words "effective" or "elastic" but in every case it is used with the word length. To some extent this is unfortunate because other methods of pile analysis, the equivalent bent method for example, also use the words "effective" or "critical" in respect of length. Indeed, buckling of piles involves a "critical length" and so a measure of confusion is bound to accompany the use of the words "effective" and "critical" when associated with pile length.

A more acceptable term might be "effective depth", or "critical depth", implying that the quantity is not solely a property of the pile like the actual pile length. Use of the term "length" tends to obscure the fact that the pile and soil stiffnesses both combine to define the critical depth, beyond which any extra pile penetration has very little effect on head load response. The word "depth" also reinforces the concept that the nature of the quantity is such that the critical depth always exists, even though the pile tip may not penetrate to that depth.

It should be noted that in the hypothesis no restriction is placed upon the form of the soil modulus distribution with depth. In fact, the critical length concept applies equally well to any soil profile that has a smooth variation of modulus with depth. Also the pile cross-section may vary with depth in a known manner. It is obvious that soil profiles which have step changes, i.e. layered profiles, will to some extent modify the approach to use of the critical length concept. If the homogeneous upper layer is sufficiently stiff then no appreciable load would reach the remainder of the pile in a softer lower layer. This case requires special treatment of the soil involving a uniform modulus with depth and the pile length equal to the layer depth.

Any pile longer than, or equal to, the "critical" length is termed flexible while shorter piles may be described as either rigid or of intermediate flexibility. For the shorter piles the head response to head load will vary with changes of pile length and so the "effective length" of such piles will be the actual pile lengths, while the "effective length" for the case of (long) flexible piles will be the critical length, since the actual pile length is no longer important. Thus, the effective length of a pile-soil system can be defined as the shorter of the actual pile length and the calculated critical pile length.

The effective length concept does not suggest that the effective length to diameter ratio is unimportant. This is only true for the simplistic approach taken by Winkler-based analyses. In general, the same effective length of pile will not mean the same head response stiffness for two piles, unless both diameters (i.e. the effective length to diameter ratios) are equal.

4.2.1 Critical Length Equation

Just as the simple Winkler model of soil behaviour can be employed to examine the trends of pile response as various parameters are changed, so too can it be used to shed light upon the requirements of an expression for predicting the critical length. By recourse to the analytic solution for pile behaviour in a Winkler uniform Subgrade Modulus soil, the variation of behaviour with increasing pile length can be examined. Recalling equ. 3.9

$$u = e^{Yz} \left(C_1 \cos Yz + C_2 \sin Yz \right) + e^{-Yz} \left(C_3 \cos Yz + C_4 \sin Yz \right)$$

it is obvious that the variation of deflection with depth is governed by the product of exponential terms and cyclic terms with a period (wavelength) of $P = 2\pi/Y$, where $Y = \left(\frac{E_s}{4E_p I_p} \right)^{1/4}$ and E_s is the Subgrade Modulus.

The values of the coefficients will depend upon the boundary conditions at the buried tip and the head of the pile. Because of the impossibility of a head load causing a deflection distribution down the pile that increases in magnitude with depth in an exponential manner, C_1 and C_2 must both be zero. Coefficients C_3 and C_4 are not bounded in this way since the exponential decay term will always enforce a value tending to zero for large depth. When it is recognised that the aim is to locate the minimum pile length that behaves fully flexibly, it can be seen that the tip boundary conditions of zero bending moment and shear force are applicable.

Hetenyi has solved this problem for the case of a pile of infinite length in a uniform Subgrade Modulus soil. His solution for deflection, u and rotation, θ down the pile in terms of head shear, H and moment, M may be written

$$\begin{aligned} u_s &= 2Y e^{-Yz} [H \cos Yz + MY(\cos Yz - \sin Yz)] \\ \theta_s &= 2Y e^{-Yz} [H(\cos Yz + \sin Yz) + 2MY \cos Yz]. \end{aligned} \quad 4.1$$

It should be noted that only the exponential decay terms of the general solution remain, thus ensuring that the deflection and rotation both decay with depth. From the cyclic nature of this solution, the deflections and rotations will also be zero at an infinite number of depths corresponding to intervals of one half wavelength. Neglecting the constants in equ. 4.1, the resulting pattern of the deflection and rotation distributions due to head shear and moment can be plotted against Yz , as in Fig. 4.1a. It is evident that for Yz greater than 2π there is very little effect upon the pile deformation due to head loads. From the reciprocal nature of the problem it must follow that the head response will suffer very little effect from the loads generated at and below the depth of one wavelength of the solution ($2\pi/Y$).

Not too much importance should be placed on the cyclic nature of the solution, i.e. the stationary points in the deflection or rotation distributions. Of much more importance is the exponential decay term which "damps" the solution, leading to very little response at a depth of π/Y . If the inverse exponent term is considered, it is found that the maximum value is unity at zero depth and by the time the depth is one half wavelength of the cyclic component it becomes less than 5% of the maximum value.

Because the smallest depth to represent a critical length of pile is required, in order to be of most advantage in producing and assessing an economical pile design, the choice of critical depth will be taken as one-half of a wavelength of the solution of a laterally loaded pile in a uniform Subgrade Modulus Winkler soil.

Thus the product of an exponential decay and a sinusoidal function governs the variation of deflection, rotation and also bending moment and shear force with depth. It follows that for the loading of a semi-infinite beam in a Winkler soil the critical depth at half a wavelength of the solution is

$$z_c = 1/2 \cdot 2\pi/Y \text{ or}$$

$$z_c = \pi\sqrt[2]{\frac{EI}{E_s P}} \quad 4.2$$

This is really a restatement of the classification proposed by Hetenyi, that piles with length greater than a critical length π/Y behave flexibly and he further suggests that piles of length less than one quarter of the critical length behave as if the pile were rigid.

The critical length is thus based upon a half wavelength of the solution of a pile in a uniform Winkler soil. The cyclic nature of the solution, expressed by equ. 4.1, ensures a zero response at points down the pile and the exponential decay rapidly damps the solution. This damping is a more important feature than the cyclic nature of the response when considering the lack of effect from pile penetration beyond the critical depth.

The exponential decay and periodic nature of the solution combine to produce a depth below which the pile deformation, and therefore stress-resultants, will be negligible when compared to their maximum values. Having predicted the form of the equation for critical length by recourse to the analysis based upon the uniform Winkler soil, it remains to investigate the expressions proposed by others in the light of this and extend the proposed expression to consider a soil with a linear increase of modulus with depth.

Other estimates for the critical length, L_c , may be broadly classed as having their basis in such work as that presented by Hetenyi or resulting from the restrictions imposed by dimensional considerations.

The former class includes the equations proposed by Barber(1953), Vesic(1961a), Broms(1965) and Oteo(1972) and have the form

$$L_c = C \left(\frac{E I}{\frac{P P}{E_s}} \right)^{1/4} \quad 4.3$$

This expression assumes the equivalence of the Young's modulus and Subgrade Modulus of the soil and has various estimates for C of 5.6, π and a range of values between 1.2 and 1.3. For a soil with a modulus proportional to depth, $E = n_z$, Broms' expression becomes

$$L_c = 4 \left(\frac{E I}{\frac{P P}{n_h}} \right)^{1/5} \quad 4.4$$

From the results of dimensional analysis and using the Winkler soil model, Matlock and Reese (1960) have proposed an expression that would predict a critical length in a soil with a Subgrade Modulus varying as

$$E_s = k z^n \quad 4.5$$

where the exponent n takes values from zero to one and k is a coefficient whose dimensional units depend upon the value of n . This expression for critical length takes the form of

$$L_c = 5 \left(\frac{E I}{k p p} \right)^{1/(n+4)} \quad 4.6$$

and can be seen to be similar to Broms' expression for the linearly increasing modulus soil when $n = 1$, and broadly agrees with the upper estimates for a uniform soil when n is zero. A close study of the curves presented by Matlock and Reese (1960) suggests that a constant of 4 would give a better approximation to the depth beyond which additional pile length causes insignificant reduction in the response of the head, as proposed by Broms.

With the exception of the work by Oteo, all the previous expressions for the critical length of a pile have been, to some degree, based upon considering the results of analyses using the Winkler model. Another, more recent exception is the work of Randolph (1981) who has also proposed an expression for the critical length of a pile in an elastic continuum soil. His equation is based upon both the results of a finite element study and the restrictions imposed upon the expression from dimensional

considerations, and can be expressed as

$$l_c = 2.93 \left(\frac{E I}{\frac{P P}{E \sqrt{d}} \frac{c}{2}} \right)^{2/7} \quad 4.7$$

where $E_{c/2} = E_o + 0.5 m l_c$ is the soil Young's modulus averaged over the pile critical length.

The use of a power of two-sevenths leads to the inclusion of a term for the square root of the diameter in order that the equation remains dimensionally correct. It should be emphasized that the form of the expression presented here is far removed from the original elegant expression of Randolph, which is in terms of $G^* = 0.5 E(1+3V/4)/(1+V)$ (which is a factored Shear modulus involving the Poisson's ratio of the soil) and an equivalent pile modulus, $E I / (\pi d^4 / 64)$, (Randolph, 1981). Strictly, the expression reproduced here as equ. 4.7 is also approximate, since the variation of Poisson's ratio from zero to one half gives only a 3% variation in Randolph's critical length and so dependence upon Poisson's ratio has been removed for the purpose of comparison.

The new expression (equ. 4.8) proposed in this work is essentially the same as equ. 4.2 and equ. 4.3, with C taking a numerical value of $\sqrt{2} \pi (= 4.44)$, but with E_s replaced by E_c , the elastic Young's modulus at the critical depth of the soil profile. One similarity with the expression of Randolph is that the expression for critical length includes a term that depends upon the value of the critical length. This means that in general, in the same manner as Randolph has described, some iteration is necessary, using an initial guess of L_c in $E_c = E_o + m L_c$ to

calculate the critical length as given by the expression

$$L_c = \left(\frac{4 \pi^4 E I}{E_c P P} \right)^{1/4} \quad 4.8$$

Using this form of expression for the critical length maintains dimensional compatibility without recourse to the inclusion of any other terms in the expression, other than the pile stiffness $E I$ and a maximum of two terms, E and m , that define the soil Young's modulus distribution with depth, where

$$E_z = E_o + m z. \quad 4.9$$

Two cases arise where iteration is unnecessary, namely a uniform modulus and a modulus proportional to depth. The case of uniform modulus does not require iteration since any depth has a modulus value identical to the value at the critical depth thus

$$L_c = \pi \sqrt{2} \left(\frac{E I}{E_o P P} \right)^{1/4} \quad 4.10a$$

where $E_c = E_o$. For a modulus proportional to depth

$$L_c = \left(\frac{4 \pi^4 E I}{m P P} \right)^{1/5} \quad 4.10b$$

4.2.2 Effective Length and Presentation of Results

Considering head response to head loading for one pile cross-section and one soil profile, the actual length of the pile may be an important parameter for normalising head response when that length is less than the critical length given by equ. 4.8:

$$L_c = \pi \sqrt{2} \left(\frac{E_p I_p}{E_c} \right)^{1/4}$$

where $E_c = E_o + mL_c$. But flexible piles, with length greater than critical, will achieve a limiting head response regardless of the pile length.

It is found that iteration using equ. 4.8 quickly converges to a value of E_c and L_c that are compatible when the modulus of the soil profile is not uniform with depth, or linearly proportional to depth. No instances of failure to converge have been found in any of the examples undertaken during this work. While equ. 4.8 could be solved and tabulated, the time spent in calculating L_c is worthwhile for the information gained about the relative importance of small changes in critical length and the changes in modulus at the depth of the critical length.

So, on the understanding that the only varying quantity is the pile length, for any pile with length longer than the calculated critical length, the head response to head loading is invariant with length of pile. Considering that the critical length is constant, because the pile cross-section properties and soil profile do not vary, then the descriptor of the soil inhomogeneity, α_c , is also constant, where

$$\alpha_c = \frac{E_o}{mL_c} \quad 4.11$$

Thus a non-dimensional representation of deflection and rotation due to shear and also moment takes the form

$$\begin{aligned}
 \frac{u}{c} \frac{E L}{c} / H &= \text{constant} = I_{1c} \\
 \frac{\theta}{c} \frac{E L}{c} / H &= \frac{u}{c} \frac{E L}{c} / M = \text{constant} = I_{2c} \\
 \frac{\theta}{c} \frac{E L}{c} / M &= \text{constant} = I_{3c}
 \end{aligned}
 \tag{4.12}$$

This system of non-dimensionalisation is basically the standard one, similar to the method used by Barber (1953), Poulos (1971a) and Bannerjee and Davies (1978), with the addition of the subscript, c , here to signify the value as being associated with the critical length. Now it is possible to investigate what effect this constant response, for increasing length, has upon the picture as given by the standard influence coefficients.

When the constant response behaviour is incorporated into the standard I_{uH} , $I_{uM, \theta H}$ and $I_{\theta M}$ system, which uses the actual pile length, it yields

$$\begin{aligned}
 I_{uH} &= \frac{u E L}{L} / H = \frac{u E L}{c c} / H \cdot k \cdot \frac{L}{L} \\
 I_{uM, \theta H} &= \frac{\theta E L}{L} / H = \frac{u E L}{L} / M = \frac{u E L}{c c} / M \cdot k \cdot \left(\frac{L}{L} \right)^2 \\
 I_{\theta M} &= \frac{\theta E L}{L} / M = \frac{\theta E L}{c c} / M \cdot k \cdot \left(\frac{L}{L} \right)^3
 \end{aligned}
 \tag{4.13}$$

where $k = \left(\frac{\alpha + L/L}{c} \right) / \left(\frac{\alpha + 1}{c} \right)$, while α and L are constant.

It is now clear that the standard system of presenting influence coefficients against a relative measure of pile-soil stiffness, involving the actual pile length, must display some special properties for piles longer than their critical length.

For a constant value of α_c (i.e. a fixed soil profile) the standard influence coefficient must be a function of the length of pile as given in equ. 4.13, leading to

$$I_i = I_{ic} (k_1 L^i + k_2 L^{i+1}) \quad 4.14$$

where $i = 1, 2$ and 3 and $I_1 = I_{uH}$, $I_2 = I_{\theta H} = I_{uM}$ and $I_3 = I_{\theta M}$

with I_{ic} as in equ. 4.12 and

$$\text{constants } k_1 = \alpha_c L^{-i} / (\alpha_c + 1) \text{ and } k_2 = L^{-(i+1)} / (\alpha_c + 1).$$

The standard method of presenting these influence coefficients, as in Fig. 4.2, is to plot their logarithm against the logarithm of the relative stiffness K_R , where

$$K_R = E I_p / E L^4 = E I_p / (E L^4 + mL^5). \quad 4.15$$

The simplest cases to investigate are the extremes of a constant modulus with depth, E and a modulus proportional to depth, $E_s = mL$. The constant modulus case has an α_c of infinity and therefore k_2 vanishes while k_1 has a finite value and K_R becomes a function of the inverse of length to the fourth power. Thus the slopes of the plot will be $-1/4$, $-1/2$ and $-3/4$ for the cases of i equal 1, 2 and 3. The equations from Hetenyi's solution for a semi-infinite beam on a Winkler foundation can easily be shown to provide results of this form.

$$u_s E L / H = 2^{1/2} K_R^{-1/4}$$

$$\theta_s E L^2 / H = u_s E L^2 / M = K_R^{-1/2} \quad \text{and}$$

$$\theta_s E L^3 / M = 2^{1/2} K_R^{-3/4}. \quad 4.16$$

The case of a modulus proportional to depth has an α of zero and so k_1 now vanishes leaving k_2 finite and K_R is now a function of the inverse of length to the fifth power. Thus the slopes on the plot will be $-2/5$, $-3/5$ and $-4/5$ for the three influence coefficients. Using the results from the analysis of a pile in a Winkler medium of section 3.2.3, the influence coefficients take the form

$$\begin{aligned}
 u_{sL} E L / H &= 2.43 K_R^{-2/5} \\
 \theta_{sL} E L^2 / H &= u_{sL} E L^2 / M = 1.62 K_R^{-3/5} \\
 \theta_{sL} E L^3 / M &= 1.75 K_R^{-4/5} .
 \end{aligned}
 \tag{4.17}$$

These results are in agreement with those of Scott (1981) and Barber (1953), and can be accurately reproduced by the BEM model using a Winkler soil influence matrix. The characteristics of flexible pile results (both uniform and proportional modulus) when presented in this standard form, rely upon the normalised results for different length to diameter ratios falling on the same curve. This happens for the simple Winkler model results, but Poulos (1971a) has shown that the standard system of non-dimensionalisation does not completely eliminate the variations in head response influence coefficient, due to changing length to diameter ratio, for the elastic-continuum model.

The elastic continuum results of various other researchers for uniform and proportional modulus soil profiles have been studied and re-expressed in the form

$$I_i = A_i (L/d)^{b_i} K_R^{c_i}
 \tag{4.18}$$

Further, the values of the exponents b and c are linked as a result of any influence coefficient based upon diameter, instead of length, being required to present a limiting value for flexible piles. Thus

$$b_i = i + 4c_i \quad \text{for } \alpha_c = 0$$

$$\text{and } b_i = i + 1 + 5c_i \quad \text{for } \alpha_c = 0. \quad 4.19$$

Table 4.1 shows the actual values presented by various authors, or values backfigured from their curves in the region $10^{-4} < K < 10^{-3}$, and results from the finite element method used in the present work for the solution of head response to head loads. The values either obey the restrictions of equ. 4.19 exactly, or in the case of backfigured numbers, are essentially correct. Blaney, Kausel and Roesset (1976) and Bannerjee and Davies (1978) both suggest that the standard influence coefficients are essentially independent of pile length to diameter ratio and thus should have exponent values exactly the same as the Winkler model predictions.

A standard parameter defining the nature of the soil inhomogeneity has been often been defined as E_o/E_L , whereas in this thesis an equivalent parameter, α has been defined. For a fixed value of the parameter

$$\alpha = E_o/mL, \quad 4.20$$

which has a similar role to α_c but is most pertinent to stiff piles of length less than critical, the soil modulus profile must change its character as the length varies, or the pile stiffness varies and the pile length remains constant.

This means that for the length of pile increasing, the basic properties of the soil E and m must change in order to preserve α as a constant. Thus the influence coefficients I_{ic} will no longer be constant and the reasoning applied previously cannot be used. If the length to diameter ratio of the pile is maintained constant, then it becomes necessary to change the pile stiffness $E I_{pp}$ in order to vary K_R and the critical length to diameter ratio will also change, which for the elastic model of soil will change the response, I_{ic} .

When α is finite and non-zero the value of α and α_c are no longer equal, i.e. the same soil profile will have one value of α_c but any number of α values as the length changes. Only when the relative stiffness $K_R = 1/4 \pi^4$ will the actual pile length be equivalent to the critical length and α equal α_c . Thus only when α is given values of zero and infinity will a simple picture evolve for the standard influence coefficients in terms of K_R .

The influence coefficient for head deflection due to head shear on a pile in a Winkler soil for intermediate values of α are plotted in Fig. 4.2 and especially for the two values $\alpha = 0.025$ and $\alpha = 0.125$ a definite curvature can be seen with respect to the logarithm of K_R for the flexible piles ($K_R < 1/4 \pi^4$). This is a function of the non-dimensional form, as chosen by Barber (1953). While this form is convenient for relatively stiff pile-soil systems it does not take advantage of the existence of a pile critical length and results in an awkward representation of the results. In section 4.3.1 a form of presentation based upon the pile critical length will be presented which simplifies the results.

4.3 Verification of Critical Length Concept and Results

The equation for critical length has been derived from the analysis of a pile in a uniform Winkler profile, so that confirmation of the existence of, and the accuracy of the expression for, the critical length in such a case will be expected to be easily proven. However, the infinite number of different cases of a Winkler soil with stiffness increase proportional to depth should not be assumed to automatically support the critical length concept, let alone allow its representation by such an equation.

The first stage in confirming that the critical length concept is valid for general laterally loaded pile analysis, is to show its applicability to the analysis of piles using the Winkler model of soil response. Here the head deflection and rotation due to head shear force and applied moment are used as measures of the response stabilisation with increasing pile length, keeping all other soil and pile parameters constant.

It should be noted that the critical length concept does not imply that the entire distribution of response down the pile becomes constant for increases of pile length; but only that pile response at a depth greater than one half-wavelength of the solution distant from the head, does not affect the behaviour of the head due to head loads. Thus the response of the pile in the entire region of the critical length may not be the same as it was before the increase of pile length.

4.3.1 Results of Winkler Analysis

The analysis of a pile in a uniform Subgrade Modulus Winkler soil has been used as the basis of the expression for the critical length of piles. The analysis of a pile in a Winkler soil with a linear increase of Subgrade Modulus with depth, m_s , results in a solution in terms of an infinite series. This solution displays a cyclic nature with rapid damping, similar to the simpler closed form uniform soil solution, see Fig. 4.1. However, a difference between the uniform and linearly varying Subgrade solutions is that the latter has a wavelength that varies with depth.

In order to extend the applicability of the equation for critical length to include the case of linearly increasing soil stiffness with depth, it has been implicitly assumed that the modulus value at the critical depth should be used in the equation. This will involve an iterative procedure for the calculation of the critical length. Essentially the iteration is solving a fifth order polynomial in L_c and convergence is achieved very quickly. Figure 4.1b shows that, as for the uniform case, the effect of head loading on response at a depth of one half of the chosen wavelength is satisfactorily small (less than 5 %, say).

Following from the discussion of the effective length concept and the presentation of results, a new form is introduced here, and is designed to cover the entire range of pile flexibilities in a Winkler soil. The standard influence coefficients are employed, but now they are plotted on a normal scale against values of L/L_c between 0 and 1.0 for various values of α . Effectively, this covers the range of rigid to flexible piles and provides a way of checking for the existence of a critical length.

By changing from the standard influence coefficients, I , to the set using the critical length, I_c , and employing α instead of α_c , it is possible to plot the new influence coefficient at an abscissa of L/L_c equal 1.0 for a pile of length twice the critical length. If the end of the curves and the plotted points, using the new non-dimensional scheme but retaining the same plot, are coincident, there has been no change in actual head response for a doubling of pile length. Therefore by viewing the results in Figs 4.3 to 4.6 the critical length can be proved to exist and be reasonably modelled by equ. 4.8.

The results presented in this section are for a pile in a Winkler soil and comprise the response of the pile head, in terms of deflection and rotation due to shear and moment loads, for,

- a) a pile with the tip free from any restraint,
- b) a pile with the tip fully socketed,
- c) a pile pinned at the tip to stop translation and
- d) a pile fixed at the tip against rotation but free to translate.

The first two cases are common boundary conditions for laterally loaded piles, while the last two are not usual, and represent extremes of behaviour that are unlikely to occur separately. Case c) may occur where the pile penetrates enough of a hard layer to limit translation, but insufficient to cause any rotation restraint. Case d) may occur if the base of the pile has been enlarged in a thin horizontal plane, such that rotation is restricted but little, if any, resistance to translation is generated. This latter case is of very little practical use but does emphasise an important feature of tip fixity conditions.

Considering Fig. 4.3b, which shows the influence coefficients for head deflection due to head shear on a pile with a socketed tip, it will be seen that the pile has a zero deflection influence coefficient if it has a length to critical length ratio less than a quarter. For all other tip conditions, Figs 4.3a, 4.3c and 4.3d, it can be seen that the rigid pile ($L/L_c < 0.25$) will have a non-zero finite deflection influence coefficient that is unaffected by the L/L_c ratio. However, it is important to note that the fixing of the tip produces the greatest decrease in deflection when compared to pinning. This means that the introduction of a moment resistance upon the tip will produce the greatest beneficial effect upon head deflections for stiff piles.

In Figs 4.3b and 4.3d, for $\alpha = \infty$ and piles with length greater than half the critical length, the prevention of rotation of the tip produces a dimensionless head response that is approximately a linear function of length. This means that as the length of the pile increases, if the tip is fixed against rotation, the pile head deflection will become constant beyond a length of half the critical length. For piles with fixed tips, the point of rotational restraint represents a point of symmetry that can be thought of as introducing a mirror image of the real pile. In much the same way that lengths used in calculating Euler buckling loads depend upon end restraints, so too the critical length may be found to depend upon the tip fixity. In the present case, by dividing the normal value L_c by two, a new critical length of one quarter of a wavelength of the long pile solution may be defined.

In Fig. 4.4 the deflection response of the pile head to moment loading of the head (and by the reciprocal nature of the

problem, the rotation of the pile head due to shear loading), is presented on four graphs. As the dimensionless head deflection due to shear for a socketed tip pile exhibited a zero value for piles with a length less than one quarter of the critical length now as well, the fixed tip results also show this response. In effect this is portraying the situation in which the pile is so stiff compared to the soil medium, that all the applied load is transferred to the tip fixing medium. This obviously requires a very strong medium in which the tip is founded; the problem of partial fixity for an elastic continuum soil model is considered by Poulos (1972).

Even though the top of a fixed tip stiff pile ($L/L_c < 0.25$) is not prevented from translating, its deflection will be extremely small under moment load, see Fig. 4.4b, since the moment is essentially not transmitted to the soil, but is carried almost completely by the tip fixity due to the large pile stiffness. Likewise a finite rotation influence coefficient cannot occur due to head shear since the pile stiffness and tip fixity preclude any significant loading of the soil. It must be emphasised that these zero value result from using the soil Subgrade Modulus in the non-dimensional influence coefficients used here. If the results were non-dimensionalised using pile stiffness $E I_p$, then the response of these zero influence coefficient cases would become identical to that given by simple bending theory for a cantilever under end shear and moment loading.

The previously described influence coefficient for deflection due to shear exhibited a linear portion to the curves for $\alpha = \infty$, and this arises as a result of the reduced critical length pertinent for piles with a rotation restraint. The influence coefficients for deflection due to moment, and rotation due to shear, will also

display this effect of a reduced critical length. However, the form of the non-dimensionalisation will mean that the function is no longer linear beyond $L/L_c > 0.5$, but is a quadratic due to the length-squared term.

For the influence coefficients of rotation due to moment loading, presented in Fig. 4.5, for the case of $\alpha = \infty$, flexible piles with a fixed tip at a depth greater than half of the critical depth present a cubic variation with length. The cases corresponding to other values of α , for this coefficient and the others, will present curves that are more complex functions of length as given by equ. 4.14. The curves simplify again for the case of $\alpha = 0$ when the exponents previously discussed for $\alpha = \infty$ each become increased by one.

The results for a fixed head pile will similarly show such a reduced critical depth and are presented in Fig. 4.6. The response of a fixed head or pinned head pile can be readily found from combination of the results presented in Fig 4.3, 4.4 and 4.5 by using the formula,

$$\begin{aligned} \frac{u}{L} E L &= I \frac{H}{uH} + I \frac{M/L}{uM} \\ \frac{\theta}{L} E L &= I \frac{H}{\theta H} + I \frac{M/L}{\theta M} \end{aligned} \quad 4.21$$

where u and θ are the translation and rotation required by the condition at the pile head. From the values of u and θ , the dimensionless ratio of shear to moment required at the pile head

$$HL/M = \left(\frac{I}{\theta M} \frac{u}{L} - \frac{I}{uM} \frac{\theta}{L} \right) / \left(\frac{I}{uH} \frac{\theta}{L} - \frac{I}{\theta H} \frac{u}{L} \right) \quad 4.22$$

can be found. With this ratio used in equ. 4.21 the desired

response of the head and the loads required can be found. This may be especially useful if a relationship exists between head deflection and rotation which will define the ratio of the shear to moment acting at the pile head at ground level.

The effect of an outstand section, at the top of which the shear load is applied, can be easily calculated using simple closed form expressions for response of a cantilever. This aspect is left until the chapter on non-linear behaviour.

This presentation of the results for a pile in a Winkler soil has relied upon the critical length and a special property of the Winkler model. This property is the way results for different length to diameter ratios non-dimensionalise to one curve as long as E_s is deemed to be a soil parameter independent of pile geometry (and $E_s = k_s d = E_h$). The points added to the rightmost side of the curves in Figs 4.3 to 4.6 demonstrate the viability of the effective length concept, in which the response of stiff piles are effectively governed by the actual pile length and the response of flexible piles by the critical length.

Thus, the results of the Winkler model with homogeneous and non-homogeneous profiles verify the existence of a critical length and can be simply expressed for the entire range of flexibilities by a plot of influence coefficient, I_i (equ. 4.13) versus actual length to critical length ratio (L/L_c) for different values of an inhomogeneity measure, α_c (equ. 4.17). The case of piles longer than L_c (equ. 4.8) is covered by using the I_i value for $L/L_c = 1$ and the appropriate α_c value and recognising these are equivalent to I_{ic} (equ. 4.12) and α_c (equ. 4.11) for a flexible pile.

4.3.2 Results of MBEM Analysis

Having shown that the Winkler analysis gives results that conform to the concept of an effective length, the problem of a pile in an elastic continuum soil is considered now. The first step is to show that, for an increasing length of pile in any particular soil, the head response reaches a limiting value. To be specific, the case of a uniform soil problem, like that considered by Evangelista and Viggiani (1976), will suffice. The results of inhomogeneity variation are accurately modelled by the MBEM analysis using a Winkler soil influence matrix. Since there is a strong similarity between the elastic analysis and Winkler analysis methods, as incorporated in the MBEM program, the inhomogeneity factor in the elastic analysis can be expected to produce similar trends to that of the Winkler analysis. Thus, a uniform soil case is adequate to show the existence of a critical length.

The approach chosen for the MBEM model uses the average of deflection across the width of an element to model the rigid nature of deformation across a pile face. This gives better agreement with finite element results than do approaches that ignore pile-soil interface stiffness. It will still be conservative, since it uses the displacement at the centre depth of the uniformly loaded element that must be near the maximum value of the displacement as it varies with depth. The results of the analysis developed in section 3.3, employing the above amended average deflection soil model, have been compared with the flexible results from the analysis of Evangelista and Viggiani in Table 2.1.

In order to maintain a consistent modelling of the effective length of the pile, the aspect ratio of the elements was held constant for the first three values of L/d analysed. This required an increase in the number of elements from 11 for the shortest pile to 51 for the $L/d = 50$ pile. The $L/d = 100$ pile was analysed using only 51 elements, resulting in a doubling of the element aspect ratio. This case of the longest, most flexible pile can be shown to have a pile length of fifteen times the effective length while the shortest, most flexible pile is only one and a half times as long as the effective length ($L_c = 6.6d$).

The result of the comparison shows that the model used provides results 16%, 25% and 12% lower, for flexible pile values of influence coefficients I_{uH} , $I_{\theta H} = I_{uM}$ and $I_{\theta M}$, than the model of Evangelista and Viggiani. This brings the results closer to those from more complex Finite Element analyses, such as those of Randolph (1981) and Kuhlemeyer (1979).

The longest pile (which was modelled using the larger element aspect ratio) compared least favourably, but considering that only three elements were assigned to cover the behaviour in the effective length of the pile it is primarily a fault of the analyser, rather than a defect of the analysis. It appears that at least six, and preferably more, elements should be assigned to the effective length in order to gain the same head response, irrespective of pile length, found above for the three shorter piles.

The results of the analyses of various researchers who used finite element methods, and those from a Boundary Element Method, are compared with the results of analyses carried out by the author using the finite element method, in Fig. 4.7. Subgrade

Reaction theory (Winkler assuming $E = E_s$) results are also plotted. The plot covers one value of $L/d = 25$ and gives the uniform soil influence coefficients as I and those of a modulus proportional to depth ($\alpha=0$) as I' , which are both the same as equ. 4.13. For this L/d ratio the Winkler results are the most conservative while the Boundary Element and finite element results generally agree.

In Fig. 4.8a to 4.8c the three influence coefficients of equ. 4.13 are plotted against K_R for $\alpha=0$ and $\alpha=\infty$ for the original modified boundary element analysis of Poulos (1971a), a similar formulation (but improved discretisation) analysis of the author (analysis A), the MBEM rigid face analysis suggested in this thesis (analysis B) and the previously mentioned finite element results of the author.

It is clear that the finite element results and those from the MBEM analysis B are in close agreement. The results of analysis A and Poulos agree well (as might be expected) except for pile-soil systems with $K_R < 10^{-4}$ where the improved discretisation of analysis A gives higher values.

Figures 4.7 and 4.8 verify that the finite element analysis used in this thesis is of comparable standard to those used by others. Boundary element and Winkler based results generally are more conservative than finite element results, but by appealing to the rigid nature of the behaviour across the face of the pile (analysis B), results nearer to those from the finite element method can be achieved.

Section 4.2.2 showed the results of elastic continuum analyses do not non-dimensionalise simply for the case of different ratios of length to diameter or critical length to diameter. For this reason the previous scheme of presenting the

results of the Winkler analyses (Figs 4.3 to 4.6) and the standard scheme of influence coefficients versus K^R for elastic continuum answers (Figs 4.7 and 4.8) becomes unwieldy.

A new scheme has been adopted, in which the extremes of rigid and flexible behaviour will provide the means of presenting the data. In this way the head response and bending moment distributions for a wide range of soil inhomogeneities can be presented without great loss of coverage. Indeed, the case of intermediate stiffness pile-soil systems can be computed using data from both extremes and interpolating using the form of the Winkler results Figs 4.3 to 4.6, or the solutions of Fig. 4.8.

Rigid Pile Results

Influence coefficients for head response to head loading as functions of L/d , and the distributions of bending moment with depth, for stiff (rigid) piles are presented in Figs 4.9 and 4.10. For each influence coefficient, Fig. 4.9 shows two horizontal lines that are the results of the Winkler analysis of piles in equivalent inhomogeneous soils for $\alpha=0$ and $\alpha=\infty$.

As can be seen, between an L/d of 20 and 40, the Winkler and elastic continuum results are nearly equal which explains why comparison of these two theories (e.g. Poulos, 1971a) for an L/d of 25 reveals no major discrepancies. As might be predicted, the smaller L/d becomes, the larger is the difference between the two results. This corresponds with a general conviction that Winkler theory is inadequate for short piers and caissons.

The range of length to diameter ratio covered by this set of curves exceeds 100 for theoretical completeness only, since rigid behaviour would be most unlikely in such slender piles. In

Fig. 4.10 the extreme of 100 and a reasonable lower value of $L/d = 10$ have been used to present the small range in the distributions of bending moment for rigid pile behaviour. By far the largest variation is associated with the inhomogeneity factor, especially for the moments generated by head shear.

Flexible Pile Results

For the flexible pile case, the corresponding curves to those of the rigid pile case are presented in Figs 4.11, 4.13 and 4.14. The critical length, L_c replaces the actual length, and the soil modulus at the critical length, E_c , replaces the modulus at the depth of the actual length, E . The measure of inhomogeneity is now $\alpha = E_c / m L_c$ and once again the two results of an equivalent Winkler analysis for $\alpha = 0$ and $\alpha = \infty$ plot as two horizontal lines as functions of L_c / d across Fig. 4.11, for each influence coefficient. Once again the region around $L_c / d = 25$ sees the Winkler results agree with those from the MBEM elastic continuum program, but now the evaluation of previous comparisons is not directly possible because of the use of the critical length.

The results of most interest are those for critical length to diameter ratios between 5 and 40, but the values at 100 are included as a guide to the shape of the curve beyond an L_c / d of 60. All the results of this case, and the rigid case, involve fifty full elements (i.e. 51 nodes) to model the full pile length. This case was modelled by using an actual pile length twice the critical length to ensure that the pile was flexible, but analysis using the actual length equal to the critical length gave no more than a maximum of 5% increase in response. This small increase is entirely comparable to that found for the Winkler results.

The results do not cover cases of L/d less than 2 since in Chapter two it was suggested that the engineering bending theory upon which the pile analysis in the MBEM program is based is unreliable for beams of length less than 3 diameters. In the next section, the finite element method, which does not rely upon simple engineering bending theory, will be used to consider piles (or rather caissons and block circular footings) as special cases of elastic continuum analysis of lateral loading.

The bending moment distributions for flexible piles in an elastic continuum soil are considered next, and a comparison is possible with the curves of Randolph (1981). In Fig. 4.12 the bending moment distributions for three values of his inhomogeneity factor $\rho_c = E_c / E_{c/2}$ (where $E_{c/2} = E_o + 0.5m_c$ and l_c is given by equ. 4.7) are reproduced for head shear and moment loads. The same trends are evident in Fig. 4.12 and Fig. 4.13, with the uniform soil presenting the smallest maximum bending moment at about the same relative level in both figures, and the maximum increasing and becoming deeper with increasing inhomogeneity. However a significant difference from Randolph's results is the MBEM prediction of a larger increase of non-dimensional moment with increasing L/d value. For the practical range of critical length to diameter ratios the variation may not be as significant as the wide range of L/d covered in the figures implies.

Figure 4.14 and Fig. 4.12 respectively display the bending moment distributions from the MBEM analysis and the results of Randolph for loading of the head by a moment. Again the trends of the two figures are the same with perhaps the two analyses agreeing most closely for L/d of 10 which is a typically encountered value

4.3.3 Results of Finite Element Analysis

In order to verify the existence of an effective length, the response of a pile with various lengths in a particular soil was analysed. This can be accomplished economically using the boundary element approach but requires excessive computer time to apply the finite element method. Thus, the finite element layer building approach was devised to analyse a large number of cases of piles of various length. Further, the piles were lengthened by only one layer of elements for each new case analysed, leading to a better defined curve of pile response versus pile length than is possible using conventional full-mesh approaches.

The "building" method was thus ideal for the task of illustrating the existence of the effective length for any combination of pile and soil. It also proved to be a good method of calculating two other aspects of foundation behaviour:

- a) The average deformation of a flexibly loaded circular area on an elastic layer of finite depth.
- b) The load-deformation response of circular foundations for a wide range of length to diameter ratios.

For generality, the three cases of a horizontal force, vertical force and lateral moment loading were considered using uniform horizontal and uniform vertical applied tractions and a linearly varying vertical traction at the free surface of the elastic layer or foundation. The three tractions that were employed have been shown in Fig. 3.9 and the average responses were defined as the uniform deflection or rotation in the direction of the applied traction based upon equivalent volumes of the displaced shapes.

The results of the "building" analysis can be directly compared with the results using the "full-mesh" finite element method, compared with results for a similar aspect ratio rigid plate foundation (as modelled by Douglas and Davis, 1964), and finally compared with the results from the MBEM program developed in this work. The last two comparisons involve considerably simplified models, with the boundary element answers expected to be the least appropriate for squat rigid foundations.

The results presented are for deformation of a circular loaded area on a finite elastic layer, the head response of circular foundations for a wide range of length to diameter ratios and the head response of flexible laterally loaded and compressible vertically loaded piles of circular cross-section. Where possible the results are compared with previous solutions.

Finite Element Analysis : Full Mesh

A standard pile to soil Young's modulus ratio of 5200 was chosen in order to keep the foundation behaviour rigid for all cases but the longest piles considered. The same basic mesh was used to analyse foundations with a length to diameter ratio of up to four, and contained three radial elements and up to six vertical elements in the foundation. For ratios of five and greater only one element was employed to model the pile radius and up to eleven elements were used to model the pile length. This was found to give an adequate representation, consistent with the reduced importance of the base in more slender foundations where the majority of support is derived from the foundation sides.

The meshes maintained a fully-fixed radial boundary at twenty foundation radii, and for the foundations with a length to diameter ratio up to four, a fully-fixed base boundary at twenty

foundation lengths except for the surface footing case where a base at twenty foundation radii was used. This system became impractical for larger length to diameter ratios and so the base was placed at twice the pile length.

The results are presented in Fig. 4.15 where the four dimensionless responses of

- a) horizontal deflection due to shear,
- b) rotation due to shear and deflection due to moment (which are identical from the reciprocal nature of the problem),
- c) rotation due to moment and
- d) vertical deflection due to vertical normal load

are presented against length to diameter ratio (and its inverse). Two apparent anomalies appear at the extremes of small and large length to diameter ratio. The deflections in the direction of applied load for the length to diameter ratio of 0.1 are not consistent with a smooth representation of behaviour. The vertical deflection response also shows a discontinuous relationship at a length to diameter ratio of five. Both of these aspects of behaviour are due to the limitations of the adopted mesh and depend on the form of loading.

Considering the case of the small length to diameter ratio, it can be seen that the mesh is only twice as deep as the diameter of the foundation. For such a thin layer it is conceivable that the vertical deflection of a rigid circular foundation due to vertical load would be smaller than that associated with thicker layers, as will be shown in the next part of this section. The case of a zero thickness layer must result in zero deflection and for the other limiting case of a layer of infinite thickness, a Boussinesqu-based solution predicts a finite vertical deflection.

It can be seen that the horizontal response to horizontal loading is not so much affected by the layer thickness, as the vertical response. However, it can still be conjectured that the proximity of the rough rigid base will reduce the deflection that would occur if the layer were of infinite thickness. It appears that the rotational response and response to moment loading are not so severely affected by the proximity of the rough rigid base.

The other extreme, of foundations with large length to diameter ratio, also exhibits a response that is a function of the mesh geometry. The vertical deflection due to vertical loading is seen to display an abrupt change at $d/L = 0.2$, and is connected with the changing of the deep mesh to one with a total depth to foundation length ratio of only two instead of twenty. It is clear that the response of vertically loaded rigid piles depends upon the layer depth to foundation length ratio.

As an example of the effect of the base boundary upon the response, a BEM program (Poulos, 1979) was used to obtain the response of two piles with an L/d of two and four with the base at a depth of twenty pile lengths and a pile with an L/d of 5 with the base at two pile lengths deep. The BEM results are plotted in Fig. 4.15 and agree well with the full-mesh FEM results.

Thus, attention must be paid to layer depth when comparing results of vertical loading analyses for shallow footings on thin layers of soil or deep pile foundations in soils of limited depth. To cater for this using a finite element analysis leads to a large number of meshes, and repeatedly solving the same problem to establish the dependence upon the ratio of layer depth to pile length. This problem is overcome by using the finite element building analysis, the results of which will now be discussed.

Finite Element Analysis : Profile Building

The profile building analysis provides an efficient means of predicting the head response of a large number of cases of foundations with various length to diameter ratios. To model foundations in an elastic continuum using this analysis, it is necessary to first establish a layer of soil that is deep enough to provide a response approximating that of a semi-infinite elastic continuum. This is achieved by checking the response of the loaded area after the addition of each layer, for the three loadings of Fig. 4.16, and stopping building when the response is essentially constant (converges) for the addition of extra layers.

The choice of response is most conveniently taken as the average deflection or rotation of a loaded circular area on the surface. This area corresponds with the position where the base of the foundation will be placed for the layers that contain the stiffer elements of the buried circular footing, pier or pile. It is necessary, but not sufficient, that the response of the surface at which the building of the foundation commences should be unaffected by the layer depth. Any analysis of a foundation on a layer whose response is affected by layer depth, will necessarily also have a response that is affected by the limited layer depth.

The average response must therefore be monitored during the building of the base layer, prior to commencing the foundation modelling. It can be conjectured that the average response of the circular loaded area will be a good measure of the response of a rigid surface footing. Therefore an approximation for the response of a rigid circular foundation on the surface of a layer of finite depth should be found for different ratios of layer depth, h , to foundation diameter, d .

Surface Loading on a Finite Homogeneous Elastic Layer

The problem is defined in Fig. 4.16, and Figs 4.17, 4.18, and 4.19 present the average-deflection and average-rotation of a circular area loaded by a uniform vertical (axial) load, horizontal uniform (lateral) shear and linearly varying vertical (moment) load for a wide range of layer depth to diameter ratios. Results were obtained for six values of Poisson's ratio and are presented as dimensionless influence factors.

Also in the figures are the results of Gerrard and Harrison from Poulos and Davis (1974), shown by arrows for the d/h ratio of zero i.e., a uniform homogeneous elastic "half-space" response. This set of results are also shown in tabular form in Table 4.2 where the average dimensionless responses, including the effects of Poisson's ratio, are compared to the average of the six responses found for the values of Poisson's ratio used in the numerical study.

The theoretical results of Gerrard and Harrison can be used to calculate the average responses by means of closed form expressions for two of the surface loading cases, but the remaining three responses require numerical integration of tabular data to find the average. This numerical treatment conforms with the way the nodal quantities are treated in the finite element building analysis to find average responses. Thus values of theoretical and numerical response are directly comparable.

All responses from the analysis compare favourably with those from Gerrard and Harrison, most errors being less than $\pm 1.5\%$. The building analysis result for vertical response, that was 3.6% smaller, is consistent with the finite depth in the analysis.

Table 4.2 presents results for the response of a layer with infinite depth to diameter ratio, non-dimensionalised with respect to Poisson's ratio. For any other values of layer depth to diameter ratio it will not do so, thus the six curves for Poisson's ratio are plotted separately in the figures. Of the five responses of Table 4.2, two are equal from the reciprocal theorem and thus only four sets of curves are drawn for variation of response with layer ratio in Figs 4.17, 4.18 and 4.19.

The influence values for layer depths less than one quarter of the foundation diameter cannot be found from the building analysis. This is due to the choice of one-eighth of the foundation diameter for the height of the elements that make up each layer. The smallest value of total layer depth that can reasonably be used requires at least two layers of finite elements and so the curves below h/d of one quarter are extrapolations to the influence values of zero that arises for a zero depth layer.

The lower set of curves in Fig. 4.19, for the cross-term responses of deflection due to moment and rotation due to shear, show an interesting phenomenon for nearly incompressible soil and small layer depth-to-diameter ratios. Whereas the rotation and deflection have normally been found to be equivalent in sense to that at the end of a tip loaded cantilever, these results indicate a reversal of this. The average rotation due to shear and average deflection due to moment loading may result in influence values less than or equal to zero. This behaviour is apparent for Poisson's ratio of one half, for any layer depth to foundation diameter ratio, and also for other values of Poisson's ratio, for small layer depths.

This behaviour appears to result from the rigid base to the mesh restricting the deformation of the material below the footing. The confining effect of the base leads to the compressive zone immediately in front of, and below, the footing, causing heave. This heave overcomes the tendency of the footing to rotate in the normal sense and is heavily dependent upon the degree of incompressibility of the soil. Likewise, the deflection from an applied moment load is affected by the confined layer depth causing the compressive region to react against the base, reversing the "normal" direction of deflection.

The increase of this "negative" deformation, with reducing layer depth and increasing Poisson's ratio, can also be found from analyses of plane strain, strip loading problems. A Finite Layer analysis, Booker and Small (1982) was modified by the writer to cater for horizontal and moment loading. Results were obtained for varying layer depths, in the same manner as for the circular loaded areas. Figure 4.20 presents the curves of non-dimensional response, for Poisson's ratio of 0.4, against the layer depth to strip width ratio, h/b and its inverse. Once again, the cross-term response involves influence coefficients less than zero for small layer-depth to strip-width ratios. This suggests that such behaviour is not a feature of the circular loaded area problem, or the finite element method, since a similar trend is seen in strip loaded problems analysed by a different method.

The results for average response of circular loaded regions on a soil of limited depth subjected to lateral, axial and moment type loads have been presented. They compare well with previous published results and show similar trends to those found for strip loading with the same load types.

The results for mean deformation of a flexibly loaded circular region presented here, do show an aspect of behaviour that is to some extent governed by the existence of a critical length for laterally loaded piles. The use of equ. 4.8 for the case of pile and soil having the same Young's modulus yields a critical length of 2.09 diameters. From the three sets of curves in Figs 4.18 and 4.19 it can be seen that for d/h values less than about 0.5 the responses have virtually reached their converged values. This provides an unexpected verification of the critical length concept for the case of a pile of very high flexibility.

Thus the building analysis has been shown to provide a set of solutions for the response of circular foundations that are sufficiently accurate to allow prediction of the behaviour of rigid loaded circular foundations on an elastic layer. This is the first step towards the calculation of the response of buried cylindrical foundations, which will ultimately lead to the modelling of flexible circular piles. By obtaining a layer of elastic soil that responds like an elastic half-space it is possible to continue building upon that layer with further layers that contain elements of the circular foundation. The method may then be used to solve problems in which the pile is modelled; with confidence in both the results obtained and also in the capability of the analysis to solve a wide range of foundation types, that are amenable to solution by the same method.

Axisymmetric Foundations of Varying Length to Diameter Ratios

For conciseness, only the case of uniform modulus with depth will be presented to show the existence of a critical length in the results of the building analysis. To each of the base layers, that provided the results for surface loading of a finite layer of elastic material, a series of new layers containing pile segments with a pile to soil modulus ratio given by $E I / E_d = 10^4, 10^{-1}, 10^0, 10^1, 10^2, 10^3$ and 10^4 , were added.

The results of the second stiffest modulus ratio have been plotted with the full-mesh results on Fig. 4.15 for Poisson's ratio of 0.49, and examination of this figure shows the two finite element methods both give essentially the same response. The slight differences between both sets of results are compatible with the previously noted effects of the mesh geometries and the existence of an effective length. The building analysis case has a stiffer pile to soil modulus ratio than the full-mesh case and this means the two curves diverge near $d/L=0$ and stabilise to give two different "converged" deflection values. The building result reaches a constant response at a larger critical length and with a smaller response than the full-mesh finite element results which are consistent with the prediction of equ. 4.8.

Flexible and Compressible Piles: Building Analysis

The building of the layers containing pile segments continued for each pile segment to soil stiffness ratio until the axial or lateral response became approximately constant. These constant values of response represent the behaviour of compressible and flexible piles, and the values of pile length at which they were achieved represent an estimate of the critical length. The

average value of the various estimates for L_c for the six values of Poisson's ratio was about 90 % of the predicted value from use of equ. 4.8. This is a result of the convergence criterion for the response necessarily providing critical length estimates that can never reach the true value since the converged response can never be achieved. The variation in response as the critical length is approached becomes smaller and means a significant change in estimated critical length will be associated with small changes in response.

Figures 4.21 to 4.24 present the "converged" response of laterally flexible and axially compressible piles from the building analysis as a function of Poisson's ratio for various values of the relative stiffness measure $K = \frac{E I_p}{E_d d^4}$, which can be used to calculate the critical length to diameter ratio from

$$L_c / d = \pi \sqrt{2} K^{1/4} \quad 4.30$$

The values of response given in these curves agree with the results of full-mesh finite element analyses and thus are slightly lower than the more conservative MBEM elastic continuum results.

Also plotted on these figures is the response of the soil layers, previously presented in Figs 4.17 to 4.19, that were used as the starting layer for each pile to soil stiffness case that was modelled. It can be seen that the soil layer response is markedly affected by changing Poisson's ratio whereas the pile response only exhibits a minor dependence. The dashed lines in the curves are from the solutions presented by Gerrard and Harrison for the response of an elastic half-space and the building results (for $h = 20d$, see Fig. 4.16) show excellent agreement.

4.3.4 Existence of Other Critical Lengths

The critical length concept is not restricted solely to the behaviour of laterally loaded piles. The results of both the Winkler analysis and Elastic theory for the problem of an axially-loaded pile also present responses that are considerably simplified by use of a critical length. Further, it is possible to see the presence of a critical length in strip raft behaviour.

The Winkler model of soil response has been presented in section 3.2 where a solution for axial loading of a pile involved exponential terms, equ. 3.17. The power to which the number e is raised, az can be treated in the same way as Yz for lateral loading and the depth to result in $az = \pi$ can be shown to be

$$z_c = \left(\frac{\pi E A_p}{E_p} \right)^{1/2} \quad 4.23$$

Thus a critical length for axial loading of piles may be proposed and compared to the results from the Winkler and elastic continuum analysis of axially loaded piles.

In Fig. 4.25 the results of the Winkler analysis of a pile in a uniform Subgrade Modulus soil are presented as a dimensionless influence coefficient for axial deflection due to axial load plotted against a measure of the relative pile-soil stiffness, $K = \frac{E_p A_p}{E_s L^2}$ for various values of soil side to base stiffness $\left(\frac{E_s d L}{E_p A_b} \right)$ ranging from zero base restraint to a vertically fixed base. For K less than $1/\pi$, as predicted by the critical length concept, all the various values of base-soil stiffness become irrelevant and show that such piles are fully compressible, i.e. the head response is independent of pile length.

Figure 4.26 presents the results of the building analysis for vertical response of circular foundations and the results of the BEM analysis of Poulos (1979), used previously. Care was taken to ensure the BEM analysis was for the same pile length to layer depth ratio as the building analysis. Both analyses agree well, even for very small pile to soil modulus ratios, and exhibit a response that reaches a constant value as the length increases. This constant response demonstrates the existence of a critical length for axial loading of pile foundations and the vertical arrows are at the predicted values of L/d for vertical response. The ratio of lateral critical length (equ. 4.8) to axial critical length (equ. 4.23) can be calculated and for most cases the axial critical length will be significantly greater. Although the difference between the two depends upon the cross sectional properties a figure of four times is perhaps typical.

The results of Brown (1978) for bending moment distribution in a strip footing, Fig. 4.27, with a length to width ratio of 10 and a low value of strip-soil relative stiffness (defined in the figure) depict distributions of bending moment and deflection that can be explained by means of the critical length concept.

- a) For a force applied at 1% of the strip length from the end of the raft ($s = 0.01$) the bending moments decay to small values over the half of the raft opposite the loaded end.
- b) Once the load has moved in from the end by 20% of the footing length ($s = 0.2$) the maximum moment has reached a peak that does not change as the force is moved to the centre of the raft.

Similar statements may be made for the reaction distribution

under the raft (not reproduced here) and the deflected shape of the raft, shown in Fig. 4.27b. Thus, considering a raft-soil combination, initially with the same relative stiffness factor and L/B , the critical length concept suggests that after extending only its length its behaviour near the load could be predicted satisfactorily using these results for a raft with an L/B of 10. If the stiffness factor, $K = 0.001$, is converted into the pile-soil stiffness factor, K_R , the raft-soil system can be shown to possess a critical length, L_c of about 0.55 of the actual length. The two responses of Fig. 4.27 indicate the raft is flexible with behaviour consistent with the above value of critical length, calculated using equ. 4.8.

The effective length concept is shown here to have other applications in soil-structure interaction problems and indeed many more problems can be approached satisfactorily, using the critical or actual dimension for non-dimensionalisation according to the relative stiffness of the structure and soil. The axial critical length is not investigated in detail here but it would help in explaining the apparent lack of complete mobilisation of shaft friction for long compressible piles. Randolph (1983) and Poulos (1982) have each implied the existence of a critical length for axial loading.

4.4 Critical Length Applied to the Design of a Test Pit

As a method of analysis, the MBEM can provide economical solutions for a range of loading conditions, and take account of limited soil depth, but is unable to incorporate the effect of a lateral boundary to the extent of the soil. To accomplish a logical treatment of the effects of a lateral boundary, the finite element method may be employed. The results can then be assessed with due regard to the effective length of the pile involved. The results presented in Section 3.4.3 were assessed in this way for a uniform soil, and here the same will be done for a soil with a Young's modulus proportional to depth by considering a hypothetical problem of field testing.

A series of tests on large scale model piles in a pit filled with a calcareous sand were to be carried out in order to investigate the response of typical off-shore piles to lateral load. The pit dimensioning was critical for the logical consideration of the far-field effects associated with the large lateral extent of the soil in the off-shore situation. Too small a pit would modify the response of the model pile to such a degree that it would change its behaviour compared to the prototype pile. Too large a pit would require expensive excavation and filling operations for no benefit in response of the piles tested.

In order to assess the minimum feasible pit dimensions a finite element analysis was used to model various pit geometries and recourse was made to the critical length to evaluate the results. The analysis employed a circular pit geometry but the use of a square cell, that completely enclosed the cylindrical model of the soil, would allow a fair comparison when more than

one pile was tested in a rectangular pit. Indeed, it seems likely that across the line of action of the loading the dimensions could be further reduced.

It is well-accepted that piles of length greater than a critical depth of penetration are flexible in response to lateral load, and have no dependence upon the actual length of pile. Thus, the use of a pit extending down to the critical depth would be required to remove the effect of the base of the pit on pile response. It remained to assess the effect, upon head response and moment distribution, of the nearness and character of the lateral boundary of the pit.

The boundary condition most relevant to the material at the pit sides was considered to be a full fixity in radial, circumferential and vertical directions. This was for two reasons.

Firstly, the decay of deflections and stresses with distance from the pile mean a realistic boundary condition to emulate far field effects in a static analysis was a fully rough boundary. Any attempt to include sliding of the material around or up the sides of the pit, would not model the far field accurately and could introduce spurious behaviour.

Secondly, the sand filling the pit would be very unlikely to experience enough shear at the boundary of the pit, due to pile loading, to cause sliding and the sides of the pit would be considered stiff enough to limit the normal deflections. A fully fixed condition at the boundary would thus appear to be the most appropriate for the present purpose.

The prototype pile size would be a maximum of 1.83 m diameter for the present requirement. The material through which the pile would be installed was not well defined but in the light of previous experience four typical profiles were assumed. These had

a linear variation of Young's modulus with depth from zero at the soil surface obeying the relationship

$$E = m.z \quad 4.24$$

where $m = 0.5, 0.75, 1.25$ or 2.0 MPa/m and z is measured in metres. For the pile of 1.83 m diameter a pile wall thickness of 75 mm was taken to be appropriate, thus leading to a bending stiffness of the steel tube pile $E I = 33494 \text{ MNm}^2$.

Employing equ. 4.8 for the critical pile length

$$L_c = \left(\frac{4\pi^2 E I}{m^2} \right)^{1/5},$$

a table of critical lengths and critical length-to-diameter ratios for the four soil parameters was produced, as in Table 4.3. Using the soil parameter $m = 0.75$ MPa/m as a conservative value, and the critical length to diameter ratio predicted by equ. 4.8, the model piles of the pit could be designed.

It was desirable to use model piles of the largest possible diameter to avoid introducing effects caused by grain size scaling. Thus, a 381 mm (15 inch) diameter pipe was chosen as a practical maximum dimension pile for testing. By recourse to equ. 4.8 the value of wall thickness for each soil profile, that ensures the critical lengths of Table 4.3 were achieved, can be calculated.

Table 4.4 displays the three wall thickness corresponding to the pile of 381 mm diameter and piles of 305 and 229 mm diameter, together with the pile critical lengths, for the soil with $m = 0.75$ MPa/m. Critical lengths corresponding to the other soil profiles may be obtained from the use of Tables 4.3 and 4.4.

The longer length of the 381 mm diameter pile would be most critical for the pit dimensioning and so this was chosen to be modelled using the axisymmetric geometry antisymmetric load finite element program. The soil modulus used involved $m = 0.75 \text{ MPa/m}$, erring on the softer side of the response so as to be conservative, i.e. a longer critical length.

Results from the investigation of moving the lateral boundary of a rectangular finite element mesh, and employing a uniform soil modulus with depth, section 3.4.3, indicate two main points:

i) a boundary must be beyond three critical lengths before the response is unaffected by the width of the mesh although the worst reduction in response for a boundary at one critical length is only 5% .

ii) there is a degree of mesh refinement necessary in order to accurately model the behaviour and if the same mesh is "stretched" too far the modelling would suffer.

As the the above points were deduced from a uniform soil analysis of the effects of different boundary positions of a finite element mesh, the analysis for the case of a Young's modulus proportional to depth was required and also a brief investigation of the possibility of sloping the sides of the pit without markedly changing the pile response.

In total, eight analyses were performed with a pit depth of 6.0 m ($L = 5.84 \text{ m}$) and using radial dimensions for the mesh of 1.5, 3.0, ^c 6.0, 9.0 and 12.0 m. Four of the eight analyses, for the surface radial boundary at 3.0 m, were used to investigate the changing response as a function of the slope of the pit side.

The results for the vertical sided pit in terms of head deflection and rotation due to a shear force and applied moment at

the head are presented in Fig. 4.28. Also shown is the response of the pile in a pit with a 1:6 sloping side.

The bending moment distributions with depth are plotted in Fig. 4.29 for the four cases of the second largest lateral boundary, the 3.0 metre boundary with both vertical and 1:6 sloping sides and the 1.5 metre boundary results.

Figure 4.28 shows that, compared with a uniform modulus, the linear modulus variation has reduced the minimum distance to the fixed lateral boundary, before reductions in head response become evident, from three to about one times the effective length. If a 3.0 metre radius pit was used the response is only reduced by 7.5%, for the worst case of head deflection due to head applied shear force. A slope of 1:6 increases this discrepancy to 9% while a 1:3 slope causes a reduction of 10.5% in the head response.

Figure 4.29 shows the bending moments generated by unit head shear force and moment loading and demonstrates remarkably little change in moment distribution between the three cases. The response plotted for the radial boundary at 9.0 metres is equivalent to that for the 12.0 metre boundary and virtually the same as that for the 3.0 metre response. The 1.5 metre boundary has the only response that differs significantly from the other cases, being smaller below a depth of 1.5 metres consistent with the proximity of the sides reducing the interaction of the upper soil with the lower layers.

The effect of slope upon bending moment distribution is negligible for the 1:12 and 1:6 slopes but showed some deviations at the point of maximum bending moment in the case of the 1:3 slope. The confined response caused by the shallowest slope actually gave larger maximum moments, which is a disturbing trend as far as modelling the far field effects is concerned.

The above results suggested that the optimum size of a pit for testing piles of a flexible nature, using a calcareous sand, and for the correct prototype to model scaling, would be a 3.0 metre radius with a slope of 1:6 on the sides. The pile of 381 mm outside diameter would require a thin wall of about 3 millimetres in order to retain the same effective slenderness ratio as the maximum diameter prototype pile. While this thickness would probably be too small to allow safe driving, it would depend upon the soil actually used whether this limiting value is required. If the soil were to have a value of modulus increase with depth equal to (say) 1.0 MPa/m and a value of critical pile length of 6.0 metres was desired, then the thickness required would become 4.5mm.

It should also be stressed that piles with actual lengths just less than their critical length also behave as if they were flexible. Thus, the above arguments could be applied again to slightly stiffer piles in order to consider the effects of varying the prototype pile size and soil properties. It would be expected that the soil property used here would be adequate and err on the conservative side, which means that a smaller dimensioned pit would be possible but would not necessarily be desirable.

4.5 Conclusion

In this chapter the linear response of a pile to lateral load has been considered using a Winkler analysis, MBEM elastic continuum analysis and elastic finite element methods, with regard to the concept of an effective length that can characterise the response. The concept of effective length requires the definition of a critical length, beyond which all piles behave flexibly, and this critical length is shown to be evident in many types of problem in foundation analysis. A comparison of the three methods of solution of the laterally loaded pile problem is informative and suggests reasons for the variable agreement found between the three methods. This comparison is facilitated by introducing the concept of an effective length for the pile and soil system.

The method of analysis of "thin" piles, i.e. the analytic Winkler solution and the numerical MBEM analysis, rely upon the modelling of the pile as a thin strip beam that behaves according to simple engineering bending theory. These "thin-pile" models demonstrate the existence of a critical length, that can be predicted by the equation developed from the simple Winkler model analysis, equ. 4.8.

The axisymmetric finite element analysis for anti-symmetric loads, models the true geometry of circular piles and does not rely upon simple bending theory. In this Thesis the finite element method has taken two forms, namely a standard (full-mesh) approach and a substructure (building) approach. The second method was developed to enable a large number of pile geometries to be economically analysed in order to provide a fine definition of the critical length.

As a by-product of the investigation of the critical length, the building analysis produces results for the response of a flexibly loaded circular region on a finite layer of homogeneous elastic soil. This response provides a further demonstration of the existence of a critical length from the depth of layer that behaves essentially the same as an elastic half-space. The critical length equation is shown to give a good prediction of the depth of layer at which this constant response is first achieved during the building process.

The results of the profile building analysis include the behaviour of rigid circular block footings, short stiff piles and long flexible piles, solutions which previously have not been obtained from a single analysis.

The existence of an effective, or critical, length of laterally loaded piles has been proposed before, Barber (1953), Matlock and Reese (1960) and Randolph (1981), and various expressions have been produced to calculate it. By recourse to the simplified method (Winkler analysis) an expression for the critical length is derived and then the other two methods are used to confirm the applicability of this expression to the elastic continuum method of analysis. Also, from the Winkler analysis of axial loading, an expression for the axial effective length, beyond which a pile is virtually fully compressible, is derived and its effect on axial behaviour is examined briefly.

The solutions for linear lateral pile response from this Chapter are directly comparable to previously-published solutions and are considered to provide a standard series of solutions for the linear response of single laterally loaded piles.

UNIFORM SOIL MODULUS WITH DEPTH

Source	A ₁	b ₁	c ₁	A ₂	b ₂	c ₂	A ₃	b ₃	c ₃
Randolph (1981)	.69	3/7	-1/7	.51	2/7	-3/7	.93	1/7	-5/7
Kuhlemeyer (1979)	.68	.32	-.17	.43	.37	-.41	.63	.35	-.66
Bannerjee and Davies (1978)	2.0	0	-.20	.80	0	-.51	1.1	0	-.78
Blaney, Kausel and Roesset (1976)	.60	0	-1/4	.94	0	-1/2	.66	0	-3/4
(Winkler) Hetenyi (1946)	$\sqrt{2}$	0	-1/4	1.0	0	-1/2	$\sqrt{2}$	0	-3/4
Present work Finite Element	.69	.28	-.18	.49	.27	-.43	.96	.14	-.72

SOIL MODULUS PROPORTIONAL TO DEPTH

Randolph (1981)	1.06	3/9	-3/9	.87	2/9	-3/9	1.20	1/9	-7/9
Bannerjee and Davies (1978)	1.89	0	-.39	1.28	0	-.59	1.23	0	-.81
(Winkler) Hetenyi (1946)	2.43	0	-2/5	1.62	0	-3/5	1.75	0	-4/5
Present work Finite Element	1.26	.24	-.35	.97	.19	-.56	1.37	.083	-.78

TABLE 4.1 Simplified Equations of Head Response from Various Authors
in the form $I_i = A_i (L/d)^{b_i} K_R^{c_i}$

Dimensionless Mean Response	Gerrard & Harrison (*numerical integration)	"Building" Analysis	Error %
$\frac{\bar{u}Ed}{H(1 + \nu)(1 - \nu/2)}$	$\frac{3.38^*}{\pi}$	$\frac{3.33}{\pi}$	-1.5
$\frac{\bar{\theta}Ed^2}{H(1 + \nu)(1 - 2\nu)}$	$\frac{2}{\pi}$	$\frac{1.97}{\pi}$	-1.5
$\frac{\bar{u}Ed^2}{M(1 + \nu)(1 - 2\nu)}$	$\frac{2}{\pi}$	$\frac{1.98}{\pi}$	-1.0
$\frac{\bar{\theta}Ed^3}{M(1 - \nu^2)}$	7.18*	7.27	+1.2
$\frac{\bar{w}Ed}{P(1 - \nu^2)}$	$\frac{3.38^*}{\pi}$	$\frac{3.26}{\pi}$	-3.6

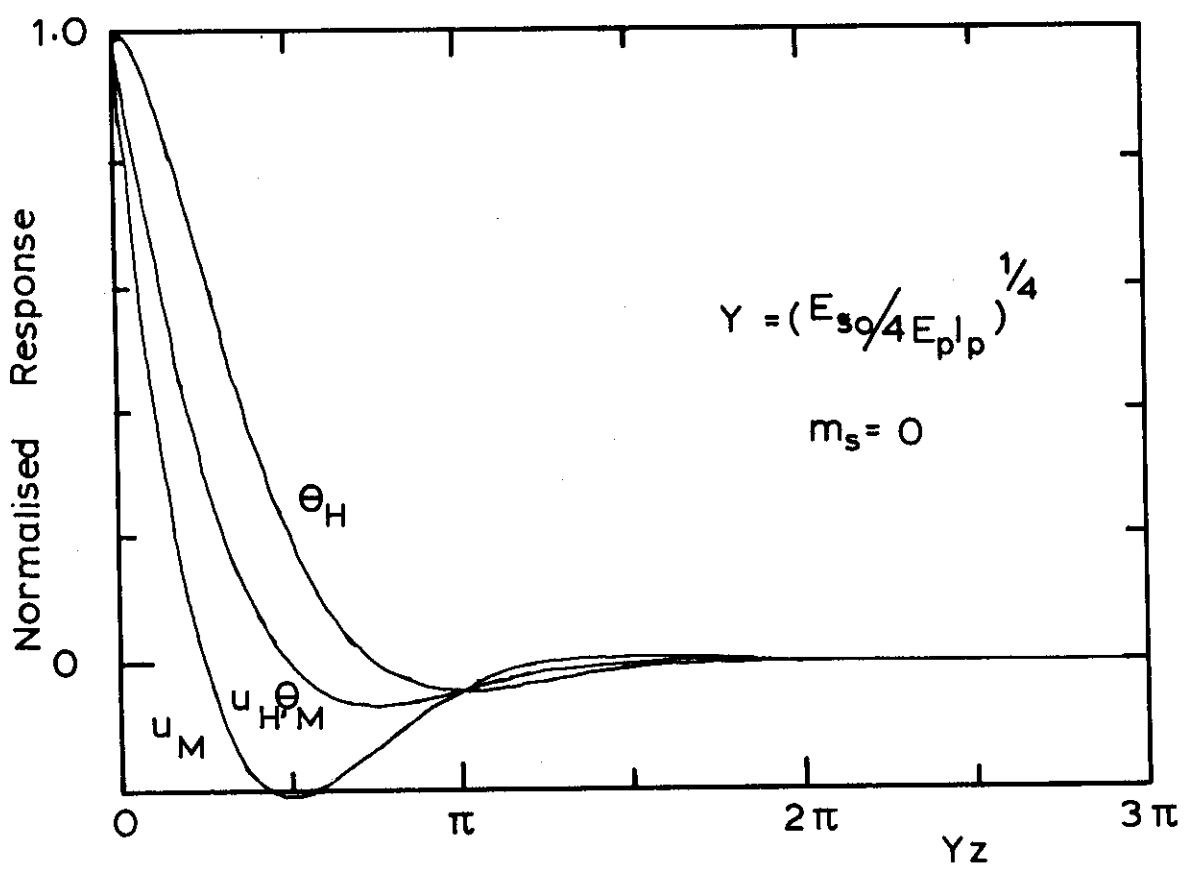
TABLE 4.2 Comparison of Influence Factors for Mean Deformation of a Circular Area on an Elastic Half-space from the Results of Gerrard and Harrison (Poulos and Davis, 1974) and the "Building" Analysis.

m (MPa/m)	0.5	0.75	1.25	2.0
L_c (m)	30.43	28.06	25.34	23.06
L_c/d	16.63	15.33	13.84	12.60

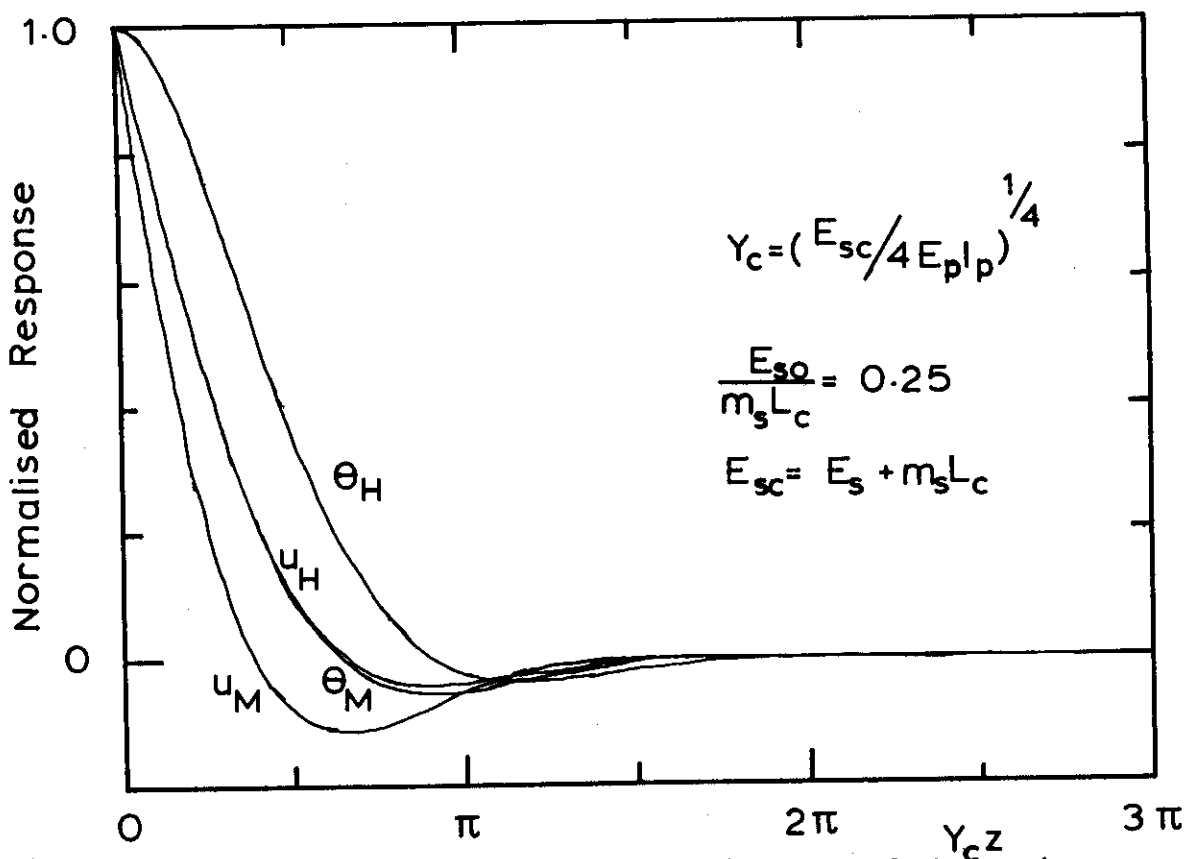
TABLE 4.3 Critical Lengths for Prototype Pile 1.83 m Diameter.

Diameter (mm)	381	305	229
Thickness (mm)	2.94	1.87	1.05
L_c ($m = 0.75$) (m)	5.84	4.63	3.50

TABLE 4.4 Pile Thicknesses for the Three Model Piles.



a) Pile in Uniform Subgrade



b) Pile in Linearly Increasing Stiffness Subgrade

FIG 4.1 THE CYCLIC AND EXPONENTIALLY DECREASING NATURE OF THE DEFLECTION AND ROTATION RESPONSE OF A PILE IN A WINKLER SOIL

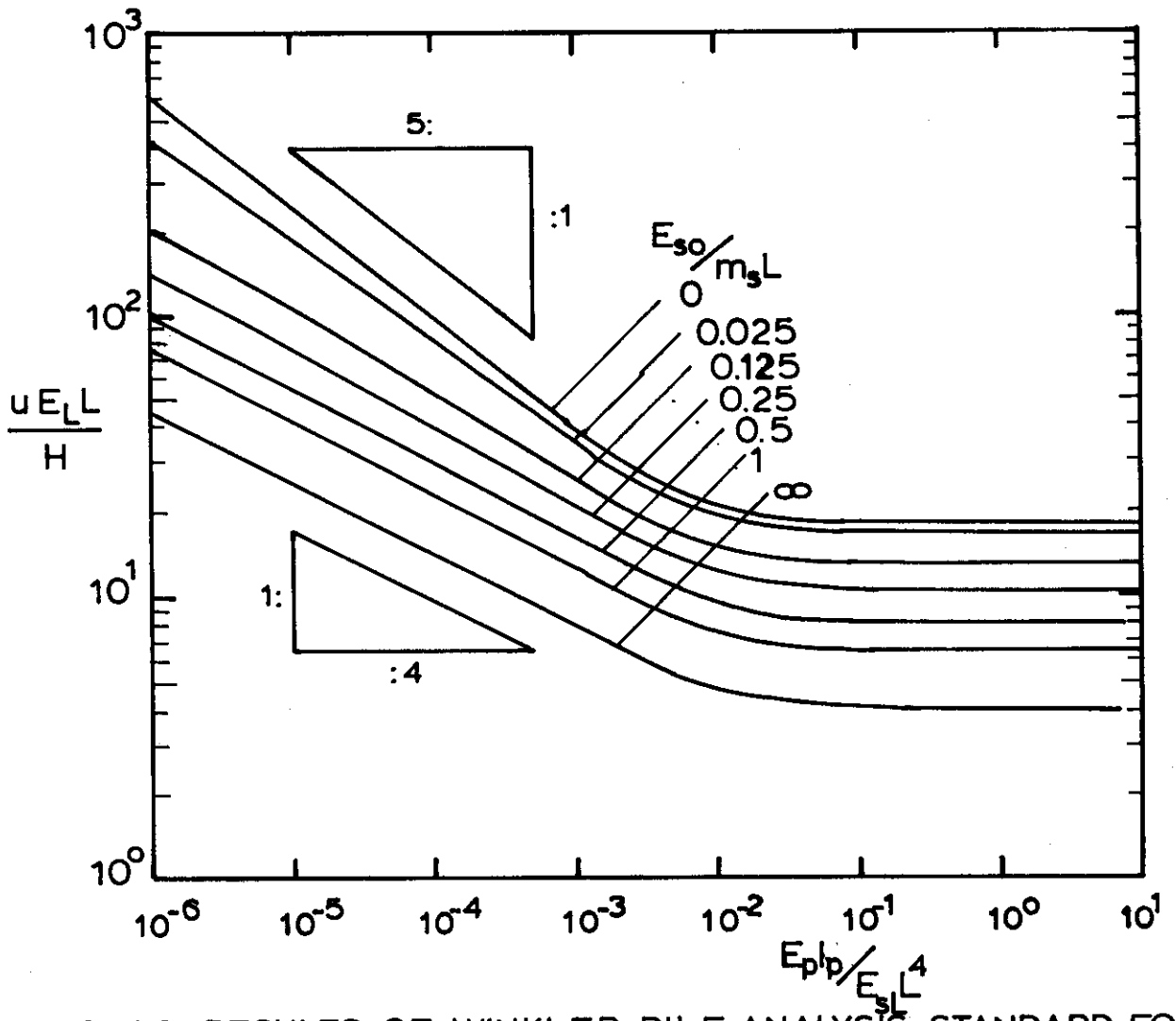
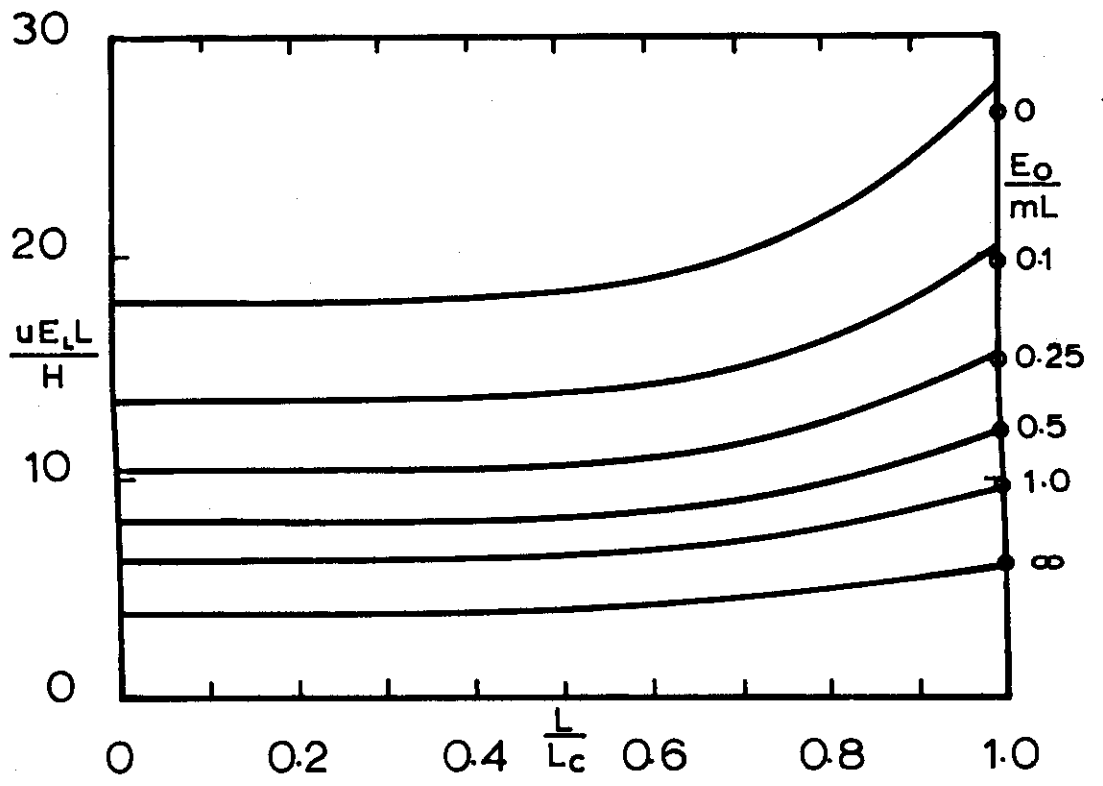
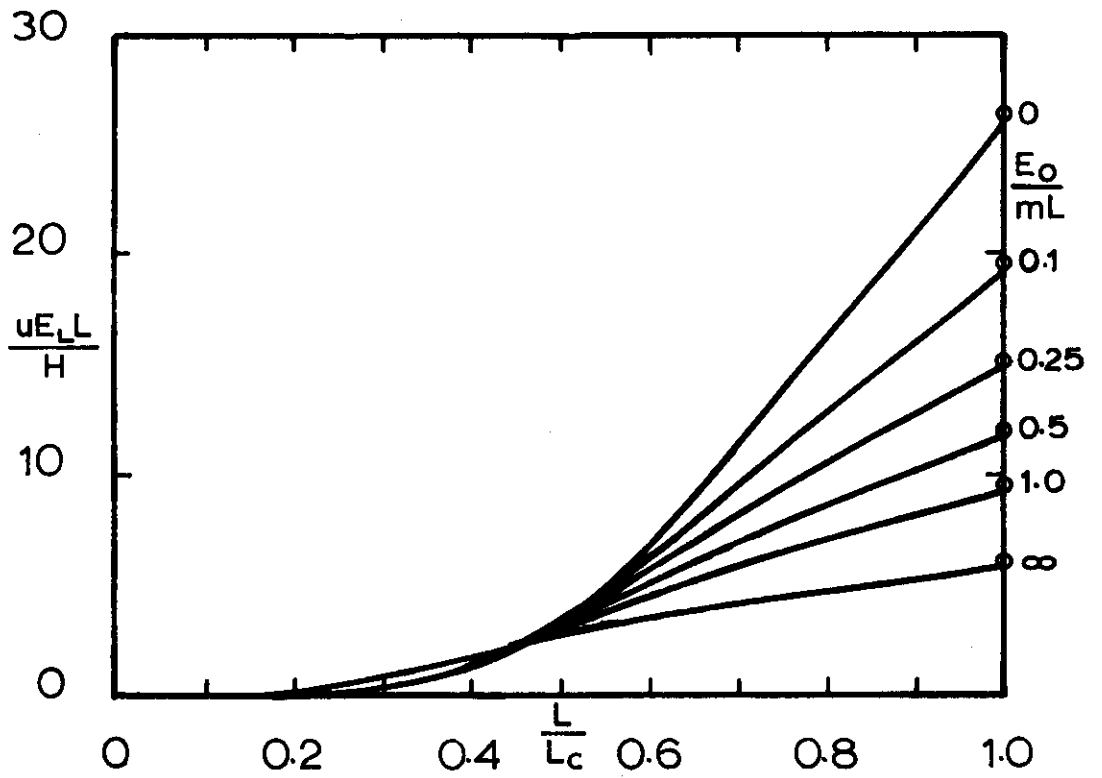


FIG. 4.2 RESULTS OF WINKLER PILE ANALYSIS: STANDARD FORM

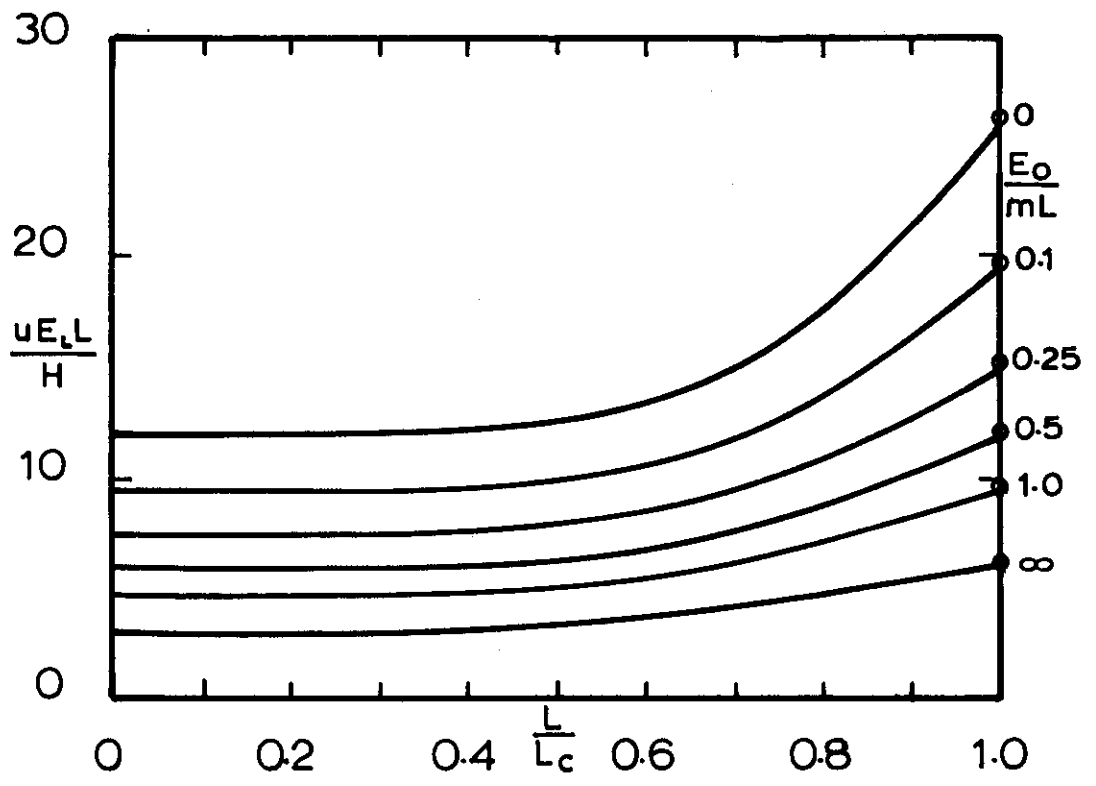


a) Free tip

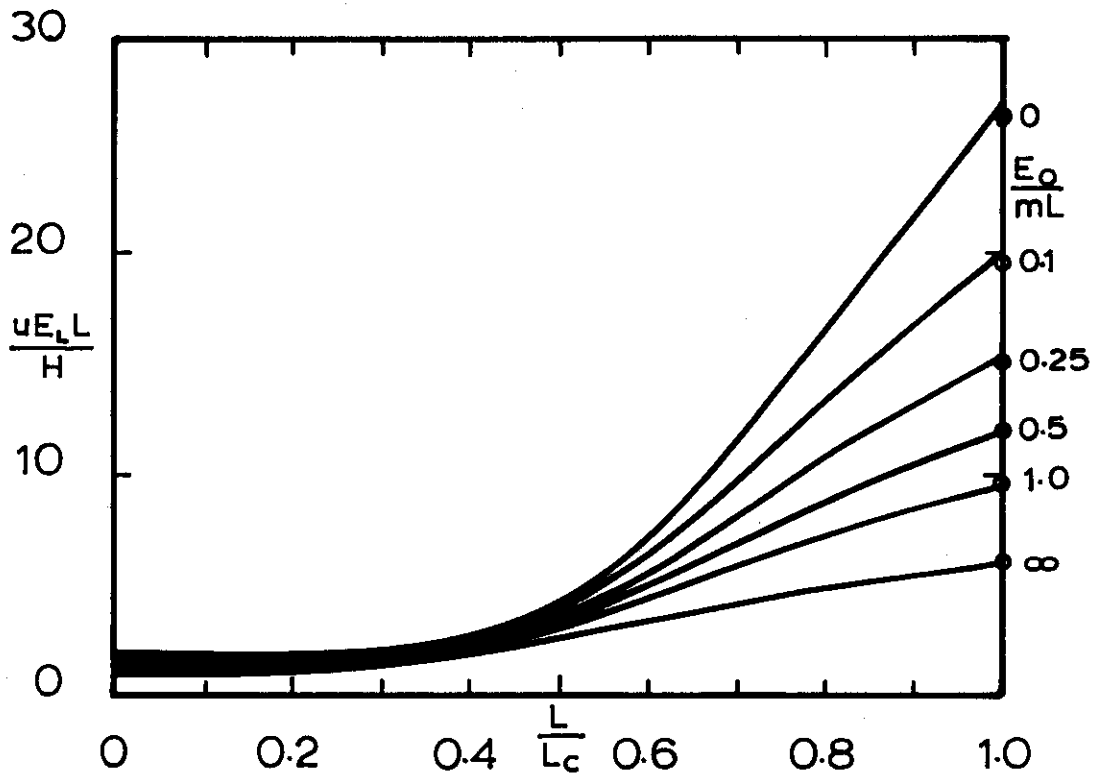


b) Socketed tip

FIG. 4.3 HEAD INFLUENCE COEFFICIENT FOR DEFLECTION DUE TO SHEAR: WINKLER SOIL.

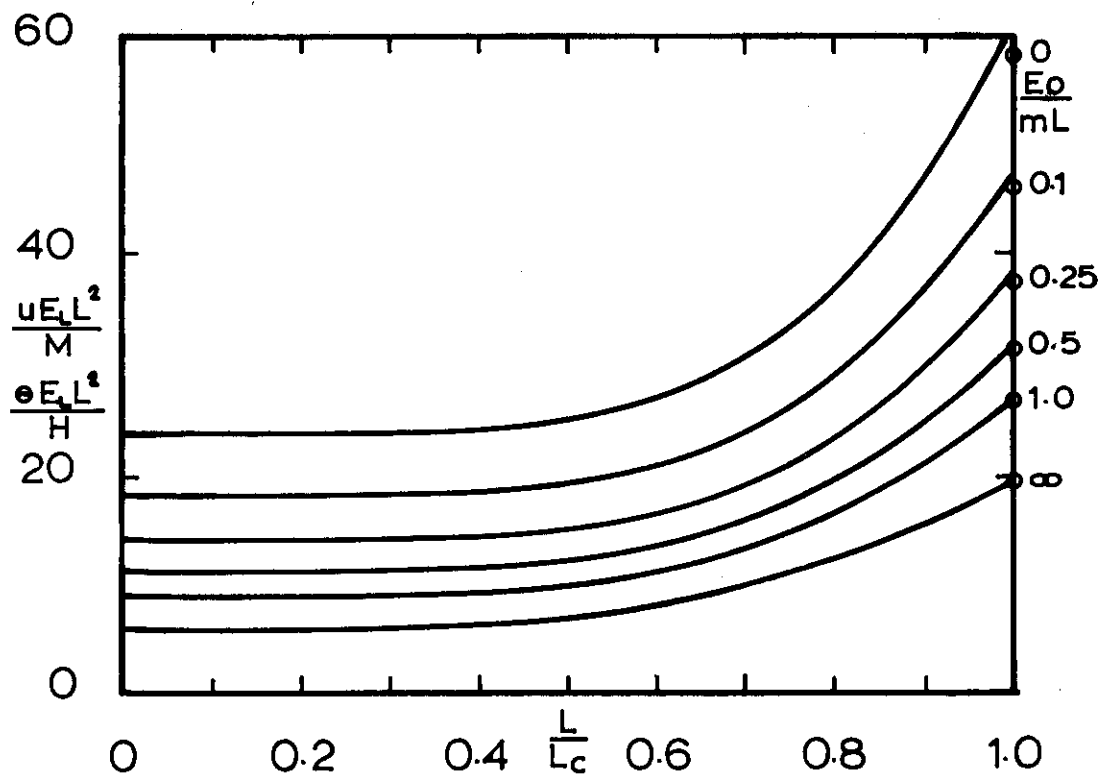


c) Pinned tip

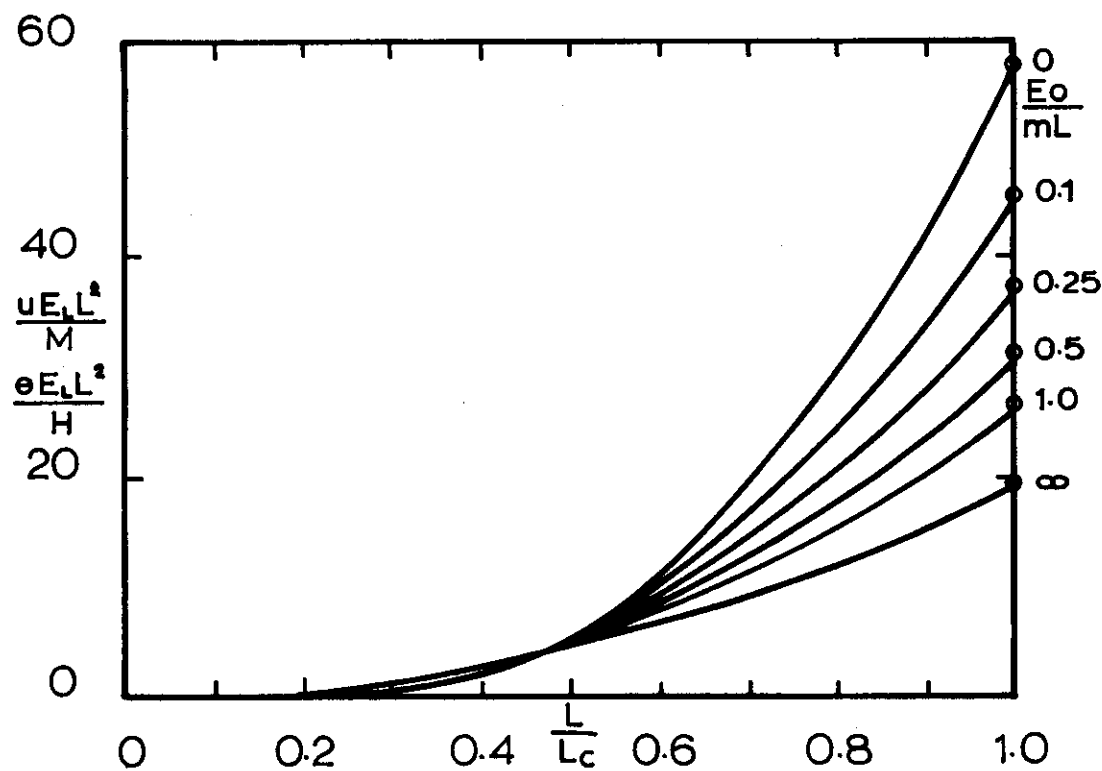


d) Fixed tip

FIG. 4.3 cont'd

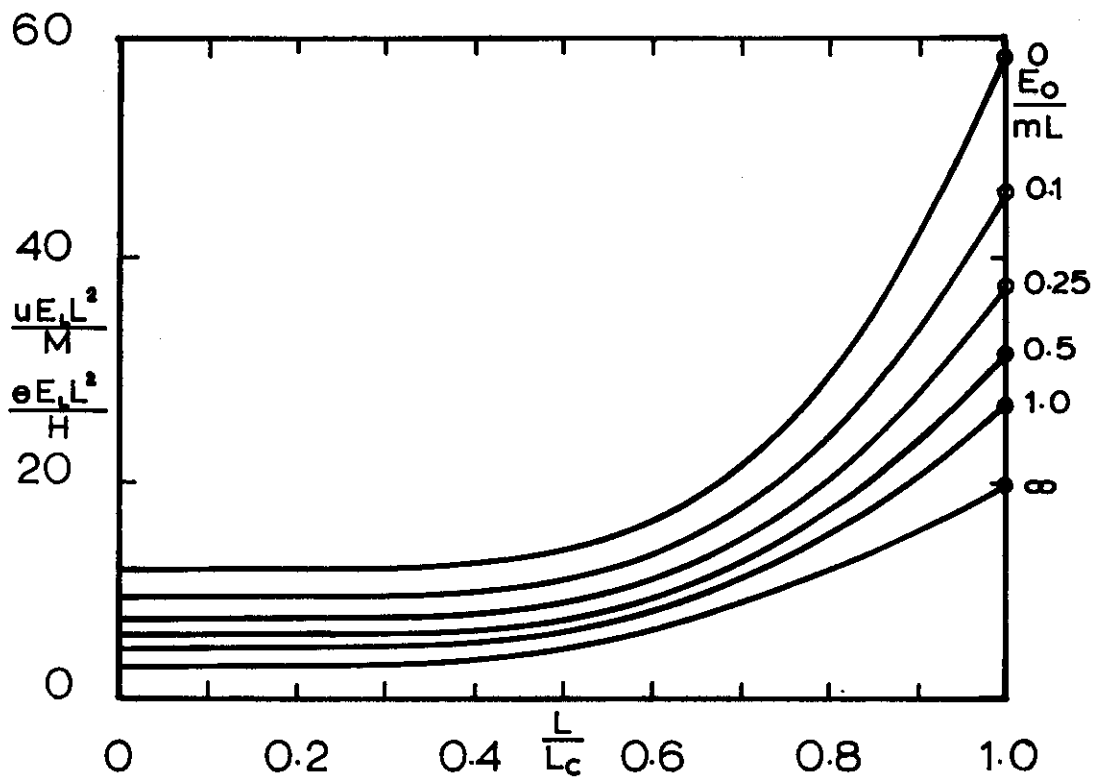


a) Free tip

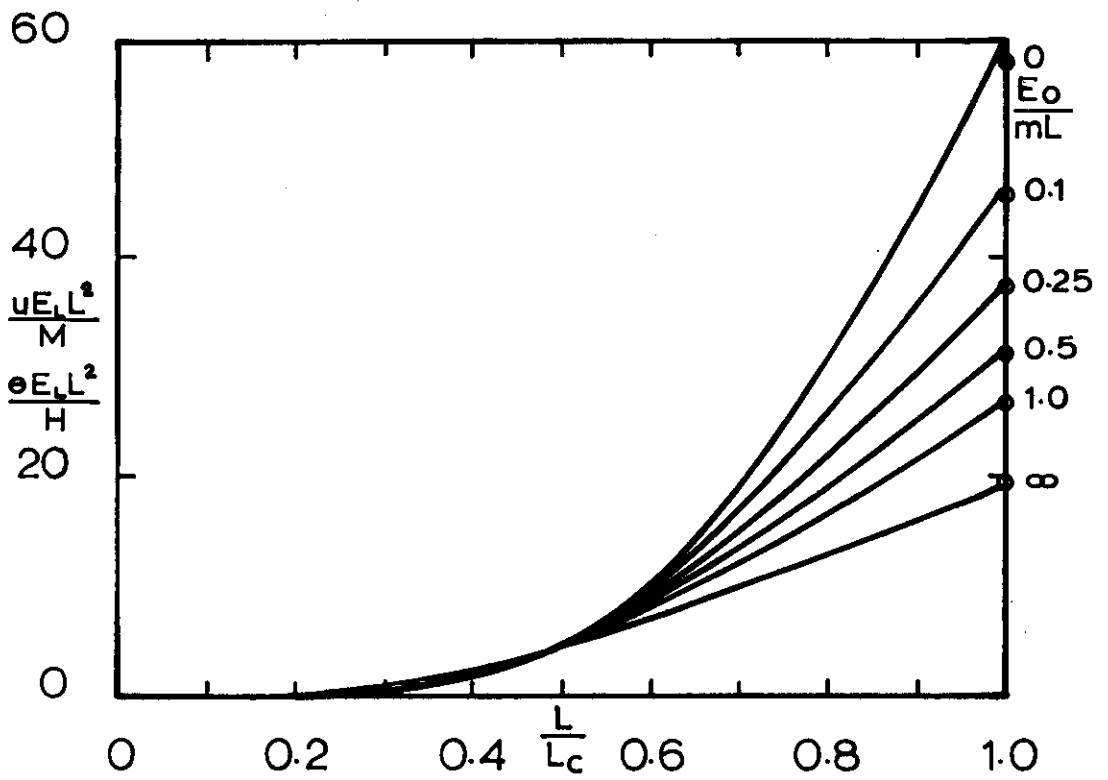


b) Socketed tip

FIG. 44 HEAD INFLUENCE COEFFICIENT FOR DEFLECTION DUE TO MOMENT AND ROTATION DUE TO SHEAR: WINKLER SOIL.

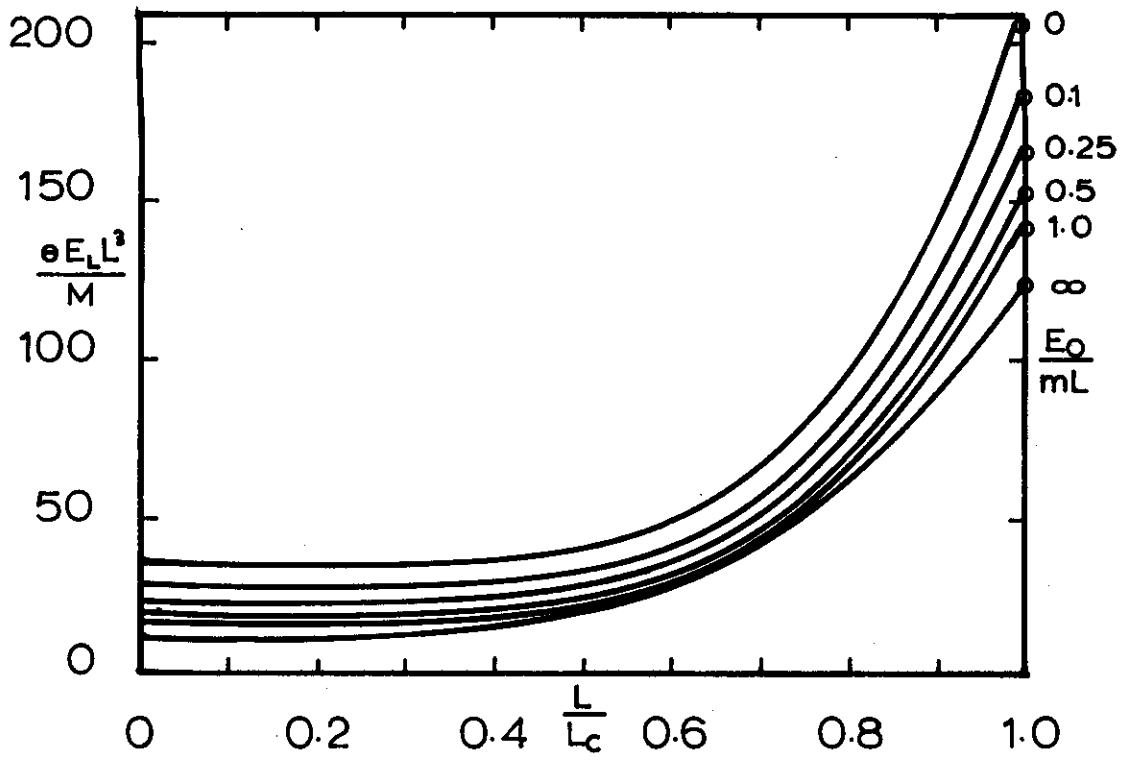


c) Pinned tip

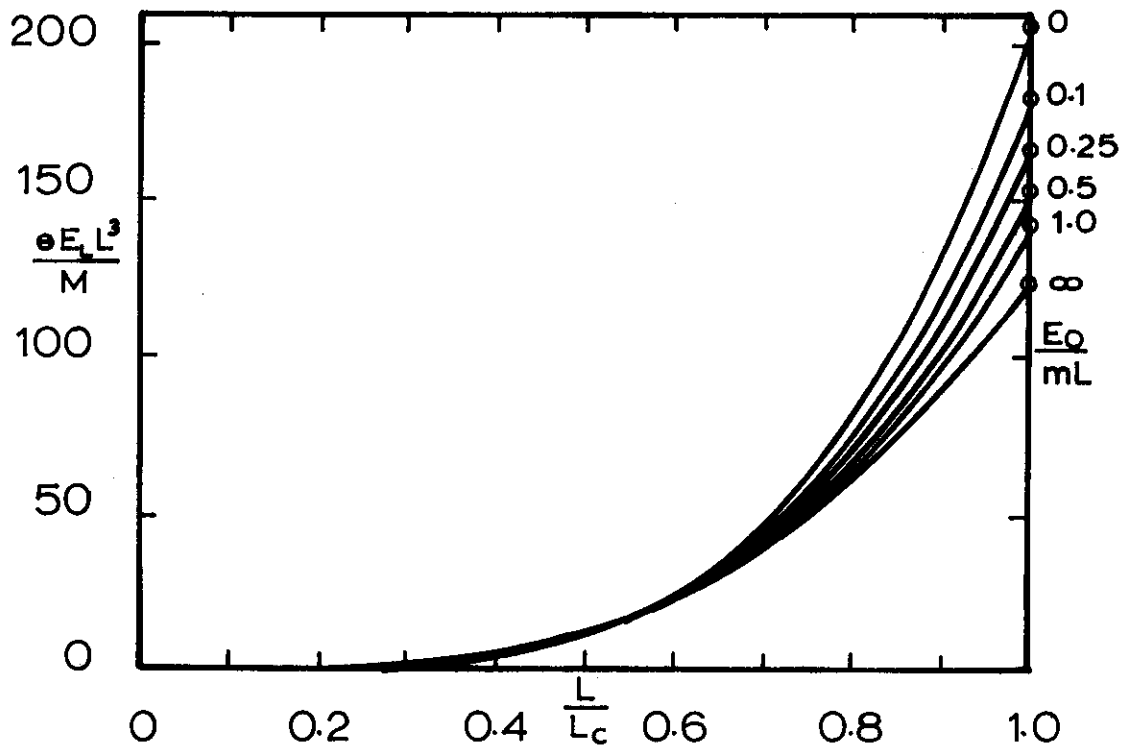


d) Fixed tip

FIG. 4.4 cont'd

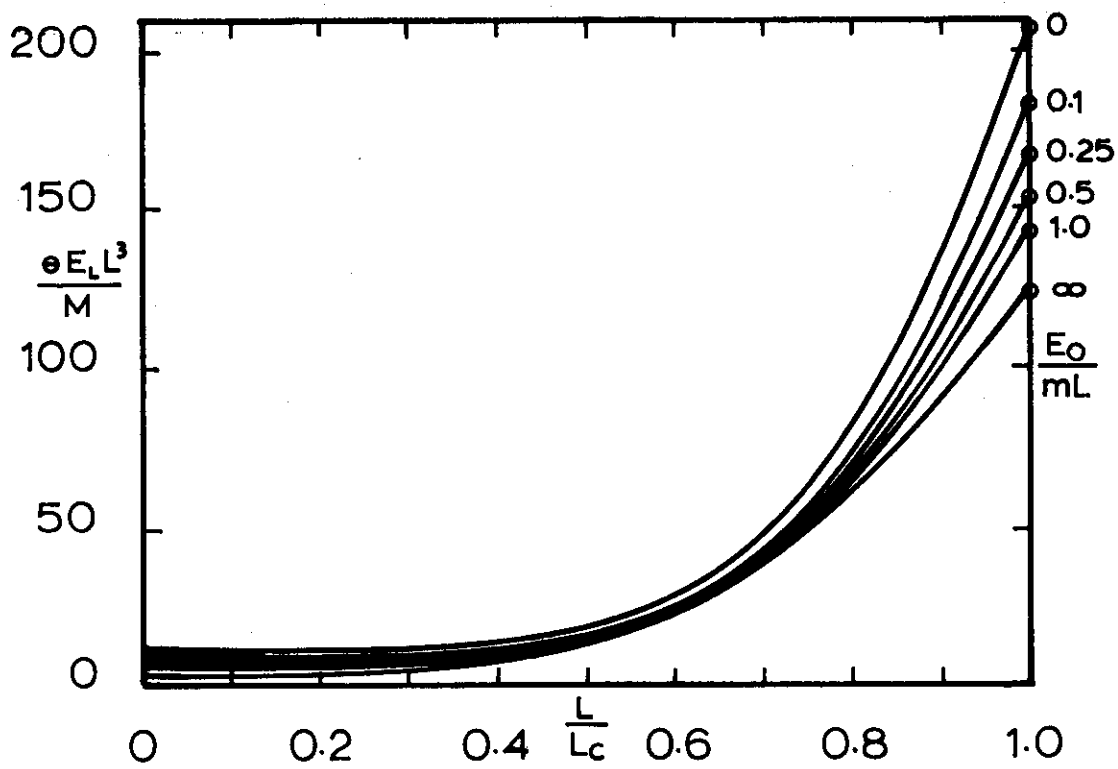


a) Free tip

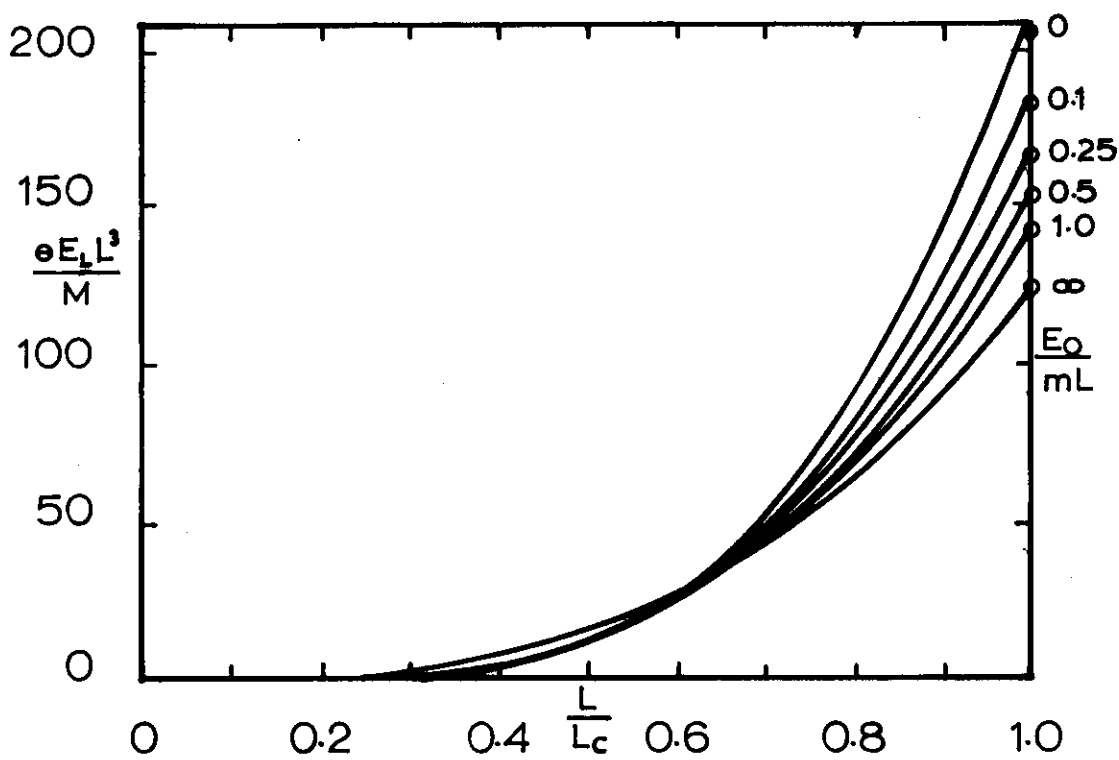


b) Socketed tip

FIG. 4.5 HEAD INFLUENCE COEFFICIENT FOR ROTATION DUE TO MOMENT: WINKLER SOIL.

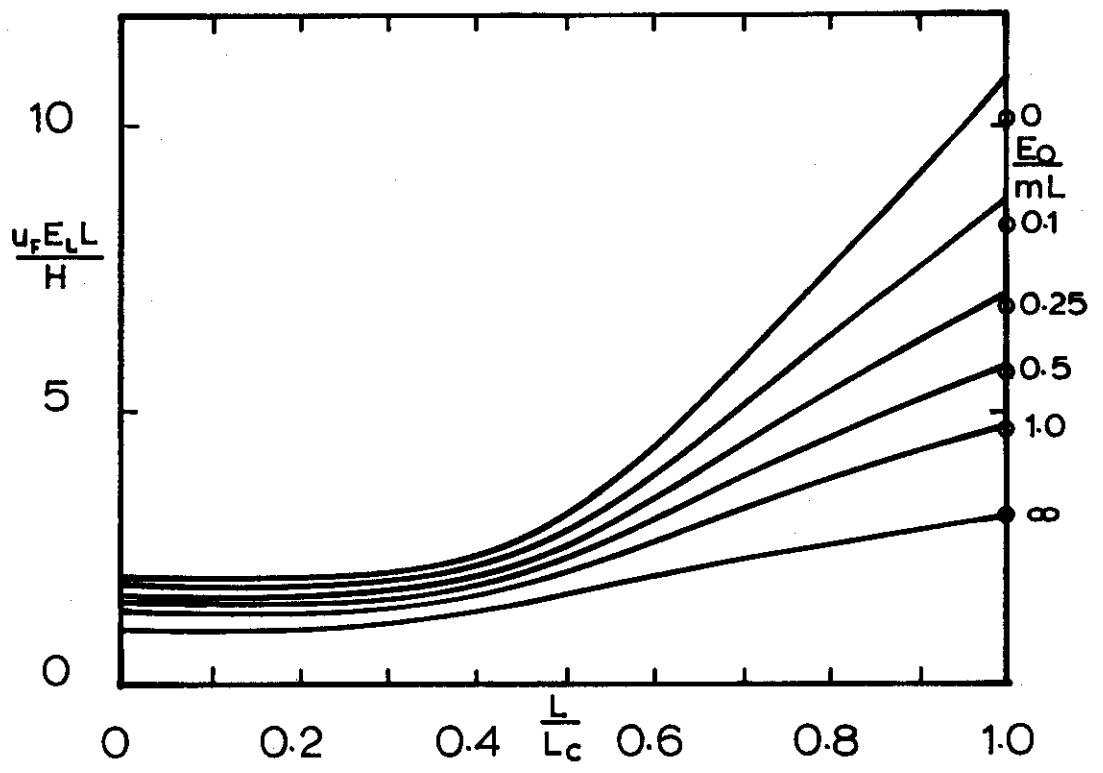


c) Pinned tip

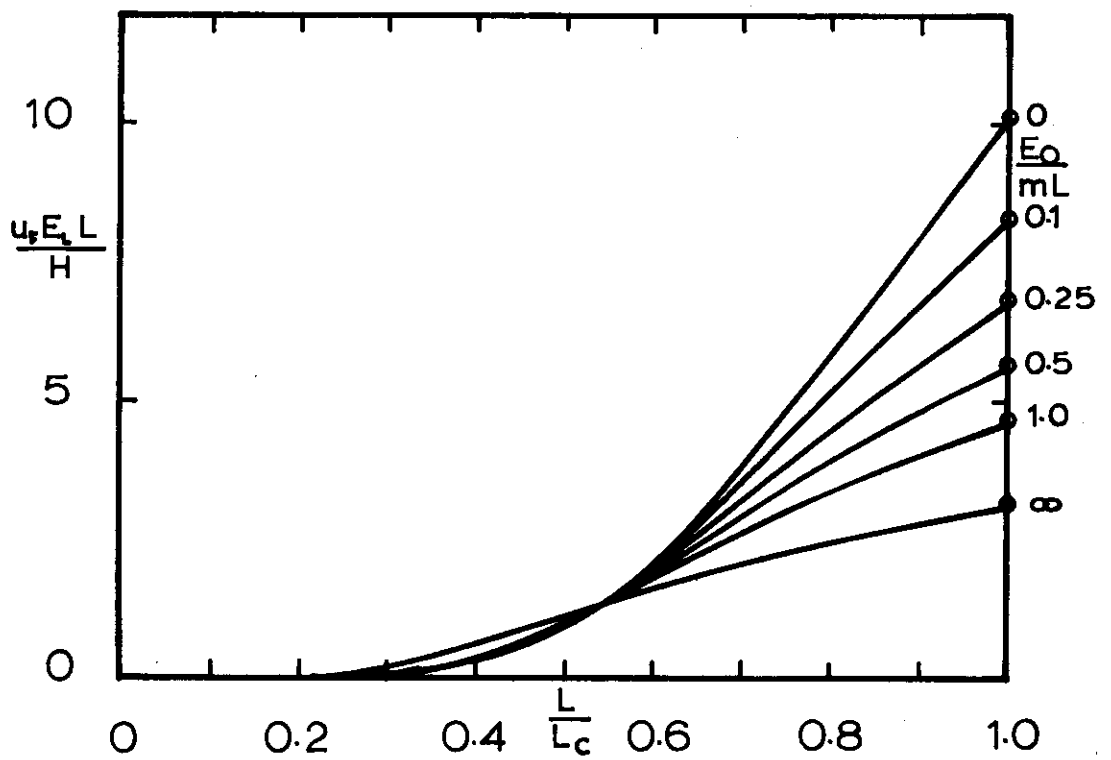


d) Fixed tip

FIG. 4.5 cont'd



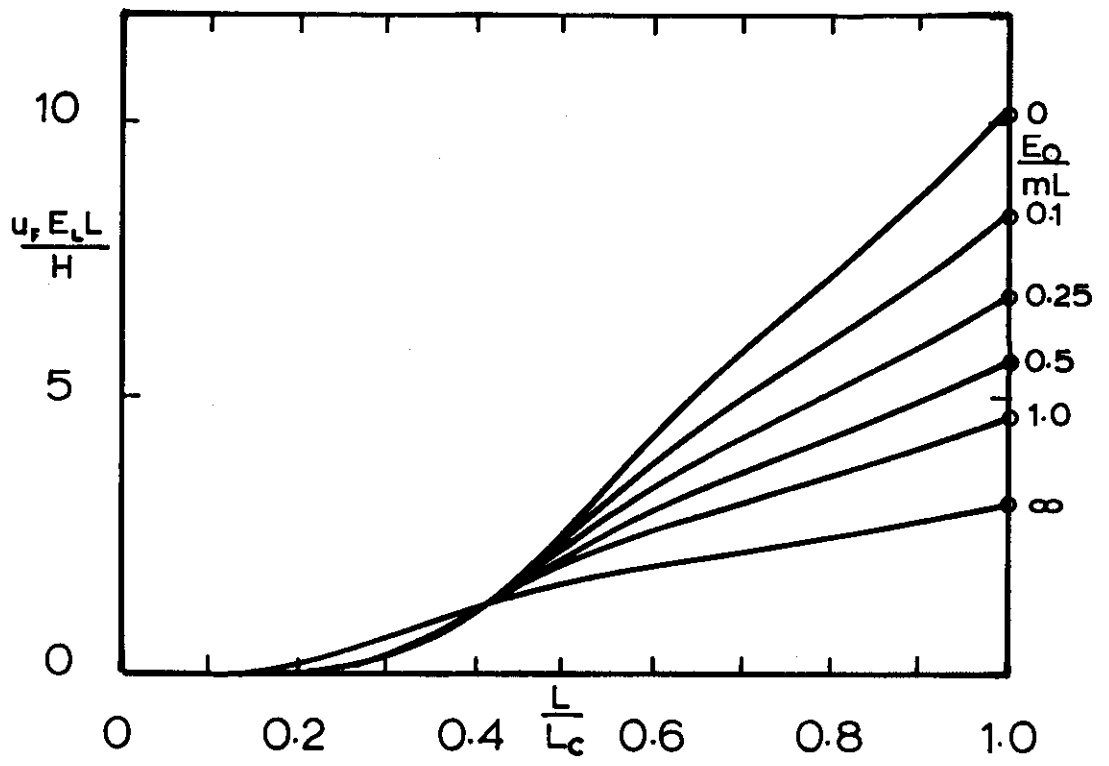
a) Free tip



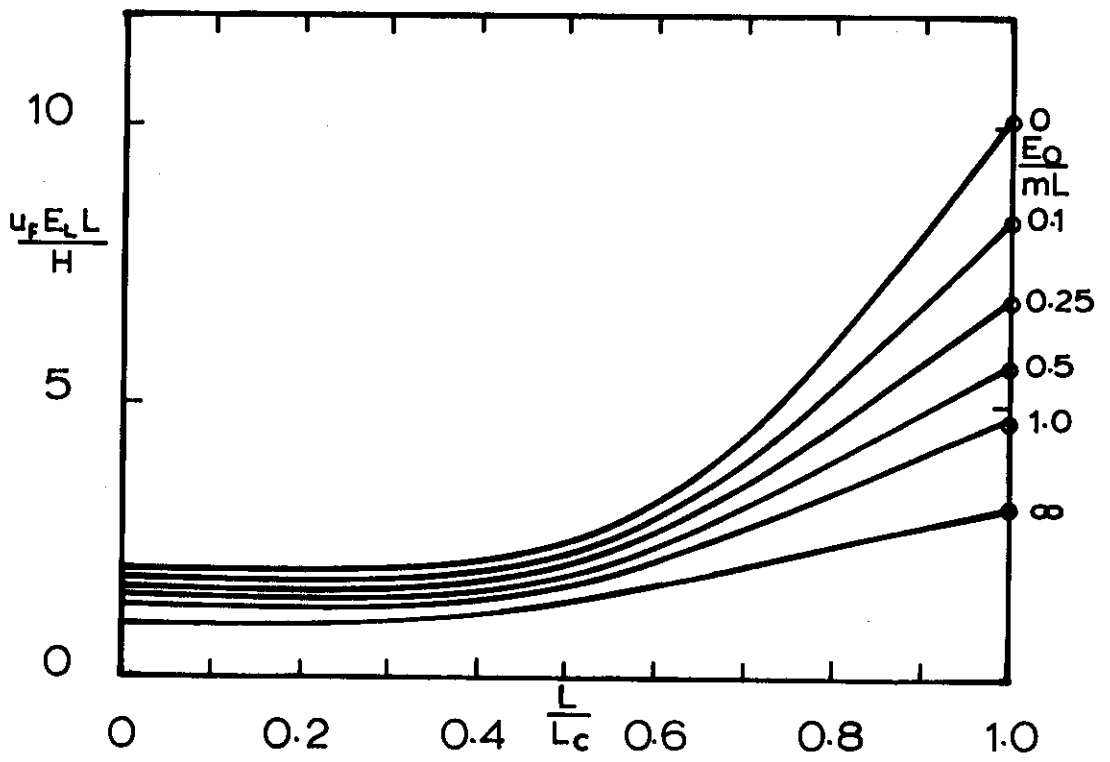
b) Socketed tip

FIG. 4.6 HEAD INFLUENCE COEFFICIENT FOR DEFLECTION DUE TO SHEAR: FIXED HEAD:

WINKLER SOIL.



c) Pinned tip



d) Fixed tip

FIG. 4.6 cont'd

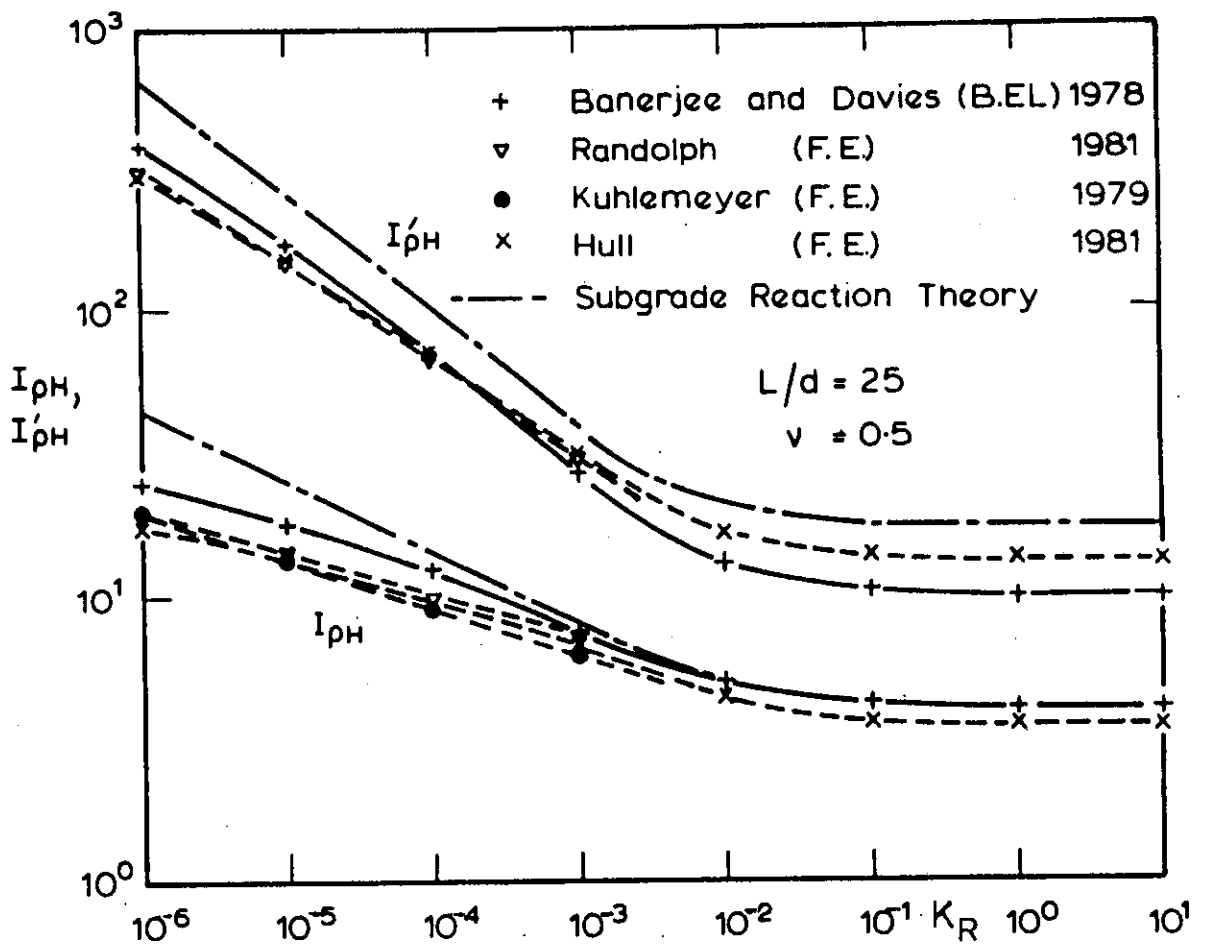


FIG.4.7 COMPARISON BETWEEN VARIOUS LINEAR SOLUTIONS

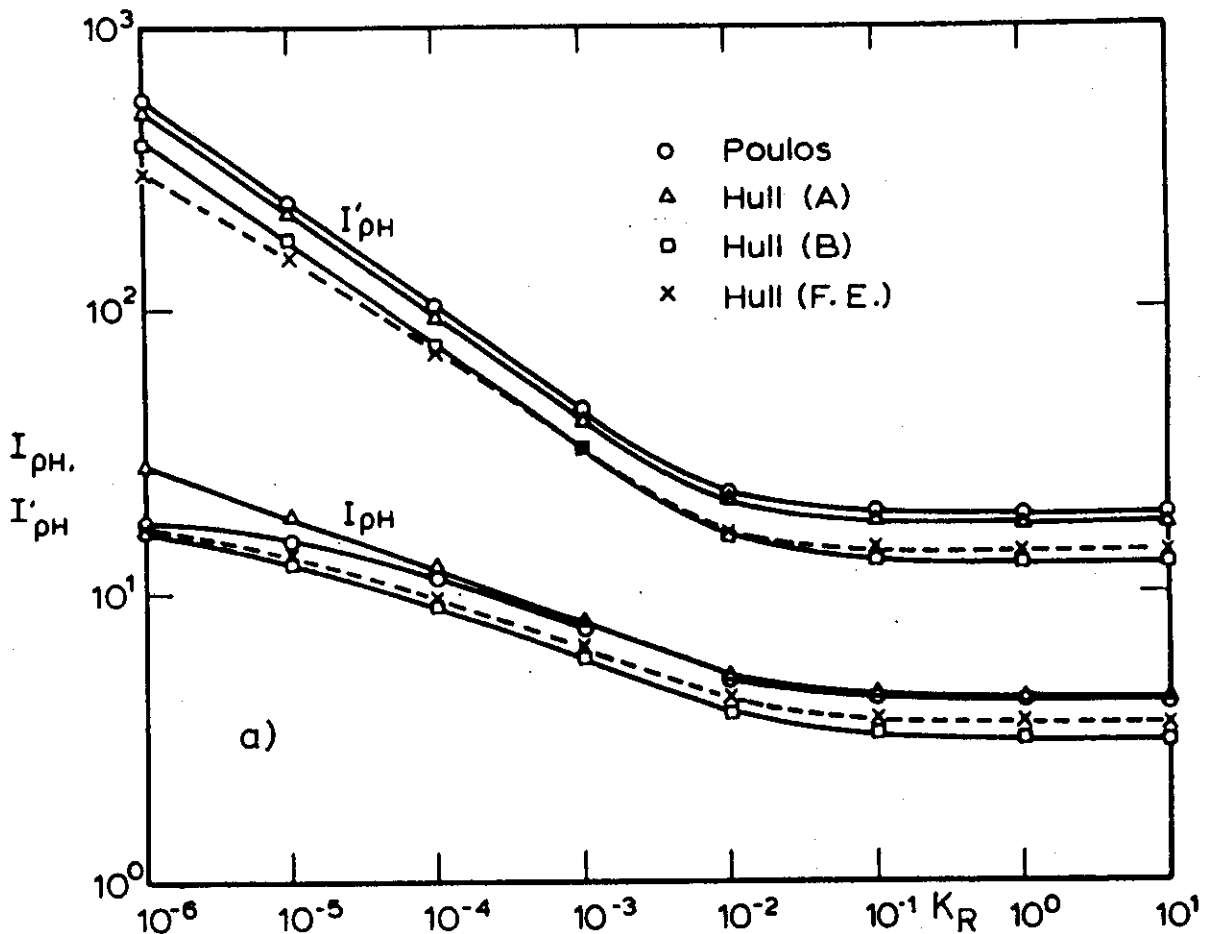


FIG. 4.8 SOLUTION FOR PILE HEAD DEFLECTION AND ROTATION

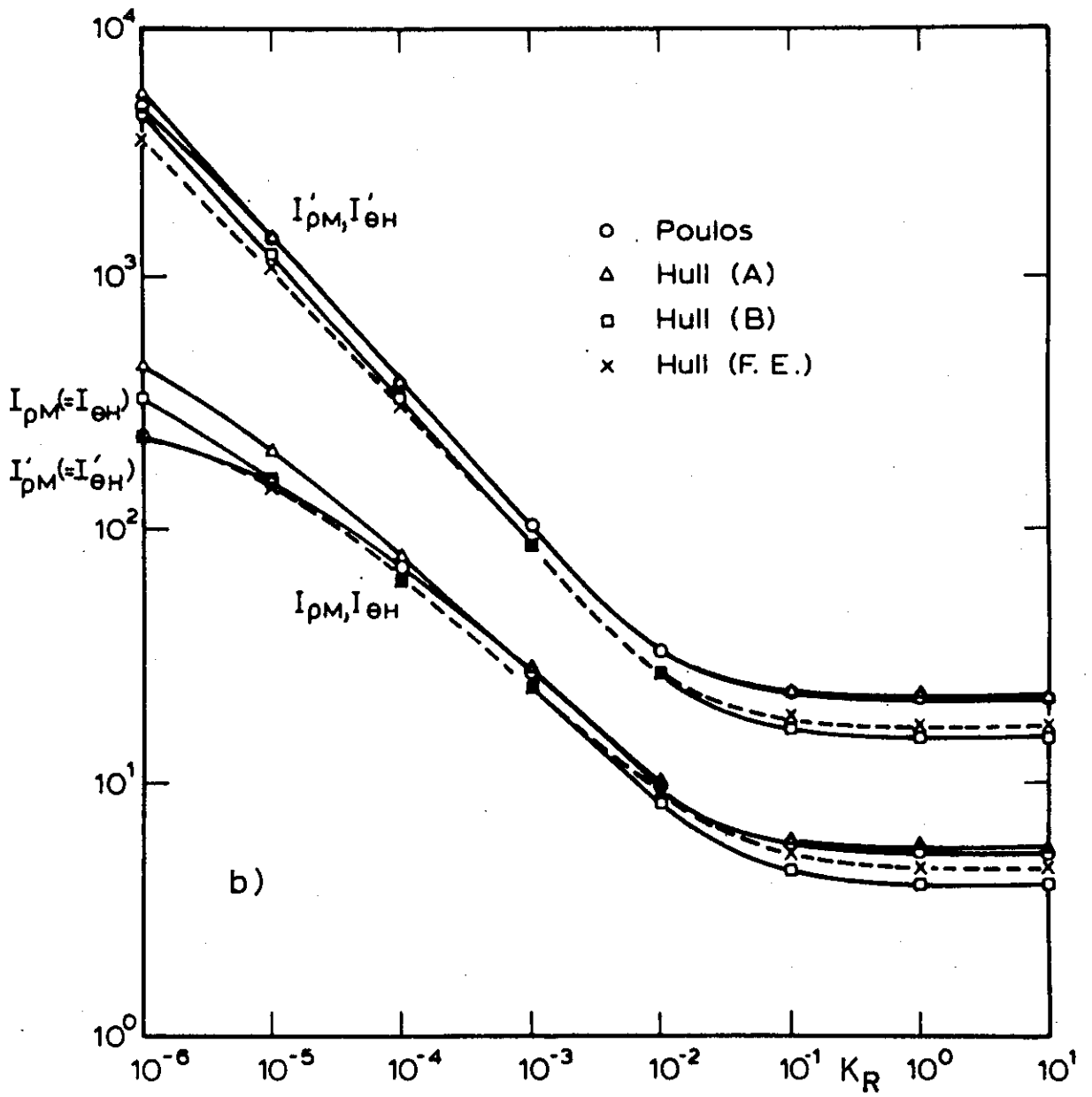
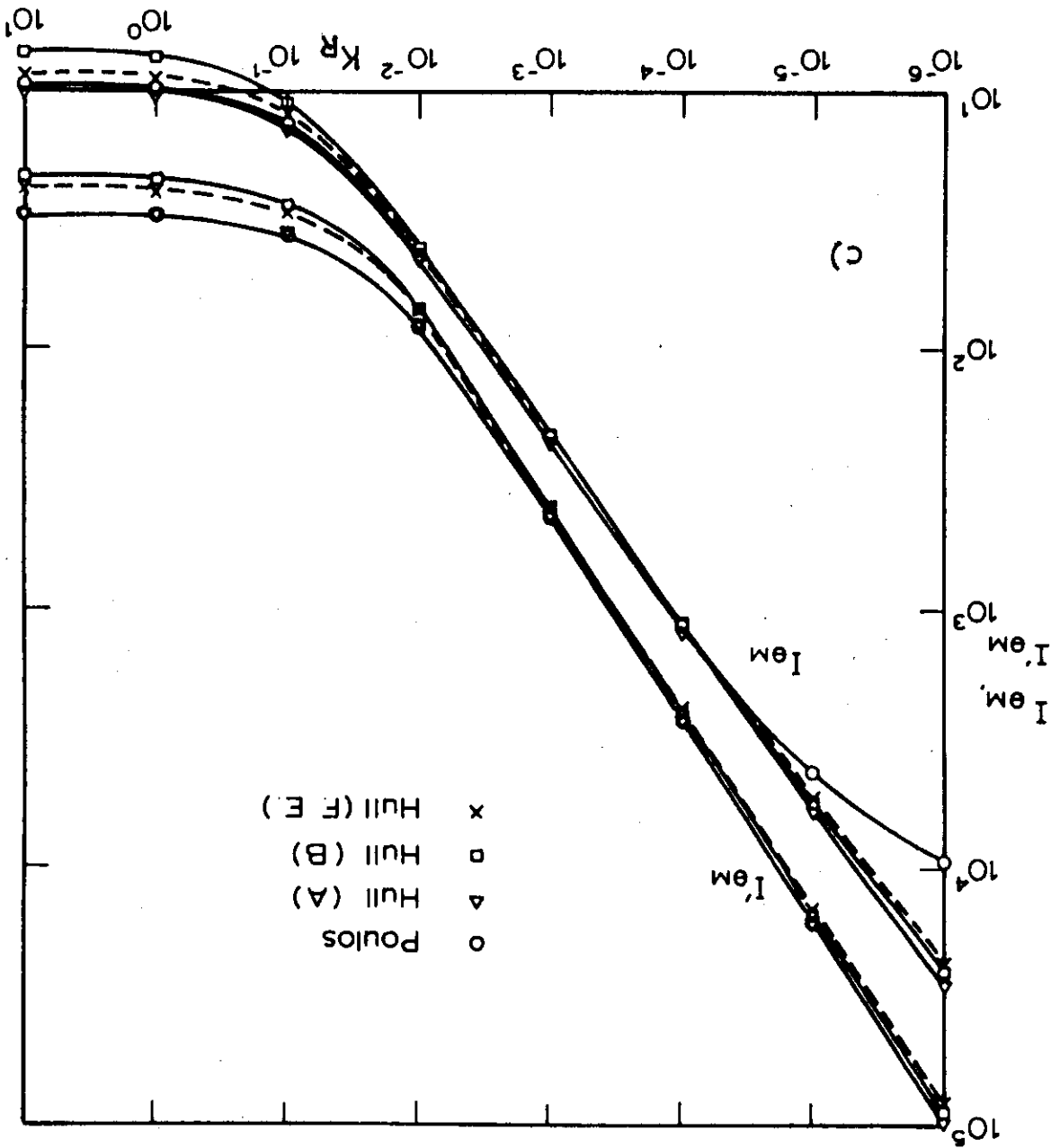
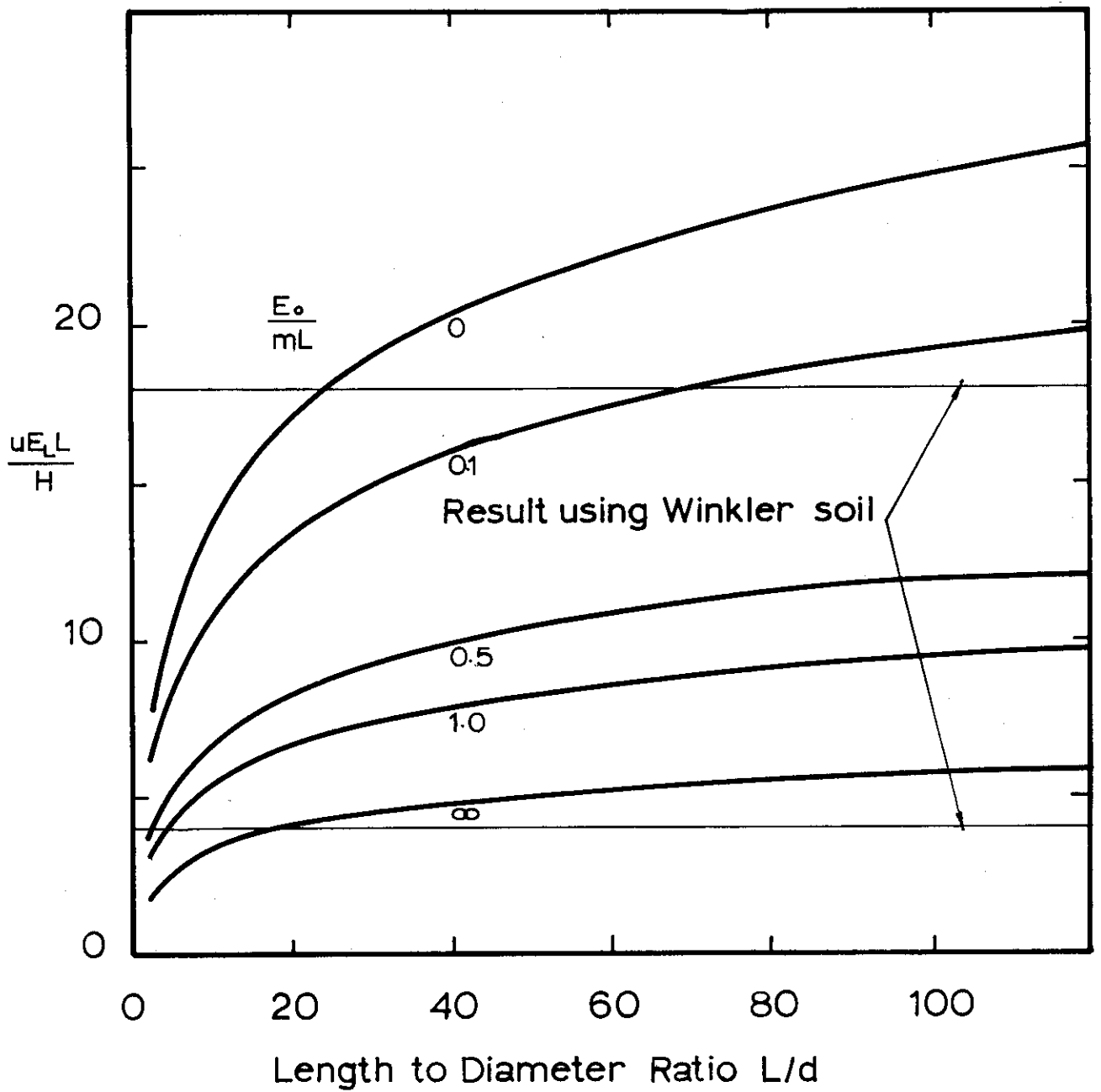


FIG. 4.8 continued

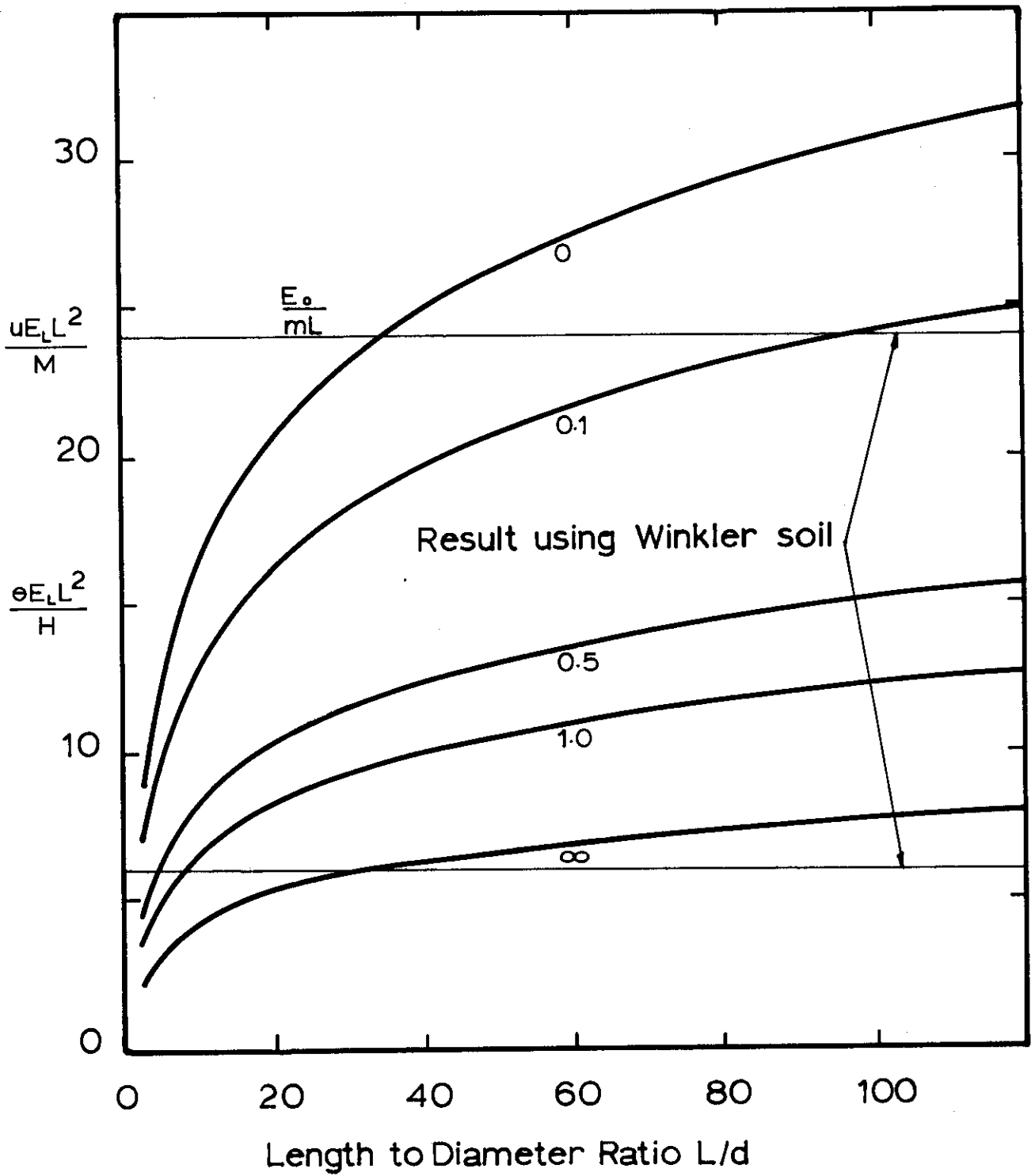
FIG. 4.8 continued





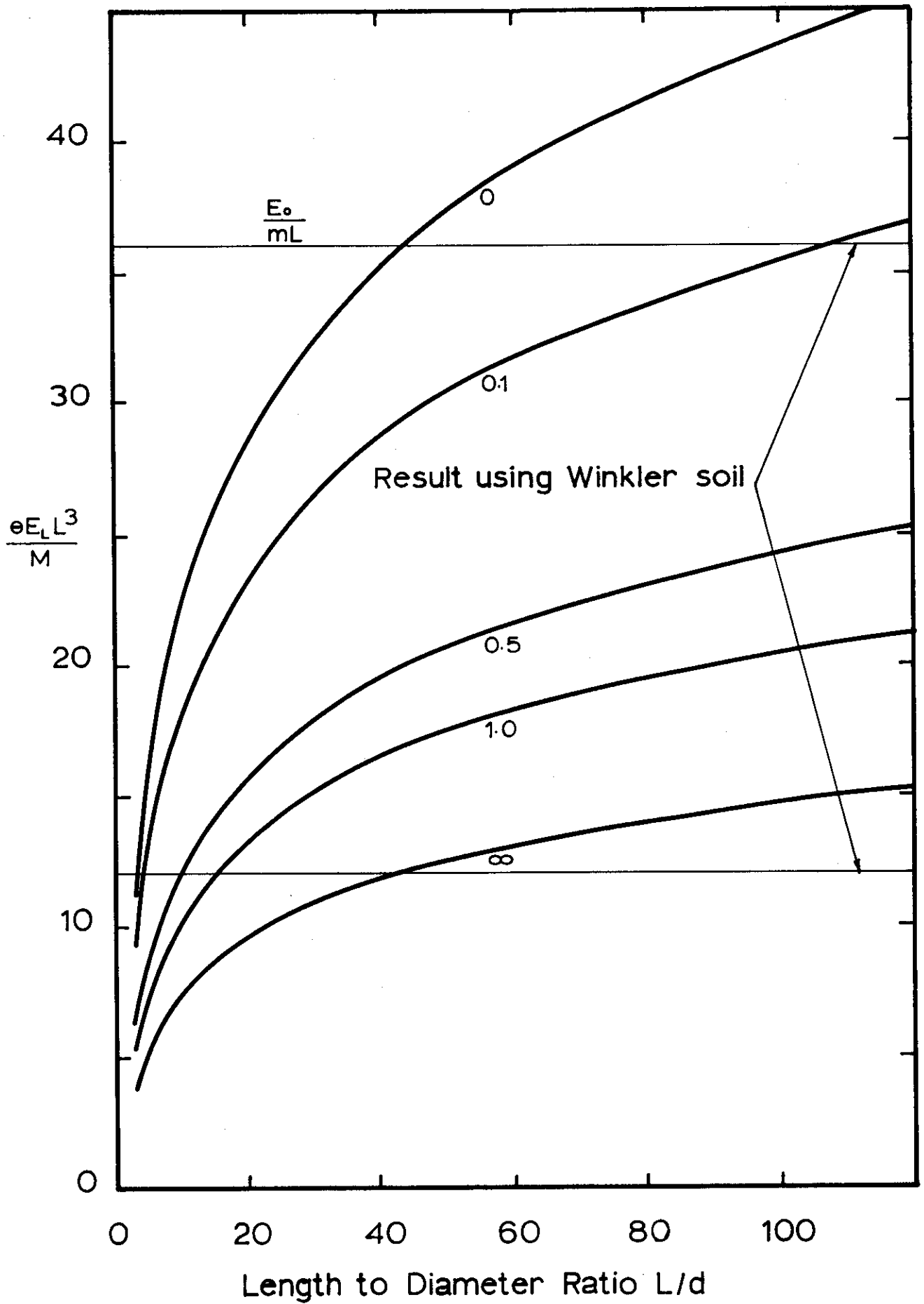
a) RIGID PILE INFLUENCE COEFFICIENT FOR DEFLECTION DUE TO SHEAR

FIG 4.9 MODIFIED BOUNDARY ELEMENT RESULTS: HEAD RESPONSE

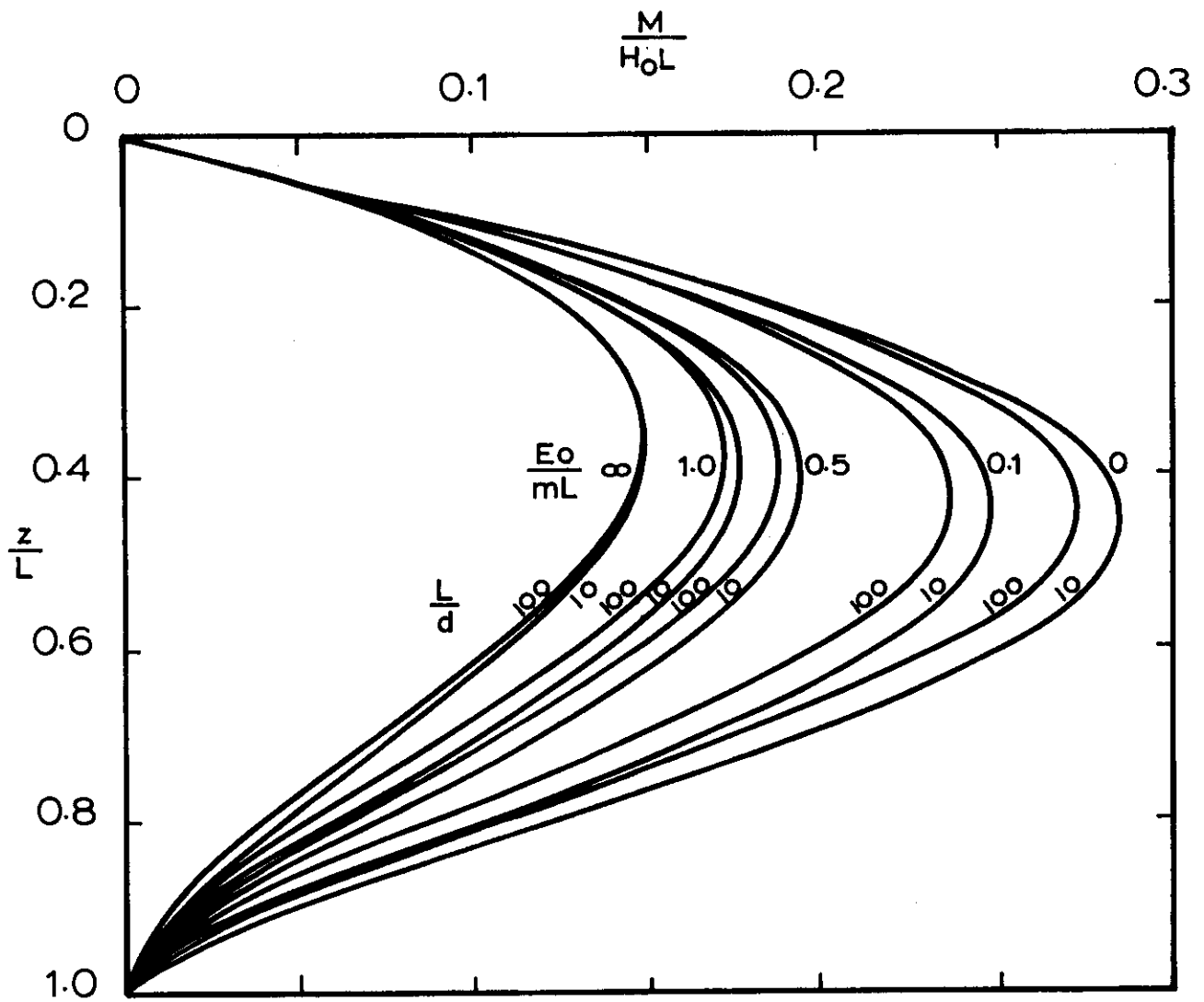


b) RIGID PILE INFLUENCE COEFFICIENT FOR DEFLECTION DUE TO MOMENT AND ROTATION DUE TO SHEAR

FIG 4.9 CONTINUED

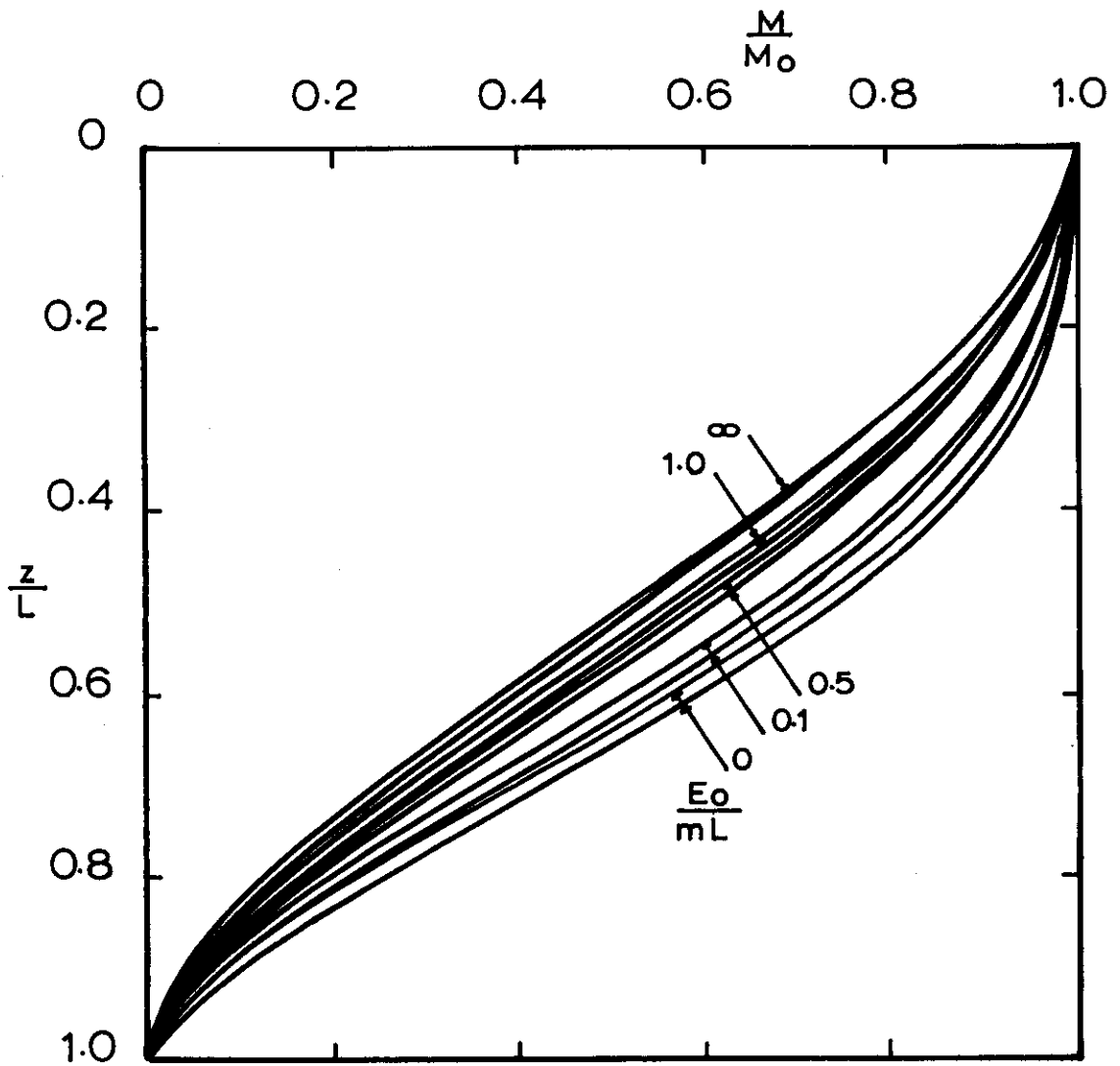


c) RIGID PILE HEAD INFLUENCE COEFFICIENT FOR ROTATION DUE TO MOMENT



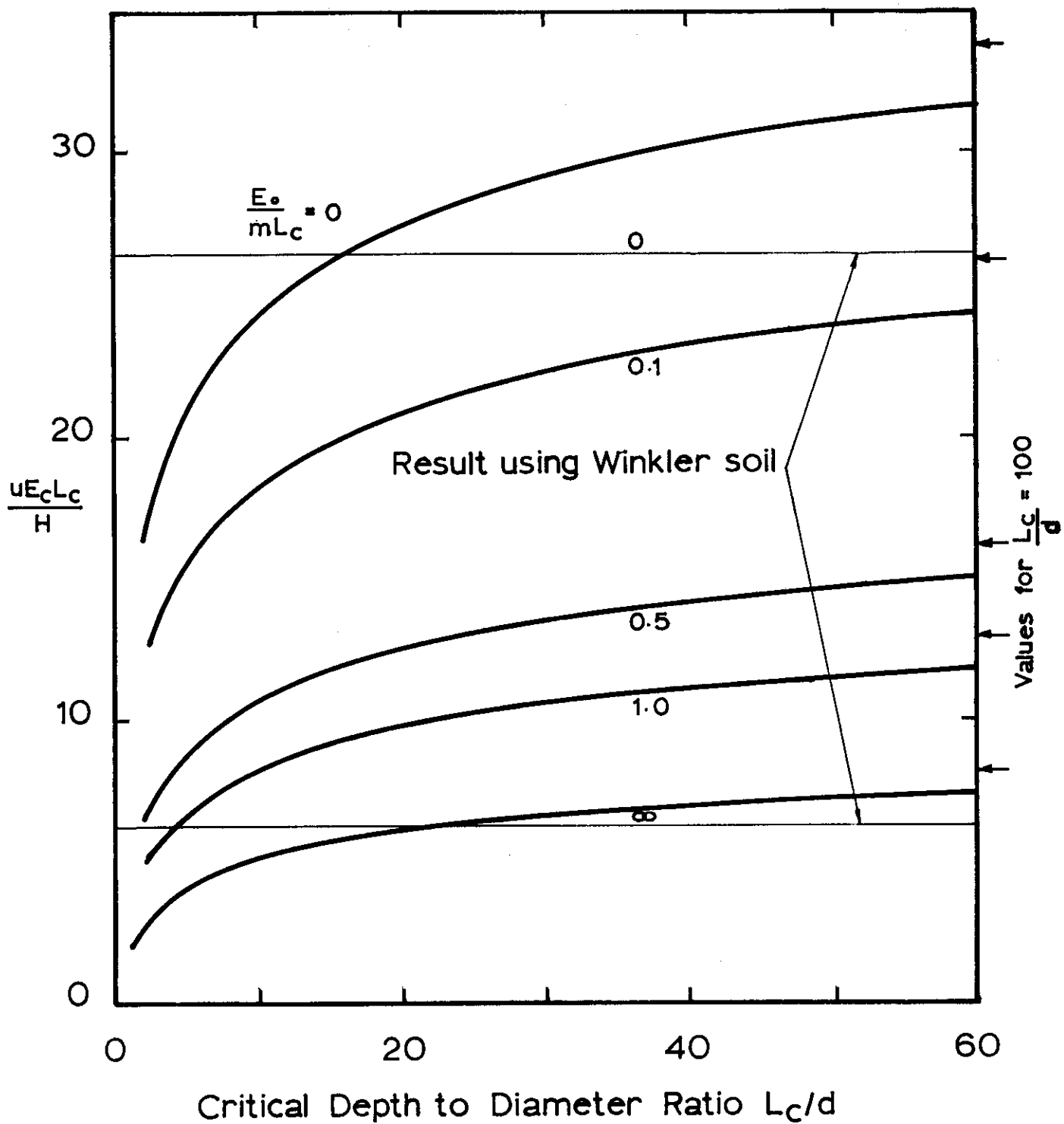
a) RIGID PILE INFLUENCE COEFFICIENT FOR
MOMENT DUE TO HEAD SHEAR

FIG 4.10 MODIFIED BOUNDARY ELEMENT RESULTS:
BENDING MOMENT DISTRIBUTIONS



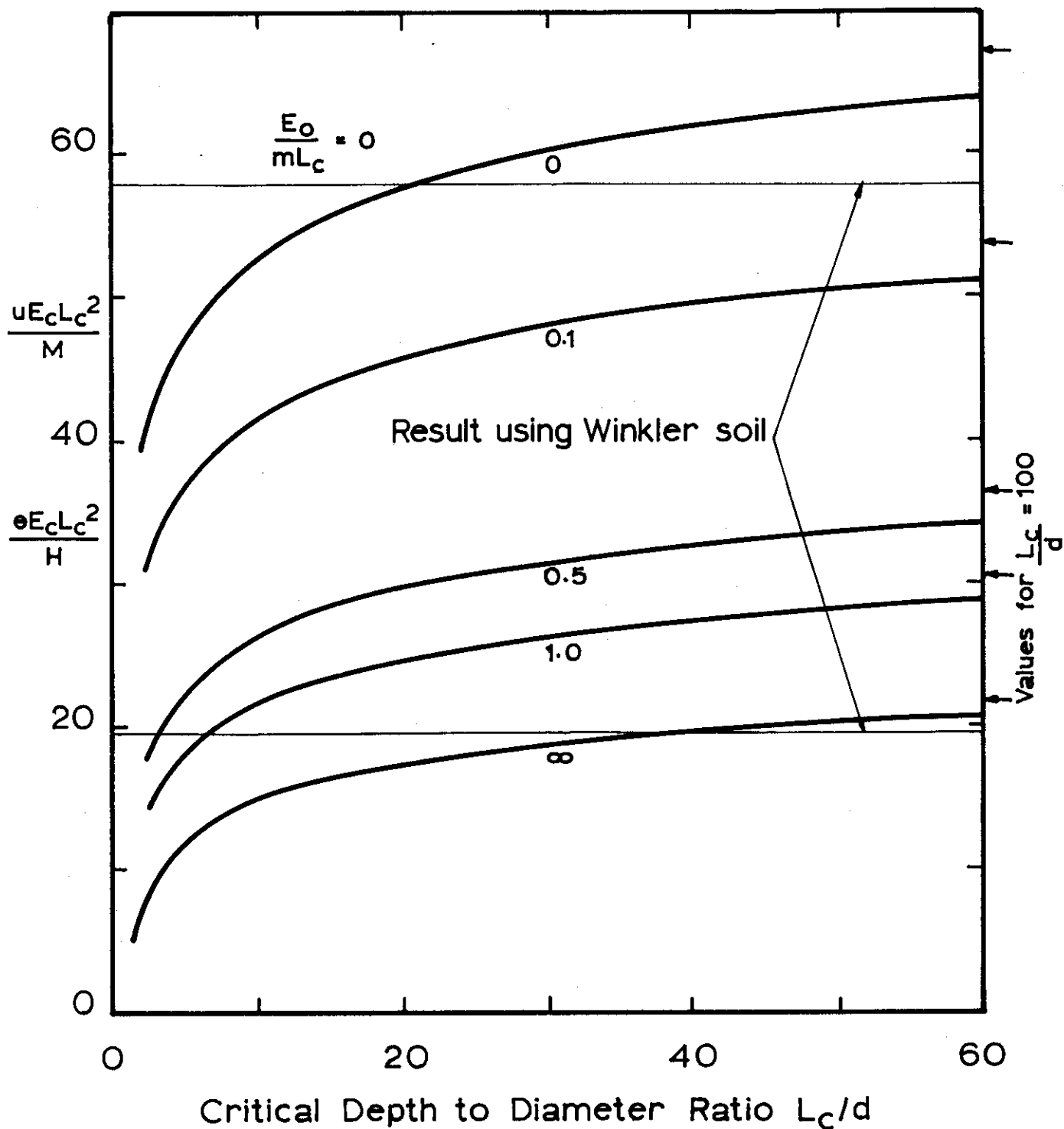
b) RIGID PILE INFLUENCE COEFFICIENT FOR
MOMENT DUE TO HEAD MOMENT

FIG 4.10 CONTINUED



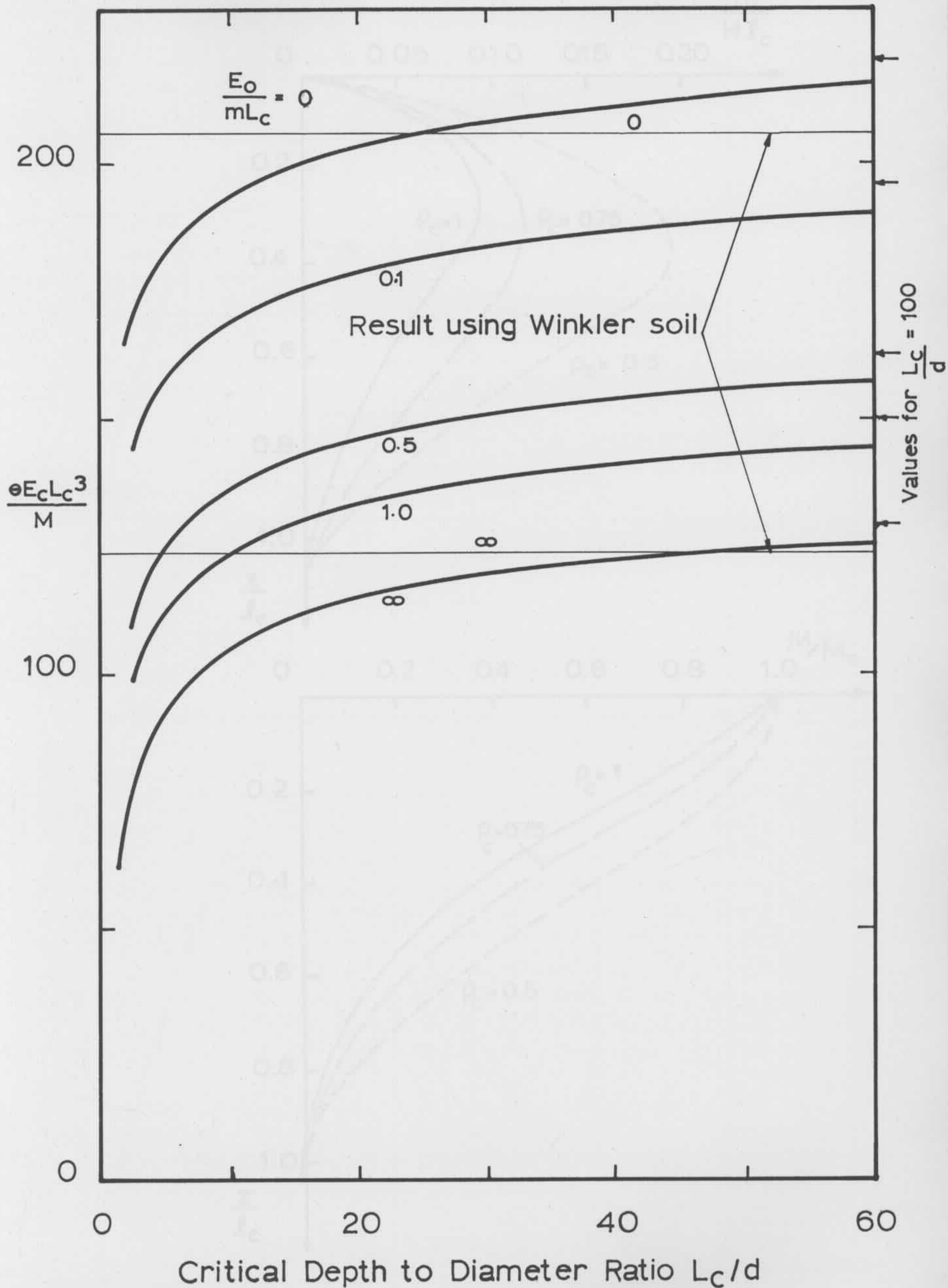
a) FLEXIBLE PILE HEAD INFLUENCE COEFFICIENT FOR DEFLECTION DUE TO SHEAR

FIG 4.11 MODIFIED BOUNDARY ELEMENT RESULTS:
HEAD RESPONSE



b) FLEXIBLE PILE HEAD INFLUENCE COEFFICIENT FOR DEFLECTION DUE TO MOMENT AND ROTATION DUE TO SHEAR

FIG 4.11 CONTINUED



c) FLEXIBLE PILE HEAD INFLUENCE COEFFICIENT FOR ROTATION DUE TO MOMENT
 FIG 4.11 CONTINUED

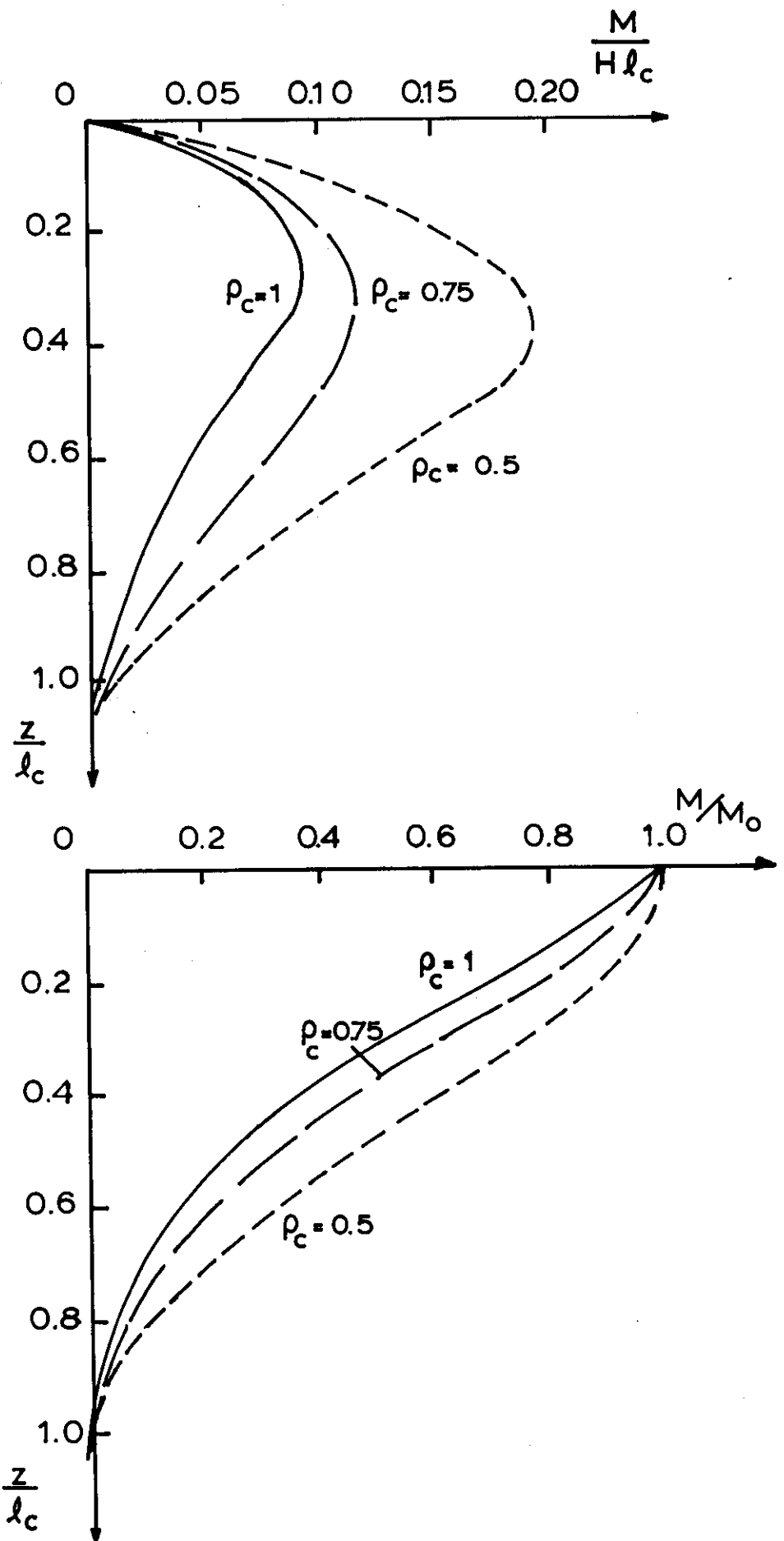


FIG. 4.12 INDUCED BENDING MOMENTS (RANDOLPH, 1977)

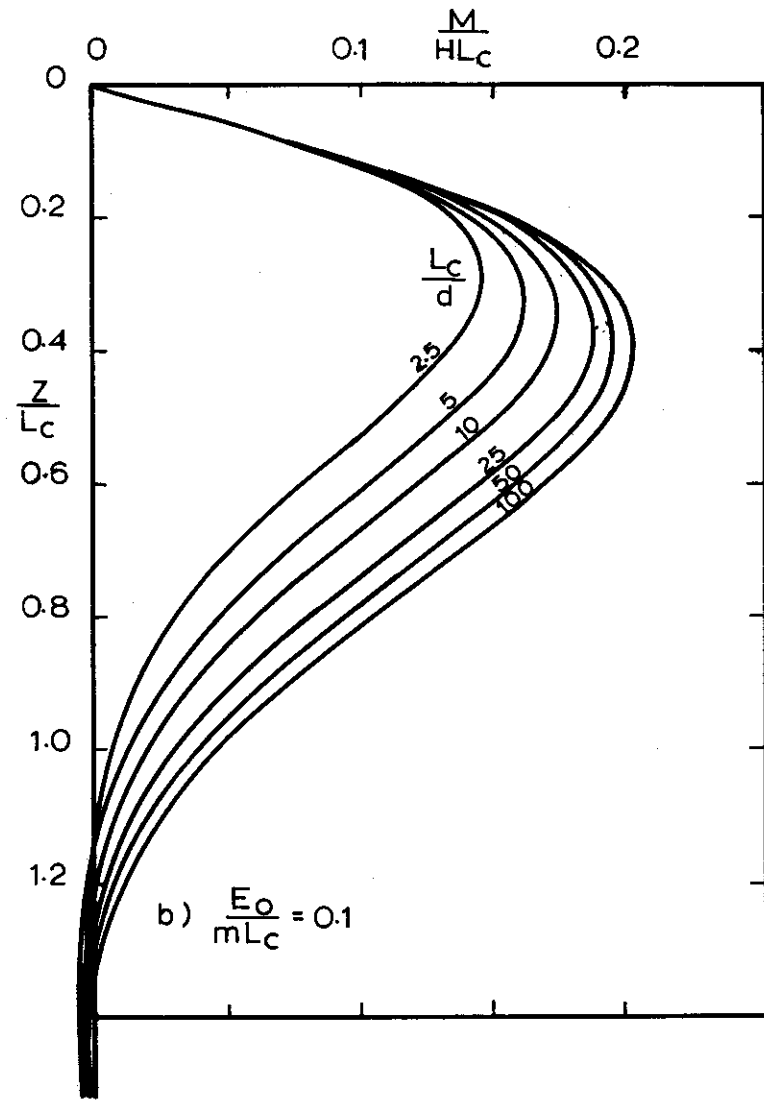
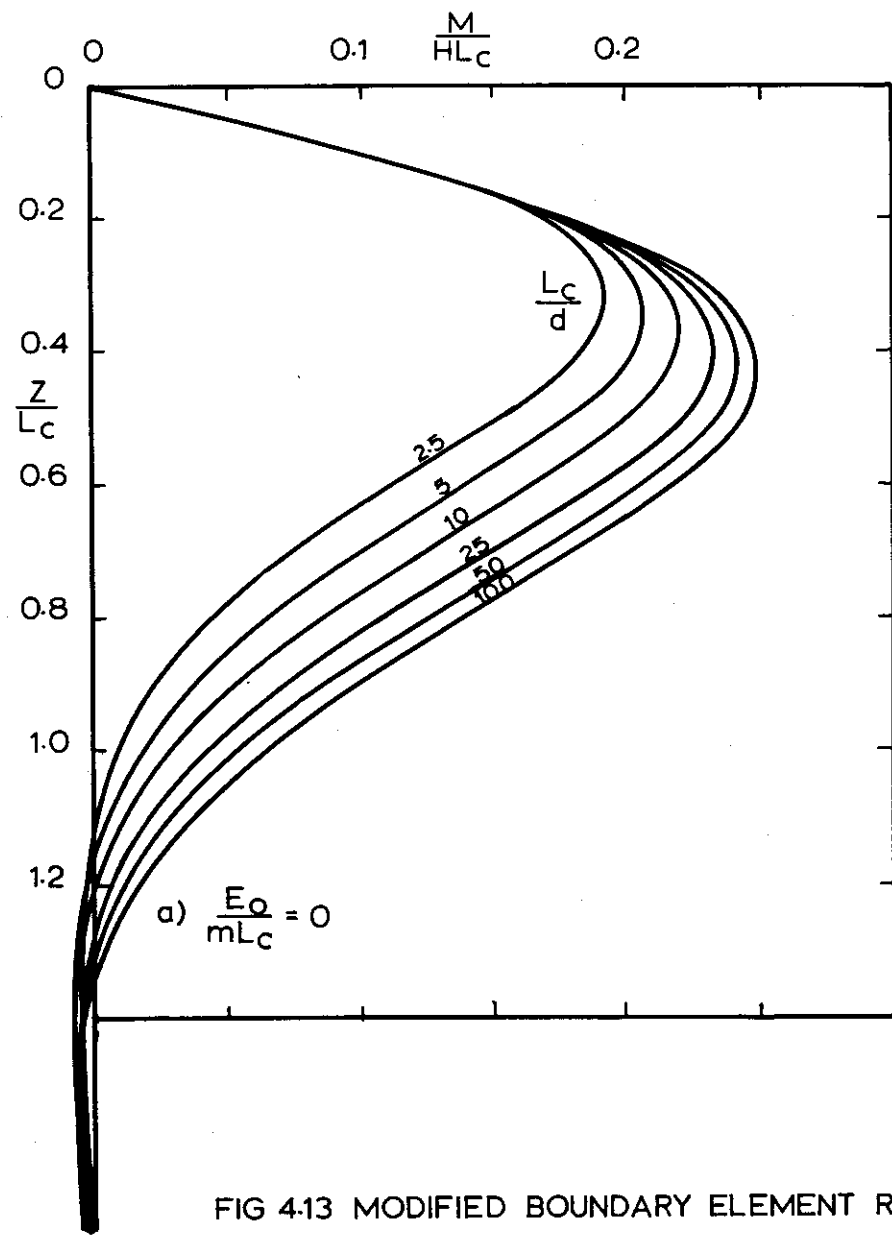


FIG 4.13 MODIFIED BOUNDARY ELEMENT RESULTS: BENDING MOMENT DUE TO HEAD SHEAR

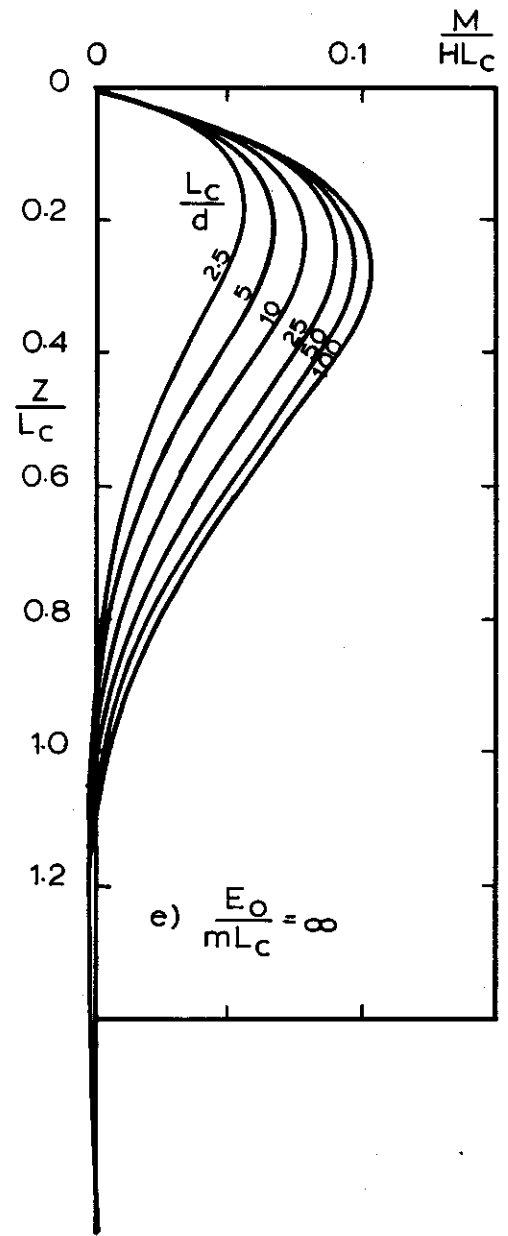
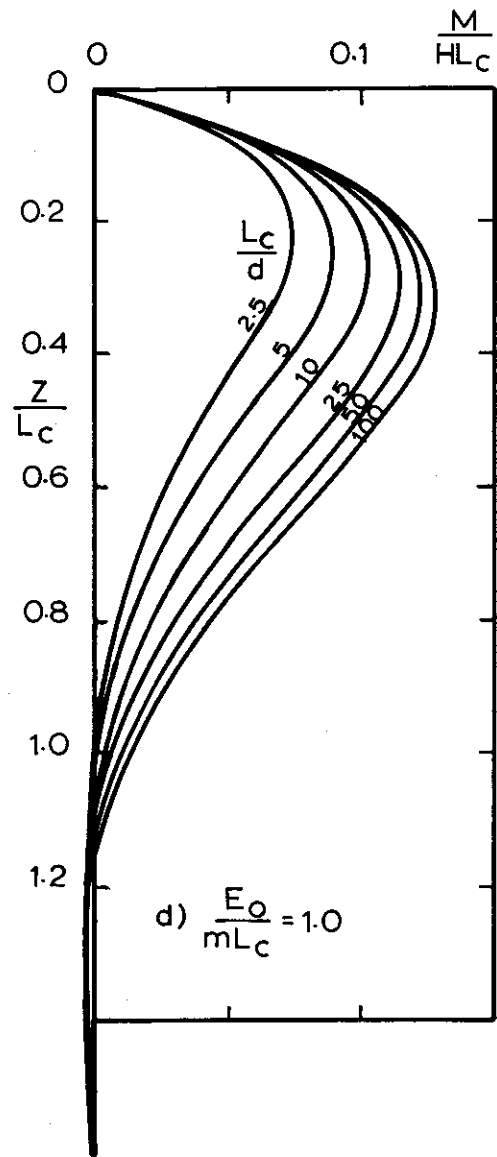
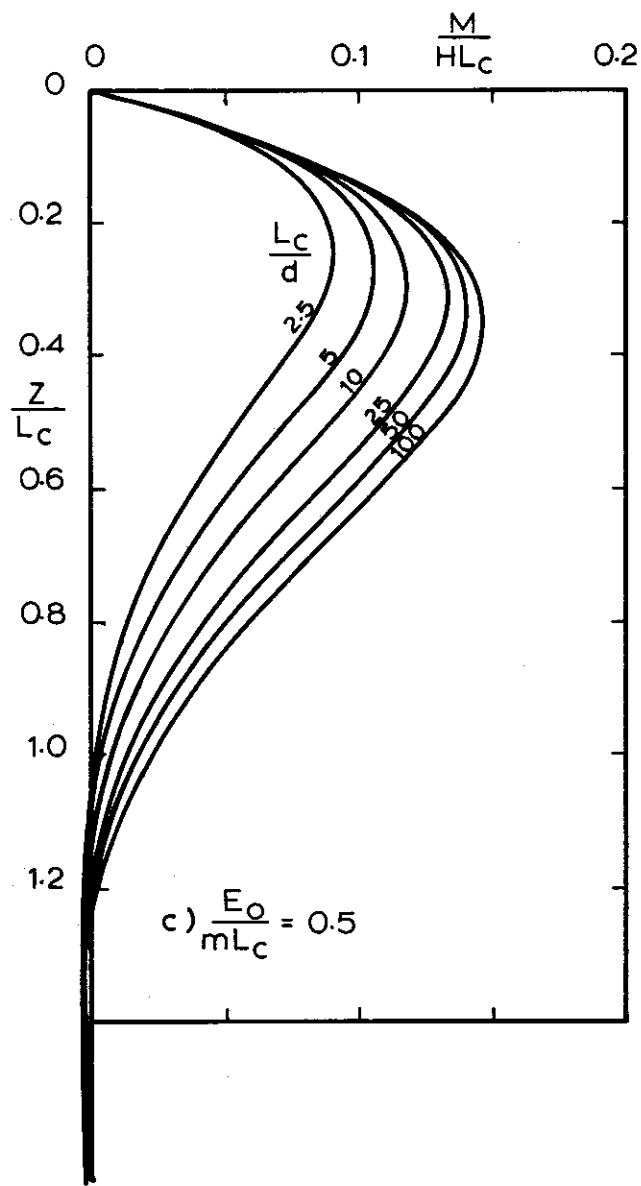


FIG 4.13 CONTINUED

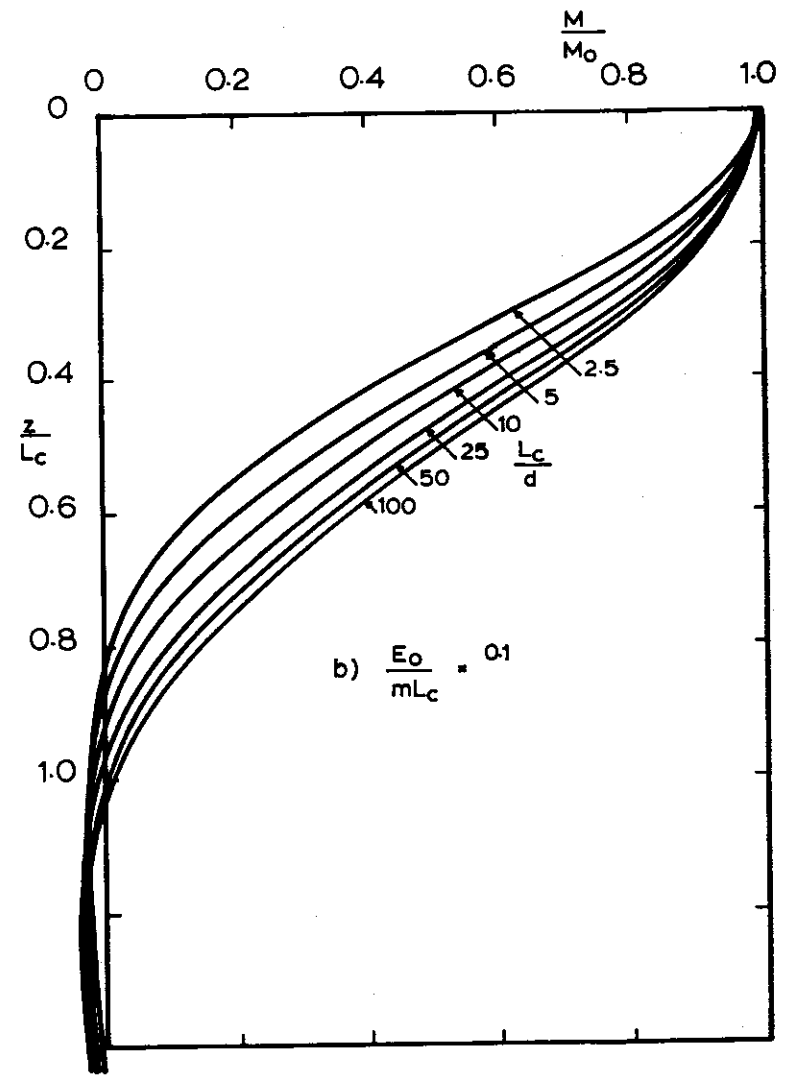
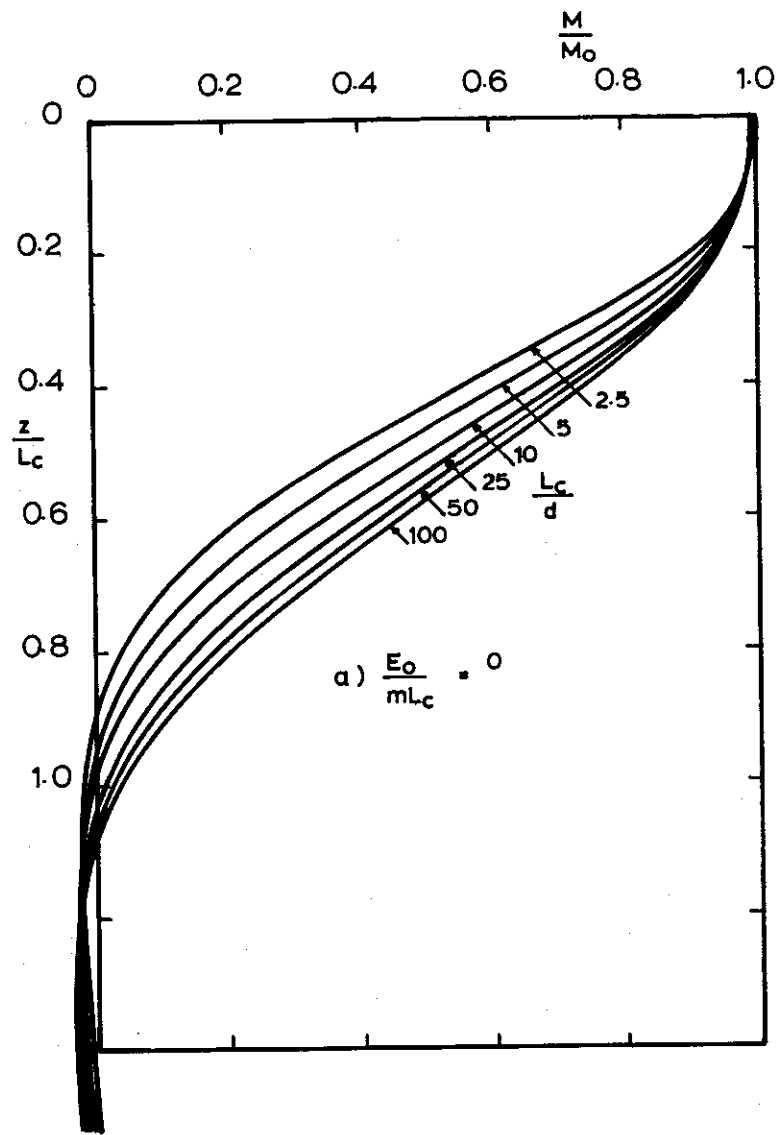


FIG 4.14 MODIFIED BOUNDARY ELEMENT RESULTS: BENDING MOMENT DUE TO HEAD MOMENT

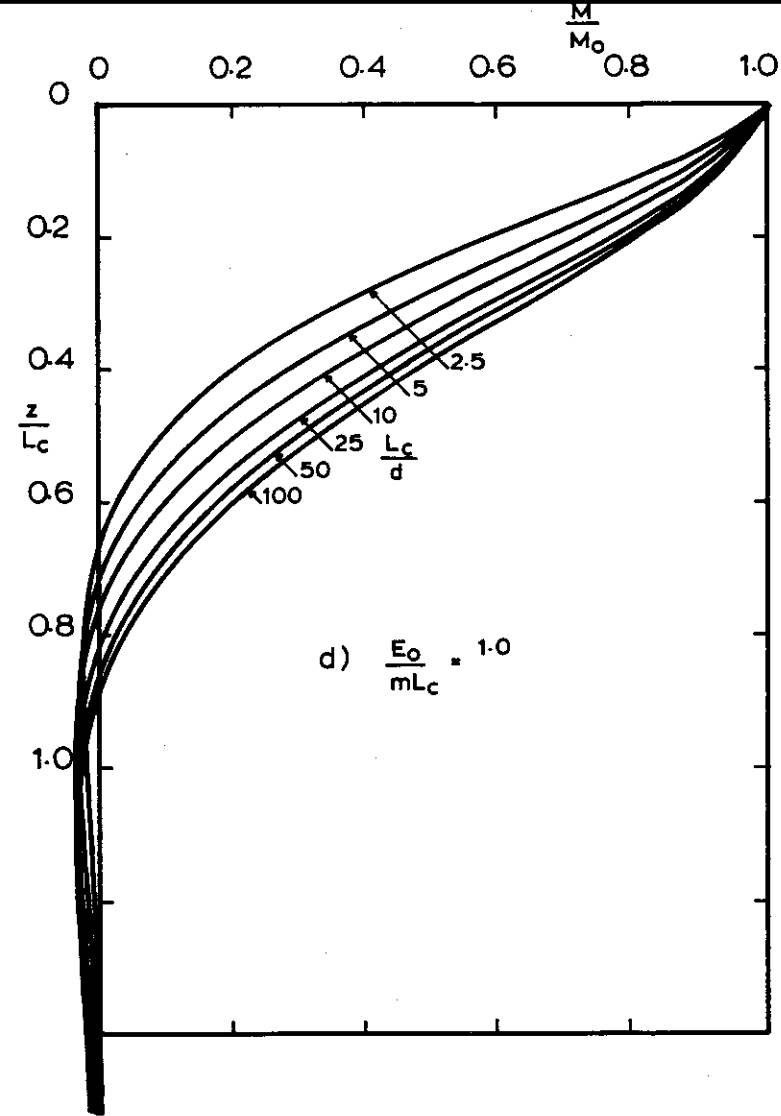
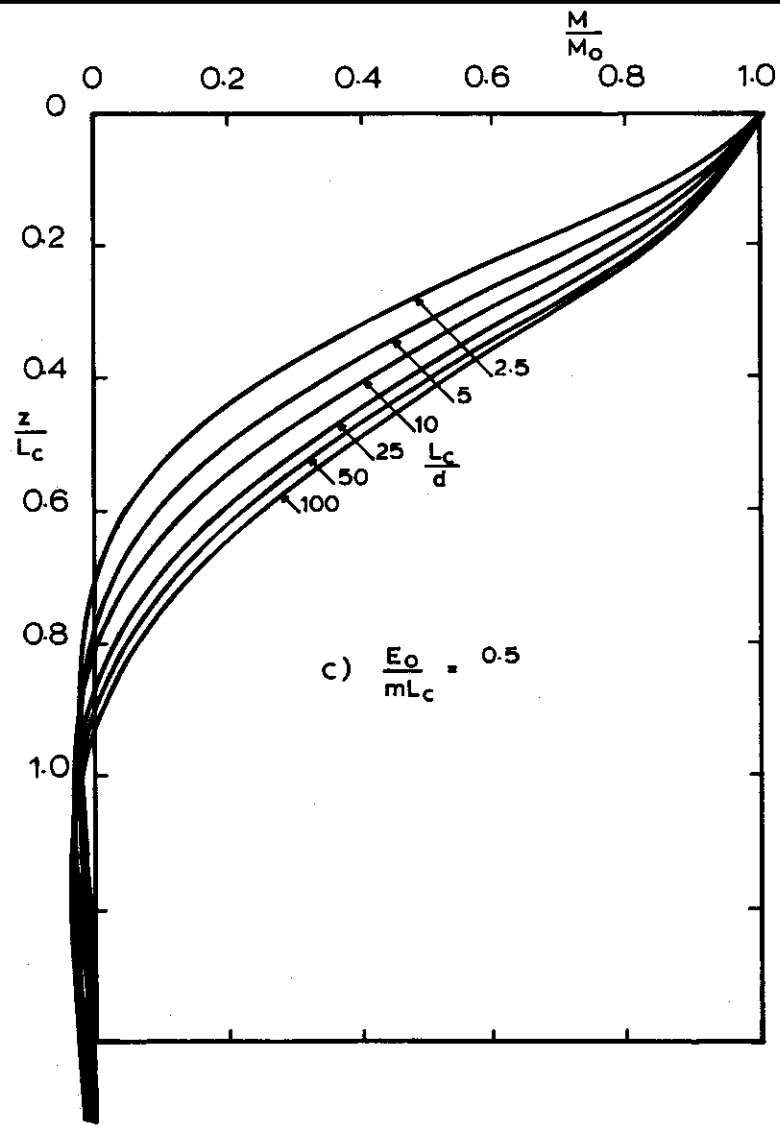


FIG 4.14 CONTINUED

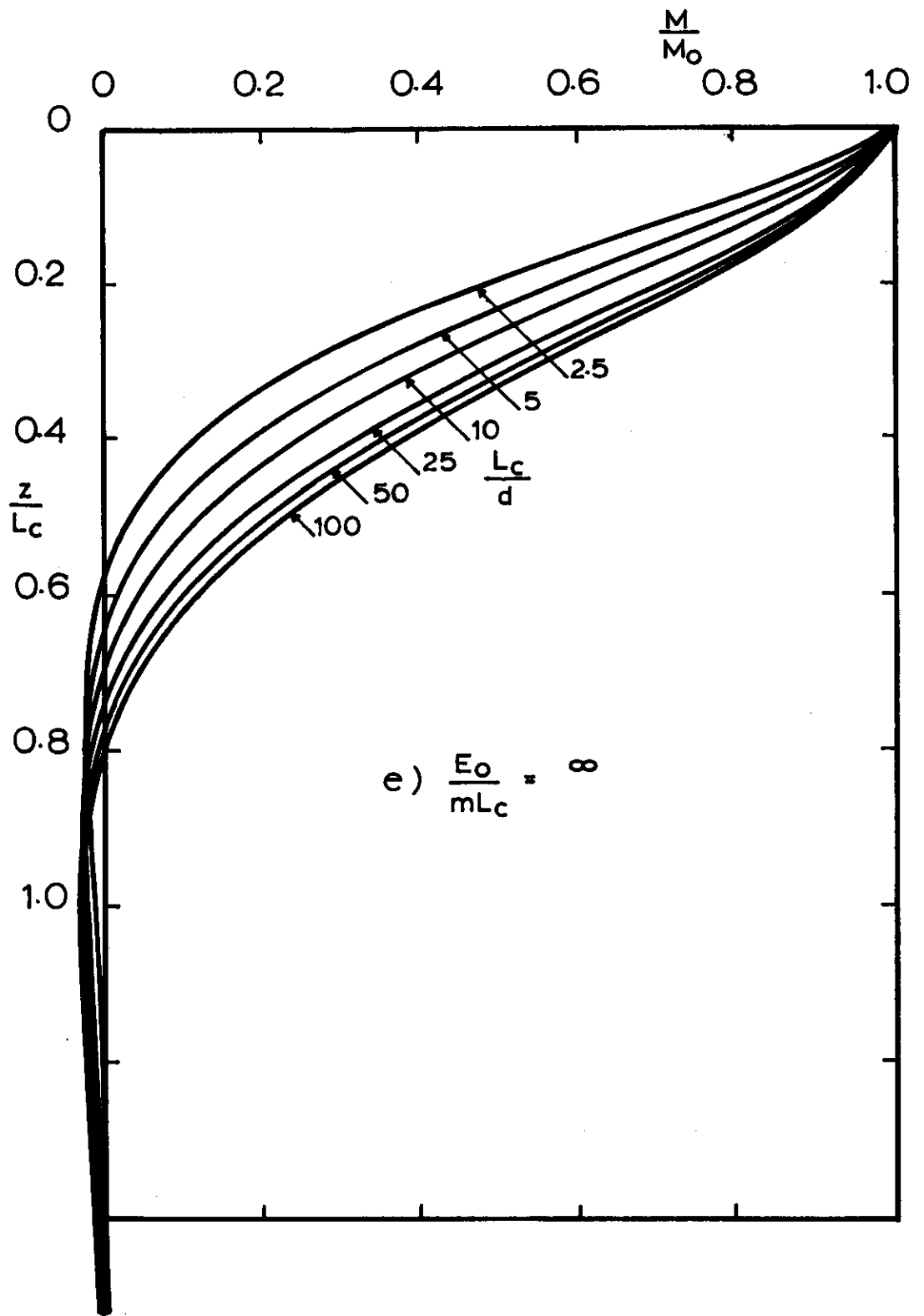


FIG 4.14 CONTINUED

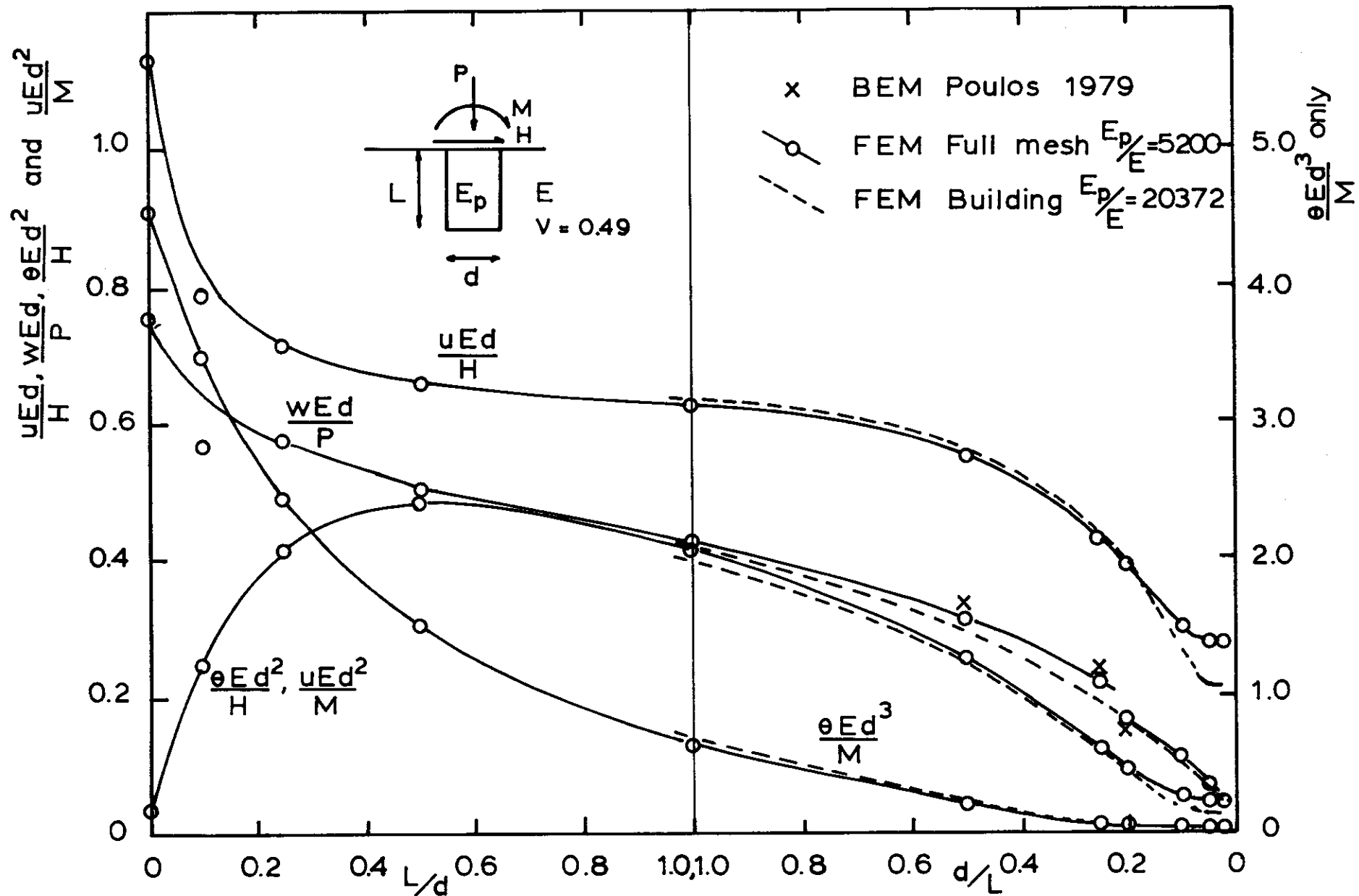


FIG.4.15 RESULTS OF THE FULL MESH FINITE ELEMENT AND BUILDING ANALYSES

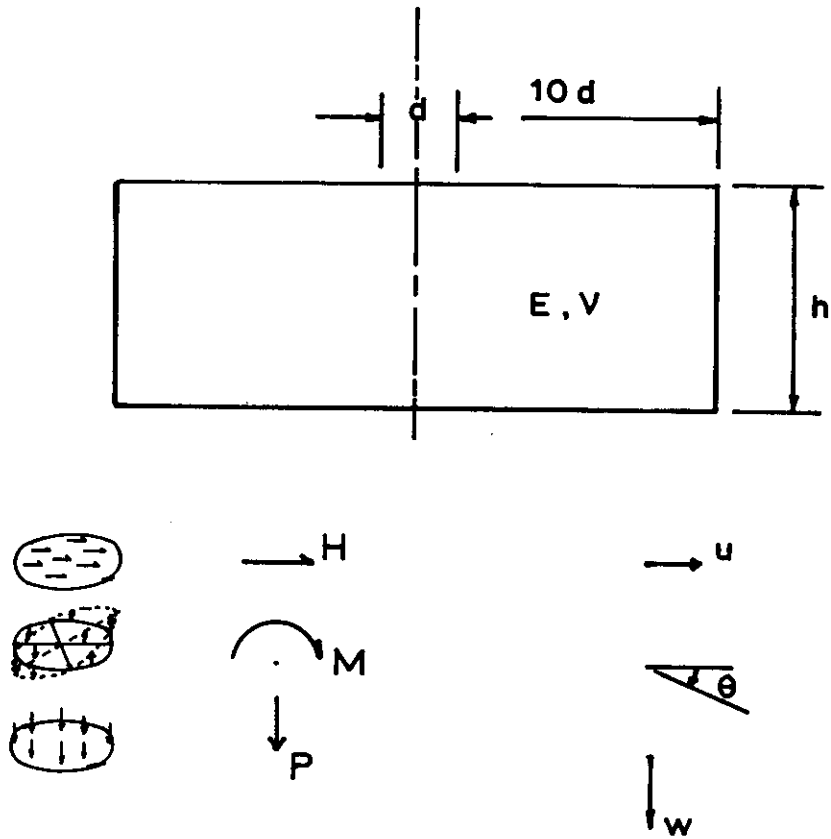


FIG.4.16 PROBLEM AND LOADING DEFINITION:BUILDING ANALYSIS

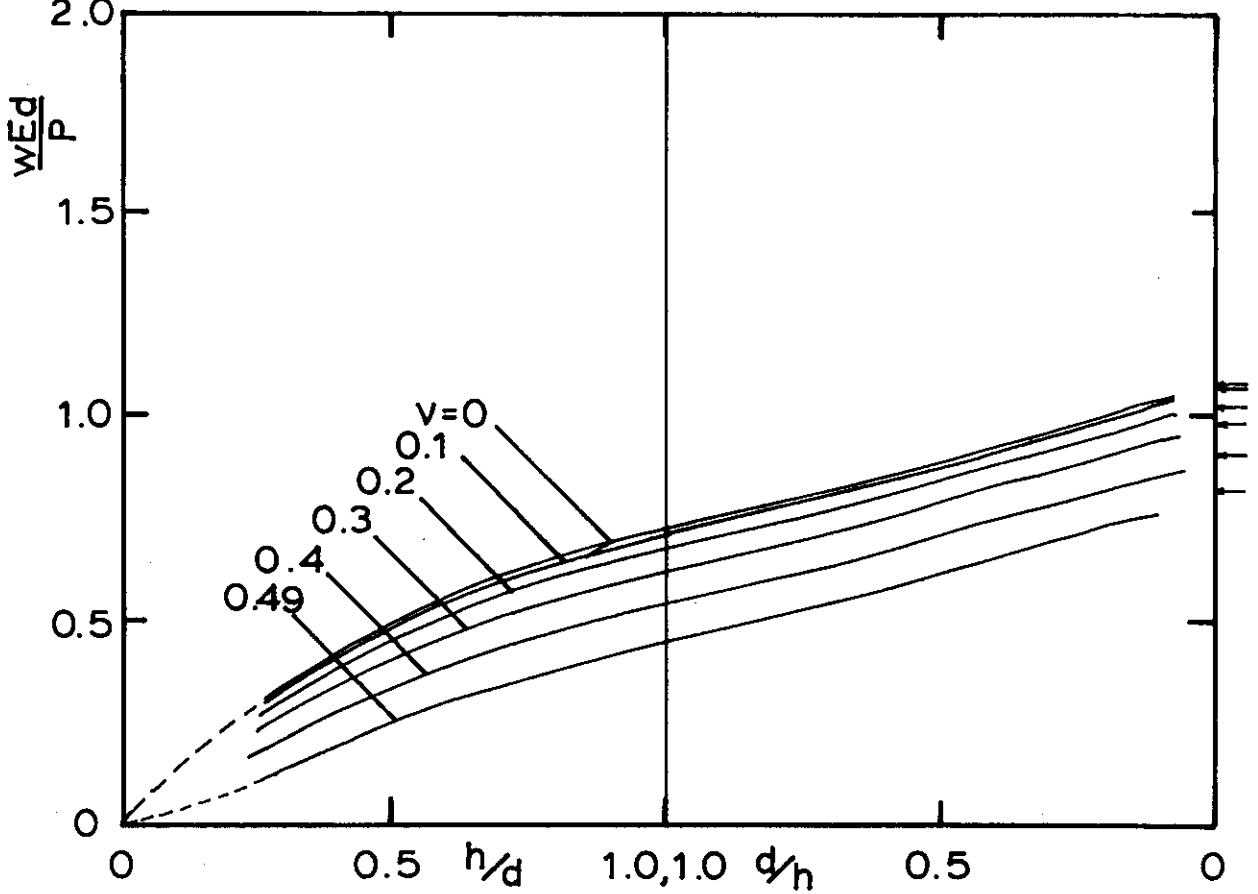


FIG.4.17 MEAN SETTLEMENT OF ELASTIC LAYER:VERTICAL LOAD

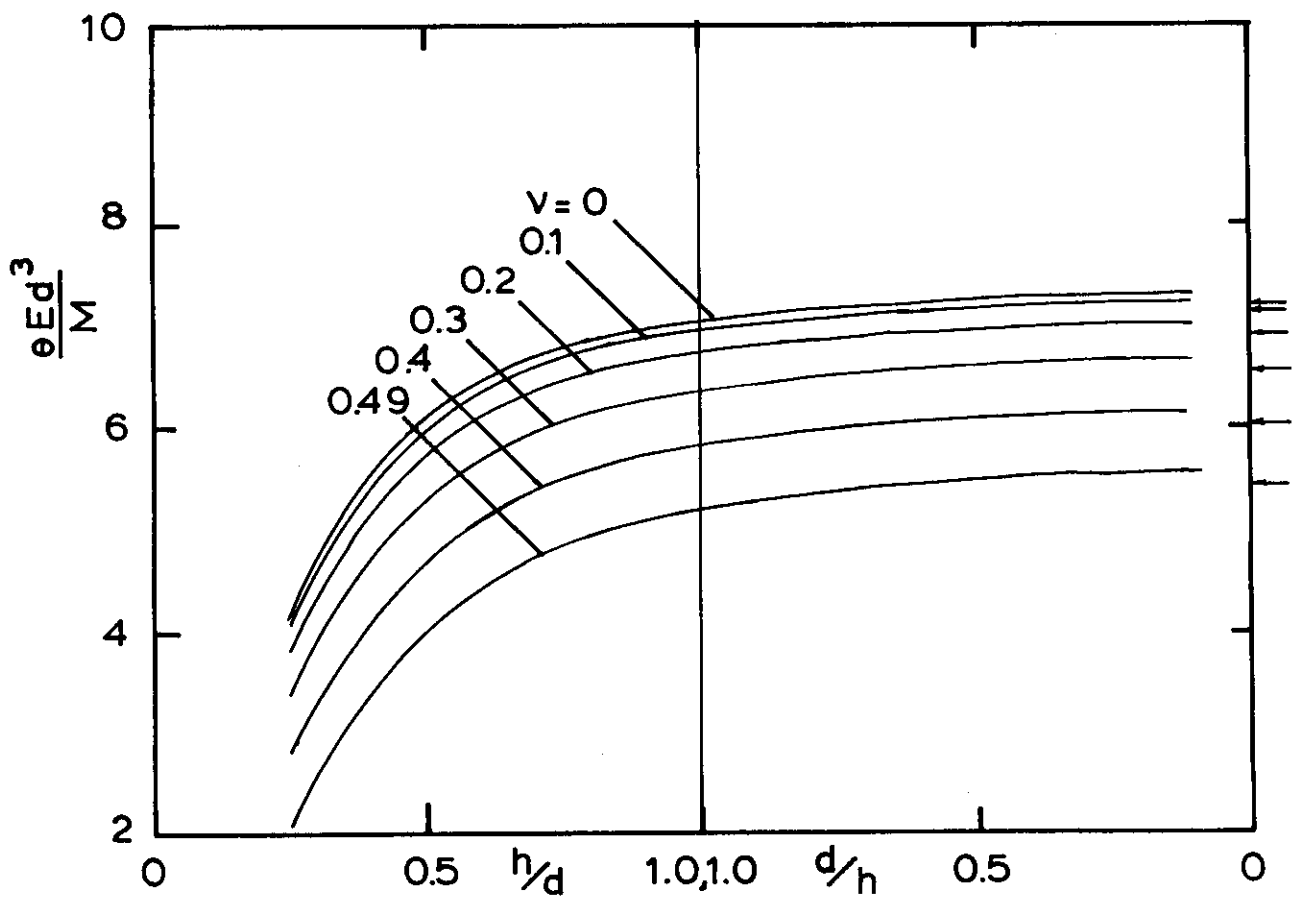


FIG. 4.18 ROTATION DUE TO MOMENT LOAD ON ELASTIC LAYER

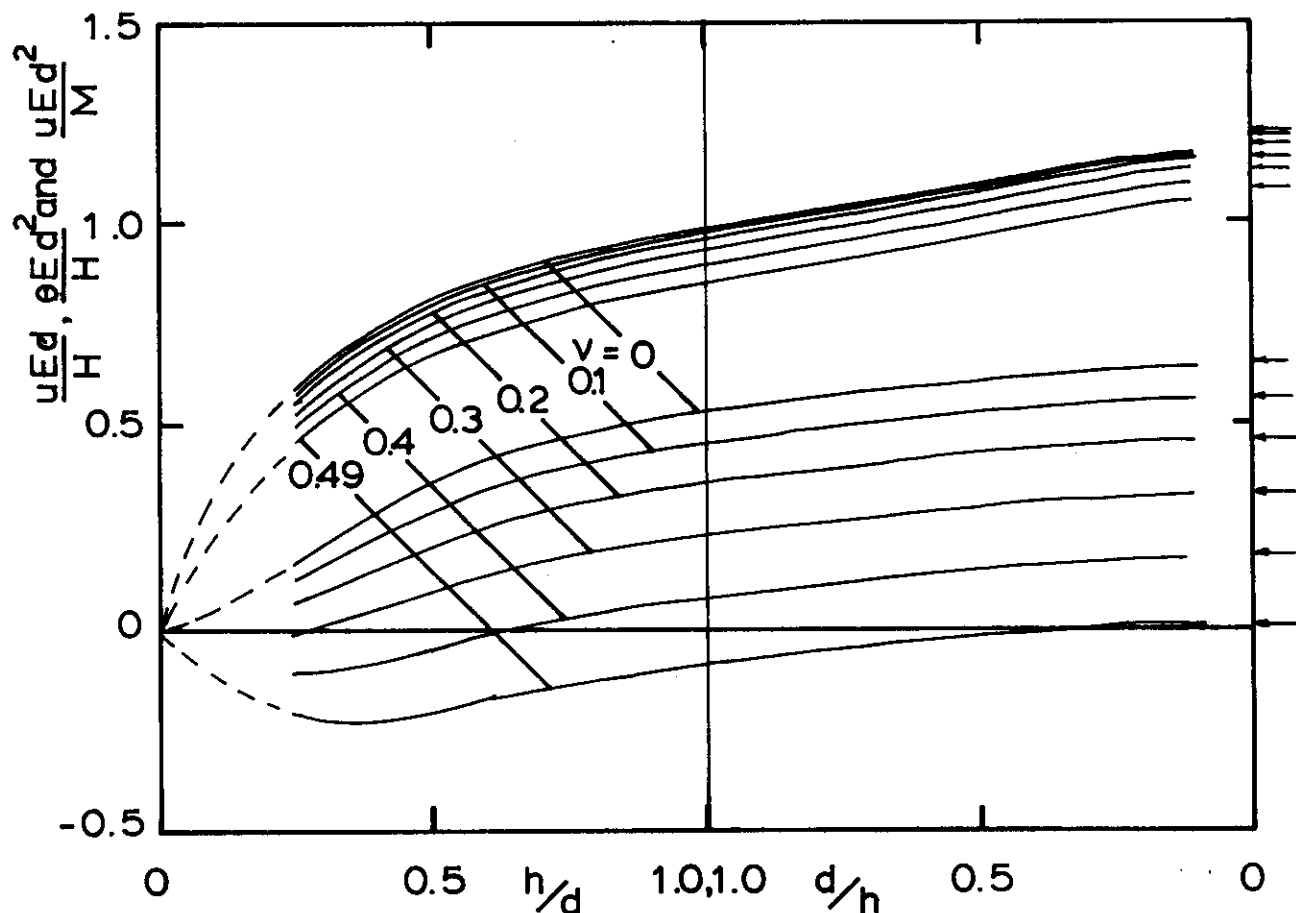


FIG. 4.19 DEFLECTION DUE TO HORIZONTAL LOAD, ROTATION DUE TO HORIZONTAL LOAD AND DEFLECTION DUE TO MOMENT

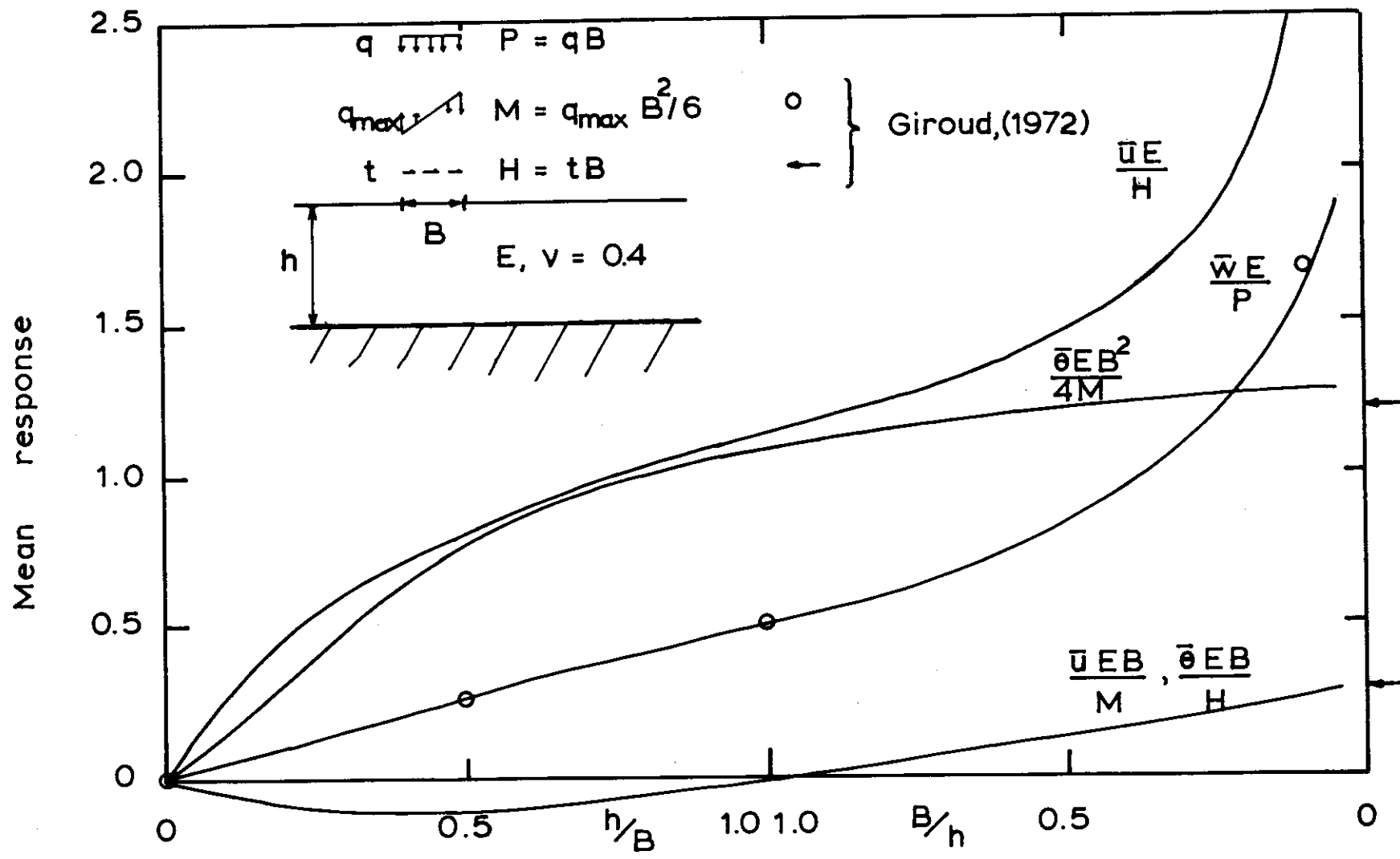


FIG. 4.20 MEAN DEFLECTION AND ROTATION OF A FLEXIBLE STRIP FOOTING ON AN ELASTIC LAYER

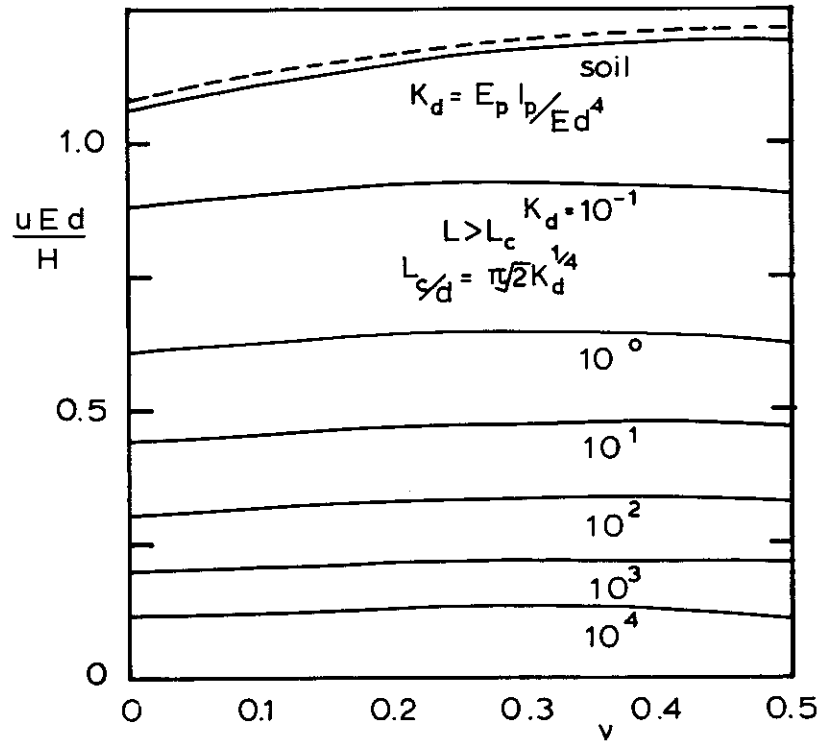


FIG. 4.21 FLEXIBLE PILE HEAD DEFLECTION DUE TO SHEAR: VARIATION WITH K_d AND POISSON'S RATIO ν

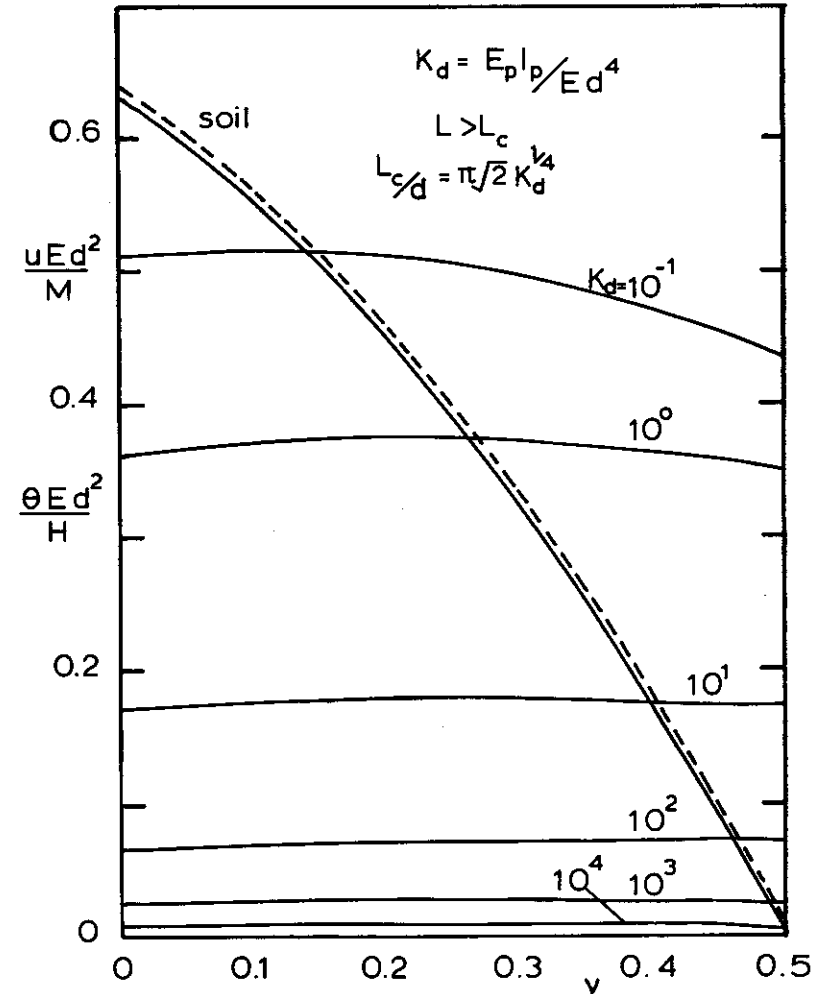


FIG. 4.22 FLEXIBLE PILE HEAD DEFLECTION DUE TO MOMENT AND ROTATION DUE TO SHEAR: VARIATION WITH K_d AND POISSON'S RATIO ν

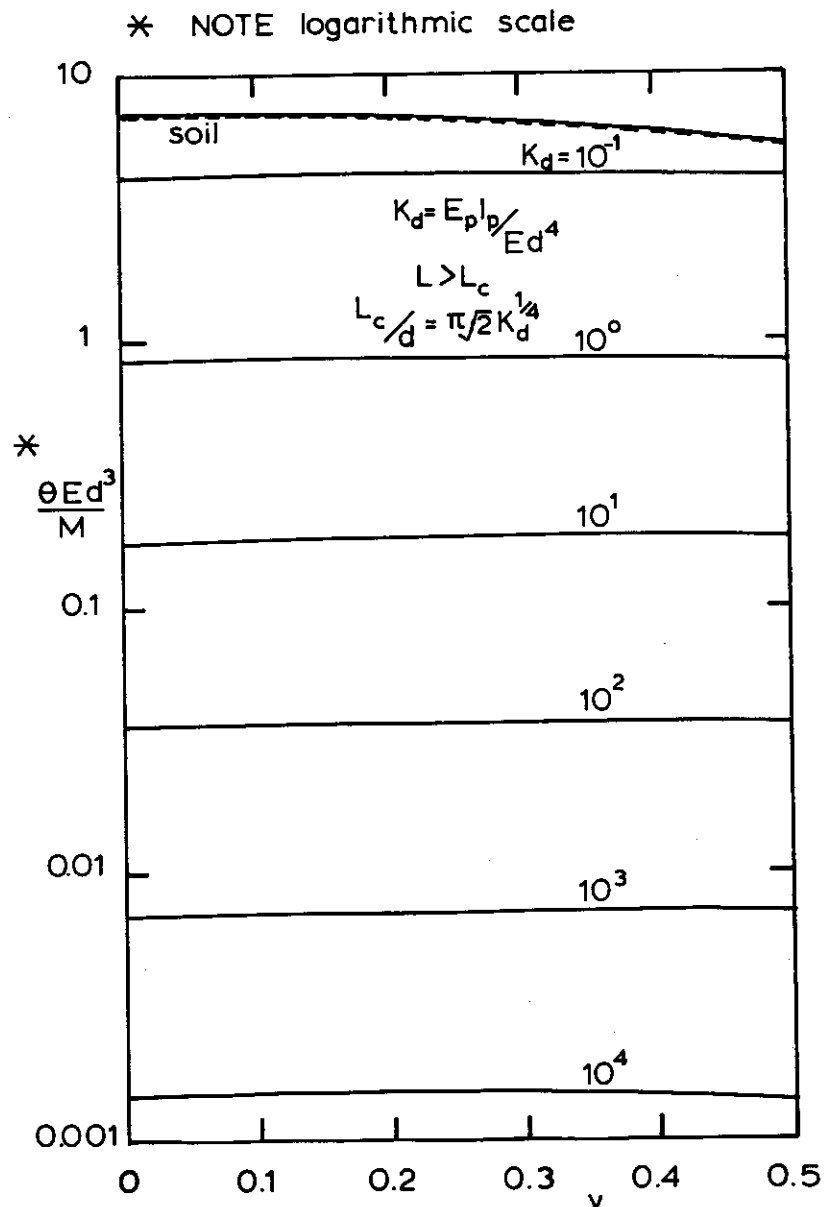


FIG. 4.23 FLEXIBLE PILE HEAD ROTATION DUE TO MOMENT: VARIATION WITH K_d AND POISSON'S RATIO ν

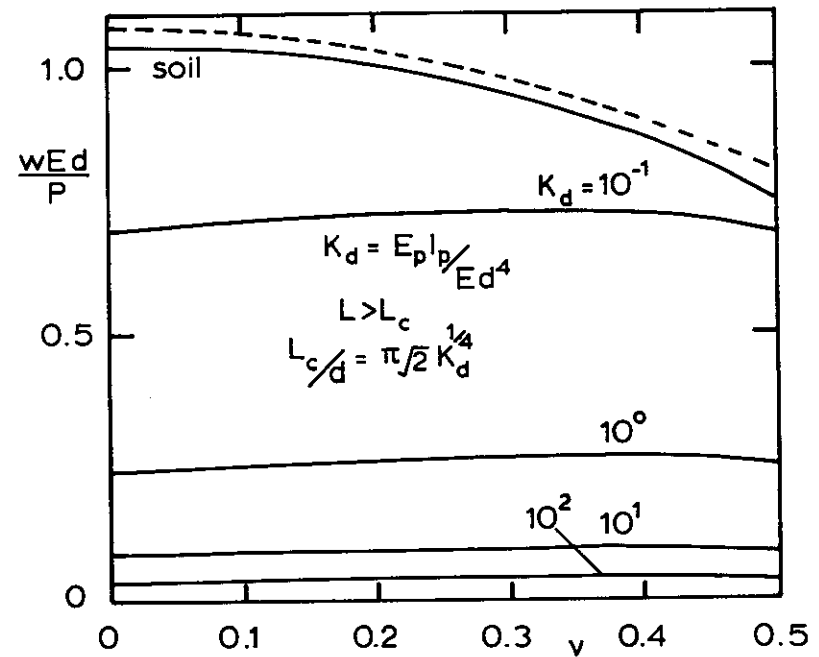


FIG. 4.24 COMPRESSIBLE PILE SETTLEMENT DUE TO AXIAL LOAD: VARIATION WITH K_d AND POISSON'S RATIO ν

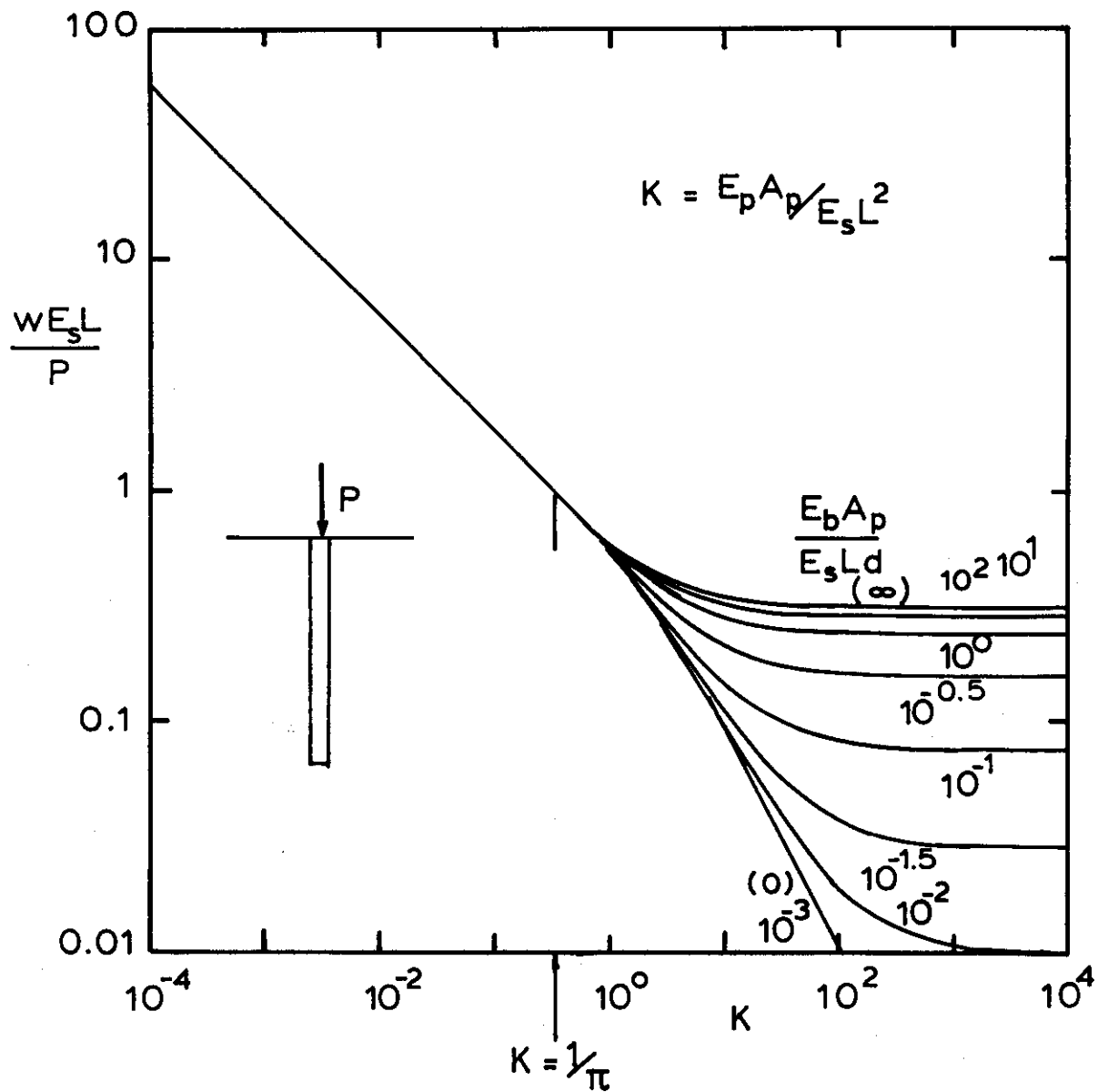


FIG. 4.25 SETTLEMENT OF AN AXIALLY LOADED PILE IN A WINKLER MEDIUM WITH SEPARATE BASE AND SIDE SHEAR SUBGRADE MODULI, E_b AND E_s

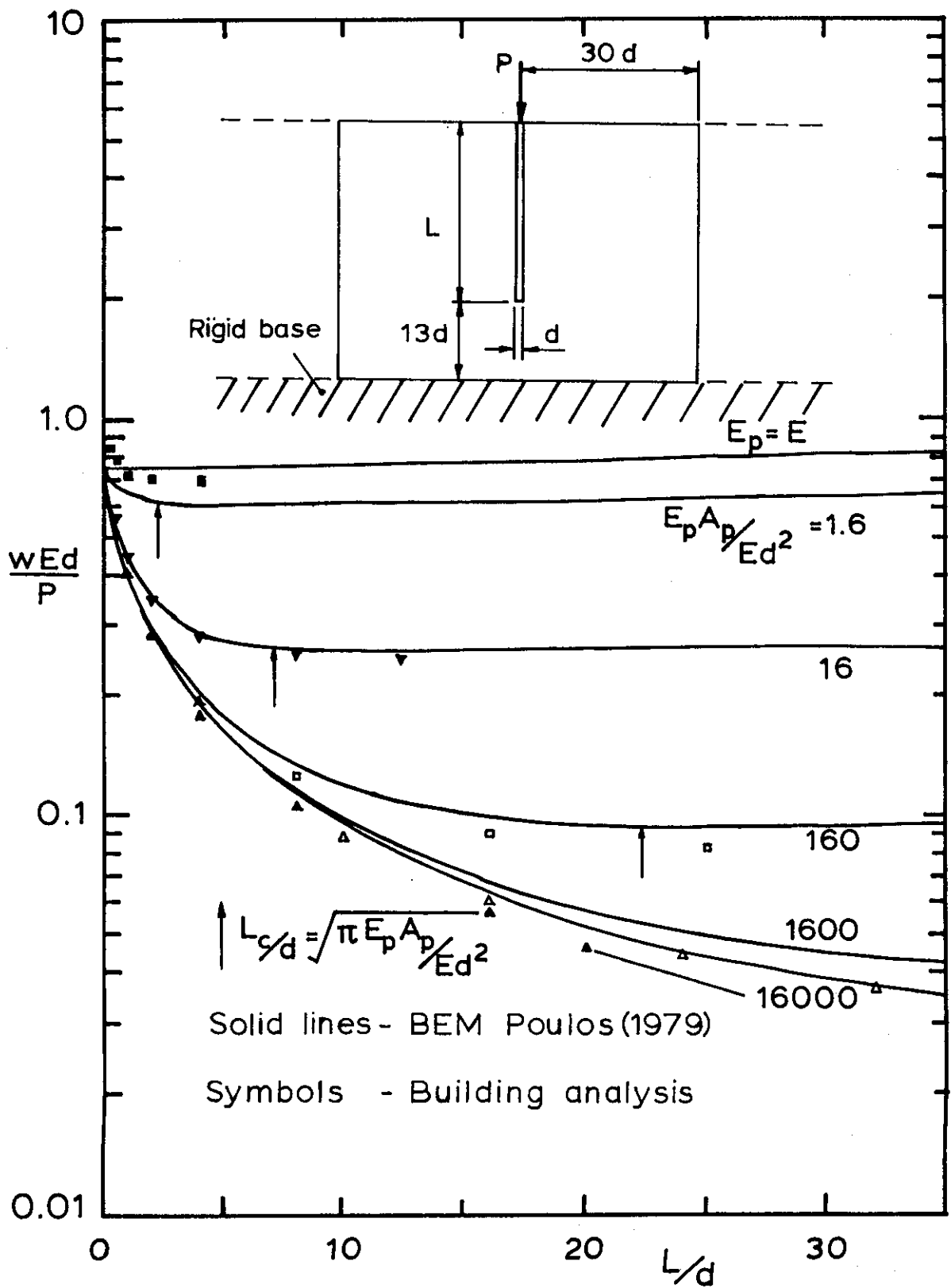
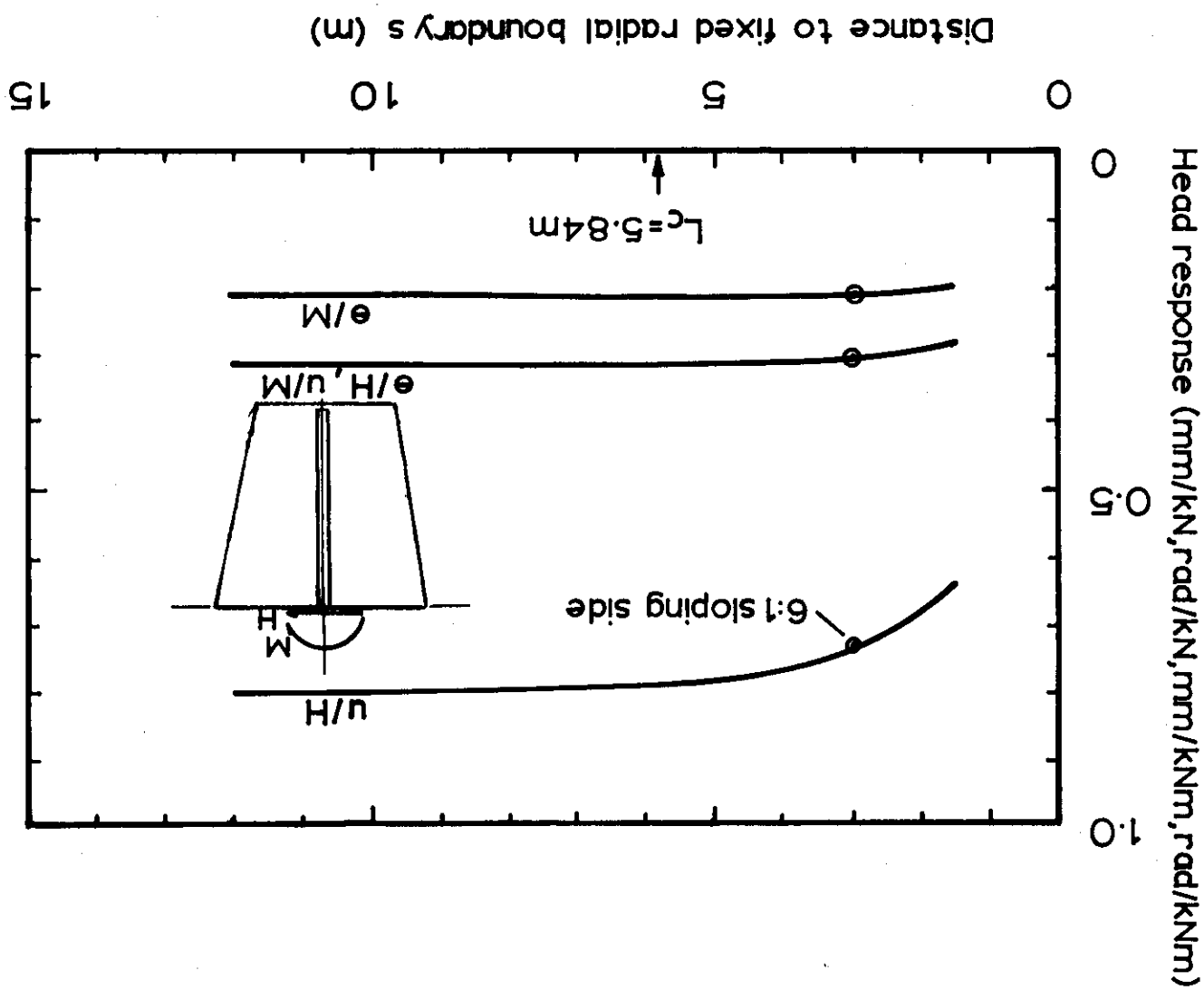


FIG.4.26 EVIDENCE OF A CRITICAL LENGTH FOR AN AXIALLY LOADED PILE : BOUNDARY ELEMENT AND BUILDING ANALYSES

FIG 4.28 PILE HEAD RESPONSE AS A FUNCTION OF DISTANCE TO A FIXED RADIAL BOUNDARY



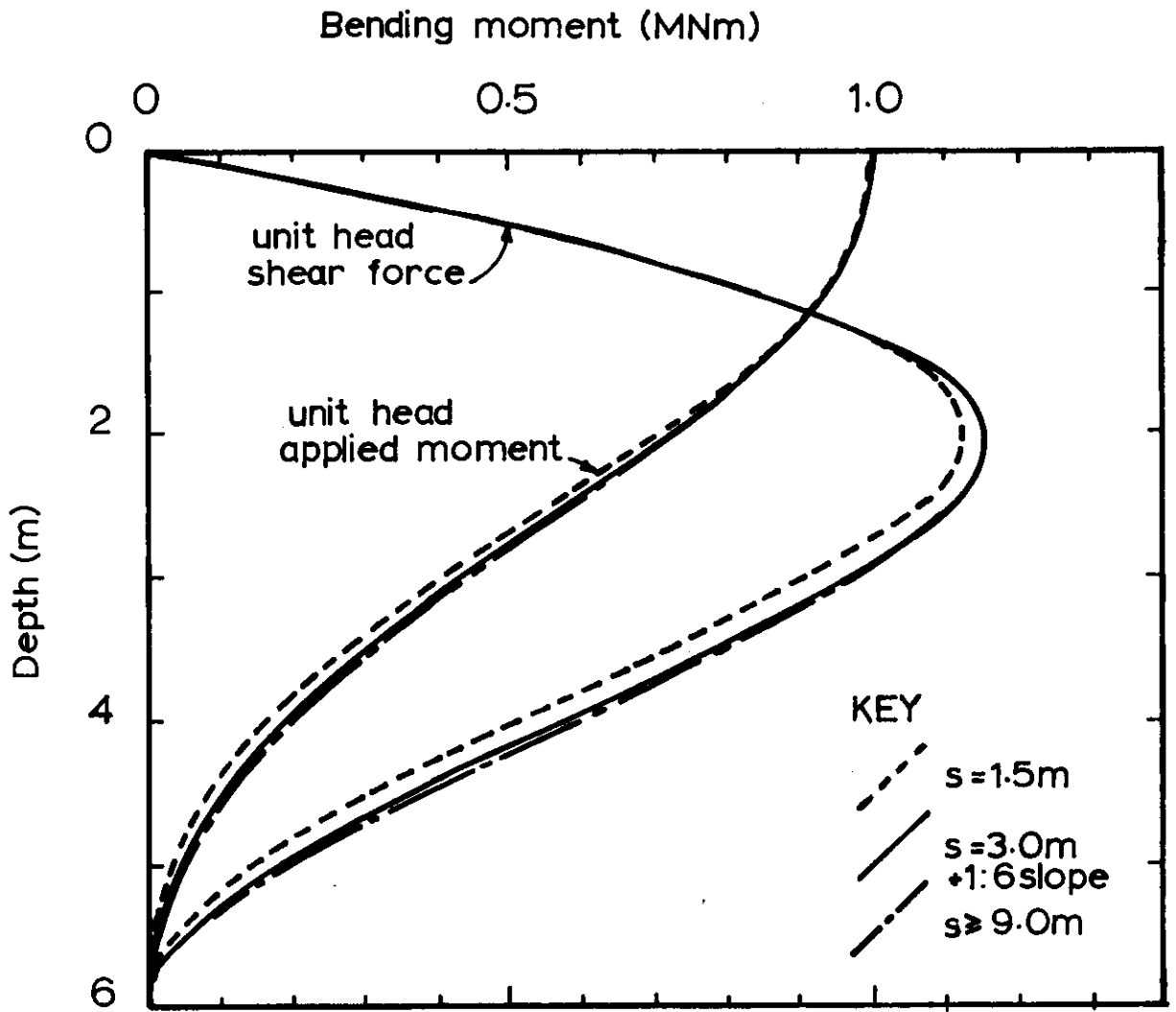


FIG4.29 BENDING MOMENT DISTRIBUTION FOR HEAD SHEAR AND MOMENT LOADING: BOUNDARY AT 1.5, 3.0 and $\geq 9.0\text{m}$ WITH VERTICAL SIDE AND 6:1 SLOPED SIDE

CHAPTER FIVE - LATERAL PILE RESPONSE : NON-LINEAR ANALYSIS

5.1 Introduction

In this chapter, the analysis of piles under lateral loading is extended to incorporate two forms of non-linear behaviour.

These are:

- i) non-linearity associated with geometrical changes, such as the formation of gaps between the pile and soil.
- ii) non-recoverable deflections, such as accompany soil yield.

The type of non-linear response arising from material property changes, such as damage and degradation, and apparent material property changes, such as those related to pore pressure generation, have not been considered.

In order to introduce gapping and soil failure it is convenient to consider both gap formation (Section 5.2.1) and soil failure (Section 5.2.2) as realistically as possible.

Means by which the effects of gap and yield behaviour can be unequivocally assessed, using analytic procedures, are then found for the Winkler soil model in section 5.3. Despite being somewhat inadequate, applying the Winkler soil model to the specific problem of full gap formation along the effective pile length during loading, illuminates the theoretical aspects of such behaviour.

Next, the MBEM technique is extended to include both types of non-linear phenomenon. By using a Winkler soil influence matrix, instead of that for an elastic continuum, the MBEM formulation can be checked against the results of the preceding section. However, the method remains limited to an exactly antisymmetric interaction traction interface element between pile and soil at any depth.

Thus, the non-linearity due to geometrical changes to the pile-soil interface brought about by gap formation, i.e. an asymmetric traction distribution, cannot be modelled properly.

A more appropriate method of analysis requires consideration of more than one interface element at any depth. To accomplish this a new Soil Structure Interaction (SSI) approach, based upon load-deflection influence matrices rather than stiffness matrices, is developed. Although more than two faces (front and back) could be used, the added complexity of more faces is not justified at this stage. The suitability of using just two faces (in a "biface" model) is given some support by analysing for the load-deflection response of a plane strain pile segment. Such an analysis has often been proposed as a useful model for lateral pile analyses, although it does have several limitations. The behaviour of this plane strain model is shown to be adequately determined using a finite element based analysis. This involves modelling the pile-soil interface by a uniform uni-directional traction around either the front or back half of the pile circumference.

The biface SSI pile analysis is shown to provide good linear results for elastic continuum based models without gapping or soil failure, by analysing a two-layer soil problem and comparing the results with those from a published solution (Pise, 1982), and the results of using both the MBEM and FEM techniques. The non-linear biface analysis formulation is also checked by using a Winkler soil influence matrix, and the results of this numerical model compare very favourably with the behaviour from direct application of Winkler theory.

The SSI approach can efficiently take account of gaps forming between the pile and soil in zones of tensile interaction stress, and also incorporate a simple interface soil failure model based upon active and passive failure of the soil. The analysis developed in this chapter is believed to be the first application of elastic continuum behaviour that avoids assumptions (save those of a biface model) about the form of interaction between the back and front interfaces used to model the soil. The analysis represents a rational means of assessing the importance, or otherwise, of gap formation upon the response of laterally loaded piles.

5.2 Aspects of Non-linear Behaviour

Before describing any of the non-linear analyses, it is convenient to introduce the concepts of separation of the pile from the soil (gapping) and the failure of the soil. Both these phenomena have been associated with laterally loaded pile behaviour, although neither have received much analytic treatment, individually or in combination. The work of Matlock, Foo and Bryant (1978), Poulos and Davis (1980) and Swane and Poulos (1982) represent examples of previous treatment where either spring-based models or assumptions about elastic interaction with gaps present have been used. This work attempts to avoid both of these courses by using the simplest model that is consistent with an elastic continuum-based soil and the current understanding of gapping and failing soil response.

5.2.1 Separation

When considering the actual behaviour of piles it must be recognised that adhesion cannot be relied upon to maintain contact between the pile and soil, thus separation will occur. This separation, due to tensile interaction tractions, will be controlled by the state of stress prior to the increment of tractions. The initial stress may arise from pile installation, i.e. driving and remoulding of the soil, or may arise from the set up of a bored pile, i.e. subsequent creep or consolidation of the surrounding soil. A particular subset of the latter is due to the effect of lateral soil movements and associated non-symmetric stresses, as evidenced by Heyman and Boersma (1961), Bernal and Romana (1977) and others. More commonly the initial stress is treated as being axisymmetric.

File installation by driving will cause modifications to the soil properties and result in a residual stress distribution. These changes from the initial conditions in clay have been considered by Carter, Randolph and Wroth (1980). Their results provide a reasonable estimate of the residual stress distribution after driving that will be employed in this chapter and Chapter 6.

Calculation of residual stresses after pre-boring and installing a pile, do not appear to be as satisfactorily treated as do those from the driven pile case. As a first approximation it is assumed here that the overburden stress will provide a reasonable approximation for the in-situ radial stress in the soil around a bored pile, i.e. a hydrostatic stress state at the pile interface. The problem of a driven pile involves extensive remoulding of the region of soil around the pile and as such is an upper limit to the range of possible disruptions to the soil caused by pile installation. The pre-bored pile installation causes relatively minor remoulding, although the soil behaviour is usually no longer considered to be in the elastic range. This mixture of elastic and limited plastic straining leads to a complex and highly individual installation history for every pre-bored pile.

The initial radial effective stress (before pile installation) can be thought of as equal to an "at rest" earth pressure coefficient, K , multiplied by the vertical effective overburden stress and may be considered a lower bound to the initial effective stress on the pile after installation. Assuming K , the one-dimensional (no lateral strain consolidation) value of K is less than one and neglecting K_a , gives the extreme lower bound to the value of lateral stress. The upper bound to the

lateral stress after moderate to extensive plastic strain behaviour may be found from empirical adjustment of the Rankine passive earth pressure or from cavity expansion analyses.

The attainment of sufficient tensile interaction stress to just eliminate the initial stress at some region on the interface leads to separation between pile and soil. Recognising that lateral stresses exist prior to loading, and assuming an axisymmetric distribution of such a stress state, the onset of separation will be dependent upon lateral load level, but not on load direction.

In general, except in highly over-consolidated or non-homogeneous soil, the distribution of lateral stress with depth will be linear after pile installation due to a linear variation of strength with depth (driven piles), and due to the linear overburden pressure (pre-bored piles). This fact leads to early, if not immediate, separation of the soil from behind the pile during loading of piles in clay. The upper portion of the pile attracts large interaction tractions and so it would be expected that separation commences at the surface. The junction between separation and full contact will move down the pile with each increase of head load, until it reaches a zone that will allow development of the tensile traction increment without producing an actual stress less than zero. The phenomenon results in a reduction in stiffness of the upper portion of the pile-soil system and a redistribution of interaction tractions to deeper sections more able to sustain the increments of tensile interaction tractions. The pile will have separation occurring along a finite (but not necessarily continuous) portion of its length, that grows with increasing head loading.

Assuming the induced interaction traction distribution down the pile, consisting of equal but opposite increments at the back and front of the pile, is unchanged by separation, results in no negative interface interaction tractions and a doubling of all positive (compressive) interaction tractions. Thus, for a Winkler soil it may be postulated that the effect of separation is a reduction in stiffness to one half of the fully contacting stiffness because, in the limiting case, no more than half the area of the pile interface will remain in contact with the soil.

It will be shown that this simple argument has some truth but, (even in a Winkler soil) the actual situation needs more attention to the modifications to pile-soil interaction caused by gap formation.

By considering a pile in an elastic medium that also has the ability to fissure, a very complex picture arises in which the back (tension side) of a pile may not completely break away from the soil, or may fissure at some distance from the pile-soil interface. Indeed, for a circular cross-section pile the prediction of the region of contact is not a trivial exercise and raises questions about the validity of small strain formulations.

To simplify the problem, and maintain a realistic analysis, the approximation of a biface soil-pile system with a front and back element at any depth is used. The onset of an average tensile total interaction traction, over the back or front element of the interface, leads to the immediate and complete separation of soil from that back or front element. In reality, partial breakaway of an element would occur at smaller interface tractions, locally within the area of the element or in the soil near the interface, but final complete separation would occur at higher tractions than

the "average" model predicts. This scheme proves most amenable to computation and if further discretisation around the circumference into more than two elements were used, the "average" model would be able to model the progressive nature of the breakaway.

5.2.2 Soil Failure

In order to model non-linear soil behaviour in the simple interaction analyses proposed in this chapter, it is necessary to specify the upper and lower limits of the interaction traction that can be sustained at the interface. Outside these limits, the soil is said to be failed, and will deform indefinitely without any increase of interaction traction. The difference between the model proposed here and previous models is that for the first time a quantity that is a measure of plastic work is defined and used as an integral part of the analysis. The sign of plastic work allows determination of when soil elements should unload and return to an elastic state.

It is useful to consider some of the concepts that have been developed to describe soil failure theoretically with the assumptions of no viscous effects or consolidation. The stresses accompanying external loading of the soil are limited to obey some failure criterion, expressed in terms of the stresses. When a region of soil fails it is assumed to be constrained by a set of rules governing the kinematics of the flowing volume of yielded soil. While the yielded soil region is contained within an elastic portion of the body and has not developed a kinematic system that allows an indefinite amount of deformation, the loading may be stopped short of collapse, and then continued without altering the load-deformation response characteristics.

Thus, time does not enter the theoretical scheme as a variable.

Real soil does behave differently from the theoretical picture presented above, in that creep under constant load, and excess pore pressure generation and redistribution (consolidation) will all modify the validity of the assumption of a solution independent of time. Further, the theoretical collapse load may well be founded upon a kinematic collapse mechanism that will only be valid for small deformations. Although large strain analyses have been produced for footing problems, and are generally thought to give little improvement over standard small strain results (Carter, 1977), the case of laterally loaded piles has not been considered in detail. It is possible for small-strain-based collapse loads to be lower or higher than those that would be found using the more complex large strain formulations, and presumably the same could be said for real soil collapse loads.

It is the possibility of a mechanism of flow occurring that is addressed by most theories used to predict the ultimate interaction traction on the pile at which soil collapse occurs. It can be seen that the attainment of a failure stress state and failure mechanism, must be accompanied by a rate of strain that is maintained. It is this aspect of failure, requiring a load path treatment of elements of soil that fail, consistent with the order in which they occur, that is often overlooked in engineering approaches to the modelling of soil failure. The requirement of positive plastic work in the plastic region is also a result of applying a rigorous theory of plasticity that is often ignored in analyses of non-linear behaviour (Davis, Ring and Booker, 1974).

Thus any model that purports to be based upon, or directly uses, plasticity theory must pay at least some regard to:

- a) the sequence of soil elements reaching collapse loads,

- b) the change from stress increment control to strain increment control at failed elements and
- c) avoiding any negative plastic work in failing soil.

It is not impossible to obtain answers of engineering use when neglecting any or all of the above three points, but it is no longer a valid use of plasticity theory. Thus the results would be based upon expectations of behaviour and not involve a reasoned argument capable of explaining the characteristics of the failure.

The modelling of soil behaviour here has been pursued using an elastic based theory to explain the transfer of stress and strain throughout the soil mass. It follows that the inclusion of non-linear, localised soil failure behaviour should also have some theoretical basis. To incorporate even the basic Mohr-Coulomb failure criterion into the behaviour of elastic soil under lateral pile loading would prove a large task. The work of Lai (1987) represents the state of the art of such approaches, e.g. the work of Winnicki and Zienkiewicz (1979), and is mainly of benefit in research investigations and application to specific foundations.

A theoretically-based and practical model of failure of soil due to lateral loading is developed in this Chapter. The main elements of a solution based upon plasticity theory, especially the concept of ensuring only positive plastic work, is incorporated into the non-linear MBEM analysis (which makes no distinction between the interface at the front and the back of the pile) and the SSI analysis (which includes failure of the front and back faces separately at any one depth in the soil). The use of this engineering approximation of behaviour at the interface proves to be of sufficient sophistication to produce a useful numerical model of the non-linear lateral loaded pile response.

5.3 Winkler Model and Non-linear Behaviour

In this section the Winkler soil model will be used as the basis of analysis for single piles where non-linear elastic gapping, non-linear soil response and non-linear pile response will be modelled. The concepts involved in the modelling of a laterally loaded pile using the Winkler soil model have been introduced in Chapter 3. Here they are further examined in the context of the new approach to modelling the soil-pile interface with a separate front and back.

5.3.1 Winkler : Elastic Non-linear Gapping

Most models assume the soil acts as one unit for the front and back, behaving according to one "pressure"-deflection relationship i.e. one value of pressure and deflection for both the front and back. The "pressure" in this sense is actually the load per unit of pile length and arises from an anti-symmetric distribution of interaction traction around the pile.

The consideration of a front and back interface at any one depth along the pile raises an important question:

Does the front face load cause deflection on the back face?

To be consistent with the Winkler model for the soil, the answer must be that no deflection occurs on the front face due to load on the back, and vice versa. For the pile however, the deflection of the pile front and back face are equal regardless of the face of the pile that is loaded.

The linear response of each soil face is unaffected by the loss of contact with the pile by other soil faces, by definition

of the Winkler model, and still may be expressed by equ. 3.6

$$W = E_s u$$

although E_s will not be the same value as the one used in the analysis that assumes contact between front and back of the soil with the front and back of the pile.

It may be argued that the Winkler approach is a poor one, because it predicts the front and back soil faces to act completely independently. This is intuitively unsatisfactory since it isolates the front from the back at any depth down the soil. The Winkler hypothesis has been acceptable for lateral pile analysis because the behaviour of the pile depends mainly upon the response of soil immediately at right angles to the pile axis. The interaction between two horizons of soil for lateral loading is thus small when compared to the interaction for the axial pile case, where the direction of load transfer is along the pile.

Now however, lateral loading would be expected to have a sizeable effect upon soil response in the same horizontal plane, in the direction of the loading, especially since the front and back soil face have common points at the sides. The Winkler hypothesis then would require some modification in order to realistically incorporate this interaction. The behaviour will thus greatly depend upon the initial state of stress and consideration of the avoidance of tension.

Thus, a rigorous application of the Winkler model exhibits an unlikely isolation of response, while a less strict approach using Winkler theory requires approximations of the behaviour to be made, but with no theoretical background to justify their choice. In this situation it is better to apply the model rigorously, and maintain simplicity while recognising the drawbacks of that

approach, rather than to incorporate assumptions that have no theoretical basis. When the front/back "biface" pile analysis technique has provided a simple but accurate solution for the Winkler soil model, its application to an improved Elastic based analysis may proceed with more confidence.

It is important to realise that conventional Winkler or Subgrade Reaction analyses lump together into one term the stiffnesses of the front and back soil elements, that now have been separated into two components. For this reason the Subgrade Modulus for the biface model differs by a factor of two when compared with the standard value of Subgrade Modulus.

To explain, it is useful to consider the basic Winkler expression (equ. 3.5), $p = k u$. When this is applied in the more common (no gap) analysis, it refers to the total traction load transferred by the pile to the soil, as being a linear function of the deflection. The total load is represented by an average pressure, p , i.e. the total force on the pile element divided by the area of the element. Thus the total distributed load on the pile is simply $W = p d$, while the same total distributed load on the soil is shared equally between the front and back face as compression and tension increments, $W_{s(front)}$ and $W_{s(back)}$, with magnitude $pd/2$.

Since the average values of the soil tractions on the front and back face govern breakaway, it is clear that these must be used in the analysis. Therefore

$$\frac{W}{p} = -W_{s(front)} + W_{s(back)} \quad 5.1$$

may be written while soil is in contact on both faces and leads to

$$W_p = -(E_{s(\text{front})} + E_{s(\text{back})}) u_p \quad 5.2$$

since

$$W_{s(\text{front})} = E_{s(\text{front})} u_{s(\text{front})}$$

$$W_{s(\text{back})} = E_{s(\text{back})} u_{s(\text{back})}$$

and $u_{s(\text{front})} = -u_{s(\text{back})} = u_p$

By assuming the soil is axisymmetric in character, the fact that $E_{s(1/2)} = E_{s(\text{front})} = E_{s(\text{back})}$ can be used with equ. 5.2 to write

$$W_p = 2 \cdot E_{s(1/2)} u_p \quad 5.3$$

which is the standard form with $E_s = 2 \cdot E_{s(1/2)}$ where the negative sense is assumed. Similar equations were presented in section 3.2.1, dealing with the Coefficient of Subgrade Reaction. The obvious uncertainties associated with measuring the actual value of E_s and $E_{s(1/2)}$ from actual pile tests, make the Winkler model parameters difficult to obtain without some ambiguity as to their applicability.

Limiting States of Breakaway

For both rigid and flexible piles, for the two cases of a Subgrade Modulus uniform and proportional to depth, the limiting case of full breakaway along the effective length will be investigated. The effective length, as defined in Chapter 4, is the lesser of the actual and calculated critical pile lengths. Consider a flexible pile in a soil with a Subgrade Modulus proportional to depth, so that there are constant influence coefficients (e.g. $u_m L / H = I_c$, noting that $E_c = m L$) and $L = (4 \pi^2 E I_p / m)^{1/5} s_c$ is the effective length.

Now suppose breakaway occurs along the entire effective length. At the element level of discretisation, the loss of contact is incrementally equivalent to a halving of the soil stiffness, since no further unloading is possible on the separated tension faces. If it did not halve it would mean the stiffness of the face remaining in contact would have to change which is not predicted by the Winkler model, so we may assume a new Subgrade Modulus distribution with $m_s^* = m_s / 2$. So a new effective length L_c^* controls where

$$L_c^* = \left(\frac{4 \pi^2 E I}{m_s^*} \right)^{1/5} \quad 5.4$$

and

$$\frac{L_c^*}{L_c} = \left(\frac{m_s}{m_s^*} \right)^{1/5} = 2^{1/5}$$

There is no change in the influence coefficients for a Winkler soil, because changing L_c/d does not alter the flexible pile response. For an elastic continuum, changing L_c/d would change the influence coefficient in general; only for longer L_c/d does the influence coefficient become nearly constant as L_c/d varies. So the original displacement

$$u = I_{uH} \frac{H}{m_s} \frac{L_c^2}{c}$$

becomes

$$u^* = I_{uH} \frac{H}{m_s / 2} \frac{L_c^{*2}}{c}$$

Thus

$$\frac{u^*}{u} = 2 \left(\frac{L_c^*}{L_c} \right)^2 \quad 5.5$$

or

$$\frac{u^*}{u} = 2^{1.2}$$

This means the incremental deflection due to shear at the pile head will increase by about 52% over the instantaneous original full contact deflection. Similar expressions can be found for the rotation due to shear and deflection due to moment (which will both be equal) and the rotation due to moment.

Now suppose breakaway occurs along the entire effective length. At the element level of discretisation, the loss of contact is incrementally equivalent to a halving of the soil stiffness, since no further unloading is possible on the separated tension faces. If it did not halve it would mean the stiffness of the face remaining in contact would have to change which is not predicted by the Winkler model, so we may assume a new Subgrade Modulus distribution with $m_s^* = m_s / 2$. So a new effective length L_c^* controls where

$$L_c^* = \left(\frac{4 \pi^4 E I_p}{m_s^*} \right)^{1/5} \quad 5.4$$

and
$$\frac{L_c^*}{L_c} = \left(\frac{m_s}{m_s^*} \right)^{1/5} = 2^{1/5}$$

There is no change in the influence coefficients for a Winkler soil, because changing L_c/d does not alter the flexible pile response. For an elastic continuum, changing L_c/d would change the influence coefficient in general; only for longer L_c/d does the influence coefficient become nearly constant as L_c/d varies. So the original displacement

$$u = I_{uH} \frac{H}{m_s} \frac{L_c^2}{c}$$

becomes
$$u^* = I_{uH} \frac{H}{m_s / 2} \frac{L_c^{*2}}{c}$$

Thus
$$\frac{u^*}{u} = 2 \left(\frac{L_c^*}{L_c} \right)^2 \quad 5.5$$

or
$$\frac{u^*}{u} = 2^{1.2}$$

This means the incremental deflection due to shear at the pile head will increase by about 52% over the instantaneous original full contact deflection. Similar expressions can be found for the rotation due to shear and deflection due to moment (which will both be equal) and the rotation due to moment.

The ratios of deformation increase due to gapping are

$$\begin{aligned} (u^*/u)_H &= 2^{3/5}, \\ (u^*/u)_M &= (\theta^*/\theta)_H = 2^{2/5}, \\ \text{and } (\theta^*/\theta)_M &= 2^{1/5} \end{aligned}$$

which numerically are 1.52, 1.32 and 1.15 respectively.

These results are possible because the soil modulus maintains the same distribution pattern, even though the magnitude of the effective length changes. This means the same non-dimensional solution covers the full contact modulus distribution and the full breakaway distribution cases. If the modulus distribution were intermediate to a proportional variation with depth and uniform ($0 < E/mL < \infty$), then the value of non-dimensional influence coefficient α_{oc} also changes with effective length (as the parameter describing the distribution of modulus E/mL varies) and the above procedure must use the solution presented in section 3.2.3.

For a uniform Winkler soil, changing the effective length does not change the pattern, or even the magnitude of the soil modulus with depth. Thus, results can also be easily found for a pile in a uniform Winkler soil for the case of complete breakaway over the effective length of a flexible pile.

The ratios of deformation increase due to gapping are

$$\begin{aligned} (u^*/u)_H &= 2^{3/4}, \\ (u^*/u)_M &= (\theta^*/\theta)_H = 2^{1/2}, \\ \text{and } (\theta^*/\theta)_M &= 2^{1/4} \end{aligned}$$

which numerically are 1.68, 1.41 and 1.19 respectively.

The influence coefficients for a stiff pile, where the critical length is longer than three actual pile lengths, will give an indication of the loss of stiffness due to complete separation along the length of a rigid pile in a Winkler soil. Since the effective length is now the actual pile length, which is unchanged by reducing the soil stiffness to half the original, it is easily found that the deflections and rotations double due to breakaway for all cases.

The implications for flexible piles from these results are:

Assuming the pile gaps along its entire effective length with gaps forming behind and in front at depths where tension occurs, the worst deterioration of the incremental deflection response is

- a) a 68% increased deformation for the uniform Winkler soil profile and
- b) a 52% increased deformation for the proportional Winkler soil profile.

The most critical situation will occur for the uniform case and the maximum possible reduction in stiffness for any linear distribution of Subgrade Modulus with depth is fairly closely bracketted by cases a) and b) above.

This result depends upon the supposition that the soil faces at the back and front of the pile have no means of influencing each other, and the total response experienced by the pile is the sum of the two equal magnitude incremental responses from the two soil faces. Because this is the only assumption that has any theoretical foundation using Winkler theory, and because it is probably true to say influence is possible between back and front soil faces, there is a need for a more involved model.

Finite Gap Length

The final analysis presented here that uses a Winkler soil model, is for the problem of the incremental response of a fixed-head pile with a pre-formed gap extending from the soil surface. A diagram of the problem is given in Fig. 5.1, where the shear forces, bending moments, deflections, rotations and dimensions used in the analysis are depicted. The pile and soil have no contact within the gapped length, and thus the response is a measure of the head stiffness, (say) about zero load, after cyclic loading has failed the soil either side of the pile.

The problem is treated as a cantilever and a pile that are joined at the bottom of the gapped length, where an initially unknown shear force and bending moment can be thought to act upon the bottom of the upper section, of length z , and the top of the lower pile, of length $L = L - z$. For the upper pile section the deflection u_f and rotation θ_f may be expressed using the equations for response of a cantilever as

$$\begin{aligned}
 E I_p u_f &= H \frac{z^3}{g} - M \frac{z^2}{g} \\
 E I_p \theta_f &= H \frac{z^2}{g} - M \frac{z}{g}
 \end{aligned}
 \tag{5.6}$$

For the embedded lower pile section, the influence coefficients from any source, including elastic continuum solutions, may be used to give

$$\begin{aligned}
 E L u_g &= H \frac{I}{g} u_H + \frac{M}{L} \frac{I}{g} u_M \\
 E L \theta_g &= H \frac{I}{g} \theta_H + \frac{M}{L} \frac{I}{g} \theta_M
 \end{aligned}
 \tag{5.7}$$

Equilibrium of the forces and moments on the upper pile section leads to the head shear load and fixing moment being expressed as

$$\begin{aligned}
 H_o &= H_g \\
 M_o &= M_g - H_g z_g .
 \end{aligned}
 \tag{5.8}$$

The compatibility of rotation at the junction between the cantilever and embedded pile sections provides the means with which to determine the unknown bending moment, M_g

$$\begin{aligned}
 M_g / L &= H_g / 2 \left[\left(\frac{z_g}{L} \right)^2 - \frac{2 K_R I_{\theta H}}{E_p I_p} \right] / \left[\frac{z_g}{L} + \frac{K_R I_{\theta M}}{E_p I_p} \right] \\
 \text{where } K_R &= \frac{E_p I_p}{E L^4} .
 \end{aligned}
 \tag{5.9}$$

By choosing a value of z_g and using equs 5.8 and 5.9 the unknown bending moment, M_g and fixing moment, M_o may be expressed in terms of the head shear, H_o .

It must be emphasised that this solution only applies while the pile makes no contact with the soil along its gapped length. Essentially the problem solved here is similar to that of a pile with an outstand. The extra factor in the problem is that the more useful case of a fixed-head pile has been modelled.

The two types of problem presented here will provide the means with which to test the validity of the programs developed in sections 5.4 and 5.5. These programs can use either a Winkler or elastic continuum soil influence matrix and will allow considerable freedom of load and head fixity conditions, as well as the ability to model soils with complex non-homogeneous properties.

5.3.2 Winkler : Plastic Non-linear Soil Failure

In section 5.3.1 the Winkler model was used to give the response of a pile within a gap that extends from the surface down to some finite depth. In this section that basic model will be extended to include the effect of soil failure tractions acting over the previously fully gapped length. Figure 5.1 shows the basic model and the distribution of ultimate traction that the soil can sustain when it fails. The idea to extend the previous solution was first suggested by Dr. M. F. Randolph in a personal communication and was then developed jointly with the writer.

The differences from the gapped analysis involve the addition of extra terms to the upper and lower pile responses, as determined by the distribution of ultimate traction employed. For the distribution that is proportional with depth the extra terms in equ. 5.6 for response due to distributed loading of a cantilever give

$$E I_{p p f} u = H \frac{z^3}{g^3} - M \frac{z^2}{g^2} + 11/120 n z^5$$

$$E I_{p p f} \theta = H \frac{z^2}{g^2} - M \frac{z}{g} + 1/8 n z^4 \quad 5.6a$$

and the extra terms in equ. 5.8 give

$$H_o = H_g + n \frac{z^2}{g^2}$$

$$M_o = M_g - H_g \frac{z}{g} - n \frac{z^3}{g^3} \quad 5.8a$$

Equation 5.9 also changes to become

$$M_g/L = H_g/2 \left[\left(\frac{z}{L} \right)^2 - 2 \frac{K}{R} \frac{I_{\theta H}}{\theta M} \right] / \left[\frac{z}{L} + \frac{K}{R} \frac{I_{\theta M}}{\theta M} \right]$$

$$+ n/8 \cdot \left(\frac{z}{L} \right)^4 / \left[\frac{z}{L} + \frac{K}{R} \frac{I_{\theta M}}{\theta M} \right] \quad 5.9a$$

The solution procedure is as before but now the depth to the change from plastic to elastic conditions is used to specify the head loads instead of the depth of the gap. With this analysis the formulation of the two numerical analyses developed in this chapter can be thoroughly checked for static loading of a pile in a Winkler soil that only fails from the surface down to a finite depth. To consider failure of soil in which the ultimate reaction load changes sign down the pile requires further sub-structuring of the pile. With the limited nature of the Winkler model, such development of the analytic based solution was not warranted.

5.3.3 Winkler : Elastic Linear Soil and Pile Failure

In this section the Winkler model will be employed to demonstrate the manner by which a pile with finite strength, and which can form plastic hinges, can be modelled in a linear elastic Winkler soil. The specific problem of a fixed-head pile, and two cases of rigid and flexible pile-soil systems will be considered.

Rigid Pile in a Uniform Winkler Soil

The head flexibility matrix of a stiff pile in a uniform Subgrade Modulus soil (where H_L and M_L act in the same sense as H_o and M_o) can be written as

$$E L_s \begin{bmatrix} u_o \\ \theta_o \\ u_L \\ \theta_L \end{bmatrix} = \begin{bmatrix} 4 & 6 & -2 & 6 \\ 6 & 12 & -6 & 12 \\ -2 & -6 & 4 & -6 \\ 6 & 12 & -6 & 12 \end{bmatrix} \begin{bmatrix} H_o \\ M_o/L \\ H_L \\ M_L/L \end{bmatrix} \quad 5.10$$

where subscripts o and L refer to the head and tip of the pile. To consider the possibility of a bending moment achieving a plastic value, the expression for bending moment as a function of

depth down the pile is required. Making use of the rigid body movements (u and θ) and the Winkler soil load deflection relationship ($W = E_s (u - \theta z)$) it is possible to obtain the expressions for the bending moment, M and shear force, $V = dM/dz$.

$$\begin{aligned}
 M &= M_o + H_o z + E_s (\theta_o z^3 / 6 - u_o z^2 / 2) \\
 V &= H_o + E_s (\theta_o z^2 / 2 - u_o z)
 \end{aligned}
 \tag{5.11}$$

In the above form the substitution of the incremental relations for a fixed-head, $\theta_o = 0$, $\dot{u}_o E_s L / \dot{H}_o = 1$ and $\dot{M}_o = -\dot{H}_o L / 2$ (where dots indicate an increment) suggest that the bending moment is a maximum at the pile tip. The value of this maximum is however zero and so the applied moment, M_o is the actual maximum value. Therefore, the head will achieve the plastic moment M_y first and subsequent loading will have $\dot{M}_o = 0$.

Expressing this non-dimensionally leads to

$$\begin{aligned}
 H_o L / M_y &= 2, & M_o &= -M_y \\
 u_o E_s L / M_y &= 2, & \theta_o &= 0.
 \end{aligned}
 \tag{5.12}$$

which represents the limit of pile linear response.

For continued loading of the head the response becomes incrementally like a free-head pile with pure shear loading. The incremental response can be obtained from equ. 5.10 and added to that existing when the load and deflection of the fixed-head pile are as given by equ. 5.12. Expressing the total bending moment as a non-dimensional function of incremental head shear, \dot{H}_o ,

$$\begin{aligned}
 M / M_y &= -1 + (2 + \dot{R}_o) z / y - (1 + 2\dot{R}_o) z^2 / y^2 + \dot{R}_o z^3 / y^3 \\
 \text{where } \dot{R}_o &= \dot{H}_o L / M_y.
 \end{aligned}
 \tag{5.13}$$

By differentiating the bending moment expression, equ. 5.13, it is possible to calculate the depth at which the maximum bending moment is located. This occurs for

$$z/L = (2 + \frac{\dot{R}}{y}) / 3\frac{\dot{R}}{y} \quad \text{or} \quad 1.0. \quad 5.14$$

The second value is the trivial solution, as found earlier, and so the first value is substituted into equ. 5.13 and the expression for M/M_y equated to ± 1 to ensure the maximum bending moment is a plastic hinge. When the value of $M/M_y = -1$ the solution involves negative plastic work at the plastic hinge and so can be discarded, leaving

$$\begin{aligned} \frac{\dot{R}}{y} &= 9.817 \quad \text{and} \\ z/L &= 0.401. \end{aligned} \quad 5.15$$

The total solution at the instant the second plastic hinge forms is

$$\begin{aligned} H L/M &= 11.82 & M &= -M \\ \circ & \quad y & \circ & \quad y \\ & \quad \quad \quad & & \quad \quad \quad \\ u E L^2/M &= 41.27 & \theta E L^3/M &= 58.90. \end{aligned} \quad 5.16$$

The second plastic hinge forming will not bring about collapse, even though it is a highly undesirable state, and collapse will not occur if more plastic hinges appear. The soil will still support the pile because it is not allowed to fail in this simple model. Thus, the loading may continue and the flexibility of the pile with two yield moments may be calculated. To do this, the deflection of the upper part of the pile above the second plastic hinge is calculated as if the remainder of the pile no longer existed. Thus, a pile with a length L_1 , that is 0.401 of the original length, is analysed and the tip deflection due to

head shear increment, \dot{H}_o and an unknown tip shear, \dot{H}_c calculated. The lower pile section is then analysed as a separate entity (a pile with a length L_2 that is 0.599 of the original length) for an unknown head load, \dot{H}_c . The two expressions are for the same deflection of the pile at the location of the second plastic hinge and by equating the two the incremental shear \dot{H}_c can be found in terms of \dot{H}_o .

$$\dot{H}_c = -\dot{H}_o / (2L_1/L_2 + 2) \quad 5.17$$

By using equ. 5.10 and equ. 5.17 the incremental behaviour of the entire pile, with two plastic hinges, can be calculated from analyses of two separate piles of lengths L_1 and L_2 . The resulting incremental head response is

$$\dot{u}_o E L / \dot{H}_o = 8.48, \quad \dot{\theta}_s E L^2 / \dot{H}_o = 26.12 \quad 5.18$$

which for some convenient value of \dot{H}_o can be calculated and added to the response of equ. 5.16 to provide a measure of the new head flexibility. This has been done and the result is plotted in Fig. 5.3, where the numbers correspond to the order in which the particular plastic hinge forms and also appear on the load-deflection curve.

The procedure could be repeated to find new plastic hinges in the section of the pile of length L_1 , but this has not been done for the results presented here. Throughout the analysis a check upon the sign of incremental plastic work at plastic pile sections must give positive values. The calculation of plastic work involves evaluating $M \cdot \Delta\dot{\theta}$, where $\Delta\dot{\theta}$ is the mismatch in the incremental rotations of the pile either side of the plastic moment.

Flexible Pile in a Uniform Winkler Soil

While it is a simple problem with which to introduce the analysis, the rigid pile is not a very practical case. The more useful problem of a flexible pile will be considered now.

The equation for a flexible pile, corresponding to the equ. 5.10 for a rigid pile response, can be written without gross errors as

$$E L \begin{bmatrix} u \\ \theta \\ u \\ \theta \\ L \\ L \end{bmatrix} = \begin{bmatrix} 2\pi^2 & 2\pi^2 & 0 & 0 \\ 2\pi^2 & 4\pi^2 & 0 & 0 \\ 0 & 0 & 2\pi^2 & -2\pi^2 \\ 0 & 0 & -2\pi^2 & 4\pi^2 \end{bmatrix} \begin{bmatrix} H \\ M/L \\ H \\ M/L \\ L \\ L \end{bmatrix} \quad 5.19$$

The linear fixed-head response continues upto the first plastic hinge forming at the head, and is limited to states less than

$$\begin{aligned} H L / M &= 2\pi, & M &= -M \\ \theta &= 0. \end{aligned} \quad 5.20$$

Expressions for the variation of bending moment and shear force with depth are

$$\begin{aligned} M &= a \cdot e^{-az} \cdot \sin az \cdot H \\ &+ e^{-az} \cdot (\cos az + \sin az) \cdot M \\ V &= e^{-az} \cdot (\cos az - \sin az) \cdot H \\ &- 2a \cdot e^{-az} \cdot \sin az \cdot M \end{aligned} \quad 5.21$$

for head loading of a flexible (semi-infinite) pile, from Hetenyi (1946), where $a = \pi/L$. From eqs 5.21 the corresponding equation to that for a rigid pile, equ. 5.13, can be found and using the

fact that $V = 0$ to determine the expression for \dot{R}_{yc} gives

$$M/M_y = e^{-az} / (\sin az - \cos az) \quad 5.22$$

where $\dot{R}_{yc} = \dot{H}_o L / M_c y = 2\pi \cos az / (\sin az - \cos az)$

Solution of equ. 5.22 for $M/M_y = 1$ gives a value for the depth to maximum bending moment, z , and the load at which this bending moment is equal to the plastic moment, namely

$$\begin{aligned} \dot{R}_{yc} &= 9.015 \quad \text{and} \\ z/L_c &= 0.3305. \end{aligned} \quad 5.23$$

Using the value of \dot{R}_{yc} , the total solution at the instant the second plastic hinge appears is

$$\begin{aligned} H_o L_c / M_y &= 15.30, & M_o &= -M_y \\ u_o E L_c / M_y &= 73.38, & \theta_o E L_c / M_y &= 177.95. \end{aligned} \quad 5.24$$

The incremental response of the pile with the two plastic hinges can then be found as before, by separating the problem into two piles with only continuity of deflection at the second plastic hinge. As a simplification the upper pile can be treated as rigid and the lower pile as flexible. This assumption has been checked by using the correct equations for response of piles of intermediate stiffness, and an original length twice the critical length. An error of less than 3% in the head deflection (at $H_o L_c / M_y = 25.30$) arises from the assumption of a rigid upper and flexible lower pile. The incremental response is given by

$$\begin{aligned} \dot{H}_c &= -\dot{H}_o / (2 + \pi L_c / L) \\ \text{and } \dot{u}_o E L_c / \dot{H}_o &= 10.11, & \dot{\theta}_o E L_c / \dot{H}_o &= 73.01 \end{aligned} \quad 5.25$$

and the total response is shown in Fig. 5.2. Once again, no attempt has been made to predict the third plastic hinge.

The curves of Fig. 5.2 and Fig. 5.3 can be used to estimate the loss of stiffness due to pile failure, for stiff and flexible piles. Providing the actual pile length is outside the range $L_c/3 < L < 1.33L_c$ the assumptions made for the flexible or rigid pile solution are appropriate. Within that range of lengths, the procedure may be used with the correct solution for a pile of intermediate stiffness (Hetenyi, 1946) to obtain precise solutions. It appears that no gross errors are involved in the use of an appropriately weighted average of both solutions, since for a pile with $L_c = 1.33L_c$ the two solutions for head deflection at $R = 15$ differ by only 3%.

^yVariations in the procedure allow treatment of piles with a defined head shear and moment ratio and soils that are not uniform. For the problem of fixed-head piles in overconsolidated clay the solutions presented here are adequate for preliminary assessment of the loss of head stiffness caused by pile failure.

The above procedure can be applied to a soil modelled as an elastic continuum, but the two pile sections will now influence each other and an incremental approach is necessary. If the pile is thought to become unserviceable as soon as the first plastic hinge forms, the analysis described here would be all that is needed to estimate the head flexibility change due to pile failure. More involved considerations such as using the continuum model, modelling progressive pile yield and including soil failure, while of use in pure research investigation, are not a significant practical advance over the linear Winkler soil model described here.

5.4 MBEM : Non-linear Behaviour

Section 3.3.3 described a modified boundary element analysis for the laterally loaded pile problem, in which the concept of complete loss of contact between pile and soil (gapping) was introduced in terms of deflection mismatch, Δ . The implementation in the MBEM analysis of the effect of soil gapping and failing will be presented in this Section, together with a parametric study for soil failure. First, there is a discussion of the interface element developed using the mismatch concept.

5.4.1 Soil-pile Mismatch Model

The concepts involved will be discussed first and then the discussion of the modification to the MBEM analysis will follow.

Soil Gapping and Yielding Interface Element Concept

Section 3.5.2 detailed the manner by which the Mindlin plate element can be extended to allow for a soil profile that is not uniform. Just as the non-homogeneous elastic behaviour of the soil can be approximated, so can the pile-soil interface response with regard to non-elastic behaviour. This is effected by using a non-linear interface element connecting an element of pile to an element of soil. The non-elastic behaviour is confined to the non-linear interface element and may take a range of forms.

Various forms of interface element have been used, mainly for finite element application to problems involving limited shear and normal stress transmission between bodies, e.g. Goodman et al. (1968). Also, Spillers and Stoll (1964), Rowe, Booker and Balaam (1978) and Poulos (1982) have employed forms of a limiting interface traction interface in basically elastic analyses of lateral

and axial pile problems. With the exception of Rowe, Booker and Balaam, no detailed descriptions are provided concerning the implementation of the limited traction rules in the pile analysis methods. In this thesis the behaviour of the interface is strictly defined, thus allowing a more complete and correct analysis.

The interface rules used here are capable of defining a wide range of responses and therefore provide a common theoretical concept connecting the range of responses. The formulation involves the assumption that the presence of the non-linear interface element has no effect upon the elastic response. For this reason, in order not to change the geometry of the pile-soil interface, the interface element is assumed to be of negligible thickness. This is consistent with the assumption of infinitely small strain that is inherent in most, if not all, of the methods currently used to analyse piles. The degree of simplicity of the non-linear interface element does not warrant the consideration of such a refinement as a finite strain formulation.

Since the pile cross-section only appears in the analysis in the form of a pile width, the actual shape of the interface element need not be determined. However, because the elastic behaviour has been found to be largely independent of pile cross-section, it is consistent to assume the same independence for the non-linear behaviour. A detailed description of the interface element will now follow in which the parameters used will be defined and then their significance discussed.

The underlying concept of the interface element is that the deflection of the pile and the deflection of the soil are not necessarily equal and the mismatch occurs within the non-linear interface element. The reaction load, W that is transmitted by u

the interface element, will increase until the limiting value, W_y is reached, without any change in the initially zero mismatch in deflections of the pile and soil. Beyond this, a mismatch in deflection, Δu occurs in the interface element, and will be a function of the response of the pile and the remaining elastic soil elements. This mismatch must be such that the product of element total reaction force and the deflection mismatch increment is always positive.

This is a much simplified form of the classical plasticity restriction that plastic work within a failed zone must be everywhere positive. If this rule is not obeyed then it would be possible to recover some of the plastic strain that has occurred. Davis, Ring and Booker (1974) have presented a clear exposition of this aspect of plastic behaviour, and illustrated how erroneous results may follow if negative plastic work is permitted.

Indeed, in any form of analysis with a changing load path it is essential to be able to predict when, and which, portions of the body return to an elastic state. A return to an elastic state may even occur in a monotonic loading sequence if a redistribution of stress away from a previously failed region occurs. This has been ignored in many other non-linear analyses and usually cannot be incorporated because of an inadequate soil model.

Depicted in Fig. 5.4a and 5.4b are the two types of behaviour that can occur. The horizontal axes are the mismatches in deflection between the pile and the soil, Δu and the vertical axes are the interaction load per unit length (W_u) transmitted by the interface element from the soil to the pile. In Fig 5.4a the three possible incrementally elastic states are shown; which one is pertinent depends upon the previous maximum deflection mismatch that has been generated and the width of the gap created.

Case (i) applies when the interface load is given by

$$\frac{|W|}{u} < f \cdot \frac{W}{y} \quad 5.26$$

Also, the pile is between the last position to which the pile failed the soil in the interface element Δu_L , and the position of the soil face in the interface element that was not just recently being failed by the pile, i.e. in a gap which has width u_g . This rigid behaviour, when referred to the mismatch deflection, leads to an elastic incremental load deflection response in the gap. It can be seen that the deflection mismatch Δu , magnitude of total gap formed, u_g , and the last position of the right hand side of the gap, mismatch Δu_L , will define the state of the non-linear interface element, i.e. $\Delta u_L - u_g < \Delta u < \Delta u_L$.

Cases (ii) and (iii) arise when the pile has regained contact on one of the sides of the already formed gap. For these cases the interaction load has limiting values for the positive and negative loads that are dependent upon the face of the soil in the non-linear interface element that is in contact with the pile. The larger magnitude allowable load corresponds to a compressive traction upon the face and the smaller load to either an adhesive traction on the face, or a minimum load arising from side resistance on the pile moving in the gap. The sign convention adopted means that positive reaction load corresponds to a compressive stress in the soil on the right hand side of the gap.

Figure 5.4b shows plastic interface behaviour and it should be noted that the failure loads only correspond to compressive stress at the soil face in contact with the pile, or a tendency to produce compressive stress on the face towards which the pile moves. This feature arises because of the requirement that the

plastic work should be positive. The sign of the sustained load and sign of the mismatch deflection increment must be the same.

Cases (ii) and (iii) correspond to having attained the compressive failure load, which is defined as having a value W_y . When the load W_y is maintained at the interface, the gap between the pile and soil, u_g , will in general grow. The growth of the gap is postulated to be a function of the plastic deflection. A simple linear dependence of gap growth on plastic deflection is the obvious first choice, when initially investigating the model response, but it is clear that more complex functions may be applied. Attention is here directed towards a model in which some fraction, g , of the plastic deflection in the interface element is converted into a gap behind the pile. In this sense "behind" is used to specify the face that is opposite to the current direction of movement of the pile.

$$\dot{u}_g = g \cdot \dot{\Delta u} \quad 5.27$$

When loading reverses, the pile will move back upon its previous course and eventually lose contact with the soil face.

Case (i) has the pile element in the gap and moving at some constant load until recontact is observed (iii). This constant load is defined as some fraction, f , of the load to cause failure, equ. 5.26. As with the failure load (ii) and (iii) any deflection mismatch increment (i) must result in positive plastic work leading to unloading and "rigid" elastic interface behaviour if the direction of pile to soil mismatch reverses.

The choice of the values of f and g will markedly influence the behaviour of the model during repeated loading, but for

monotonic loading these parameters do not affect pile response until near to collapse. This means that in this model the introduction of gapping does not affect the maximum load capacity of the pile or the load-deflection response for virgin load paths until near the collapse load. Only the cyclic response at loads less than the previous maximum will be affected. The changes in elastic interaction behaviour due to gapping require a more complex model and will be considered in detail in Section 5.5.

Varying the value of f from zero to one will model an interface behaviour that for a pile element within the gap, provides no resistance at one extreme, and causes no reduction in resistance from the fully contacting case at the other extreme. The value of f will only change the response while the load is varying, i.e. as would occur with cyclic loading. It would be possible to link the failure load W to the amount of plastic straining and so produce a hardening or softening response. At this stage this aspect is not pursued, since the chosen model of constant ultimate load is considered adequate to model many aspects of the non-linear behaviour of piles under lateral loading.

A non-zero value of f allows for the generation of some resistance within the gap. This resistance may arise from

- a) side shear acting upon the pile or
- b) some reduced strength available in a disturbed zone as defined by the gap width.

In reality if a complete gap forms, with loss of pile contact from the back and front soil face, the two sides of the pile may still remain in some degree of contact with the soil and attract some shear resistance. In this case, it may be realistic to allow this resistance to reduce during cycling, much as has been done

with skin friction in cyclic analysis of axially loaded piles Poulos (1982).

Varying the value of g from zero to one corresponds to the transition between the extremes of no gap formation and complete gap formation during plastic deflection. A value greater than unity seems to be unlikely, but relief of horizontal stress may cause collapse or spalling of the hole over the upper sections of the gapped length, thus causing the infilling of the lower section of the gapped length of the pile. This form of behaviour has been observed in tests performed on piles on loose sand, (Swane, 1983).

It should be noted that in the case of a full gap, with no reduction in soil strength within that gap, the model performance is identical to that if no gap forms. When the gap that forms is a fraction of the plastic deflection (less than unity), the gap formation is an expression of the extent to which soil flows around the pile. Zero gap formation implies complete flow, while complete gap formation corresponds to no flow of soil in the non-linear interface element around the pile.

An important feature of this model is that the deflection mismatch, which corresponds to plastic deflection, must be understood to be a relative measure of deflection. It is helpful to consider the non-linear interface element as a small region of soil through which a pile segment passes when the failure state is reached. The model may be visualised as shown in Fig. 5.5. The thickness of the pile has no part to play in this representation although, in fact, it may have a profound effect upon the resistance encountered by the pile whilst in a gap; this effect is dealt with by choice of an appropriate f factor.

Figure 5.5a shows diagrammatically the pile segment connected to the soil by the interface element before loading commences. For

simplicity it is assumed that no initial gap exists but this may not be true and is not a requirement of the method. The dimension of the pile gap is thus taken as zero, as are the unloaded values of deflection and mismatch in deflection of the pile and soil.

Figure 5.5b shows the result of loading that remains within the elastic state; with the interaction traction, W less than the failure traction, W^u . The pile deflection, u^y , and the soil deflection, u^s , are both equal and no gap, u^g , or mismatch in deflection, Δu , can occur.

After the first plastic state has occurred the pile has deflected more than the elastic soil by the amount, Δu . This mismatch in deflection, Δu , is equal to the plastic deflection in the interface element and is accompanied by the growth of a gap behind the pile, u^g . This gap growth is governed by the g parameter and the value of the increment in mismatch of pile and soil deflections. This is depicted in Fig. 5.5c.

In Fig. 5.5d elastic unloading takes place and the increment in pile and soil deflection are again equal but the total pile deflection is not the same as the total soil deflection.

In Fig. 5.5e the pile has broken away from the front of the soil and is moving towards the soil at the back. This is assumed to happen with a constant resistance to movement that is defined by some fraction of the ultimate available resistance, i.e. $f \cdot W^y$. The mismatch in pile and soil deflection is again changing but now the gap, u^g is not growing. Further, the product of the inter-gap resistance and the increment in deflection mismatch must be positive, following from the restriction of positive plastic work.

Upon recontact with the back of the soil, the situation reverts to a state somewhat similar to that in Fig. 5.5d and if the reversal of loading continues, the mirror image of Fig. 5.5c

is arrived at. Thus two states are defined, one elastic and one plastic, and within each state there is a further subdivision. The elastic state may be elastic within the gap or at one extreme of the gap, and similarly with the plastic state. Therefore, the previous and current values of the deflection of the front and back of the interface element must be known at any time throughout the analysis in order to specify the state that exists.

The final non-linear interface response is shown in Fig. 5.6, where interaction load W and gap width u are plotted against the relative measure of deflection Δu , for a hypothetical cycling of load. Thus, the plot is not the same as the normal p - y plot of the theory of Subgrade Reaction which includes elastic as well as plastic deflection components. It will be apparent that there is no theoretical restriction on the product of interface failure load and the increment in total deflection. Providing the increment in deflection mismatch is of the same sign as the interaction load the sign of the pile total deflection is immaterial.

In terms of W and u versus Δu , Fig. 5.6 demonstrates the element response obtained from a hypothetical cycling of a load on the pile. Symbols (a) to (e) in the diagram correspond to the states possible in the interface element, as depicted in Fig. 5.5. The only possible responses while the load is less than the ultimate are:

Points (a) which correspond to the initial elastic loading.

Points (b) which correspond to elastic loading and unloading.

Points (c) depict the growth of the gap, u , during failure.

Points (d) represent the same behaviour as (a) and (b) but now at one extreme of the gap.

Points (e) correspond to the pile moving in the gap.

5.4.2 Description of Non-linear MBEM Analysis

First, an allowable fraction of the head load increment is calculated, so that the next critical condition (failure, gapping or recontacting) at one element, will just occur. For the pile-soil system the allowable fraction of the induced interface load increments, \dot{W}_u , may be found for a head load increment and added to any existing loads at the interface. The result is that the current load increment causes no new failure, recontacting or gaps in the soil. There are many possible criteria for introducing soil failure or gapping, and these may depend upon critical deflection, load, strain or stress conditions in the soil or pile.

Major differences between this and previous approaches to implementing non-linear behaviour, lie in the manner in which the return to an elastic state, or recontacting of the soil and pile interface, is accomplished. A valid set of critical conditions can be defined and the solution proceed with the correction required for the pile-soil system response. The possibility and details of reversal of those critical conditions can be deferred for the moment, i.e. the critical conditions are assumed to be maintained.

Information concerning the nodes which have gapped or failed for the present valid state is then used to rearrange equ. 3.33 to give the unknown quantities on the left and known quantities on the right of the equality. The program ensures that only one new yielding, gapping or recontacting node will be involved each time a new fraction of load is considered. If any node involves negative plastic work the incremental solution for the current fraction of load must be recalculated with the elements having negative plastic work allowed to return to an elastic state.

Failure of a soil node when the soil reaches a limiting stress, or load, means further increments in \dot{W}_u are normally equal to zero. It is possible to incorporate hardening of the soil response by allowing a certain interaction load increase, after yielding, dependent upon (say) the accumulated plastic deflection Δu . Here it will be assumed that an isolated region of soil has failed, but that the elastic geometry of the soil system is unchanged, and further that \dot{W}_u is zero until a return to an elastic state is achieved. The vector containing the failure loads will be specified as W_y and is a total, not incremental quantity.

When the node fails or gaps there is a known total interaction load and so the allowable incremental interaction load \dot{W}_u on that node may be calculated. For generality we introduce a finite load available when the pile moves in the gap, $f.W_y$, that may be zero. The incremental deflection mismatch between pile and soil, $\dot{\Delta u}$, is non-zero for gapped and failed nodes and every non-zero occurrence of the quantity $\dot{\Delta u}$ must be transferred to the left of the equality.

The original equ. 3.33 from section 3.3.3, neglecting the soil-movement-induced term, W_s , can be expressed in the form

$$\begin{bmatrix} I & 0 \\ 0 & I \end{bmatrix} \begin{bmatrix} \dot{W}_{u1} \\ \dot{W}_{u2} \end{bmatrix} = \begin{bmatrix} \dot{W}_{e1} \\ \dot{W}_{e2} \end{bmatrix} + \begin{bmatrix} B_{11} & B_{12} \\ B_{21} & B_{22} \end{bmatrix} \begin{bmatrix} \dot{\Delta u}_1 \\ \dot{\Delta u}_2 \end{bmatrix} \quad 5.28$$

Upon rearranging equ. 5.28 the system may be reduced to two sets of known and unknown quantities and will take the form

$$- \begin{bmatrix} B_{11} & 0 \\ B_{21} & I \end{bmatrix} \begin{bmatrix} \dot{\Delta u}_1 \\ \dot{W}_{u2} \end{bmatrix} = \begin{bmatrix} \dot{W}_{e1} + \dot{W}_{u1} \\ \dot{W}_{e2} \end{bmatrix} + \begin{bmatrix} B_{12} \\ B_{22} \end{bmatrix} [\dot{\Delta u}_2] \quad 5.29$$

in which one group of unknowns consists of a vector containing $\dot{\Delta u}$ values at gapped or failed elements and the remaining group of unknowns consists of a vector of interaction load increments, \dot{W}_{u2} at linear elements. The right hand side of equ. 5.29 includes the known externally induced incremental elastic loads, \dot{W}_e plus the necessary interaction load increments \dot{W}_{u1} and a term for the effect of the pile-soil deflection mismatches that occur at elastic nodes, $\dot{\Delta u}_2$ which are usually taken to be zero. Elements of \dot{W}_{u1} can be found from the load required to maintain the critical condition and will be taken as zero in the current method, which uses load steps defined by the attaining of critical conditions one at a time and uses a constant plastic failure load.

The form of equ. 5.29 allows for solution of the matrix B_{11} for the righthand side $\dot{W}_{e1} + \dot{W}_{u1}$ and the determination of $\dot{\Delta u}_1$ with little computational effort. The values of $\dot{\Delta u}_1$ then permit equ. 5.28 to give the interaction loads \dot{W}_u directly. Thus, the procedure only involves solution of the full matrix B of equ. 5.28 when all the nodes have become non-linear.

- In summary, the elastic-plastic model includes the effect of,
- a) a constant reaction load at a failed element of soil,
 - b) the growth of a gap as a function of plastic deflection,
 - c) a residual reaction load when the pile moves in the gap,
 - d) changes of state from plastic to elastic and
 - e) recontact of the pile and soil at the limits of the gap.

Discussion of Model for Soil Yield and Gapping

The proposed three-parameter model will produce a response at an interface element as seen in Fig. 5.6. The parameters f and g are arbitrarily chosen here to be one-quarter and one-third respectively; varying the values will only change the degree of the response, not the general form.

In Fig. 5.6a the first, second and third cycles of response caused by some cyclic load on the pile head are plotted. It is assumed that the range of the pile and soil deflection mismatch is unaltered by cycling. It is obvious that the response is not symmetric but is heading towards an anti-symmetric final response. This final response is the same as the one obtained after the first cycle when using a unit value for g . Physically this means the gap is continually growing, as shown in Fig. 5.6b and this growth is linked to repeated returns to the ultimate load. It is considered that this assumption, with gap growth independent of previous load history of the interface element, is unrealistic. The gap is increased even though the pile is passing through the already heavily remoulded soil of the non-linear interface.

If it is assumed that any plastic deflection, of both previously failed as well as unfailed soil interface material, will result in gap growth, then the response gradually "shakes down" towards a final response after a large number of cycles. This final behaviour is the same as if one hundred percent of plastic deflection were converted to a gap, i.e. g equal unity. Previous pile analyses have suggested that shakedown occurs after the first cycle of load, Swane (1983). Thus, the three parameter model may require alteration.

It is considered that allowing every excursion to the yield load to cause gap growth is unrealistic. So a new model is proposed in which only upon the initial passage of the pile through the failing interface material will the mechanism of gap growth come into play. The subsequent failing of the soil will happen with the re-failed soil flowing around the pile. The total width of the gap will not again increase until new extremes of plastic deflection are attained.

This situation is presented in Fig. 5.7 and as shown the response now "shakes down" after the first cycle of load. Regardless of which of the two responses of Figs 5.6 and 5.7 are more correct, the second model provides the limiting soil response of the first with much less computing effort. The limiting response can be taken to be the one of interest in most applications.

As noted previously, the presence of gapping will only become evident when loads are less than the previous maximum load. Thus, the MBEM analysis will provide results comparable to previous non-linear pile analyses for monotonic static load paths, using an improved theory.

5.4.3 Non-linear Soil-pile Response : Parametric Study

The non-linear MBEM analysis can be used to solve for a wide variety of soil types and load forms. Here, attention is limited to piles in a uniform elastic continuum soil with a constant soil failure load with depth. Results are obtained for two piles with length to diameter ratios equal to their critical length to diameter ratios, which are then shown to provide good estimates for piles with lengths longer than critical. Thus the effective length concept (L_e being the shorter of the actual and critical lengths) is also an aid for assessing non-linear pile response.

With a soil failure load W and an effective length of 25 diameters, a pile was analysed^y for 8 ratios of head shear to moment. The ratio for a flexible pile is defined as

$$\beta_c = M_o / H_o L_c \quad 5.30$$

and took values over half the entire range of possible head shear and head moment combinations, because the problem possesses symmetry, with two possibilities associated with the one value of β_c , e.g. negative shear and negative moment gives a positive β_c just as positive shear and moment does. The values begin at -0.5 and end with 0.5. The two values involve a change of sign of both the head shear and moment, and give half of an anti-symmetric plot as in Fig. 5.8, where non-dimensional head shear and moment are plotted against head deflection and rotation respectively.

The values of β_c are chosen so that between each value at the collapse load of the pile, as calculated using the theory of Appendix I, the point of sign change in the load distribution moves one tenth of the pile length, starting at the surface. This ensured an even spread of curves and meant that the point of sign change in the pressure distribution was at the junction of two elements at collapse, which gives an improved modelling.

The form of result presentation of Fig. 5.8 has the drawbacks of hiding the response for deflection due to pure moment, and rotation due to pure shear, and not presenting a well-normalised response with respect to the collapse load. Thus, the head shear and moment loads were converted into a vectorial quantity in H_o vs M_o / L_e space with a magnitude given by

$$R_o = \sqrt{H_o^2 + (M_o / L_e)^2} \quad 5.31$$

and direction given by ω , where $\tan(\omega) = M / H L$.

Values of R at collapse are designated as R_o and for the entire range of values of β , Fig. 5.9 plots R_u for five distributions of soil failure loads, where W_o is the value of W_y at the surface and \bar{W} is the average value over the effective length of the pile. By using R_o and normalising with R_u , the correction factors are defined by the expressions

$$u = F \frac{u}{u_e}$$

$$\text{and } \theta = F \frac{\theta}{\theta_e} \quad 5.32$$

where u_e and θ_e are linear-based deformations from Chapter Four.

Figures 5.10 and 5.11 present the non-linear soil failure deflection factors for piles with both actual and critical lengths of 10 and 25 diameters respectively. There is some difference between the responses of the two piles with different length to diameter ratios, but the general form is consistent. The cases of negative values have factors that do not conform to the accepted monotonically-softening response associated with non-linear behaviour. A reversal of deflection is even predicted for the $\beta = -0.388$ case, which can be seen more easily in Fig. 5.8.

The apparently abnormal behaviour becomes understandable when the problem is considered in more detail. A clue to understanding comes from the fact that the point of zero pressure, which has already been mentioned in connection with the collapse load, will normally move down the pile as more non-linear behaviour appears in the soil. However, for certain negative β values (to be specific, when a negative moment is assumed) the elastic distribution of pressures will have a small compressive component near the surface from the positive head shear, while the negative moment is

sufficient to induce a larger component of compression in the opposite face of the soil. Thus, a small zone near the surface with a compression inconsistent with the sign of head shear, results in a negative initial deflection of the pile head.

When loading is continued to collapse, the point of zero pressure actually moves down the pile, toward the tip. This result is the only one possible from the requirement that the failure load distribution and plastic deflections (which are several times larger than the elastic ones) should not result in negative plastic work. So collapse of the pile-soil system is accompanied by deflections consistent with the direction of head shear, i.e. a positive deflection, rather than the elastic-based deflection. For this to happen, previously failed soil will become elastic, and then fail in the opposite sense. Therefore, the importance of obtaining solutions without negative plastic work is paramount, if a sensible method of following load-deflection response to collapse is required.

The particular case of fixed-head piles presents an interesting feature of non-linear lateral loading. The boundary conditions at the head become mixed, with shear load defined and rotation defined. The result is that the head fixing moment will vary during shear loading, much in the same way that the head rotation will be non-linear for head shear loading with zero head moment for a free-head pile. The initial elastic fixing moment and the fixing moment at collapse can be calculated easily from the linear influence coefficients of Chapter Four and the equations in Appendix I, and represent the limits of the possible values of fixing moment.

From Fig. 5.8b it can be seen that for $\beta = -0.233$ the

rotation of the head, for the free-head pile, is initially small and negative, but collapse is preceded by the rotation reversing and momentarily passing through the fixed-head state. This β value represents one of the intermediate values for head fixing moment for a fixed-head pile. It is also seen from Fig. 5.8b that the collapse value of $\beta (= -0.5)$ does not give a fixed-head response, although near collapse incremental rotation is small.

The case of a fixed-head pile has been analysed and the results are presented in Fig. 5.8c. Head shear is plotted against head deflection and fixing moment in two plots, for four values of length-to-diameter ratio. The manner in which the head fixing moment varies with head shear is clearly non-linear and becomes up to three times that predicted by linear-elastic analysis.

The curves of Figs 5.10 and 5.11 were produced using a pile length equal to the critical length and so the non-dimensional collapse load ratio R/R_u always has a value of one at collapse. The curves can also be applied to piles that have a length longer than critical and this aspect is investigated in Figs 5.12 and 5.13 for the two L/d ratios chosen. To investigate the validity of applying the curves of Figs 5.10 and 5.11, three values of β_c were chosen and four piles of various lengths analysed to produce load-deflection correction factors for non-linear soil response.

Figure 5.12 depicts the response for a pile with L/d of 10 for values of L/d of 7.5, 10, 12.5 and 20. The case of $\beta_c = 0$ shows the pile response indicating collapse at a load of 75% of the normalised critical length collapse load R/R_{uc} for piles with $L/d = 7.5$. This is the correct response and for other values of β_c the correct response can be calculated using Fig. 5.9.

Figure 5.13 depicts the response for a pile with L/d of 25

for values of L/d of 20, 25, 30 and 50. The case of $\beta_c = 0$ the pile response indicates collapse at 80% of the normalised critical length collapse load R/R_{uc} for piles with $L/d = 20$. Again, this is the correct response and for other values of β_c the correct response can be calculated using Fig. 5.9.

Both Fig. 5.12 and Fig. 5.13 illustrate clearly that the non-linear response of piles longer than the critical length (flexible), is conservatively predicted by the curves for a pile with length equal to the critical length. Great simplifications are possible when this fact is employed, as long as it is understood that the critical length collapse load does not always refer to collapse of the soil, but the attaining of a deformation consistent with an unserviceable pile foundation.

The analysis used to obtain these curves has been thoroughly checked against answers for a pile in a Winkler soil from Section 5.3. Further, the incremental response of piles in a non-linear continuum soil from the MBEM analysis has been checked. This was done for cases where soil failure extends from the surface down to a finite depth. The pile-soil interaction equations may be assembled with the failed portion of pile assumed to not be in contact with the soil. This direct solution was found to agree exactly with that from the non-linear MBEM program.

While the results presented in Chapter Four included the bending moment distributions due to head shear and moment, no such curves are given here. Instead, it is recommended that the theory of Appendix I, in providing the equation for bending moment distribution at collapse, is sufficient for design of pile cross-sections. If the effective length is used, adequate values of maximum bending moment and its location can be determined.

5.4.4 Comparison with Previous Non-linear Results

The results presented in this thesis can be compared to previous solutions for lateral loading of piles in non-linear elastic continuum soil models. The analyses of Poulos and Davis (1980) and Davies and Budhu (1986) are used and represent the only comprehensive sets of results available in the literature.

Davies and Budhu have presented a wealth of data on the non-linear response of laterally loaded piles, derived from a boundary element analysis where the soil is modelled as an elastic continuum and the pile as an elastic flexural member. By assigning limiting values of tensile and compressive normal traction and shear traction that act on the pile, an incremental form of the equation of flexure of the pile is used to define the nature of the redistribution of interaction tractions to interface elements that are still linear elastic. The modified boundary element model used in this thesis is somewhat closer to that of Poulos than the model used by Davies and Budhu.

In the technique used in this thesis the mismatch in deflection which would have occurred in the elastic soil (under the total interaction traction distribution with soil failure) and the pile (under an equal but opposite set of tractions), is evaluated directly. This mismatch is an integral part of the solution and is a measure of the plastic deflection. It is not clear from the paper of Davies and Budhu how the authors' incremental algorithm treats this problem.

It is not possible to determine from the paper of Davies and Budhu whether negative plastic work, the definition of which varies according to the non-linear model used, has occurred in the

analysis of the authors. In the MBEM analysis this quantity is evaluated by multiplying the incremental "mismatch" displacement by the total interface traction. Since negative plastic work is an indication of soil stresses being wrongly held on the yield surface, it occurs when soil should be returning to an elastic state. Thus, for failed elements, the sign of incremental plastic work and elastic unloading are inextricably linked.

A comparison is made of results from the MBEM analysis, those of Poulos and Davis (1980) and those of Davies and Budhu for the example of a solid circular pile in a soil, as given in Fig. 5.14. The results, also in Fig. 5.14, show the non-linear load-deflection response of the head according to Davies and Budhu, Poulos and the MBEM analysis, for a pile with an installed length of 10 diameters. The results are derived from reading dimensionless curves designed to modify elastic predictions of response. The correction curves of Fig. 5.10, those presented in Poulos and Davis (1980) and those of Davies and Budhu (1986) were used.

In Fig. 5.14, the results of Poulos and the Author agree well, as might be expected, but Davies and Budhu's results exhibit an earlier departure from linear behaviour and a larger deflection until near the ultimate collapse load (considering failure of the soil only). Davies and Budhu's sets of curves and equations are intended to be applied to piles longer than their predicted effective length ($L/d = 4.8$). This is also true of the results from the MBEM analysis, provided the critical length proposed in Chapter Four is used. As an illustration, Fig. 5.14 shows results from direct use of the MBEM analysis for four piles with the same properties as the example pile, but now with values of length to diameter ratio = 5, 10, 15 and 20. For these cases 20 elements

were used to model either the critical length or the installed length of the pile (whichever was smaller, i.e. "effective").

It may be seen from Fig. 5.14 that the three curves for $L/d = 10, 15$ and 20 are essentially the same for loads up to about 80% of the collapse load for piles with an actual length equal to the critical length, viz $H/C d^2 = 41.4$. Piles longer than the critical length will have collapse loads larger than $H/C d^2 = 41.4$, and for such cases (i.e. $L/d = 15$ and 20) the responses are almost the same, see Fig. 5.14, until their individual collapse loads are approached. Davies and Budhu's predictions, which essentially provide a "backbone" curve for all "flexible" piles, are more conservative than those of the Author for low loads, but comparison of the responses in Fig. 5.14 demonstrates a reversal of this when loading exceeds the Author's critical length based collapse load.

The MBEM analysis predicts a sensibly different linear response for piles of length 5 and 10 diameters, but according to Davies and Budhu's effective length they should behave identically. Even allowing for the differences between the models used to analyse the non-linear response of piles in a failing soil, it appears that the results of the two techniques are inconsistent.

Further, a comparison of the non-linear correction curves of Davies and Budhu with those of the MBEM analysis, suggests a more complex non-linear form may be required than the essentially parabolic load-deformation relationship (linear correction) they propose. While some of the curves of Fig. 5.10 may be closely approximated by straight lines, e.g. for head loads with a positive moment ratio, by no means can the curves with $M/HL < 0$ be

simplified to linear corrections.

The results of the MBEM analysis and those presented by Davies and Budhu represent a new method in a field that has very little established work with which to make comparisons. The widely used p-y approach does not represent a solution with which the formulation of the method may be assessed, rather it represents a different method of analysis of the same problem. The type of comparison made here represents one way with which to establish the elastic-plastic method as a reliable and convenient alternative to the more established and empirical p-y methods of analysis.

5.5 Finite Element Method : Non-linear Behaviour

Although the MBEM analysis has been developed to model non-linear response based upon soil failure and gapping, it still remains a method with no intrinsic differentiation between the front and back faces of the soil-pile interface. The only way in which the effect of a separate front and back is included is within a non-linear pile-soil interface element. The finite element method described in Chapter Three, presents a method by which the soil and pile may be assigned a separate front and back face at any depth, upon which unequal interface stresses act; thus extending the elastic continuum model to take account of a different interaction stress on the back and front face in a gapping and failing soil.

First a Soil Structure Interaction analysis for laterally loaded piles is described, without specifying the source of the soil or pile model, nor assuming the restriction of a biface model of interaction. The biface approach is then developed with the help of a plane strain pile segment analysis, of the type discussed in Chapter Two. The linear elastic response from the pile analysis is checked with existing solutions for a two-layer soil problem and the non-linear response is assessed by using the analytic response for a Winkler soil found in Section 5.3. The response of the biface model is then investigated for soil failure with unequal pressures on the front and back faces, for both a Winkler and an elastic continuum model of the soil.

5.5.1 Soil-Structure Interaction:Analysis

Most methods of analysing laterally loaded piles in an elastic soil employ the modified boundary element approach for the soil response, and the equation of flexure from simple bending theory for the pile. When the stiffness matrices of the pile and soil have been found their combination may take many forms. The resulting equation is some expression of a soil-structure interaction problem. Rowe, Booker and Balaam (1978) have presented a general form for soil-structure interaction problems and it is this form, using influence matrices rather than stiffness matrices, that provides the basis for the analysis used here.

The first step is to produce the relationship connecting forces due to uniform soil loads to average soil displacements at elements of the discretisation.

$$u_s E_d = [I] \begin{pmatrix} F_s \\ F_{se} \end{pmatrix} \quad 5.33$$

Similarly the pile relationship is evaluated,

$$u_p E_d = [I] \begin{pmatrix} -F_p \\ F_{pe} \end{pmatrix} + [A]\theta \quad 5.34$$

where $[I]_s$, $[I]_p$ are the soil and pile influence matrices,
 E_s , E_p are representative soil and pile moduli,
 u_s , u_p are the deflections of soil and pile,
 F_{se} , F_{pe} are the external loads on the interface,
 F_u is a vector of pile-soil interaction loads,
 $[A]$ is the kinematic matrix connecting element deflections to the rigid body movements and
 θ is a vector of rigid body movements, u_o and θ_o .

The extra terms $[A]\theta$ for the pile relationship, arise from

the need for restraint of the pile in order to apply loading and obtain an influence matrix. Once the pile is attached to the soil, the pile restraint arises from compatibility of pile and soil and equilibrium of the forces and moments generated at the arbitrary points of restraint.

For the case of the pile it is found convenient to choose restraint conditions at the head of the pile, where the loading is usually applied. The simplest fixity is that of no lateral deflection or rotation at the ground level. This choice then determines the rigid body motions as the displacement, u and rotation, θ of the pile head and also the form of the $[A]$ matrix.

Having produced them by some means, eqs 5.33 and 5.34 may be used to provide an expression of the mismatch in pile and soil deflections,

$$E_d (u_r - u_p) = -([I']_p + [I']_s) F_u + [I']_p F_{pe} - [I']_s F_{se} + [A] \theta E_d \quad 5.35$$

where $[I']_p = E_r / E_p [I]_p$

$$[I']_s = E_r / E_s [I]_s$$

and E_r is a convenient reference modulus.

The reference modulus can be varied according to the relative magnitude of the elements of the influence matrices in order to maintain the elements in $[I']_p$ and $[I']_s$ of the same magnitude.

The kinematics matrix may now be used again, transposed, to provide the statics matrix for the equations of equilibrium of the forces acting on the pile

$$- [A]^T F_u = - \emptyset \quad 5.36$$

where $\underline{\phi} = \begin{pmatrix} H \\ 0 \\ M \\ 0 \end{pmatrix}^T$

If the A matrix is non-dimensionalised and represented as \underline{A} then the two equations 5.35 and 5.36 may be combined to yield.

$$\begin{bmatrix} 0 & -\underline{A}^T \\ -\underline{A} & I \end{bmatrix} \begin{bmatrix} \underline{\theta} \\ F \\ u \end{bmatrix} = \begin{bmatrix} \underline{\phi} \\ b \end{bmatrix} \quad 5.37$$

with $[I] = [I'] + [I']$
 $b = E d \begin{pmatrix} u_p \\ r \end{pmatrix} - u_s \begin{pmatrix} u_s \\ p \end{pmatrix} + [I']_p F_{pe} - [I']_s F_{se}$

$$\underline{\phi} = \begin{bmatrix} -H \\ 0 \\ -M/d \\ 0 \end{bmatrix}$$

$$\underline{\theta} = \begin{bmatrix} u E d \\ 0 \\ \theta E d^2 \\ 0 \end{bmatrix}$$

From this formulation it is readily seen that the head influence coefficients can be easily recovered in dimensionless form, from the two vectors $\underline{\theta}$ and $\underline{\phi}$, as follows:

$$\begin{matrix} u E d/H & , & u E d^2/M & , & \theta E d^2/H & \text{and} & \theta E d^3/M \\ \text{or } 0 & & \text{or } 0 & & \text{or } 0 & & \text{or } 0 \end{matrix}$$

Equation 5.37 relating loads to pile-soil deflection mismatches, is seen to be similar to equ. 5.28 in Section 5.4.2, and so with Δu replaced by $u_p - u_s$, the scheme of allowing for pile-soil deflection mismatches can be repeated for the new SSI model to give non-linear behaviour. Also, the external loads applied to the pile and soil, F_{se} and F_{pe} , can normally be taken as zero

unless (say) surface loading is applied to the soil.

In determining the soil and pile response, finite element, finite difference or analytic methods could be used. The specific method used here for the soil is finite elements with axisymmetric geometry, using Fourier series to allow for the variation of quantities in the circumferential direction. This has already been presented in Chapter Three (the AGFEM analysis), and the extensions necessary to employ "patch" loadings are given in Appendix II. The soil is fixed at the mesh boundary, so that only a finite volume of soil is modelled. The case of an elastic half space requires zero strain at an infinite distance from the applied load, but for practical purposes there is a finite region beyond which the load has negligible influence. It is this limited region of influence that allows a finite bounding of any elastic finite element discretisation to still reproduce good approximations to half-space response characteristics.

At least two broad alternative representations are possible for the pile. A model utilising the same finite element technique as used for the soil may be employed to create the pile influence matrix or a completely different representation may be used. Such alternative representations include the use of simple bending theory with a finite difference scheme (as has been employed in the boundary element approaches), or an analytic solution for a cantilever loaded by isolated uniform distributed loads.

The analysis is not necessarily restricted to one plane of loading or a biface model and can also be extended to include axial and torsional loading. For a single pile subject to lateral loading, the biface model and loading in one plane however was considered sufficient.

5.5.2 Biface Analysis

For a circular cross-section pile the biface model is depicted in Fig. 5.15, where the geometry of the interface and the extent of the traction applied to one face are given. The effects of the simplification of using just two faces at one depth cannot be judged, because other solutions for this problem do not exist. To gain complete vindication of the applicability of the biface model to problems of lateral pile loading, would require complex three dimensional analyses with progressive soil breakaway. The biface model must be accepted as being an improvement over existing models and the most accessible analysis of the possible ones that can address this problem.

The technique used to give the response for the biface model involves modelling uniform directed tractions, around half of the pile-soil interface, using a limited number of the Fourier terms of a series that in the limit would provide the desired traction distribution. This aspect of the biface model can be checked and, to this end, the plane strain pile segment is employed.

Modelling of Plane Strain Pile Segments

A plane strain pile segment analysis has been suggested as a method of obtaining soil response to pile loading. The assumption often made is that the soil behaves as thin discs at stations down the pile, with the behaviour of each disc isolated from all others. In fact, a plane stress disc might be more appropriate, Yegian and Wright (1973), however, it may be said without question that the plane strain pile segment is a problem that is similar to that of a laterally loaded pile. To be precise, it represents a pile of infinite length loaded in such a manner as to induce a constant interaction load along its entire length and no rotation.

Without relying on the plain strain pile segment being a good way to represent a laterally loaded pile, it can be used to:

- a) provide a means of assessing the difference in behaviour between rough and smooth interfaces.
- b) verify the applicability of the biface analysis approach to an elastic soil-structure interaction problem.
- c) with an elastic-plastic soil model it can assess the effect of gapping upon the failure load.

a) Rough and Smooth Pile Segment

It is normally considered that sufficient pile-soil interface shear can be generated without vertical or circumferential slip. However, it is useful to bound the magnitude of increase in deflection, above that occurring for a rough interface segment, caused by the interface being unable to sustain any shear tractions in the circumferential direction.

In order to model the smooth case, the axisymmetric geometry finite element method (AGFEM) is used with dual nodes at the interface between the pile segment and elastic soil. This is depicted in Fig. 5.16a, where the two (AGFEM) meshes for direct analysis of the plane strain pile segment and the biface modelling of the plane strain rigid pile segment problem are drawn. The upper mesh is for the antisymmetric direct analysis, with Fourier term $k = 1$ in which the rigid pile segment is modelled by stiffer finite elements for the first three radial elements and the constraint $U_{ri} = U_{ri+3}$ is imposed for nodes numbered i equal to 16, 17 and 18 at the interface between the rigid pile segment and the soil.

It is a feature of the finite element program that the linear

constraint may be applied to the coordinate-based degrees of freedom of one particular node. This allows a direction-defined constraining boundary to the finite element mesh to be used, which may be an important feature in specialised applications. If the direction in a vertical plane is given by α then, as in Fig. 5.16, $U_z = U_r \tan \alpha$ will apply, with α measured anti-clockwise from the horizontal plane. An application of a similar type has already been mentioned in Chapter Three, for radial and circumferential deflections along the centre line of the axisymmetric elastic body, where $U_\theta = -U_r$ for $k = 1$.

For the present problem, because the radial and vertical deflections (u_r and u_z) are both modelled by a cosine variation with circumferential position, deflection maxima (U_r and U_z) may be visualised as being in the same plane ($\theta = 0$) while the circumferential deflection, u_θ with a sine variation is a maximum, U_θ in a plane at right angles ($\theta = 90^\circ$). Thus the imposed constraint at the pile-soil interface for a Fourier analysis with $k = 1$ can be interpreted as a rigid body lateral translation of the pile segment.

The results of the analysis of the plane strain pile segment predict an increase in deflection of the smooth pile segment when compared to the rough case of the order of 19%, since

$$\bar{u}_x \frac{Eh}{F_x} = 0.532 \quad (\text{Rough}) \text{ and}$$

$$\bar{u}_x \frac{Eh}{F_x} = 0.633 \quad (\text{Smooth})$$

where h is the thickness of the plane strain disc, E the Young's modulus of the soil, Poisson's ratio of the soil is 0.3 and F_x is the total force in the x -direction.

This difference is understandable, since the smooth interface has no contributions to resistance from the shear, caused by

circumferential compatibility, which is symmetrical about the line of action of the resultant of the external loading for the rough pile. The result does not follow the grossly simplified concept of halving the stiffness that Winkler type theory would suggest (assuming shear and normal Coefficients of Subgrade Reaction are equal). The elastic continuum model predicts a more complex redistribution of strain throughout the body.

The Fourier coefficients for the stresses near the interface are given in Table 5.1. These values are obtained by linear extrapolation to the interface, of the stress values at the Gauss points and generally are within 5% of the Gauss point values, thus verifying the adequacy of the mesh discretisation.

From these results it can be seen that the interface tractions take the form.

$$p_{rr} = \frac{F}{x} \frac{1}{r_0} \cos \theta \quad (\text{Smooth}),$$

$$p_{rr} = \frac{F}{x} \frac{1}{2 r_0} \cos \theta \quad (\text{Rough}) \text{ and}$$

$$t_{r\theta} = - \frac{F}{x} \frac{1}{2 r_0} \sin \theta \quad (\text{Rough}).$$

These tractions are consistent with the equilibrium of the generated interface tractions and the x-directed force, F in both cases. The rough case agrees with the analytic solution of Baguelin, Frank and Said (1977) for tractions, see later, equ. 5.41, and the load-deflection behaviour which was presented in Fig. 2.6 of Chapter Two, see also later, equ. 5.42.

From the cosine variation of the vertical stress with circumferential position, it can be deduced that both the rough and the smooth interface cases involve a bending moment. However, the stresses that produce the bending moment are not a linear

function of position from the neutral axis and so simple bending theory is not applicable. The pile segment neither hogs nor sags, since the restriction of no vertical strains enforces longitudinal elements of the pile segment to suffer no relative displacement along its (infinite) length. However, it still may support a hogging or sagging "bending moment" from the "Poisson's effect" that generates stresses without accompanying strains.

If the vertical axis is viewed as being horizontal and the x axis (i.e. the direction of loading) is directed downwards, the problem is similar to a long pipe buried deep in an Elastic soil. The pipe is loaded by gravity acting upon material passing through the pipe. The indications are that the assumption of a fully bonded, rough interface will lead to a "sagging moment" being generated while the smooth interface assumption, with only radial compatibility, predicts a "hogging moment". These moments are an indication of the restraints required to satisfy the plane strain restriction of the analysis. How much of this behaviour is a result of the fixing of the boundary of the mesh used is open to conjecture. Thus the application of this result to the settlement of a long, buried pipe is somewhat questionable.

With regard to the behaviour of laterally loaded piles, the only case that might provide a true plane strain condition is that of a fixed head, rigid, long pile under lateral load. Such a large pile to soil relative stiffness would rarely, if ever, occur for piles that are long enough to allow consideration of the deep pile segments as a plane strain problem.

Of more concern is the circumferential stress generated within the soil near the interface. The smooth case predicts tensile stresses in the soil near the front face with a magnitude

of the order of one-quarter of the compressive radial stress. This is in contrast to the circumferential compression of nearly half the radial compression predicted for the rough case. Thus, the rough and smooth interface assumptions tend to cause tension in the soil near the interface but on different sides, i.e. in front of, or behind, the advancing pile segment.

When deciding which of the two assumptions is more appropriate, it is useful to consider the kinematics involved in each case. For the rough interface case the pile and soil will undergo the same average deflection in the x coordinate direction, i.e. the direction of the resultant of the applied load. Consideration of the smooth case however will lead to the soil and pile having different average deflections. This arises from the definition of the average deflection \bar{u}_x as

$$2 \pi r_o \bar{u}_x = \int_0^{2 \pi} u_{x o} r_o d\theta \quad 5.38$$

where $u_x = U_r \cos^2 \theta - U_\theta \sin^2 \theta$.

This is the value of uniform x-directed deflection, that when multiplied by the arc length of the back or front half of the pile circumference, produces the same sum as if the actual variation of x-directed deflection were integrated around the back or front half of the pile circumference. The integration leads to

$$\bar{u}_x = (U_r - U_\theta) / 2. \quad 5.39$$

The smooth pile-soil interface will undergo a smaller average deflection in the x direction since the relative slipping around the sides of the pile leads to a smaller magnitude circumferential

deflection, given by U_{θ} , than that which occurs for the rough case. A more complete investigation of this aspect requires a change to finite, as opposed to infinitely small, deformation theory. This aspect is outside the scope of the current work.

The assumption preferred for the laterally loaded pile biface analysis is to take the average deflections of the pile and soil when analysed separately, and as defined by equ. 5.38. The average is extended vertically over the area of the interface element by recourse to numerical integration of the shape function of the finite element. By this manner, the average deflection of the soil from an analysis using the applied tractions as shown in Fig. 5.17a (i.e. just the anti-symmetric term $k = 1$) and the lower mesh of Fig. 5.16a yields a value of

$$\bar{u}_x \frac{Eh}{F} = 0.532.$$

This value agrees exactly with the answer from the analysis that actually modelled the pile segment, and this value is within 0.3% of the analytic answer for the rough pile-soil interface.

Thus, the average deflection used to model the response of the plane strain pile segment interacting with the soil, provides an adequate means of representing the soil and pile. The effect of assuming a smooth pile-soil interface is to increase the deflection by only 19% and involves behaviour more suited to analyses capable of modelling large deflection/strain behaviour. The plane strain analysis suggests an average deflection-based influence coefficient and a rough interface represent a suitable form for soil-structure interaction analyses.

b) Biface Test Problem

It has been proposed by Baguelin, Frank and Said, (1977) and others, that the behaviour of the soil and pile at depth can be approximated by a horizontal plane of soil containing the pile segment acting in plane strain, i.e. no vertical strains. This approximation of plane strain has also been the basis of much work concerning the non-linear and plastic collapse behaviour of deep pile segments, Poulos and Davis (1980), Randolph & Houlsby (1984). Therefore a precedent for such an approach as an aid to analysis of laterally loaded piles exists.

While the three dimensional nature of the pile problem does not necessarily contain any strictly plane strain behaviour, it seems that a plane strain analysis is a closely related simple test problem that can be considered when assessing the accuracy of the proposed front-back biface method. It must be emphasised that the results of this test problem are not proposed as being of value in any pile analysis that is contained in this work. It is merely the ability of the proposed method to analyse the test problem, which also has often been applied to analysis of laterally loaded piles, that is considered here.

The plane strain pile segment problem can be solved in three ways:

- a) analytic solution, as presented by Baguelin et al. (1977).
- b) the conventional plane strain finite element analysis, see Figs 5.16b and 5.16c.
- c) the axisymmetric geometry finite element analysis, see Fig. 5.16a.

Of these, the analytic solution has been commonly restricted to a full contact analysis, although Pyke and Beikae (1984) have presented a solution designed to model breakaway, while the finite

element solutions can allow for soil-pile breakaway.

The mesh of Fig. 5.16c has been constructed in such a way that the pile and soil make no contact over a specified section. Actually, the nodes at which separation is forced are dual nodes with no compatibility between deflections, which does not eliminate the possibility of the pile and soil elements overlapping. The finite element employed here uses a quadratic shape function and therefore cannot exactly model the circular geometry which involves trigonometric functions. Thus, attempts at calculating the regions of overlap are not conclusive.

The axisymmetric finite element meshes for the plane strain problem are given in Fig. 5.16a, and can be seen to provide a much more economical analysis than the normal plane strain meshes of Figs 5.16b and 5.16c. Further, the geometry of the region discretised corresponds exactly to the circular geometry of the pile segment problem. From this regard, the AGFEM results are more accurate than the plane strain FEM results, given the same radial arrangement of elements.

Because the analysis is not required to model an infinite extent of soil and to improve the accuracy of the plane strain FEM analysis, it is appropriate to make no attempt at modelling an infinite lateral extent to the plane strain problem. Baguelin et al. (1977) have indicated that a model with a fixed boundary at more than thirty pile radii was a fair approximation to pile behaviour. Therefore, the rough circular boundary was chosen to be at a distance of ten pile-segment radii from the centre of the pile segment. This provides a domain that can be accurately discretised and the circular geometry is matched precisely by that of the axisymmetric geometry in the AGFEM analysis.

The mesh chosen for modelling breakaway is shown in Fig. 5.16c and schematically indicates the restraints employed to take advantage of the symmetry of the geometry and the loading. The inner radius of the pile segment is one-half while the outer radius is unity. The circumferential discretisation gives sixteen equal-angled segments, while radially the element widths grade from small values near the soil-pile interface to larger values near the fixed outer boundary at 10 interface radii. The inner three radial elements model the pile segment and are assigned a Young's modulus that is one thousand times that for the remaining eight radial soil elements. This ensures that the pile has an essentially rigid response when compared with the soil.

By using such a stiff pile-to-soil modular ratio, for the full contact problem, shown in Fig. 5.16b, the load can be applied on the inner surface of the pile segment in virtually any form (discrete nodal forces or distributed load) that has an imbalance in total x-directed forces. A unit depth and a unit positive radial load over the front half (and from the symmetry of the problem a negative radial load over the back half of the plane strain pile segment) at a radius of one-half, gives a resultant x-directed load, F of unity. This loading is transferred to the soil at the interface radius of unity. Because of the rigidity of the pile the stress distribution in the soil near the interface is unaffected by the distribution of the applied load.

Baguelin et al. (1977) have presented equations for the stress state in the soil and at the interface these result in the approximate expressions

$$\sigma_{rr} = \frac{F}{2\pi r} \cdot \cos \theta$$

$$\begin{aligned} \sigma_{\theta\theta} &= \frac{F}{2\pi r_o} \cdot \frac{V}{1-V} \cdot \cos \theta \\ \tau_{r\theta} &= - \frac{F}{2\pi r_o} \cdot \sin \theta \end{aligned} \quad 5.41$$

As seen in Fig. 5.17a, the finite element results for the interface stresses (which are the same from both meshes, Fig. 5.16b and Fig. 5.16c) fit the above equations very well, especially when it is considered that the stresses from the finite element method are at Gauss points some small distance from the interface.

Thus the finite element and theoretical solutions for interface stresses both agree for the case in which the pile segment and soil remain in contact. The case of a smooth pile-soil interface was considered in the previous section using the axisymmetric geometry finite element method. This solution for a full contact case is a result consistent with the assumptions made by most researchers, who have assumed that full contact is preserved.

Also provided by Baguelin et al. (1977) is enough information to derive an expression for the deflection of the rigid pile segment as a function of Poisson's ratio. This has been plotted in Fig. 2.6 as a dimensionless influence coefficient using the equation

$$\frac{uEh}{F} = \frac{1}{8\pi} \left(\frac{1+V}{1-V} \right) \left\{ (3-4V) \ln(R/r_o)^2 - \frac{2}{(3-4V)} \right\} \quad 5.42$$

where R is the fixed outer radius.

Also plotted are two sets of points corresponding to an approximate solution found in Chapter Three for the average deflection of a rigid square situated vertically, both at the surface and at infinite depth in a homogeneous elastic half-space.

It can be seen that the solution is very sensitive to values of Poisson's ratio as the incompressible limit of behaviour ($\nu = 0.5$) is approached. The rigid square behaviour is seen to bracket the plane strain result, suggesting that the plane strain behaviour is not vastly different from the fully three-dimensional response. However, the three-dimensional behaviour is known to be insensitive to variation of Poisson's ratio. The opposite applies to the results of the plane strain problem, and thus it could be inappropriate to use it for undrained conditions.

The mesh of Fig. 5.16c, with the dual nodes, is used to analyse the problem where the back of the pile segment has no compatibility of deflections over the chosen arc length. For the biface analysis this arc is from $\pi/2 < \theta < \pi$ (and $\pi < \theta < 3\pi/2$ from symmetry) and the resulting interface stresses are given in Fig. 5.17b. Clearly the stress distribution becomes more complex than that in Fig. 5.17a, since stress concentrations arise at the junction of the full-contact region and the stress-free face.

The average deflection of the front face of the soil (and pile segment) u_{FF} , and the average deflection of the back face of the soil u_{BF} , due to loading of the front face, are the quantities that are required in a biface SSI analysis. From the plane strain finite element results these deflections are

$$u_{FF} \frac{Eh}{F} = 0.719 \quad \text{and}$$

$$u_{BF} \frac{Eh}{F} = 0.351.$$

Thus, the AGFEM analysis must be shown to produce adequate estimates of these deflections and the first stage is to define the form of the interface traction that will be used for the half-contact analysis. Fig. 5.17b presents the form of the interface

traction found from the finite element analysis and shows one of possible method of approximation. By defining the radial normal traction to be a cosine function and the circumferential shear traction to be a sine function of circumferential position θ , within the range $-\pi/2 < \theta < \pi/2$, and both tractions to be zero elsewhere, there is reasonable agreement with the finite element result. Another alternative is to assign the radial normal traction a cosine squared variation and take the shear traction as the product of a sine and cosine function.

The former traction distribution results in an x-directed uniform traction around the interface, while the latter induces a uniform normal stress in the x coordinate direction in the soil. Both of these forms were considered as possibilities and, using Table II.1, could be synthesised by the AGFEM analysis using the "patch" loading of Appendix II. Table 5.4 presents the intermediate results in the form of the Fourier coefficients of deflection due to unit Fourier load term, the deflections after multiplying by the Fourier terms for x-directed traction load, p_x and the deflections after multiplying by the terms for loading as an x-directed uniform stress in the soil, σ_{xx} .

The last column does not contain entries for Fourier terms, k higher than two. This is because of the use of an average x-directed deflection in the model. The definition of the average deflection, equ. 5.38, leads to the front and back deflections due to loading of (say) the front face being calculated by

$$\begin{aligned}
 u_{\text{FF}} = u_{\text{BF}} &= \left(\frac{1}{r} U_r - \frac{1}{\theta} U_\theta \right) / 2 + \frac{2}{\pi} \left[\frac{0}{r} U_r + \left(\frac{2}{r} U_r - \frac{2}{\theta} U_\theta \right) / 3 - \left(\frac{4}{r} U_r - \frac{4}{\theta} U_\theta \right) / 15 \right. \\
 &\quad \left. + \left(\frac{6}{r} U_r - \frac{6}{\theta} U_\theta \right) / 35 - \dots \right] \quad 5.43
 \end{aligned}$$

Since, for k greater than 2, the Fourier terms used to model the uniform-stress load case only have non-zero values for odd terms, and only even terms are involved in the average deflection calculation, there is no influence for any term greater than 2, i.e.

$$p_r = p_r^0 + \frac{1}{r} p_r \cos \theta + \frac{2}{r} p_r \cos 2\theta + \dots$$

$$p_\theta = \frac{1}{\theta} p_\theta \sin \theta + \frac{2}{\theta} p_\theta \sin 2\theta + \dots \quad 5.44$$

where $p_r^0 = 1/4$, $\frac{1}{r} p_r = 4/3 \pi$, $\frac{2}{r} p_r = 1/4$

$$\frac{1}{\theta} p_\theta = -2/3 \pi \text{ and } \frac{2}{\theta} p_\theta = -1/4$$

which is all that is required from the series in order to provide an exact value for the average deflections.

However, the x -directed traction loading does not present such a feature, since the load form is now given by the series

$$p_r = \frac{1}{\pi} + \frac{1}{2} \cos \theta + \frac{2}{3\pi} \cos 2\theta - \frac{2}{15\pi} \cos 4\theta + \frac{2}{35\pi} \cos 6\theta \dots$$

$$p_\theta = -\frac{1}{2} \sin \theta - \frac{4}{3\pi} \sin 2\theta + \frac{8}{15\pi} \sin 4\theta - \frac{12}{35\pi} \sin 6\theta \dots$$

5.45

which contains even terms that coincide with those of the equation for the average deflection, equ. 5.43. The results from Table 5.4 for the deflections in the case of an x -directed traction, p_x are

$$u_{FF} \frac{Eh}{F} = 0.771 \text{ and}$$

$$u_{BF} \frac{Eh}{F} = 0.292.$$

While those for the uniform x -directed stress, σ_{xx} are

$$u_{FF} \frac{Eh}{F} = 0.808 \text{ and}$$

$$u_{BF} \frac{Eh}{F} = 0.255.$$

Comparing these results with those from the plane strain control problem, reveals a closer modelling is possible using the x-directed traction scheme of loading. The analysis has used six terms in the x-directed traction case and the effect of the last three terms is not very significant. Indeed, the use of only the first three terms gives an answer closer to that from the control problem than that from using six terms, u_{FF} being 6% higher and u_{BF} 17% lower than the control answers. Considering the fact that the AGFEM mesh and analysis are likely to be more accurate than the plane strain FEM analysis, and the greater degree of uncertainty associated with the actual form of the biface condition with respect to a real soil, the x-directed traction model is seen to give sensible and adequately accurate results.

c) Non-linear Model of Soil-Pile Interface

Standard methods of incorporating non-linear soil behaviour have involved estimating the ultimate lateral load required to cause collapse of an element of soil containing the pile. The loads can be found by engineering approximation analyses, results from classical plasticity for simplified problems or from experience with previous full scale tests, e.g. Matlock and Reese (1960), Poulos and Davis (1980) and Broms (1965).

These failure loads for an element of soil take no account of the proximity of other failed soil elements and do not incorporate three-dimensional behaviour except in an approximate manner. The loads are also implicitly linked with the behaviour of the full pile cross-section, i.e. they include the back and front in the one element. There is no formulation for loads on a pile segment where the front and back are treated separately. The closest any method of analysis comes to this is when a gap is assumed to have formed behind the moving pile, (Matlock, Foo and Bryant, 1978).

For this reason a new approach has been adopted herein, employing elements of previous work but being strictly applied to the behaviour of the front and back soil elements. Swane (1983) has introduced a degree of rational organisation to the various modes of pile movement through the soil at failure. He divides the soil response into three categories namely

- a) adhesive,
- b) gapping and
- c) flowing soil behaviour.

He recommended the situations within which each type of failure may occur. The method of incorporating the various stages of behaviour was an assignment of separate tension and compression properties to the Winkler springs.

Within the framework of elastic soil behaviour, applied here to the analysis laterally loaded piles, it is not possible to change spring stiffnesses since none are assumed in the method. The approach adopted here has been to use a deflection mismatch between the pile deflection and the soil deflection that would have occurred if the interface only transmitted a limited amount of load. All the while the soil is elastic and linear the mismatch in pile and soil deflections is seen to be zero.

As an element of soil reaches a critical state the pile and elastic soil can be thought of as losing contact and a mismatch in deflection arises. If the pile is moving away from a soil face, a gap situation may arise or the soil may flow to fill in the mismatch in deflection. Alternatively, if the pile is moving into the soil the mismatch between the pile and the elastic soil may be interpreted as a plastic deflection. This plastic deflection or

flow may be thought of as existing in a thin film of soil at the pile-soil interface and is non-recoverable.

If axial behaviour is considered this would be quite realistically a case of slip between two elastic bodies. For lateral behaviour however the slip becomes an actual penetration of the pile into the failed region. If it is considered that the soil which is failing does so in a thin band, then the elastic region of soil involved in interaction with the pile is essentially unaltered.

A limited investigation into the non-linear response of an elastic-plastic soil model for the specific problem of a circular pile section acting in a plane strain soil that obeys the Tresca failure criteria is considered. Both full contact and the half-contact situation associated with the biface model are analysed for a soil with an undrained shear strength, c_u . In a total stress analysis, the initial stress value makes no difference to the result, since it is assumed that there is no change in effective stress and thus the back and front soil has the same shear strength.

The elastic-plastic plane strain finite element program was first checked against the solution of Koiter (1953) for the problem of a plane strain elastic-plastic cylinder under internal pressure. The results are given in Fig. 5.18 as a plot of internal pressure against the deflection of the internal radius. The indications are that the deflection for a given load level, and also the collapse load, will be slightly overestimated.

The mesh of Fig. 5.16b was used to analyse for the load-deflection behaviour of the pile segment upto collapse of the soil. Figure 5.19 shows the load-deflection curve resulting from

the analysis. The collapse load predicted by Randolph and Houlsby (1984) is indicated in the figure, and as might be expected, the finite element analysis overpredicts the collapse load. However, the fine discretisation and the nature of the problem do allow a definite value of the collapse load to be found, which has often not been the case for other attempts at calculating collapse loads using finite elements, e.g. Baguelin et al. (1977).

Also in Fig. 5.19 is a curve resulting from analysis using the mesh of Fig. 5.16c with half-contact. The larger size of the mesh and the large strains associated with the amount of load that could be applied before computing time became grossly excessive, precluded loading to collapse. The results obtained suggest that the load may well continue to increase but that excessive deflections would occur long before true collapse was achieved, although an apparent collapse lower than that for full contact might be proposed.

Rowe and Davis (1982) have presented results for the problem of a soil anchor using an elastic-plastic finite element model with allowance for breakaway. They also conclude that the collapse load with breakaway is the same as that with no breakaway, but failure of the anchor is evident long before this from excessive deflection.

For the biface model the soil failure load is not affected by breakaway of soil from the opposite face. This assumption is consistent with the findings of this section and those of others. Until a more advanced analysis of the three-dimensional nature of pile-soil interaction is forthcoming, the biface model, as presented here, remains the most promising tool with which to account for non-linear behaviour.

5.5.3 SSI Analysis Verification

The SSI analysis using the finite element-based soil and pile influence matrices is checked by analysing a simple two-layer soil problem. This establishes the correctness of the analysis for linear elastic problems and provides some more proof of the effectiveness of the non-homogeneous modification method used in the MBEM analysis. The non-linear behaviour is checked by modelling a non-linear elastic gapping problem using the influence matrix from an analytic solution of a cantilever with uniformly distributed loading over elemental areas and a Winkler-based soil influence matrix. Finally, the method of approximation for the interface traction distribution is assessed for the SSI biface analysis using an elastic continuum soil.

Two-layer Soil Problem

A set of solutions for laterally loaded piles in a two-layered elastic continuum soil has been presented by Pise (1982). He employed the point force solution of Mindlin (1936) in an unspecified manner that allowed treatment of a non-homogeneous, layered soil. His results cover three values of relative pile-soil stiffness, given by $E_p I_p / E_b L^4$ values of 10^{-1} , 10^{-3} and 10^{-5} , using twenty elements in a model similar to that of Spillers and Stoll (1964). The modulus of the base layer, E_b has been used as the representative soil modulus for non-dimensionalising the response and a top modulus, E_t to base modulus ratio, and, together with a ratio of the top layer thickness L_t to full pile length L_s , defines the problem. The variation of response with length to diameter ratio has not been presented and the results are strictly only valid for the chosen length to diameter ratio of twenty five.

The three methods developed in this thesis for analysis of piles in an elastic continuum have been used to analyse this problem and the results are in good agreement with one another. Figure 5.20 depicts the deflected shapes of the stiff and flexible piles from the three methods of analysis. As might be expected the MBEM analysis predicts larger deflections, consistent with the infinitely larger volume of soil that is modelled compared to the SSI and full mesh direct FEM analyses. The bending moment distributions for the stiff pile are presented in Fig. 5.21 and again the agreement between the SSI and FEM direct analyses are very good and the MBEM analysis, with its modification of the uniform soil response, predicts less than 10% more for the maximum bending moment.

The results of Pise are very close to those from the MBEM analysis, typically being within 10% of each other for the head deflection due to head shear and the value of maximum bending moment. For this reason the results of the MBEM analysis only are plotted in Figs 5.22 and 5.23, where the above-mentioned head deflection and maximum bending moment from the SSI and FEM analyses are compared. The results for small layer and modulus ratios provide the least satisfactory agreement, where the effects of the coarseness of the SSI discretisation become evident.

The SSI analysis for a pile in an elastic continuum agrees with results found from direct analyses using the FEM meshes and the MBEM analyses, and further, all the methods are in good agreement with the results presented by Pise for a pile with a length to diameter ratio of 25 in an elastic continuum. Thus, the SSI analysis gives satisfactory results for a linear elastic continuum based laterally loaded pile.

Non-linear Elastic Gapping

While the study of the Winkler soil model is a good way to introduce soil-pile breakaway behaviour, questions arise about the applicability of such an approach that limits the usefulness of the Winkler results. One use for the Winkler results is to confirm the modelling technique used in the biface Soil Structure Interaction (SSI) program. By comparing the predictions from the SSI approach for a Winkler soil with results from the theoretical analysis of section 5.3, it is possible to quantify the errors of the SSI numerical method.

Since the Winkler solution is independent of the value of length-to-diameter ratio it is only necessary to use one value of this ratio. To non-dimensionalise the rigid pile solution it is best to use the pile length and soil modulus at the tip. If a flexible pile is considered, the critical length should be used, together with the modulus at that depth. An intermediate flexibility pile solution is most conveniently made dimensionless by using the actual pile length and tip modulus. These two schemes are used in an unconventional presentation of the limiting cases of rigid and flexible piles where SSI results for head shear and moment loading are compared with those from Winkler Theory.

The results for a rigid pile in a uniform Winkler soil are plotted in Fig. 5.24, and are presented as four curves, two for deflection and rotation with full contact and another two for full breakaway. The standard response of head deflection and rotation to head shear and moment are shown in a non-standard form, each response being multiplied by quantities that ensure the slopes of the lines represent the incremental form of the influence coefficients given in Section 4.2.2, I_{uH} , $I_{\theta H} = I_{uM}$ and $I_{\theta M}$.

Each curve is actually two curves super-imposed, each

starting at zero load and being the result of two loadings of the pile head; first with a unit shear alone, ($H=1, M=0$) then the unit shear is reduced to zero while at the same time applying a value of moment numerically equal to the effective length of the pile ($H=0, M=L$); the procedure was then reversed, applying the moment first, then the unit shear as the moment was removed.

Because no non-recoverable deflections are involved, the solution cannot produce locked in residual stresses upon load removal, above those existing before loading. With no permanent deflections all load paths leading to the same total load must result in the same total response, although the individual paths may be very different. Both load paths result in the same deflection and rotation at the same head loads which verifies that the elastic nature of the linear and non-linear problems is correctly modelled. The deflection and rotation responses meet along the horizontal axis, for each of the two cases of breakaway and no breakaway, since the solutions obey the reciprocal theorem.

The results for full separation have been obtained by using very small self-equilibrating loads for the unloaded state, in order to model the insitu lateral stress condition. The program was organised to allow progressive breakaway and so is unable to model the case of breakaway occurring at the instant of loading. It would be possible to do this by using large initial stresses which inhibit all breakaway, and employing a Subgrade Modulus of half the normally chosen value, but this would also avoid checking the solution scheme.

The preceding analyses assume a simple model in which equal support from front and back of the soil at any one depth will be available up until separation of a front or back face occurs.

Swane (1983) has used a model wherein the stiffness of tension and compression elements at one depth are allowed to vary. However the simplest assumption is most convenient to use here, in order to quantify the errors arising from the SSI method. From the above it is obvious that some small region of the loading history will involve the progressive growth of zones of separation. The small initial stress chosen has minimised the extent of this region but it is not possible to completely remove such behaviour and still maintain a stable solution.

It was noticed that the load level at which the response is virtually equivalent to full separation can be well short of that at which all elements have separated. This indicates the minor influence that some individual elements have upon total response. However, too coarse an arrangement of elements will negate the validity of the above statement. The insitu stresses chosen ensured full separation at the maximum head shear and moment loads that were applied to the rigid piles in Winkler soils with both a uniform and linear distribution of stiffness.

Careful study of the response of a rigid pile in a proportionally distributed stiffness (linear) Winkler soil, Fig. 5.25, shows that the "full-contact" rotation due to moment load ($\theta, M=L$) and the "complete-breakaway" deflection ($u^*, H=1$) due to shear load are not on the same point at maximum applied load. This coincidence might be expected since analytically

$$u_E \frac{L}{H} = 18 \quad (\text{full contact})$$

$$\text{thus leading to } u^* \frac{E L}{H} = 36 \quad (\text{complete breakaway})$$

$$\text{which is the same as } \theta \frac{E L}{M} = 36 \quad (\text{full contact}).$$

However, this coincidence of the complete breakaway and full contact results relies upon complete breakaway forming at the instant the load is applied. It has already been mentioned that such behaviour is not available from the program and indeed, such a response is most unlikely to occur practically. Thus, the responses will only be comparable to the analytic solution when incremental behaviour is considered, i.e. the slopes are equal.

Table 5.2 compares the incremental response values of derived ratios of breakaway to full contact response of rigid piles from the numerical results with the analytic answers from Section 5.2. Also included in the Table are the values of response ratio achieved from considering a flexible pile in both a uniform and linearly increasing stiffness Winkler soil. The numerical results are very good, the maximum error being less than 0.25%.

It is clear that rigid and flexible piles in both a uniform and linearly varying stiffness Winkler soil profile, reach a limiting response where all effective elements of the pile have separated from the soil where tension is imminent. The rigid pile has separation throughout the full length of the pile. A flexible pile may achieve separation along its full length, but at least must have gapped over its effective length before the incremental response stabilises. Both rigid and flexible piles essentially attain full separation response before all elements have separated within the effective length. This shows the lack of importance of the response of single elements upon the head behaviour, especially when those elements are not near the head of the pile.

An element near the head will naturally produce a larger change in head response as it separates than an element at greater depth. But, providing the pile has sufficient elements in its effective length, the contribution of each element is small enough

to produce a relatively smooth head response curve.

Figure 5.26 shows an enlarged view of the early stages of loading for the flexible pile in a uniform stiffness with depth Winkler soil. The smooth curve is a result of using 30 elements in the pile discretisation. To gauge the effect of the number of elements the analysis was repeated using 20, 10 and 5 elements and these results are also plotted.

The linear elastic portions of the curves exhibit a variation of response as the number of elements increases, with the 20 and 30 element results agreeing and giving a response only 1% less than the true deflection. Because of the low initial stresses specified in the problem, the non-linear elastic response deviates from the linear one at very low loads and essentially reaches a complete breakaway response at the top of the plot. The 5 element analysis shows distinct points where the response changes as new elements breakaway, but the more finely discretised curves are much smoother. Thus, the SSI analysis is shown to give excellent results for the effect of breakaway upon a pile in a Winkler soil, provided there is an adequate number of elements (say between ten and twenty) in an effective length.

Effect of the Form of Interface Traction and Head Restraint

The two traction distributions discussed in Section 5.5.2 were both used to analyse a pile in an elastic continuum soil for comparison of the results with those from a direct finite element analysis. As well, the effect of the manner of fixing the head of the pile, to obtain the influence coefficients, was investigated.

The results are presented in Table 5.3 where the difference in response from fixing the deflection of the entire cross-section of the head of the pile and just fixing that of one node

at the circumference is seen to be very small. Thus the more easily applied case of full fixity was chosen, because fixing just sufficient nodes to generate the restraints necessary to allow load to be applied will require the definition of the traction at the pile head. It is simpler to assume the pile head cross-section does not deform in the horizontal plane than to introduce the extra variable of a traction distribution that does not give any significant change to the results.

The choice of uniform stress or uniform traction loading does not appear to be important for the response of the head, since both methods overestimate, almost equally, the results when compared to the full mesh answer. Thus, with regards also to the results from section 5.5.2 the uniform traction load was employed.

Non-linear Elastic Gapping Results

The results for behaviour with gapping and soil yield (involving unequal soil pressures on the front and back of the pile), depend upon the number of Fourier terms modelling the uni-directional uniform traction, see Appendix II. The SSI results for analyses of laterally loaded piles in a continuum here employ three terms only (0,1 and 2), since a comparison with results found using up to 8 terms showed negligible differences (less than 1%) for the incremental response at limiting states of breakaway, as defined for the Winkler response of section 5.3.1.

The results from the elastic continuum analysis show a variation with critical length to diameter ratio that was not evident in the results from the Winkler analysis. Another major difference is that the rigid pile solutions, although following the Winkler trend in possessing a higher breakaway to contact deformation ratio than the flexible pile solutions, do not achieve the one unique value that is numerically two for a Winkler soil.

$$(u^*/u)_M = 1.451; (\theta^*/\theta)_H = 1.452,$$

and $(\theta^*/\theta)_M = 1.466.$

These results conform to the trends exhibited by the Winkler-based answers and differ in the aspects that characterise the additional elements found for linear response continuum solutions, namely:

- a) the added importance of the effective length to diameter ratio.
- b) the stiffening of response associated with soil-soil interaction.

Thus, the SSI biface model can give accurate analyses of lateral loading of piles in a linear elastic continuum, non-linear gapping analyses for piles in a soil modelled as a Winkler medium, and also present reasonable results for a pile in a linear elastic continuum modelled soil with gapping.

5.6 Non-linear Biface Model Response

A soil-structure interaction method for linear analysis has been presented in Section 5.5 and in Section 5.4 it has been shown that non-linear behaviour can be included, based upon rules of a general type commonly held to be obeyed by soil. To illustrate the model a rigid pile in a non-linear Winkler soil is presented, since it is the simplest problem that illustrates the major points of the model used for the soil-pile interface behaviour.

The soil parameters have been chosen such that the head load-deformation linear response and the head loads at collapse are equal for each of four cases. To this end, the slopes of the interface stress-deflection curves for the soil elements are all the same and the difference between passive and active failure stresses is maintained constant.

The four assumed interface stress-deflection responses of a Winkler soil interface element, at either the front or back, are depicted in Fig. 5.27, namely the responses when:

- 1) the initial stress is midway between the active and passive values.
- 2) the initial stress is at the active value.
- 3) the initial stress is at the passive value.
- 4) the low initial stress and zero or negative active failure stress means a tendency to cause tension results in a gap.

The loading consists of two sets of two-way load cycling, the first just beyond the elastic range of the pile-soil system, followed by cycling at just below the failure load. The resulting pile element reaction load per unit length at a typical station

near the surface is plotted against pile deflection in Fig. 5.28 for all the cases. The reaction load is a result of the difference between the unequal stresses acting on the front and back faces. This is the typical "p-y" response commonly used in some lateral pile analyses.

In cases 1), 2), and 3) the soil remains in full contact, by flowing around the pile, and it is possible that a combination of passive and then active failure states can cause a return to the initial stress-zero deflection state, although this is most unlikely to be the case. More commonly the active and passive stages of the element response will alter the value of interface stress associated with zero deflection. It can be seen in the figure that in case 4) if the soil interaction stress reduces to zero, thereafter the deflection remains constant until recontacting is predicted. In all four cases the attainment of a passive failure stress would cause plastic deflections that would not be recovered and alteration or even removal of the stress associated with the original zero deflection position is possible.

If the Winkler soil face breaks away from the pile, producing a gap as in case 4), it will undergo no further movement until recontact, unlike the continual deflection experienced by an elastic continuum based soil interface element. Since only passive failure is possible at any gapped element, the permanent deflection always occurs in the same direction and eventually may lead to zero interface stress at zero deflection. Even more likely is a state in which zero soil deflection and contact is no longer obtainable, i.e. a permanent gap is formed. This gap response assumes the soil will not flow around the pile at passive failure to fill in the gap.

Thus the case of full contact may be readily associated with both sand and clay, while gap formation is more relevant to clay response. It would not be expected that sand would be able to maintain a stress-free face, but would experience flow. This flow would then result in an active pressure on the pile, controlled by the movement of the pile. Some calcareous sands appear to be an exception to the above argument. It would appear that the platy, relatively degradable particles do not promote a stress-free flowing situation and exhibit an apparent cohesion.

Zero Bias Response

For the case of an interface with an initial stress value midway between the active and passive stresses, curve 1) of Fig. 5.27 is relevant. It must be remembered that an average stress on the individual front and back soil element faces, along the line of head loading, is being considered here. Since there is no bias towards either failure stress, this state is described as having a "zero bias".

Upon head loading of the pile, an interaction load must develop at the interface elements to preserve equilibrium. For a typical case, this load is the result of the front face stress increasing and the back face stress decreasing. Since the stiffness of both faces are the same, with an equal magnitude deflection, an equal but opposite sense stress change must occur on the front and back faces of the pile/soil. Since the total reaction is found from the difference in compressive stresses on the front and back faces, a pile reaction load-deflection response will arise that is twice as stiff as the individual component soil reaction load-deflection responses, see Fig. 5.28a.

The front and back face must reach their passive and active failure state at the same deflection (i), because of the symmetric

nature of the problem. This means that when the back soil remains in contact with the pile, both the front and back faces undergo the same amount of plastic deflection that is non-recoverable. It is only the sense of the stress on each of the two faces that is different and so a symmetrical response must follow as long as the head loading is symmetric. Thus, closed hysteretic reaction load-deflection loops characterise the response of the zero-bias case. The combination of the bilinear elastic plastic responses at each station results in a multi-linear response at the head, as seen in Fig. 5.29a. Since the applied head load is symmetrical, the pile element response and the head response are also symmetrical.

Such a response is typical of many soil behavioural models, notably the class of hysteretic model often termed the Ramberg-Osgood model. Unlike models such as the Ramberg and Osgood one, the response here is directly attributable to simple rules of elemental soil behaviour and does not rely upon empirically derived data to fix the shape of the response curves. The rules used, here with the Winkler model, are equally applicable to the more consistent elastic soil model. This enables the combination of the benefits of the linear soil response model with commonly accepted concepts of limiting stresses in non-linear soil models.

While the zero bias response may be typical of undrained clay behaviour, it does not typify the response of drained clay or sand. Undrained behaviour means that total stress analysis is appropriate and undrained shear strength controls the failure stresses. In the section using the plane strain pile segment it was proposed that proceeding from the at-rest state to failure, the stress increments on the front and back of the pile were of equal magnitude and opposite sign. As long as the pile-soil inter-

face can withstand tension, or while the initial stress is sufficient to eliminate tension, the zero bias model is appropriate for undrained response.

If drained conditions exist, then the increase in mean effective stress at the front element is accompanied by a decrease in effective stress at the back element. Since the soil strength in general is a function of mean effective stress, the active and passive limiting stresses will be affected differently (one decreasing, the other increasing).

A commonly accepted method of predicting the drained ultimate reaction load, is to use a distributed failure load based upon three to five times the passive failure stress as given by Rankine earth pressure theory and the pile frontal width. This simple device has been found to agree reasonably well for a limited range of lateral pile tests in frictional soil. For drained conditions, the active pressure acting behind the pile will be much smaller than the passive stress and so is often neglected in other methods. The factor of three to five may be seen as an attempt to allow for the three-dimensional nature of the problem and the fact that plane strain conditions do not apply. These "real-life" variations from the theoretical model may one day be accommodated in a range of theories based upon pressuremeter results. Until such theories are formulated and tested, relatively crude but apparently reliable approximations must be used.

Active and Passive Bias Response

The drained case with no gapping is similar to the undrained case, but now the absolute magnitude of the interaction stress changes, from the initial stress state at the interface, that are required to produce active and passive failure will not be equal.

The usual case will involve the active face failing before the passive face and so an active bias state is defined. If a situation arises in which the soil is initially close to passive failure on both sides then a passive bias state results.

Observing the response at the improbable two limit states of a fully active and fully passive bias, would be expected to provide bounds upon the response of the model. Thus the limiting cases 2) and 3) can be analysed and are shown in Fig. 5.28b.

With the fully active bias case, initially the back face will not accommodate any reduction in stress and so will move with the pile and allow a mismatch between the interface element and the remaining elastic soil. Since the only resistance arises from the linear behaviour at the front face, the total pile reaction load-deflection response will be equivalent to the front face soil reaction load-deflection response alone (i).

The front face at one depth reaches passive failure and at that element of the pile, assuming positive plastic work only is involved, deflection at a constant reaction load occurs until the head load is all applied (ii). At this stage, a large amount of permanent deflection has occurred in the positive direction. However upon unloading only the same amount of elastic response is available as was available for the zero bias case.

The unloading of the head of the pile results in the interfaces returning to the linear response state and unloading of compressive stress from the front face, with an increasing compression of the back face. Because both faces now contribute to the response, the unloading proceeds with an incremental stiffness of twice the original value, (iii). Swane (1983) has predicted similar behaviour, although his model was based upon a somewhat

different approach to modelling the pile and soil behaviour.

The initial purely active flow phase introduced an apparent compression of the soil at the back of the pile and a reduced compression on the front face. This effectively results in a deflection offset accompanying the state of zero reaction load upon the pile. Subsequent to the initial load, the symmetric nature of the response means the front and back soil elements at any one depth will both fail at the same time, and never again will just active flow alone occur. Thus a permanent offset is apparent in Fig. 5.28b that was not present in Fig. 5.28a, although the shape of the stabilised reaction load-deflection loops are the same.

Upon first application of the larger cyclic load, the new active flow phases occurring at stations down the pile that were previously fully linear, mean large plastic deflections arise at all previously non-linear elements (iv). These non-recoverable deflections mainly occur in the same sense as those during the initial load, since the cyclic head load was first increased in the same direction as the initial head loading. Thus the load deflection loop is offset further in the direction of initial loading. If the load were increased in an opposite sense to the initial load, i.e. increasing the amplitude on the negative load leg of a cycle, the larger plastic non-recoverable deflections, associated with the higher cyclic load, cause the load-deflection loops to shift in the opposite direction to the initial load.

This has important implications for tests where successive trains of cyclic loads are applied to a pile. The sense in which the additional cyclic load is first applied will affect the load-

deflection response of the head. This will be true for any situation in which the value of initial stress gives rise to an unequal bias with respect to the active and passive stress states.

If the other limiting case of an initial stress state fully biased to the passive pressure is considered, it transpires that no material changes to the active bias case response are observed. The equivalence of the active and passive bias cases may be understood when it is realised that equivalent incremental responses are achieved whether a face unloads from ultimate compression to a lower limit or loads from a lower limit to ultimate compression. The head response for both cases is given in Fig. 5.29b.

This equivalence of the pile response for the two limiting cases of active and passive biased initial stress is also evident in any pair of initial stress states that are equally removed from the zero bias stress state. This means that the behaviour of a pile in a soil can be normalised according to the deviation of the initial stress state from the mean value of the passive and active stresses. An initial stress equal to the mean value of the active and passive failure stresses being the zero bias stress state.

While the theoretical model predicts such a feature it must be realised that, practically, it relies upon the flow of soil in an active state. There is some evidence from model pile tests carried out in sand, that flow may not occur or at best an incomplete flow of soil around the pile may arise. It seems that a measure of the soil flow ability could be made by measuring the difference in response from model lateral pile tests with an active and then a passive biased initial stress. However until the active and passive character of the soil response is clearly understood this must remain only a theoretical possibility.

Figure 5.30a presents results for static loading to failure of a rigid pile in a uniform Winkler soil, for various values of initial stress. The initial stress, p_o , the mean of the active and passive failure stresses, p_m and the difference between the passive and active failure stresses, p_y are defined in the figure and used to specify the initial stress state. The use of a "bias parameter" based upon the absolute value of the difference between p_o and p_m divided by p_y allows two cases of equal active and passive bias to be defined by one curve. A zero value for the parameter is associated with a zero bias and a value of one half signifies a fully active or fully passive bias.

It can be readily seen that the zero bias case presents the largest range of linearly elastic response to initial head load, while the fully biased cases exhibit an immediate reduction in stiffness. Although the initial response is again linear for the fully biased cases, it is linearity associated with the formation of non-recoverable deflections. It is the instant attainment of a fully failed state at one of the two soil elements at each depth down the pile, that produces linear behaviour totally controlled by the remaining unfailed element faces.

Interestingly, a picture similar to the results from the elastic-plastic soil plane strain pile segment problem is evident. There is an initial difference of stiffness between the responses, just as there was between the fully contacting and half contact pile segment responses. The fully contacting plane strain case corresponds to a zero bias case and the half contact pile segment to the fully biased case of a rigid pile in a Winkler soil. There is a large increase in pile deflection required to achieve the full collapse load, which was held constant for all cases of initial stress. This parallels the results of Rowe (1978) where he

states that breakaway of soil from behind a plane strain anchor will not change the collapse load, but will greatly increase the deflection at which that load is achieved.

Thus, if the collapse of a pile-soil system is to be considered, great care must be taken over how it is defined. A deflection definition based upon a percentage of the pile diameter contains no information about soil strength or the initial state of stress. As such it must not be interpreted as a collapse load, but may be viewed more correctly as a serviceability condition.

The intermediate bias states show a transition from the zero bias state with progressively less pure linear behaviour, until the active, or passive, flow-based linearity of the fully biased states is reached.

Apparent in the curves is the stepwise linear nature of the solution. This follows from the finite discretisation of the pile-soil system, where only the points corresponding to critical states occurring represent exact solutions for load-deflection response. Although smooth curves could be drawn through these points, corresponding to the states at which a critical condition has arisen, this has not been attempted. In some cases two curves may thus seem to touch, which is a result of linear interpolation between the load-deflection points at which elements first become failed. The points at which critical conditions of elements arise for the various bias states, will always present a progressive change of behaviour with no overlap.

Soil-pile Breakaway

The Winkler model with a limiting stress cutoff, used with the biface soil-structure interaction approach, displays a complexity of response that is not usually associated with such a

simple model. By introducing two faces at any depth along the pile, the opportunity exists for soil-pile separation governed by the state of initial stress and also the inability of a soil to sustain tension.

Separation will now be considered by referring to Fig. 5.28c, which displays the 'p-y' response of the top element of the discretised pile. Beginning at the origin, the first increase of head load is mirrored by the interface reaction load increasing until (i), a state at which the most severely tensioned element face reaches zero traction. This is the state at which breakaway occurs on the back face and the pile reaction load-pile deflection response is governed by the remaining contacting element face.

The curve denoted by a single arrow head is followed on the initial load and illustrates the change in response due to break-away of the back face as a change of slope at (i). Upon reaching the front element failure load at (ii), a deflection-defined response, governed by the remaining linear elastic elements, ensues until negative incremental plastic deflection would occur if no change of state were made. Reversal of the head load causes such a negative plastic deflection at (iii) and so unloading of the front face occurs in a linear elastic manner until the back soil face is recontacted by the pile at (iv). That face was left by the pile and, true to a Winkler model, had not moved since no load acted upon it, so the point of breakaway (i) and recontact (iv) occur at the same pile deflection but different pile reaction loads.

The original incremental stiffness is regained during unloading after (iv), until the front face reaches a zero interaction traction at (v). Since irrecoverable plastic deflection had been produced in the first load, and there is still only the same

deflection available in the linear range, the breakaway of the front face occurs at a smaller magnitude of negative deflection than the positive deflection for separation of the back face. Thus, there is a lack of symmetry in the front and back face behaviour, controlled by the direction of first load and the amount of plastic deflection.

With continued unloading, the pile element again experiences the reduced stiffness of response due to breakaway and then yields the soil of the back face until (vi). In the two-way cycling applied, the plastic deflections occur at maximum load in each direction and are equal. Because no unloading at element faces is associated with the cycling of the head load, except when the head load reverses, subsequent cycles do not cause soil failure unless the head load magnitude increases, i.e. plastic deflections only occur in the first load cycle leading to first cycle shakedown.

The single arrows represent paths that are only followed during the first cycle of load and the second and subsequent cycles occur along the paths with double arrowheads. This response is a result of shakedown during the first load cycle, and, because no irrecoverable deflections are permitted, the response has a symmetry that was not evident during the first cycle. No new plastic deflection will occur in this state although the yield loads may be repeatedly reached.

This shakedown state will continue to exist until an increase of maximum load on the pile head forces more irrecoverable plastic deflection to occur. The new plastic deflection is in response to the need for equilibrium of the extra applied force, which can only be achieved by increasing the load carried at previously linear elements. Such load increases will, in turn, cause elements to reach their limiting values of load and so introduce

irrecoverable deflections governed by the behaviour of an increasingly smaller set of remaining linear elements.

The physically shrinking zone of soil, along the pile with purely linear response, cannot be accurately modelled by numerical means that involve spatial discretisation, as employed here. The continued reduction in the physical size of the linear zone forces the modelling of response by progressively fewer elements. It has already been emphasised in this thesis that a sufficient number of elements must be maintained in the effective length of a pile. Since the size of the linear response zone of the pile length is small, it seems almost certain that a rigid response is appropriate and so analytical expressions for the response of rigid piles for a Winkler soil model could be used. Swane (1983) has commented upon the need for adequate numerical modelling in order to obtain unique shakedown loads and employed such an analytic approach.

The progressively poorer modelling of the shrinking linear region, will affect the response of piles when head loads close to the static collapse loads are applied. As such, the pile would normally be considered unsatisfactory, without a real need to investigate the load-deflection response. However one possible exception, is when piles of unequal sizes are used in a group and the collapse of one of the weaker foundation elements is an integral assumption made in the design.

Thus, the cycling near static collapse of the next stage of loading, must be viewed as possibly being affected by the problem of poor discretisation of the small linear response region. This is also true of the second stage of cycling for the previous cases considered. It becomes more apparent for the case where soil

gapping is incorporated because the loss of lateral pile support is more easily visualised as breakaway rather than failure of the soil. Indeed, care must be exercised when only two element faces remain in a linear and contacting state. Both elements must be at different depths in order to allow equilibrium of any increment of moment caused by extra load at the pile head, or an ill-conditioned set of interaction correction equations result.

The second stage of cycling employed here, did not remove all linear soil response, which would have involved a deformation-defined rather than load-defined problem. The first increase to the larger cyclic load introduces new plastic deflection at the front face first. Reversal of the head load causes an incremental response for the unloading that is purely a result of linear unloading of the front face. The amount of permanent deflection is so large that it exceeds the amount of linear deflection available for the front face. No change in the pile element response load around zero total reaction load signifies the pile passing through a complete gap, i.e. the pile is free-standing over the length of the element. Recontacting occurs at the same deflection at which recontact occurred during the shakedown response of the previous load, because the back face of the soil has no knowledge of the permanent deflection at the front face.

For further loading, there is no response for this pile element that involves both soil faces acting together. This is partly a result of using the Winkler model, in which no interaction occurs between the front and back soil faces, and partly due to the "lumping" of all side-face behaviour into the front and back faces. A more complex model would involve four instead of two faces to the pile at any depth, but this added complexity has been deferred in favour of establishing the two-face model as a first

and necessary step. The elastic continuum soil model does not have the limitation of no interaction that is inherent in Winkler theory, but will incorporate the assumption of biface behaviour.

The two-way nature of the applied head load again results in a shakedown response that is symmetric and the path shown by three arrowheads in Fig. 5.28c is obtained after the first cycle of the new load. The portion of the curve passing through zero reaction load represents the pile in a gap between the two soil faces, and the two sloping portions either side represent the linear loading of each isolated soil face. Figure 5.29c presents the load-deflection response of the head of the pile for the gapping model. The hysteresis loop for the small cyclic load is seen to be much smaller than those for the zero and fully biased cases, shown in Figs 5.29a and 5.29b where the shakedown response of the larger cyclic load is denoted by two arrowheads.

The shakedown head load-deflection response is seen to have its lowest stiffness for small loads around zero, but does not achieve a zero stiffness, since this would indicate no contact between the pile and soil along its entire length. The reduction in head stiffness is nevertheless alarming and may well give cause for concern when the effects of small displacements or loads, say due to vibrations, are important.

The initial load-deflection curves for all the cases with an equal bias are the same and the end points of the cycles of load are also equivalent. Even the cases with an unequal bias have hysteresis loops for the full contact case that are equivalent. The effect of an increasing bias is seen to be a translation of the hysteresis loop and the effect of gapping is to leave shakedown loops with a zero area, implying only geometrical non-

linearity with no non-recoverable deflections. All of these responses are available from the one soil-structure interaction analysis using the same basic soil properties, with only the bias of the initial stress and the magnitude of the active failure stress varying.

The problem of a rigid pile in an elastic continuum has been modelled using the axisymmetric geometry finite element analysis to produce the influence coefficients for the SSI program, and the results for static loading are presented in Fig. 5.30b. This figure may be directly compared to the one above, which is for a rigid pile in a Winkler soil. The most noticeable difference is the much smaller effect of the bias parameter upon the load-deflection response, which is a result of the interaction now existing between all the faces of the soil.

The integrity of the soil in the elastic continuum model, reduces both the deflection for a given load and the effect of the initial stress bias upon response, when compared to the Winkler results. The interface traction-deflection curves, as depicted in Fig. 5.27 for the Winkler model, cannot be drawn for the elastic continuum soil beforehand, since the elastic slopes of the curves depend upon the ratio of head shear to moment and will be affected, to some extent, by any change of state arising at any other element face because of interaction through the soil.

Despite the added complexity of the elastic continuum model, the general conclusions from the study of the Winkler results still apply to the continuum results. This does not mean that the Winkler results are suggested as being preferable to the continuum results, but rather that the basic laws governing soil-pile behaviour are evident in both models. The lack of interaction in

the Winkler model is still a serious deficiency that can be overcome, by the continuum model, which can include interaction. The Winkler model represents a highly simplified approximation to continuum behaviour that is unnecessary, but does serve as a useful means of simplifying the presentation of the behaviour of the SSI analysis.

Broadly, the response of the model of gapping behaviour with respect to head load level has two regions, in which:

- a) the effect of the initial stress has not been lost.
- b) there is no remnant of the effect of the initial stress state evident in the response.

These two features are also often present in models of soil behaviour and it seems likely that both lateral pile behaviour, as modelled here, and many soil behavioural models are closely linked by underlying premises of soil response. The existence of non-recoverable deflections or strains, the impossibility of any form of negative plastic work, and the importance of the level of the load or stress, represent three such features that are present in both types of model.

In essence, a parametric study would be possible to present the effects of both gapping, and active and passive failure of the soil using the elastic continuum based SSI analysis. From the results presented in this section it may be seen that separation does not greatly alter the response due to monotonic loading but is important when repeated loading is considered. Because of the multiplicity of parameters involved and the restriction to static loading for the topic of this Thesis, it is not feasible to present a parametric study at this stage.

5.7 Conclusions

The same broad categorisation, into three classes of analysis of single piles subjected to lateral loading, has been employed to present the theoretical non-linear behaviour arising from soil-pile separation, soil failure and pile failure. Each class has beneficial aspects to commend it, but only the discrete analysis by the finite element method is able to accurately take account of varying the extent of the region over which interaction between the pile and soil occurs during loading in a continuum.

The ease with which solutions can be produced using the Winkler soil model, make it ideal for investigating the major effects of non-linear soil and pile response, and developing analytic results that can be used to check the behaviour of more complex analyses. The lack of a basic material property in the formulation of the Winkler soil, reduces the practical usefulness of its results.

Versatility is the major attribute of the modified boundary element method when applied to single pile analyses, since the soil interaction response provides the basis of the model and remains unaltered by the conditions applied to the pile-soil interface. By defining a mismatch in deflection between the pile and elastic soil as being non-recoverable, an improved non-linear soil interface model is achieved which allows for "unloading" of failed soil in response to the need to avoid negative plastic work. However, nowhere in its formulation does it allow for the fact that the region over which the interface interaction loads act can change during loading, i.e. soil-pile breakaway at the interface is only modelled within a non-linear interface element.

Inclusion of soil-pile breakaway is accomplished by developing a new soil-structure interaction analysis in which the regions over which the interaction tractions may act are modelled separately, as a Winkler soil or a continuum soil using a finite element technique, thus allowing loss of contact between pile and soil. The biface model is used to introduce the analysis and its use is supported by analysing a plane strain pile segment by traditional finite elements and the axisymmetric finite element-based technique. The linear elastic continuum and non-linear elastic gapping Winkler response are shown to be adequately modelled by the SSI pile analysis and the behaviour resulting from non-linear soil response is presented. Further, the SSI analysis reproduces the results of direct application of the MBEM analysis for the pile analysed in Fig. 5.14.

Several commonly observed aspects of non-linear response are evident in the results and this suggests that the continuum-based models are capable of predicting pile response directly, rather than relying upon pre-determined empirical devices to reproduce the soil response. Further, the SSI analysis represents a useful way to assess the importance of gap formation upon pile response, without relying entirely upon assumptions about soil behaviour that limit the predictive capabilities of any resulting model.

Developed Interface Stress	Smooth Interface		Rough Interface	
	Pile	Soil	Pile	Soil
S_{rr}	0.318	0.318	0.161	0.161
$T_{r\theta}$	0.000	0.000	-0.157	-0.157
$S_{\theta\theta}$	0.072	-0.088	-0.441	0.068
S_{zz}	0.078	0.069	-0.056	0.069

TABLE 5.1 Stresses Developed near the Interface between the Soil and the Plane Strain Pile Segment for unit Force.

Pile Type	Soil Modulus Profile	Response due to Head Shear		Response due to Head Moment	
		u^*/u	θ^*/θ	u^*/u	θ^*/θ
<i>Num'l Analytic</i> RIGID	UNIFORM	2.000	2.000	2.000	1.999
		2.000	2.000	2.000	2.000
<i>Num'l Analytic</i>	LINEAR	2.000	2.000	2.000	2.000
		2.000	2.000	2.000	2.000
<i>Num'l Analytic</i> FLEXIBLE	UNIFORM	1.679	1.411	1.410	1.187
		1.682	1.414	1.414	1.189
<i>Num'l Analytic</i>	LINEAR	1.518	1.321	1.322	1.150
		1.516	1.320	1.320	1.149

TABLE 5.2 Ratios of Incremental Response with Complete Breakaway to Full Contact Response for the Winkler Model.

Load Type	Pile Fixity	uEd/H	$\theta Ed^2/H$	uEd^2/M	$\theta Ed^3/M$
Uniform σ_{xx}	Full	0.3872	0.1038	0.1039	0.06396
	Just	0.3883	0.1049	0.1051	0.06599
Uniform p_x Traction	Full	0.3874	0.1039	0.1039	0.06399
Finite Element Full Mesh Results		0.3638	0.0950	0.0951	0.06055

TABLE 5.3 Comparison of Full Contact Response for the SSI Model for Different Head Fixity Conditions and Assumed Pile-Soil Interface Traction with a Full Mesh FEM Analysis. ($L/d=10$, $L_c/d=11.8$).

Fourier Term k	$p_r = k p_{r0} \cos k\theta$ $k p_r = 1$		$p_\theta = k p_{\theta 0} \sin k\theta$ $k p_\theta = 1$		p_x		σ_{xx}	
	U_r	U_θ	U_r	U_θ	U_r	U_θ	U_r	U_θ
	0	1.256	0	0	0	0.400	0	0.314
1	1.988	-1.346	-1.346	2.003	1.667	-1.674	1.129	-0.966
2	1.326	-0.893	-0.893	1.326	0.660	-0.788	0.555	-0.555
4	0.520	-0.260	-0.260	0.520	-0.066	0.099		
6	0.327	-0.141	-0.141	0.327	0.021	-0.038		

TABLE 5.4 Plane Strain Pile Segment : Deflections for Unit Fourier Load Terms and Resultant Deflections after their Combination to Model a Uniform x -directed Traction, p_x and a Uniform x -directed Normal Stress in the Soil.

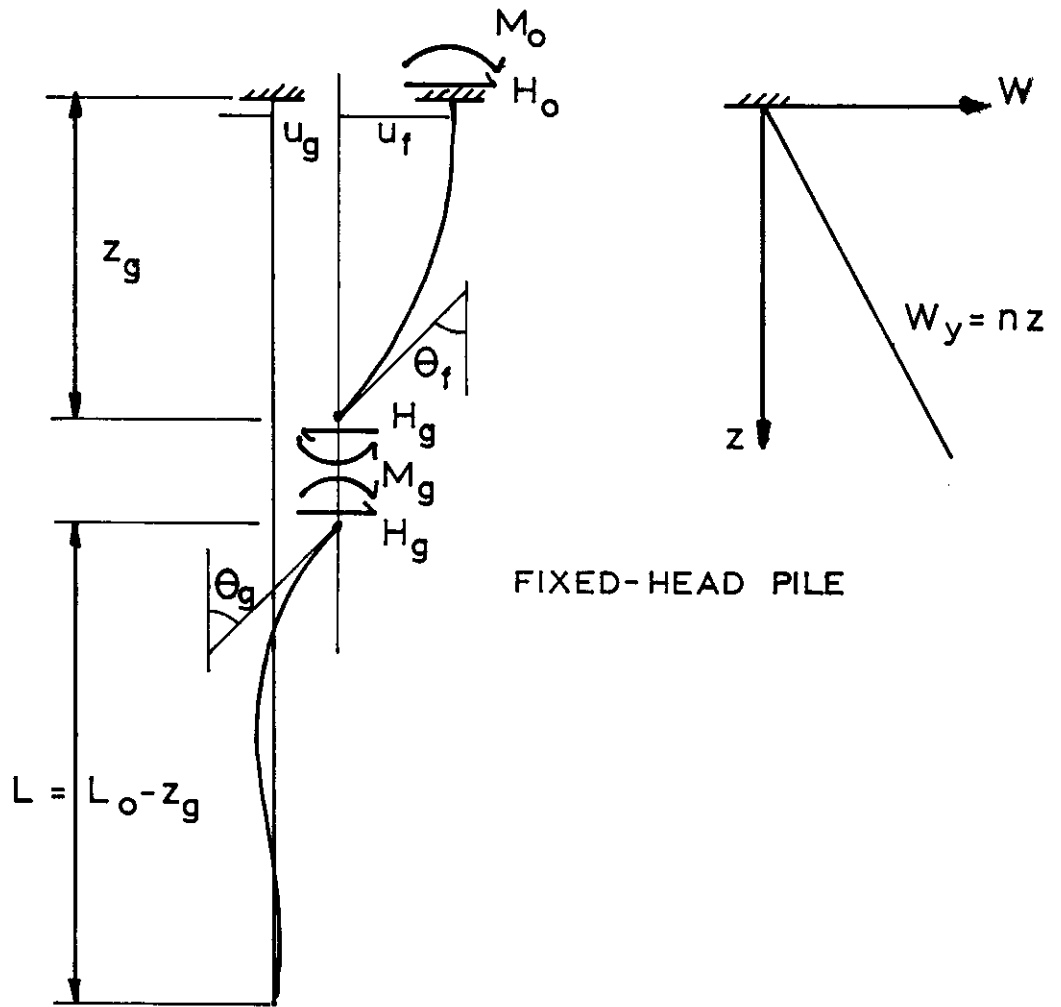


FIG. 5.1 THE PROBLEM OF A PILE WITHIN A GAP AND ASSUMED DISTRIBUTION OF SOIL FAILURE LOAD

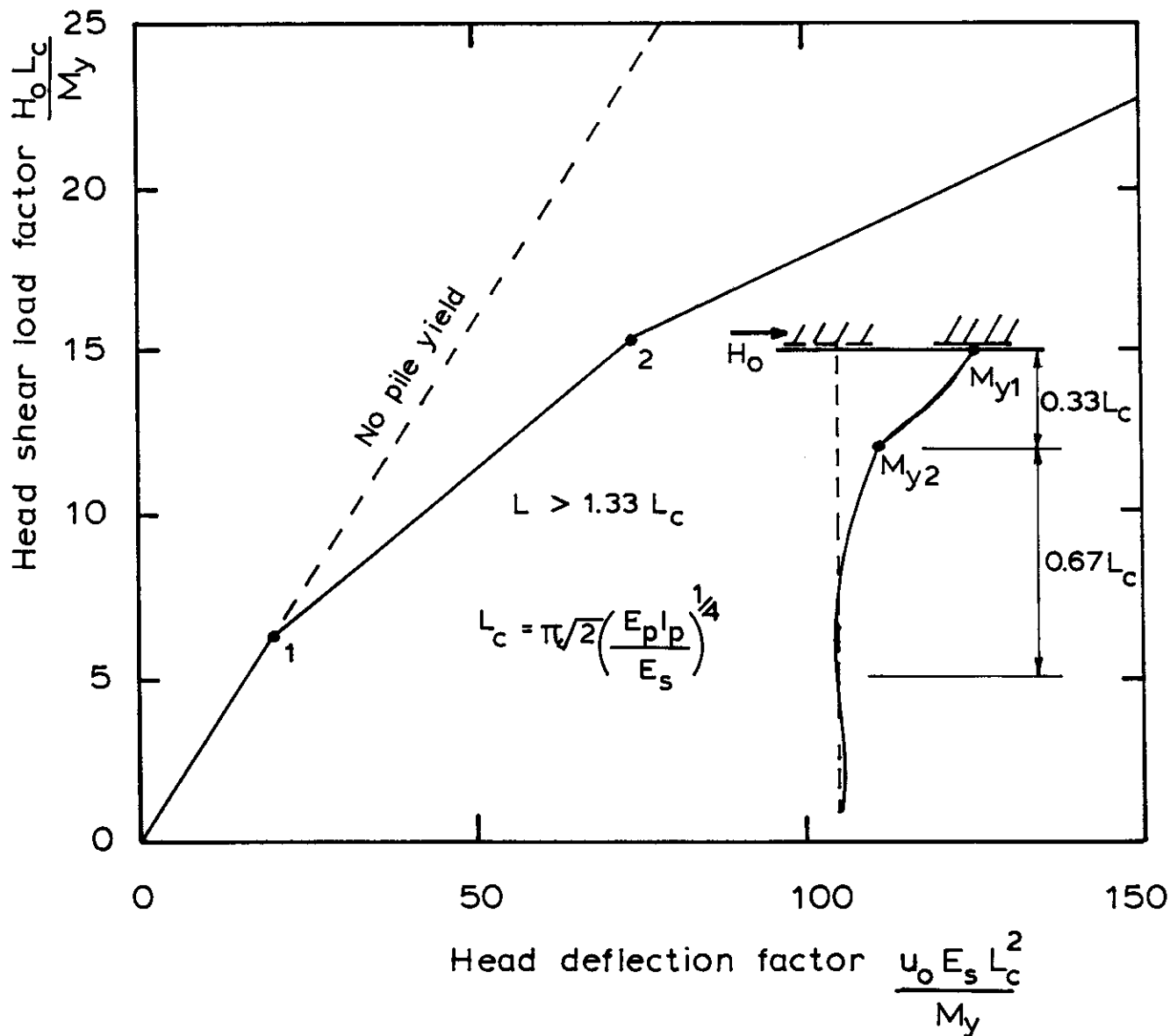


FIG. 5.2 THE HEAD LOAD-DEFLECTION RESPONSE OF A FLEXIBLE FIXED-HEAD PILE IN A UNIFORM WINKLER SOIL

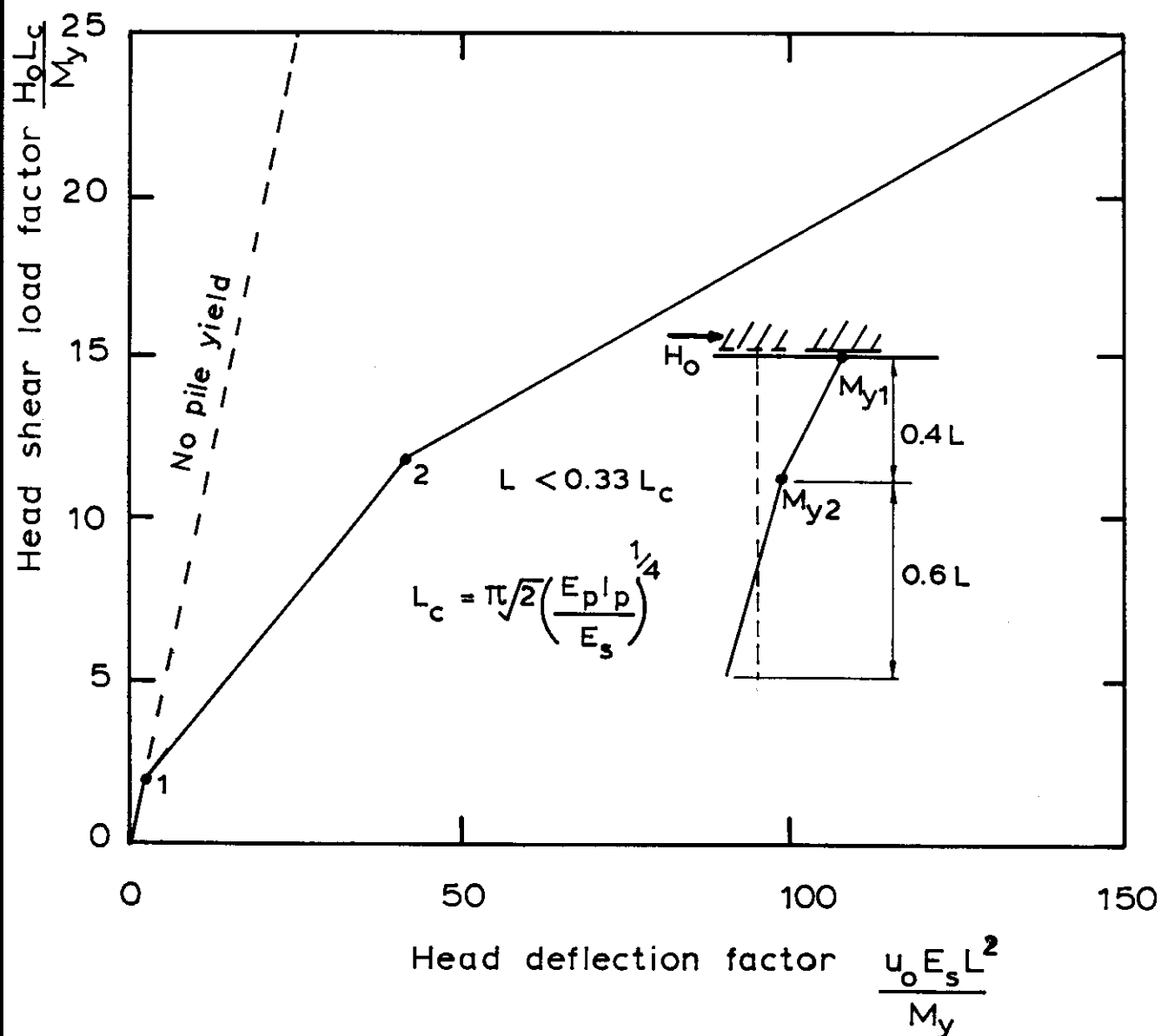
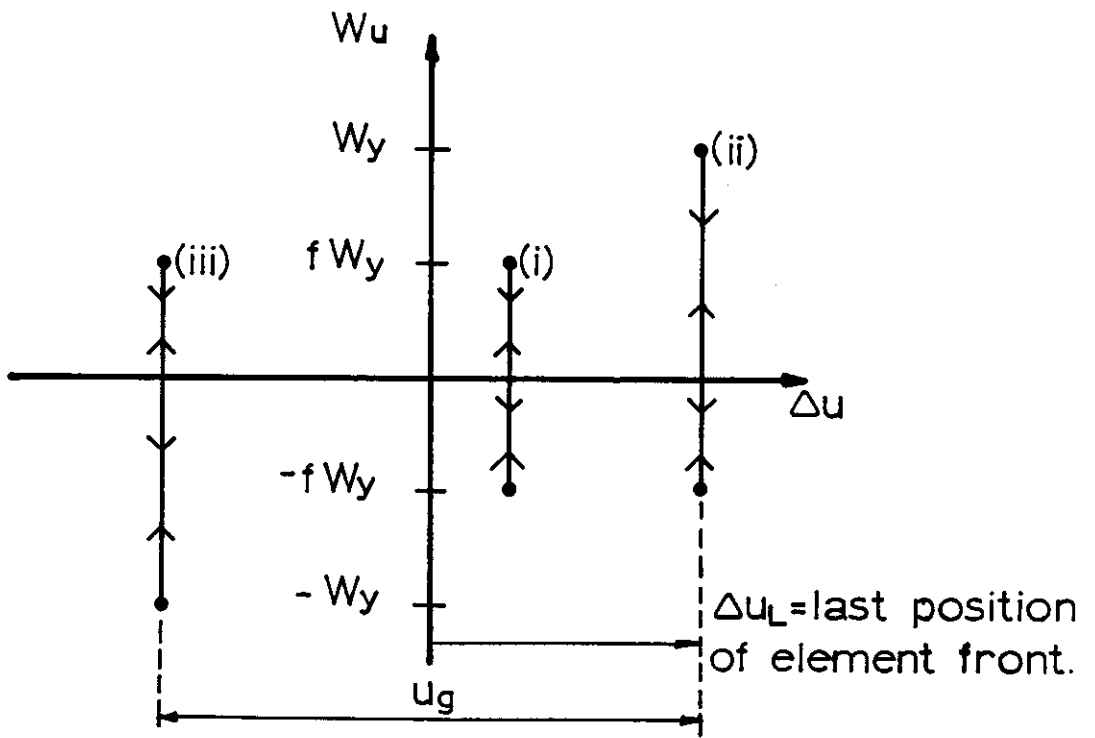
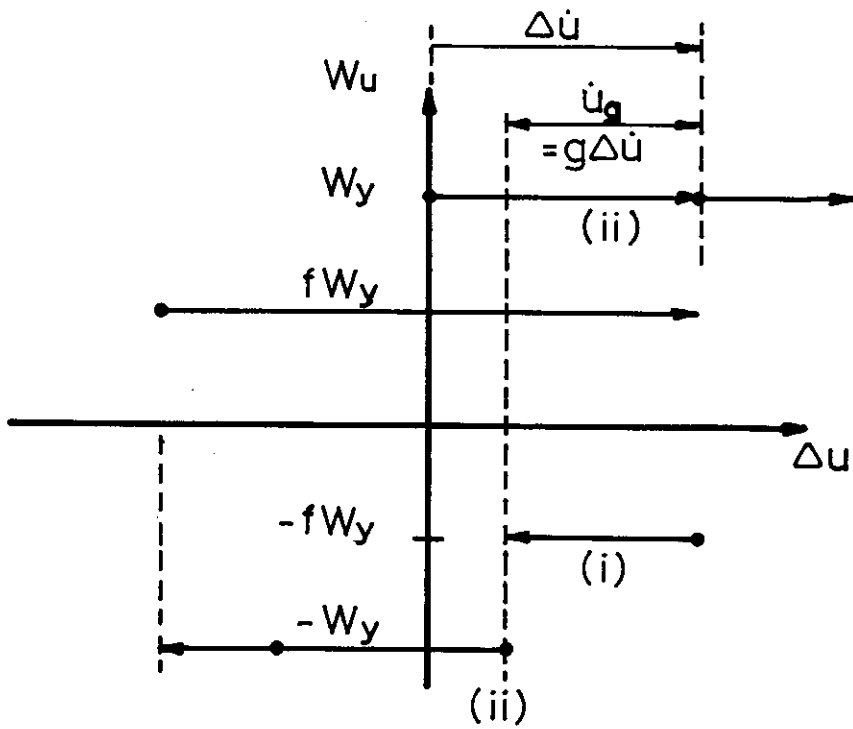


FIG. 5.3 THE HEAD LOAD-DEFLECTION RESPONSE OF A RIGID FIXED-HEAD PILE IN A UNIFORM WINKLER SOIL



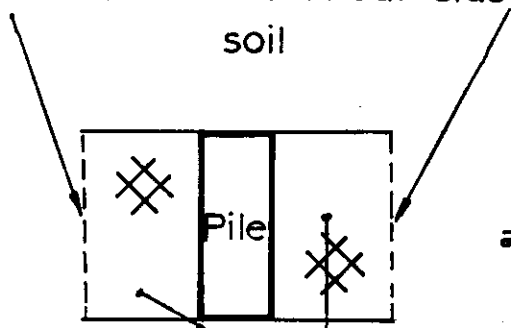
a) Elastic Interface Behaviour



b) Plastic Interface Behaviour

Fig 5.4 DEFINITION OF ELASTIC-PLASTIC MBEM NON-LINEAR SOIL-PILE INTERFACE BEHAVIOUR

Interface with linear elastic soil

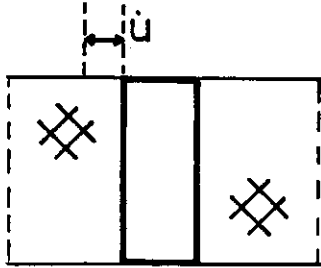


a) Initial state

$$\Delta u = u_g = 0$$

$$u_s = u_p = 0$$

Non-linear interface element



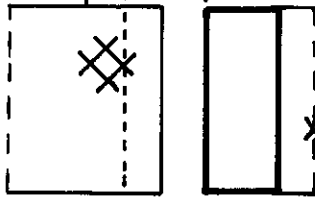
b) Elastic load

$$\Delta \dot{u} = \dot{u}_g = 0$$

$$\dot{u} = \dot{u}_s = \dot{u}_p \neq 0$$

$$W_u < W_y$$

$$\dot{u}_s \quad \dot{u}_g \quad \dot{u}_p$$



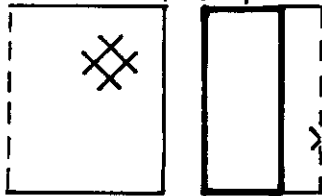
c) First yield

$$\Delta \dot{u} \neq 0 \quad \dot{u}_g = g \Delta \dot{u}$$

$$\dot{u}_s \neq \dot{u}_p \quad W_y \Delta \dot{u} > 0$$

$$W_u = W_y$$

$$\dot{u}_s \quad \dot{u}_p$$



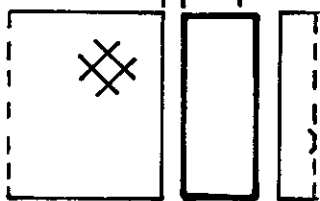
d) Elastic unload

$$\Delta \dot{u} = \dot{u}_g = 0$$

$$\dot{u}_s = \dot{u}_p \quad (u_s \neq u_p)$$

$$-fW_y < W_u < W_y$$

$$\dot{u}_s \quad \dot{u}_p$$



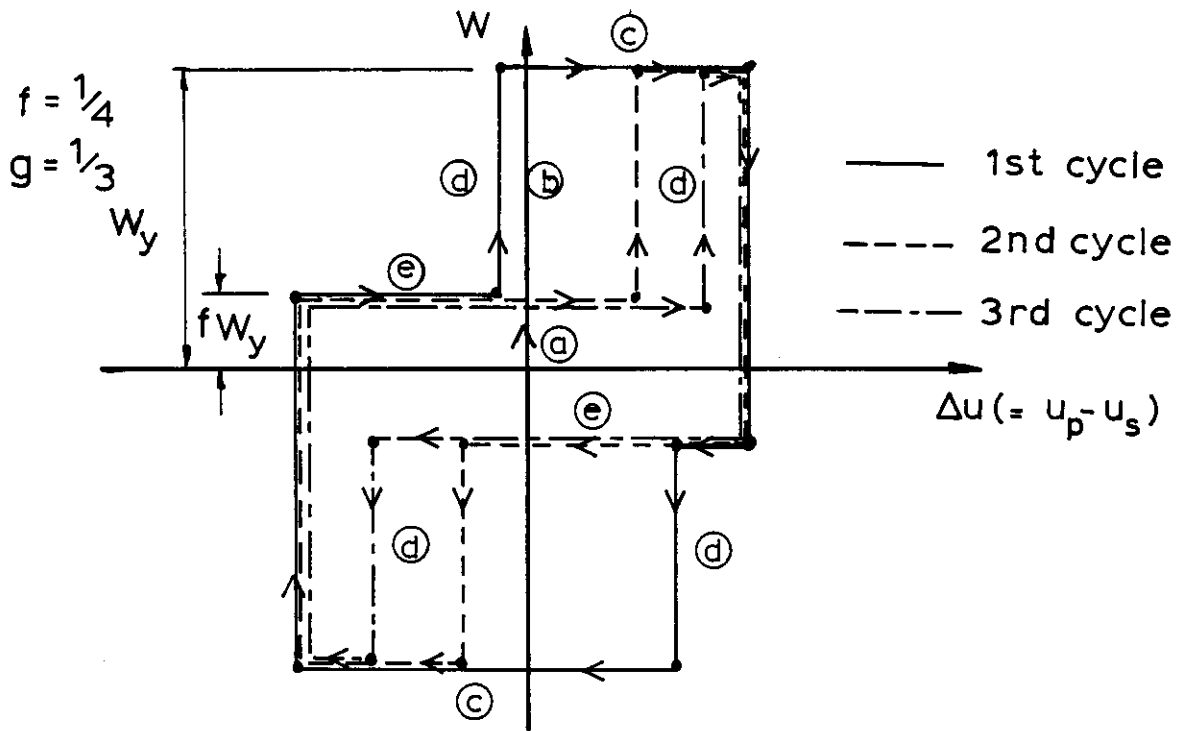
e) Gap

$$\Delta \dot{u} \neq 0 \quad \dot{u}_g = 0$$

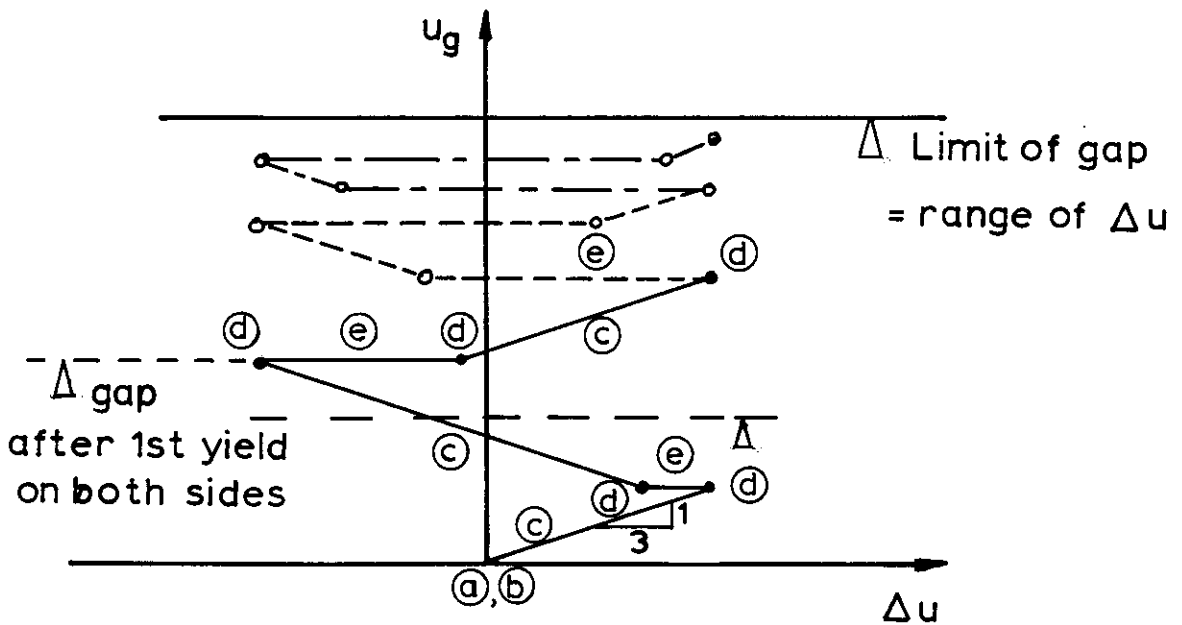
$$\dot{u}_s \neq \dot{u}_p \quad fW_y \Delta \dot{u} > 0$$

$$|W_u| = fW_y$$

Fig. 5.5 SCHEMATIC DIAGRAM SHOWING THE INTERFACE MODEL FOR NON-LINEAR BEM ANALYSIS



a) Interface load - deflection mismatch ($W - \Delta u$)



b) Gap growth - deflection mismatch ($u_g - \Delta u$)

FIG. 5.6 NON-LINEAR INTERFACE ELEMENT RESPONSE: 1st MODEL WITH GAP GROWTH FOR ANY PLASTIC DEFLECTION, Δu

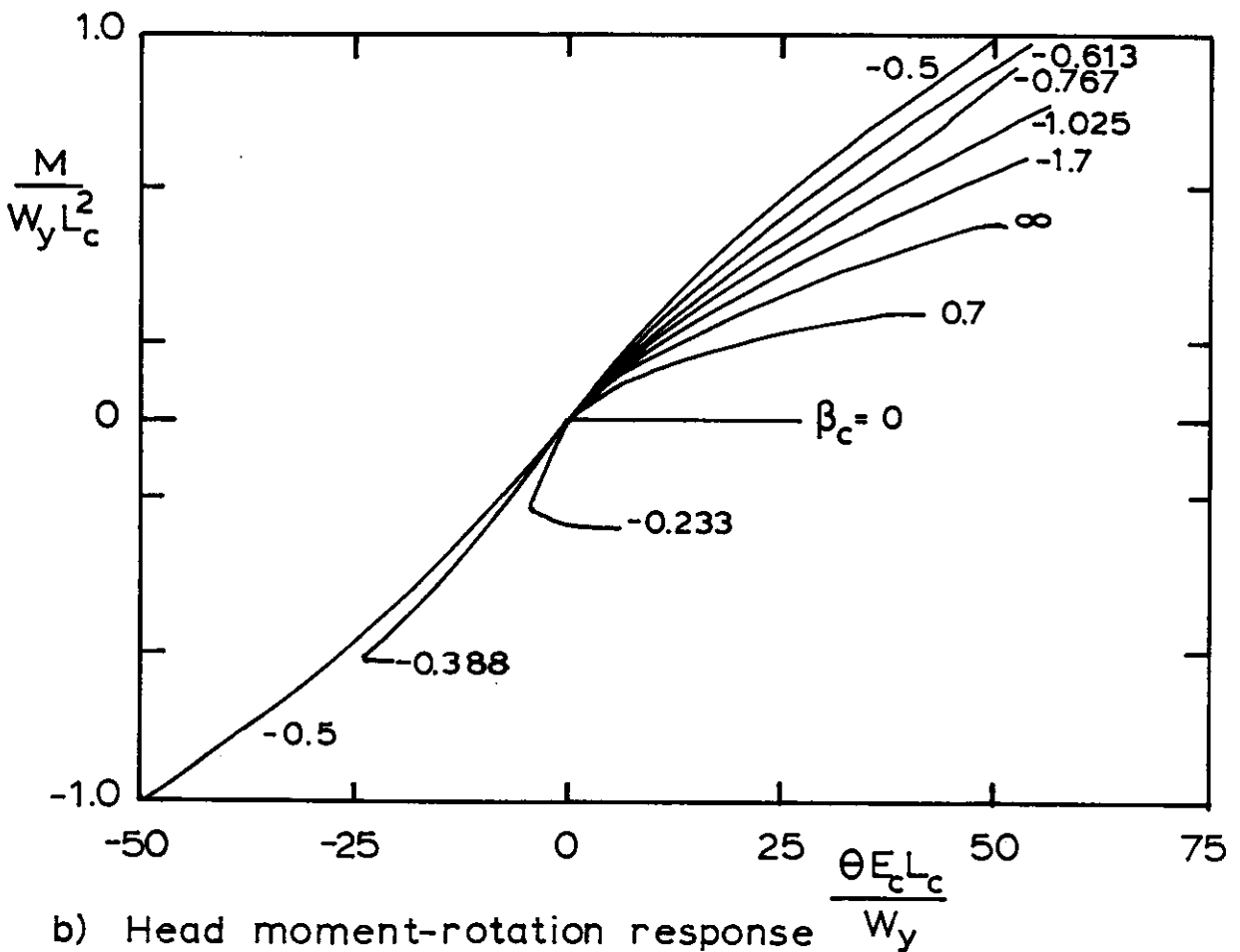
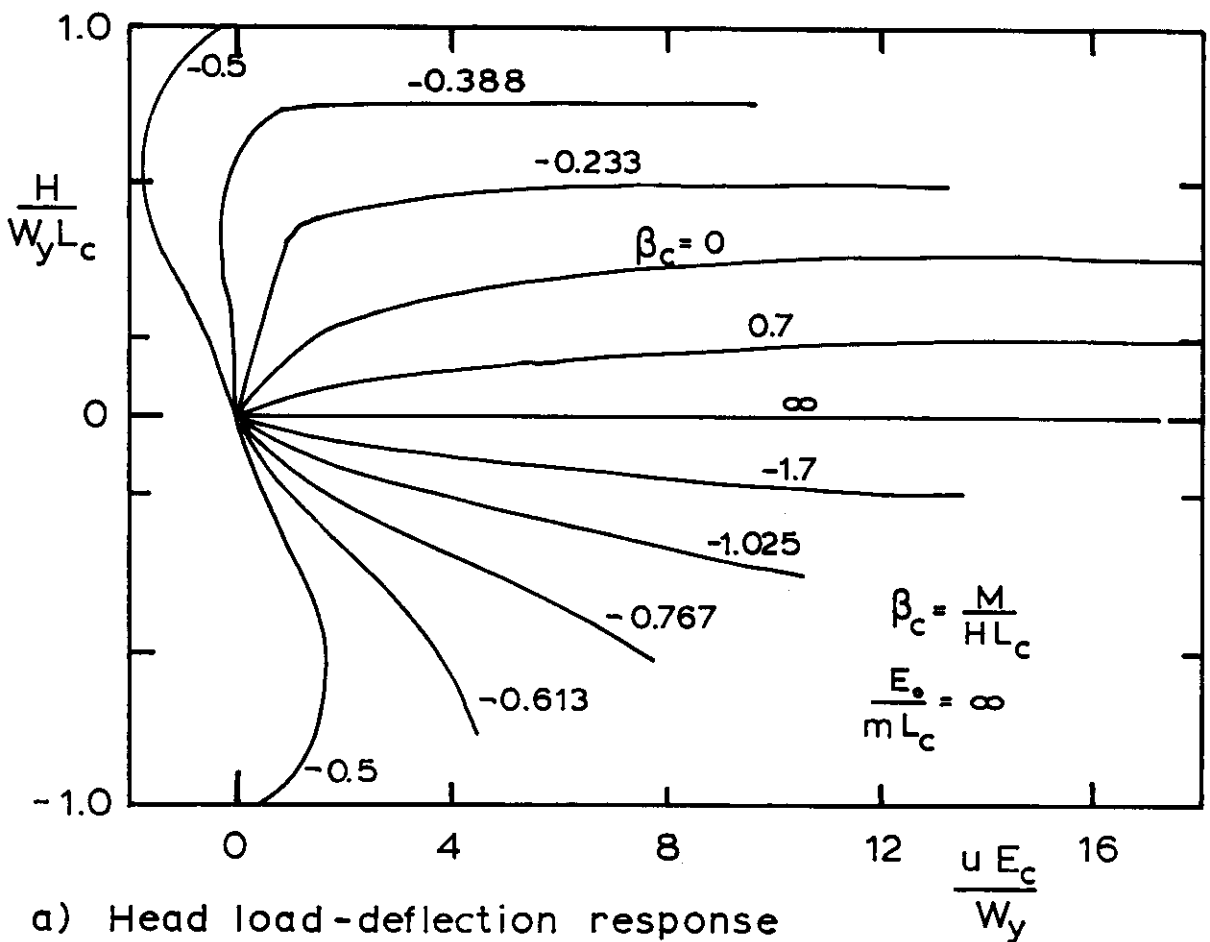
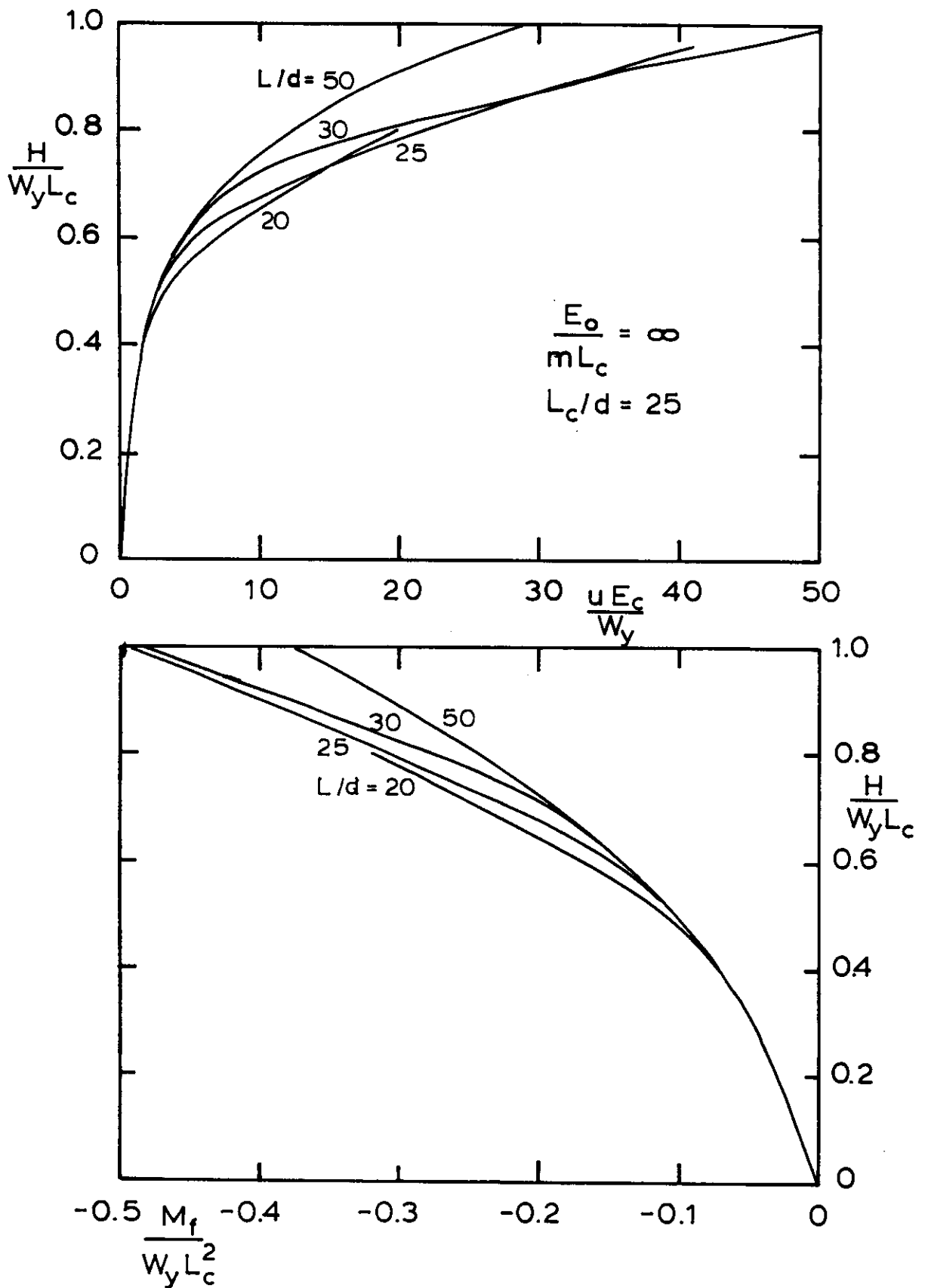


FIG. 5.8 NON-DIMENSIONAL HEAD RESPONSE FOR NON-LINEAR CONTINUUM: MBEM ANALYSIS $L_c/d = 25$



c) Head shear- deflection and fixing moment:
fixed-head pile

FIG. 5.8 CONTINUED

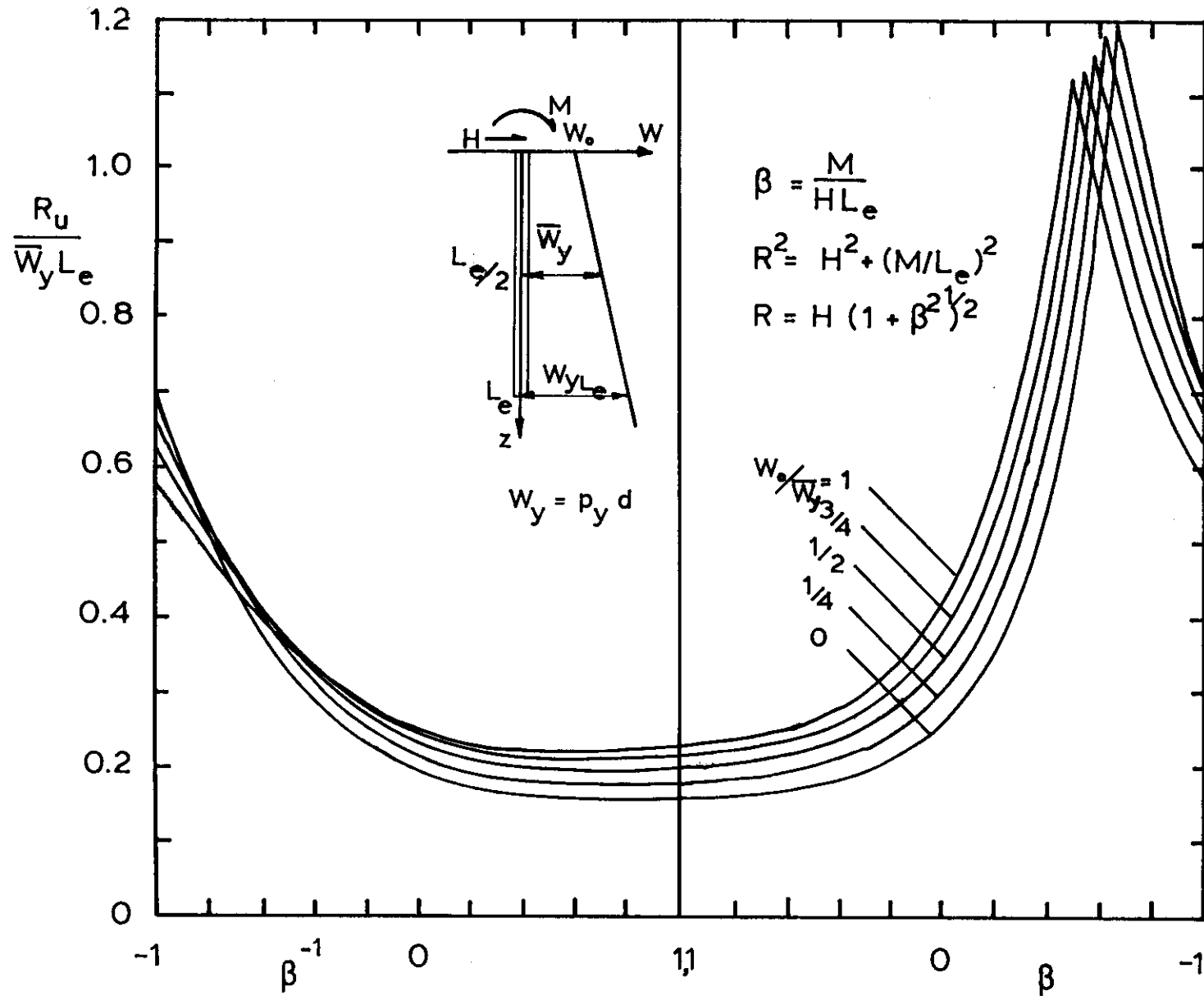
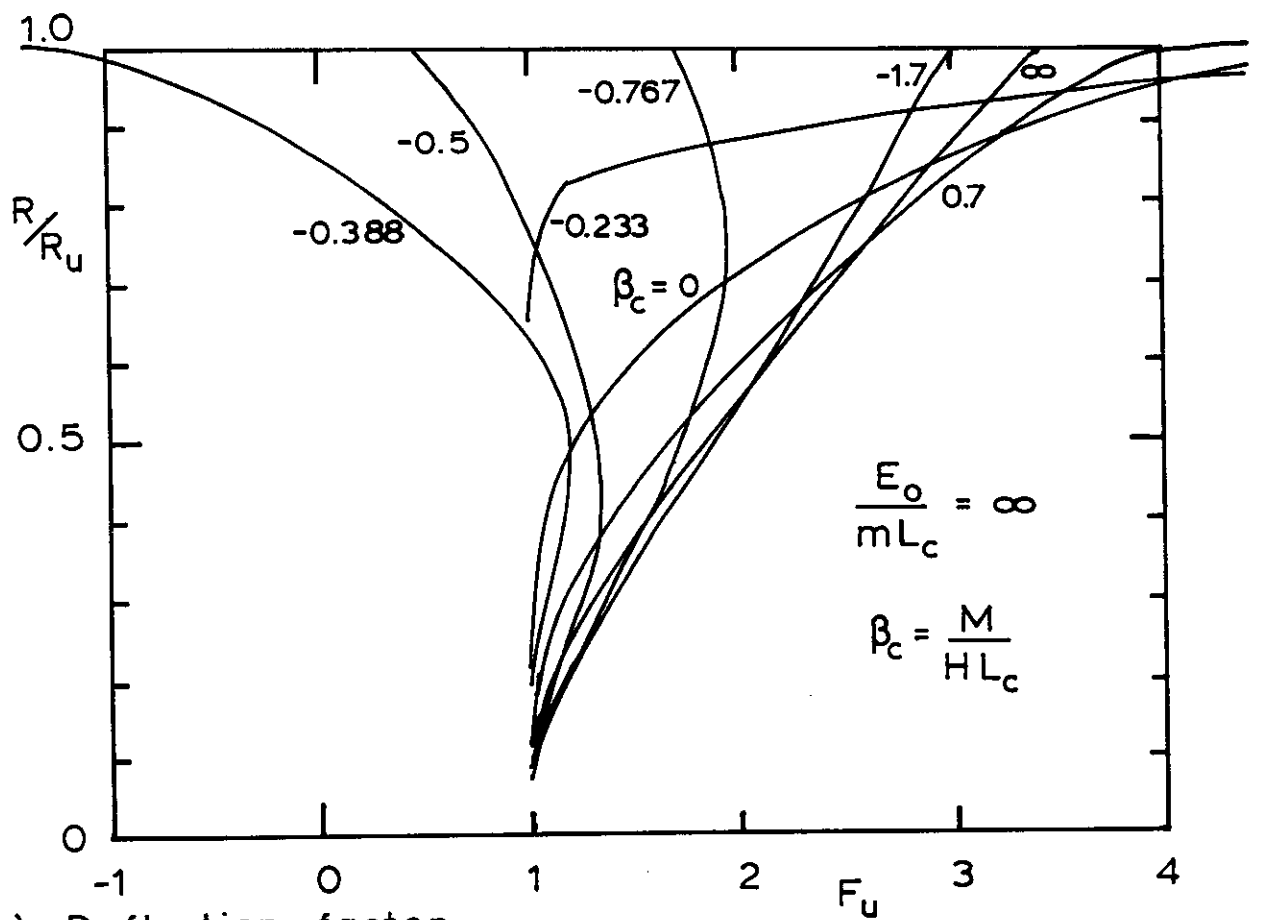
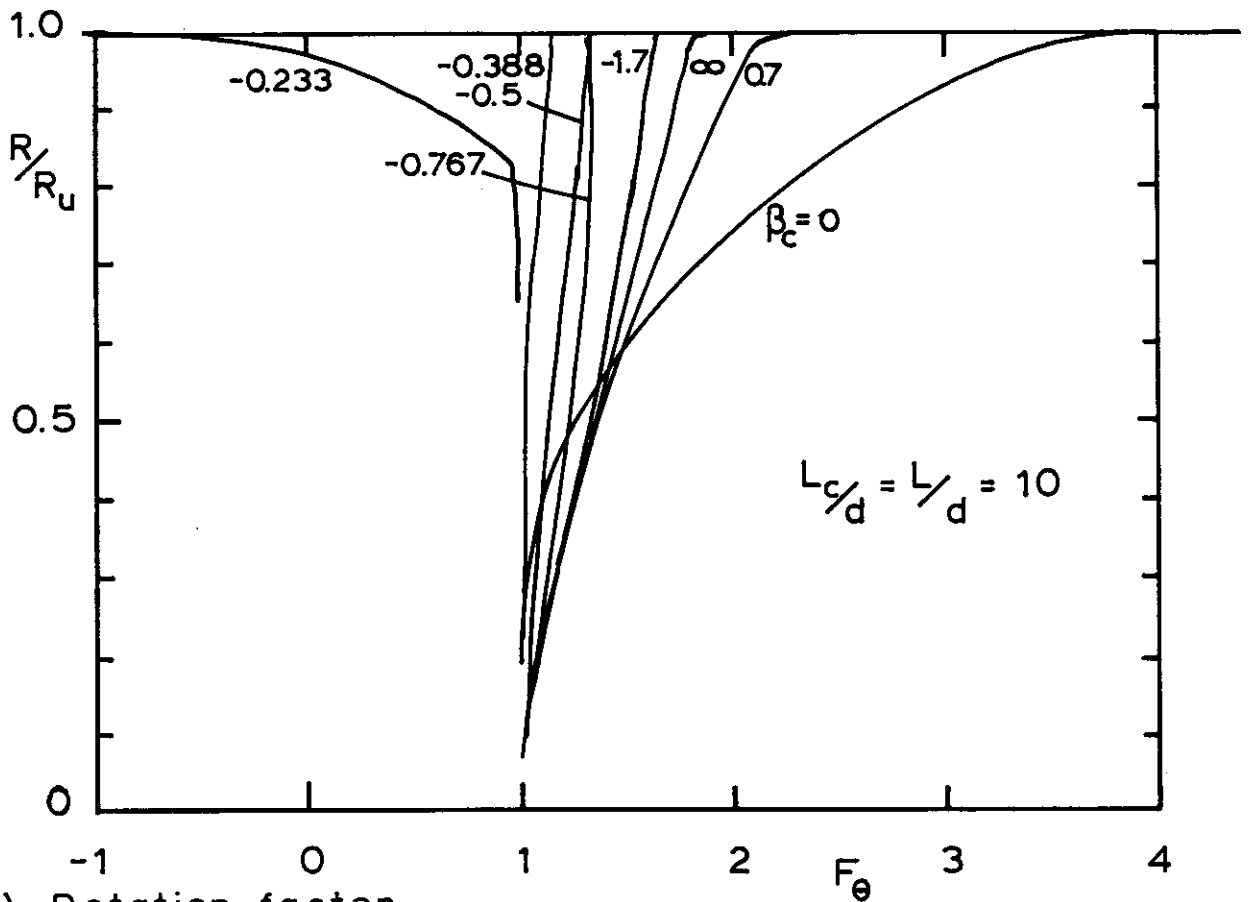


FIG. 5.9 ULTIMATE LOAD, R_u AT COLLAPSE OF SOIL WITH A LINEAR DISTRIBUTED LOAD, W_y

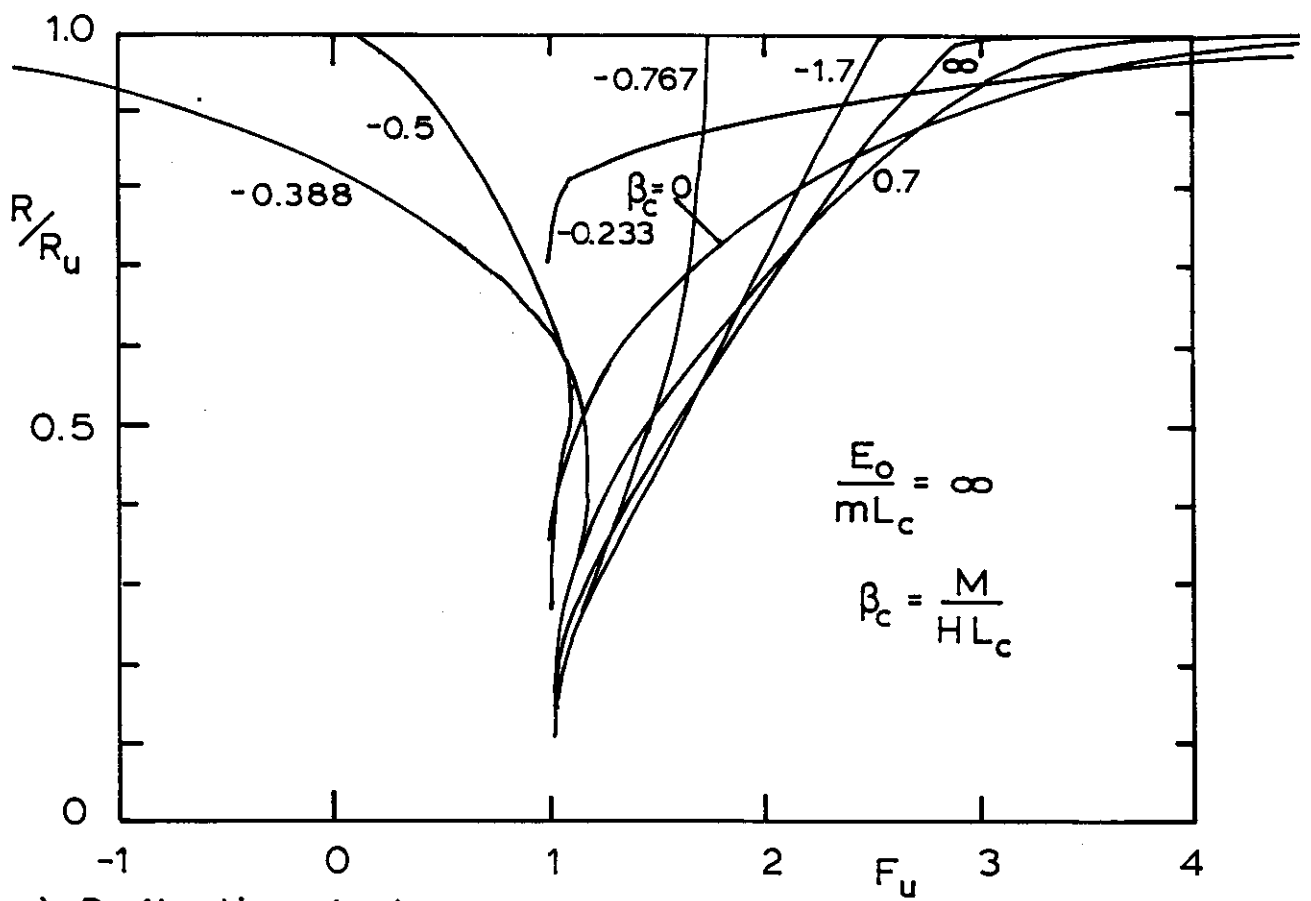


a) Deflection factor

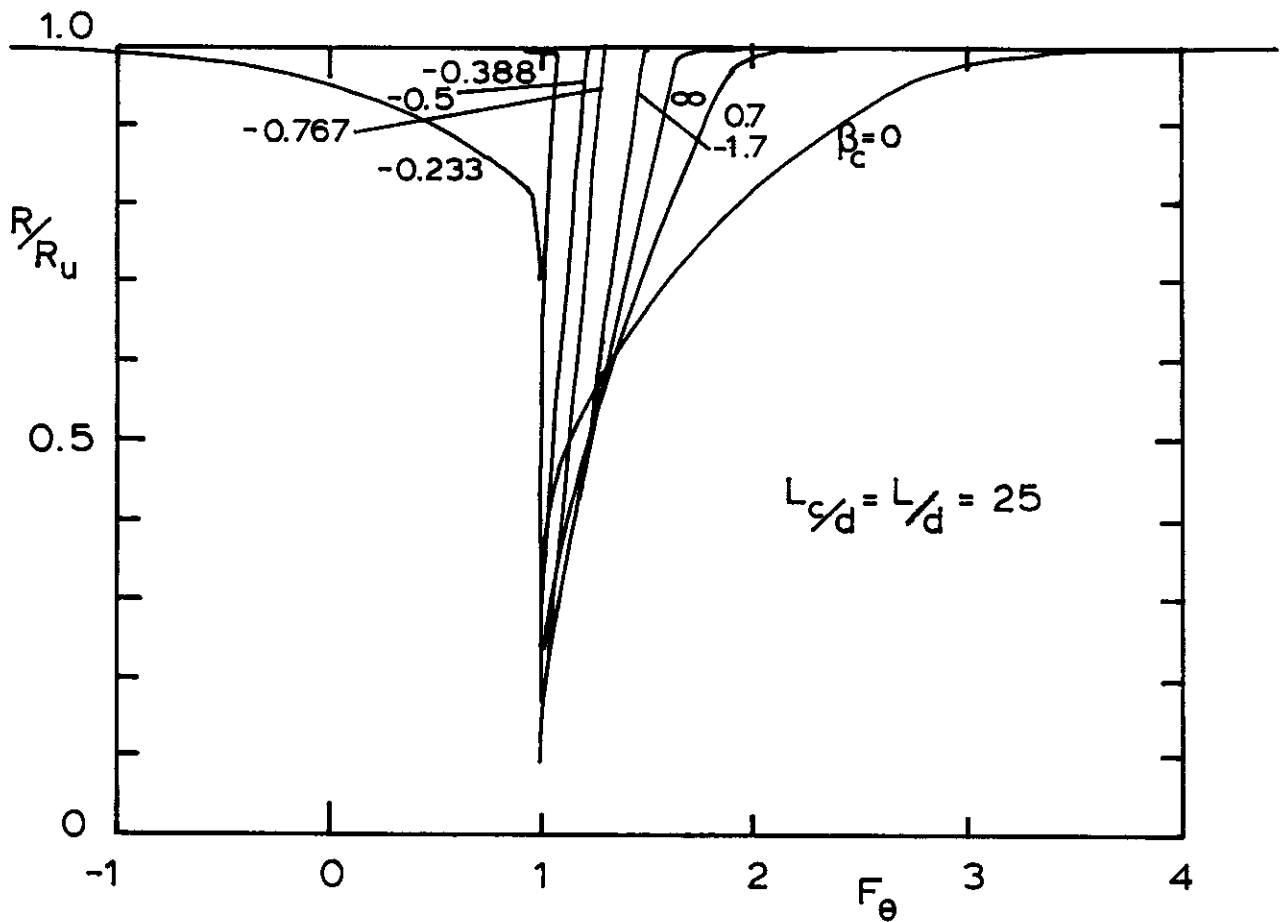


b) Rotation factor

FIG. 5.10 NON-LINEAR MBEM ANALYSIS: PILE HEAD RESPONSE MULTIPLYING CORRECTION FACTORS F_u AND F_θ $L_e/d = 10$



a) Deflection factor



b) Rotation factor

FIG. 5.11 NON-LINEAR MBEM ANALYSIS: PILE HEAD RESPONSE MULTIPLYING CORRECTION FACTORS F_θ AND F_u , $L_e/d = 25$

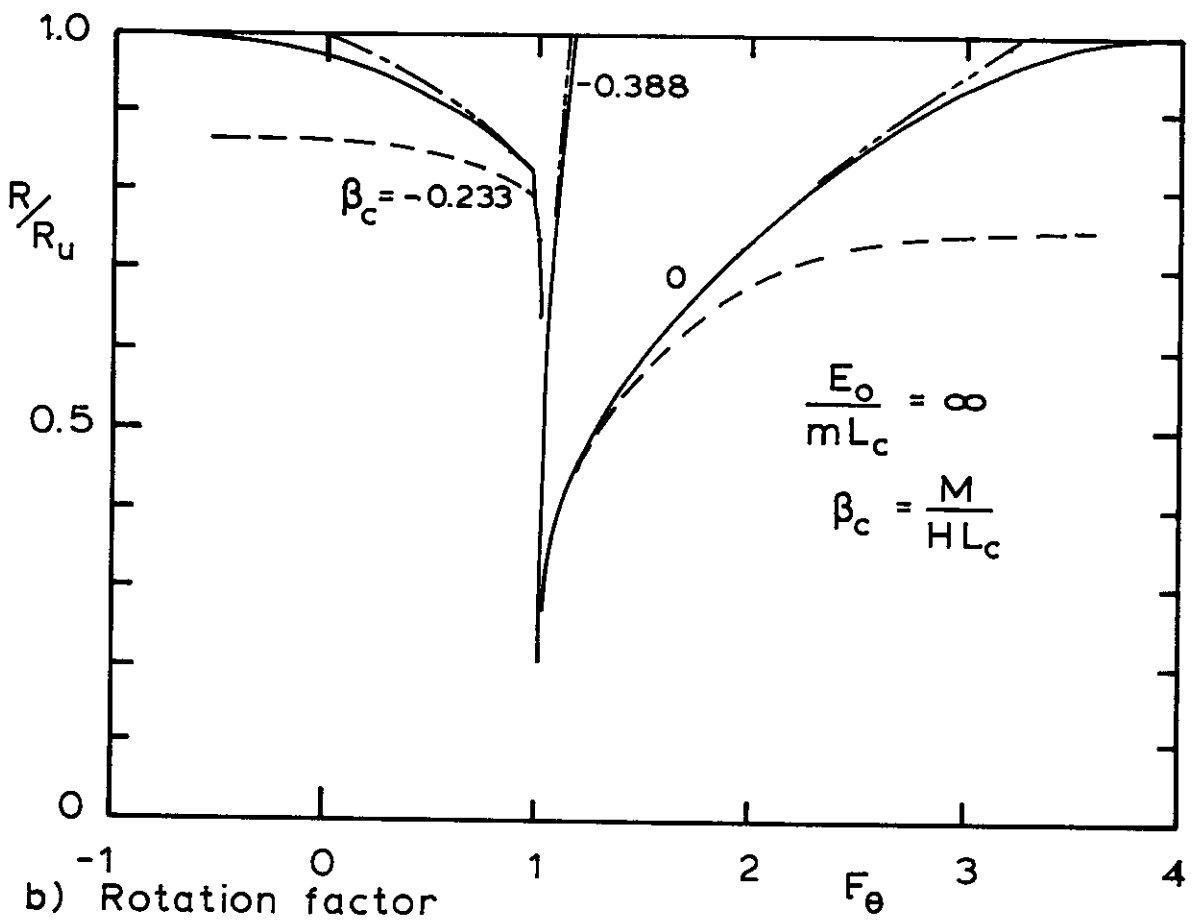
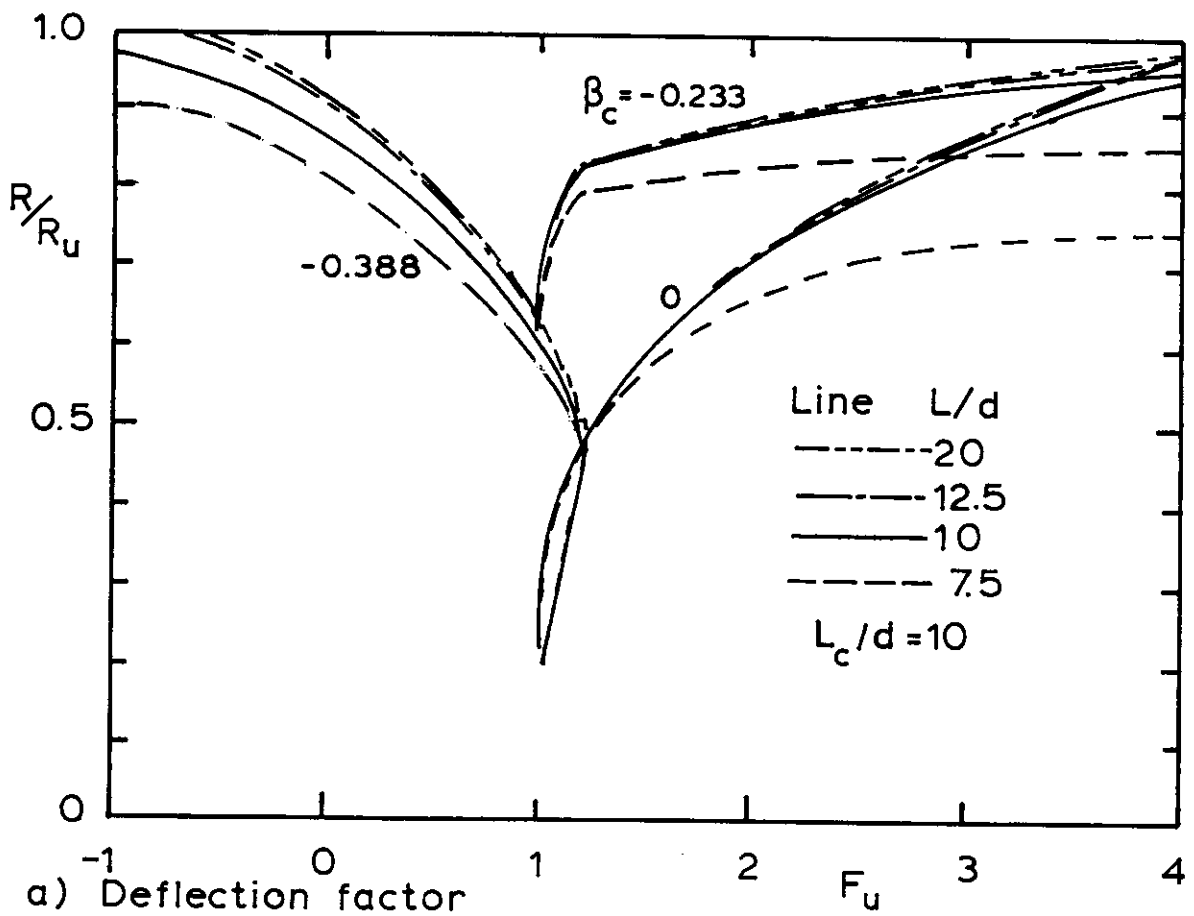
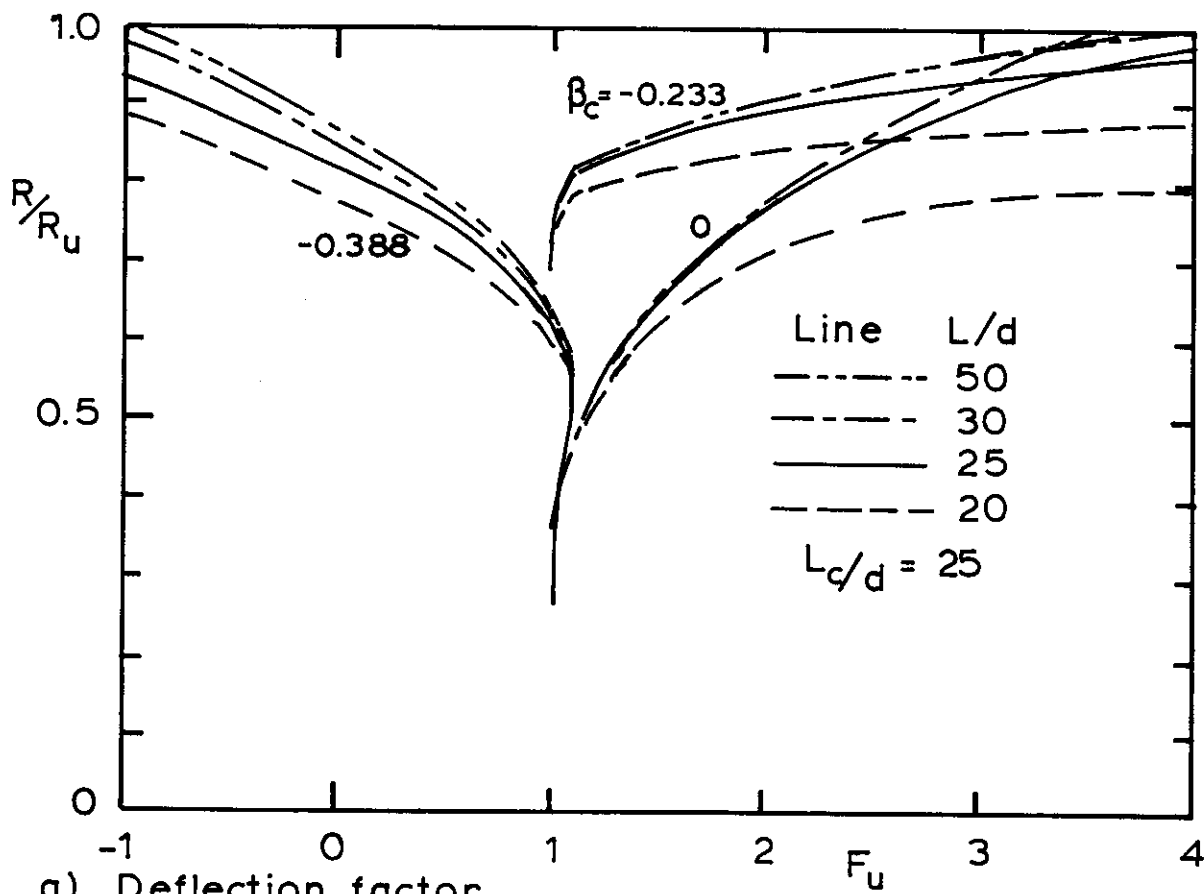
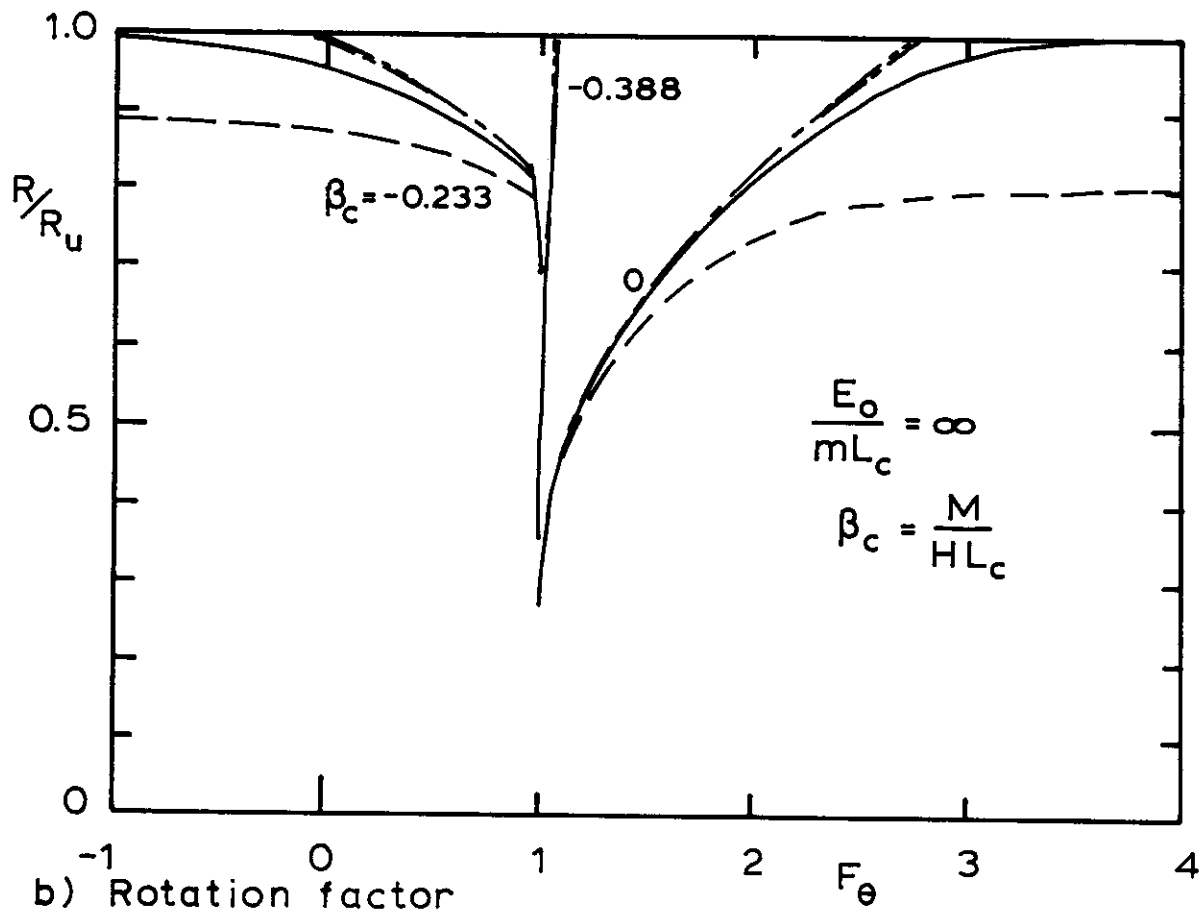


FIG. 512 COMPARISON OF CORRECTION FACTORS FOR DIFFERENT PILE LENGTHS : $L_c/d = 10$



a) Deflection factor



b) Rotation factor

FIG. 5.13 COMPARISON OF CORRECTION FACTORS FOR DIFFERENT PILE LENGTHS : $L_c/d = 25$

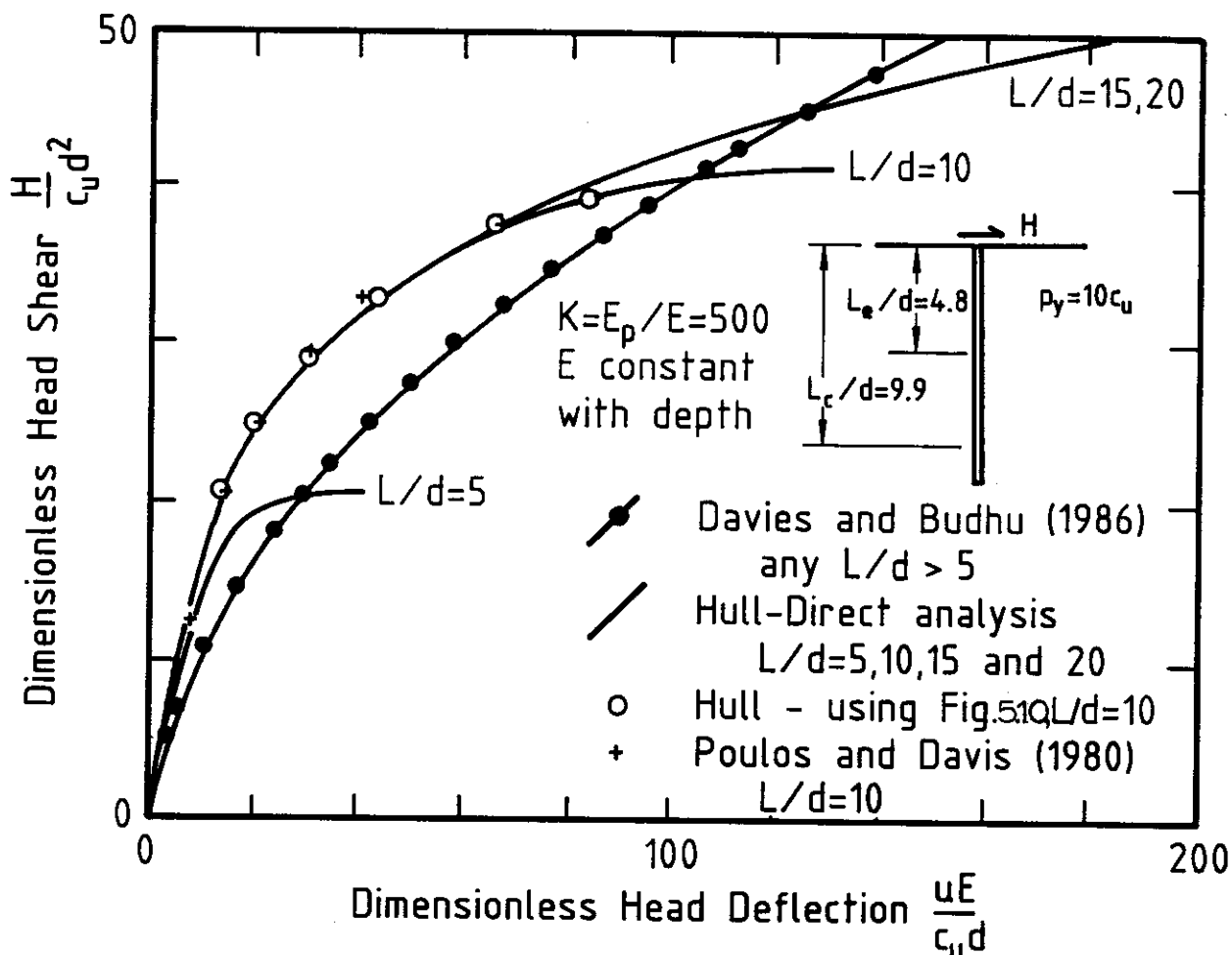
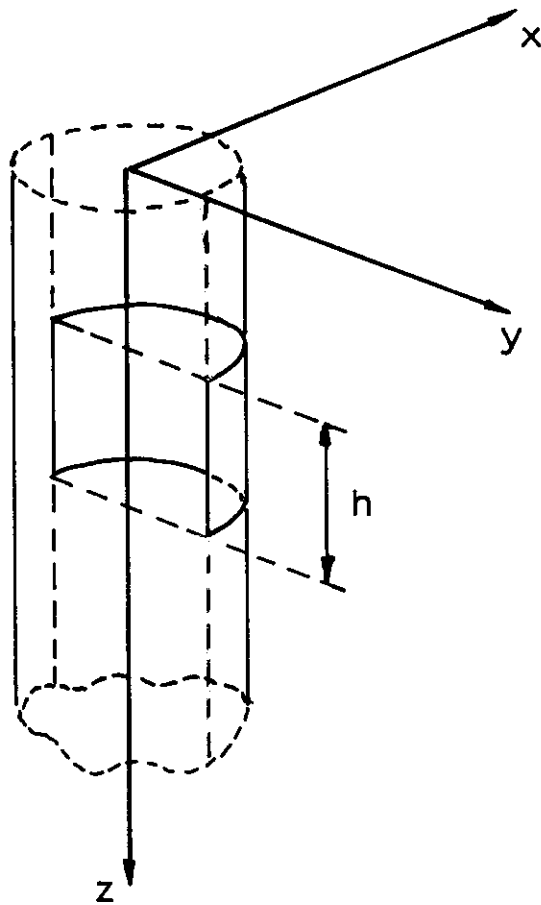
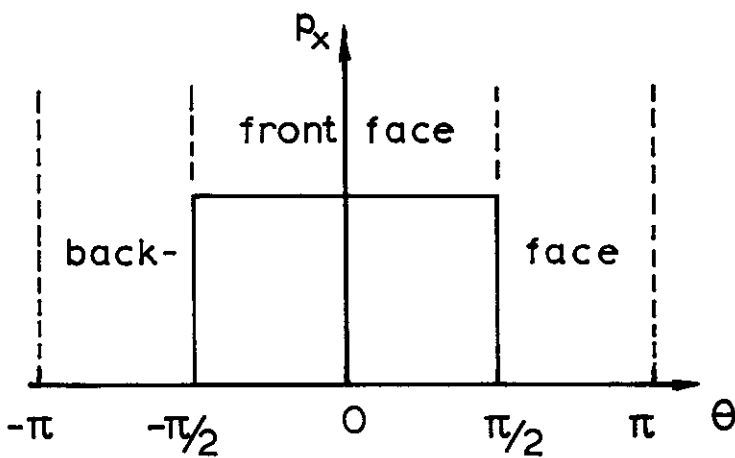


FIG 5.14 DIMENSIONLESS HEAD RESPONSE TO HEAD LOADING



a) Definition of an element front face in the biface soil-structure interaction model



b) x-directed traction, p_x over a front face

FIG. 5.15 THE BIFACE ELEMENT FOR LATERALLY LOADED PILE ANALYSIS

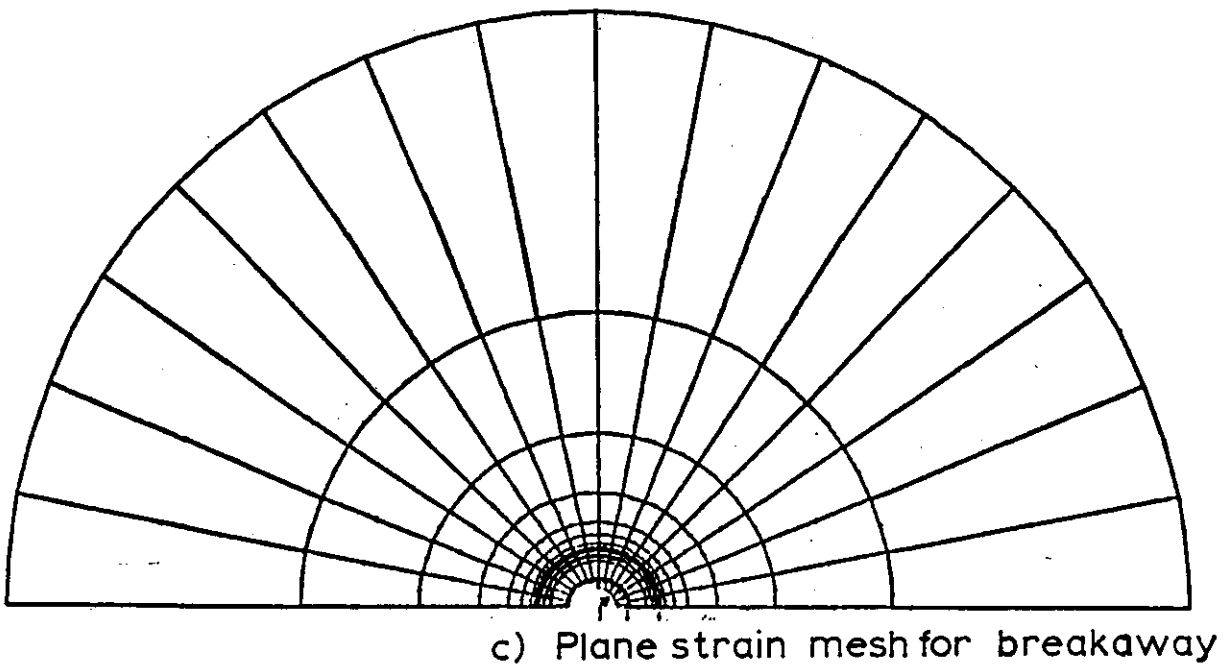
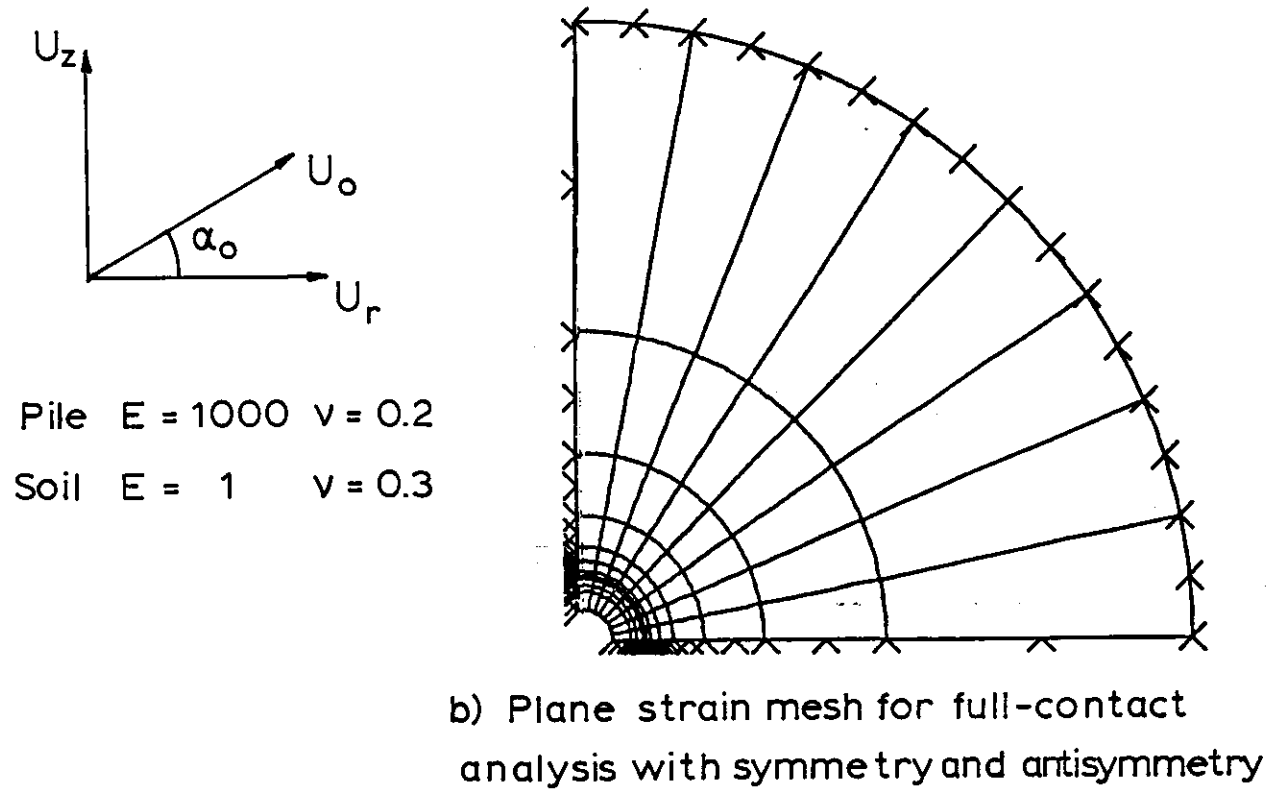
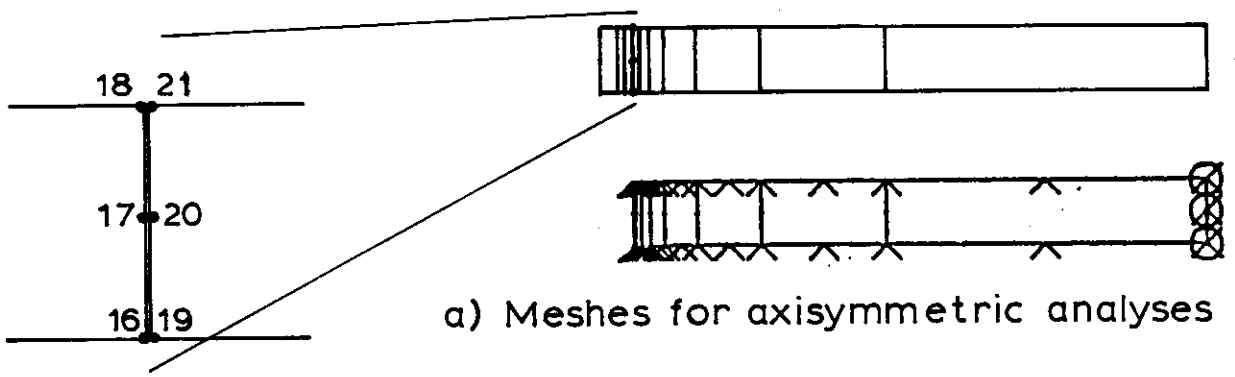


FIG. 5.16 FINITE ELEMENT MESHES FOR THE PLANE STRAIN PILE SEGMENT ANALYSES

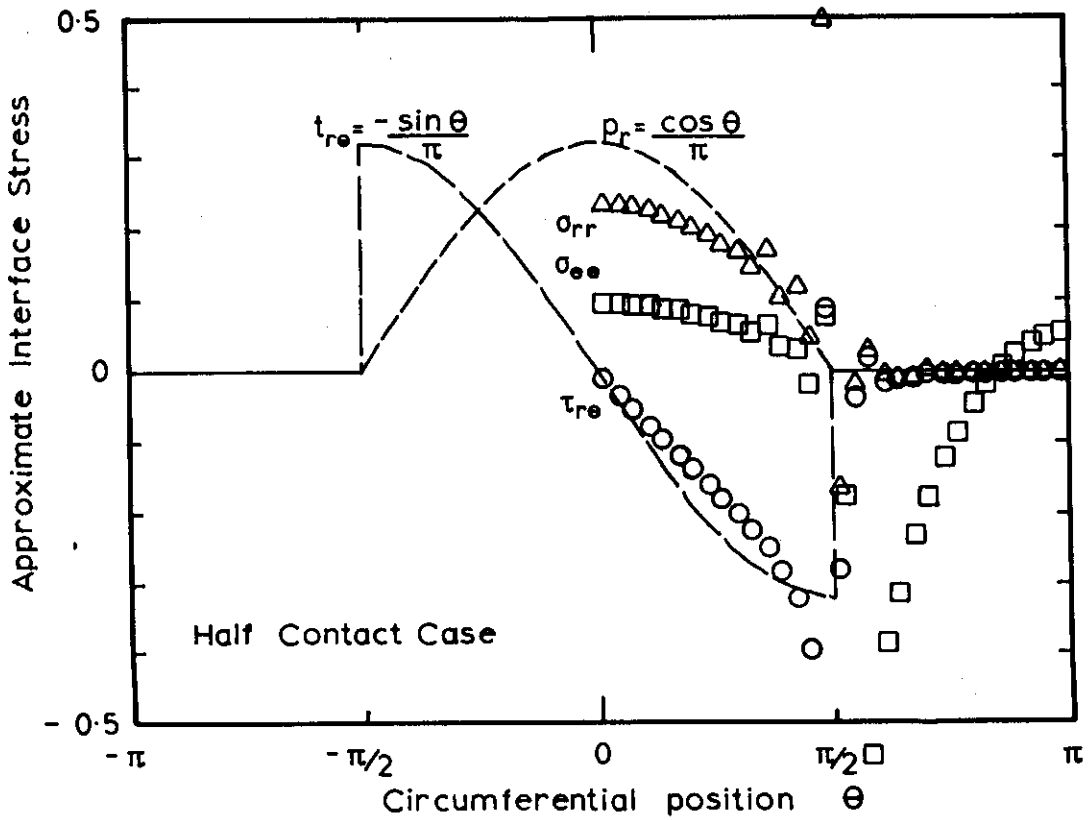
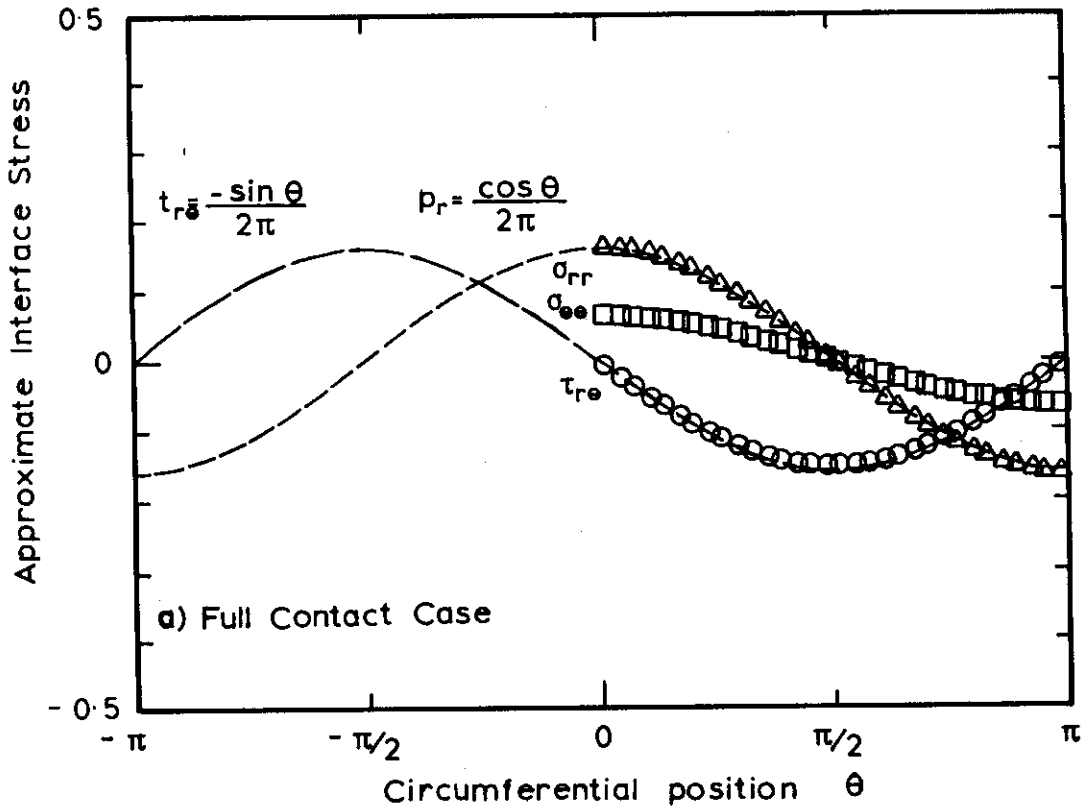


FIG. 5.17 PILE SEGMENT IN PLANE STRAIN SOIL PROBLEM:

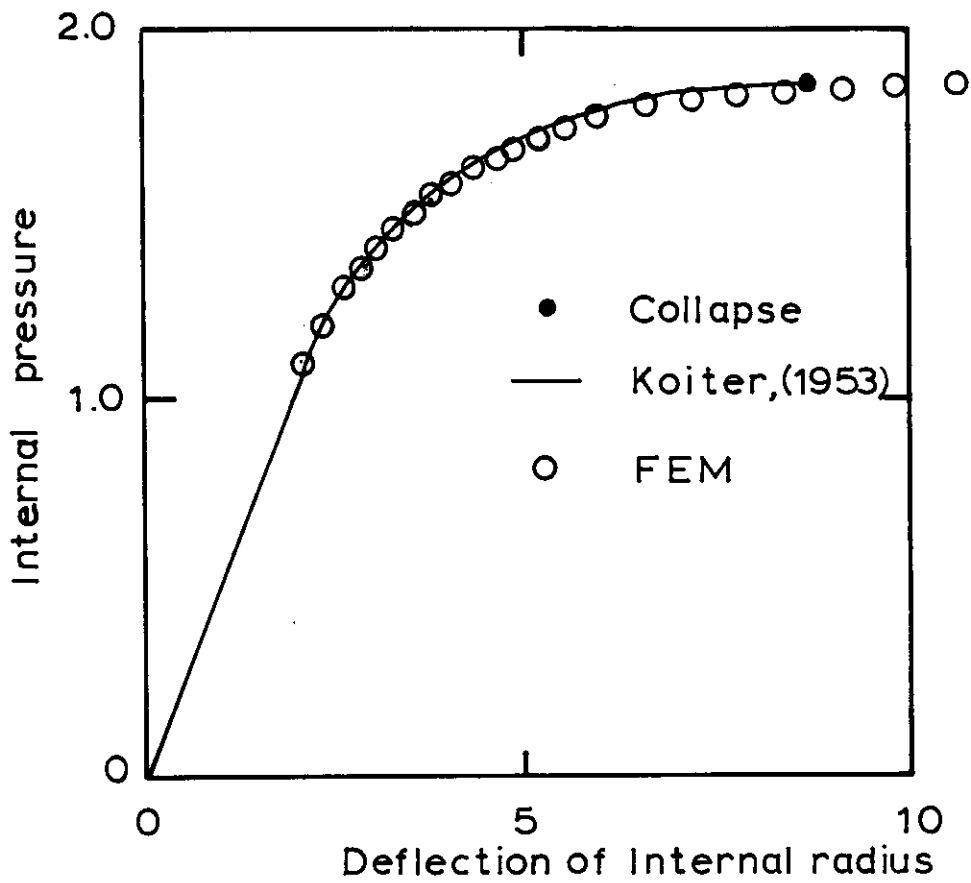


FIG. 5.18 FINITE ELEMENT MODELLING OF ELASTIC-PLASTIC COLLAPSE OF A CYLINDER WITH INCREASING INTERNAL PRESSURE

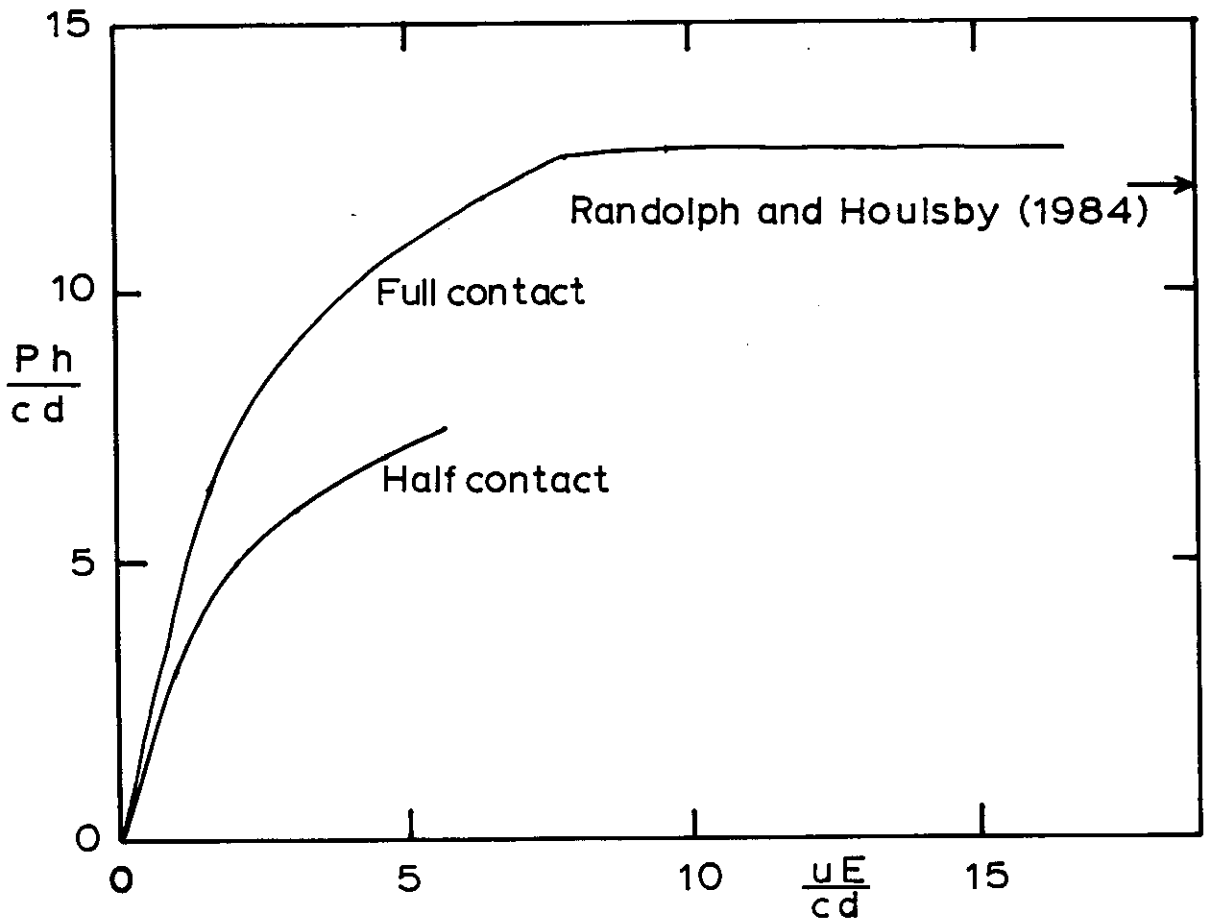


FIG. 5.19 FINITE ELEMENT MODELLING OF ELASTIC-PLASTIC PLANE STRAIN PILE SEGMENT

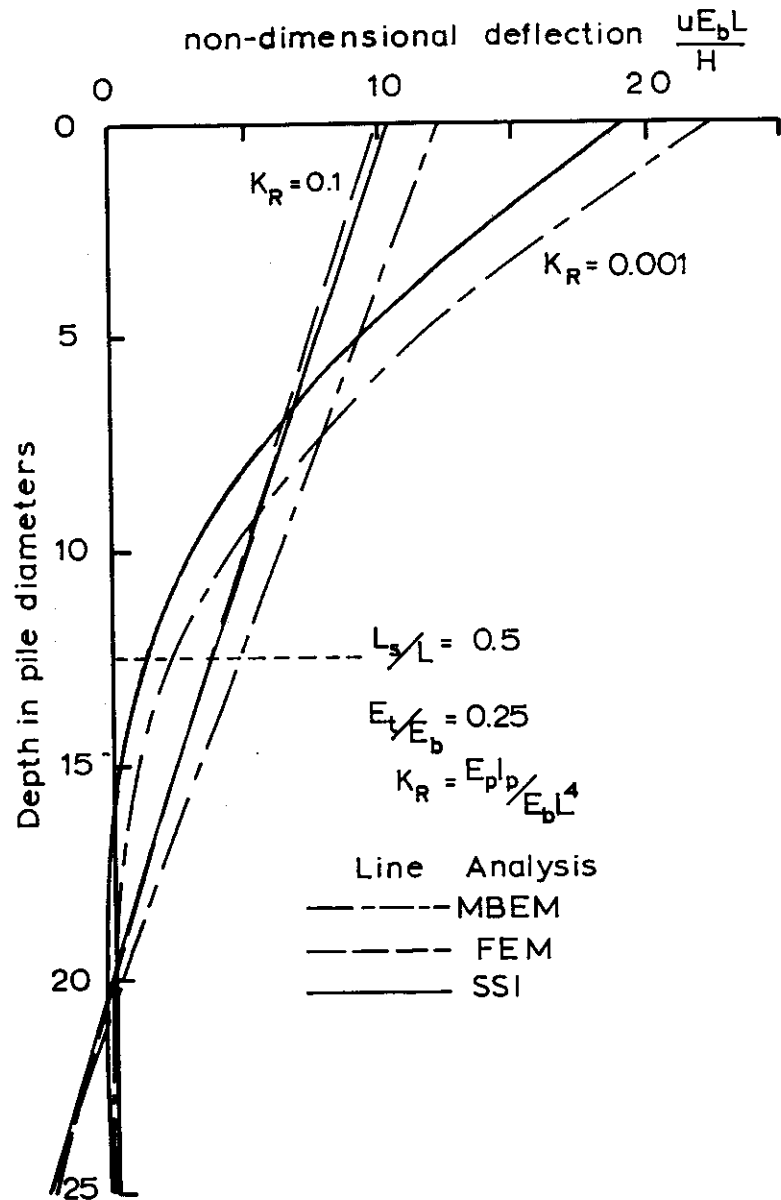


FIG. 5.20 COMPARISON OF PILE DEFLECTED SHAPES FROM THE THREE ANALYSES FOR A PILE IN A LAYERED SOIL

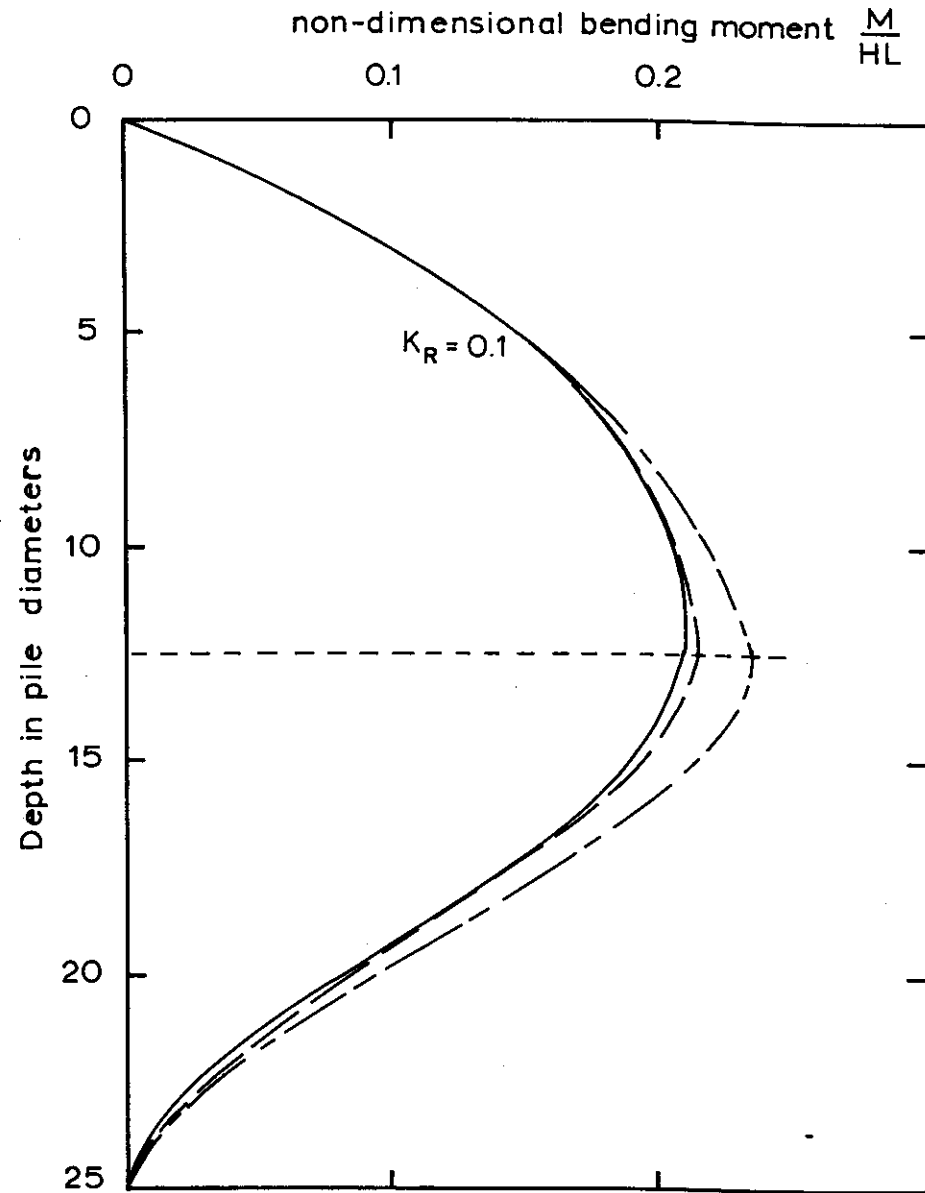


FIG. 5.21 COMPARISON OF PILE BENDING MOMENTS FROM THE THREE ANALYSES FOR A PILE IN A LAYERED SOIL

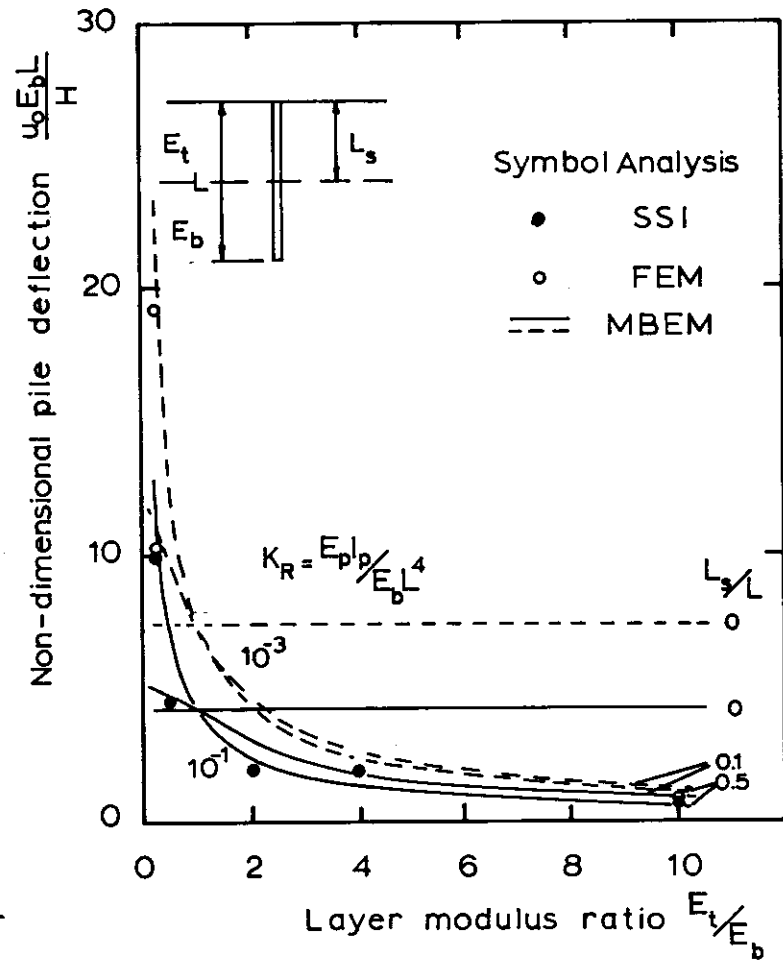


FIG. 5.22 COMPARISON OF HEAD DEFLECTIONS FROM THE THREE ANALYSES OF A PILE IN A LAYERED SOIL

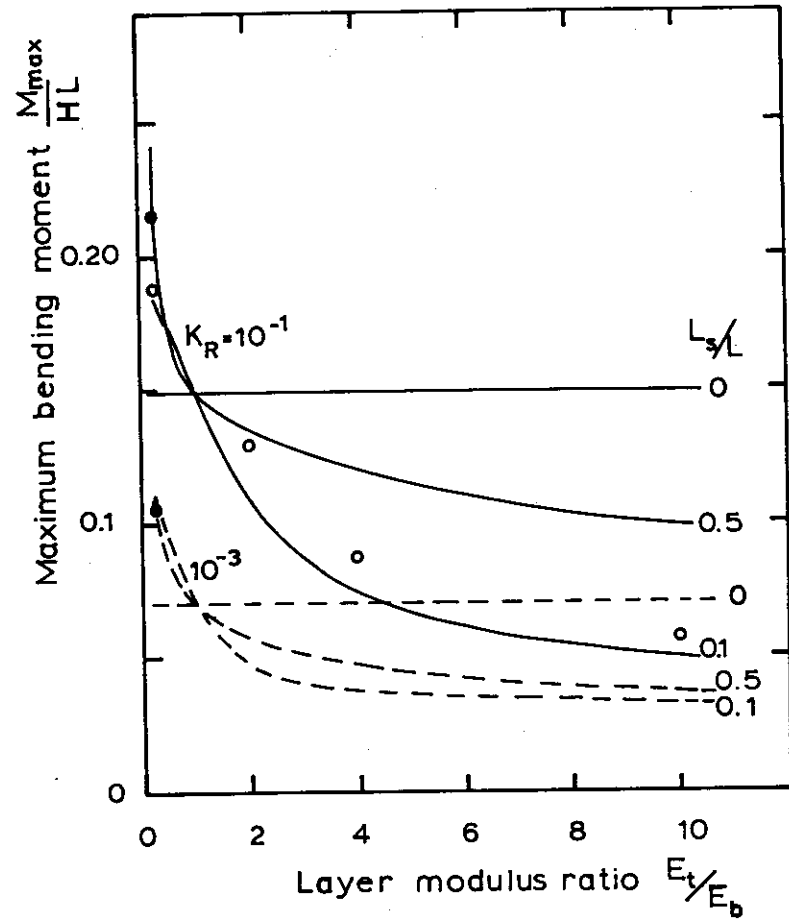


FIG. 5.23 COMPARISON OF MAXIMUM BENDING MOMENTS FROM THE THREE ANALYSES OF A PILE IN A LAYERED SOIL

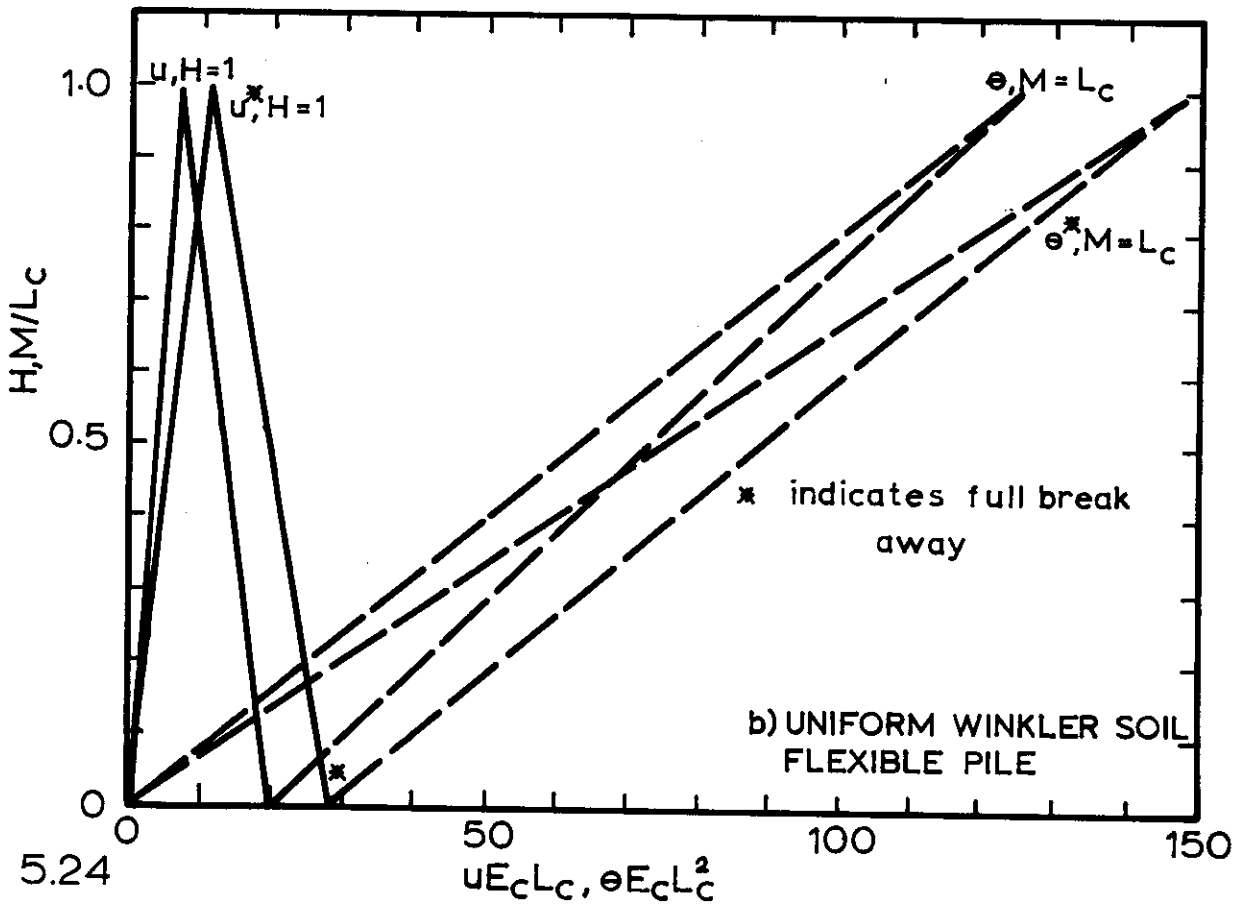
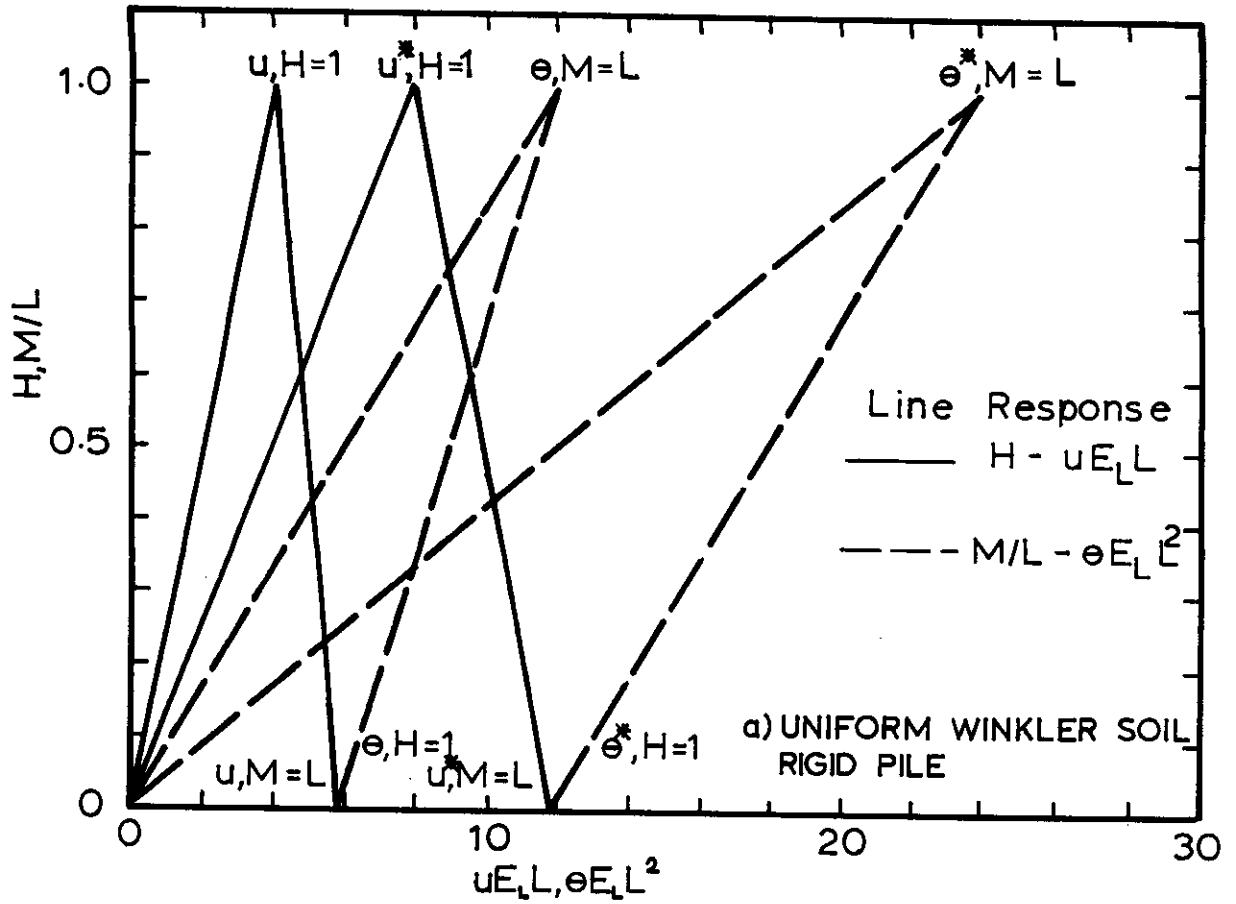


FIG. 5.24

LIMITING GAPPING BEHAVIOR FOR RIGID AND FLEXIBLE PILES
 IN UNIFORM SUBGRADE MODULUS WINKLER SOIL

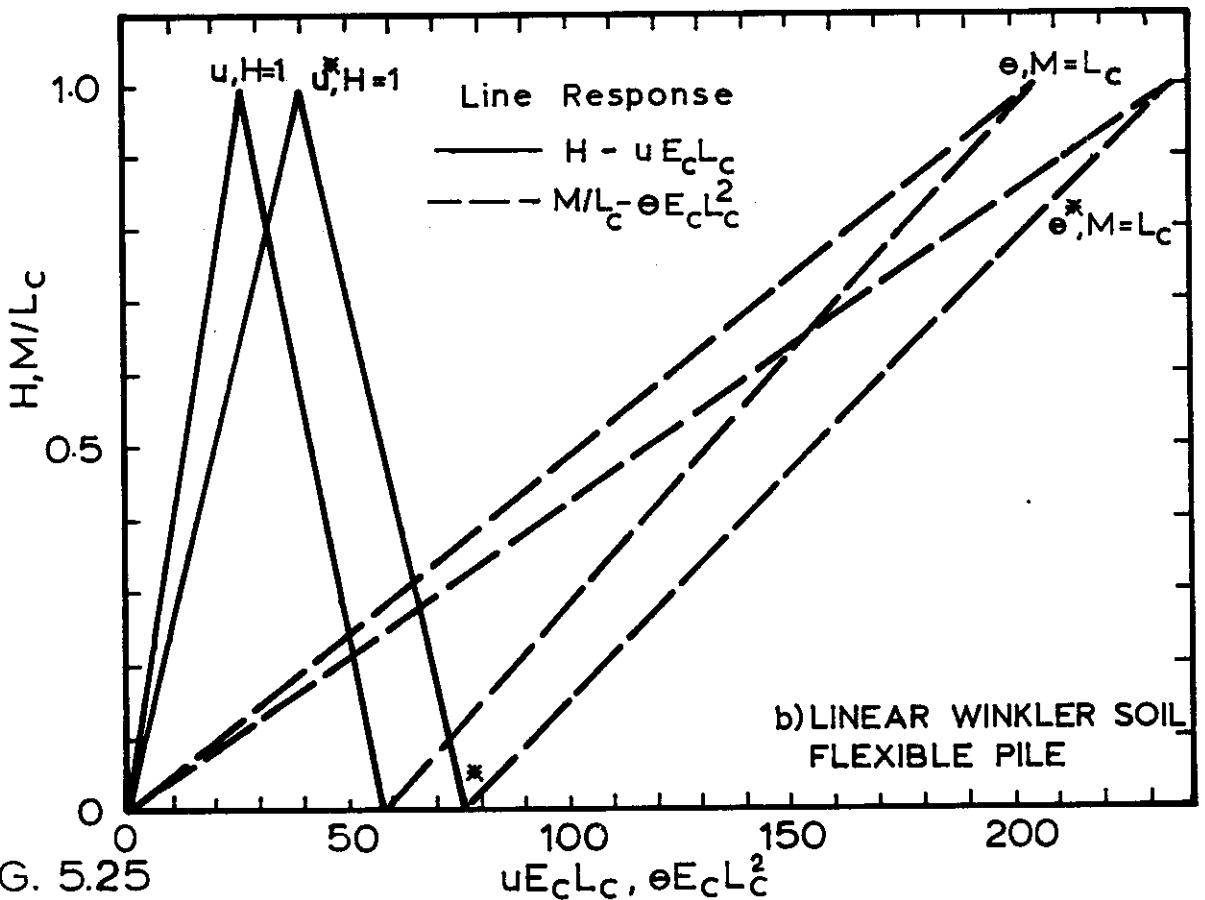
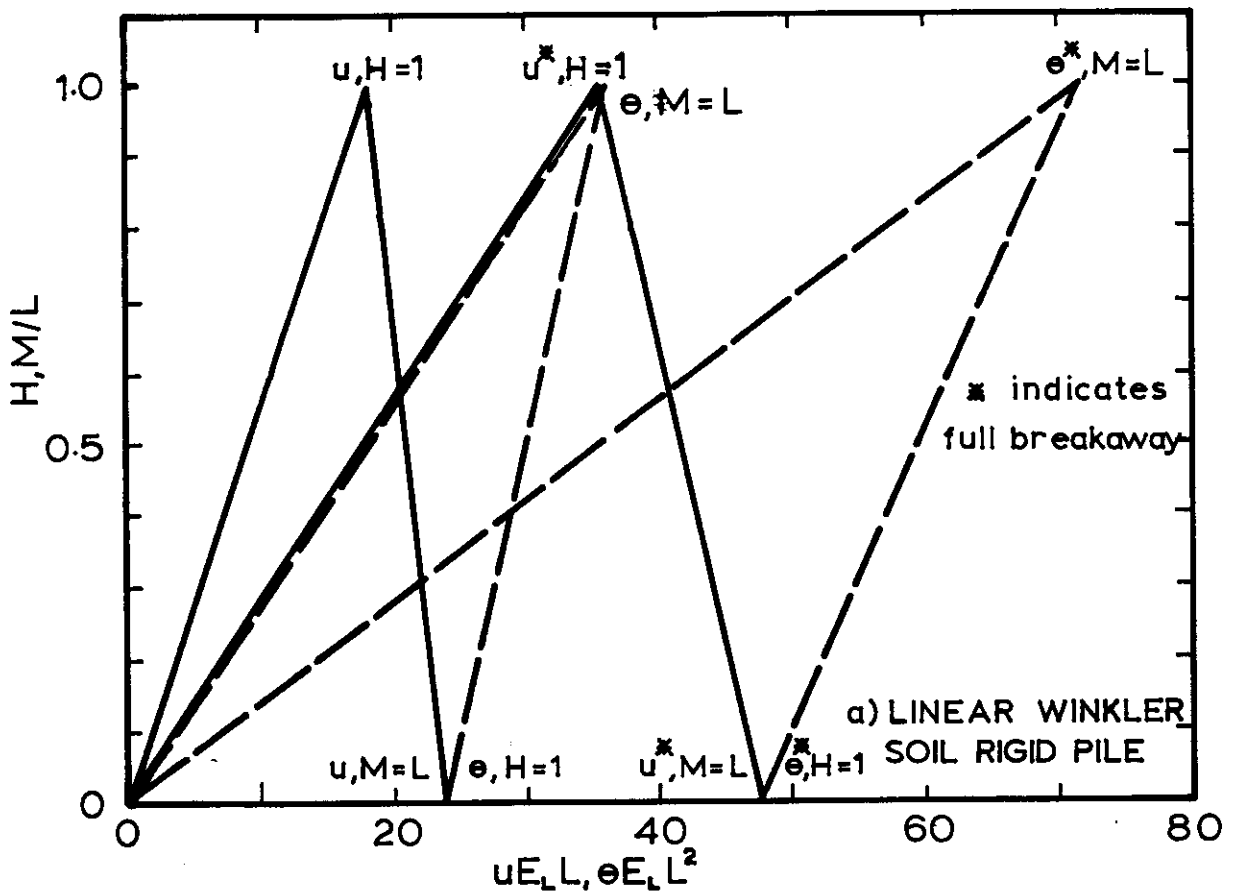


FIG. 5.25
 LIMITING GAPPING BEHAVIOR FOR RIGID AND FLEXIBLE PILES
 IN A LINEAR SUBGRADE MODULUS WINKLER SOIL

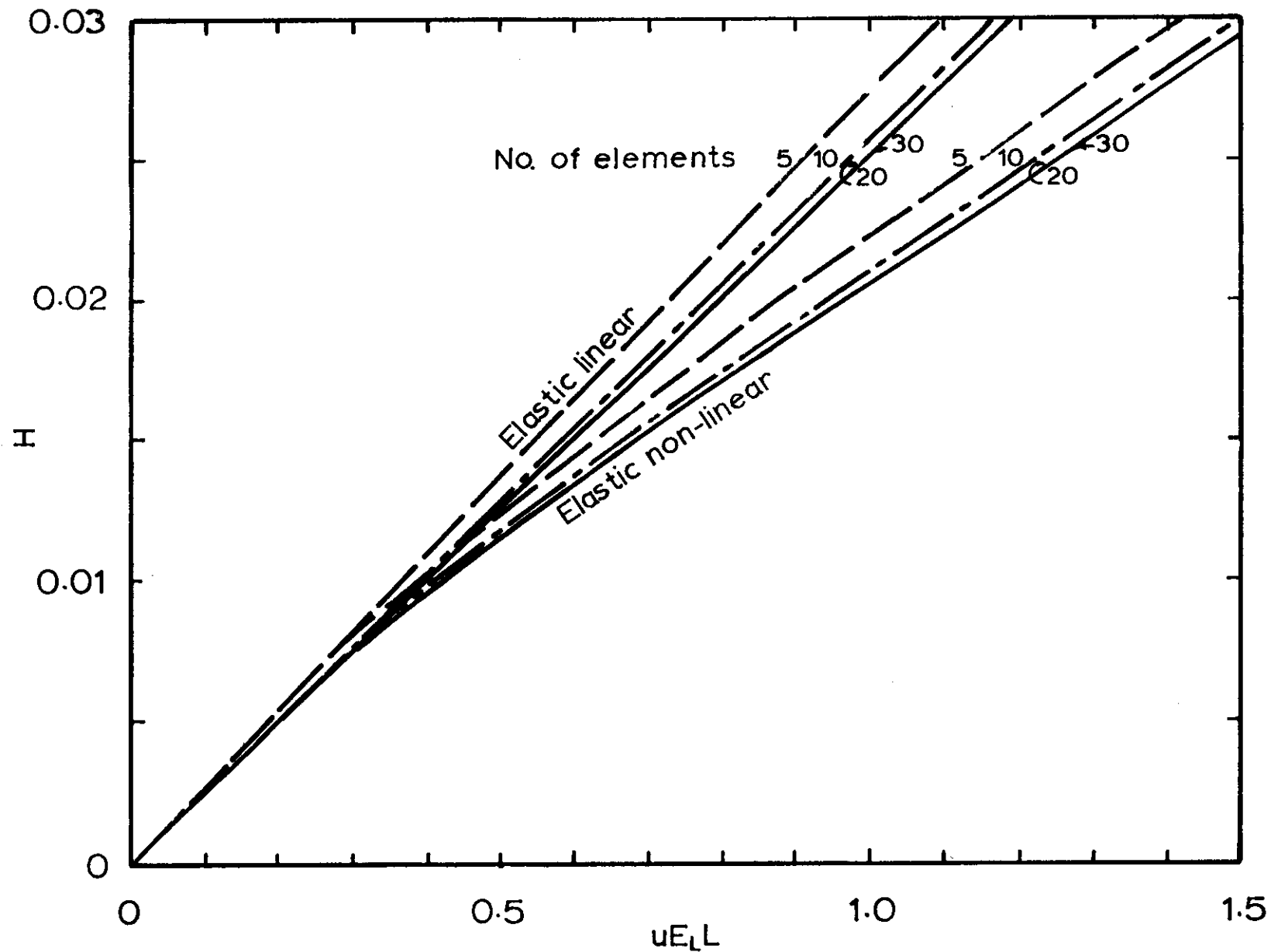


FIG. 5.26 NON-LINEAR ELASTIC BEHAVIOR-PROGRESSIVE GAPPING:
UNIFORM WINKLER SOIL MODEL

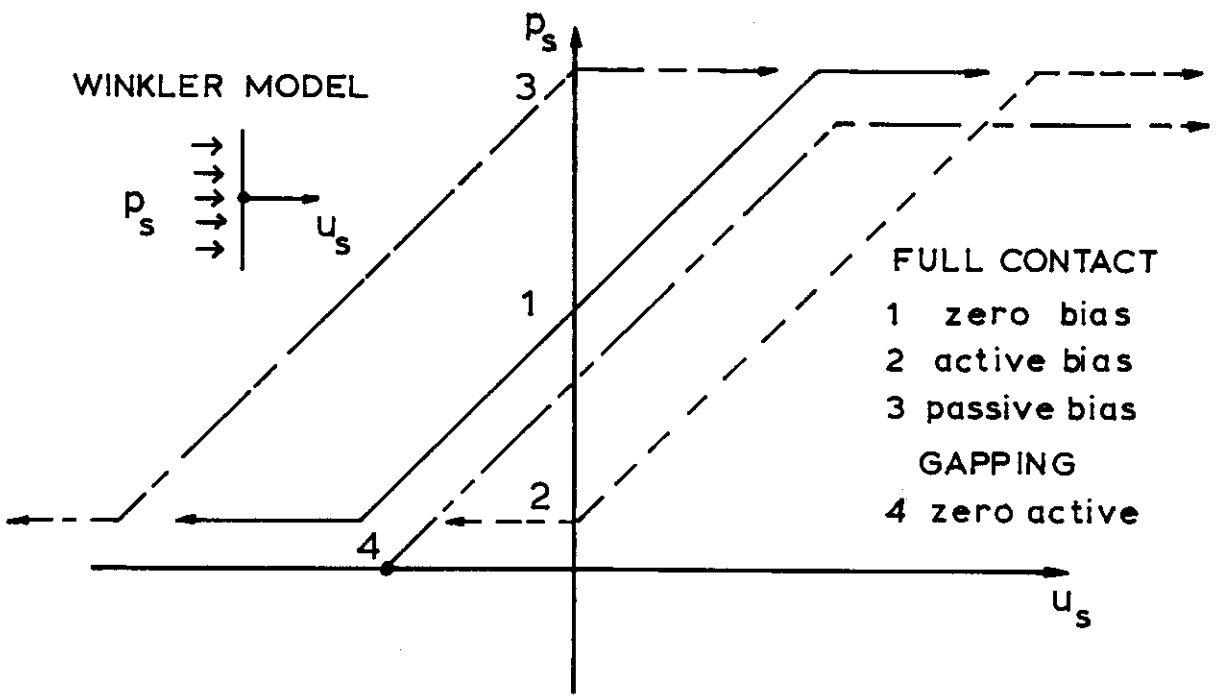
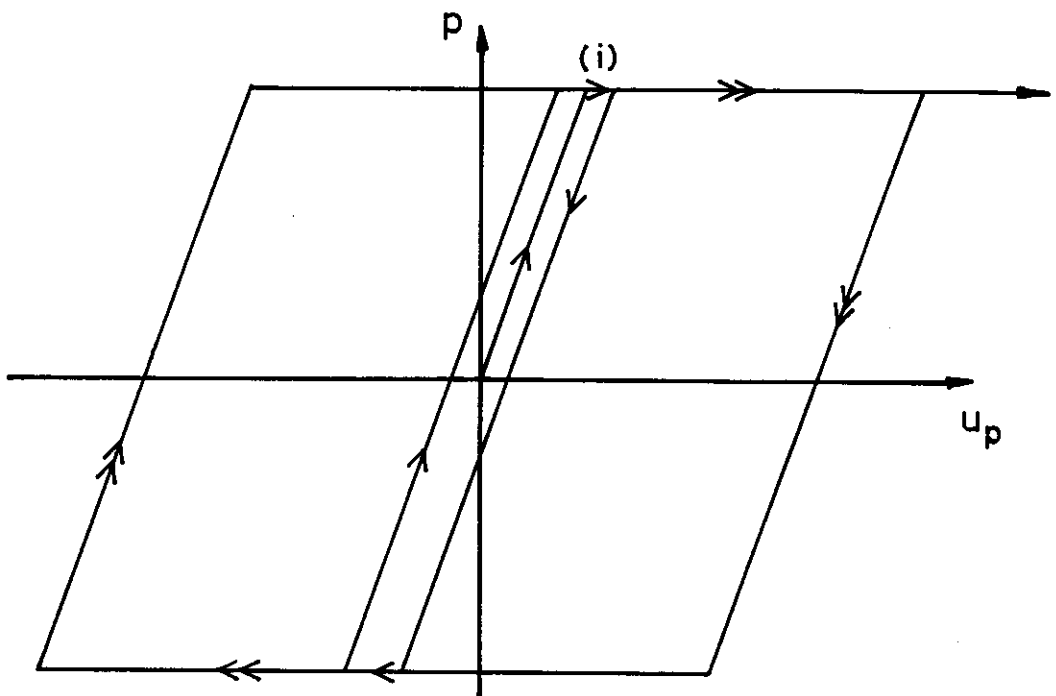
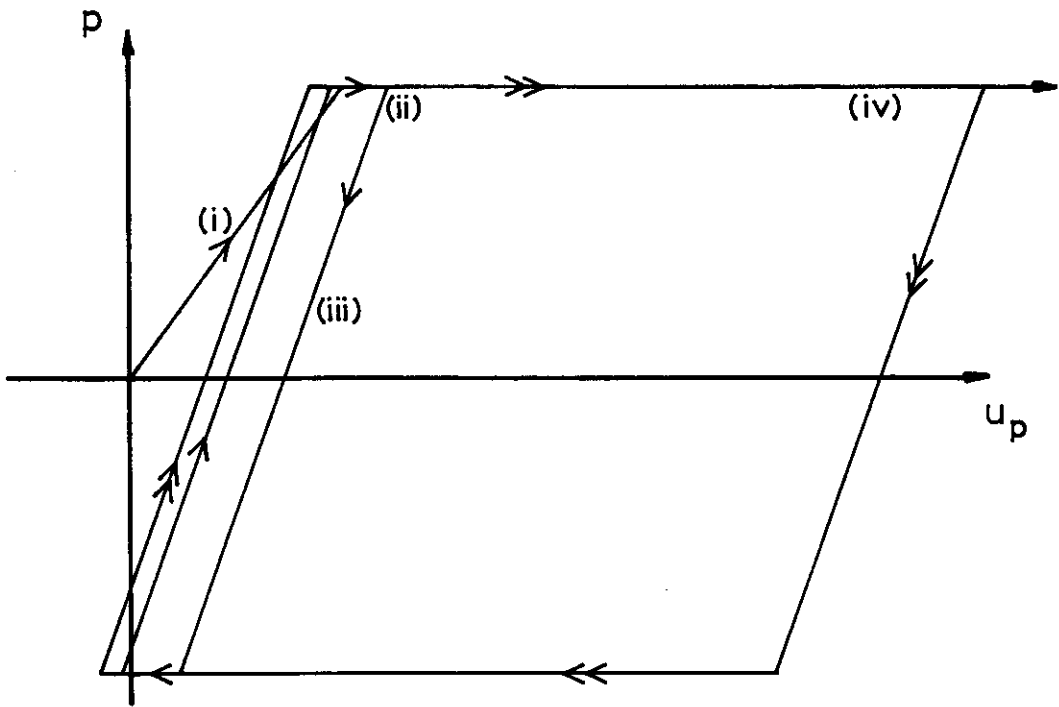


FIG. 5.27 SOIL INTERFACE STRESS-DEFLECTION RESPONSES

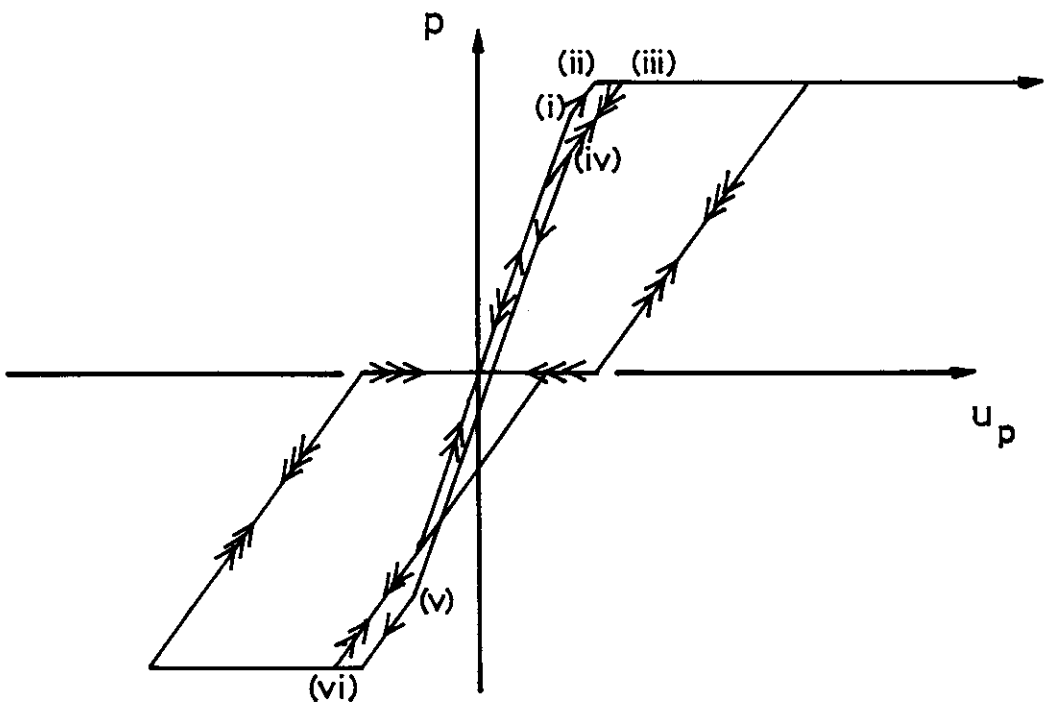


a) Full contact, zero bias case 1

FIG. 5.28 TYPICAL PILE REACTION LOAD - DEFLECTION RESPONSE AT ONE DEPTH



b) Full contact, fully active and fully passive
biased cases 2 and 3



c) Gapping, zero (or negative) active case 4

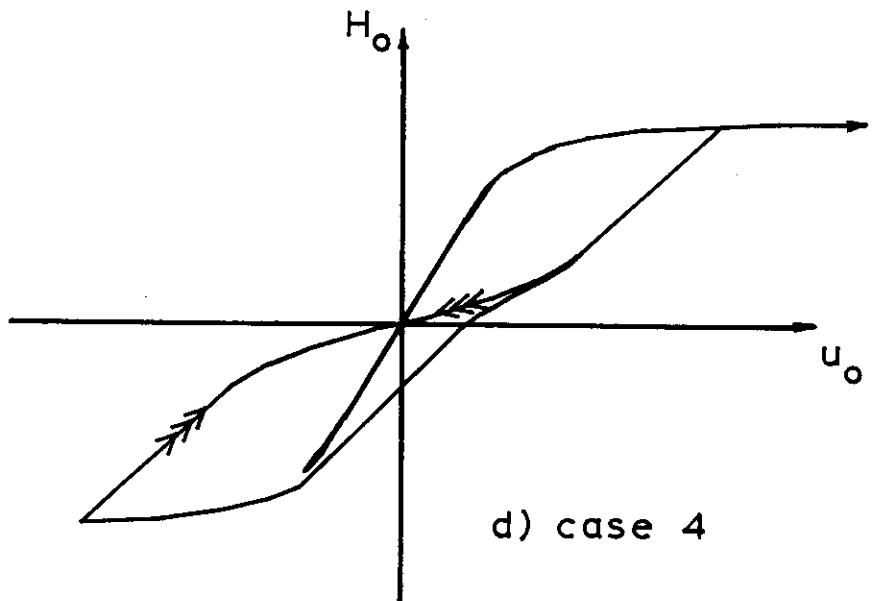
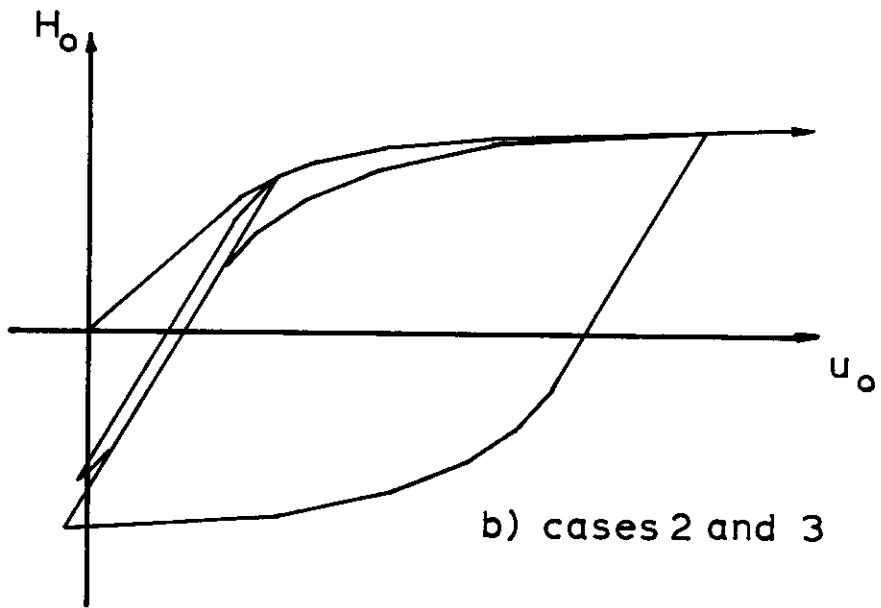
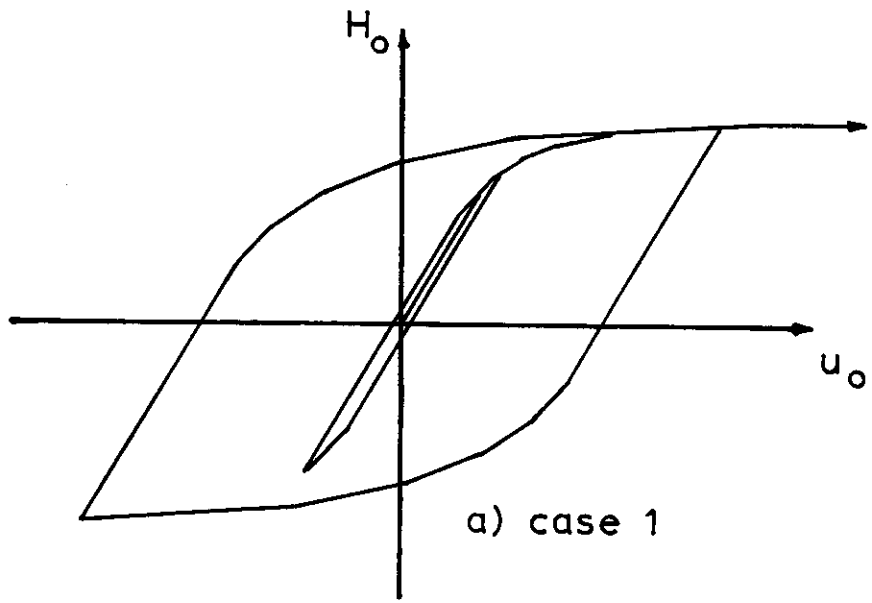


FIG. 5.29 RIGID PILE IN A WINKLER SOIL : HEAD LOAD-
DEFLECTION RESPONE

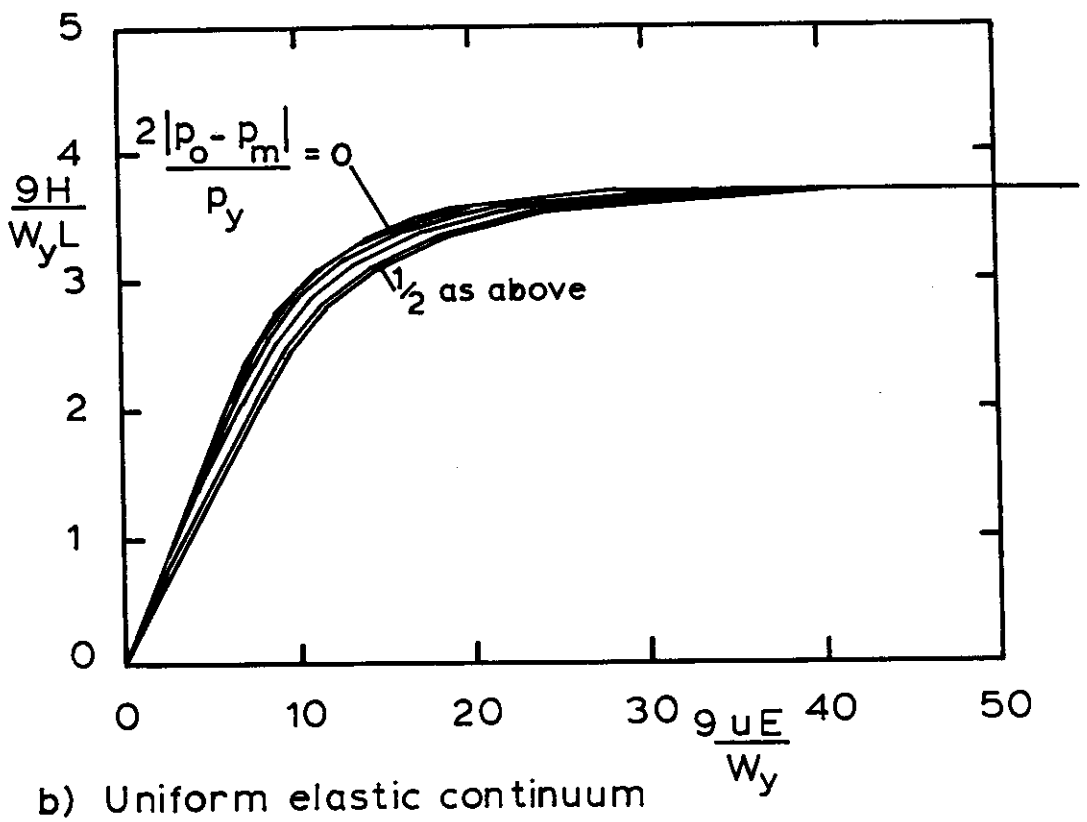
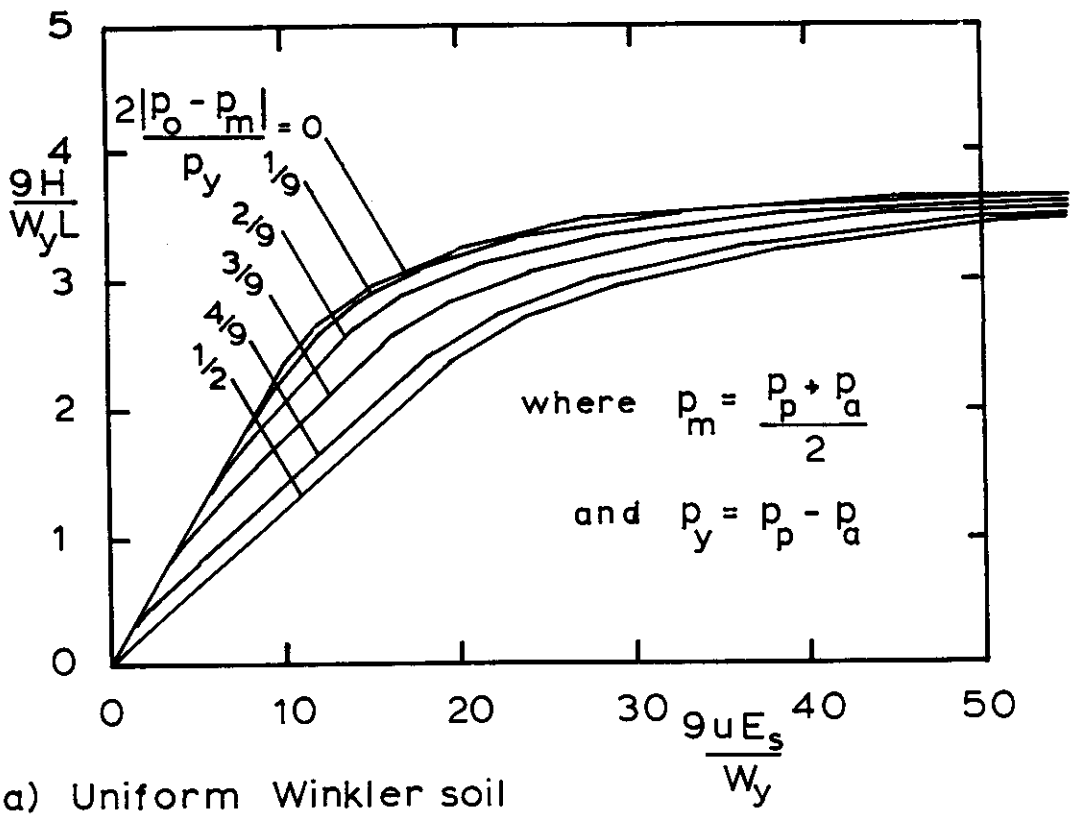


FIG. 5.30 EFFECT OF BIAS PARAMETER ON THE STATIC HEAD LOAD-DEFLECTION RESPONSE OF A RIGID PILE

CHAPTER SIX - LATERAL PILE RESPONSE : EXPERIMENTAL AND FIELD CASES

6.1 Introduction

This Chapter reports comparisons between experimental and theoretical pile behaviour, using a series of model pile tests performed by the writer. Also, the measured response in reported full-scale lateral loading pile tests is compared to the response predicted by the analysis method developed in Chapter 5.

Broadly the experimental investigation comprised two phases:-

- a) small model pile lateral load tests in beds of clay consolidated and tested under vertical overburden pressure.
- b) larger-scale pile tests using a strain-gauged pile in prepared beds of clay without overburden pressure present during the test.

Connected with the lateral pile tests were a number of Quick Undrained (QU) triaxial tests performed upon samples cored from the bed of clay after the lateral pile tests.

Tests in category a) were conducted to provide experimental results for a soil body in which the stress state can be reasonably predicted. Due to limitations of the testing equipment, it was impractical to test, under an overburden pressure, piles of sufficient dimensions to allow strain gauging. This necessitated the series of tests b) on larger beds of clay prepared under a consolidation pressure and then allowed to swell back to atmospheric pressure. The pile used in these tests was strain-gauged (see Swane, 1983) in order to record values of bending moment at several locations, and the "open vessel" technique of testing allowed free access to the outstand of the pile for deflection and rotation measurement.

6.1.1 Data Acquisition and Manipulation

Before presenting the closed-vessel, open-vessel and tri-axial test results there follows a description of the method by which data from these tests was gathered, stored and reduced.

The nature of the tests required accurate and frequent measurement of deflections, loads, pore water pressures and bending moments. In order to accomplish these measurements a data acquisition system was used. A Hewlett Packard Data Acquisition System was available for this purpose, but had not been commissioned. During the procedure of readying the system for actual use, much was learned about the requirements and limitations of electronic measuring equipment, but also the large range of its capabilities was recognised.

The use of electronic data acquisition methods led to a number of benefits:-

- a) the readings could be taken more frequently than is possible by manual methods.
- b) the readings were more accurate and consistent than manual readings.
- c) the reading of instruments continued overnight.
- d) the received data was immediately available in result form.
- e) the system could also be used to actuate switches and fully automate the test procedure.
- f) the data could be stored on disk to be accessed later for comparison with other tests.

The main components of the system and their tasks will now be described.

Digital Voltage Measurement

The majority of electronic measurement devices provide a voltage output that varies as a function of the measured quantity. To supply the computer-based system with digital data a voltmeter, or rather an analog to digital signal converter, is required. This converter is the Digital Volt Meter (DVM), and the quality of the data collected by the system is directly governed by its quality.

The HP3455A DVM has a 6 digit display, measuring to one micro-volt. This resolution is more than adequate for most transducer outputs and proved useful for identifying problems of drift and transducer instability. Accurate readings require long signal integration times and so less readings per second are possible than with less accurate readings. This conflict means that if very fast readings are required, the scatter in such a set of readings may reduce the accuracy to an undesirable level. For the system used in the high resolution mode the maximum reading rate was about ten per second. This rate is adequate for the tests undertaken and any faster reading rate is well into the realm of dynamic behaviour and so outside the scope of the present work.

Scanner

The scanning system consists of a plugboard that allowed data lines from the tests to be connected to any desired input channel of the scanner. The scanner directs the instrument signals to the DVM where they can be read individually and also closes switches to operate loading machines.

Controller

The device used to control the data acquisition system is a HP9825 micro-computer. This micro-computer provides the means by which the experimenter interacts with the testing and alters the flow of data and course of the test.

Peripherals

When the data has been collected into the memory of the micro-computer, it remains to present this data in an acceptable form and store it for future reference.

A thermal printer provided a means of rapid and immediate communication with the operator and also gave an immediate hard-copy of the test results. Legibility and long term readability of the thermal type printer paper was poor and a high quality daisy wheel impact printer was employed to provide permanent tables of data as required after the end of a test.

A single line, light emitting diode display on the HP9825 was the quickest form of communication with operator, but also the most temporary. All important warnings and messages were printed as well as displayed.

A hard bed plotter was used for obtaining graphs of the variables measured in the tests and had the ability to digitise and change pen colour automatically. Any test that required long term plotting used the fact that the plotter caps and returns the pen on command from the controller, to avoid drying out the pen.

The available mass storage peripherals included mini-disk drives and magnetic cassette tapes. The cassettes were of a type peculiar to the manufacturer of the controller and the disk drives were 8inch with 1500 records available for data. The disk drives proved very reliable and allowed very quick transfers of data during testing and after for data reduction.

The magnetic cassette is a serial access system, meaning the required information must be searched for from wherever the tape

was positioned. If the data was at the end of a tape and the tape rewound to the beginning, delays of approximately 30 seconds to 2 minutes could occur while the tape is being searched. This delay was critical when data was being acquired from a test while other data was transferred onto a cassette. This delay was minimised by positioning the tape during a period of inactivity in the data acquisition phase.

The problem of time delay in data transfer was overcome with the use of a disk drive storage system and direct access to the data by storing the values in data records. Blocks of data were formed and then transferred to a specific record within a file. This means that the data can be retrieved by skipping directly to the record required instead of reading all the data in the records between the file pointer and the required record.

Power Supply for Measuring Instruments

Just as the accuracy of the DVM directly controls the quality of data recorded, so does the performance of the power supply used to energise the measuring instruments. If the power supply does not maintain the voltage and/or current that the instrument requires, the output that is read from that instrument can be badly affected. The power supply used had a very low (virtually unmeasurable) drift in its output and was capable of recovering the desired output value when extra demands were made.

Most measuring devices require a constant voltage. However, some strain gauge applications may benefit from a constant current source. The option of constant voltage or constant current was investigated for the strain gauging operation and for simplicity the constant voltage method was used.

SYSTEM OPERATION

Signal Sources

The measuring instruments can be thought of as signal sources that, given a constant power supply, will vary their output signal as a function of the response being measured.

Linear voltage deflection transducers to measure deflections as small as 0.001 mm upto 50 mm were used, depending upon the expected magnitude of deflections. It is important to use the correct range transducer; the larger the deflection range of the transducer, the less likely it is to sense a small change in deflection accurately. Most transducers were found to be very nearly linear in output versus deflection within the range of the maker's specifications.

The transducers available were of a wire wound resistance change type or used an electronic circuit to sense the position of a metal core in the body of the transducer. The wire wound type was linear but produced step changes in its lower limit of readability. The metal core in an electro-magnetic field type can be slightly non-linear but has a definition of change dependant only upon the accuracy of the system DVM and was the type used for the measurement of deflection in all tests.

Pressure transducers rely upon movement of a strain-gauged plate, and thus need a volume change of the fluid in which the pressure is measured, i.e. measuring the pressure may change its value if the volume change is significant. This effect will only be important in a few specialist applications, e.g. K_0 one-dimensional triaxial tests; for the Quick Undrained triaxial tests carried out, the effect was negligible for the triaxial sample volumes used.

The conventional proving ring was converted to a load cell by using a deflection transducer to replace the dial gauge, using a more accurate small-stroke transducer for very stiff proving rings and longer-stroke transducers for more flexible rings. If it is assumed that the proving ring has a linear load-deflection behaviour and the transducer is linear in the range in which it will deflect, the voltage changes linearly with change in load.

The measurement of strain gauge resistance is best accomplished using some form of a bridge circuit to measure a null balance or potential difference. Using a full bridge and a temperature-controlled environment, readings were repeatable within 5 microstrain over a long period of time.

Signal Conditioning

The signal that is generated by the measuring device may depend upon many factors apart from the response it is meant to be measuring. The temperature, proximity of electrical machines, and radiation from equipment, may all modify the signal on its journey from source to DVM. As well, most transducers and load cells are temperature sensitive to some degree and the application determines whether the effects are serious enough to warrant temperature control. All test equipment was housed in constant temperature rooms and so this potential problem did not arise.

Any system of data lines connecting measuring instruments to the DVM may allow a stray current to return to the DVM via an earth loop. The "earth" between the instrument end of the data lines and the DVM measuring terminals may allow such loops of current, which will modify the signal that is measured. A system whereby this earth loop is allowed, but also eliminated from the measured value was used, which routed this current away from the

DVM measuring terminals in all tests. This constitutes a "Guarded" measurement, not to be confused with a "common earth" method of eliminating earth loops, which may produce measurable potential differences between signal receiver and source.

Shielding signal protection was also employed, in which a screen of metal around the data lines intercepted and earthed any induced currents from surrounding electrical activity. The shield must be free at one end and earthed at the other to eliminate possible earth loops.

The signal conditioning system used for the tests here was found to be more than adequate for the measurements required.

Calibration

The majority of measuring devices used were designed to give a voltage response proportional to the measured quantity. However, commonly the output voltage with respect to the change in the measured quantity was not exactly a linear function. One way of obtaining a more accurate measure is to fit a function to the voltage response. The basic polynomial was used to find a polynomial curve to fit a set of data consisting of voltage response versus measured quantity. The choice of the degree of the polynomial fit will be governed by the required accuracy and the amount of work needed to use the calibration practically. A tenth-order polynomial may provide good correlation between measured response and input response, but take too long to convert voltage readings to measured responses.

As with all calibrations, the use of any device outside its calibrated range can cause serious errors. This is particularly evident for high order polynomials which can approach infinity outside the range very quickly. The lower the order of the poly-

nomial the less chance there is that this asymptote to infinity will occur just outside the calibration range. Indeed the linear fit will never suffer from this problem and is to be preferred if measuring outside the calibration range is unavoidable. The tests undertaken here were always carefully carried out to ensure that no measurements were made outside of the calibrated range.

Summary

At the University of Sydney, School of Civil and Mining Engineering, the Soil Mechanics Laboratory has been using a micro-computer to control and read a wide range of tests. The computer is a Hewlett Packard HP9825 and controls a HP3052A Data Acquisition System containing a HP3455A DVM and HP3495A Scanner. A HP9872A Plotter with four pens and a HP9871A Impact Printer provide hard-copies of the test results. The HP9825 has a cassette tape drive and a HP9885M Master Disk Drive and a HP9885S Slave Disk Drive provide a system of mass data storage and retrieval that is quick and safe. The HP9825 also has a one line display and a small thermal printer.

Communication on the system is via an HP-IB interface bus which links the Controller, Impact Printer, Plotter, Disk Drives, DVM and Scanner. A second interface is used to connect to a quartz time-clock that has the ability to interrupt the main controller in order to service a required function at set time intervals.

Power is supplied by a very accurate HP-6113-A DC Variable Current and Voltage power supply for strain gauge work and a constant 5 volt HP-1818-A power supply for all other transducers.

6.2 Closed-vessel Clay Tests

In order to gain some experimental data on laterally loaded pile response, a series of loading experiments were carried out using equipment designed for closed-vessel lateral pile tests in clay. The clay was Kaolin, as used by various researchers at The University of Sydney, Rowe (1977), Balaam (1978), Redman (1980) and Swane (1983). Since very little data on laterally loaded piles with regard to undrained and drained behaviour is available, this aspect was addressed in the test program.

The clay was maintained under a uniform vertical pressure in a cylindrical steel vessel with a 305mm diameter and of length 420mm, and so did not model the commonly assumed situation in which the vertical stress increase is approximately proportional to depth. As such, the test is not designed to be a full scale model of a prototype, but is an attempt to indicate the behaviour of the clay at one depth, i.e. one overburden pressure.

The pile will behave flexibly or rigidly depending upon the cross-section bending stiffness, and the overburden pressure used, because the clay Young's modulus is commonly found to vary with consolidation stress-level. The results were reviewed for:

- a) the consolidation response to dead loading.
- b) the overall load-deflection response characteristics.

A series of exploratory cyclic lateral loading tests on piles in clay and calcareous sand under overburden stress and on clay with zero overburden were also performed, but due to both limitations of space and the necessity to expand the topic of this Thesis to properly discuss their results, they will not be presented.

6.2.1 Apparatus and Procedure

The apparatus consisted of essentially the same equipment as was used for the previously referred to open and closed-vessel clay tests of Rowe, Balaam, Redman and Swane, but now the pile was tested under a lateral load, as shown in Fig. 6.1. The model piles, of solid aluminium rod with lengths from 75 to 290 mm with 5, 8 and 10 mm, diameters, were tested without any head restraint, and the force applied at an eccentricity of between 10 and 17 mm.

The clay had a Liquid Limit of 46% and Plastic Limit of 35% and was remixed to a moisture content of between 55 and 60% prior to filling the vessel to prepare the clay bed for each test. For the range of vertical consolidation pressures employed (from 100 to 250 kPa), the void ratio ranged from 0.95 to 0.83 in oedometer tests carried out on samples from the vessels and samples prepared in pre-consolidation tubes at 100 kPa vertical stress and trimmed to oedometer size. The Compression Index, C_I was typically found to be 0.235 and the Recompression Index, C_R took a value of 0.080. The value of the Coefficient of Consolidation was measured as 40.0 mm²/minute for the vertical stress range 100 to 200 kPa.

Values of the Young's modulus and undrained shear strength of this clay from QU triaxial tests have been reported (see authors named above), and range from 2.0 MPa to 15.5 MPa and 25 to 60 kPa respectively. These two properties depend upon the vertical stress used to consolidate the clay beds and this varied from 100 to 200 kPa for the quoted values. The range of values of Young's modulus is highly dependant on the level of loading of the clay at which the value is determined. Typically, the value at 50% of the ultimate deviator stress in the undrained triaxial tests carried out here was up to 10 times smaller than the initial value.

After placing circular filter paper drains in the base of the vessel the pre-mixed clay slurry was poured into the vessel, with an immersion vibrator used on each 150mm deep layer to remove entrapped air. The top drains were then placed and a rubber membrane on the top ensured the consolidating pressurised air did not mix with the clay. The slurry was placed with a domed top and approximately 20kPa of consolidating pressure applied. After one or two days the measured volume of expelled water indicated the membrane would have reached an excessive amount of deflection, and the top was removed and more clay slurry placed over the partially consolidated surface. The pressure was then reapplied to a value of about a half of the final desired pressure and consolidation was allowed to proceed to completion, as determined by less than 1% of the total volume of expelled water being expelled during one day.

The top was removed and the pile jacked in carefully, manually winding a constant rate of penetration loading machine. Figure 6.2 presents a typical plot of penetration load against time for a pile of length 200mm and diameter 10mm. The filter and membrane were replaced, taking care to eliminate trapped air by forcing it out to the edges. The loading equipment was lowered along guide rods and the pile head connected to the loading linkages to provide the desired eccentricity. The whole vessel was then firmly bolted together and the free standing portion of the exposed loading plunger locked from moving. This locking prevented accidental loading and effectively stopped the upward force of the internal air pressure acting over the area of the plunger from being transmitted to the pile head.

A very small settling air pressure of the order of a few

kilopascals was applied, in order to press the membrane onto the clay surface and expel any free water, and then the full consolidation pressure was applied. The complete procedure, from first filling the vessel to end of consolidation with a pile installed, took two to three weeks. Following consolidation, a proving ring and deflection transducer were rigidly attached to the exposed end of the now-locked loading plunger. At this stage the load was zeroed, according to a previously established reading taken with the base of the proving ring unconnected, in free air.

The system of loading was designed to exert a pre-load on the loading machine in order to eliminate a zone of slackness in the machine when passing through zero load, and to allow static dead loading. Essentially the maximum downward load was fixed by the hanger weight, and the amount of load transferred through the proving ring was controlled by the movement of the loading machine, which always worked with a tension load.

Having achieved the aforesaid zero reading, the loading plunger was unlocked and the test commenced. The deflection and generated load were recorded digitally throughout the test and saved for later inspection. The time of each reading was also stored to enable consolidation effects to be assessed. However, the rapidity of the consolidation necessitated a data recording program that was limited to one channel in order to obtain sufficient data about the rate of deflection of the pile. This program was used to monitor the "dead load" series of tests, which will now be presented.

6.2.2 Dead Load Tests

The first response considered is that of constant lateral load (dead loading) of the pile, giving information about the undrained and drained behaviour of a laterally loaded pile, as well as an indication of the creep.

The simplest problem that can be analysed is that of dead loading, but it is actually a very difficult test to perform in the laboratory. The small size of the model pile makes its response susceptible to even the slightest interference from friction in the loading mechanism. Further, the small magnitude of the response requires careful observation techniques and specialised equipment is needed in order to apply the load quickly and smoothly since:

- a) The immediate undrained response is virtually dynamic and thus is subject to a large degree of uncertainty.
- b) The progressive deflection with time during consolidation, is more accurately known but still takes place rapidly.
- c) Behaviour after consolidation is markedly affected by the presence of creep and, in turn, the creep can be modified by the "hangup" of load from friction in the loading mechanism.

A stick-slip response occurs when the stiffness of the friction assembly gradually attracts load until a limit is reached and slips the full load onto the pile. Deflection of the soil then sheds load back to the loading mechanism until the slipping load is reached. Linear ball races were used in the bushing that carried the loading rod to minimise friction, and the tension-inducing hanger system ensured true alignment of the proving ring and loading rod to eliminate sideways thrust on the bushing.

The curves of Fig. 6.3 show the deflection response as a function of the logarithm of time for four model piles subjected to a constant lateral load while under a constant vertical overburden pressure, and the response of one pile tested without overburden pressure. The loads were applied using the hanger system without the loading machine engaged, i.e. the loading machine was used to set up the test, then manually wound downwards to leave the hanger alone acting.

The deflection of the pile was data logged using a program that sampled all the test outputs every two seconds. This method of reading was able to measure the creep behaviour, but was too slow to give the actual consolidation response. Evident in the results is the "stick-slip" behaviour previously described. The creep deflection response is seen to be a significant proportion of the total response change to load with time, and presents a linear increase as a function of the logarithm of time.

Poulos and Davis (1980) have presented results obtained by Druery and Ferguson in 1969, for the time dependant deflection of a pile in Kaolin. It appears that their measured response consists mainly of creep and the manual reading of the deflection values has not given the actual consolidation response. The extra deflection above that expected for consolidation of an elastic two-phase material, was consistently reflected in their ratio of immediate to final deflection, with typical values of 0.56 instead of a quoted theoretical ratio equal to 0.73.

The results of the tests carried out with and without overburden pressure are presented in Table 6.1 and the average value of the ratio of initial deflection, u_0 to final deflection, u_{100} is 0.82. If it is accepted that the theoretical deflection influence factors are not dependant upon the value of Poisson's

ratio, it is possible to use the relationship $E = 3E' / 2(1 + \nu')$ to derive the expression

$$(u_{100} - u_o) / u_{100} = (1 - 2\nu') / 3$$

$$\text{or } u / u_o = 2(1 + \nu') / 3. \quad 6.1$$

This expression can be used to estimate the value of the drained Poisson's ratio, ν' as 0.23, which is slightly lower than would be expected for soft normally consolidated clay.

A theoretical solution for the degree of lateral displacement $U = (u_t - u_o) / (u_{100} - u_o)$, with time, t has been presented by Carter and Booker (1981) for a pile in a continuum-soil model and their results are reproduced here in Fig. 6.4, together with those from two model pile tests. The theoretical and experimental degrees of consolidation are seen to be almost equal at any time.

The assumed value of c_v of $40 \text{ mm}^2 / \text{min}$ was consistent with data from the oedometer tests and, with a T_{50} value of 0.25 and pile radius, r_o of 5 mm, gives a time to 50% consolidation of the order of 9 seconds. This small value corroborates the finding that consolidation occurs very quickly for the size of model piles used here. Thus, using continuum theory, it is possible to account for the effects of consolidation with respect to time. The results using the standard program are presented in Figs 6.5, 6.6 and 6.7, where the load-deflection curves and the deflection-time curves are shown.

Figure 6.5b clearly shows the two-second separation between data points and also illustrates some delay that arose between the load being applied to the plunger and the pile commencing to exhibit the classic consolidation curve shape. This delay could

have been due to "hangup" of load in the bushing and linkage mechanism or from the pile having an initial gap to close before loading of the soil properly commenced. The "hangup" explanation is reinforced by the response evident at the end of the time-deflection curve and the gapping possibility is supported by an early flat portion to the load-deflection curve of Fig. 6.5a.

The procedure for locating the end of primary consolidation is shown in Fig. 6.5b, where two straight lines are drawn, one tangent to the curve at the point of inflection and one through the creep portion of the curve, with the intercept taken as the estimate of the end of primary consolidation. In this way, the effects due to creep are, to some degree, removed and a consistent set of deflection values result.

After the consolidation test, the load was cycled in three stages and then taken to the extremes defined by the limits of travel of the loading linkages. Another consolidation test was then performed. The cycling had caused several changes to the response, including an increased deflection, a delayed end of consolidation and a slightly better defined shape to the curve. Despite the previous loading, the general characteristics of the consolidation behaviour remain unchanged. This implies that a two-phase elastic soil model is still an appropriate model, provided some account is taken of the changes made to the geometry of the soil-pile interface, i.e. gap formation, and the changes to soil properties, i.e. degradation.

Figure 6.7 presents another consolidation response, now after cycling the load between -100 and 200 N until no observable change in response occurred, i.e. shakedown. The consolidation load was then applied relatively slowly by manual winding of the loading

machine until the hanger load alone acted. As before, the time to 50% consolidation increased and the curve became better defined. It was felt that the pre-loading had removed some of the capacity of the clay to creep and made the pile and soil contact region more intimate, i.e. any gaps were well defined and the soil-pile contact was well established.

In an attempt to better define the initial part of the primary consolidation curve a program designed to monitor quickly just the deflection was required. This program monitored the deflection before load was applied, to sense small changes in deflection and then start reading as fast as possible (about 8 readings/second) the deflection and time. Examples of the resulting curves are given in Fig. 6.8 for two pile tests. Curves a) and b) are for the same pile test, with curve b) depicting the response of the second load increment applied one week after the first. The ratio of the immediate total deflections for the first and second load increments is 0.613 while the ratio of the respective total loads is 0.620, thus exhibiting a very linear response to loading. However, it is evident that at the higher load level the creep rate has increased. This increase in the rate of creep is also seen in the response for the higher load of 360 N in Fig. 6.7b.

Figure 6.8c shows in more detail the type of consolidation response measured, with the initial zero reading not included on the figure. The curve is seen to initially waver slightly due to swinging of the hanger and later to oscillate, showing the dependency of the deflection transducer reading upon the temperature fluctuations as the air conditioning system turned on and off.

6.2.3 Load-deflection Response

While previous investigators have presented information on the laterally loaded static response, and the so-called cyclic response of piles, very little data has been presented on the overall deflection response to general loading. It is a very difficult task to perform tests that have a direct correlation to real situations, since the stiffness of the supported structure and variability of imposed load forms cannot be simply obtained. However, a necessary first step is to investigate more complex load forms than initial static (dead) loading, and static loading after cycling of the load is one such load form.

It would be hoped that the characteristics associated with cyclic loading, such as increased bending moments and deflections, could be explained by recourse to the history of the loading that preceded the after-cycling static load test. The methods of analysis developed here will be able to provide the means with which to follow more complex load paths, but attention in this section is restricted to the initial response of the pile to load. Once the initial, largely linear response has been modelled, the observed cyclic and after-cycling responses could be investigated using the parameters found to fit the initial response.

Figures 6.6a and 6.7a present the load-deflection responses that preceded the two dead-load tests depicted in Figs 6.6b and 6.7b. To obtain the results in Fig. 6.6a, a symmetric cyclic load was first applied and the resulting hysteretic load-deflection loops can be clearly seen in the inset. Following the initial train of cycles was a non-symmetric train, then a reload and unload to zero and finally a large cycle of load reaching the

limits of travel of the loading system. From the early portion of the curve an estimate of the initial pile stiffness can be made, and for a range of tests will later be compared to theory.

The flat section (i) to the load-deflection loop can be interpreted as a combination of a pile-soil gap and the looseness of the fit of the pins connecting the linkages, that is necessary to reduce friction. If the flat section ("gap" length) were solely due to pin clearances then it would be expected to maintain the same width, regardless of the stage of loading. The "gap" length can be seen to be larger at a later stage of loading (ii) and thus it was concluded that a gap existed in some degree over a reasonably large proportion of the pile length. The slight mismatch in load between the two gapped responses corresponding to the two directions of travel, is a measure of the friction in the loading linkages and the amount of soil resistance available, (say) on the sides of the pile, in the gap.

Regardless of the gap being a physical space between the pile and soil or being the result of the soils inability to sustain a load increase, the gap phenomenon is present in all cyclic test results and increases in magnitude with increased load level, while decreasing with increased overburden stress.

It can be seen that to some degree, the initial stiffness of the measured response can be recovered during reversals of load direction, which is consistent with failed regions of soil returning to a stiffer, elastic state. Also, a measurable amount of consolidation remains in the dead load test (iii), even after the extremes of loading as evidenced in Fig. 6.6b. The dead loading stage at the end of the test did not commence at the original zero-load deflection, although the load was zero at the start of dead-load application. This indicates a permanent

deflection of 2.5mm was associated with the last leg of the final load cycle and further, more than 32 N would be required in order to recover the original zero-load deflection position. Thus, any pile that appears not to have moved, does not necessarily have zero load applied to it.

Figure 6.7a presents results for a longer pile, with a larger diameter and at a higher overburden pressure; thus higher loads and greater deflections are generated. The load in this test was cycled non-symmetrically until the deflection response stabilised, and then the dead-load test was commenced. Once again, the soil-pile response depicted in Fig. 6.7b is a classic consolidation curve. Resuming the load test saw the original stiffness almost restored for some 50 N of load increase before the non-linear effects again appeared. This may well be associated with the pile and soil, at the end of the dead-load test, being in intimate contact, with some potential for plastic-deflection exhausted at the current load.

All load-deflection responses presented here have some degree of uncertainty associated with their classification as being either undrained or drained. With the time to 50% consolidation for low load levels being of the order of 5 to 10 seconds, it must realistically be argued that a fully undrained test is unlikely. Attendant to this is the certainty that creep will be responsible for a large proportion of the measured deflections.

These tests were thus most useful, for the present purpose, in providing estimates of the initial load-deflection relationship, that would be least affected by consolidation and creep of the soil. Figure 6.9 presents the results of a number of tests in the form of a flexibility measure as a function of pile length-to-

diameter ratio. Since the majority of the piles might be classed as flexible (i.e. longer than the critical length which depends upon the soil Young's modulus), this form does not allow for simple presentation of the theoretical responses. Instead, it was found convenient to separately analyse each case, using the MBEM analysis, with its own value of length, diameter, load eccentricity, e and overburden pressure.

The, commonly quoted, limiting cases of a soil with an undrained Young's modulus, E_u to shear strength, c_u ratio of 500 and 250 were used, assuming a realistically conservative value of the ratio of c_u to vertical overburden stress, σ'_{vc} of 0.3. The agreement is encouraging, but does reflect the difficulties encountered with the small size of model pile used. Considering the likelihood that both consolidation and creep have also been measured, the test results suggest the higher E_u/c_u ratio would be more appropriate for undrained response. Nevertheless, the experimental results do conform with the trend of the theoretical results in having an increased flexibility coefficient with increasing length-to-diameter ratio and a decreasing coefficient with increasing overburden pressure.

6.2.4 Summary of Closed-vessel Tests

The tests covered a range of laterally loaded pile responses, including dead-loading with undrained response, drained response and the isolation of creep, and gave some indication of pile response to cycles of load. Using the closed-vessel technique it proved difficult to obtain sufficient good quality repeat tests because of equipment malfunctions and the problem of setting up the loading linkage system inside the pressurised top. The small size of the pile, chosen to enhance the modelling of a large extent of soil, added to the problems, since the slightest preload of the pile during setup could result in the pile already having a gap formed before starting the test. The reapplication of the overburden pressures was not sufficient to close the gap, especially for the lower two pressures.

The above, taken with the uncertainty with which undrained, or drained, conditions were felt to have been achieved, led to the major conclusion that larger size model piles, and thus larger times for consolidation, would be required in order to obtain more accurate measures of pile response. The responses that were obtained were consistent with a two-phase (solid and fluid) soil model and proved to be capable of being realistically modelled using an elastic continuum based soil model.

6.3 Open-vessel Clay Tests

The linear-elastic behaviour of the pile-soil system is much simplified by the use of the effective length concept. The test program using the open-vessel technique culminated in an attempt to illustrate the existence of a critical length, by considering the linear and non-linear response of piles with different lengths in the same soil. In Chapter Four the existence of a linear-elastic critical length was investigated, and in Chapter Five the critical length was shown to allow a parametric study of non-linear pile response. Here, some experimental evidence for the existence and utility of the critical length is presented.

The apparatus used for the tests of Swane (1983) was modified slightly and used to test a series of piles in a large open-vessel containing overconsolidated Kaolin clay. The procedure for preparing the beds of clay for the open-vessel test reported here, was the same as that for the closed-vessel tests. The final consolidation pressure used was 200 kPa and was applied in stages, topping up the clay to maintain the surface at the top of the vessel at the end of the final stage. After two months the pressure was removed, with the drainage tubes held under water in measuring cylinders situated below the base of the vessel. This procedure ensured the attainment of as fully-saturated a bed of clay as was possible. After a further three weeks, the top of the vessel was removed and a number of layers of rubber membrane and plastic were used to limit water loss from the surface.

Each pile was installed by preboring a 17 mm diameter hole and then jacking the 20 mm diameter pile by hand, with observations taken at 90°^o apart to ensure the verticality of the

pile. Moisture content samples were taken at every 50 mm penetration, down to the final depth required for each pile. Typical values, in order down one of the 300 mm deep holes, were 37.7, 38.8, 39.1, 38.8, 39.6 and 37.3%, while the extreme values of all holes were 37.3 and 40.0%.

The vessel had a diameter of 590 mm and a height of 480 mm and allowed the same strain-gauged pile to be tested five times using the centre and the four "compass points" 140 mm distant from the centre. When another test of the 300 mm pile was required, it was located at the same radial position but intermediate between two of the "compass points", i.e. NE.

6.3.1 Tests with Different Pile Lengths

Five different pile lengths of 100, 150, 200, 250 and 300 mm with the cross-section properties given in Fig. 6.11, were chosen to be tested, using the same lateral loading condition in the same clay bed. Due to a problem with the installation of the longest pile, this test had to be repeated, making six tests in total. This particular bed of clay was the fourth of a series which had concentrated upon cycles of load, and prior to this last open-vessel test the strain-gauged pile had been overloaded when buried to a depth of 400 mm.

The overload made one strain gauge inoperable and introduced a permanent curvature to the pile above a distance of approximately 250 mm from the base. The problem that arose during installation was that this curvature produced a non-uniform radial displacement pattern in the soil when the last 100 mm of the pile was installed. This left a small gap and a region of indistinct contact between the pile and soil, which was reflected in a lower than expected stiffness that recovered with increasing deflection.

A repeat test of the 300 mm long pile was made, attempting to maintain the pile vertical according to the embedded length, not the outstanding length. An improvement was evident but it was still not as stiff as the 250 mm long pile, suggesting the permanent curvature was still affecting the response.

6.3.2 Test Results and Theoretical Predictions

The actual pile tests took two days, with three tests each day, and at least two hours elapsed between pile installation and pile loading commencing. The assumed distributions of Young's modulus E , initial interface stress p_0 and ultimate interface traction p_u with depth are presented in Fig. 6.10. The initial response of the piles to loading, see Figs 6.11 and 6.12, together with the distribution of bending moments in the pile at low loads, see Fig. 6.13, and the results of unconsolidated, quick undrained triaxial tests on clay samples cored from the clay bed, see Fig. 6.14, were used to determine the parameters.

Overconsolidated clay has often been treated as possessing a uniform Young's modulus with depth, but the results from these tests suggest a linear variation with depth was more appropriate. Both a linear distribution (case 1) and a uniform modulus (case 2) were investigated, in order to assess the importance of the choice of distribution on the fit of the continuum-based model. For both distributions of modulus the initial stress and ultimate interface stresses were considered to have zones of reduced efficiency that were modelled by a linear correction to the "deep" values, giving zero at the surface, increasing to the "deep" values at a depth of 5 pile diameters. The deep values were based upon the undrained shear strength from the triaxial tests, see Fig. 6.14, which gave

an average for tests from vertically and horizontally oriented samples of $c = 20$ kPa with a variation of ± 2.5 kPa.

The initial stress was approximated by the expression

$$p_o = 2 c_u \quad 6.2$$

which was based upon an upper limit from the work of Carter, Randolph and Wroth (1980), where values of p_o of about $4c_u$ are suggested for driven open-ended tube piles, and the relatively small volume of soil displaced by the pile. From various empirical and theoretical solutions for deep pile segment ultimate interaction loads, notably Randolph and Houlsby (1984), the increase of total stress on the passive face Δp_p and decrease on the active face Δp_a were chosen to be

$$\Delta p_p = -\Delta p_a = 5c_u \quad 6.3$$

which represents a pile-soil interface that is almost completely rough. Evidence, in the form of small triangular regions of clay, in plan view, adhering to the back of piles pulled from the soil after testing, suggests a rough interface is most likely to be the real situation.

The ultimate interface traction in Fig. 6.10b results from a passive stress of $7c_u (= 2c_u + 5c_u)$ and an active stress that, to avoid being tensile, is given the value of zero. In this way the resultant ultimate traction on the pile p_y and the passive stress on the soil p_y are the same, but the analysis still takes account of the active and passive faces of the pile and soil separately.

For case 1 and case 2 the empirical ratio,

$$E_u / c_u = 375 \quad 6.4$$

has been chosen, in line with commonly quoted values of between

250 and 500 as used in section 6.2.3. A modulus distribution that was proportional with depth was tried but gave responses for the shortest pile that were much too flexible. Obviously any fit between experiment and theory can be improved, but here it is the ability of the model to provide reasonable comparisons without departing from uncomplicated, and commonly accepted, parameter distributions that is demonstrated.

Load-deformation Response

A comparison of the initial load-deflection and load-rotation results from the tests, and the theory using a linear modulus distribution, is presented in Fig. 6.11, and for the uniform modulus distribution in Fig. 6.12. Each set of results is presented in two groups. The first group consists of the results for the limiting length cases of 100 and 300 mm long piles, with the intermediate lengths in the second group. This is to allow the limit cases to be easily recognised and because the two tests in the first group are not expected to be entirely reliable. The small length to diameter ratio case may well have considerable influence from the base, and the problem with the longer piles has already been discussed.

The consistent trends in both theory and experiment are that:

- a) the longer the pile, the stiffer the response at high loads.
- b) the three longest piles have very similar response curves.
- c) the two shorter piles present highly non-linear responses near their theoretical collapse loads.
- d) the two longer piles behave essentially the same at any time during the imposed loading.

The results for a soil modelled with a linear distribution of modulus presented a marginally better agreement with the test

results than the uniform case. Both distribution cases over-estimated the shortest pile responses and under-estimated the longest pile deflection response, and consistently overestimated the rotation response.

The four trends can be explained in terms of pile collapse loads being achieved and the existence of a critical length of the pile when it is associated with this particular clay bed. The linear distribution of modulus predicts a critical length of 272 mm and the uniform modulus yields a value of 310 mm. Both these values are consistent with the load-deformation response of the five pile lengths tested here.

Bending-moment Response

Figure 6.13 shows experimentally- and both theoretically-derived bending moment distributions for a head shear load of 10 N, and compares the experimental bending moments generated by loads of 20 and 40 N with the linear-modulus-based theoretical results. The two stations that recorded bending moments on the free-standing section of the pile are in good agreement with the values calculated from static equilibrium. The uppermost station demonstrates a reduced measured moment, but this was considered to be a result of the confinement of the clamp used to transmit lateral load to the pile.

The 100 and 150 mm long piles both show excellent agreement between theory and experiment for the 10 N load, with slightly better correspondence for the linear modulus case. The 200 and 250 mm long piles also show a good correspondence between theory and experiment, with the worst agreement at a depth of 85 mm where the theory predicts only 80% of the actual bending moment. However, in terms of the maximum bending moment from theory and

experiment, the worst error is less than 10%. The two tests for the 300 mm long pile can be seen to provide the least satisfactory degree of comparison between experiment and theory; this is not surprising considering the problems associated with the lack of straightness of the pile beyond 250 mm from its base. The presence of gaps probably led to increases of measured bending moment above those which might be expected.

The last two sets of curves of Fig. 6.13, for the two higher loads, sees the bending moment distribution curves congregate near the surface to define a unique curve that is consistent with the theoretical predictions. This unique curve is associated with failure stresses in the soil being reached and maintained. By observing where the bending moments diverge from this curve it is possible to postulate the depth to which the soil has failed. There was good agreement between observed and theoretical depths of soil failure, but a higher density of gauge stations is required to accurately locate this depth. Again, the two tests with the longest pile length present the least satisfactory agreement, but the agreement for the more-carefully-installed long pile becomes significantly better at the higher load.

Load-Deflection Loops

The piles were tested by increasing the load to 60 N, the results of which have already been discussed, and then the load was reversed and cycled for six times, or until the deflection became excessive. The results of this procedure are shown in Fig. 6.15, in the form of the entire load versus groundline deflection response of the six tests.

It can be seen that for piles that are shorter than their critical length, cyclic loading at load levels close to the

ultimate collapse load can lead to severe performance degradation.

The flat portions of the curves reflect the passage of the pile through a well-defined and extensive gap and the small peaks of load prior to entering the gapped zone were associated with a tensile failure in the soil behind the pile. Withdrawing of the piles from the clay after the tests caused some of the clay to be wiped off the surface of the piles, but sufficient clay remained adhering to the piles to indicate that tensile failure of the soil had occurred along large sections of the shorter pile lengths.

The extra embedment of the two longer piles (and consequently the higher initial lateral stresses acting) is reflected in a finite stiffness of the head response associated with movement of the piles in the gap. The 200 mm long pile presents an intermediate response, in which the initial load cycle shows the pile has a finite head stiffness when the pile passes through the original (zero-deflection) position, but by the fifth load cycle this stiffness has disappeared.

The analysis of a rigid pile in a soil that can form gaps (in Chapter Five, Fig. 5.29c) shows a similar type of response to these test results. The gapping, theoretically, causes a reduced head stiffness near the zero-deflection position and maximum stiffness at the end-points of the load cycle. Further, the theoretical results of Chapter Five emphasise the importance of the direction in which loading is commenced. In the results from the model pile tests, it is obvious that only on the first leg of the first cycle of load is the maximum stiffness achieved, and that upon unloading to the opposite leg of the cycle a different path is taken. This behaviour is also evident in Fig. 5.29c.

6.3.3 Summary of Open-vessel Tests

The open-vessel tests have shown that a continuum model of soil behaviour, with allowance for soil failure and soil-pile gap formation, is capable of modelling the non-linear response of model pile tests. The major features of the pile tests are reproduced by the theory and extension of the model to predict the response during a few cycles of load seems possible.

A feature of the theory developed to consider the non-linear response of piles to lateral loading, is the importance of the pile critical length. It has been shown that non-linear response, as well as linear response, is controlled by the existence of a pile critical length. Any pile that is longer than its critical length will present the same non-linear response to loading until the different "short pile" collapse loads are approached. By using piles of length longer than critical, the non-linear response, especially the cyclic response, does not appear to involve excessive deformations. Further, once the "short pile" collapse load, defined by using the pile effective length, is reached, the pile may be considered as unserviceable.

Comparison between the three load-deflection curves of Fig. 5.29 and the results of these model pile tests, Fig. 6.15, suggests that a combination of the plastic flow loops of the non-gapping soil model and the stiffness reduction of the gapping soil model, at the zero-deflection position, is required to faithfully model the test responses. It must also be said that the degradation of response and sudden loss of tensile interface traction in the model pile tests, represent types of behaviour that are currently beyond the capability of any theory to rigorously model.

6.4 Field Case

The field case chosen for study in this section is that of Reese, Cox and Koop (1975), where two different diameter piles were tested under the same load eccentricity (0.305 m or 1 foot), at the same site. In choosing this test, regard was given to the need to have high quality data, tests with different pile dimensions, and a well-established acceptance of the tests by previous researchers. All these features are found in these tests.

A soil profile at the site of the tests is presented in Fig. 6.16, and the adopted distribution of undrained shear strength, c_u with depth is shown. Although the penetrometer and unconfined test results indicate a relatively uniform strength at depth, a distribution proportional to depth compares favourably with the triaxial test results. Since it is the response of the upper 2 to 4 metres of soil that was found to control the pile response the following linear distribution proved to be most appropriate,

$$c_u = 0.080 z \text{ MPa where } z \text{ is measured in metres.}$$

The prediction of pile response is divided into two phases, namely linear and non-linear response.

Linear Response

From inspection of the bending moments induced in the larger of the two piles at the lowest reported load, a value of critical length was chosen to be about 5.6 m (15 ft). With the bending stiffness of the pile, $E I_p$ of 482.5 MNm^2 and assuming a Young's modulus for the soil that is proportional to depth, the use of the expression for critical length, equ. 4.8 leads to

$$E_u = 110 z \text{ MPa where } z \text{ is measured in metres.}$$

This combination of values produces an E_u/c_u ratio of 1375, which is higher than is normally reported for lateral loading of piles in clay, but is more consistent with values reported for surface foundations.

The bending moment curves of Fig. 4.13 were used to obtain the theoretical solution for comparison with the test results and the dimensionless deflection influence factors of Fig. 4.11 are used to predict the initial head stiffness of the two piles.

24 inch pile

With L_c of 4.43 m and a critical length to diameter ratio of 6.9, from the curves of Fig. 4.11 with $E_o/mL_c = 0$

$$\frac{uE_c L_c}{c c} / H = 22.7 \text{ and } \frac{uE_c L_c^2}{c c} / H = 49.5$$

which gives

$$\begin{aligned} u/H &= (22.7 + .305 \times 49.5/4.43) / 2158.7 \\ &= 0.0121 \text{ m/MN (or 0.34 inch at 60 kips)} \end{aligned}$$

6 inch pile

With L_c of 1.78 m and a critical length to diameter ratio of 2.8, from the same curves

$$\frac{uE_c L_c}{c c} / H = 18.2 \text{ and } \frac{uE_c L_c^2}{c c} / H = 42.3$$

which gives

$$\begin{aligned} u/H &= (18.2 + .305 \times 42.3/1.78) / 348.5 \\ &= 0.0730 \text{ m/MN (or 0.256 inch at 20 kips)} \end{aligned}$$

Two straight lines on Figs 6.18 and 6.19 correspond to the theoretical initial stiffness, and the agreement is found to be satisfactory.

Non-linear Response

The choice of undrained shear strength distribution having been made, it remains to estimate the initial lateral stress and failure stress distributions. Randolph, Carter and Wroth (1979) and Carter, Randolph and Wroth (1980) have presented results that suggest the initial radial effective stress near the pile face after the excess pore pressures due to driving have dissipated is of the order of between 4 and 5 times the undrained shear strength measured prior to pile driving, see Fig 6.17. Thus,

$$p_o = (0.36 \text{ to } 0.40) z \text{ MPa where } z \text{ is in metres.}$$

From empirical data, e.g. Stevens and Audibert (1979), theoretical plasticity solutions, e.g. Poulos and Davis (1980) and notably Randolph and Houlsby (1984), it may be proposed that the increase of total stress on the passive face, Δp_p and decrease on the active face Δp_a are equal to 5 times the p_o undrained shear strength. Thus,

$$p_p = p_o + \Delta p_p = (0.76 \text{ to } 0.8) z \text{ MPa and}$$

$$p_a = p_o - \Delta p_a = 0 \text{ since tension is not allowed.}$$

These parameters (using the upper estimates of p_o and p_p) were used in an analysis by the Soil Structure Interaction method, presented in Chapter Five. The resulting head response and maximum induced bending moments of both piles is presented in Figs 6.18 and 6.19. The bending moment distributions from the test and theory at a number of load levels is drawn in Fig. 6.20 for the 24 inch pile.

Before discussing the agreement between theoretical results and the test results, the ultimate load capacity of the pile will

be considered. A calculated effective collapse load, employing the effective length of a pile instead of the actual length (i.e. the critical length of a flexible pile), is suggested here to be a realistic upper limit to the loads capable of being sustained by a flexible pile. Using the curves of Fig. 5.9, with the average failure load per unit depth, \bar{W}_y , taken over the effective length, the effective collapse loads of both piles can be calculated.

24 inch pile

With a diameter of 0.641 m and L of 4.43 m the moment ratio $\beta_c = M_o / H_o L_c$ is 0.069, which indicates a dimensionless failure load

$$r_u = \left(H_u^2 + \left(M_u / L_c \right)^2 \right)^{1/2} / \bar{W}_y L_c$$

equal to 0.25 from Fig. 5.9. The value of head shear load is thus

$$H_u = 1.26 \text{ MN (or 282 kips).}$$

6 inch pile

With a diameter of 0.168 m and L of 1.78 m the moment ratio $\beta_c = M_o / H_o L_c$ is 0.171, which indicates a dimensionless failure load

$$r_u = 0.22$$

from Fig. 5.9. The value of head shear load is thus

$$H_u = 0.046 \text{ MN (or 10.4 kips).}$$

The 6 inch pile obviously presents unsatisfactory head response at the effective collapse load calculated above and it might be conjectured that the 24 inch pile would also be unserviceable at the calculated effective collapse load. It must be emphasised that neither pile would necessarily stop attracting load at their respective effective collapse loads, unless the

critical and actual pile lengths were equal, but the piles have effectively failed.

The agreement between theoretical and field case results gives encouragement to use of the uncomplicated approach to the choice of model parameters. The simple assumption of a zone within which there is a reduction factor with which to multiply the values of initial and ultimate traction, here leading to a parabolic increase of traction from the surface down to a depth of five pile diameters, see also Fig. 6.10b, proves adequate. Such devices take account of the proximity of the free soil surface, which inhibits the generation of "deep" limiting stress values.

Figure 6.18 displays good agreement between the results of the SSI analysis and the test results, being a conservative predicted response and following closely the measured response. The results of using the p-y curves actually derived from the pile test, and the p-y curves of the proposed criteria of Reese et al., have a slightly better agreement, as might be expected, since they were fitted to this pile test, but are less conservative than the SSI-based results. Figure 6.19 presents the results of the test on the six-inch pile, together with the results from the SSI analysis and the use of the p-y criteria which were produced for the 24-inch pile. Without changing the soil parameters, the SSI analysis has provided a superior degree of agreement with the test results than the p-y criteria.

The bending moments generated at four load levels during the test on the 24-inch pile are presented in Fig. 6.20, as are the comparable bending moments from the SSI analysis. Since the p-y method is essentially a curve fit of the bending moment distribution of the pile test, a comparison of p-y criteria-based

moment distributions is only a check upon the accuracy of the curve fitting and will not be made here. The SSI analysis shows promising agreement over the entire range of loads, with the increasing depth of the point of maximum bending moment being particularly well-modelled. A tendency of both the p-y and SSI analyses to overpredict the pile bending moment at the groundline suggests some source of error, possibly in the calibration of the pile for bending moments or in the loading arrangement, which could further improve the already adequate agreement.

With more refinement of the soil parameters, the degree of agreement between theoretical and test results may be improved further, but the predictive capability of the elastic continuum-based analysis has been adequately proven.

6.5 Conclusions

In this Chapter, the elastic continuum model of soil, used in theoretically-sound linear and non-linear analyses, has been shown to provide a competent means of assessing, and predicting, model pile and full-scale pile test results. The applicability of the effective length concept to the results of model pile tests has been demonstrated, as well as the existence of a drained and an undrained response in model pile tests, that are adequately addressed by using an elastic continuum two-phase soil model.

The critical length has also been shown to be useful in back-analysis of the bending moment distribution of a full-scale pile test, in order to obtain soil properties. The presence of gapping has been observed in the model tests and, using an analysis that incorporates gapping, the slightly increased flexibility of the response has led to use of higher values of Young's modulus, which are more consistent with surface foundation-based experience.

σ'_{vc} kPa	L d e mm	u_0 u_{100} mm	H N	u_0/u_{100}
100	110 8 12	0.208 0.244	30.5	0.852
	170 10 10	0.190 0.253	34.0	0.751
	170 10 10	0.473 0.576	49.0	0.821
	170 10 10	0.126 0.250	49.0 to 79.0	0.504
	110 8 12	1.750 2.330	0 to 32.0	0.751 *
150	200 10 17	0.508 0.580	50.0	0.876
250	75 10 12	0.103 0.136	30.0	0.757
	220 10 12	1.440 1.555	99.0	0.926 **

* Reloading of pile after cycling of load, see Fig. 6.7a.

** Total overburden pressure reduced to zero for test.

TABLE 6.1 *Deflection Results of Laterally loaded Model Pile Consolidation Tests Carried out with and without Overburden Pressure*

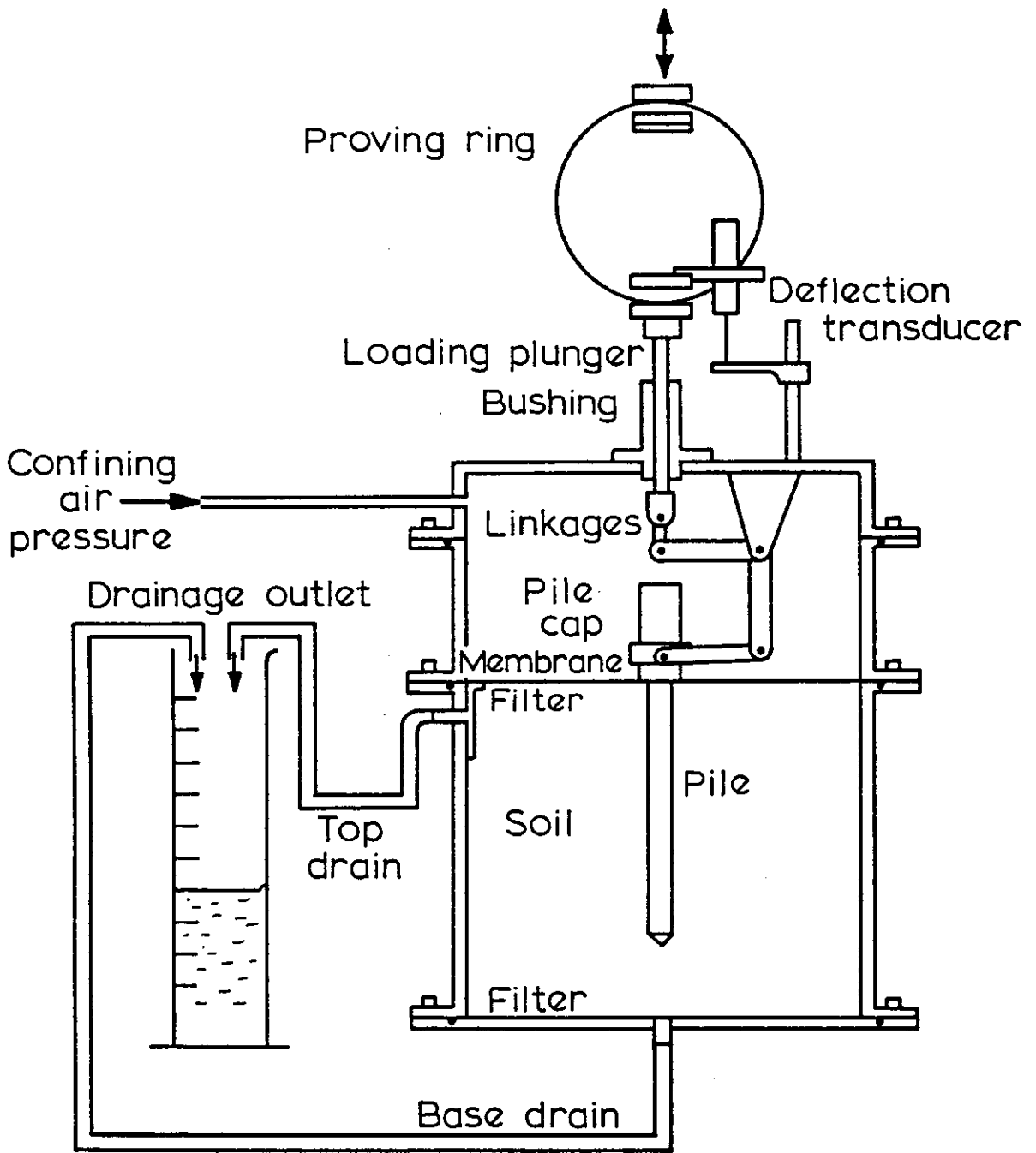


FIG. 6.1 APPARATUS FOR MODEL PILE TESTS

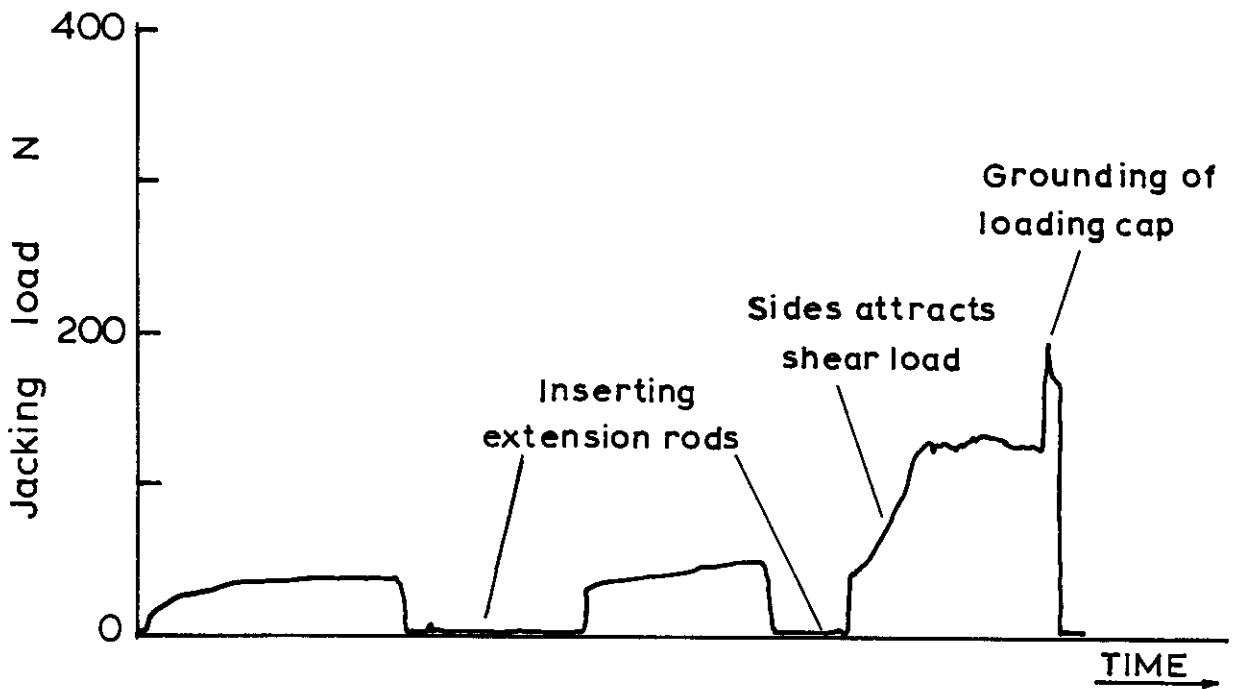


FIG. 6.2 DEVELOPMENT OF JACKING LOAD (TYPICAL)

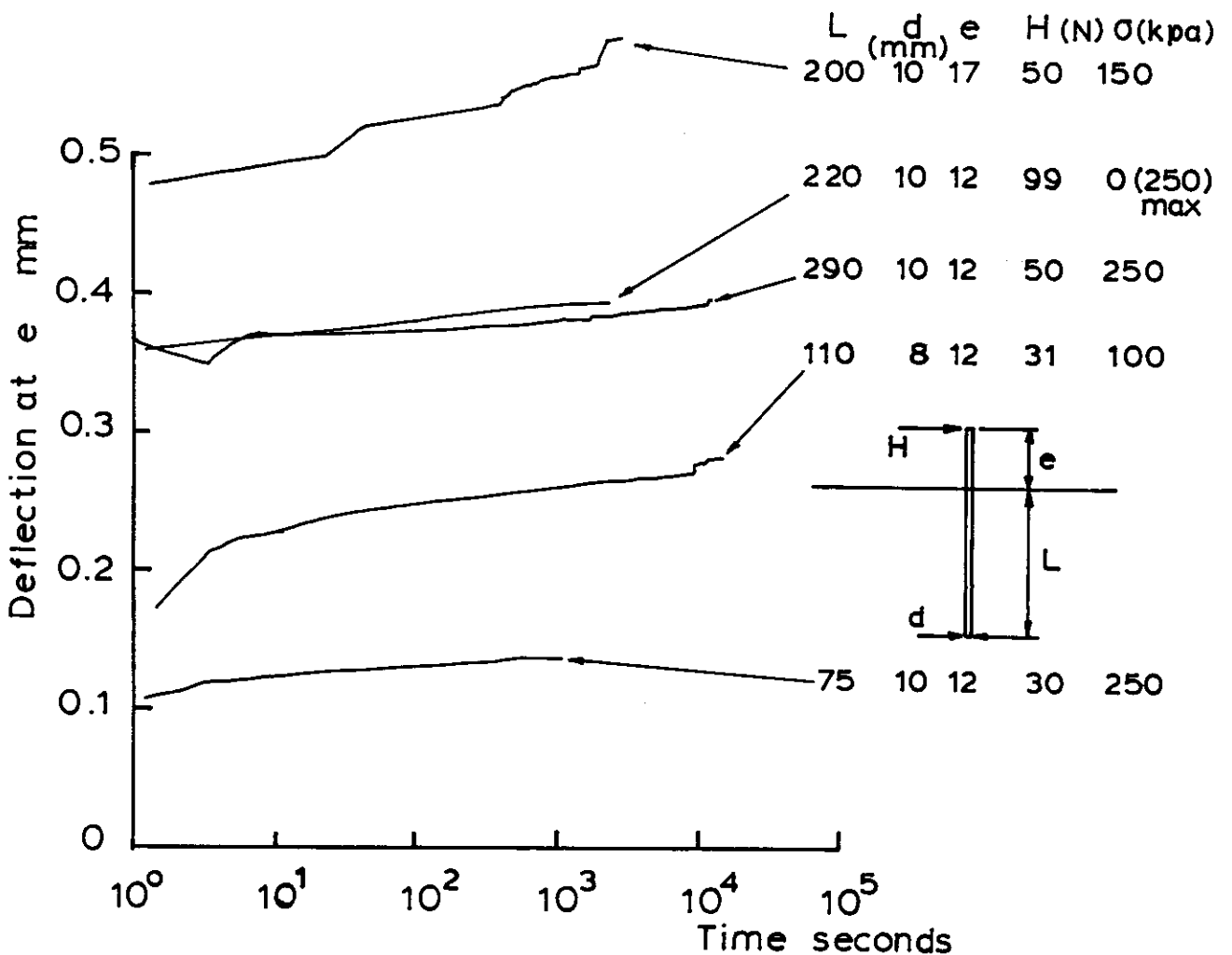


FIG. 6.3 DEFLECTION-TIME RESPONSE : CLOSED-VESSEL MODEL PILE TESTS

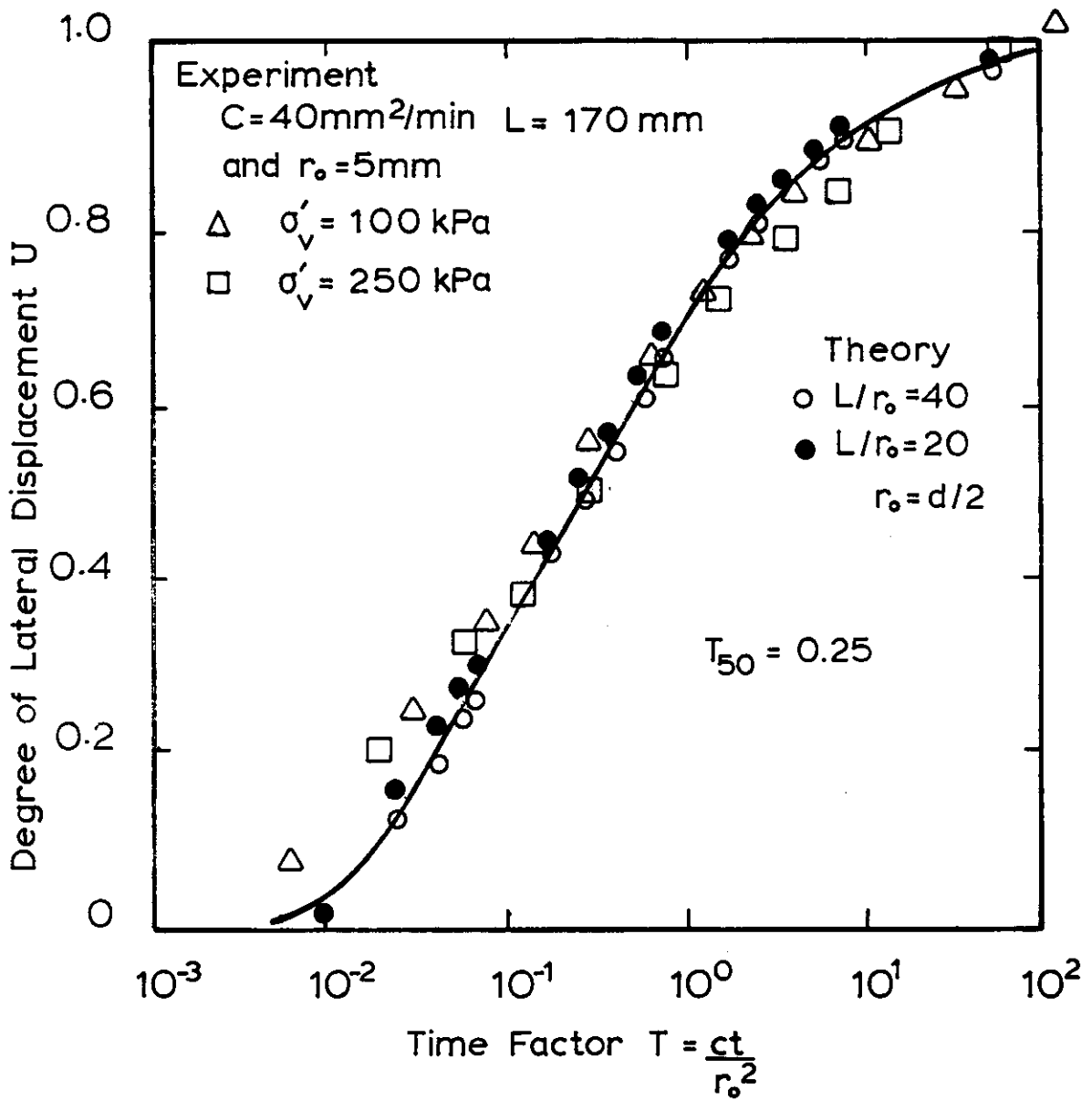
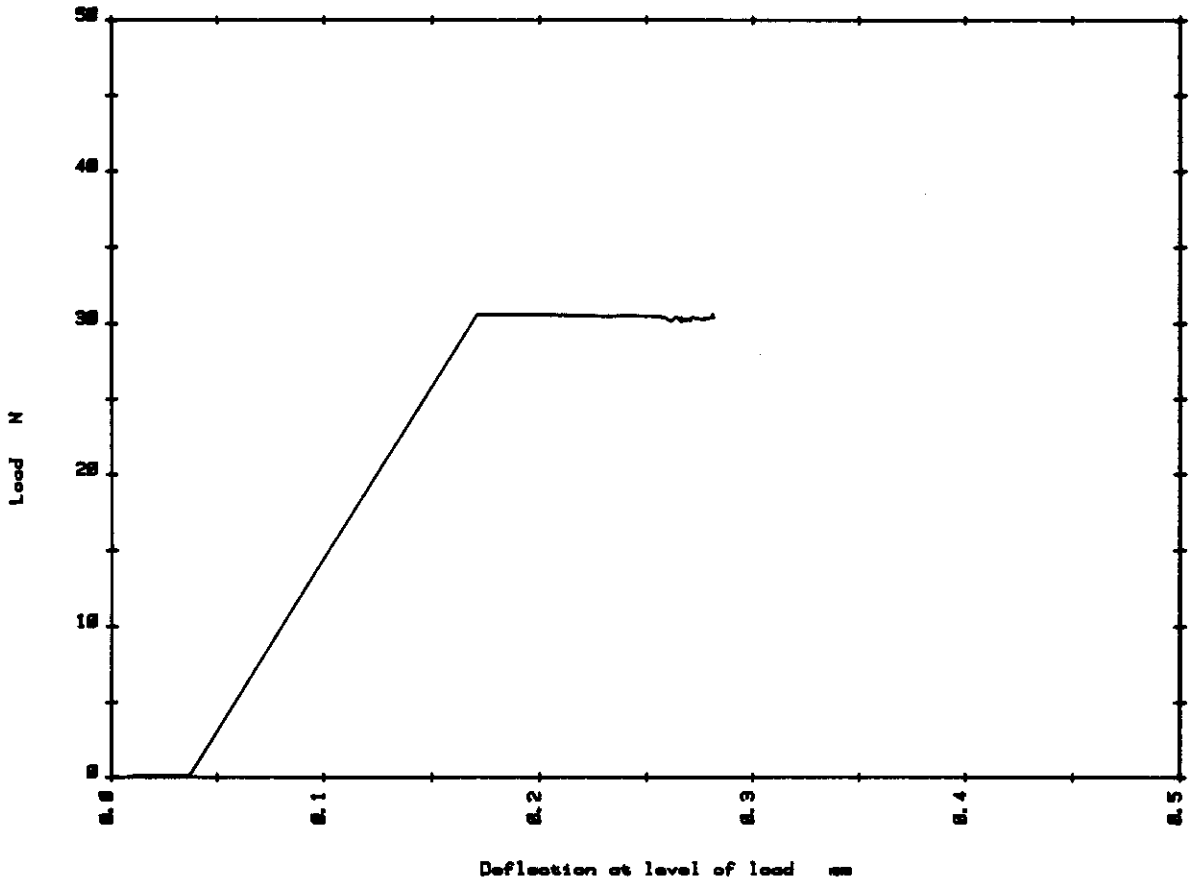
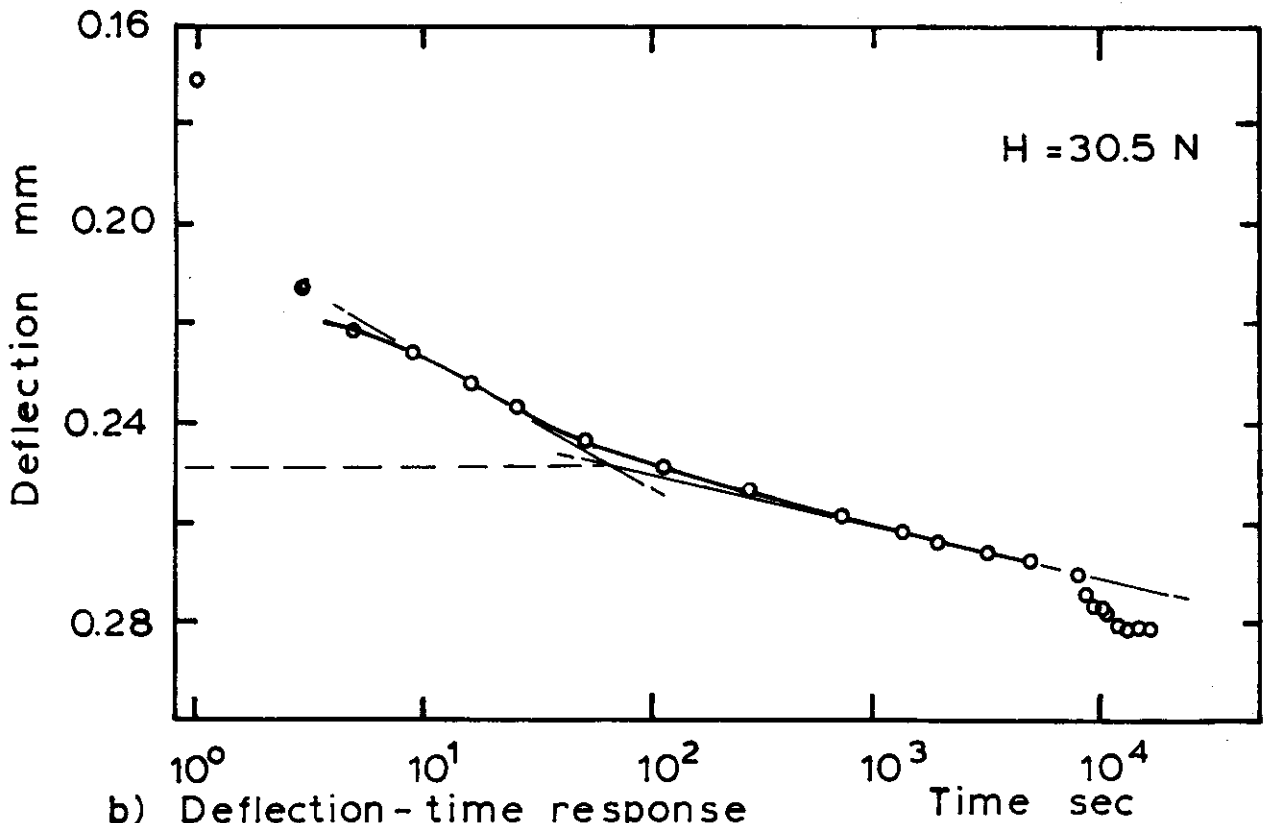


FIG. 6.4 DEGREE OF LATERAL DISPLACEMENT vs TIME; THEORY
 $E_p/G_s = 10^3$, $H/G_s r_0 = 1$, $\nu_s = 0.4$ (Carter & Booker, 1981)
 AND EXPERIMENT

Test of pile #8 pos #1 : L=110 d=8 mm : min σ : 300/2000 Pa.



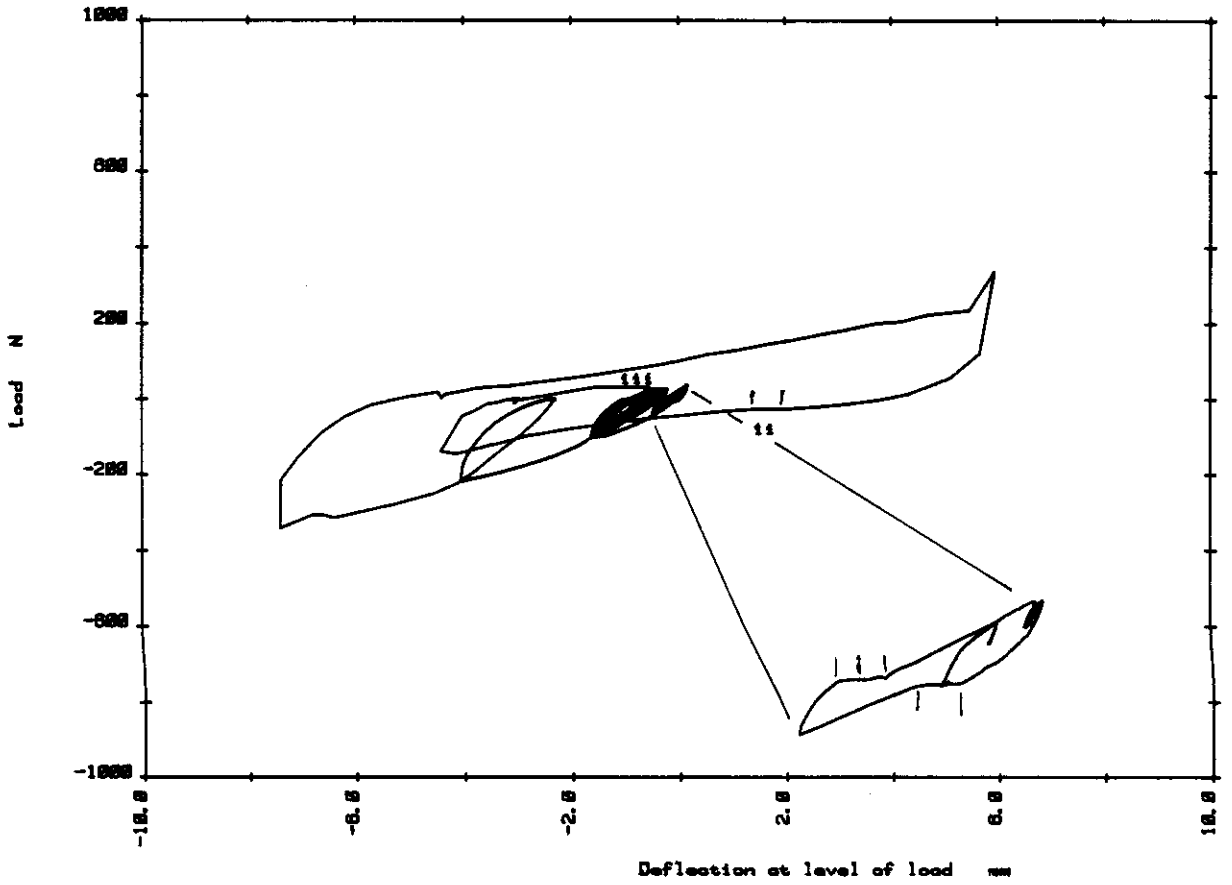
a) Load-deflection response



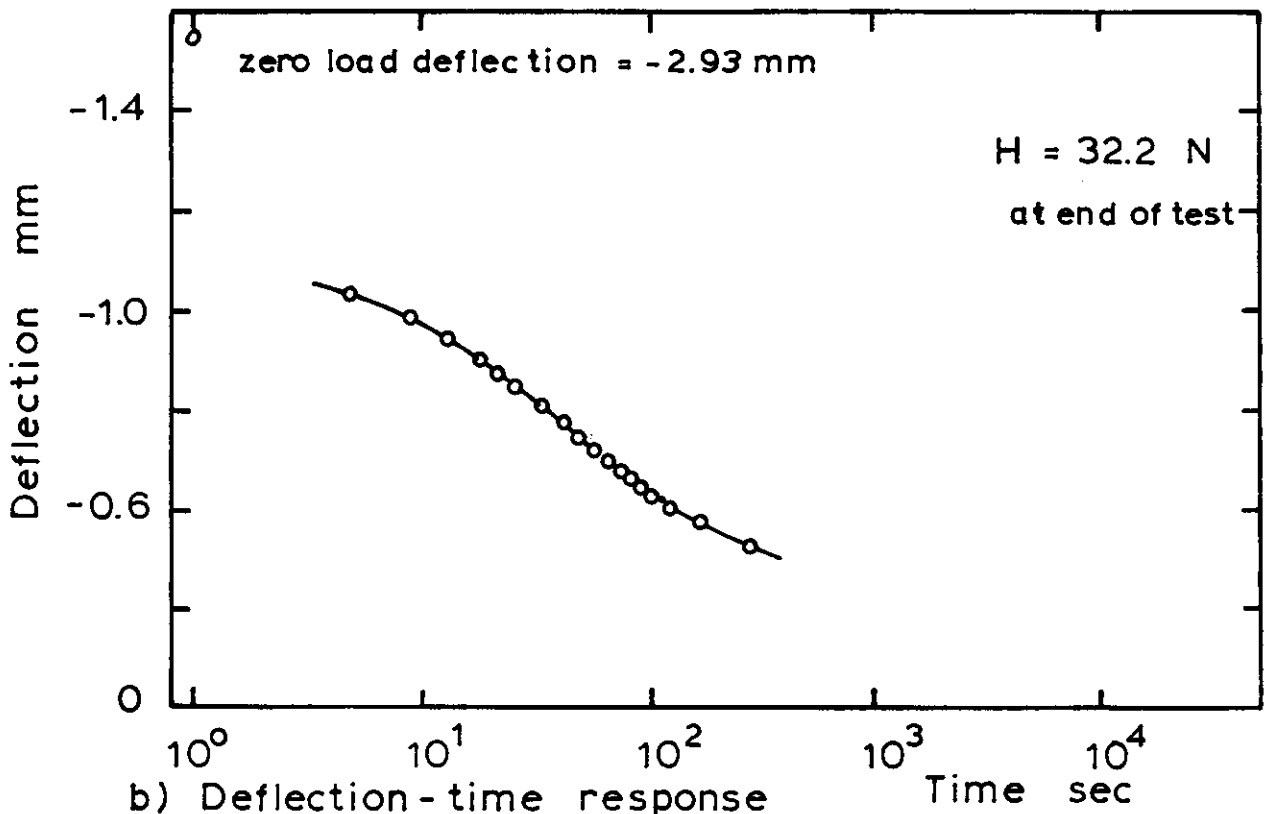
b) Deflection-time response

FIG. 6.5 CLOSED-VESSEL TEST RESULT: L=110 d=8 e=12 $\sigma'_V=100$

Cyclic loading pile #B pot #I : 300/200 kPa : L=110 d=8mm : min e



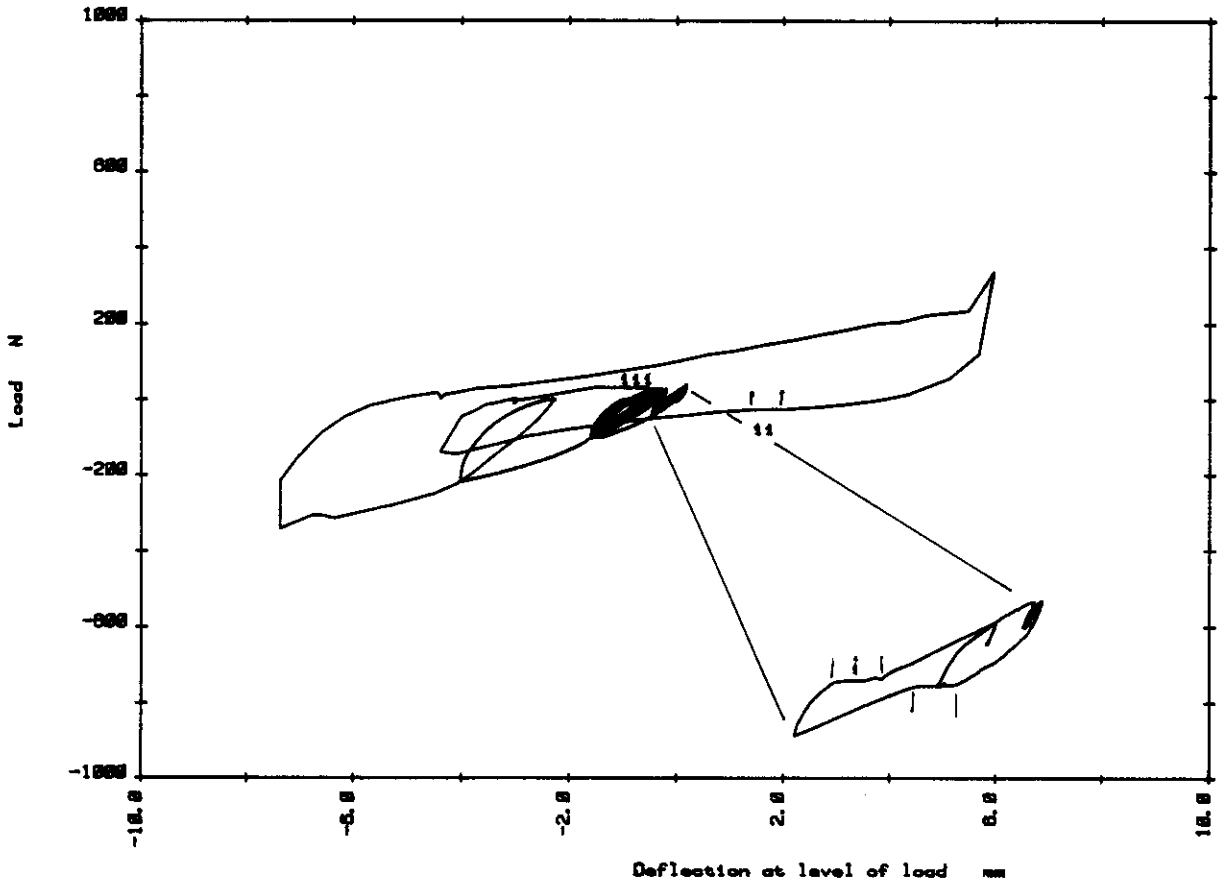
a) Load-deflection response



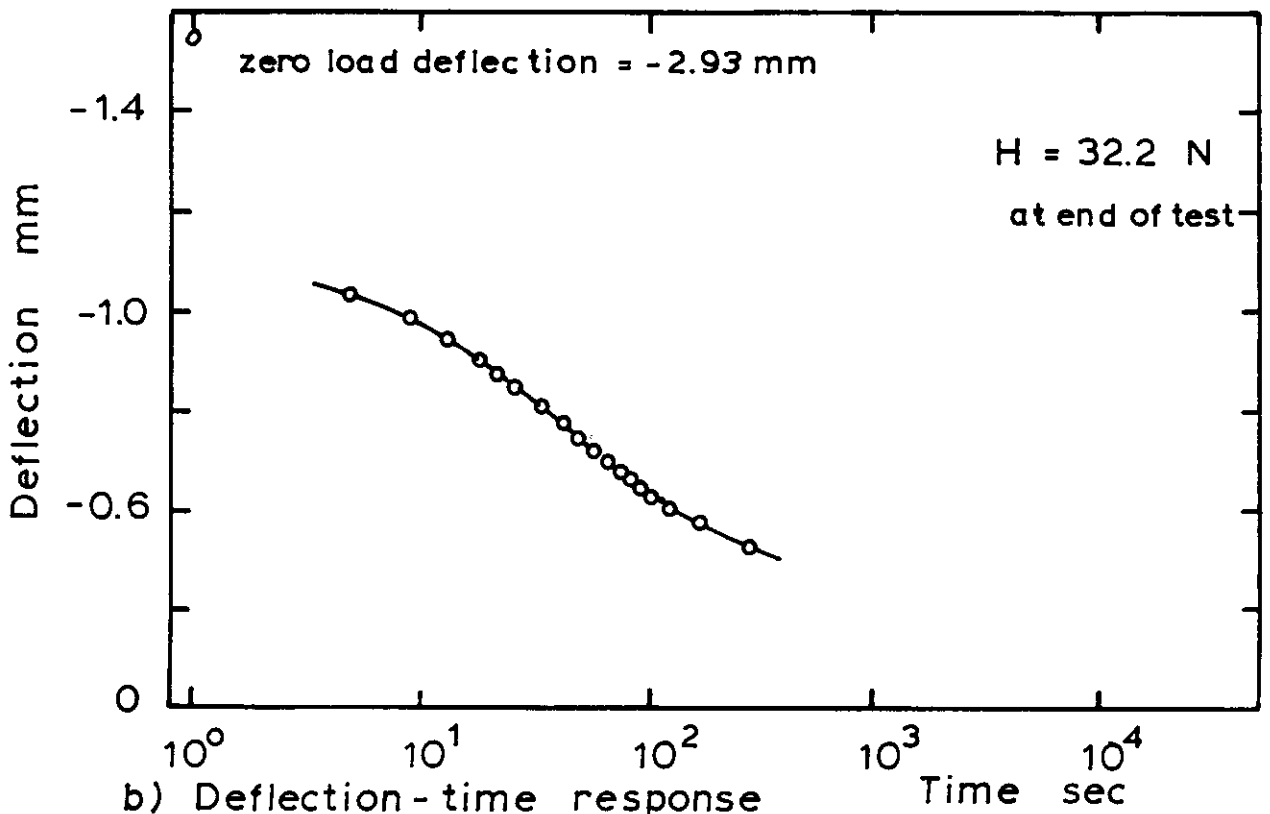
b) Deflection-time response

FIG. 6.6 CLOSED-VESSEL TEST RESULT: L=110 d=8 e=12 $\sigma'_V=100$

Cyclic loading pile #B pot #1 : 388/288 kPa : L=110 d=8mm : min e

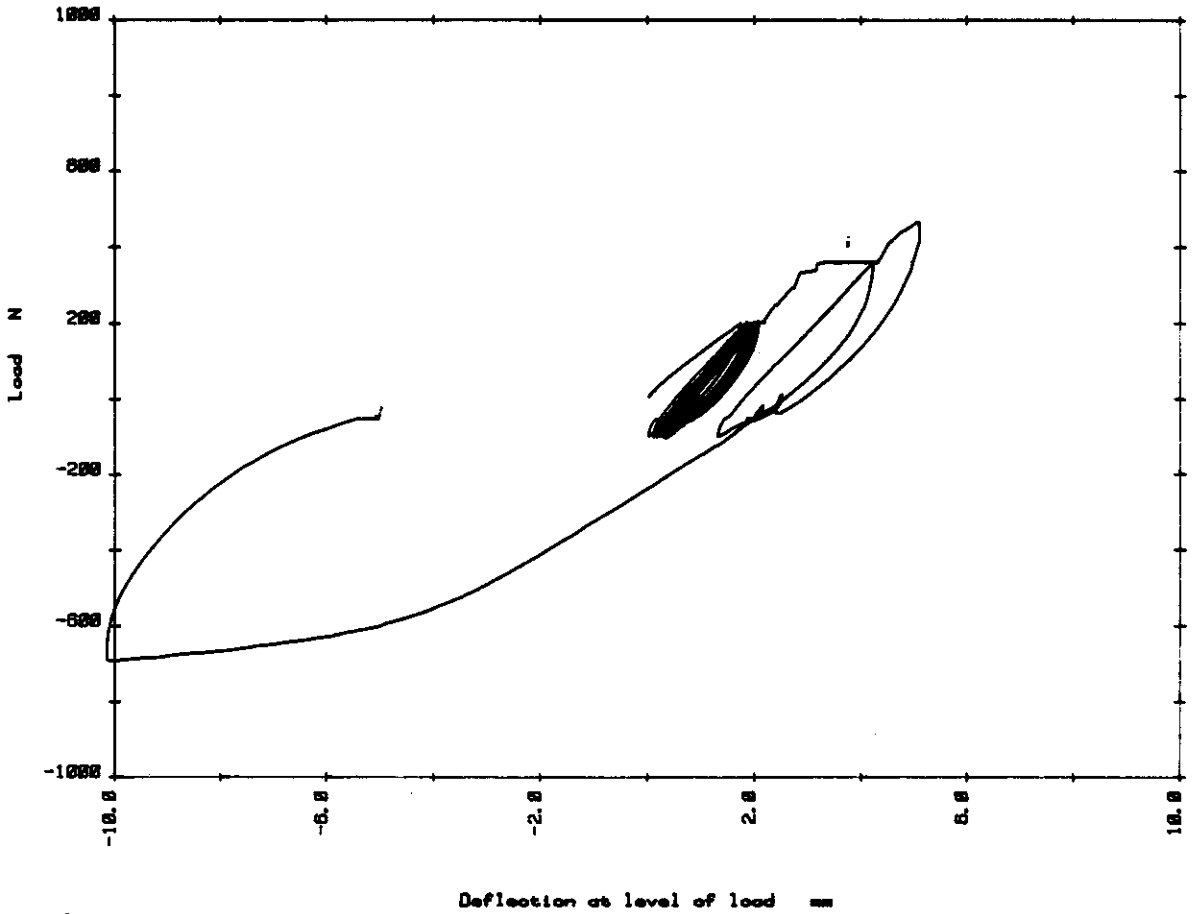


a) Load-deflection response

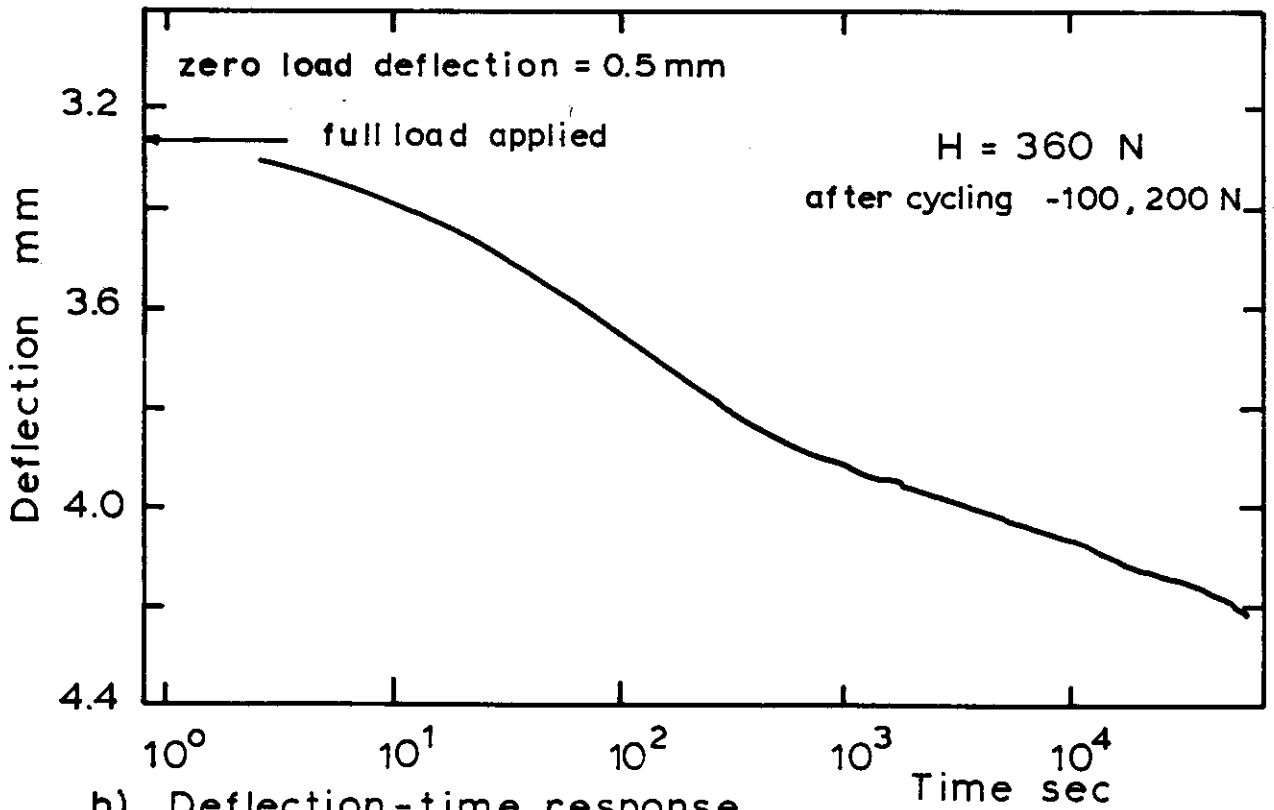


b) Deflection-time response

FIG. 6.6 CLOSED-VESSEL TEST RESULT: L=110 d=8 e=12 $\sigma'_V=100$



a) Load-deflection response



b) Deflection-time response

FIG. 6.7 CLOSED-VESSEL TEST RESULT: L=165 d=10 e=12 $\alpha'_V=250$

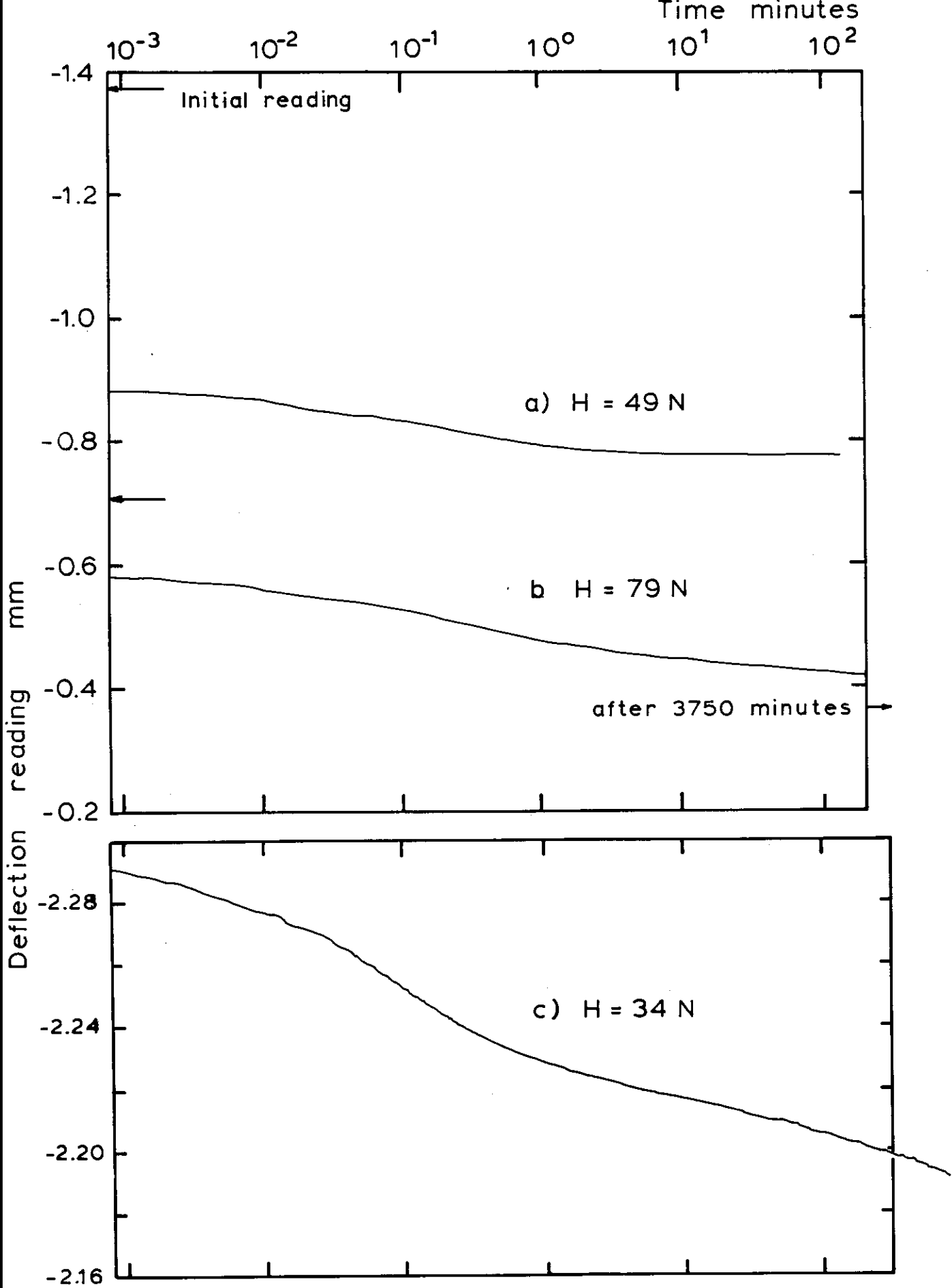


FIG. 6.8 LOG-TIME - DEFLECTION RESPONSE FROM TWO CLOSED-VESSEL TESTS, BOTH $L=170$ $d=10$ $e=12$ $\sigma'_v=100$ kPa

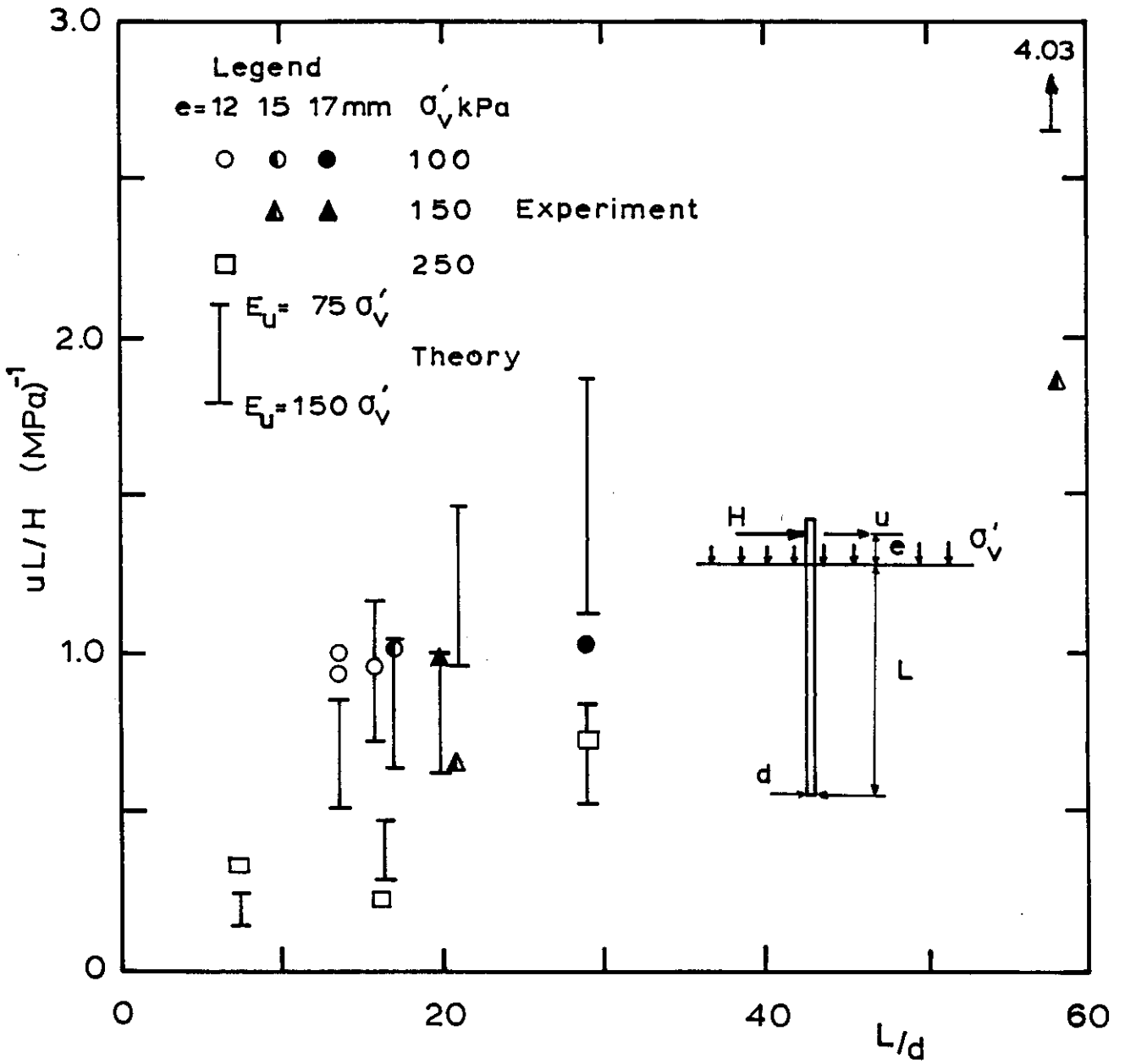
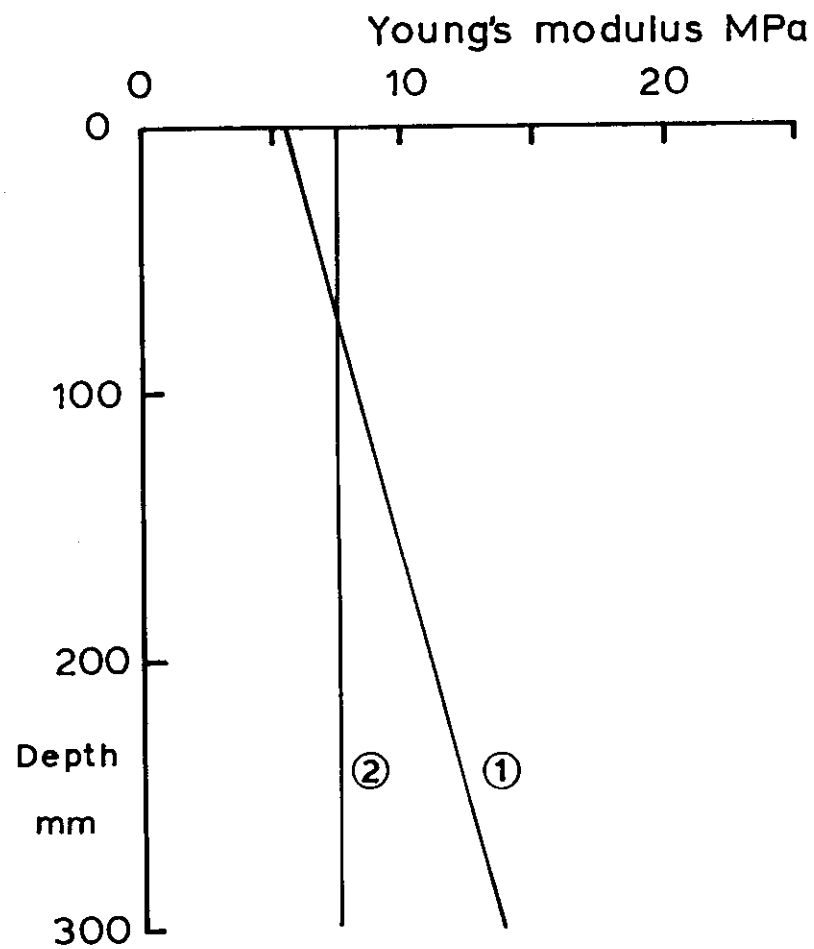
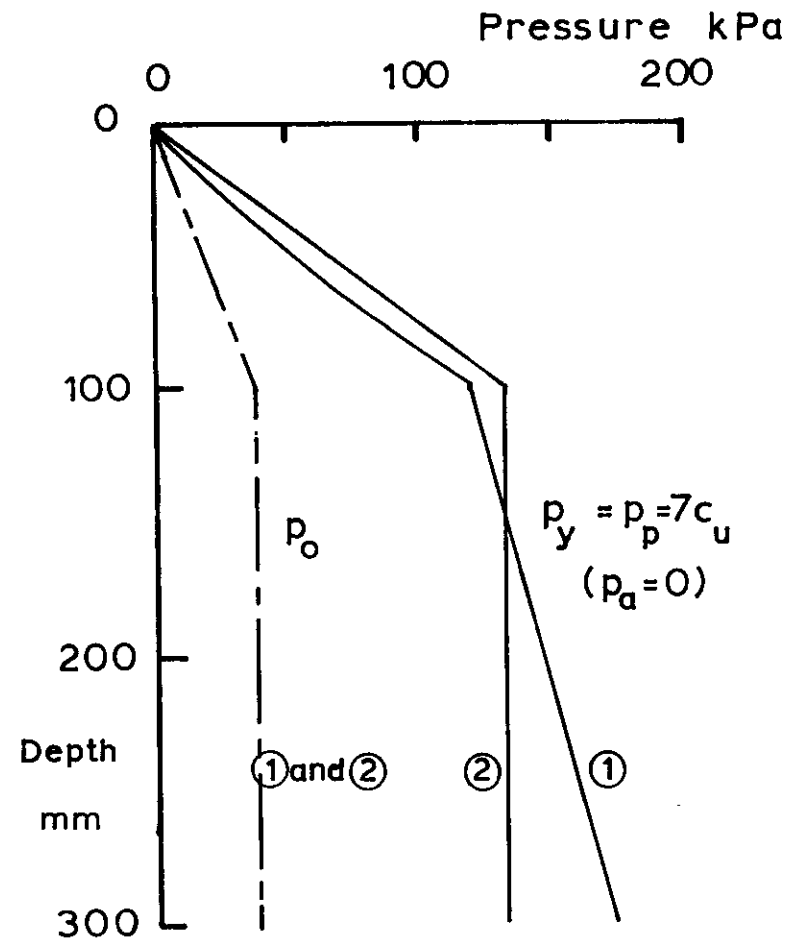


FIG. 6.9 CLOSED-VESSEL TEST RESULTS: COMPARISON WITH THEORETICAL RESULTS USING $E_u = 75$ to $150 \sigma'_v$



a) Assumed distributions of Young's modulus



b) Assumed distributions of ultimate and initial interface tractions

FIG. 6.10 THEORETICAL VALUES OF SOIL PROPERTIES FOR THE OPEN-VESSEL TESTS

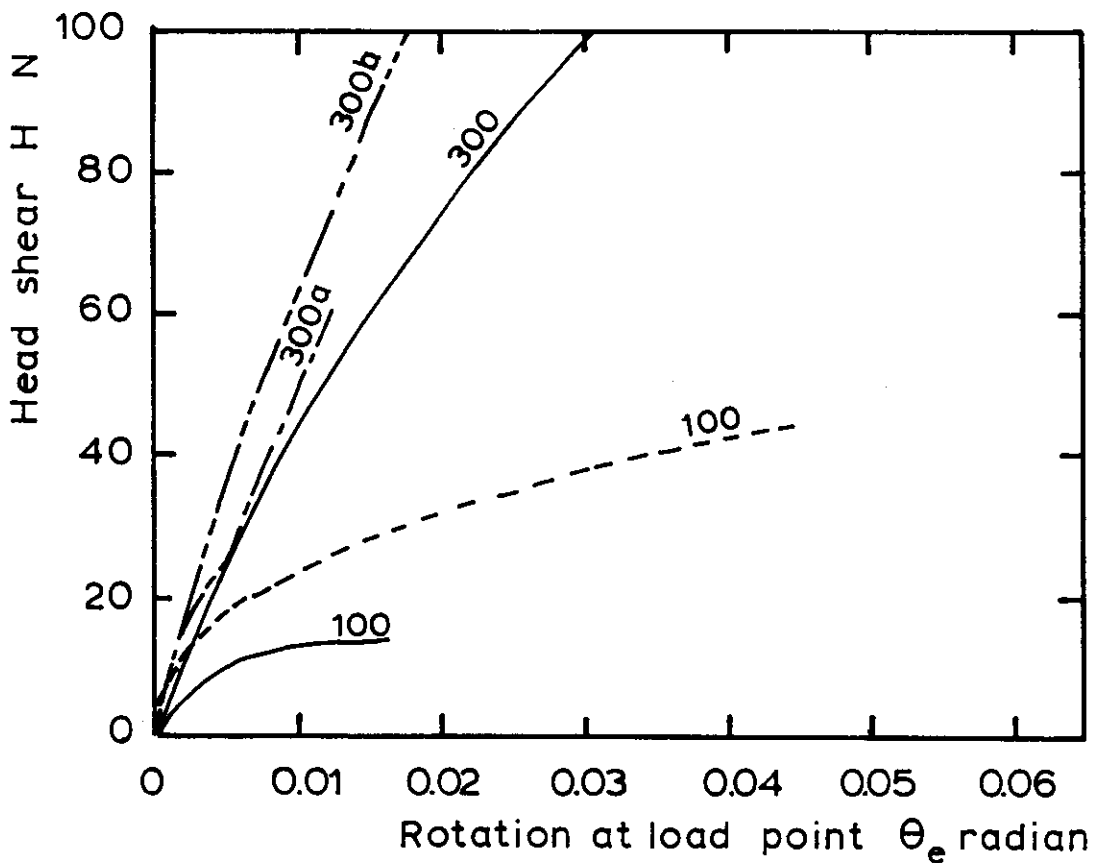
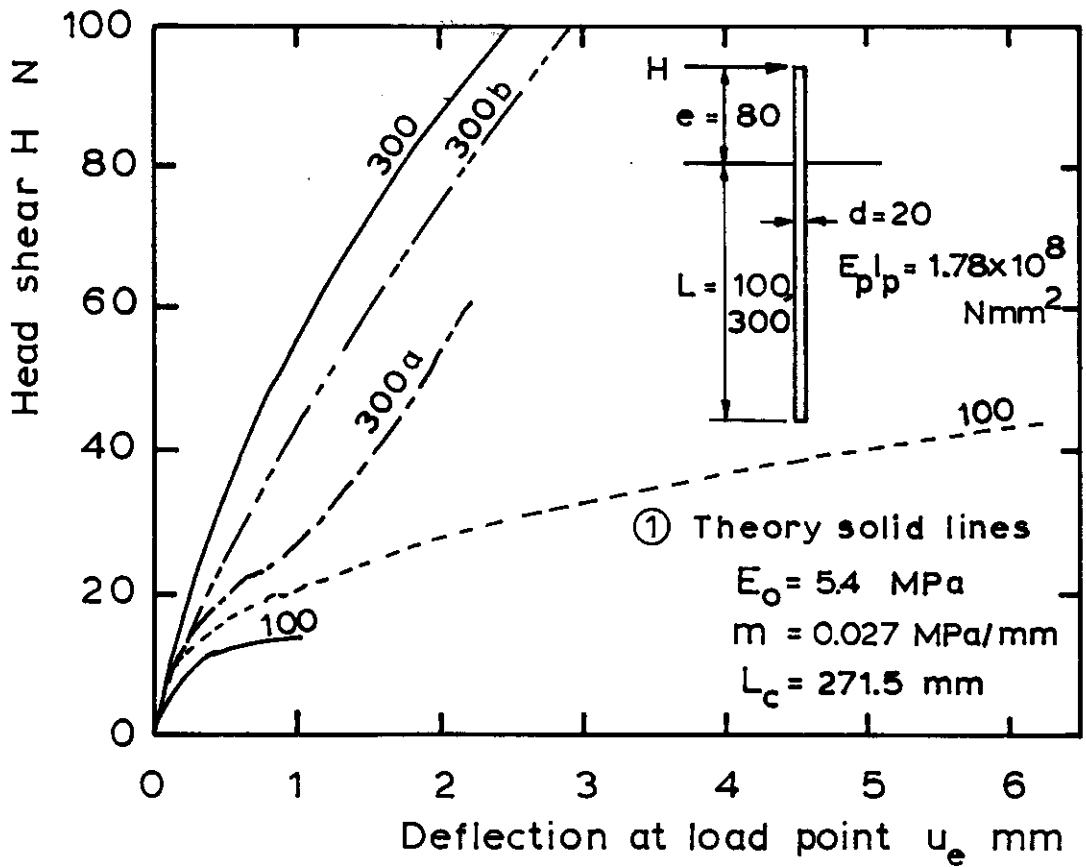


FIG. 6.11 COMPARISON OF THEORETICAL AND EXPERIMENTAL LOAD-DEFORMATION RESPONSE: $L/d = 5$ and 15

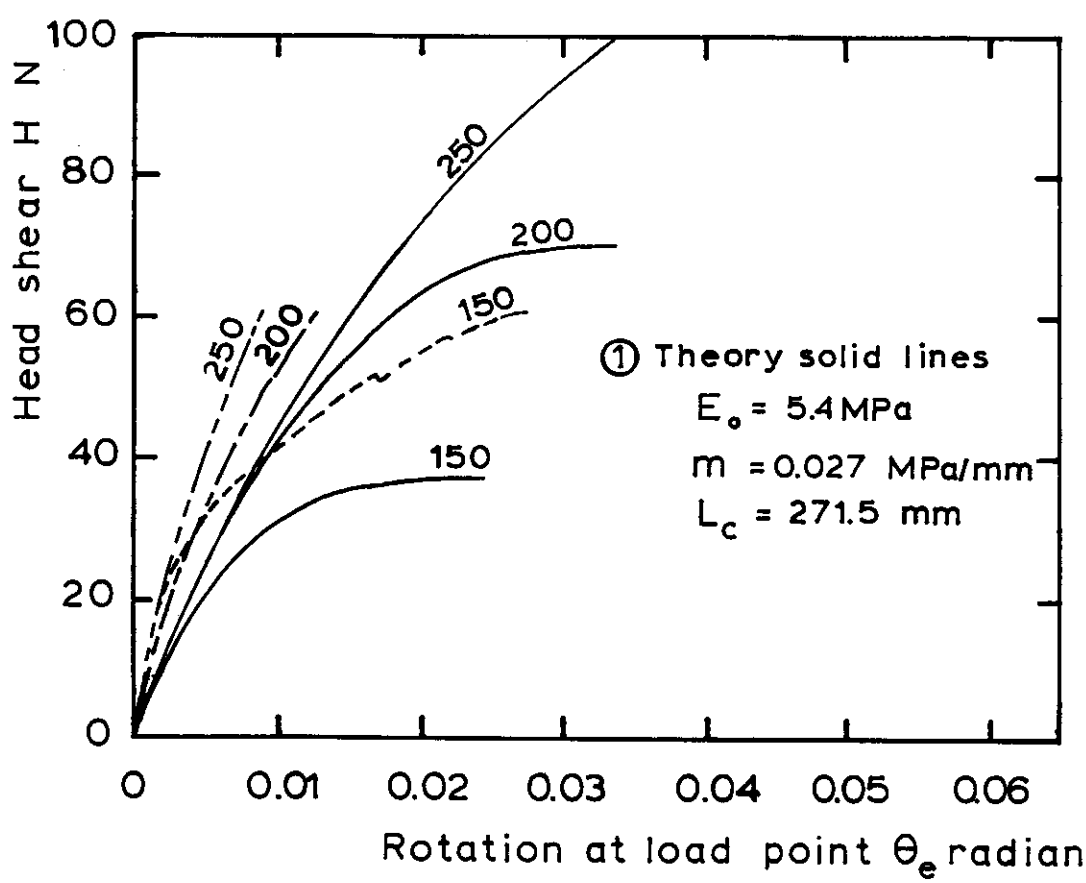
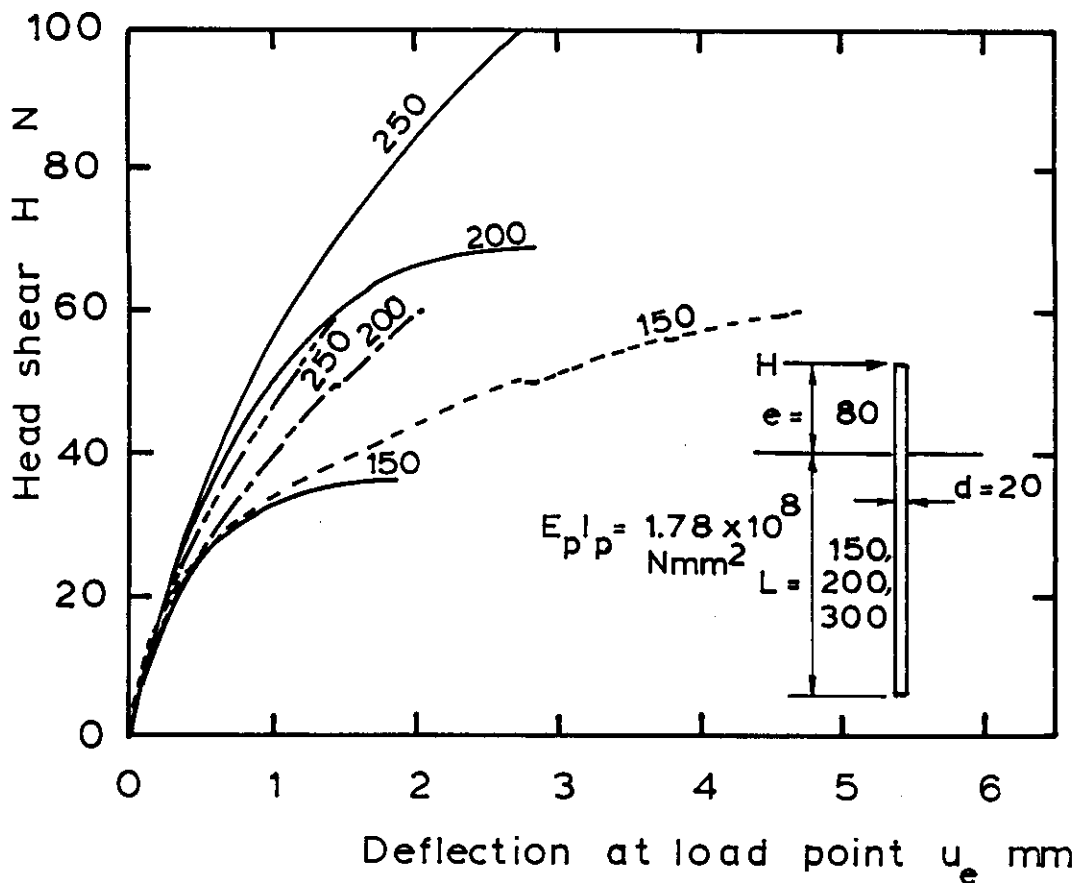


FIG. 6.11 CONTINUED: $L/d = 7.5, 10$ and 12.5

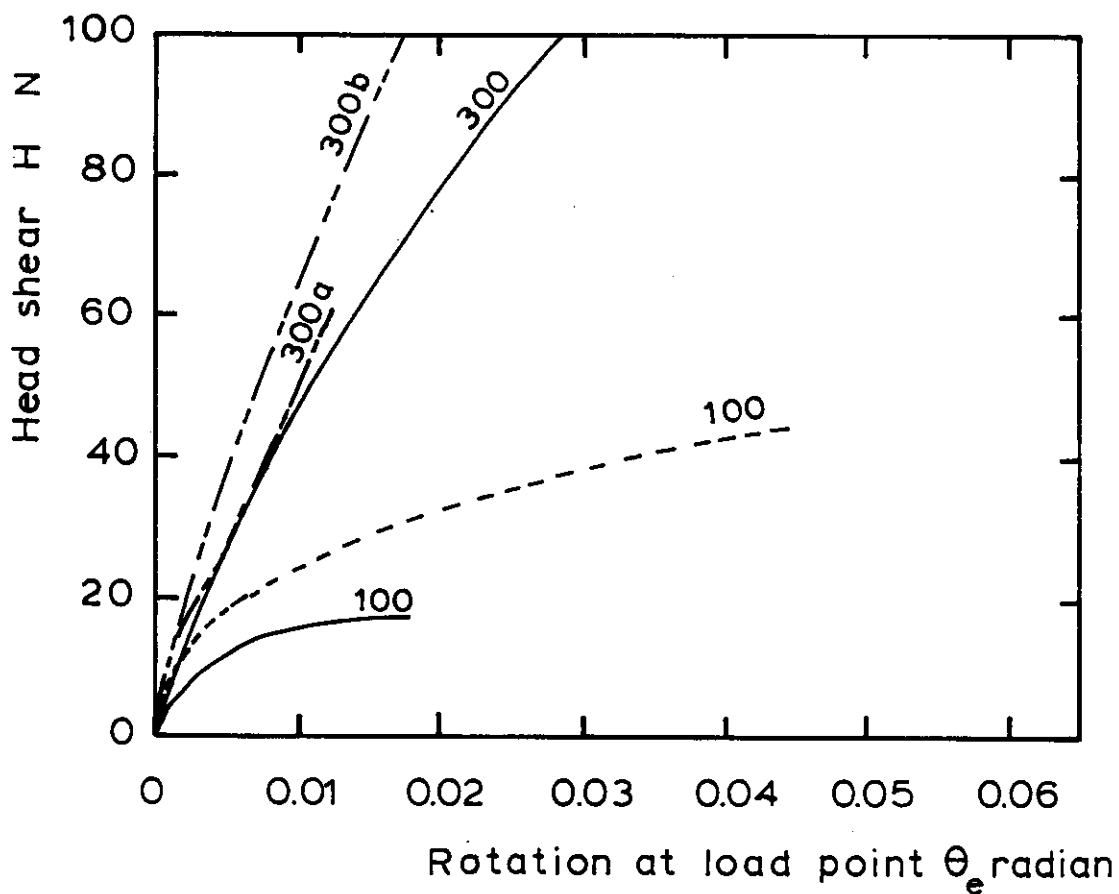
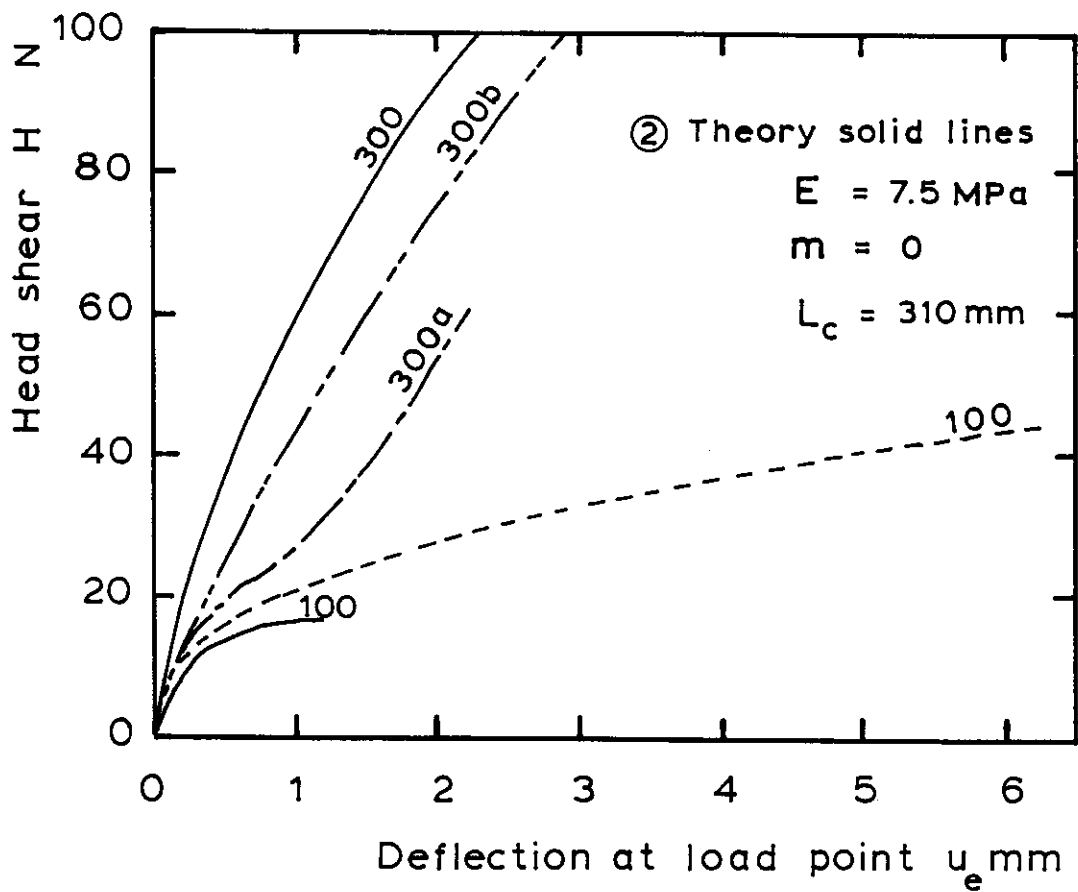


FIG. 6.12 COMPARISON OF THEORETICAL AND EXPERIMENTAL
 LOAD-DEFORMATION RESPONSE: $L/d = 5$ and 15

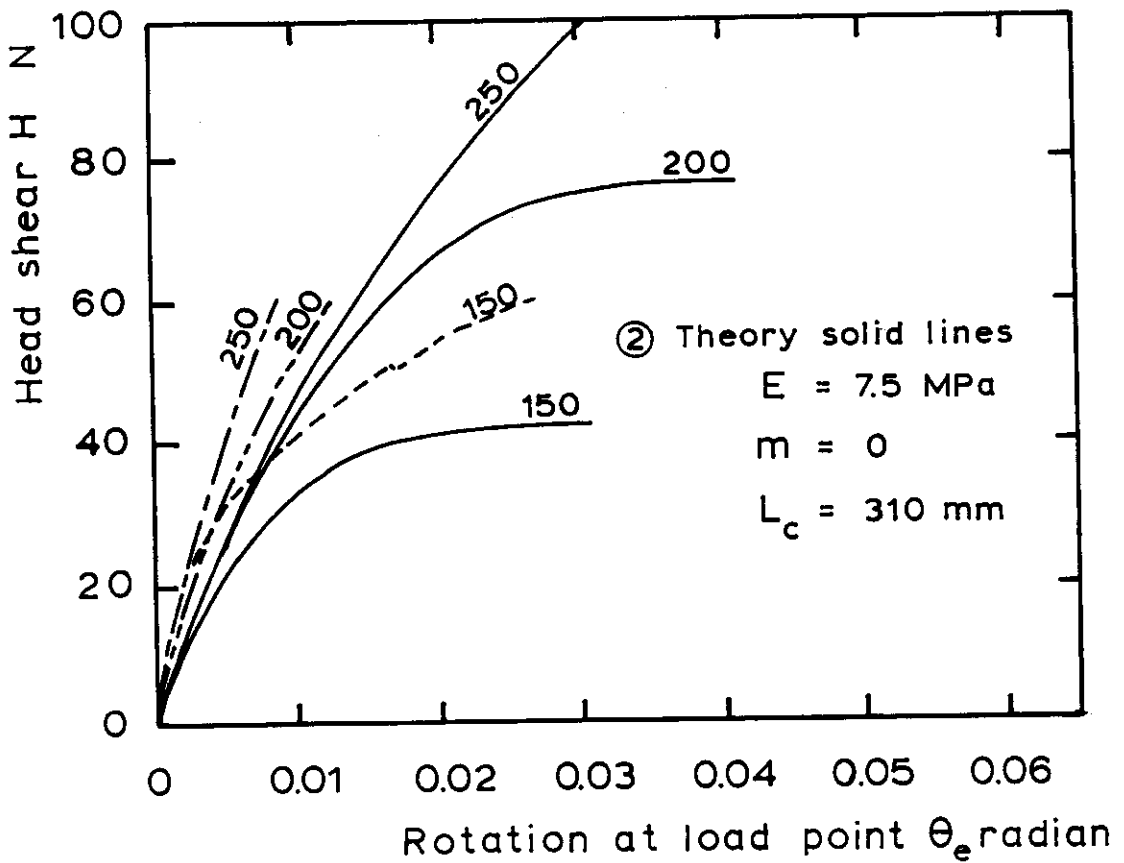
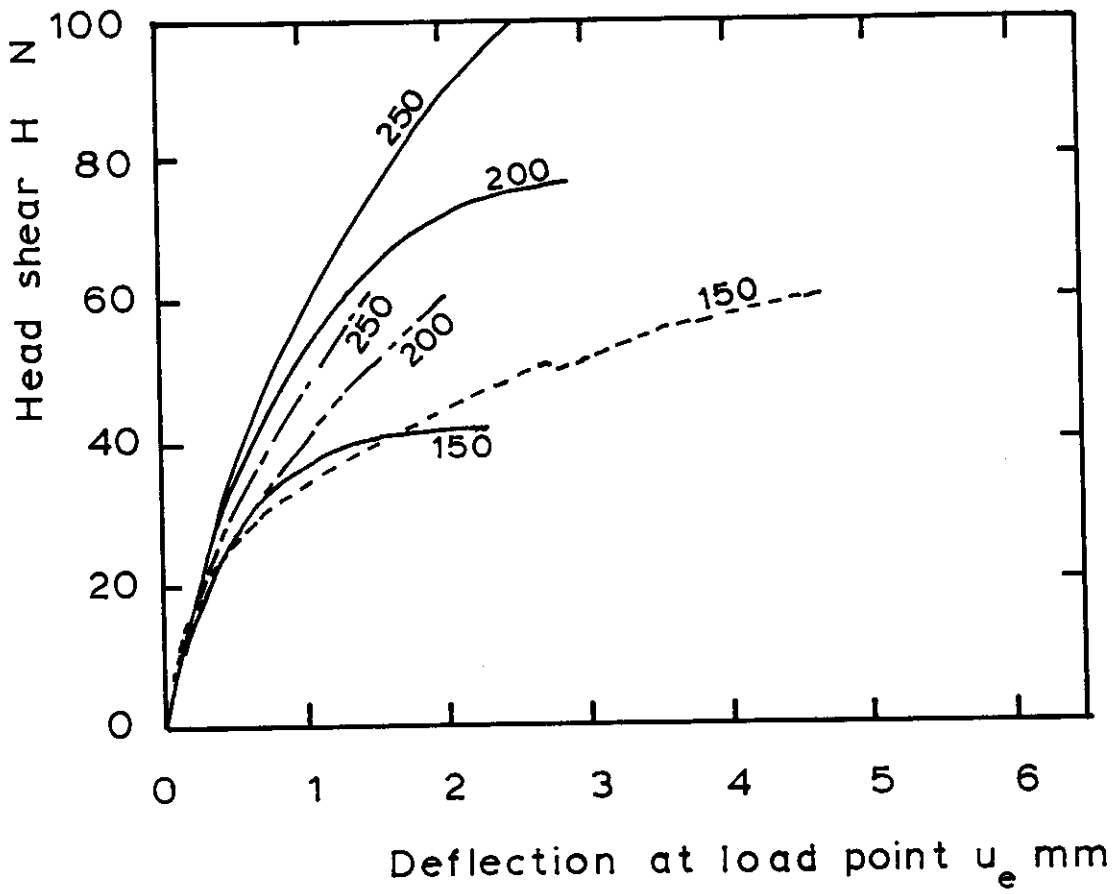


FIG. 6.12 CONTINUED: $L/d = 7.5, 10$ and 12.5

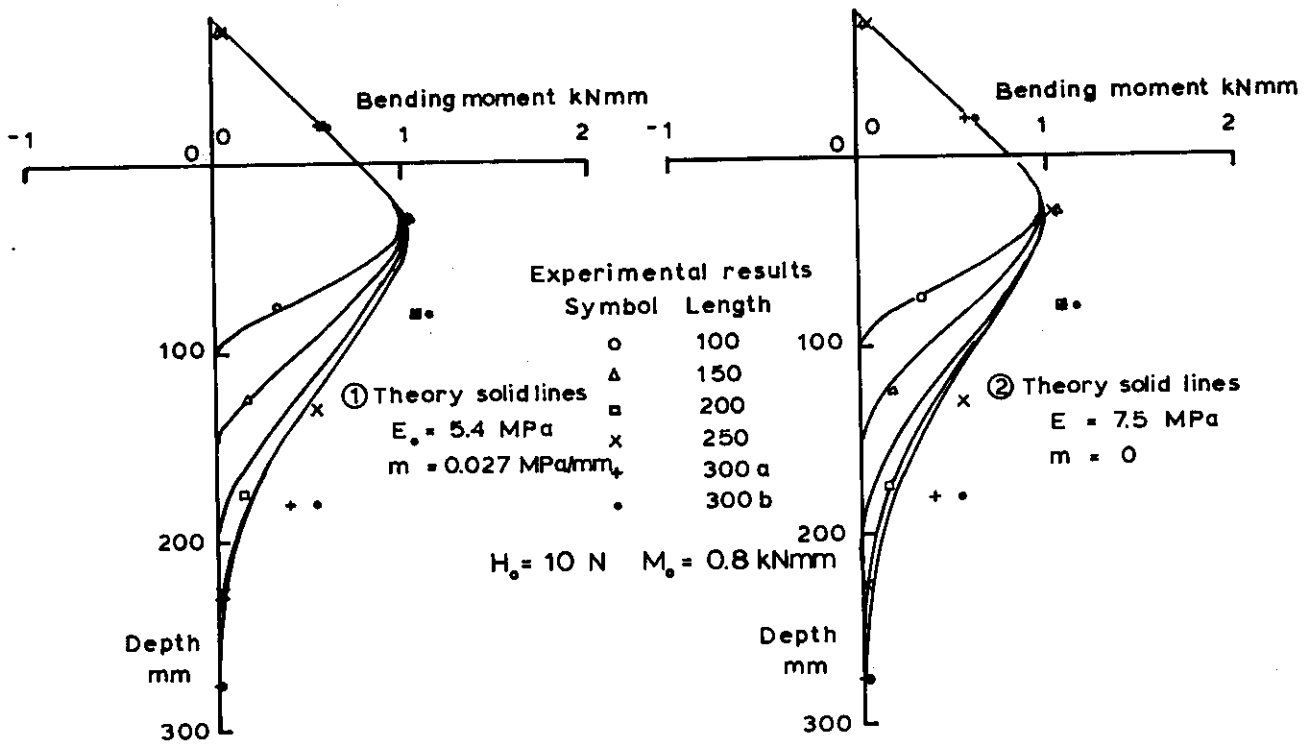


FIG. 6.13 COMPARISON OF THEORETICAL AND EXPERIMENTAL BENDING MOMENT DISTRIBUTIONS : OPEN-VESSEL TESTS

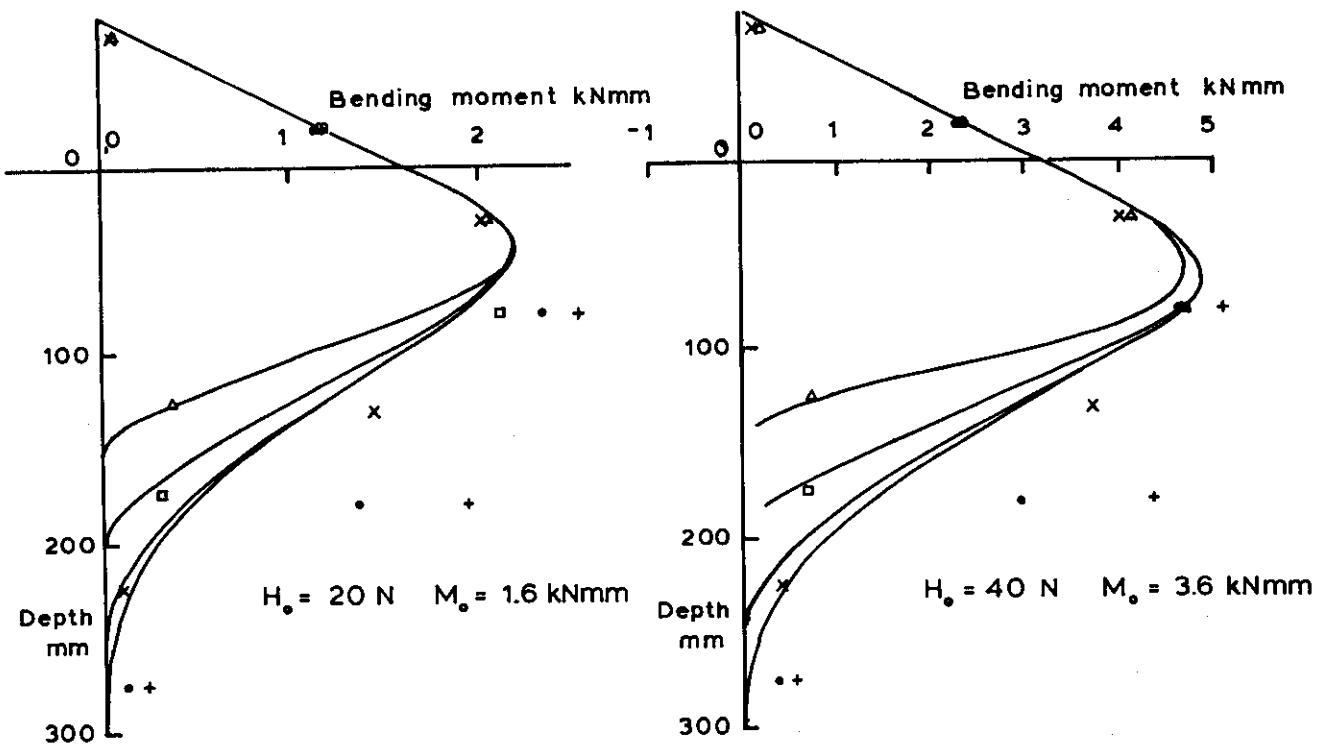
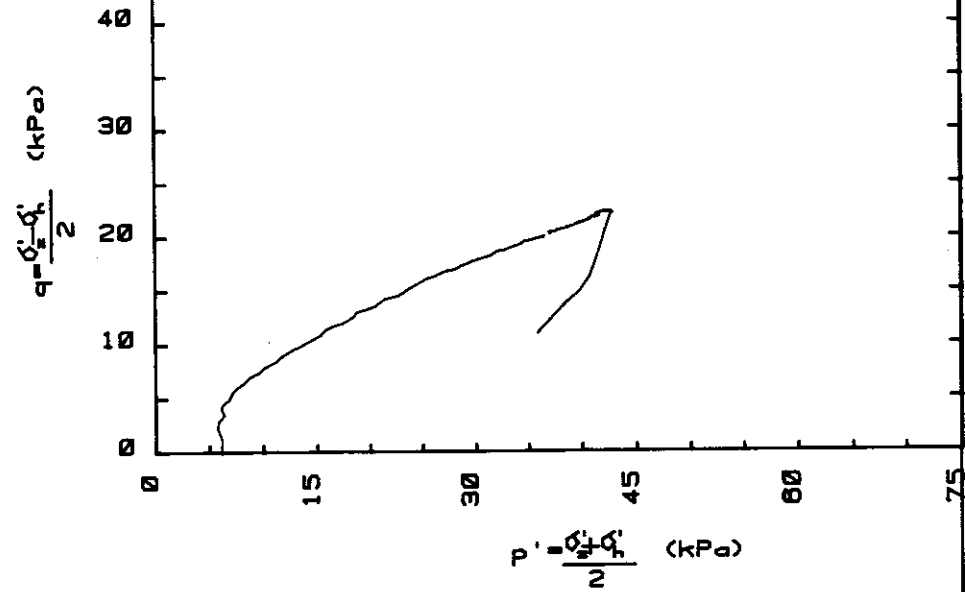
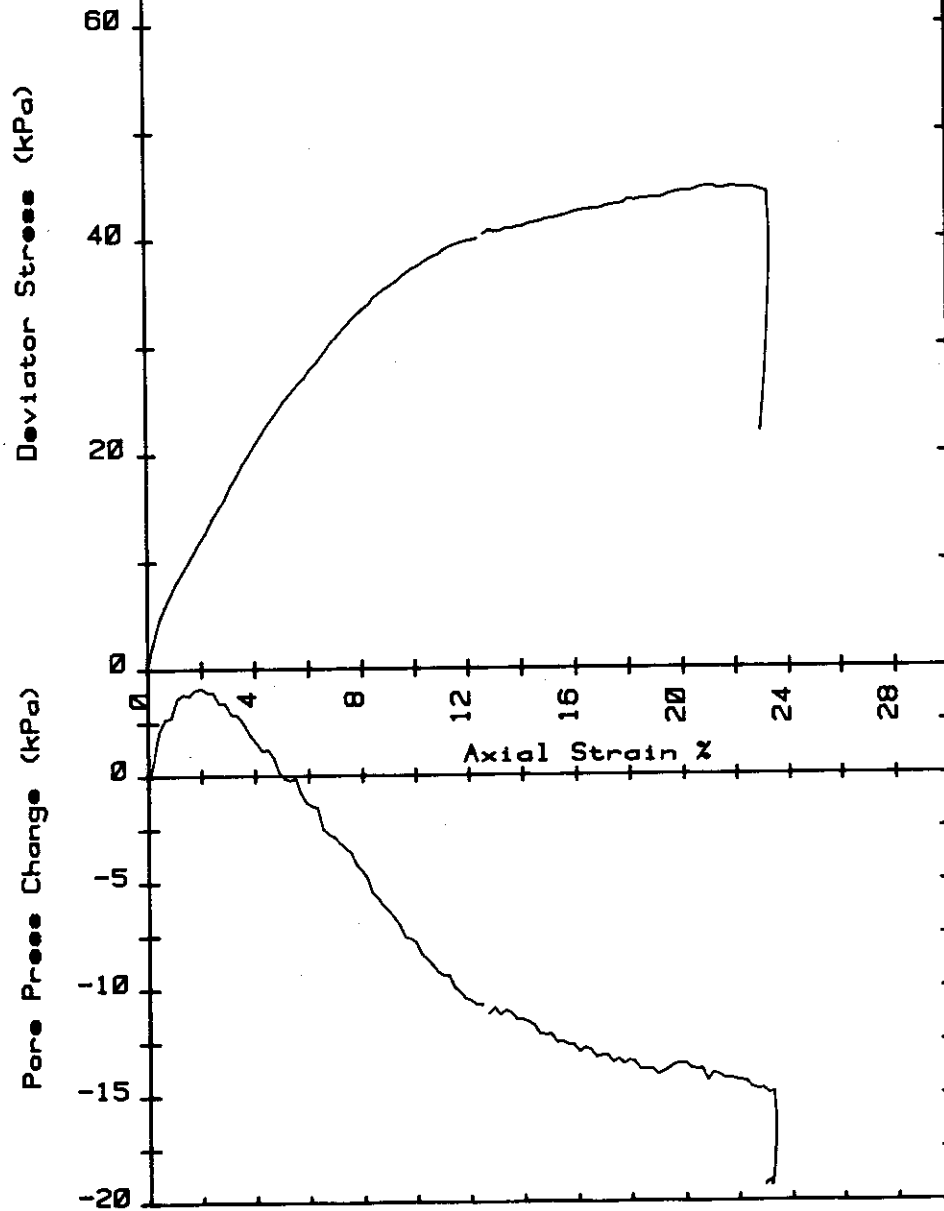


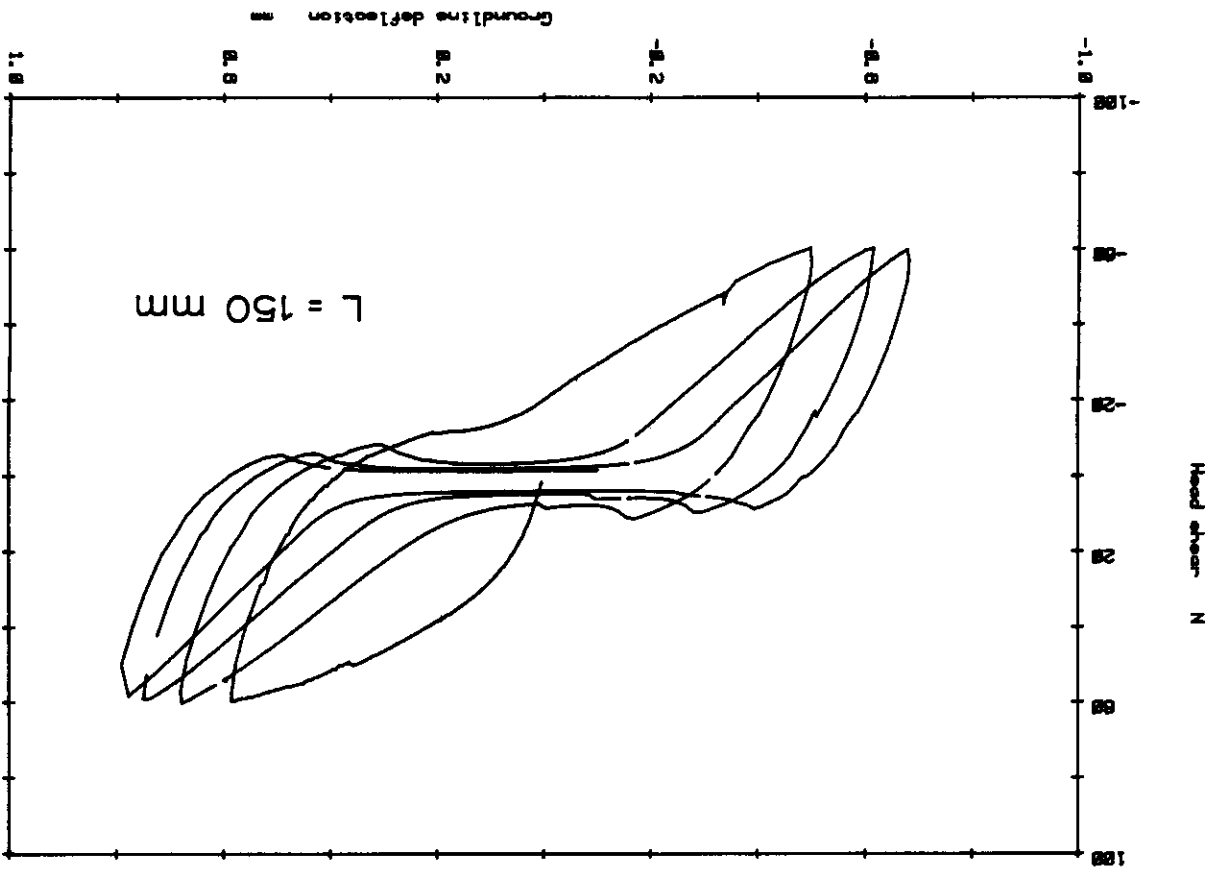
FIG. 6.13 CONTINUED ① Theory solid lines $E_s = 5.4 \text{ MPa}$ $m = 0.027 \text{ MPa/mm}$



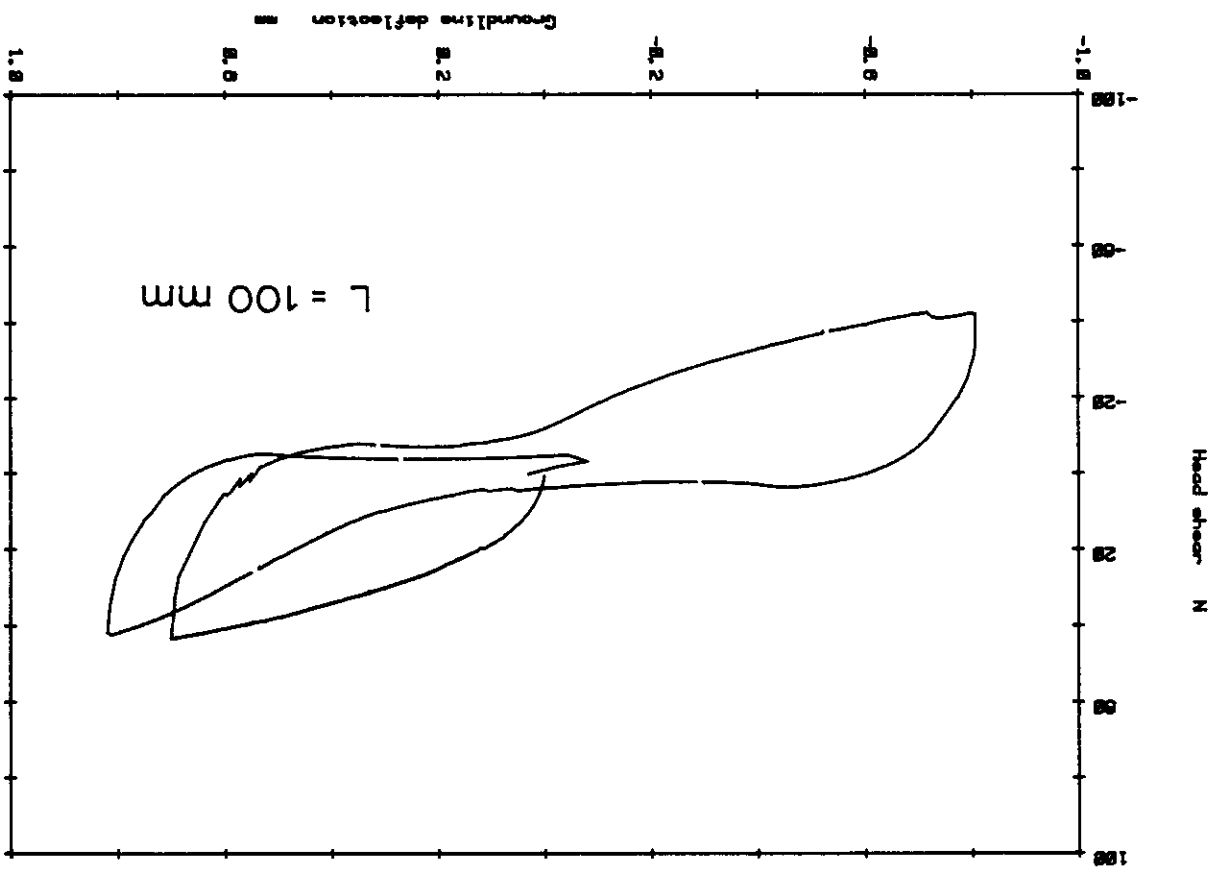
CENTRE Quick T/X. Big Pot. 200 kPa(OC). 09/01/85. 100 kPa.: RUN DATED : 20:05:11:51:41

FIG. 6.14 TYPICAL UNCONSOLIDATED UNDRAINED TRIAXIAL TEST ON CORED SAMPLE: OPEN-VESSEL

FIG. 6.15 LOAD-DEFLECTION LOOPS : OPEN-VESSEL TESTS

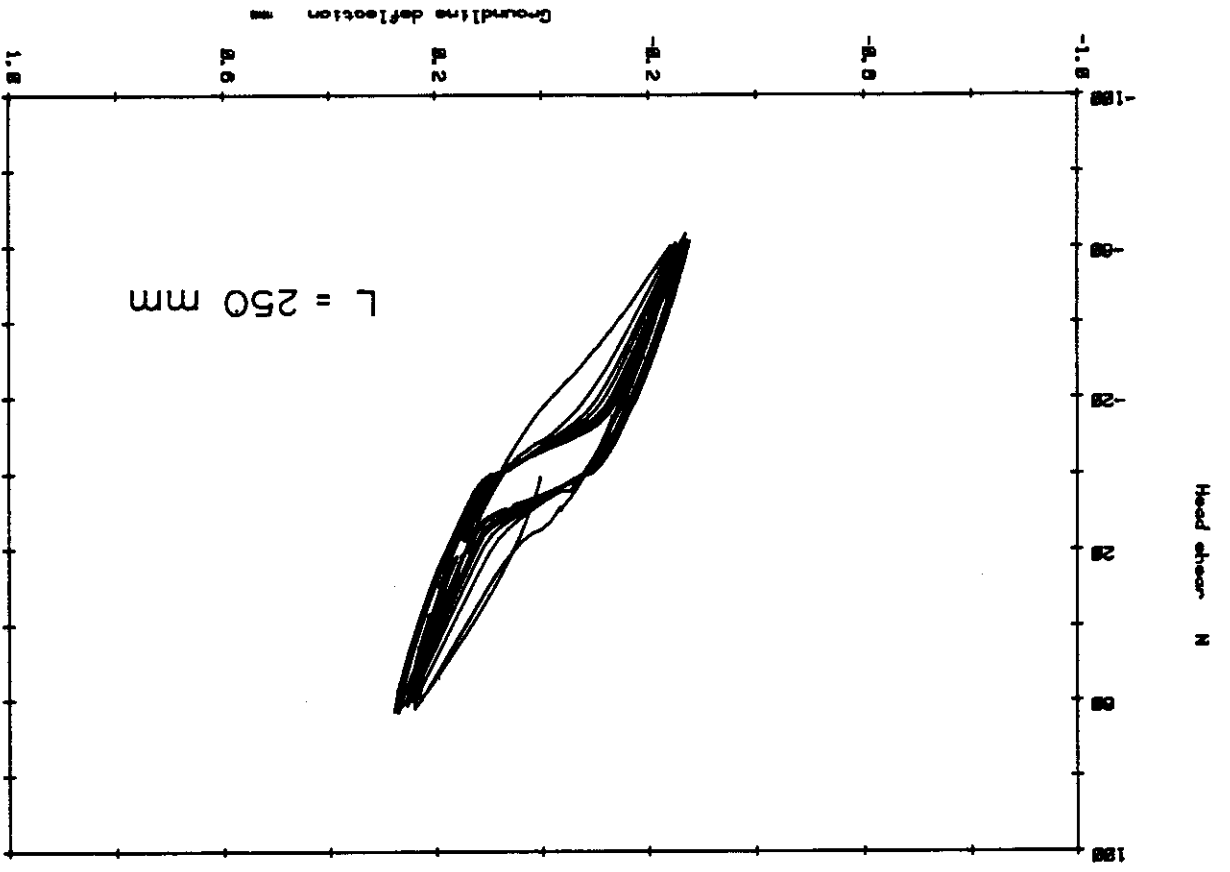


Big Pot #4, L=150 D=28 ab=4-88 ac=158, (CC2884P), 21/12/84.

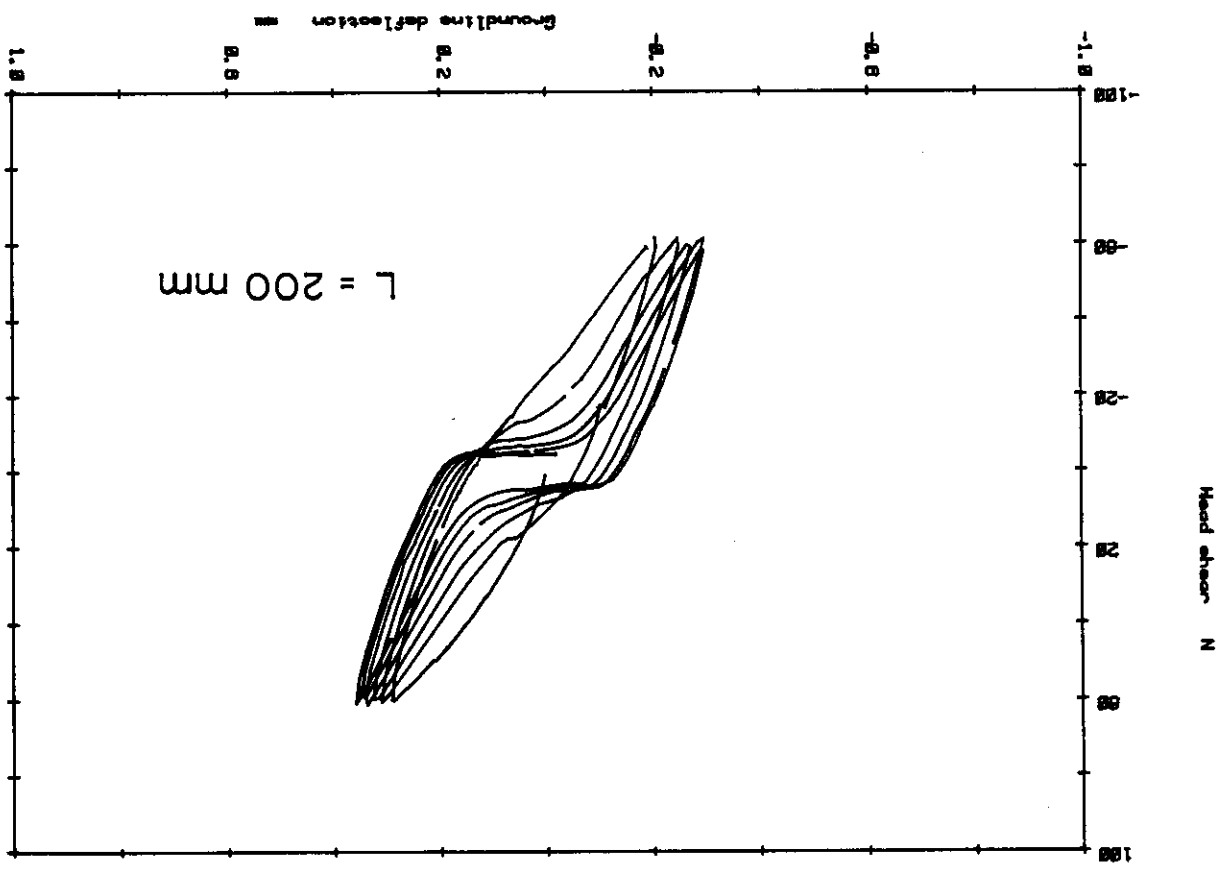


Big Pot #4, L=100 D=28 ab=4-88 ac=158, (CC2884P), 28/12/84.

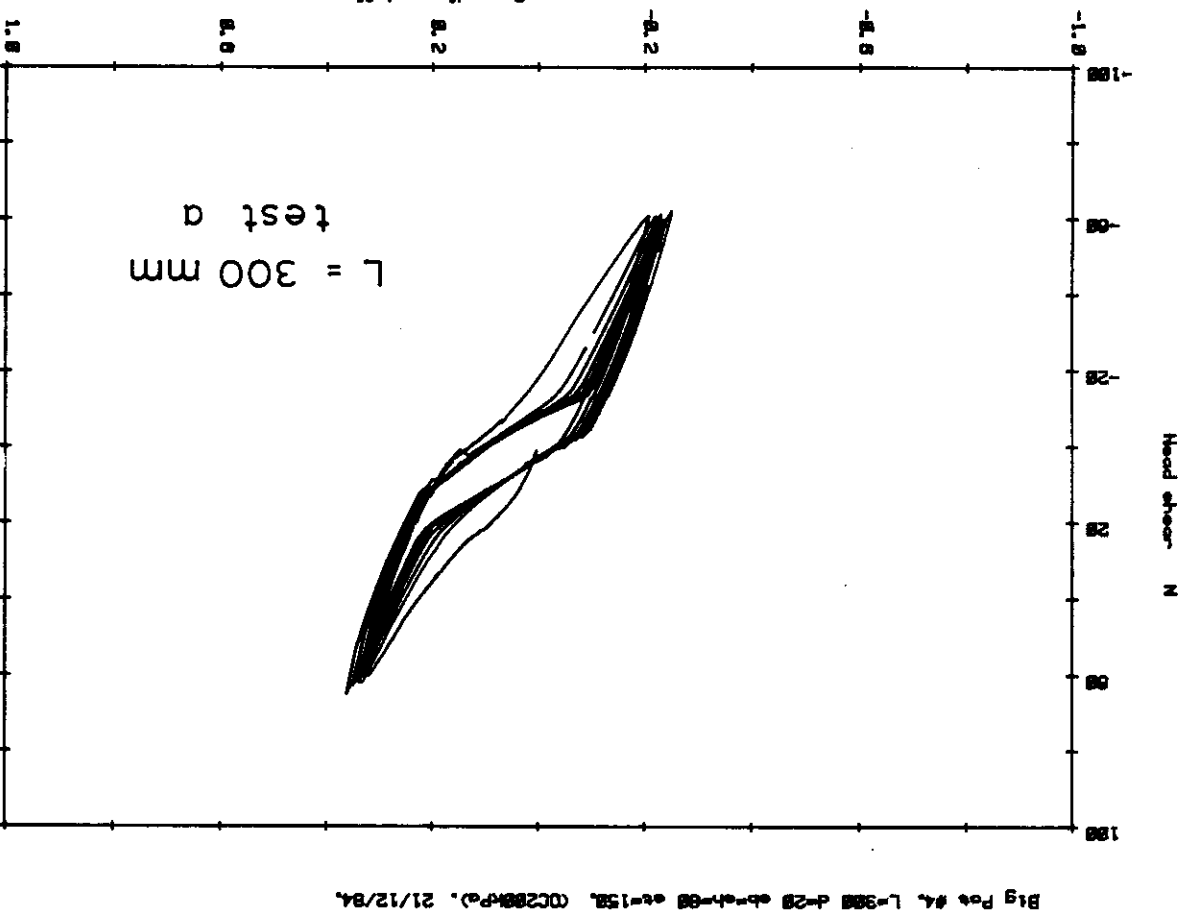
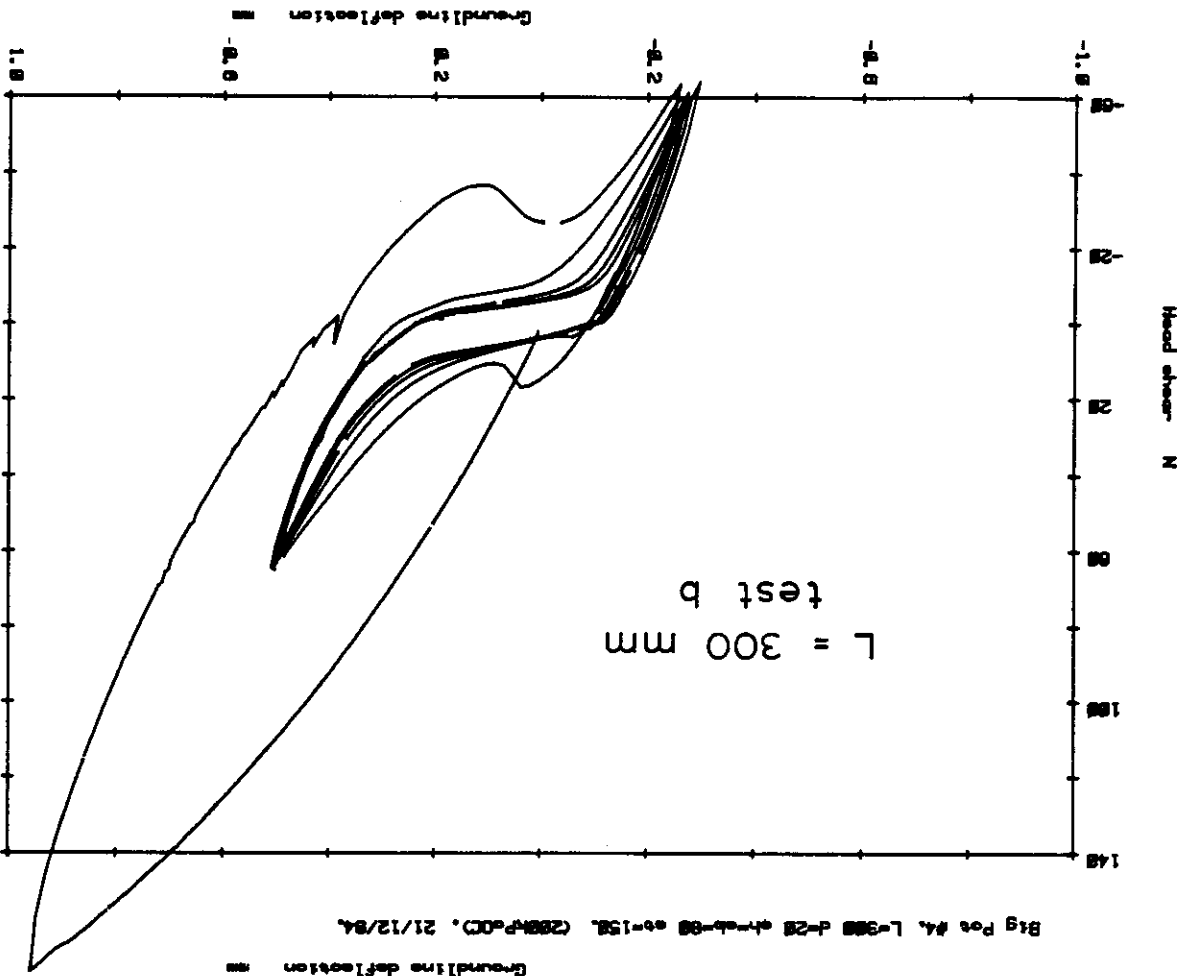
FIG. 6.15 CONTINUED



Big Pos #4, L=250 d=28 ab=41=88 at=158mm, (DC288KPa), 28/12/84.



Big Pos #4, L=200 d=28 ab=41=82 at=152mm, (DC288KPa), 28/12/84.



Depth Below Groundline (ft)

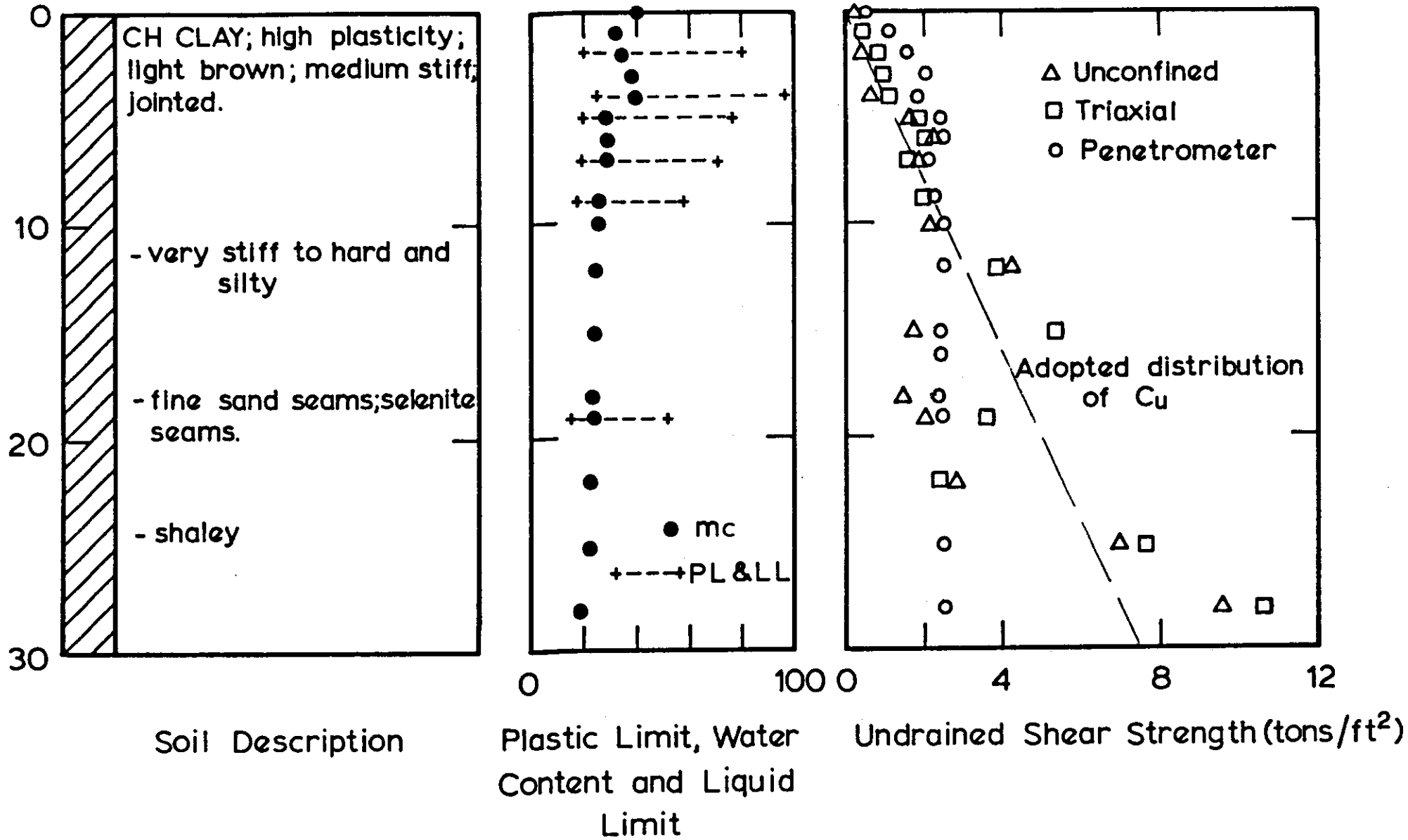
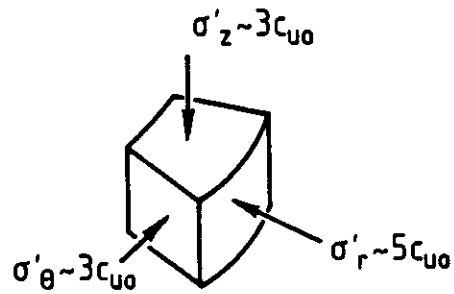
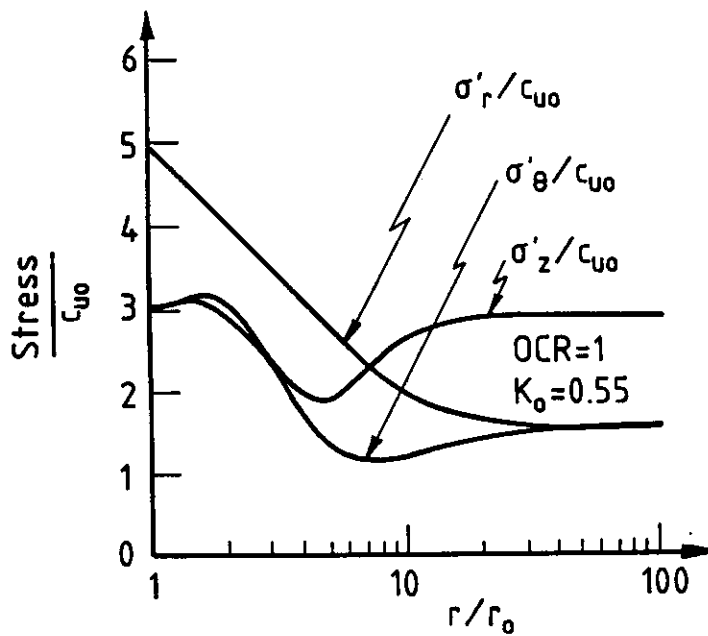


FIG.6.16 COMPOSITE SOIL PROFILE
REESE ET AL. (1975)



(a) Stresses on Element Adjacent to Pile



(b) Stress Distribution Around Pile

FIG. 6.17 THEORETICAL STRESS STATE AFTER CONSOLIDATION AROUND PILE IN NORMALLY CONSOLIDATED SOIL (from Randolph et al. (1979))

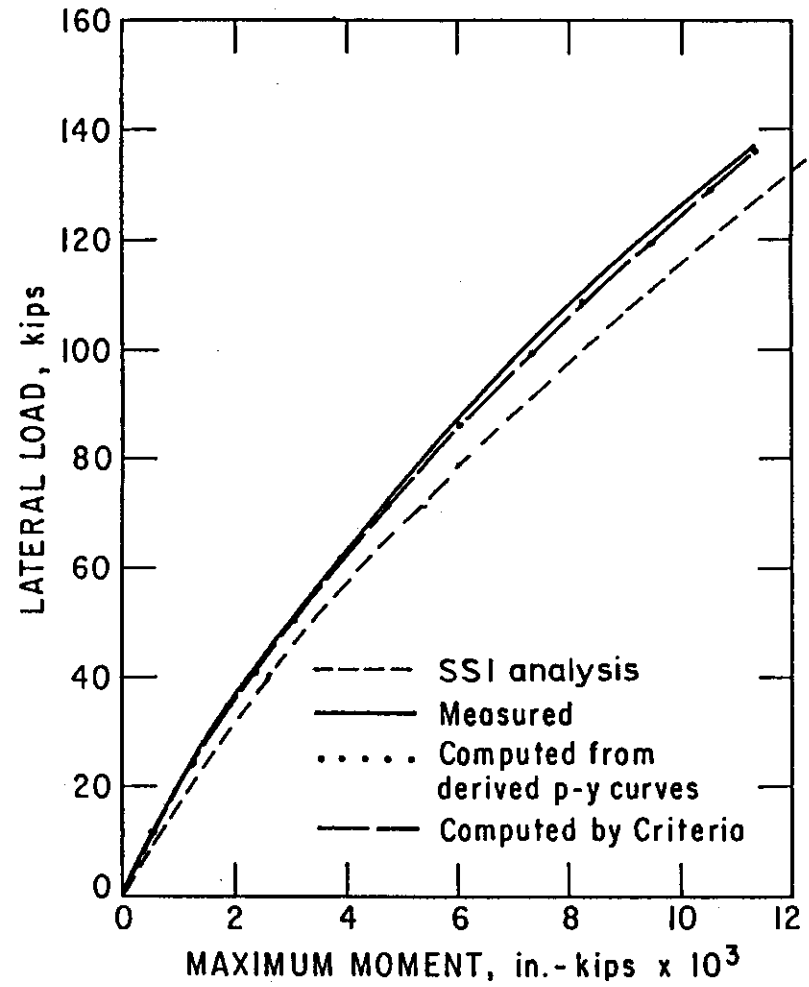
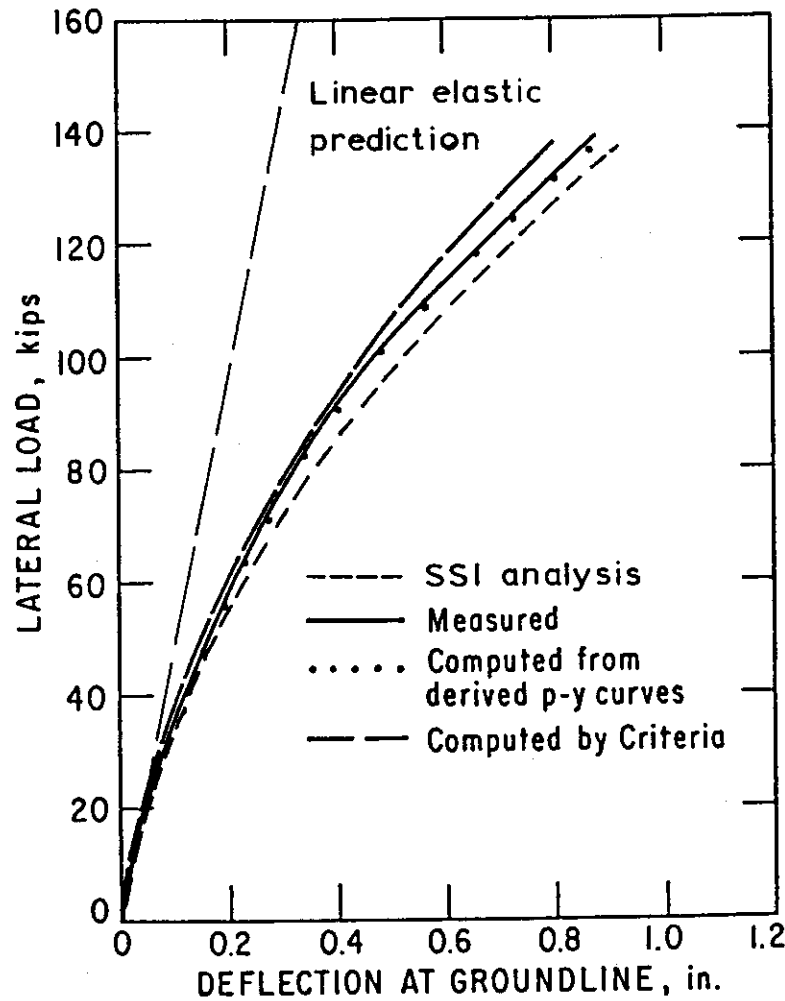


FIG. 6.18 THEORETICAL AND TEST RESULTS FOR 24 INCH PILE OF REESE ET AL.(1975)

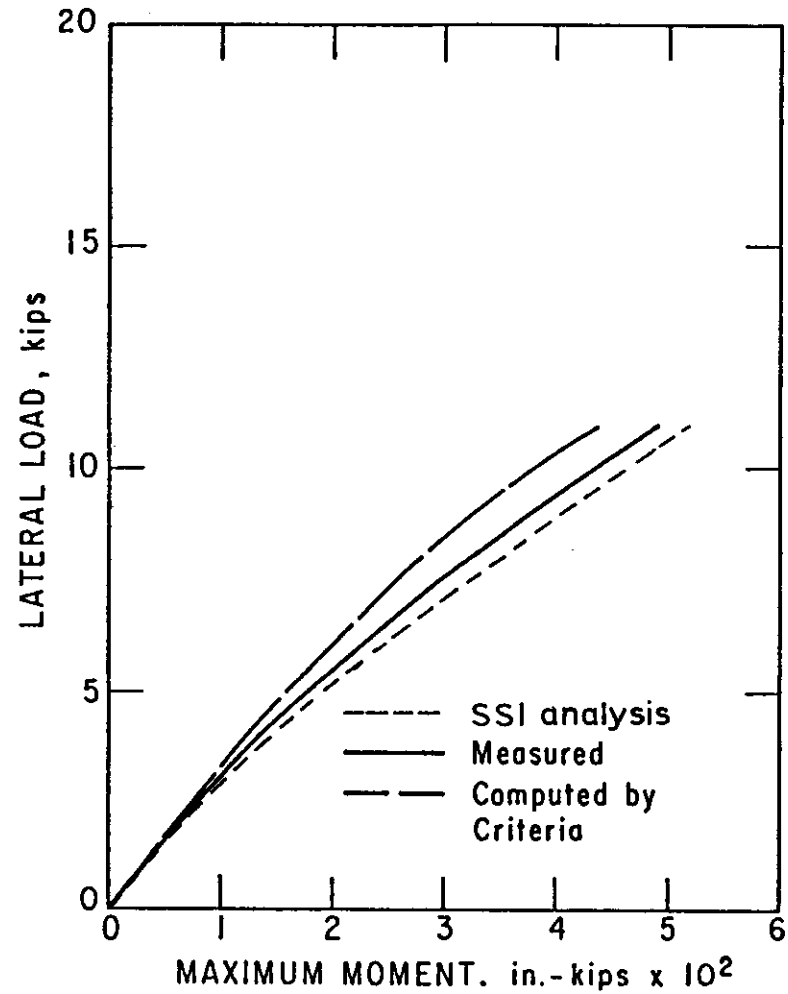
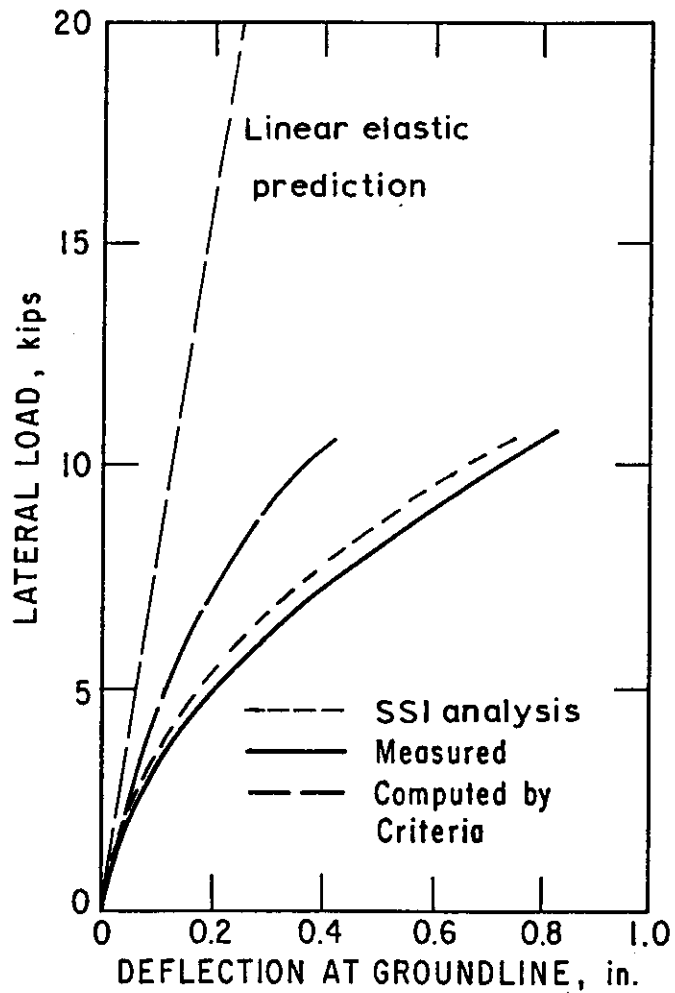


FIG. 6.19 THEORETICAL AND TEST RESULTS FOR SIX INCH PILE OF REESE ET AL. (1975)

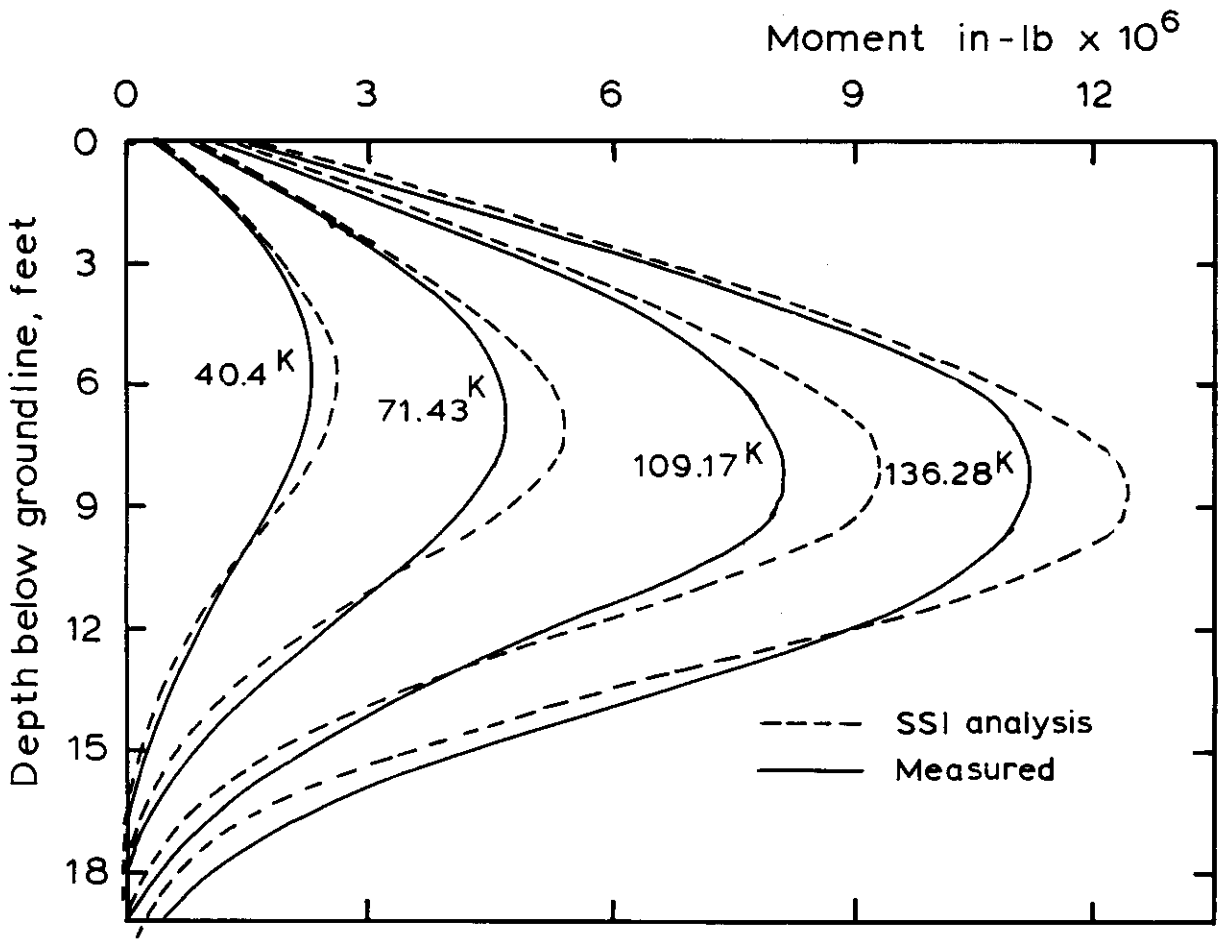


FIG. 6.20 THEORETICAL AND TEST RESULTS FOR BENDING MOMENT DISTRIBUTIONS: 24 INCH PILE OF REESE ET AL.

(1975)

CHAPTER SEVEN - SUMMARY OF CONCLUSIONS

The analysis of single laterally loaded piles has been the subject of many, and varied approaches. Each approach has arisen from perceived ideas of which factors are important in determining lateral response and the accessibility of an appropriate solution technique. This Thesis has sought to improve the linear elastic-continuum method of analysis and extend it to encompass non-linear response.

The various approaches to this problem fall naturally into two groups: those based upon linear response of the soil; and those directly addressing the non-linear nature of the overall pile response. Analyses in the first group are included in Chapters Three and Four, and Chapter Five directs attention at the extensions necessary for non-linear analysis. It is convenient to consider the analyses in each chapter using the same classification of the model type, namely:

- a) Winkler-type empirical models.
- b) Boundary element, elastic-continuum models.
- c) Finite element elastic models.

This classification scheme is used in the review of literature presented in Chapter Two, from which the following major conclusions are made.

The limitation of Winkler-based approaches to the particular set of conditions under which their parameters were derived, is the main drawback of these approaches. Elastic-continuum models using boundary element analysis techniques are useful for prediction of response based directly upon fundamental soil properties, although simplifying assumptions about the effects of soil non-homogeneity and limited depth are required to allow a

tractable and effective analysis. The finite element method can theoretically take into account aspects of the laterally loaded pile problem that require assumptions to be made in the boundary element method.

In Chapter Three, several Winkler-based analyses are developed and, while being of limited practical use, provide linear solutions against which the numerical technique of the boundary element analysis can be checked by employing a Winkler soil influence matrix.

The boundary element analysis based upon linear response of the soil, using either a homogeneous elastic-continuum (Mindlin) model or a Winkler model, is presented and the concept of a deflection mismatch between nodes of the pile and the soil is introduced. This mismatch is an integral part of the analysis of non-linear response developed in Chapter Five.

In Section 3.4.2 the finite element model analysis is subjected to a comprehensive verification with solutions for the response of cantilever beams (to end, distributed and self-weight loads), axisymmetric elastic bodies (under pressure loading), surface foundations (to axial, torsional and lateral loading) on both a homogeneous and non-homogeneous (Gibson) half-space and a cylinder subjected to periodic loading. The boundary conditions and boundary positions used for the finite element model are investigated to determine their effect upon lateral pile response. Thus, the finite element model is shown to give accurate results, especially for non-homogeneous soil profiles, and can be used confidently to predict the lateral response of a pile in an elastic medium.

By recourse to all three models, a recommended method of linear analysis of laterally loaded piles is presented in Section 3.5. In the analysis, account is taken of the stiff nature of response across a pile face, and of the modifications to a homogeneous half-space response caused by limited soil depth and a non-homogeneous Young's modulus distribution. The approximate method of modifying the homogeneous solution, to obtain the solution for a non-homogeneous soil, proves capable of predicting, quite accurately, the actual non-homogeneous response as determined from a finite element analysis.

In Chapter Four the concept of an effective length for any laterally loaded pile is studied and it proves to allow great simplification in the presentation of results. The effective length is defined to be the actual pile length for relatively stiff piles and the critical length of flexible piles.

By tracing its history, and studying the analytical closed-form solution of the uniform Winkler soil model, an expression for the critical length is found in terms of relative pile-soil stiffness. The critical length expression is also shown to provide adequate values of critical length for piles in a Winkler soil with a linearly varying stiffness with depth.

The boundary element elastic model exhibits behaviour that supports the concept of an effective length, but an important feature of the results is a dependence upon the effective length to diameter ratio of the pile, which is absent in Winkler results.

The finite element model has the capability to analyse foundations with a wide range of length-to-diameter ratios and to make allowance for layers of finite depth. These solutions place the analysis of laterally loaded piles within a broader class of

foundation problems, those capable of solution using elastic-continuum soil models. The finite element results are mostly obtained using the layer building method of Section 3.4.4, which ensures a finely discretised geometry, and consequently the results are considered to be as accurate as possible.

The finite element results reinforce the conclusions about the suitability of the equation for critical length and further, exhibit behaviour in non-pile related analyses that supports the existence of a critical length. This is further investigated by considering the response of surface strip raft foundations and axial pile response. In both cases an expression for a critical length is found that is consistent with the calculated response.

The existence of a critical length, and the concept of an effective length, are the major findings of Chapter Four, and the linear results for pile foundation response to head loads, using the recommended boundary element analysis, are presented in non-dimensional forms that employ the effective length.

The non-linear response of laterally loaded piles is studied in Chapter Five, where again the chosen three categories of model type are used.

The Winkler model proves capable of extension to consider non-linear response caused by soil-pile gapping, failure of the soil to some predetermined depth, and the generation of plastic hinges in the pile. An analytic treatment of gaps reveals that a simple halving of pile head stiffness is not always necessary to account for the effects of gapping. The theoretical solution, allowing for the effect of soil failure, is used to confirm the accuracy of the numerical solution procedure (using a Winkler-based soil) developed for the soil-structure interaction analysis

in this Chapter. The formation of plastic hinges, in both stiff and flexible piles, is seen to markedly alter the head response of a fixed-head pile in a Winkler soil, more so for the flexible than the rigid pile.

Section 5.4 develops a boundary element model which takes account of soil failure, and also allows for the possibility of forming a gap, dependent upon the deflection mismatch developed between the pile and the soil (plastic deflection). The increment of plastic deflection and the total load transmitted by the non-linear interface are multiplied together to obtain a measure of plastic work. By checking the sign of incremental plastic work, it is possible to return failed elements to an elastic state and recalculate the incremental response, based upon the need to avoid negative plastic work.

Cyclic loading is not studied directly, but to properly take account of unloading of elements during static loading (i.e. due to movement of the point of "zero pressure"), the model is required to admit the possibility of "cyclic" loading at the element level of discretisation. An important practical situation where such behaviour is evident is the case of a fixed-head pile, and results are presented to illustrate the non-linear response.

Section 5.4.3 presents the results of a parametric study of the effect of soil failure upon head response, using the boundary element method with a non-linear soil-pile interface, in the form of correction factors to be applied to the linear results for a uniform soil presented in Chapter Four. The critical pile length is again proposed as having significance, now for non-linear response, to allow a large range of flexible pile to soil stiffness ratios, head shear to moment ratios and soil Young's modulus to undrained shear strength ratios to be treated.

The non-linear MBEM analysis results are consistent with a direct modelling of interaction over only the linear-elastic portion of a pile length and a distributed failure load over the failed portion (similar to the analysis of Section 5.3.2) and compare very favourably with one previously published study, which uses a similar boundary element approach. Agreement is less satisfactory with a study employing a more complex boundary element approach and is an instance of comparison between two dissimilar models, even though both use an elastic-continuum modelled soil, possibly giving misleading information, as is discussed in Chapter Two.

Section 5.5 develops a new soil-structure interaction (SSI) analysis using the axisymmetric geometry finite element method. In the SSI analysis, interaction tractions are modelled over a finite arc length of the pile circumference at interface elements, thus gapping between the pile and soil (a deflection mismatch) is theoretically possible. By assuming a biface model for the interface (i.e. a 180 degree arc-length) and an x-directed interaction traction, the analysis provides estimates of response when gaps develop behind a pile or unequal interaction tractions occur.

The SSI analysis reproduces the results predicted by Section 5.3 for a non-linear Winkler soil, gives good agreement with boundary element and finite element results for a linear-elastic soil and also agrees with the predictions of non-linear response from the MBEM analysis. The comparison between the MBEM and SSI analyses is only made for the case of equal magnitude active and passive failure stress, since this is the only case which the theory of the MBEM analysis can model. The effect of gapping is shown to be less severe for a linear-elastic continuum than a Winkler modelled soil, and the bias of the axisymmetric initial

stress, that exists before loading of the pile, also has less effect on the non-linear response of a continuum model.

Chapter Six presents the results of experimental work on model piles in clay beds and predictions of the test results, as well as a study of two full-scale piles tested at the same site.

The model pile tests, performed with overburden pressure, isolate the undrained and drained phases of clay response and give measures of initial (linear) pile response. Both these features of soil-pile response are adequately modelled by the MBEM analysis using a continuum soil model. The occurrence of gapping is evident in the test results and is found to be less prevalent at higher overburden pressures, as would be expected for the deep response of a pile which is discussed in Chapter Two.

In Section 6.3, larger scale model piles, without overburden present during the tests, allow the occurrence of gapping to be visually verified during testing, measurement of rotation and strain gauging of the piles to measure bending moments. The effects of gapping introduced during jacking of the bent pile are found to greatly influence both the load-deflection response and the bending moment distribution. The larger scale model tests clearly illustrate the existence of a critical length of the pile in the clay bed and using the SSI analysis the same behaviour, consistent with a critical length, is predicted.

The final section of Chapter Six considers two full-scale pile tests and uses the critical length to find a Young's modulus distribution with depth by fitting theoretical linear bending moment distributions for a flexible pile to low load level test results, i.e. the depth at which the moments are negligible is taken to be the critical length. The back-calculated Young's modulus

distribution is consistent with the distribution of undrained shear strength, from triaxial tests on samples of soil taken from various depths, and empirical E/c ratios. The assumed in-situ stresses and failure stresses in the clay soil are based upon plane strain analyses and rational adjustments for the effect of the free soil surface and an inability of the soil to sustain tension.

Pile head loads, for the imposed conditions, that cause soil failure along the effective length of the pile (i.e. the pile is treated as being as long as the critical length), are calculated for both piles tested and sensible ultimate load predictions result. These effective ultimate loads are not strictly collapse loads but represent loads at which the pile becomes very inefficient, since the incremental response is essentially that of a pile with load applied at an eccentricity of one critical length.

The chosen parameters for the soil are based upon the response of one test and thus, their application to the other pile with a much smaller diameter tests the predictive ability of the elastic continuum based analysis. The agreement between theory and test result for head load-deflection and maximum bending moment responses for both piles, amply illustrates the utility of the effective length concept when married with the elastic continuum soil model.

This Thesis considers the response of laterally loaded piles, with particular emphasis on the predictive ability of the elastic-continuum based method of analysis. Winkler type analyses are included as means with which to verify the more complex analyses

(that can employ a Winkler soil model) with precise solutions. The precision of the Winkler solution is not proposed as intimating that the solution provides a good model of lateral pile response. The more complex MBEM and SSI analyses are then applied to the analysis of laterally loaded piles using the elastic continuum model for soil response with confidence that the numerical techniques are accurate.

The linear and non-linear response of the improved MBEM and the SSI analyses is checked against other published results and linear results of the AGFEM analysis which use the direct, as opposed to the interaction, approach. A series of solutions, from the one method of analysis (profile building), places pile response as one limit of the range of foundation responses which the linear elastic continuum model encompasses and thus makes the method unique, in that one set of soil parameters (in theory) can be used for a range of problems.

The concept of effective length, which requires the existence of a critical length for a pile in a particular soil to be proven, is shown to simplify presentation of theoretical pile response. Further, the effective length concept provides a powerful tool for examining the results of model tests and field cases. For non-linear response the concept also allows much simplification in the presentation of results and supports the idea of an effective ultimate load for a pile. This effective ultimate load, by including a measure of pile-soil stiffness, replaces to some extent the concept of long pile and short pile collapse loads, which do not directly consider the deformations at which collapse occurs.

Soil-pile separation has previously received little attention and here it is addressed using an elastic continuum-based analysis

which relies on the finite element method. The solutions suggest gapping is not as severe a problem as a Winkler model of soil theoretically predicts, but the increased flexibility does tend to permit higher (more realistic) values of Young's modulus to be used when fitting test results.

While some refinements may be required, the MBEM analysis and, more precisely, the SSI analysis are capable of modelling cyclic loading because of the logical way failed soil elements can return to a linear elastic state and the efficient manner by which non-linear response is incorporated in both analyses.

The SSI analysis can be extended to take account of combined axial and torsional response as well as lateral response. The bi-face analysis introduced here could be used, or one with a more finely discretised circumference.

Pile group interaction could be investigated using the commonly employed approximation of the presence of the pile and removal of the soil having negligible influence upon interaction. The added dimension would be the inclusion of gapping (laterally) and slipping (axially and circumferentially).

Several advances in the understanding and analysis of laterally loaded piles are made in this Thesis by:

- a) recognising the importance which the pile effective length has in determining the entire response of laterally loaded piles.
- b) taking into account the possibility of mismatches developing between pile and soil.
- c) admitting the possibility of recontacting at gapped element interfaces and the impossibility of negative plastic work.

REFERENCES

Apirathvorakij, V. and Karasudhi, P. (1980),
Quasi-Static Bending of a Cylindrical Elastic Bar Partially
Embedded in a Saturated Elastic Half Space.
Int. Jnl of Solids and Structures, Vol. 16, No. 7, pp 625 - 644.

Baguelin, F., Frank, R. and Said, Y.M. (1977),
Theoretical Study of Lateral Reaction Mechanism of Piles.
Geotechnique, Vol. 27, No. 3, pp 405 - 434.

Baguelin, F., Trezos, C.S. and Frank, R. (1979),
Reaction Laterale des Pieux: Effects de forme et Effects
Tridimensionnels.
Bull. Liaison Lab. P. et Ch., Vol. 104, pp 33 - 47.

Balaam, N.P., Poulos, H.G. and Booker, J.R. (1975),
Finite Element Analysis of the Effects of Installation on Pile
Load-Settlement Behaviour.
Geot. Eng., Vol. 6, No. 1, pp 33 - 48.

Balaam, N.P. (1978),
Load-Settlement Behaviour of Granular Piles.
Ph.D. Dissertation, Univ. of Sydney, Australia.

Banerjee, P.K. (1978),
Analysis of Axially and Laterally Loaded Pile Groups.
Ch. 9, Developments in Soil Mechanics, Ed. C.R. Scott, London,
App. Sci. Publishers.

Banerjee, P.K. and Davies, T.G. (1978),
The Behaviour of Axially and Laterally Loaded Single Piles
Embedded in Non-Homogeneous Soils.
Geotechnique, Vol. 28, No. 3, pp 309 - 326.

Barber, E.S. (1953),
Discussion to S.M. Gleser. Symposium on Lateral Load Tests on
Piles
ASTM STP154, pp 96 - 99.

Bernal, A. and Romana, M. (1977),
Pile Behaviour at Torreonillas Dock (Huelva Spain).
Proc. 9th Int. Conf. on Soil Mech. Fndn Eng., Tokyo, Vol. 1,
pp 399 - 405.

Blaney, G., Kausel, R. and Roesset, P. (1976)
Dynamic Stiffness of Piles.
Proc. 2nd Int. Conf. Num. Meth. Geomechanics, Blacksburg, Vol. 2,
pp 1001 - 1012.

Booker, J.R. and Small, J.C. (1982),
Finite Layer Analysis of Consolidation, Part II.
Int. Jnl for Num. Anal. Meth. in Geom., Vol. 6, pp 173 - 194.

Bowles, J.E. (1982),
Foundation Analysis and Design.
McGraw-Hill, 3rd Edn.

Briaud, J-L., Smith, T. and Meyer, B. (1984),
Laterally Loaded Piles and the Pressuremeter : Comparison of
Existing Methods.
Laterally Loaded Deep Fndns : Analysis and Performance, ASTM
STP835, pp 97 - 111.

Broms, B.B. (1965),
Design of Laterally Loaded Piles.
Jnl Soil Mech. Fndn Div., ASCE, Vol. 91, No. SM3, pp 79 - 99.

Brown, P.T. and Gibson, R.E. (1972),
Surface Settlement of a deep elastic stratum whose modulus
increases linearly with depth.
Can. Geot. Jnl, Vol. 9, No. 4, pp 467 - 476.

Brown, P.T. and Booker, J.R. (1976),
Numerical solution of rafts on visco-elastic media using Laplace
transforms.
Proc. Int. Conf. Finite Elem's in Eng., Adelaide, pp 27.1 - 27.14.

Brown, P.T. (1978),
Stiff rectangular rafts subject to concentrated loads.
Aust. Geomech. Jnl, Vol. G8, No. 1, pp 40 -49.

Carter, D.P. (1984),
A Non-Linear Soil Model for Predicting Lateral Pile Response.
University of Auckland, Dept of Civil Engineering, Report No. 359.

Carter, J.P. (1977),
Finite Deformation Theory and its Application to Elastoplastic
Soils.
Ph.D. Dissertation, Univ. of Sydney, Australia.

Carter, J.P., Randolph, M.F. and Wroth, C.P. (1980),
Some Aspects of the Performance of Open-and-Closed Ended Piles.
Proc. Num. Meth. in Offshore Piling, ICE, London, pp 165 - 170.

Carter, J.P. and Booker, J.R. (1981),
Consolidation due to Lateral Loading of a Pile.
Proc. 10th Int. Conf. Soil Mech. Fndn Eng., Stockholm, Vol. 2,
pp 647 - 650.

Chang, Y.L. (1937),
Discussion to Feagin (1935), Trans ASCE, Vol. 102, p 272 - 278.

Coyle, H.M. and Reese, L.C. (1966),
Load Transfer for Axially Loaded Piles in Clay.
Jnl Soil Mech. Fndn Div., ASCE, Vol. 92, No. SM2, pp 1 - 26.

Davies, T.G. and Banerjee, P.K. (1978),
The Displacement Field due to a Point Load at the Interface of a
Two Layer Elastic Half-space.
Geotechnique, Vol. 28, No. 1, pp 43 - 56.

Davies, T.G. and Budhu, M. (1986)
Non-linear Analysis of Laterally Loaded Piles in Stiff Clay.
Geotechnique, Vol. 36, No. 4, pp 527- 538.

Davis, E.H. and Poulos, H.G. (1968),
The Use of Elastic Theory for Settlement Prediction Under Three-
Dimensional Conditions.
Geotechnique, Vol. 18, No. 1, pp 67 - 91.

Davis, E.H., Ring, G.J. and Booker, J.R. (1974),
The Significance of the Rate of Plastic Work in Elasto-plastic
Analysis.
Proc. Int. Conf. Finite Element Methods in Engng, Univ. New South
Wales, Australia, pp 327 - 335.

Desai, C.S. and Appel, G.C. (1976),
3-D Analysis of Laterally Loaded Structures.
Proc. 2nd Int. Conf. Num. Meth. Geomechanics, Blacksburg, Vol. 1,
pp 405 - 418.

Douglas, D.J. and Davis, E.H. (1964),
The Movement of Buried Footings Due to Moment and Horizontal Load
and the Movement of Anchor Plates.
Geotechnique, Vol. 14, No. 2, pp 115 - 132.

Evangelista, A. and Viggiani, C. (1976),
Accuracy of Numerical Solutions for Laterally Loaded Piles in
Elastic Half-Space.
Proc. 2nd Int. Conf. Num. Meth. Geomechanics, Blacksburg, Vol. 3,
pp 1367 - 1370.

Feagin, L.B. (1935)
Lateral Pile Loading Tests.
Proc. ASCE, Vol. 61, No. 9, Paper No. 1959, pp 1335 - 1353.

Gibson, R.E., Brown, P.T. and Andrews, K.R.F. (1971),
Some results concerning displacements in a non-homogeneous
elastic layer.
Zeit. ang. Math. Phys., 22, pp 855 - 864.

Giroud, J.P. (1972)
Tables pour le calcul des fondations.
Mecanique des sols, Dunod, Paris.

Goodman, R.E., Taylor, R.L. and Brekke, T.L. (1968)
A Model for the Mechanics of Jointed Rocks.
Jnl Soil Mech. Fndn Div., ASCE, Vol. 94, No. SM3, pp 637 - 659.

Hardin, B.O. and Richart, F.E. (1963)
Elastic Wave Velocities in Granular Soils.
Jnl Soil Mech. Fndn Div., ASCE, Vol. 89, No. SM1, pp 33 - 65.

Hardin, B.O. and Black, W.L. (1966)
Sand Stiffness under Various Triaxial Stresses.
Jnl Soil Mech. Fndn Div., ASCE, Vol. 92, No. SM2, pp 27 - 42.

Hetenyi, M. (1946),
Beams on Elastic Foundations.
Ann Arbor, Michigan, Univ. of Mich. Press.

Heyman, L. and Boersma, L. (1961),
Bending Moments in Piles Due to Lateral Earth Pressures.
Proc. 5th Int. Conf. Soil Mech. Fndn Eng., Paris,
Vol. 2, pp 425 - 429.

Horvath, J.S. (1983),
New Subgrade Model Applied to Mat Foundations
Jnl Geot. Eng. Div., ASCE, Vol. 109, No. 12, pp 1567 - 1587.

Koiter, W.T. (1953)
On Partially Plastic Thick Walled Tubes.
Biezeno Anniversary Volume in Applied Mechanics, N.V.de Technische
Uitgeverij H. Stam, Haarlem, pp 232 - 251.

Krynine, D.P. (1937),
Discussion to Feagin (1935), Trans ASCE, Vol. 102, pp 278 - 283.

Kuhlemeyer, R.L. (1979a),
Static and Dynamic Laterally Loaded Floating Piles.
Jnl Geot. Eng. Div., ASCE, Vol. 105, No. GT2, pp 289 - 304.

Kuhlemeyer, R.L. (1979b),
Bending element for circular beams and piles.
Jnl Geot. Eng. Div., ASCE, Vol. 105, No. GT2, pp 325 - 330.

Lai, J.Y. (1987)
Personal communication, University of Sydney.

Lambe, T.W. (1964),
Methods of Estimating Settlements.
Jnl Soil Mech. Fndn Div., ASCE, Vol. 90, No. SM5, pp 43 - 67.

Lee, P.Y. and Gilbert, L.W. (1979),
Behaviour of Laterally Loaded Piles in Very Soft Clay.
Proc. 11th Off. Tech. Conf., Houston, Paper OTC3401, Vol. 1,
pp 387 - 395.

Lin, T.H. (1968),
Theory of Inelastic Structures.
Wiley.

Love, A.E.H. (1928),
A treatise on the mathematical theory of elasticity.
Dover Publications, New York.

Matlock, H. and Reese, L.C. (1960),
Generalised Solutions for Laterally Loaded Piles.
Jnl Soil Mech. Fndn Div., ASCE, Vol. 86, No. SM5, pp 63 - 91.

Matlock, H. (1970),
Correlations for Design of Laterally Loaded Piles in Soft Clay.
Proc. 2nd Off. Tech. Conf., Houston, Paper OTC1204, Vol. 1,
pp 577 - 594.

Matlock, H., Foo, S.H.C. and Bryant, L.M. (1978),
Simulation of Lateral Pile Behaviour under Earthquake Motion.
ASCE Speciality Conference, Earthquake Engineering and Soil
Dynamics, Pasadena, Vol. 2, pp 600 - 619.

McClelland, B. and Focht, J.A. (1956),
Soil Modulus for Laterally Loaded Piles.
Jnl Soil Mech. Fndn Div., ASCE, Vol. 82, No. SM4, pp 1 - 22.

Mindlin, R.D. (1936),
Force at a Point in the Interior of a Semi-Infinite Solid.
Physics, Vol. 7, pp 195 - 202.

- Murff, J.D. (1975)
Response of Axially Loaded Piles, Technical Note:
Jnl Geot. Eng. Div., ASCE, Vol. 101, No. GT3, pp 356 - 360.
- Oteo, C.S. (1972),
Discussion of Poulos (1971b),
Jnl Soil Mech. Fndn Div., ASCE, Vol. 98, No. SM2, pp 226 - 231.
- Peck, R.B., Davisson, M.T. and Hansen, W.E. (1958),
Discussion to McClelland and Focht (1956),
Trans ASCE, Vol. 123, Paper No. 2954, p 1063.
- Pender, M.J. (1983),
Earthquake-Soil Structure Interaction, Spring and Dashpot Models,
and Real Soil Behaviour.
3rd South Pacific Regional Conf. on Earthquake Eng.
- Pise, P.J. (1982),
Laterally Loaded Piles in a Two-Layer Soil System.
Jnl Geot. Eng. Div., ASCE, Vol. 108, No. GT9, pp 1177 - 1181.
- Poulos, H.G. (1971a),
Behaviour of Laterally Loaded Piles: I - Single Piles.
Jnl Soil Mech. Fndn Div., ASCE, Vol. 97, No. SM5, pp 711 - 731.
- Poulos, H.G. (1971b),
Behaviour of Laterally Loaded Piles: II - Pile Groups.
Jnl Soil Mech. Fndn Div., ASCE, Vol. 97, No. SM5, pp 733 - 751.
- Poulos, H.G. (1972),
Behaviour of Laterally Loaded Piles: III - Socketed Piles.
Jnl Soil Mech. Fndn Div., ASCE, Vol. 98, No. SM4, pp 341 - 360.
- Poulos, H.G. (1979),
Settlement of Single Piles in Non-homogeneous Soil.
Jnl Geot. Eng. Div., ASCE, Vol. 105, No. GT5, pp 627 - 641.
- Poulos, H.G. (1982a),
Developments in the Analysis of Static and Cyclic Lateral Response
of Piles.
Proc. 4th Int. Conf. Num. Meth. Geomechanics, Edmonton, Vol. 3,
pp 1117 - 1135.
- Poulos, H.G. (1982b)
The influence of shaft length on pile load capacity in clay.
Geotechnique, Vol. 32, No. 2, pp 145 - 148.

Poulos, H.G. and Davis, E.H. (1974),
Elastic Solutions for Soil and Rock Mechanics.
New York, Wiley.

Poulos, H.G. and Adler, M.A. (1979),
Lateral Response of Piles of Non-Uniform Section.
Proc. 6th Asian Reg. Conf. Soil Mech. Fndn Eng., Singapore,
pp 327 - 331.

Poulos, H.G. and Davis, E.H. (1980),
Pile Foundation Analysis and Design.
New York, Wiley.

Pyke, R. and Beikae, M. (1984)
A New Solution for the Resistance of Single Piles to Lateral
Loading.
Laterally Loaded Deep Fndns : Analysis and Performance, ASTM
STP835, pp 3 - 20.

Randolph, M.F. (1977),
A Theoretical Study of the Performance of Piles.
Ph.D. Dissertation, Univ. of Cambridge, UK.

Randolph, M.F. (1981),
The response of flexible piles to lateral loading.
Geotechnique, Vol. 31, No. 2, pp 247 - 259.

Randolph, M.F. (1983)
Settlement considerations in the design of axially loaded piles.
Ground Engineering, Vol. 16, No. 4, pp 28 - 32.

Randolph, M.F., Carter, J.P. and Wroth, C.P. (1979),
Driven piles in clay - the effects of installation and subsequent
consolidation.
Geotechnique, Vol. 29, No. 4, pp 361 - 393.

Randolph, M.F. and Houlsby, G.T. (1984),
The limiting pressure on a circular pile loaded laterally in a
cohesive soil.
Geotechnique, Vol. 34, No. 4, pp 613 - 623.

Redman, P.G. (1980),
Analysis of Undrained Creep of Foundations and Embankments on
Clays.
Ph.D. Dissertation, Univ. of Sydney, Australia.

Reese, L.C. and Matlock, H. (1956),
Non-dimensional Solutions for Laterally Loaded Piles with Soil
Modulus Assumed Proportional to Depth.
Proc. 8th Texas Conf. Soil Mech. and Fndn Eng., Austin, Special
Publ. No. 29, pp 94 - 98.

Reese, L.C. and Cox, W.R. (1969),
Soil Behaviour from Analysis of Tests on Uninstrumented Piles
Under Lateral Loading.
ASTM STP 444, pp 160 - 176.

Reese, L.C., Cox, W.R. and Koop, F.D. (1974),
Analysis of Laterally Loaded Piles in Sand.
Proc. 6th Off. Tech. Conf., Houston, Paper OTC2080, Vol. 2,
pp 473 - 483.

Reese, L.C. and Welch, R.C. (1975),
Lateral Loading of Deep Foundations in Stiff Clay.
Jnl Geot. Eng. Div., ASCE, Vol. 101, No. GT7, pp 633 - 649.

Reese, L.C., Cox, W.R. and Koop, F.D. (1975),
Field Testing and Analysis of Laterally Loaded Piles in Stiff
Clay.
Proc. 7th Off. Tech. Conf., Houston, Paper OTC2312, Vol. 2,
pp 671 - 690.

Robertson, P.K., Hughes, J.M.O., Campanella, R.G. & Sy, A., (1984),
Design of Laterally Loaded Displacement Piles Using a Driven
Pressuremeter.
Laterally Loaded Deep Fndns : Analysis and Performance,
ASTM STP835, pp 229 - 238.

Rotter, J.M. and Hull, T.S. (1985)
Wall loads in squat steel silos during earthquakes.
School of Civil and Mining Engineering, Research Report No. R509.

Rowe, R.K. (1977),
The Behaviour of Anchor Plates.
Ph.D. Dissertation, Univ. of Sydney, Australia.

Rowe, R.K., Booker, J.R. and Balaam, N.P. (1978),
Application of the Initial Stress Method to Soil-Structure
Interaction.
Int. Jnl for Num. Meth. in Eng., Vol. 12, pp 873 - 880.

Rowe, R.K. and Davis, E.H. (1982)
The behaviour of anchor plates in clay.
Geotechnique, Vol. 32, No. 1, pp 9 - 23.

- Scott, R.F. (1981)
Foundation Analysis.
Prentice-Hall Civil Engineering and Engineering Mechanics Series.
- Selvadurai, A.P.S. (1976),
The Load-deflexion Characteristics of a Deep Rigid Anchor in an Elastic medium.
Geotechnique, Vol. 26, No. 4, pp 603 - 612.
- Selvadurai, A.P.S. and Rajapaske, R.K.N.D. (1985),
On the load Transfer from a Rigid Cylindrical Inclusion into an Elastic Half space.
Int. Jnl of Solids and Struct's, Vol. 21, No. 12 , pp 1213 - 1229.
- Spillers, W.R. and Stoll, R.D. (1964),
Lateral Response of Piles.
Jnl Soil Mech. Fndn Div., ASCE, Vol. 90, No. SM6, pp 1 - 9.
- Stevens, J.B and Audibert, J.M.E. (1979),
Re-examination of p-y Curve Formulations.
Proc. 11th Off. Tech. Conf., Houston, Paper OTC3402, Vol. 1,
pp 397 - 403.
- Sullivan, W.R., Reese, L.C. and Fenske, C.W. (1980),
Unified Method for Analysis of Laterally Loaded Piles in Clay.
Proc. Num. Meth. in Offshore Piling, ICE, London, pp 135 - 146.
- Swane, I.C. (1983),
The Cyclic Behaviour of Laterally Loaded Piles.
Ph.D. Dissertation, Univ. of Sydney, Australia.
- Swane, I.C. and Poulos, H.G. (1982),
A Theoretical Study of the Cyclic Shakedown of Laterally Loaded Piles.
Proc. 4th Int. Conf. Num. Meth. Geomechanics, Edmonton, Vol. 3,
pp 853 - 864.
- Swane, I.C. and Poulos, H.G. (1985),
Shakedown Analysis of a Laterally Loaded Pile Tested in Stiff Clay.
Civil Engg Trans, I.E. Aust., Vol. CE27, No. 3, pp 275 - 279.
- Terzaghi, K. (1955),
Evaluation of Coefficients of Subgrade Reaction.
Geotechnique, Vol. 5, No. 4, pp 297 - 326.
- Timoshenko, S.P. and Gere, J.M. (1972)
Mechanics of Materials.
Van Nostrand-Reinhold Co., New York, N.Y.

Velez, A.B., Gazettas, A.B. and Krishnan, R.C. (1983),
Lateral Dynamic Response of Constrained-Head Piles.
Jnl Geot. Eng. Div., ASCE, Vol. 109, No. GT8, pp 1063 - 1081.

Vesic, A.B. (1961a),
Beams on Elastic Subgrade and the Winkler Hypothesis.
Proc. 5th Int. Conf. Soil Mech. Fndn Eng., Vol. 1, pp 845 - 850.

Vesic, A.B. (1961b),
Bending of Beams Resting on Isotropic Elastic Solid.
Jnl Eng. Mech. Div., ASCE, Vol. 87, No. EM2, pp 35 - 53.

Wilson, E.L. (1965),
Structural Analysis of Axisymmetric Solids.
Jnl Am. Inst. Aer. Astr., Vol. 3, pp 2269 - 2274.

Winnicki, L.A. and Zienkiewicz, O.C. (1979),
Plastic (or Visco-Plastic) Behaviour of Axisymmetric Bodies
Subjected to Non-Symmetric Loading - Semi-Analytic Finite Element
Solution.
Int. Jnl for Num. Meth. in Eng., Vol. 14, pp 1399 - 1412.

Yegian, M. and Wright, S.G. (1973),
Lateral Soil Resistance - Displacement Relationships for Pile
Foundations in Soft Clays.
Proc. 5th Off. Tech. Conf., Houston, Paper OTC1893, Vol. 2,
pp 663 - 676.

Yeung, S.K. and Carter, J.P. (1987),
Finite Element Studies of the Pressuremeter Test.
Paper submitted to the 5th Int. Conf. in Australia on Finite
Element Meths, Melbourne.

Zienkiewicz, O.C. (1971),
The Finite Element Method in Engineering Science.
McGraw-Hill, London. pp 254 - 270.

Appendix I

Ultimate Loads : Strong Pile in a Failing Soil

From consideration of static equilibrium of a rigid pile in soil that is failing, with a general linear variation of ultimate pressure with depth, a solution for the head loads and maximum moment can be found. The solution proceeds by assuming some depth along the pile at which the soil failure pressure changes sign. Only one such depth is considered here, since no more than one depth of sign change may occur for a rigid pile. For, if the pile is to produce positive plastic work when failing, a restriction similar to the Winkler law connecting positive load to positive deflection will apply.

If W_o is the value of the distributed failure load W at the surface and n is the increase of W per unit length of pile, then equilibrium requires that

$$\begin{aligned} \pm H_u &= W_o (2z_s - L) + n/2 (2z_s^2 - L^2) \\ \pm M_u &= W_o /2 (L - 2z_s^2) + n/3 (L - 2z_s^3) \quad \text{I.1} \end{aligned}$$

with z_s the depth to failure load sign change.

The uncertainty of sign is linked to the assumed sign of the soil failure traction and produces a point-wise symmetry, about the origin of the H_u versus M_u space, for the locus of ultimate load points. The values of shear and bending moment can be found for any depth of cross-section again from equilibrium. Thus the shear force

$$\begin{aligned} \pm V_{z < z_s} &= W_o (2z_s - L - z) + n/2 (2z_s^2 - L^2 - z^2) \\ \pm V_{z > z_s} &= W_o (z - L) + n/2 (z^2 - L^2) \quad \text{I.2a} \end{aligned}$$

and bending moment

$$\begin{aligned} \frac{+}{-} M_{z < z_s} &= \frac{W}{o} / 2 [(L - z)^2 - 2(z - z_s)^2] \\ &+ n/6 [(L - z)^2 (z + 2L) - 2(z - z_s)^2 (z + 2z_s)] \\ \frac{+}{-} M_{z > z_s} &= \frac{W}{o} / 2 (L - z)^2 + n/6 (L - z)^2 (z + 2L) \end{aligned} \quad \text{I.2b}$$

Using the fact that true bending moment maxima occur when the shear force is zero, a value of z and depth to maximum bending moment is found. This maximum need only be considered for the depths occurring within the pile length. It can also be shown that this depth to maximum bending moment is always less than or equal to the depth to ultimate pressure sign change. In many load cases the maximum bending moment is the applied moment at the head.

Special attention must be paid to solving for the maximum bending moment when either of W or n are zero. In particular if $n = 0$

$$z_{\max} = 2z_s - L \quad \text{I.3a}$$

$$\text{and } M_{\max} = \frac{W}{o} (z_s - L)^2$$

and if $n \neq 0$

$$z_{\max} = \left[\left(\frac{W}{n} \right)^2 + 2(2z_s - L) \left(\frac{W}{n} \right) + 2z_s^2 - L^2 \right]^{1/2} - \frac{W}{n}$$

$$\text{or } z_{\max} = 0. \quad \text{I.3b}$$

and M_{\max} is obtained from substitution in equation I.2b.

Noting that if $z < L/\sqrt{2}$ and $W = 0$ the expression to the power of one half is negative and corresponds to the case of zero ultimate head shear or a negative head shear with the maximum bending moment being the applied ultimate head moment.

Equations I.1, I.2 and I.3 may be used to determine z_s by assuming the ratio of head shear to moment is known. This is only generally true and one important exception is the case of a stiff, essentially rigid fixed head pile. If the distribution of W_y changes sign, a point of rotation within the pile is required to avoid negative plastic work. This rotation would violate the fixed head condition. This situation requires a z_s equal to the pile length, or zero, to avoid a sign change in the distribution of W_y and thus the solution may proceed directly.

The fixed head condition is an extreme of behaviour occurring if the supported structure is very stiff. The other extreme is pure shear when the supported structure is very flexible. Between these are the cases of load on the head consisting of combined moment and shear and the less common case of pure moment.

It is generally possible, during the application of external load to the structure, that the ratio of moment to shear at the pile head will vary, as is the case for a fixed head pile. Here only the ultimate values of head load are considered and this ratio is assumed to exist throughout the loading. Details of the behaviour of the supported structure are required to further develop this aspect of the effect of pile-structure interaction upon load transmitted at a pile head.

By assigning a value to the ratio H_u / M_u it is possible to obtain a cubic in z_s to be solved for the value of z_s that corresponds to the H_u / M_u ratio chosen.

This cubic is

$$a_0 + a_1 z_s + a_2 z_s^2 + a_3 z_s^3 = 0 \quad \text{I.4a}$$

with

$$a_0 = -L [3W_0 (2 + \beta_u^{-1}) + nL(3 + 2\beta_u^{-1})]$$

$$a_1 = 12 W_0$$

$$a_2 = 6 (\beta_u^{-1} / L W_0 + n)$$

$$a_3 = 4 \beta_u^{-1} / L n$$

$$\text{and } \beta_u = M / H L. \quad \text{I.4b}$$

A cubic solver Fortran program, written by Dr. J.M. Rotter at The University of Sydney, was modified and used to solve this equation for the z required. The equation may reduce to a quadratic, or even linear, equation for certain values of β_u , W_0 , and n . For example if $\beta_u = c = 0$ then $z = L/2$ as would be expected for two stress blocks of equal size and opposite sign. The quantity β_u^{-1} will become very large when the applied moment approaches zero and an alternative formulation is required.

$$a_0 = -L(3W_0 (2\beta_u L + L) + nL(3\beta_u L + 2L))$$

$$a_1 = 12 W_0 \beta_u L$$

$$a_2 = 6 (W_0 + n\beta_u L)$$

$$a_3 = 4 n \quad \text{I.4c}$$

The parameters involved in this analysis are W_0 , n and β_u . Of these β_u is a function of the loading system acting on the pile and W_0 and n are constants that characterise the soil. From the definition of distributed load at failure $W_y = p_y d$, where p_y is the ultimate pressure that can be carried by the soil at any depth z and d is the frontal width of the pile, $W_y = W_0 + n z$.

Various values of W and n can be extracted from the literature such as

$$n = 0 \quad W / c_d = 9 \text{ to } 11 \text{ for clays.}$$

$$W = 0 \quad n z / K \sigma'_v d = 3 \text{ to } 5 \text{ for sands.} \quad I.5$$

where K is the Rankine passive earth pressure coefficient, c_u is the undrained shear strength and σ'_v is the effective vertical stress at z the depth considered.

From using simple approximations and plasticity theory p_y varies from $2 c_u$ or $4 c_u$ at the surface to $9 c_u$ or $11 c_u$ at depths greater than about three pile diameters depending upon the assumed pile shape and roughness. A simplified model for the reduced p_y values near the surface of a uniform strength soil profile is often used and is enhanced by allowing a free standing portion of pile of e diameters and reducing the buried pile length by e diameters. This reduces the ultimate moment derived using this analysis so that

$$H_u = H'_u$$

$$M_u = M'_u - e d H'_u \quad I.6$$

Where M'_u and H'_u are derived using a pile of length $L - e d$ and $n = 0$ and for example it can be assumed that $W = 9 c_d$ and $e = 1.5$ diameters, (Broms, 1965). The normally used p_y approximations do not consider the special form of p_y distribution assumed in the above method but are more often the extremes of $n = 0$ or $W = 0$, e.g. Swane (1983). If however, there is some reason why the generation of soil resistance to some depth z cannot be relied upon then the above form may be used.

It can therefore be seen that a wide variety of problems can be approached by using a simple static solution to the failure of soil with the simple equation

$$W_y = W_o + nz. \quad \text{I.7}$$

Figure 5.9 presents the information concerning the values of ultimate head loads for any given head shear to moment ratio, β_u for different values of a soil failure load distribution parameter. Figures I.1 and I.2 present more information for only one soil strength profile. The ultimate head shear load, depth to maximum shear force and its value are presented in Fig. I.1 as a function of β_u . The ultimate head moment load, depth to bending moment maximum and its value are presented in Fig. I.2.

In addition, the values of pile resultants that are generated at failure assuming an infinitely strong pile and the value of, and depth to, the maximum values can be obtained from the equations of this appendix. The maximum bending moment can then be compared with the yield or full plastic moment of the pile cross-section. This gives an indication of the applicability of assuming a strong pile failure mode, i.e. no plastic hinge formation in the pile is allowed.

This consideration of pile and soil failure requires attainment of complete failure of the pile and/or soil. In practice the pile behaviour will give unserviceable response long before complete structural failure. This facet of pile behaviour is simplified by the concept of an effective length which allows the effective collapse load of a flexible pile to be based upon the collapse of a strong pile, as considered here, with the critical length replacing the actual pile length in all equations.

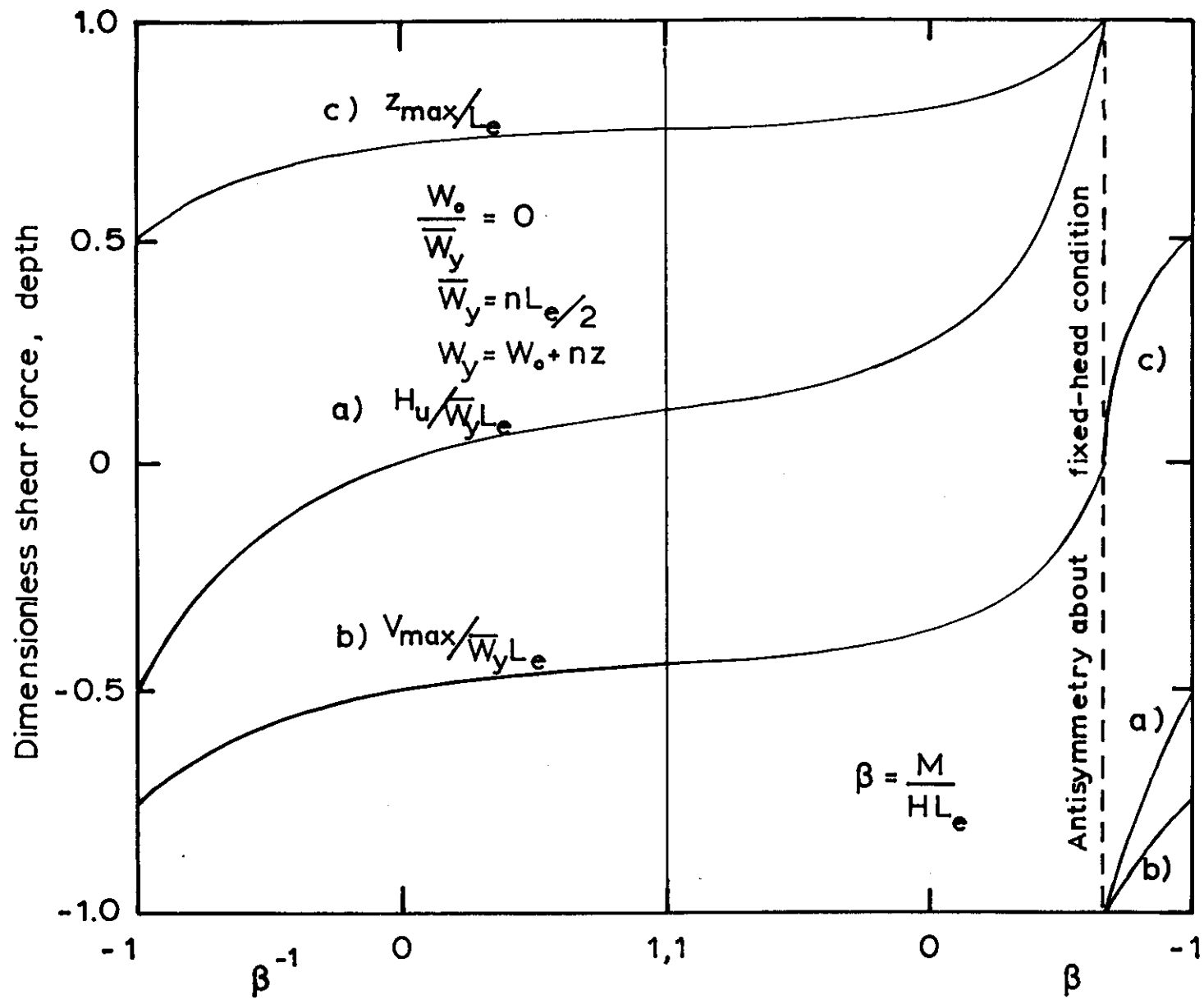


FIG. I.1 ULTIMATE HEAD LOAD, H_u , DEPTH TO AND VALUE OF THE MAXIMUM SHEAR, V_{max}

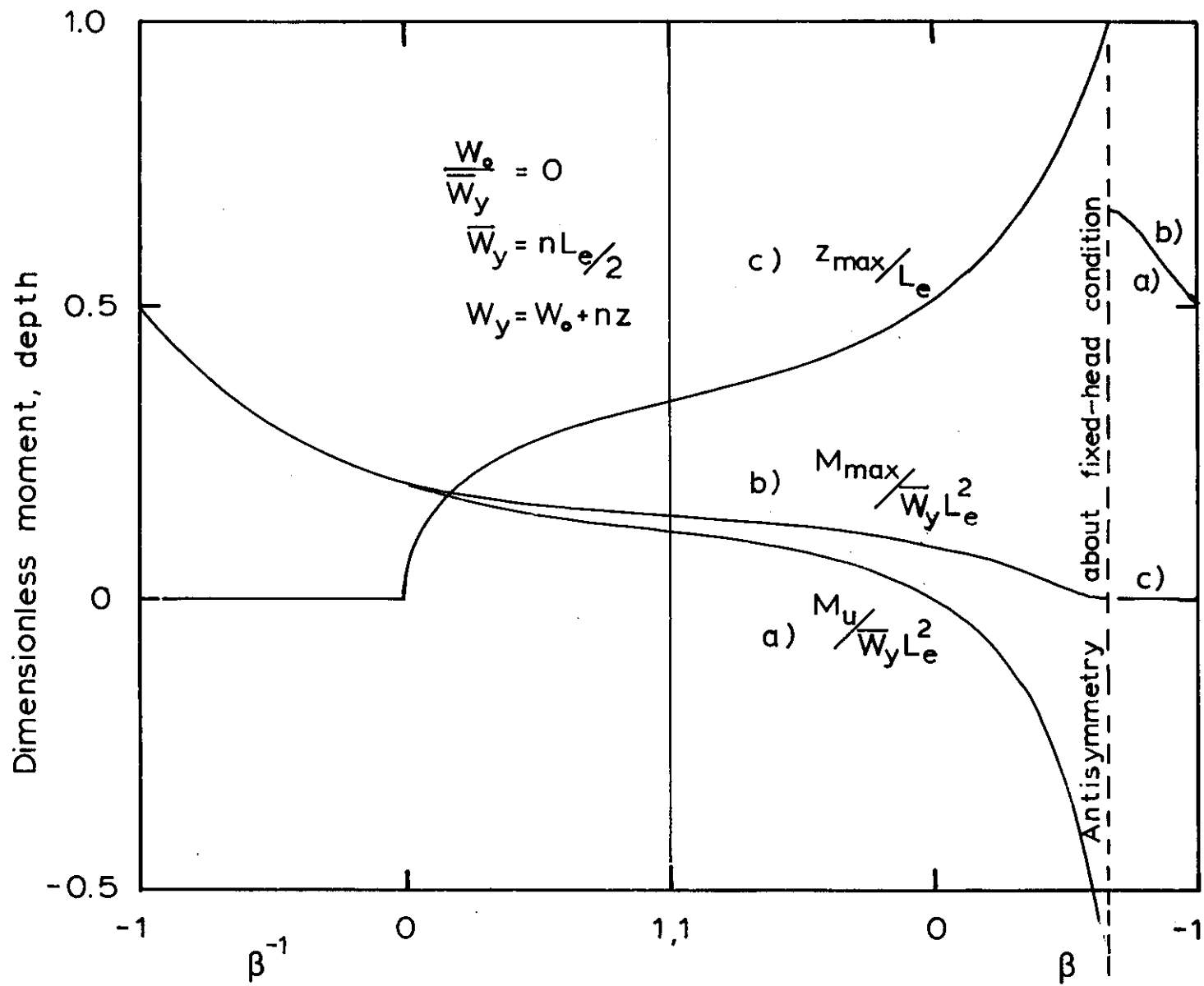


FIG. 1.2 ULTIMATE HEAD MOMENT, M_u , DEPTH TO AND VALUE OF THE MAXIMUM MOMENT, M_{\max}

Appendix II

Patch Loading : Fourier Series Approximation

The two forms of tractions studied for modelling of the pile-soil interface can be synthesised by trigonometric functions over the loaded half of the biface element and by zero traction over the gapped half. Thus, a need arises for the approximation of a trigonometric function over a prescribed arc and depth of the hole in the soil in which the pile is located, and a compatible area of the pile itself. This approximation is taken from a truncated Fourier series of the form

$$\begin{aligned} f(\theta) = & a_0 + a_1 \cos \theta + a_2 \cos 2\theta + a_3 \cos 3\theta + \dots \\ & + b_1 \cos \theta + b_2 \cos 2\theta + b_3 \cos 3\theta + \dots \end{aligned} \quad \text{II.1}$$

The Fourier coefficients a_k and b_k can be determined from the values of integrals of the function $f(\theta)$, given by

$$2\pi a_0 = \int_0^{2\pi} f(\theta) d\theta$$

$$\pi a_k = \int_0^{2\pi} f(\theta) \cdot \cos k\theta d\theta \quad \text{and}$$

$$\pi b_k = \int_0^{2\pi} f(\theta) \cdot \sin k\theta d\theta. \quad \text{II.2}$$

For generality, the loading may be taken to be in the direction θ_0 and act over an arc of the circle defined by $\theta_0 - c < \theta < \theta_0 + c$.

Thus, in order to model the trigonometric functions given by $\sin n\theta$ and $\cos n\theta$ it is necessary to evaluate the integrals given by

$$2\pi a_o = \int_{\theta_o - c}^{\theta_o + c} \cos n\theta \, d\theta$$

$$\pi a_k = \int_{\theta_o - c}^{\theta_o + c} \cos n\theta \cdot \cos k\theta \, d\theta \quad \text{and}$$

$$\pi b_k = \int_{\theta_o - c}^{\theta_o + c} \cos n\theta \cdot \sin k\theta \, d\theta. \quad \text{II.3}$$

for $\cos n\theta$ and a similar set of integrals for $\sin n\theta$.

These integrals have been evaluated and are presented in Table II.1. The special case of a uniform load, p_o over the arc length is presented, although it is obtainable from the approximation of a Cosine function with n equal to zero. From this table, the effect of any loaded area may be synthesised and in particular the two cases of $n = 1$ and 2 , needed to model the two load forms assessed in Chapter Five, can be calculated for $\theta_o = 0$ and $c = \pi/2$.

Load Case	Fourier Term Coefficient		
	a_0	a_k	b_k
<i>Uniform</i> $p=p_0$	$\frac{p_0 c}{\pi}$	$\frac{2p_0 c}{\pi} \cdot \frac{\sin kc}{kc} \cdot \cos k\theta_0$	$\frac{2p_0 c}{\pi} \cdot \frac{\sin kc}{kc} \cdot \sin k\theta_0$
<i>Cosine</i> $p=p_0 \cos n\theta$	$\frac{p_0 c}{\pi} \cdot \frac{\sin nc}{nc} \cdot \cos n\theta_0$	$\frac{p_0 c}{\pi} \left(\frac{\sin(k+n)c \cdot \cos(k+n)\theta_0}{(k+n)c} + \frac{\sin(k-n)c \cdot \cos(k-n)\theta_0}{(k-n)c} \right)$	$\frac{p_0 c}{\pi} \left(\frac{\sin(k+n)c \cdot \sin(k+n)\theta_0}{(k+n)c} + \frac{\sin(k-n)c \cdot \sin(k-n)\theta_0}{(k-n)c} \right)$
<i>Sine</i> $p=p_0 \sin n\theta$	$\frac{p_0 c}{\pi} \cdot \frac{\sin nc}{nc} \cdot \sin n\theta_0$	$\frac{p_0 c}{\pi} \left(\frac{\sin(k+n)c \cdot \sin(k+n)\theta_0}{(k+n)c} - \frac{\sin(k-n)c \cdot \sin(k-n)\theta_0}{(k-n)c} \right)$	$-\frac{p_0 c}{\pi} \left(\frac{\sin(k+n)c \cdot \cos(k+n)\theta_0}{(k+n)c} - \frac{\sin(k-n)c \cdot \cos(k-n)\theta_0}{(k-n)c} \right)$

TABLE II.1 Fourier Terms for Trigonometric loading of an arc from $\theta_0 - c$ to $\theta_0 + c$

UNIVERSITY OF SYDNEY LIBRARY



0000000300075744